2009

BEACH MORPHODYNAMICS AND ASSOCIATED HAZARDS IN THE UK

SCOTT, TIMOTHY MARK

http://hdl.handle.net/10026.1/1850

BEACH MORPHODYNAMICS

AND

ASSOCIATED HAZARDS IN THE UK

by

TIMOTHY MARK SCOTT

A thesis submitted to the University of Plymouth
in partial fulfilment for the degree of

DOCTOR OF PHILOSOPHY

School of Marine Sciences and Engineering
Faculty of Science and Technology

In collaboration with the
Royal National Lifeboat Institution

November 2009

ABSTRACT

Name: TIMOTHY SCOTT

Title: BEACH MORPHODYNAMICS AND ASSOCIATED HAZARDS IN THE UK

In this thesis the relationship between beach morphodynamics and recreational hazards was investigated for the first time within the United Kingdom (UK). Four field experiments, conducted during 2006–2008 provided new insights into the spatio-temporal dynamics of UK beach types and their associated hazard signatures. The extent of data collection ranged from national (UK beach classification) to regional (temporal morphologic variation) to site specific (macrotidal rip current dynamics).

Detailed morphodynamic characteristics of 98 beaches within the UK were collected. Twelve distinct beach groups were identified through cluster analysis, each having a unique morphodynamic signature. Conceptualisation within a relative two-dimensional framework using the dimensionless fall velocity (Ω) and the relative tide range (RTR) required an absolute wave energy flux threshold to differentiate between intermediate beaches with ($H^2T > 5$) and without ($H^2T < 5$) three-dimensional bar morphology. The role of geologic control, sediment abundance and drainage characteristics in constraining beach morphodynamics was shown to be significant within the sites studied.

Rip currents were responsible for 68% of all recorded incidents between 2005-2007 throughout all 76 beaches patrolled by the Royal National Lifeboat Institution (RNLI). Hazard type and severity varied between morphodynamic beach types. Intermediate beaches with low-tide bar/rip morphology (Ω = 2–5 and $RTR < 7$), including Low-Tide Terrace and Rip (LTT+R) and Low-tide Bar/Rip (LTBR) beaches, presented the greatest risk to the insea beach user. These high risk beaches, representing 59% of the west coast beaches in Devon and Cornwall, also attracted the greatest visitor populations.

Seasonal monitoring of hydrodynamics and morphology at LTT+R and LTBR beaches in Devon and Cornwall (annual $H_{s10\%}$ = 3–4 m; mean spring tidal range = 4.2–8.6 m) identified key mechanisms controlling the temporal hazard signature (THS), a term used here to describe the spatio-temporal variation in type and severity of bathing hazard within a specified region both in the alongshore as well as in the cross-shore (significant in macrotidal environments). The morphological template controlled the presence, extent and intensity of beach rip current systems, where the development of low/tide transverse and inter-tidal bar/rip systems during summer presented the greatest morphological hazard. Typical summer wave forcing by

relatively small, long period swell ($H_s \sim 0.5\text{-}1$ m; $T_p \sim 6\text{-}10$ s) over this morphology provided conditions conducive to hazardous rip currents. Under these conditions hazard exposure was increased due to the accessibility of the relatively low energy surf zone. Both spring/neap and semi-diurnal tidal variations were identified as key controls on the THS. Variable tidal excursion modulates rip current activity, and tidal translation rates control the rate of change of the THS. The 'optimum' combination of these mechanisms results in the 'switching' on and off of rip currents during spring low tides and the subsequent rapid alongshore migration of rip channel/hazard location as the surf zone inundates the landward inter-tidal bar system. In conjunction with high insea population, these 'optimum hazard scenarios' drove the high risk, coast-wide 'mass rescue' events identified in the incident records.

This work provides a scientific, standardised basis for a beach risk assessment model and lifeguard training programs within the RNLI. Improved understanding of macrotidal rip currents has initiated new field and modelling efforts to further general quantitative understanding of these systems, vital to the improvement of beach safety services.

AUTHOR'S DECLARATION

At no time during the registration for the degree of Doctor of Philosophy has the author been registered for any other University award without prior agreement of the Graduate Committee.

Except for Chapter 6, there was no other significant collaborative contribution to the research documented in this thesis, the contents of which are the results of original research carried out by the author.

Relevant scientific conferences and symposiums were regularly attended at which work was often presented; external institutions were visited for knowledge exchange and consultation purposes and several papers prepared for publication.

Word count of main body of thesis: 64,071.

Signed

Date 22/6/2010

Publications (journal and conference proceedings):

Austin, M.J. and Scott, T.M., submitted. *Temporal observations of rip current circulation on a macro-tidal beach*. Continental Shelf Research.

MacMahan, J., Brown, J.W., Reniers, A., Brown. J.A., Thornton. E., Stanton.T., Austin. M.J. and Scott. T.M., *Mean lagrangian flow behaviour on a open coast rip channeled beach: a new perspective*. Marine Geology. *(in press)*.

Scott, T.M., Russell, P.E., Masselink, G. and Wooler, A., 2009. *Rip current variability and hazard along a macrotidal coast*. Journal of Coastal Research, SI 56, 895-899.

Austin, M.J., Scott, T.M., Brown, J.W., Brown, J.A. and MacMahan, J.H., 2009. *Macrotidal rip current experiment: circulation and dynamics*. Journal of Coastal Research, SI 56, 24 - 28.

Scott, T.M. , Russell, P.E., Masselink, G., Wooler, A., 2008. *High volume sediment transport and its implications for recreational beach risk*. International Conferenence on Coastal Engineering 2008 (Hamburg, Sept 2008), 4250-4262.

Scott, T.M., Russell, P.E., Masselink, G., Wooler, A. and Short, A., 2007. *Beach rescue statistics and their relation to nearshore morphology and hazards: a case study for south-west England*. Journal of Coastal Research, SI 50, 1-6.

Dawes, P., and Scott, T.M., 2007. *Developing a risk assessment model for practical application in the UK*. ILS World Water Safety 2007, Porto, Portugal, 27th-29th September.

Wills, S. and Scott, T.M., 2007. *The research, development and implementation of the UK national guidelines and specifications for coastal public rescue equipment*. ILS World Water Safety 2007, Porto, Portugal, 27th-29th September.

Other presented work:

Scott, T.M., 2009. *University of Plymouth: Student Data Use*. Plymouth Coastal Observatory, Third Annual Partners Meeting. Oral presentation. Forde House, Newton Abbot, October 2009.

Austin, M.A., Scott, T.M., Masselink, G. and Russell, P.E., 2009. *Macrotidal rip current experiment: circulation and dynamics*. Plymouth Marine Sciences Partnership (PMSP) Symposium 'Science for a Changing World', 7 April 2009. Oral presentation and abstract.

Scott, T.M., Russell, P.E., Masselink, G. and Wooler, A., 2008. *Seasonal and geographical variations in rip current systems and beach morphology: implications for beach safety in the UK*. British Geomorphological Association conference, July 2008. Abstract.

Scott, T.M., Russell, P.E., Masselink, G., Wooler, A. and Short, A., 2007. *Spatiotemporal dynamics in beach morphology and their implications for assessing UK beach hazards: a case study for SW England*. Marine Institute Conference presentation and abstract. University of Plymouth, December 2007.

Scott, T.M., 2007. *Risk Assessment Update*. Full-time Lifeguards Conference (RNLI). Oral presentation, Poole, UK, September 2007.

TABLE OF CONTENTS

3.   BEACH RESCUE STATISTICS, NEARSHORE MORPHOLOGY AND HAZARDS: A CASE STUDY FOR SOUTHWEST ENGLAND

4.   UK BEACH CLASSIFICATION

LIST OF FIGURES

LIST OF TABLES

ACKNOWLEDGEMENTS

1. INTRODUCTION

1.1 PREAMBLE

Due to its location and geologic setting, the United Kingdom (UK) possesses a very broad spectrum of beach environments around its more than 5,000-km long shoreline. UK beaches attract a large number of visitors annually due to their aesthetic, sport and recreational appeal, providing pivotal support to the tourism industry in many regions. However, the beach environment is inherently hazardous and exposes people to risk. To manage this risk a comprehensive understanding of UK beach environments and their associated hazards is needed.

Historically, beach hazards have been addressed in terms of the vulnerability of coastal areas to damage, often financially with regard to loss of property or infrastructure. Since the late 1980's interest within the scientific community for developing understanding of hazards and risk to the beach user has grown (Engle et al., 2002; Hartmann, 2006; Lascody, 1998; Leahy et al., 1996; Lushine, 1991; Sherker et al., 2008; Short, 2001; Short, 1999; Short and Hogan, 1994a) and the application of our improved knowledge of beach dynamics to the public domain and safety was initiated through the work of Short (1999). Nearshore currents such as rip currents have long, been documented as significant hazards to beach users swimming in the surf zone (McKenzie, 1958; Shepard, 1949). Lascody (1998) stated that, in Florida, rip currents, on average, result in more deaths than hurricanes, tropical storms, lightning and tornadoes combined.

In the UK the significance of beach hazards has been considered serious enough for lifeguard provision to be deemed necessary around the nation's coasts for the past 50 years. Therefore, the attention of the scientific community to this application of knowledge is long overdue. With increased professionalism within the lifeguarding community and increasing availability of both data collection techniques and advanced scientific quality datasets of the coastal environment, a higher quality dataset of the state of beach hazard is becoming available.

This project is concerned with the nature of physical beach hazards at UK beaches, specifically hazard levels, their spatio-temporal distribution and the relationship

1

between beach hazard and type. This requires an assessment of the applicability of present understanding of beach morphodynamics to a UK beach environment that is dominated by large tides, a mixed often high-energy wave climate and a complex geological history. Identified as a knowledge deficit, Short (2006) highlighted the need for further research in these afore-mentioned beach environments, endemic in the UK, which have morphodynamically received little previous attention.

The Royal National Lifeboat Institution (RNLI), the principal provider of lifeguard services to the UK, commissioned this project. The project was conceived to further the understanding of beach morphodynamics and hazard within the UK to provide a basis for the development of practical hazard assessment tools and improved lifeguard training. These elements are an integral part of the risk assessment and mitigation programs within the RNLI.

1.2 AIMS AND STRUCTURE OF THESIS

The broad aim of this study is to improve our understanding of beach morphodynamics and associated hazards within a UK coastal environment. Through a review of the UK coastal environment and relevant previous research specific to beach morphodynamics and hazards, specific targeted project aims were defined:

1) Identify the nature and specific causes of beach hazards through the assessment of RNLI incident records and assess the resulting hazard signatures.

2) Identify beach type variability in UK and investigate the appropriateness of using a beach classification system to describe beach type groups though the use of traditional morphodynamic parameters.

3) Investigate the spatial distribution of the identified beach types and their associated morphodynamic characteristics.

4) Investigate the relationship between hazard and beach morphodynamics within the UK environment and assess whether it is similar to that observed in previous research.

5) Identify the extent to which rip currents are a hazard in UK and identify and quantify the location, circulation and dynamics of high-risk rip current scenarios.

The structure of the thesis, illustrated in Figure 1.1, comprises four main sections, each representing distinct field campaigns and associated analysis.

This chapter highlights the research problem, project aims and the process of development of a baseline understanding through a review of the UK coastal environment and relevant literature. Chapter 2 provides a description of field and laboratory techniques used to collect and analyse data that are either common to the varied field campaigns or more appropriate as reference material to avoid duplication in subsequent chapters.

Chapters 3-6 pertain to each of the four field campaigns, each addressing the aims identified above. Chapter 3 provides an introduction to the physical environment of the

OBJECTIVES

- DEFINE RESEARCH PROBLEM AND PROJECT OBJECTIVES
- PROVIDE INFORMATION OF THESIS STRUCTURE
- IDENTIFY KEY RESEARCH AND CONCEPTS
- INITIAL DATA COLLECTION AND REVIEW OF THE UK COASTAL ENVIRONMENT

- DEFINING CORE DATA COLLECTION AND ANALYTICAL TECHNIQUES

- IDENTIFYING BEACH HAZARD CHARACTERISTICS
- INVESTIGATING RELATIONSHIP BETWEEN HAZARDS AND BEACH TYPE

- INVESTIGATING SPATIAL BEACH TYPE VARIABILITY IN UK
- DEFINING UK BEACH CLASSIFICATION
- INVESTIGATING TEMPORAL VARIABILITY OF BEACH MORPHODYNAMICS AND ASSOCIATED HAZARDS
- IDENTIFYING RIP CURRENT CHARACTERISTICS AND ASSOCIATED HAZARDS

- INVESTIGATING HIGH RISK MACROTIDAL RIP CURRENT SCENARIOS
- INVESTIGATING RIP CIRCULATION AND DYNAMICS

- COLLATION, INTEGRATION AND DISCUSSION OF KEY CONCEPTS AND FINDINGS
- APPLICATION OF RESEARCH

Figure 1.1 – Flow chart detailing the structure of thesis. Pentagons represent field campaigns and their links to relevant chapters. Summaries of key objectives for each chapter are provided to the left of the flow chart. To the right are indications of the outputs for each section of work, specifically relating to conference presentations and published articles (Appendix 5).

study region, the RNLI lifeguard service and documents an initial field campaign designed to provide the context for subsequent investigation by providing an assessment of the type and spatial distribution of beach morphology and environmental setting within the study region. This morphological assessment is combined with an analysis of RNLI beach incident statistics and beach population data to provide an insight into hazard characteristics and an initial assessment of the link between beach type and hazard.

Chapter 4 examines in detail the diversity and spatial distribution of beach environments within England and Wales investigating their morphodynamic regimes and proposing a beach classification system and associated conceptual morphodynamic framework.

Chapter 5 provides a comprehensive analysis of beach hazards in the context of the classified beach types identified in Chapter 4. This analysis informs the third field campaign that investigated the temporal variation of morphology and environmental forcing at a selection of the high hazard beach types within the study region, concluding with an assessment of the hazard and beach safety implications of temporal morphodynamic variation on a scale of years to minutes.

Chapter 5 identified a number of high risk rip current scenarios which were investigated further in Chapter 6 through a fourth field campaign, focussing on a low-tide, macrotidal rip current system that resembled, as close as was possible, the morphology and forcing conditions that were observed to generate 'optimum' high hazard scenarios. An investigation of the forcing mechanisms and tidal modulation under these conditions provided a new quantitative insight into a previously unstudied type of rip current system.

Finally Chapter 7 provides a synthesis and discussion, bringing together the key findings and evaluating them in the context of the project aims and previous research, finishing with the key conclusions.

1.3 REVIEW

1.3.1 The UK coastal environment

The coast of England and Wales is one of the most diverse coastlines in the world and a large variety of coastal landforms are represented, including dunes, sand and gravel beaches, barriers and spits, various types of estuaries, tidal flats and salt marshes, rapidly eroding soft-rock cliffs and resistant hard-rock cliffs with shore platforms. Many publications over the years have addressed the coastal geomorphology of England and Wales, such as the seminal work by Steers (1946) and regional guides pertaining to interesting stretches of coastline of particular relevance for this study (Bridges, 1998; Brunsden and Goudie, 1997; Castleden, 1996; Keene, 1996; Motterhead, 1996)

The large variety in coastal systems along the coastline of England and Wales is mainly attributed to the along-coast variability in static and dynamic environmental factors, or boundary conditions. The three most important environmental factors are geology, sediments and external forcing (wind, waves, storms and tides), with sea level serving as a meta-control by determining where coastal processes operate. When contemporary coastal systems and processes are considered, human activity should also be taken into account. Spatial variability in the boundary conditions is responsible for geographical variations in coastal morphology and morphodynamics (Davies, 1980).

1.3.1.1 Sea level

Long-term coastal evolution is largely driven by changes in (relative) sea level. At the end of the glacial maximum, around 18,000 years ago, sea level started to rise rapidly from ~ 120 m below present sea level, attaining its present level around 4,000 years ago (Fairbanks, 1989). The effect of this sea-level rise on the coastline of England and Wales must be considered in combination with the changes in the land level associated with glacio-isostatic effects, in particular isostatic rebound of the formerly glaciated areas in the north, and collapse of the forebulge of areas near the ice margin in the south. Shennan and Andrews (2000) reconstructed the relative sea-level in NW Europe during the Holocene. The situation at 7,500 BP, when global mean sea level was ~ 15 m below present, highlights the contrast between the east coast of England and the rest of the country (Figure 1.2). At this time, the coastline of east England had a very different shape and was located more than 10 km seaward of the present coastline. Therefore the implication is that the modern day coast is very young,
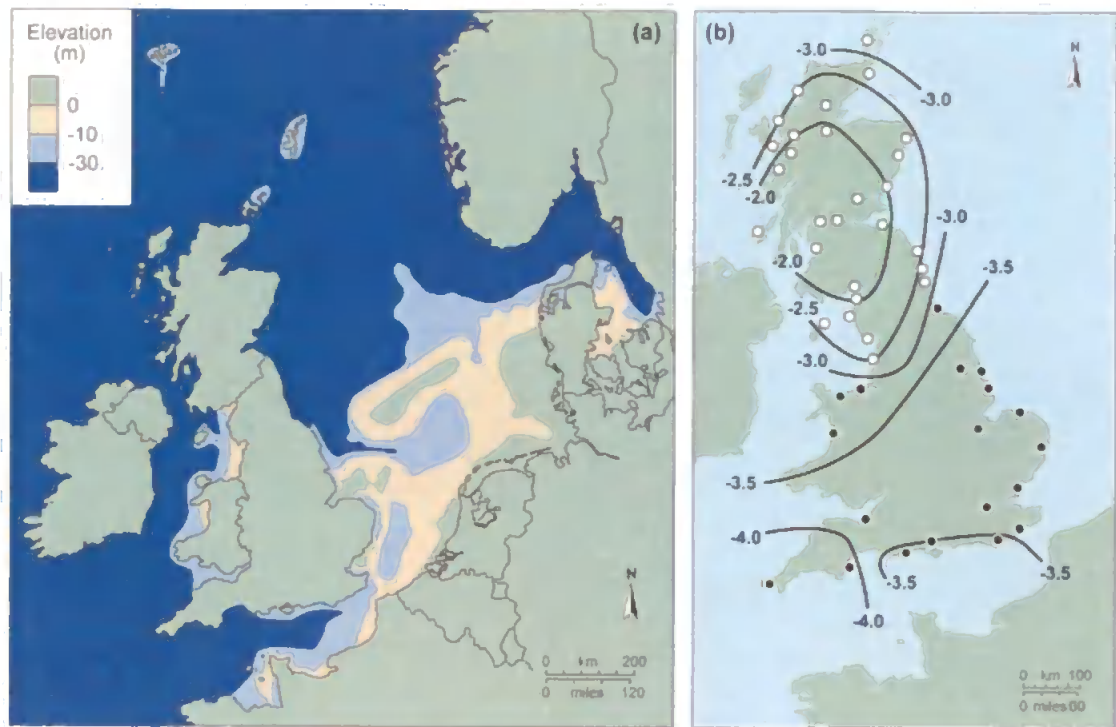
Figure 1.2 – (a) Coastal configuration of NW Europe 7,500 years BP (Shennan and Andrews, 2000) and (b) estimated current relative land-level changes (mm yr^{-1}) in England and Wales obtained by combining current land-level change (Shennan and Horton, 2002) with current eustatic sea-level change (Church and White, 2006). The open and solid circles indicate rising and falling absolute land levels, respectively.

and is unlikely to have equilibrated to present day sea-level conditions; therefore, it is likely to be significantly affected by relaxation time effects. The post-glacial sea-level rise ceased about 4,000 years ago, but over the last 130 years sea level has begun rising again by 0.2 m, equating to a rate of rise of 1.5 mm yr^{-1} (Church and White, 2006). The current rate of sea-level rise, based on a decade of satellite altimeter data, is 3 mm yr^{-1} (Church and White, 2006). Combining the current rate of global mean sea-level rise with Shennan and Horton's (2002) recently revised estimates of rates of land-level change in England and Wales suggests that the relative rate of sea-level rise in north and south England is ~ 2 and 4 mm yr^{-1}, respectively (Figure 1.2).

1.3.1.2 Geological history

Steers (1960) attributed the diversity in coastal geomorphology in England and Wales mainly to the variety of rocks in the country. The large-scale solid geology, characterised by a decrease in age from west to east, forms the template of the overall coastal topography and the outline of the coast. The geology exerts its control on coastal
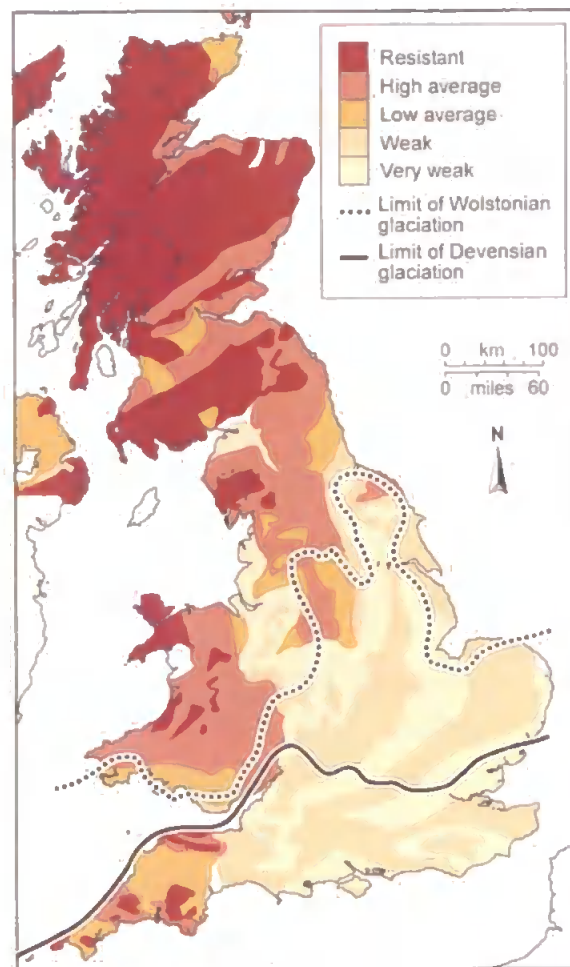
Figure 1.3 – Map of Britain showing resistance of the geology to denudation (Clayton and Shamoon, 1998).

morphology mainly through the resistance of the rocks to denudation (Figure 1.3) and this provides the explanation for the contrast between the high-relief, mainly rocky coasts of west England and Wales, and the low-relief, mainly unconsolidated coasts of east England (Clayton and Shamoon, 1998). On a smaller scale, coastal landforms such as headlands, bays and inlets reflect contrasts in rock strength, and it is the local contrasts that lead to the detail and diversity of our coasts (May and Hansom, 2003).

1.3.1.3 Sediments

In addition to the solid geology, the drift geology is also important, mainly a legacy of the most recent and penultimate glaciations, the Devensian and Wolstonian, respectively. During deglaciation, large quantities of glacial and paraglacial sediments, comprising the full spectrum of sediment sizes from mud to boulders, were left by the retreating glaciers. The coarser material, most of which was deposited on what is now

the continental shelf has been transported onshore during the post-glacial transgression and has been incorporated in dunes, beaches, barriers and estuaries (Anon, 2002). This sediment source is now mostly depleted and offshore sediment supply to the coast by natural processes is very limited. However, most of the material that was deposited on what is now land is still present and represents an important sediment source to the nearshore system through cliff erosion (Bray and Hooke, 1997). The finer fractions of these eroded glacially-derived sediments (mud and silt) are being deposited on salt marshes and tidal flats in estuarine environments, or are transported to the southern North Sea by tidal currents (Dyer and Moffat, 1998). The coarser fractions (sand and gravel) enter the littoral system and are distributed along the coast.

1.3.1.4 Coastal processes: waves, tides and extreme events

Coastal sediment transport processes are the result of external forcing, mainly in the form of tide- and wave-driven currents. The wind climate is of significance as well, either indirectly through the generation of waves and currents, or directly by inducing aeolian sediment transport and dune development. The tidal regime and wave climate exhibit a large spatial variability (Figure 1.4) and play an important role in explaining the diversity in coastal landforms on England and Wales.

The tidal range varies along the coast due to the presence of several amphidromic systems and the interactions between the tidal motion and the coastal topography. The largest tides occur in the Bristol Channel due to the 'funnelling effect' of the coastal topography and the smallest tides are experienced in the lee of the Isle of Wight in proximity to the degenerate amphidromic point near Bournemouth. For the majority of the coast, the amplitude of the M2 tidal component is larger than 1.5 m and the mean spring tide range exceeds 4 m.

Within England and Wales the most energetic wave conditions are experienced in the southwest, where the 50% exceedence significant wave height ($H_{s,50\%}$) is larger than 1 m and the wave climate is a mixture of Atlantic swell and locally-generated wind waves. The lowest wave conditions prevail in Northwest and East England, where waves are predominantly wind waves and $H_{s,50\%}$ is generally less than 0.5 m. The influence of exposure to the Atlantic Ocean in the southwest of England and to a lesser extent the Irish Sea increases the contribution of long-period, swell waves to the wave spectrum. The complexities of coastal orientation and exposure around the coasts of
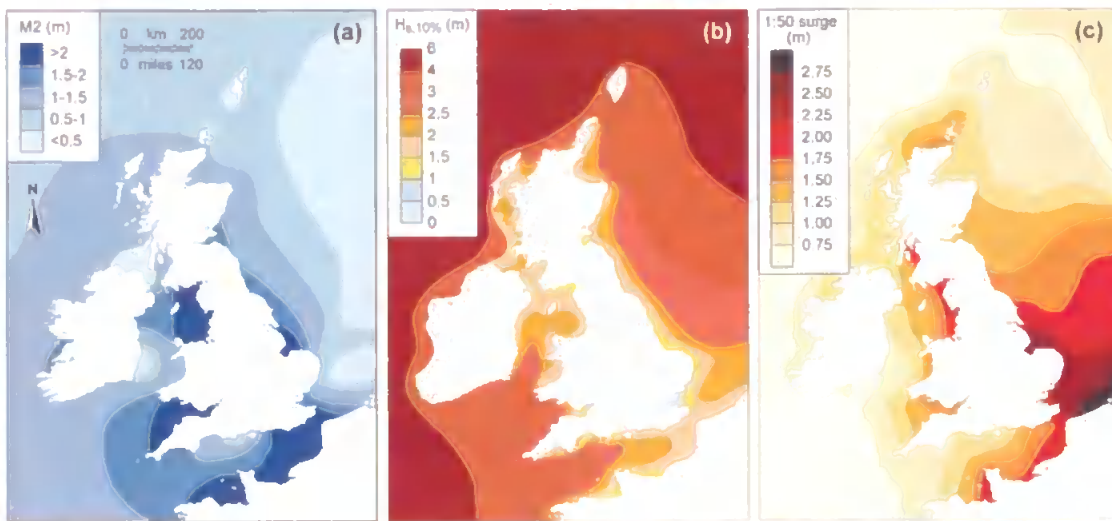
Figure 1.4 – Map of Britain with: (a) M2 tidal amplitude (adapted from Proudman and Doodson, 1924); (b) 10% exceedence significant wave height, $H_{s10\%}$ (Draper, 1991); and (c) 1-in-50 year storm surge level (Flather, 1987).

England and Wales lead to a dynamic balance of clearly defined high-/low-energy, and wind/swell wave components that is often characterised by a bi-modal wave energy spectrum (Figure 1.5) with multiple directional sources in many regions (Bradbury et al., 2004). Mean seasonal variation in wave climate is significant in many coastal regions with strong summer-winter wave energy variations illustrated in Figure 1.6 where wave buoy data from the Atlantic southwest coast of England (2003–2008) shows 10% exceedence significant wave heights ranging from 2 m to 5 m from summer to winter, respectively. Joint wave distributions from the same location clearly show that a significant portion of the increase in energy during winter months is due to high-energy storm events with associated mean wave periods of up to 14 s (Figure 1.7), whereas the modal joint wave events increase on average by approximately 1 m (1.5–2.5 m) with a similar mean wave period. Characteristics of storm frequency variations are shown in Figure 1.8.

Coastal morphological changes that occur as a result of extreme water level conditions during storms, such as coastal dune erosion and barrier breaching can be equally as important as waves and tides. Storm events are particularly relevant due to the associated flooding and indeed, the most serious natural hazard to have affected England during the last 100 years was the 1953 storm surge that struck the east coast of England (Baxter, 2005). The distribution of extreme surge height around the UK coast
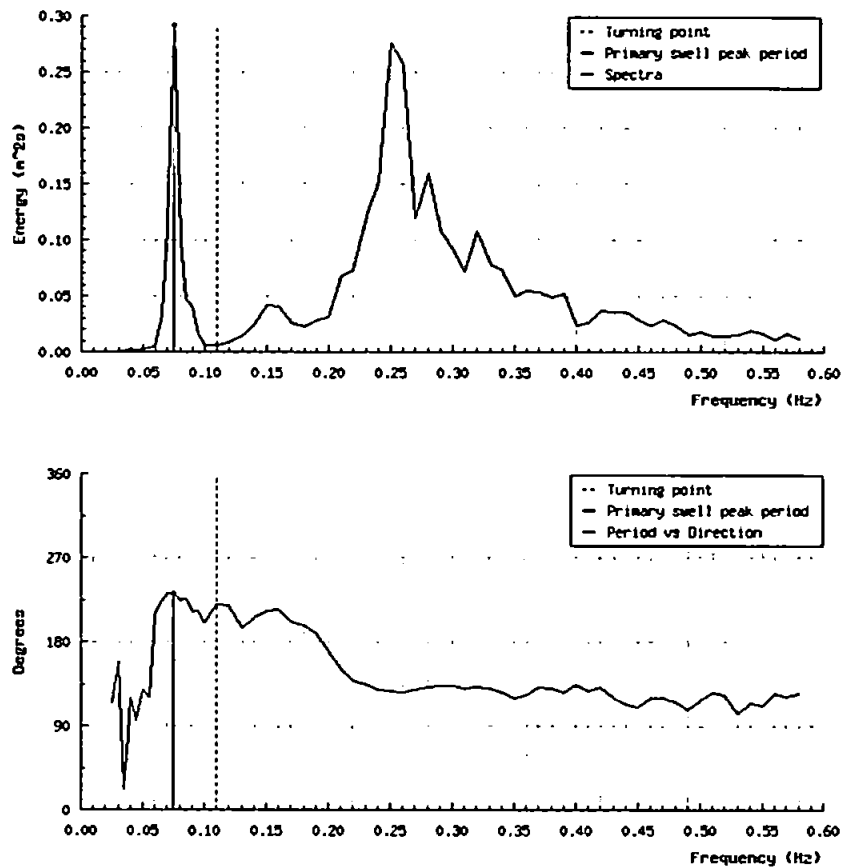
Figure 1.5 – Typical spectral wave output from Looe on the South Cornwall Channel coast showing a bi-modal, bi-directional sea (data courtesy of the Channel Coast Observatory).

is plotted in Figure 1.4 and indicates that the areas particularly prone to storm surge are the east coast of England with a 1:50 year storm surge height of 1.5–2.5 m, and the NW coast of England and the Bristol Channel with a 1:50 year storm surge height of ~1.5 m.

An analysis of storm wave characteristics along the Atlantic west coast from 2003 to the present illustrates the extreme high wave conditions experienced in west coast regions. On average, 17.4 storm events (peak H_s > 4 m) and 5 severe storm events (peak H_s > 6 m) occur annually. Figure 1.8 illustrates the strong seasonal variation in both storm intensity and duration with the peak H_s of the highest storm events exceeding 8 m and on one occasion reaching > 10 m. Sustained periods of high-energy storm conditions during winter are common averaging > 40% of storm days per month (Figure 1.8). The seasonal high-energy character of much of the west coast of England and Wales plays a key role in the evolution of the coastal geomorphology of the region.
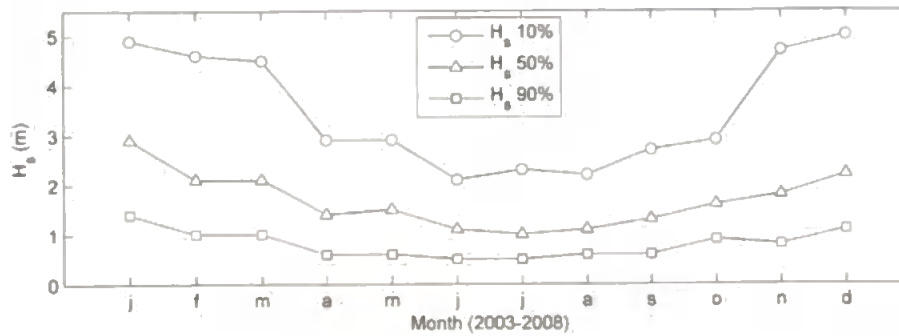
Figure 1.6 – Monthly wave height exceedence statistics for Seven Stones offshore wave buoy (50.10°N 3 6.1°W) between 2003 – 2008.
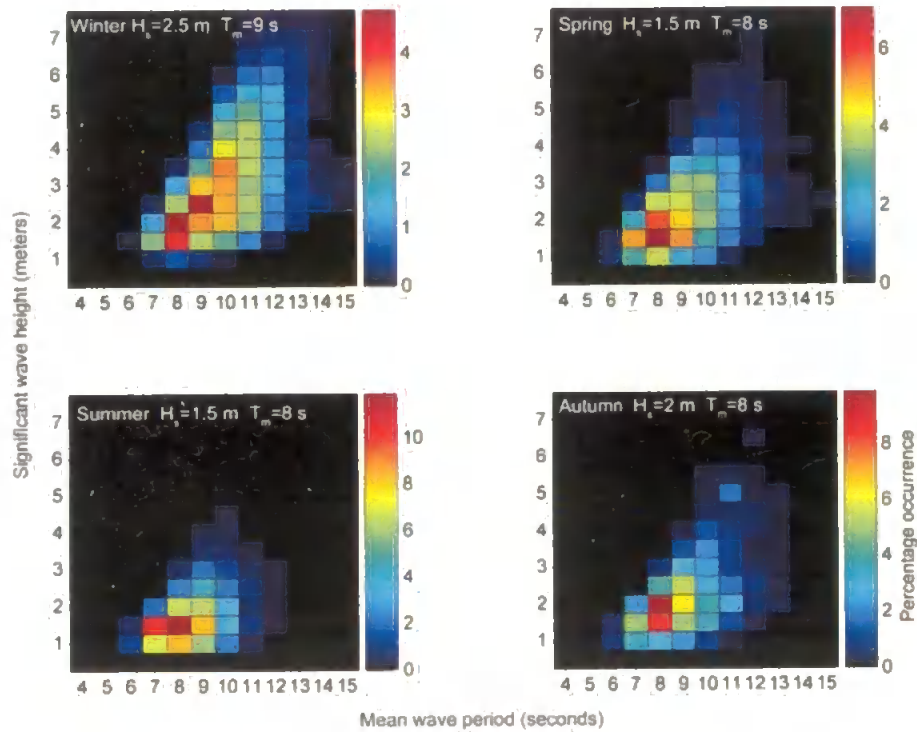
Figure 1.7 – Seasonal joint distribution wave climate statistics for significant wave height and mean period for Seven Stones offshore wave buoy (50.10°N 3 6.1°W) from 2003 to 2008.
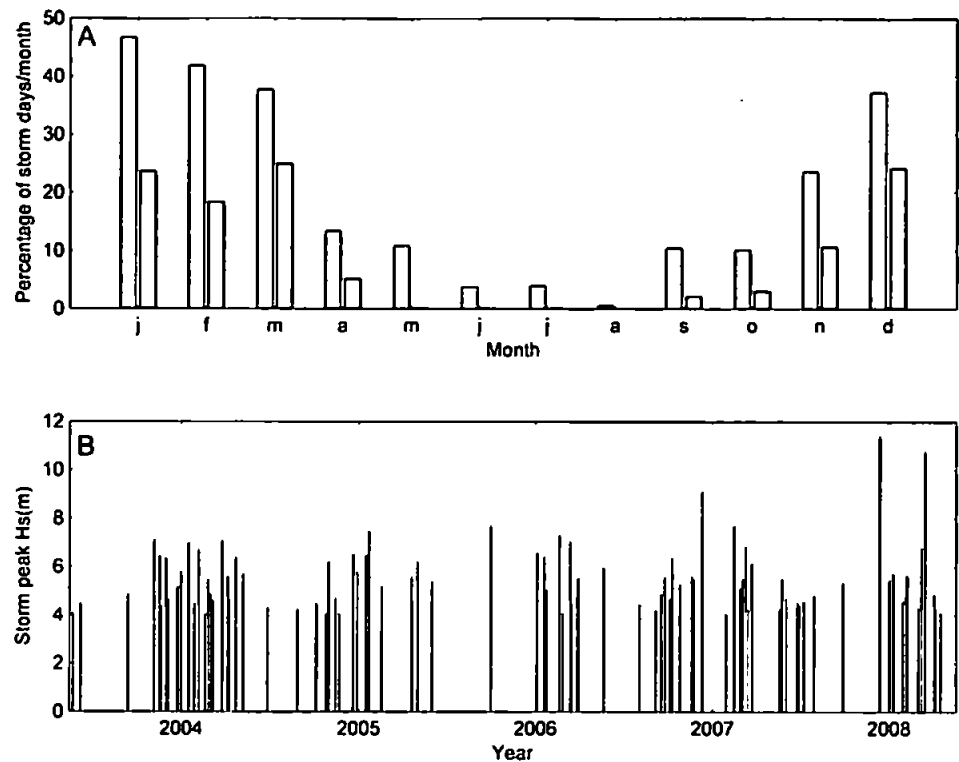
Figure 1.8 – Temporal characteristic of storm events in the southwest of England (Seven Stones offshore wave buoy, 2003 – 2008). Storm duration defined as the time over which the mean hourly H_s remained above 2 m: (A) storm days per month, grey and white bars represent storm peak > 4 m and > 6 m, respectively; (B) Peak wave heights (H_s) for storms identified between 2003 and 2008.

Table 1.1 – Storm event statistics for Seven Stones offshore wave buoy (50.10°N 6.1°W) from 2003 - 2008.

	Storm frequency (2003-2008)		Storm duration (2003-2008)			
	Peak H_s > 4 m	Peak H_s > 6 m	Peak H_s > 4 m		Peak H_s > 6 m	
	Mean events	Mean events	Mean hrs	sd	Mean hrs	sd
Annual	17.4	5.0	100.1	89.2	162.9	101.4
Winter	5.8	2.0	155.1	123.3	231.3	109.5
Spring	5.4	1.6	78.1	51.3	82.2	46.9
Summer	1.8	0.0	27.7	6.0	0.0	0.0
Autumn	4.0	1.2	77.1	34.6	85.8	28.6

1.3.1.5 Coastal modification

Most of the coastline of England and Wales is developed, often modifying coastal morphodynamic systems (Figure 1.9). In England alone, the total length of man-made coastal defences is at least 860 km (Herlihy, 1982; MAFF, 1994). These defences restrict the natural landward movement of coastal systems under the influence of rising relative sea level, resulting in a steepening of the inter-tidal profile. In England and Wales, almost two thirds of the inter-tidal profiles have steepened over the past hundred years, whereas only one third has flattened (Taylor et al., 2004). Direct human intervention in nearshore and inshore sediment transport processes is also important. These include fragmentation of the coast by engineering structures that interrupt the littoral drift (e.g., groynes, breakwaters, marinas and jetties), removal of sediment by dredging and provision of sediment through beach recharge (French, 2004).
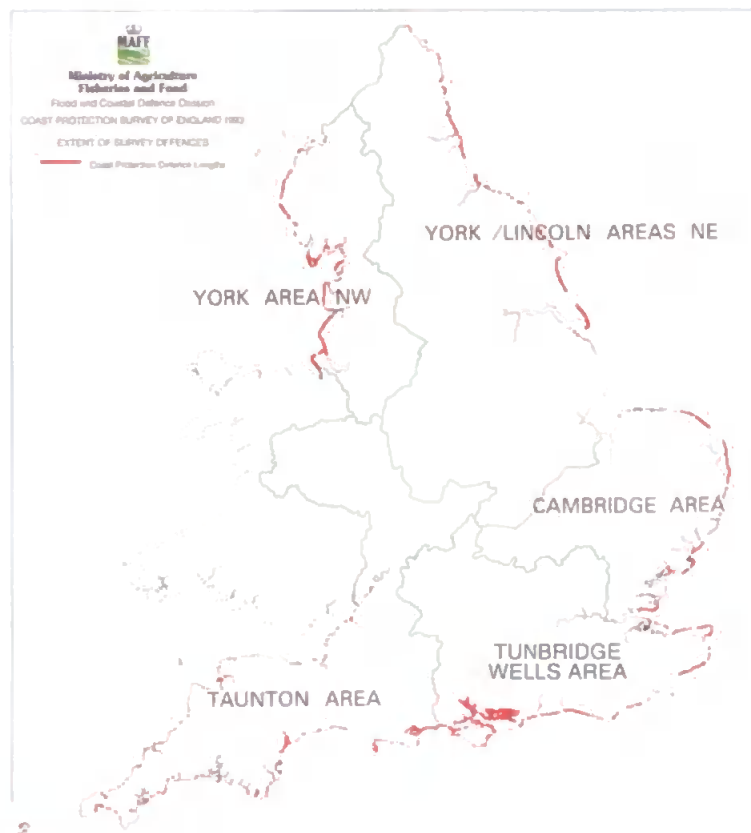
Figure 1.9 - Extent of coastal protection around England in 1993. Survey results courtesy of Ministry of Agriculture and Food (1994).

1.3.2 Beach morphodynamics and state

Beaches, acting as the border between land and sea, are composed of mobile sediments from mud to boulders lying upon and constrained by their surrounding geologic framework and influenced by the dynamics and characteristics of the surrounding coastal and shelf systems. Beaches lie between a submerged seaward point at which no significant sediment movement occurs due to waves, and a landward point that marks the maximum height that the waves act on the beach sediment. Although driven principally by wave action, this sediment is also mobilized through tidal forcing and wind driven currents. Beach shape and characteristics vary greatly around the globe depending on numerous environmental factors and their complexity and beauty has been a source of fascination to coastal scientists for decades.

Within a geologic timescale, many factors such as shelf dimensions and gradient, sediment supply, and relative changes in sea-level exact an overarching control on the coastal system within which a given beach resides (Reading and Collinson, 1996). These factors, among others, affect the coastal geomorphologic setting of beach environments within the UK, which include high hard-rock cliffs, low soft-rocks cliffs, embayed coves and open ocean coast beaches, river mouths, tidal inlets, estuaries, spits and barriers. The temporal context of beach systems considered within this thesis range from an 'instantaneous' morphodynamic response (a single forcing cycle of seconds to days), to one of intra- and inter-annual 'event' change (Cowell and Thom, 1997). Due to this, the dominant characteristics under consideration are those that are known to have the greatest influence on the state of the beach system on this timescale, namely waves, tides and sediment size distribution. The geologic framework and rate of sediment supply of the beach are considered important, but stationary.

1.3.2.1 The morphodynamic approach

An important concept in the understanding of beach processes and form is that of beach morphodynamics. This systems approach, now widely used within coastal research, was introduced to coastal morphology and evolution by, among others, Wright and Thom (1977) who stated 'Coastal evolution is the product of morphodynamic processes that occur in response to changes in external conditions', resulting in the 'mutual adjustment of topography and fluid dynamics involving sediment transport'. It is the close coupling and feedback between fluid dynamics and form that drives sediment transport and produces morphological change over time. This morphological change in turn alters the boundary conditions for the fluid dynamics, affecting further morphological changes (Figure 1.10). This hydrodynamic coupling enables the possibility of identifying particular nearshore morphologies through their characteristic nearshore dynamics (e.g. Wright and Short, 1984). Apart from energy input to the system through hydrodynamic processes, characteristics of the environmental setting exert an influence on the morphodynamic system through sediment properties (abundance and characteristics), geologic characteristics (solid boundaries and geometry) and stratigraphy (antecedent morphology). The spatio-temporal variations in these environmental conditions form the boundary conditions of the morphodynamic system (Masselink and Hughes, 2003).
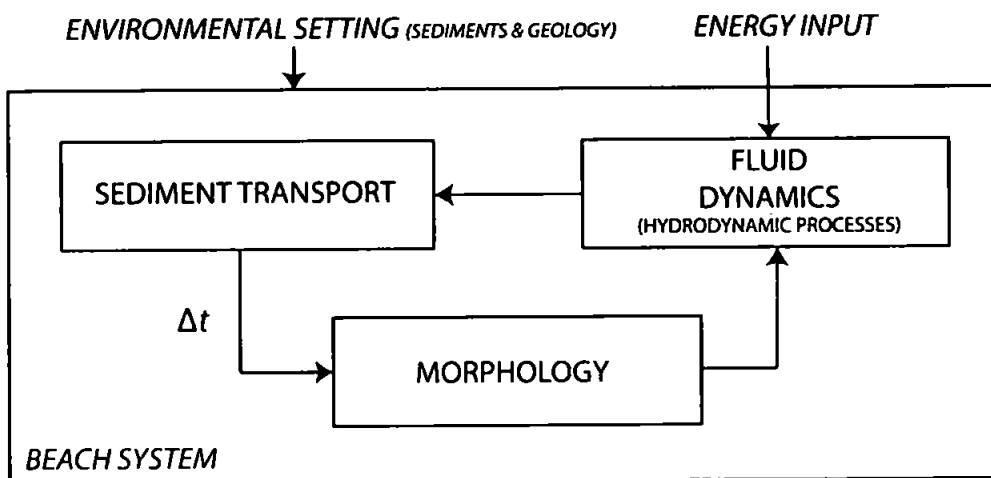
Figure 1.10. – Primary components involved in beach morphodynamics. The feedback loop is responsible for the fundamental complexities in beach morphological evolution. Δt represents the time dependence inherent in morphological evolution due to the process of sediment redistribution.

While hydrodynamic processes respond instantly to changes in morphology, morphological change requires sediment redistribution that takes a finite time (relaxation time). Due to this lag in morphological adjustment and the constantly changing nature of the forcing conditions a beach may never attain its 'equilibrium' condition. With strongly stochastic forcing conditions, evolving morphodynamic states are affected by morphological inheritance from previous states due to memory effects associated with relaxation times. Due to this non-linear behaviour in addition to associated properties of feedback (positive and negative) and self-organisation (Cowell and Thom, 1994) inherent within the coastal morphodynamic system, prediction of coastal evolution is a very difficult task (Cowell and Thom, 1994; Masselink and Hughes, 2003).

1.3.2.2 History

Early investigations of beaches, often through analysis of sequential two-dimensional beach profiles, attempted to understand the relationships between environmental factors like waves, tides, and sediment size, and the beach systems under study. Work by King (1972) gave descriptions of a number of different beach systems in Europe and the USA, from high energy open-coast beaches, to fetch-limited ridge and runnel beaches, to those associated with cresentic bars. This work successfully linked certain beach types to associated environmental conditions, but did not provide a relationship between the huge range of beach types seen globally and the variety in their morphodynamic response (Short, 1999).

The first classification of beaches began in California where Shepard and LaFond (1940) observed distinct seasonal profiles. Termed 'cut and fill', describing a cycle of erosive and accretionary conditions, where winter storm waves remove sediment to an offshore bar and a summer calm promotes beach accretion and a steep barless beach form with berm. This basic model was only applicable in a climate where distinct differences in seasonal wave climate existed, i.e. the Northern hemisphere. The two end member profiles were not linked until the first work on sequential beach profiles was conducted by Sonu and van Beek (1971) in North Carolina where they generated a completely wave dominated two-dimensional sequence of sub-aerial beach change involving an erosion and an accretion sequence (Figure 1.11).
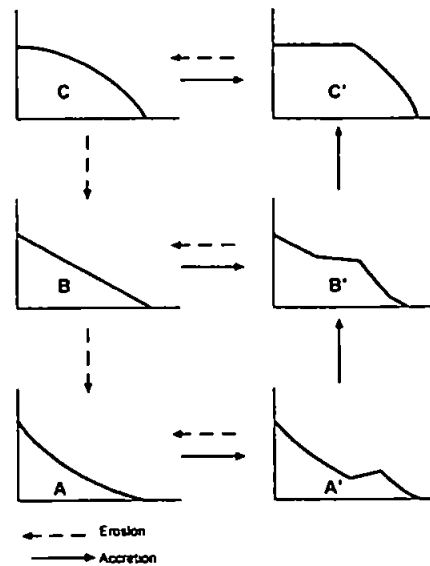
Figure 1.11. - Two-dimensional sequence of sub-aerial beach profile change (Sonu and VanBeek, 1971).

The next development was to acknowledge the three-dimensional behaviour of beach systems and incorporate the sub-tidal beach and the role of bars (Figure 1.12). The recognition of sub-tidal rhythmic bar morphologies, which had been documented by researchers since 1938, led to the first three-dimensional sequence of beach change by Sonu (1973), driven by his previous interest in rip current systems on the Florida coast (Sonu, 1972). This model involved the formation of rhythmic bars and their subsequent migration towards, and welding to, the shoreface. These cycles were associated with edge waves and the cycle of erosion during storm events and accretion during calms. Increased understanding of surf zone hydrodynamics, such as sub harmonic and infragravity wave activity, originally termed 'surf beat' (Munk, 1949); standing waves and edge waves; and radiation stress and wave set up (Tucker, 1950) aided the improved understanding of rip current circulations (Bowen and Inman, 1969), swash and nearshore cell circulation. Following these advances the relationship between net bottom currents and resultant sediment transport was developed and coupled with beach morphodynamic states (Wright and Short, 1984).

With the exception of sandy microtidal environments, which are almost completely wave dominated, in the vast majority of cases some kind of tidal effect will play a role. The degree to which tide related processes affect beach morphodynamics will be directly linked to tide range. Hence, as the tidal range increases from meso (2–4 m) to
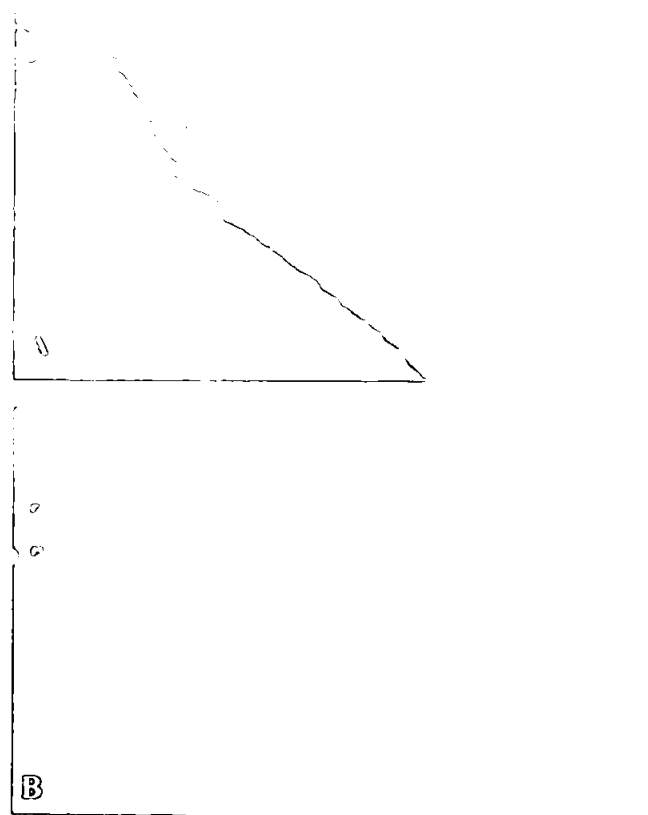
Figure 1.12. Oblique time stack images from the Duck, Field Research Facility, North Carolina. High intensity patterns are suggestive of sub tidal bathymetry. A indicates a detached bar trough system with bar breaking and swash, B illustrates a classic rhythmic/cresentic bar morphology (Lippman and Holman, 1989).

macrotidal (>4 m) (Davies and Hayes, 1984) and megatidal (>8 m) beaches (Levoy et al., 2000), the system becomes progressively more tidally dominated (Short, 1999).

Wright *et al.* (1982b) conducted experiments investigating low-energy macrotidal beach morphodynamics in Cable Beach, Western Australia (MSR = 9.5 m). They found that rhythmic and aperiodic longshore irregularities such as cresentic/transverse bar and rip channels, commonly associated with microtidal beaches were generally absent. They divided the inter-tidal beach into 3 zones, from a dissipative to an intermediate/reflective surf zone from the low- to high-tidal zones respectively. Each zone was characterised by its morphodynamic character, including frequency of inundation. Wright *et al.* (1982b) suggested that each zone is dynamically different, proposing that the dynamics of the lower inter-tidal zone is similar to the sub-tidal zone of a microtidal beach due to the dominance of shoaling wave processes.

Therefore, under macrotidal conditions, beach states could be considered to change morphodynamically throughout the tidal cycle. More recently, studies on the high-energy, meso- to macrotidal Aquatine coast of France (e.g. Castelle et al., 2007; Castelle et al., 2009; Masselink et al., 2008) have described highly three-dimensional sub- and inter-tidal bar dynamics of similar form to their well-studied high-energy microtidal counterparts within an environment with a significant tidal range. Davidson *et al.* (1993) and others have suggested that key beach processes are essentially identical on both micro- and macrotidal environments, but differ in the extent of tidally induced surf zone translation. The concept of a 'shape function', developed by Russell *et al.* (1999) and later extended by Marino-Tapia *et al.* (2007) and Tinker *et al.* (2009), describes the cross-shore variation in cross-shore sediment transport across the shoaling and surf zones, and can be used to simulate bar building and bar migration processes. This concept of a morphodynamic template was used by Masselink (2004) to simulate, with some success, the mechanisms of inter-tidal bar formation on macrotidal beaches in relation to surf zone processes, translating a 'shape function' across the inter-tidal profile to simulate the tidal-cycle.

Inter-tidal bar morphologies, present on wave-dominated beaches with a significant tide range, have received less attention than sub-tidal bars in the coastal morphodynamic literature (Masselink et al., 2006). A range of inter-tidal bar formations have been observed around the coast of the UK (Davidson, 1997; King, 1972; King and Williams, 1949; Kroon and Masselink, 2002; Selma van Houwelingen et al., 2006) and identified in literature (Carter, 1988; Short, 1991; Short, 1999; Wijnberg and Kroon, 2002). Three key types were usefully defined by Masselink *et al.* (2006), based principally on morphology, as: (1) 'slip-face bars', with the largest amplitude (generally >1 m). These are the most dynamic and develop as breaker bars and move onshore through wave asymmetry (Roelvink and Stive, 1989). Common in higher-energy environments and mesotidal settings, slip-face bars are often fronted by/in the lee of sub-tidal systems. They usually form low on the inter-tidal beach after storm-induced beach erosion and develop into a berm under prolonged calm wave conditions. Often present as a single inter-tidal bar they represent the bar type that occurs in the ridge and runnel beach state defined by Wright and Short (1984); (2) the more static 'low-amplitude ridges' (generally <1 m). These occur as a series of shore-parallel bars, distributed across the inter-tidal profile, dissected by shore-normal drainage channels. This type of inter-tidal bar morphology, termed 'ridge and runnel' by King and Williams (1949), features in

Group II meso- and macrotidal intermediate beaches identified by Short (1991); and finally (3) the very subdued, marginal, 'sand wave' formations, which are not relevant in the context of this study. As well as wave forcing, inter-tidal bar morphology is significantly affected by relaxation time effects and morphodynamic feedback, particularly on multiple barred beaches (Masselink et al., 2006). The main difference between inter-tidal and sub-tidal bar morphodynamics is the importance of tidal water level variations and shallow water surf zone processes (surf, bores and swash), rather than just wave height variability (surf and shoaling) (Masselink et al., 2006). The inter-tidal bar forms should not be considered distinct, rather part of a continuum of morphologies.

1.3.2.3 Morphodynamic state models

Identification of beach morphodynamic states through classification schemes can be a useful conceptual tool to help assess the different forcing mechanisms and controls behind observed beach types globally. Much of the pioneering work on the classification and modelling beach morphodynamic states was conducted in Australia. Wright and Short (1984) developed a beach classification model that was the culmination of a large body of previous work (e.g. Short, 1975; Short, 1978 ; Wright et al., 1979; Wright et al., 1982a; Wright et al., 1982b; Wright and Short, 1983) to describe the morphodynamic character of a beach system. Based around morphodynamic states of surf zones and beaches, they identified a succession of intermediate states that exist with characteristic signatures of both beach morphology and associated surf zone dynamics. These states were constrained between the relatively stable fully dissipative and highly reflective extreme states corresponding to flat, fine grained, shallow beaches with large sub tidal sediment storage capacity and steep, coarser grained beaches with small sub tidal sediment storage capacity, respectively. These two extremes can be morphologically described through their surf zone characteristics using the surf scaling parameter (Carrier and Greenspan, 1958):

$$\varepsilon_b = a_b \omega^2 / g \tan^2 \beta \qquad (1.1)$$

where a_b is breaker amplitude, ω is radian frequency ($2\pi/T$, where T = period), g is acceleration due to gravity and $\tan\beta$ is beach slope. The parameter recognizes that the continuum from surging to spilling breakers represents an increase in the amount of energy dissipation across the surf zone (Short, 1999). When ε_b < 2.5 surging breakers

and a highly reflective surf zone are expected, permitting strong standing wave and edge wave motion (Guza and Inman, 1975; Short, 1999), and when ε_b > 20 spilling breakers dominate a highly dissipative surf zone characterized by turbulent dissipation of incident wave energy across the surf zone, and an increased influence of infragravity standing waves exists towards the shore, often dominating dynamic processes in the inner surf zone (Wright and Short, 1984).

Wright and Short (1984) identified a link between wave height, period and sediment size, described by the dimensionless parameter Ω, often termed the dimensionless fall velocity, first combined by Gourlay (1968), redefined by Dean (1973) and eventually adapted for use on natural beaches by Wright and Short (1984):

$$\Omega = H_b / w_s T \qquad\qquad (1.2)$$

where H_b is breaking wave height, w_s is sediment fall velocity and T is wave period. This attempted to describe the beach and surf zone morphology and the shoaling, surf and swash zones interacting with it for microtidal, wave-dominated coasts. This work was based upon datasets collected by both Wright *et al*.(1979), investigating a range of beach types, and Short (1978; 1979) who recorded 18 months of daily observations at Narrabeen beach, Australia. Ω was used to differentiate between reflective (Ω < 1), intermediate (Ω = 1–6) and dissipative (Ω > 6) regimes. This work produced a series of sequential beach types (Figure 1.13) linking them to their associated environmental conditions (H_s, w_s and T) and the sensitivity of Ω to each parameter (Figure 1.14).

A series of sequential intermediate beach states are presented that illustrate the three dimensional evolution of bar morphology as environmental conditions change temporally and/or spatially. As Ω reduces from a highly dissipative state, to a reflective state (Ω > 6 to Ω < 1) the intermediate beach states move from a longshore bar and trough beach (LBT) state to the low tide terrace (LTT). This is represented by the onshore migration of a detached straight/rhythmic longshore bar towards the beach face setting up a rhythmic bar and beach (RBB) system characterised by the presence of well developed rip current cells that are enhanced as the bar attaches to the shoreline generating transverse bars, perpendicular to the shore and segregating individual rip current systems. Further onshore bar migration leads to the LTT beach state where a steeper upper beach (often coarser) is attached to a shallower flat or slightly convex
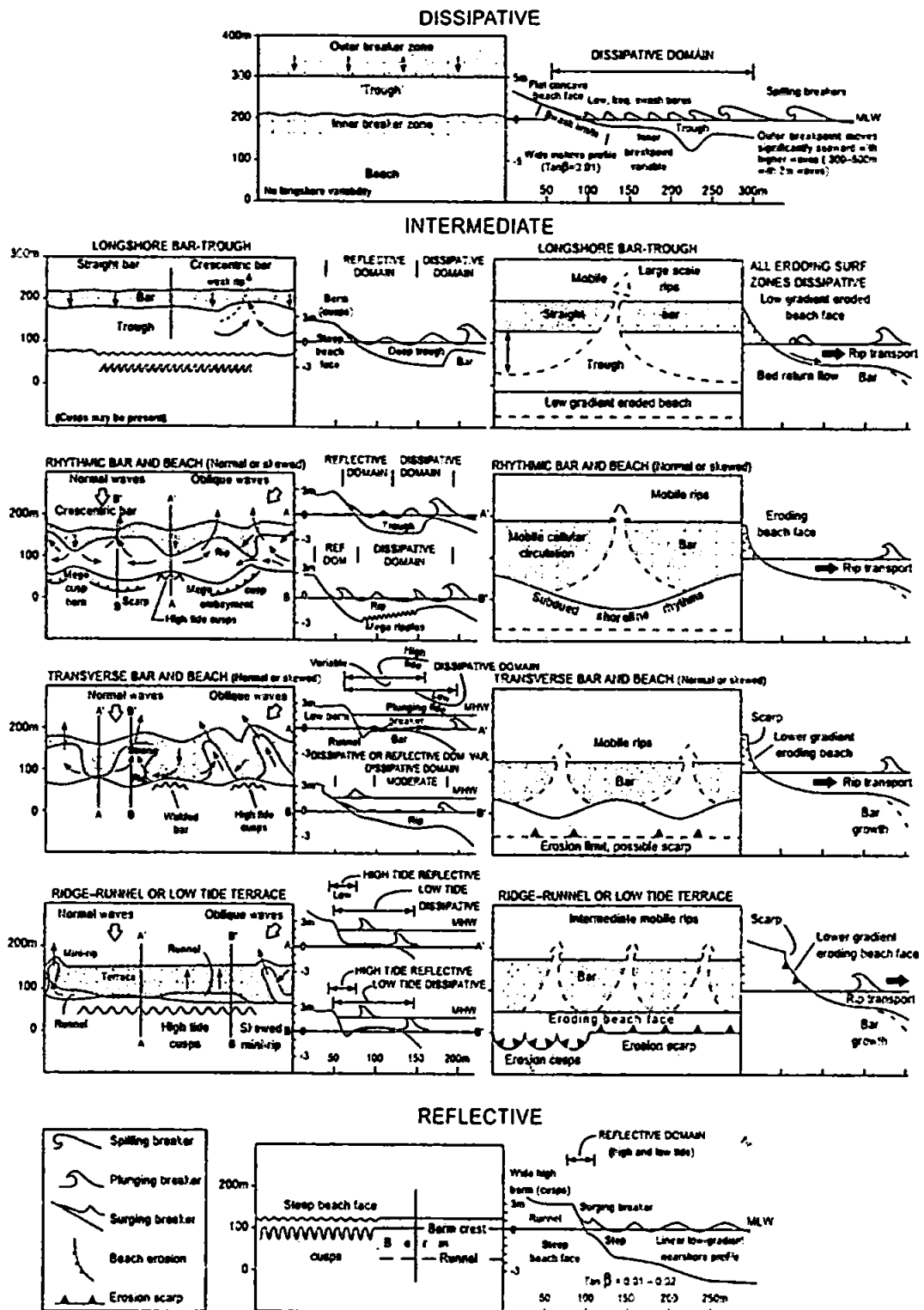
Figure 1.13. - Morphodynamic classification of micro tidal wave dominated beaches (Wright and Short, 1984).
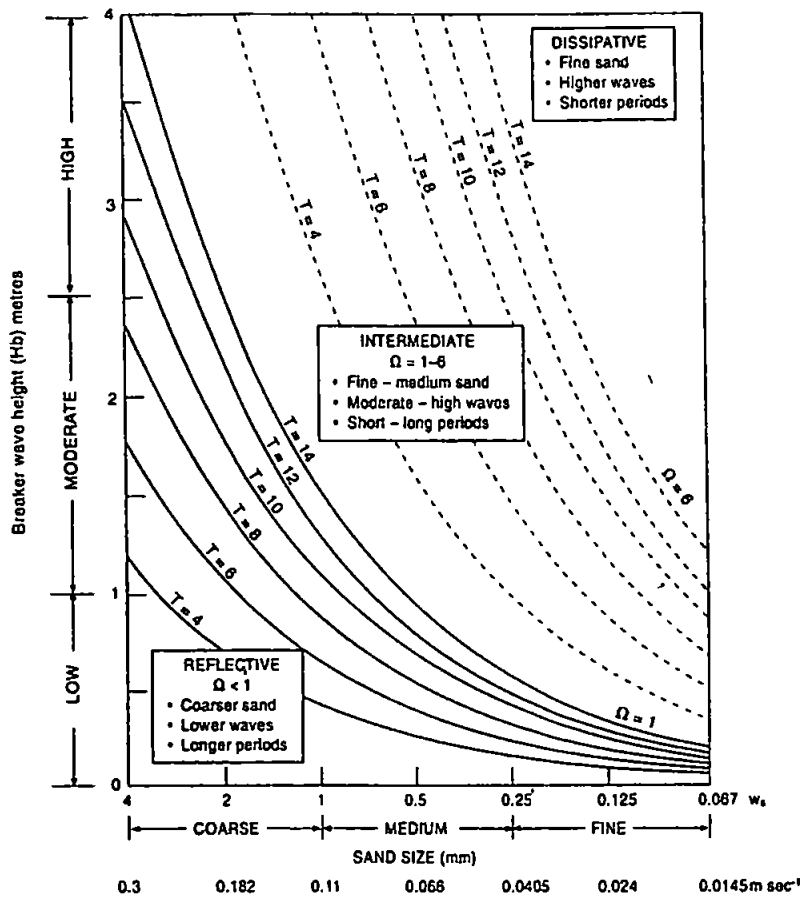
Figure 1.14. - Sensitivity plot of the contribution of wave breaker height, wave period, and sediment size to Ω and beach type (Short, 1999).

terrace. Associated with the combined presence of dissipative and reflective wave breaker characteristics, intermediate beaches possess complex surf zone dynamics but generally move from a predominantly dissipative to predominantly reflective regime as Ω reduces.

1.3.2.4 Tide-modified beach state model

The majority of research relating to beach morphodynamic state and particularly bar dynamics, has been carried out in relatively tide-less (micro- and mesotidal) environments. As a result, the effects of large tidal range on beach morphodynamics have received relatively little attention until the last few decades. Beginning with the research from the B-BAND project in the UK (Davidson et al., 1993) and research along the macrotidal coast of Queensland, Australia (Masselink, 1993; Masselink and Hegge, 1995; Short, 1991; Turner, 1993) a number field experiments have been conducted in this study area in recent years addressing this identified gap in scientific knowledge (Anthony et al., 2005; Anthony et al., 2004; Castelle et al., 2007; Kroon and

Masselink, 2002; Levoy et al., 2000; Masselink, 2004; Masselink and Anthony, 2001; Masselink et al., 2008; Michel and Howa, 1999; Reichmüth and Anthony, 2007; Sedrati and Anthony, 2007).

Increasing the tidal range to a mesotidal (2–4 m) or macrotidal (< 4 m) beach environment significantly modifies morphodynamic processes in a number of ways. The lateral translation or 'sweep' of surf zone processes (swash, breaker zone, shoaling) across the beach during the tidal cycle, controlled by the tidal range and beach slope, can be greater than 500 m in some macrotidal environments and acts to subdue morphological development. The extent of these smearing effects are controlled by the rate of tidal translation, determining the length of time any of the surf zone processes act on a specific point on the beach. The sinusoidal nature of the tidal oscillation means that maximum translation rates occur over the mid stages of the tide (Figure 1.15). In areas where tide ranges are in excess of 8 m, termed mega-tidal, as in Normandy, France (Levoy et al., 2000), translation rates can exceed running speed. Finally, tide induced fluctuation of the beach groundwater table determines the time varying saturation characteristics of the inter-tidal beach profile (Turner, 1993), where a saturated beach promotes erosion and an unsaturated beach, deposition. It is important to note that the tidal effects discussed above have an effect on both semi-diurnal and lunar spring-neap cycles. With increasing tidal range, these processes play a progressively more significant role in determining the character of the prevailing beach state.

Masselink and Short (1993) extended this work to the development of characteristic meso-/macrotidal beach environments, furthering the previously discussed microtidal beach state model of Wright and Short (1984). An additional dimensionless parameter to describe the relative importance of shoaling, surf zone and swash processes across the inter-tidal profile was defined, the relative tidal range:

$$RTR = MSR/H_b \qquad (1.3)$$

where MSR is mean spring tide range in meters, and H_b is wave breaker height in meters. This provided a useful parameter with which to quantify the tidal effects within a beach system. The principal importance of the RTR is that it distinguishes the relative effects of waves and tides, a concept first established by Davis (1984), suggesting that coastal geomorphology is a function of the relative contribution of waves and tides
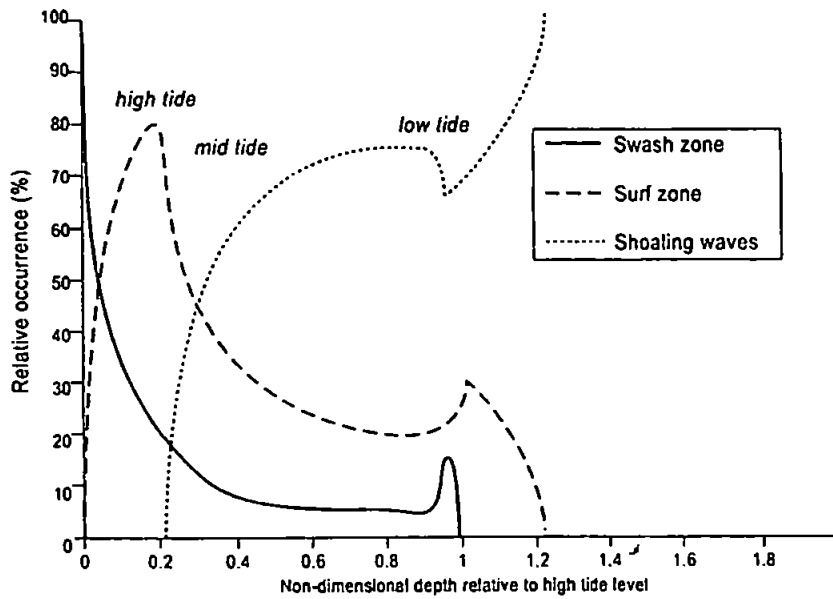
Figure 1.15. - Relative occurrence of swash, surf and shoaling wave processes across the beach profile calculated over one tidal cycle where $H = 1$ m, $T = 8$ s, $w_s = 0.03$ m s^{-1}, breaker criterion $\gamma = 0.8$ and tide range $TR = 6$m from a simulated tidal excursion model by Masselink and Short (1993).

(Short, 1999). The modified conceptual beach state model includes the parameter RTR and defines a number of identified beach types through four physical constraints, the modal wave breaker height, modal wave breaker period, upper beach face sediment size and mean spring tidal range. Incorporated in the two parameters Ω and RTR, these variables describe the surf zone characteristics (reflective to dissipative) and the relative importance of swash, surf and shoaling zone processes respectively.

This extension enables the inclusion of a number of well documented beach types that commonly occur in regions of meso- and macrotidal regimes (Figure 1.16). Masselink and Short (1993) took profiles observed from 19 beach sites from Australia and the UK that represented mean spring tidal ranges from 3.6 m to 9.5 m, and modal wave breaker heights from 0.3 m to 0.8 m to develop their model. From the classic reflective beach type, the increased RTR led to the compound profile of a LTT beach type characterized by a distinct steeper upper beach and flat/convex low gradient terrace. Then the barred and barred dissipative states, represented within the Wright and Short (1984) model as intermediate and dissipative regimes, represent increasingly subdued morphology as RTR increases. As RTR increases from 3 to 7 the bar/rip morphology is displaced seaward towards low water and becomes increasingly subdued until the beach is flat and
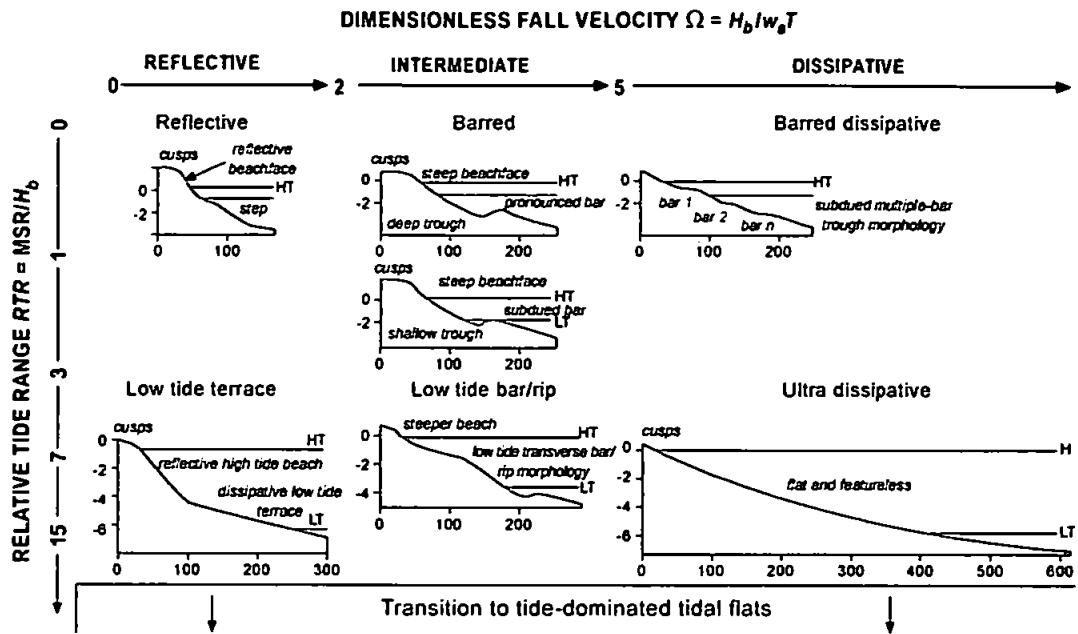
Figure 1.16. - Modified conceptual beach state model (Masselink and Short, 1993).

featureless ($RTR > 7$). It is important to note that these points of division are not intended to be absolute.

In summary, Masselink and Short (1993) generalised that beaches with an $RTR < 3$ are best classified according to the microtidal model of Wright and Short (1984), whereas beaches with an RTR that lies between 7 and 15 are expressed as macrotidal beaches with planar, concave profiles with the transition to tidal flats occurring when $RTR > 15$. Where RTR is between 3 and 7 they suggest that beaches are typically high to moderate energy macrotidal beaches not included in previous beach state models. Inclusion of relative values of wave height and tide range enables the incorporation and description of a number of varieties of beach type in a single model, although it is acknowledged that absolute values are of importance in a number of ways (Masselink and Short, 1993).

Wave height

Absolute wave height is crucial in determining a minimum wave energy threshold for transport below which no morphological change occurs. There will also be a threshold energy level required for the presence of infragravity and edge waves (Guza and Inman, 1975), potentially important in the generation of the rhythmic and bar morphology described within all the beach classification models. Therefore, application of models at

27

low energy levels, H_b < 0.25 m Masselink and Short (1993), should be pursued with care.

Tide range

The transition to a LTT beach, as documented in previous study by Turner (1993) and Masselink and Short (1993), is suggested to be related to the drainage capacity of the beaches concerned, where the water table can become decoupled from the tide level during the falling tide, resulting in a seepage face where the water table outcrops into the beach producing a saturated lower beach. Generally associated with fine sediment, mixed beaches often exhibit a seepage face at or near a textural break between coarse upper and fine lower beaches. This de-watering effect can have significant implications for cross-shore sediment transport pattern and hence the profile development exemplified by the LTT beach form and is controlled by complex beach sediment characteristics, beach slope and the absolute tide range. Masselink and Short (1993) state that: 'the RTR value of 3 separating the reflective beaches from the LTT beaches is rather arbitrary'.

Finally, at low values of tide range and wave height, the morphological situation of the beach system becomes very sensitive to small changes in environmental factors. This is an area where further study is required to assess energy thresholds controlling the separation of different morphological states (Masselink and Short, 1993).

Masselink and Short (1993) also commented that unlike in previous models (Short, 1991), 'ridge and runnel' beach systems (low-amplitude ridges) are not identified as an individual beach type, but are a phenomenon that occur on any beach where the environmental conditions are characterised by fine sediments, limited fetch wind waves (short period), and a large tidal range, where RTR > 3.

It is important to note that this is a conceptual model, and is developed with a limited amount data that represents macro tidal regimes. Therefore threshold values separating beach types should be used with caution and with an understanding of the nature of the model as a framework for future development (Masselink and Short, 1993).

1.3.2.5 Present perspectives: The UK beach environment

A recent study by Jackson *et al.* (2005) has highlighted that although the Australian beach state models describe well processes in the highly dynamic, steep inner shelves of the Australian coasts, there are a number of other factors that may also control beach dynamics in other coastal environments. Their application of these aforementioned classification models in the UK beach environment highlights some of these controlling factors and indicates areas where further study is needed (Jackson et al., 2005).

Geologic features play a significant role in controlling beach morphodynamics, especially in the UK environment, where a huge number of geologic settings and sediment sources are present. These factors constrain the shape and accommodation volume of beaches. This affects their morphological evolution, and controls the often finite sediment supply to the system, characterising the sediment size and distribution. Constraining geologic features control beach length, shape and morphology through physical boundaries, such as headlands, islands and rock outcrops and shore platforms/reefs. Geologic inheritance also plays a major role in controls of inner-shelf gradient and roughness, and hence wave energy transfer to the shore (reducing wave breaker height), coastal tidal currents and the modification of nearshore hydrodynamics such as topographically controlled rip currents (Short, 2006). Further evidence of the importance of geologic control was provided by McMinch (2004) who identified a number of shore-oblique sandbars along the North Carolina Outer Banks and Southeastern Virginia, through geophysical surveys suggesting that the underlying framework geology exerted a first order control on nearshore morphology, by influencing the stability and re-establishment of large-scale sandbar morphology.

Short (2006) has classified Australian beaches into 15 types, including those defined by Wright and Short (1984) and Masselink and Short (1993) as well as recently defined tide dominated and two geologically constrained states accounting for rock flats and fringing coral reefs. Short (2006) highlights Australia's lack of tide-modified beaches exposed to higher ocean swell and storm seas and gravel beaches.

The mixed sediment and gravel dominated beaches of the UK coast, comprising 2900 km of the Nation's shoreline (May and Hansom, 2003) provide beach environments not present in the Australian studies. Many of these beaches are composed of relict structures (in some cases older than 5500 years old) created through post glacial marine

transgression and contemporary transport processes. Characterised by a range of sediment sizes, these environments are being reworked over time scales of years to minutes.

The presence within UK and northern Europe of tide ranges > 9 m, termed 'mega-tidal' by Levoy (2000), in combination with high-energy open coast locations creates another unique beach environment. As documented by Levoy (2000) when studying beaches in Normandy, France, high-energy mega-tidal beaches often possess the classic combination of a reflective upper beach and a dissipative lower beach exhibited by meso-/macrotidal beaches, but also show, at low-tide, an extremely dissipative zone that is characterised by very rapid tidal translation of the shoreline. This low-tide zone, dominated by shoaling wave conditions during high-tide, is wave dominated due to the high-energy conditions. These environments are unlike many of the descriptions in the literature of beaches characterised by large tides and tidal sand flats that are only affected by waves during storms. Strong tidally driven currents are therefore present in addition to wave driven processes. The study by Levoy (2000) provides extra beach types that are not present within the Australian beach state models.

Finally, the contribution of anthropogenic modification of the beach environment can significantly alter the freedom of sediment movement, constraining and distorting the reaction of the beach environment to the forcing environmental conditions. This is a significant issue within the UK as 23% of the coastline of England possesses coastal defence structures (MAFF, 1994).

1.3.3 Rip currents

Rip currents form an integral part of many wave dominated surf zones and beach systems around the globe (Shepard, 1941; McKenzie, 1958; Sonu, 1972; Bowman, 1988; Huntley et al., 1988; Aagaard et al., 1997; Brander, 1999; Brander and Short, 2001; MacMahan, Thornton et al., 2005). Most often associated with the intermediate beach states within microtidal environments, as defined by Wright and Short (1984), rip current systems have also been observed in wave dominated systems in meso- and macrotidal environments (e.g. Castelle et al., 2007; Masselink et al., 2008; Masselink and Hegge, 1995) although, in comparison to their microtidal counterparts, relatively little is known about macrotidal rip currents, particularly in regions where tidal range exceeds 6 m.

Rip currents, driven by cross-shore and longshore gradients in the mean water surface, result from wave energy dissipation patterns associated with bar/rip morphology and wave-current interaction (Sonu, 1972) and are traditionally known as relatively narrow, seaward-flowing currents that originate in the surf zone and extend seaward of the breaking region (Bowen, 1969). Rip currents are most often observed when the waves approach at near shore-normal incidence and where there are alongshore variations in bathymetry and incised sandbars. The pre-existence of template morphology on the beachface will act to drive alongshore gradients in radiation stress focusing wave energy over the bars forcing wave breaking and an associated increase in onshore directed radiation stress that decreases in the alongshore in the deeper incised channels. In the classic example, a nearshore circulation is set up comprising of onshore mass transport over the bars, which then, via longshore currents, driven by the alongshore variations in pressure gradient in the feeder channels, most efficiently exits offshore through a rip channel creating a rip current (Figure 1.17). The seaward flow is generally characterised by the narrow jet through the 'rip neck' that decelerates and widens into a 'rip head' (Figure 1.17).

Most rip currents are topographically constrained by bar morphology, rocky outcrops or coastal structures, but they also occur in the absence of topographic expression when they are referred to as 'transient rips' or 'flash rips'. Short (1985) classified rip systems into 4 categories: accretionary and erosional, associated with beach rips that are fixed
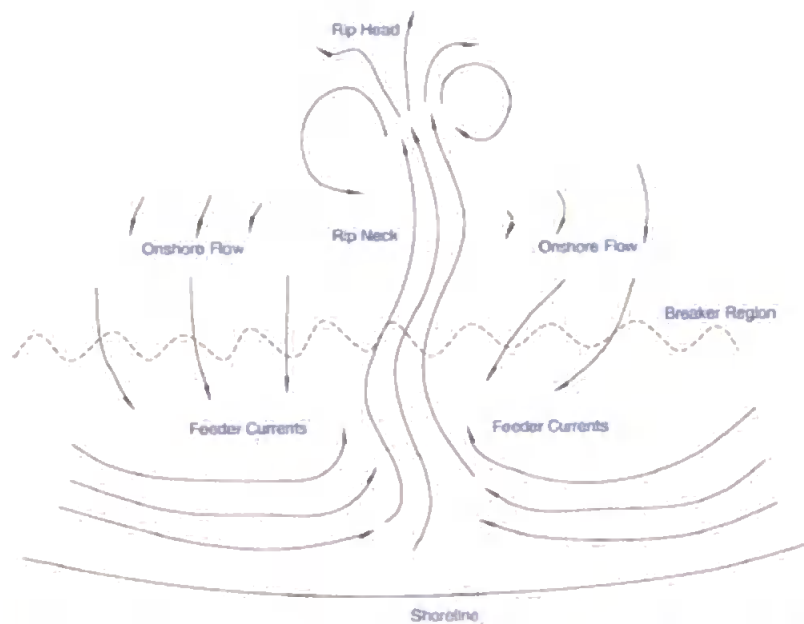
Figure 1.17 – Schematic of a simplified rip current system from MacMahan et al. (2006).

(low-energy) and migratory (high-energy) respectively; topographic rips that are generated through the influence of solid structures such as groynes or jetties; and large scale mega rips that occur during high waves.

Our understanding of rip current dynamics has increased significantly over the last decade due to a number of comprehensive field and laboratory experiments (reviewed by MacMahan *et al.*, 2006). This has enabled a quantitative and theoretical evaluation of previous more qualitative observations. Data from these laboratory and field experiments suggest that the rip current strength increases with increasing wave energy and decreasing water depths. Rip currents can occur under various bathymetric perturbations, even for beaches with subtle alongshore variations.

Rip channels are a key component of rhythmic nearshore morphology, such as transverse/crescentic bars, and are typical of morphodynamically intermediate-type beaches (Wright and Short, 1984). Brander (2001) suggested rips are a key sediment transport mechanism, qualitatively associated with the development and migration of a rip head bar during evolving beach states (accretionary down-state transition). He suggests elements of morphodynamic feedback are critical in low-energy accrectionary beach rip current evolution.

Rip channel morphology is commonly observed to have a quasi-periodic alongshore spacing. Attempts to explain this observed alongshore spacing of rip morphology, commonly $O(100$ m$)$ in relation to measured wave height, period and sediment characteristics have not been particularly successful (Ranasinghe et al., 2004). Recent modeling efforts suggest that the rip spacing may not be sensitive to wave height or mean period of the incident waves, but is dependent on the alongshore length scale of the wave group energy and the direction of the incident waves. Reniers *et al.* (2004) demonstrated that group wave forcing could produce low frequency vortices which perturbed the initially alongshore uniform barred beach at the length scale of the groups. Subsequent morphological coupling and positive feedback with the hydrodynamics is then suggested to lead to the development of the rip channel morphology.

Flow velocities associated with cell circulation can be very significant with mean and maximum flows in the rip neck of 0.2–0.65 m s^{-1} and 1–2 m s^{-1} respectively (MacMahan et al., 2006). The flow variation is due to a number of mechanisms. When considering rip current flow contributions over a given morphology, an approach, suggested by MacMahan *et al.* (2006), provides a useful method of summarising rip current flow characteristics by partioning frequency bands that represent key forcing mechanisms:

$$U_{rip} = U_{ig} + U_{VLF} + U_{tide} + U_{mean} \qquad (1.4)$$

where U_{ig} is the contribution within the infragravity band 25–250 s, U_{VLF} is the contribution within 4–30 min, U_{mean} is the mean based on the rip current system and wave conditions, and U_{tide} is the modulation associated with slow variations in the water level. U_{ig} and U_{VLF} are responsible for what is known as 'pulsing' of the rip flow. Largely driven by U_{ig}, the two main explanations of this 'pulsing' phenomenon are standing infragravity waves, which are higher over the bar profile than the rip channel (MacMahan *et al.*, 2004) and wave group related-variations in mass flux over nearshore bars, causing ponding of water in the trough and periodic releases through the rip channels (Brander and Short, 2001). Hourly variations in flow are principally driven by the U_{tide} component, a phenomenon identified in a number of field investigations (e.g. Sonu, 1972; Aagaard et al., 1997; Brander, 1999; Brander and Short, 2001; MacMahan et al., 2005), where decreasing tidal elevation over the bar crest corresponds to an associated increase in rip flow velocity through modulation of the wave dissipation (MacMahan et al., 2006). Brander and Short (1999) found a direct relationship between

rip morphology and flow with rip velocity increasing as cross-sectional rip channel area decreases due to tidal modulation. Finally, over a period of days, U_{mean} is controlled by the forcing wave conditions (e.g. wave height, period and angle).

As well as being an integral component of a range of intermediate beach morphologies, the characteristics of the rip current, as outlined above, represent a potential hazard to beach users interacting with the surf zone. As such, improving the understanding of these systems and their spatio-temporal variation, specifically in environments with significant tidal ranges, is paramount when striving to improve management of beach hazards.

1.3.4 Beach Safety

1.3.4.1 Hazard and Risk Assessment

The findings of this thesis will provide a scientific knowledge base of beach morphodynamics and hazards within the UK coast that will feed into the RNLI risk assessment and management program. This section outlines the approach to risk assessment within the RNLI and summarise some key internationally accepted concepts of hazard and risk, crucial to understanding the framework of the project aims and objectives. The World Health Organization offers the following advice in relation to the assessment of hazard and risk in its *Guidelines for safe recreational water environments* (coastal and fresh waters) (WHO, 2003): 'Assessment of hazard and risk inform the development of policies for controlling and managing risks to health and well-being in water recreation. The assessment of a beach or water should take into account several key considerations including:

- the presence and nature of natural or artificial hazards
- the severity of the hazard as related to health outcomes
- the availability and applicability of remedial actions
- the frequency and density of use
- the level of development.'

Several of these considerations are being taken into account in the development of the RNLI's risk assessment model for use on UK beaches. The RNLI's programme considers the implementation of beach risk assessments/safety audits through a process that takes advantage of established scientific principles, established best practice and benchmarking against available standards and guides.

In developing a proactive approach to managing risks at beaches, the RNLI established a safety management system based on acknowledged good practice. After review, the best practice in risk management was assessed to be represented by the Australian/New Zealand Standards *Risk Management* AS/NZS 4360:2004 (AS/NZS, 2004). This provides a generic framework illustrated in Figure 1.18.

The scope of the project documented in this thesis falls within the 'establishment of context' and 'risk assessment' boxes in Figure 1.18. Within the risk management system, establishing the context requires an assessment of the basic parameters within
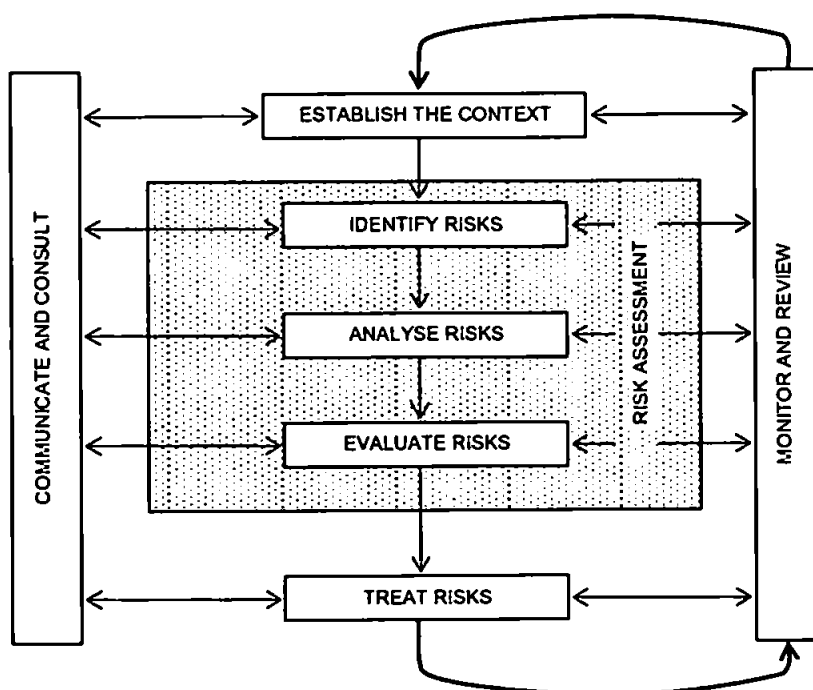
Figure 1.18 – Risk management process – an overview (AS/NZS, 1999; AS/NZS, 2004).

which risks must be managed, setting the scope for the rest of the risk assessment process. This study is concerned only with the risk posed to beach users that are interacting with the surf zone and specifically those risks that are driven by physical hazards (i.e. not biological or chemical). The context to be established is that of the beach and near-shore environment and the specific types and levels of hazard inherent within that environment. The first two steps of practical risk assessment guidance provided by the Health and Safety Executive (HSE, 2006) involve the identification of hazard, who may be harmed, and how.

In order to be clear in establishing terminology, it is useful to define the meanings of both hazard and risk within the context of this study: a 'hazard' is anything with the potential to cause harm and 'risk' is the chance or probability that a person will be harmed (HSE, 2006). It is therefore crucial to gain a comprehensive understanding of the hazards in order to perform a successful risk assessment.

The risk assessment model under development by the RNLI will allow beach managers to gain positive benefits from conducting a risk assessment process. Managing risk in the coastal environment requires the systematic application of management policies, procedures and practices to the tasks of identifying, analysing, treating and monitoring

risk. Risk assessment must take a holistic approach when determining the most effective actions and control measures to implement.

1.3.4.2 Beach hazard research

As discussed previously, the beach is a highly dynamic environment, with constantly changing morphology and hydrodynamics, both spatially and temporally. Due to this, it is an inherently hazardous place for humans in many ways. Since the late 1980's, interest within the scientific community for developing understanding of hazards and risk to the beach user has grown (Engle et al., 2002; Hartmann, 2006; Lascody, 1998; Leahy et al., 1996; Lushine, 1991; Sherker et al., 2008; Short, 2001; Short, 1999; Short and Hogan, 1994) and the application of our improved knowledge of beach dynamics to the public domain and safety has begun (Short, 1999).

Risk to the beach user entering the coastal/beach environment becomes a product of the physical hazards present within the surf and nearshore zones and their severity, and the number of beach users interacting with the beach system (frequency and density of use). Identification of these hazards is site specific and varies depending on a number of environmental factors (Short and Hogan, 1994). Short (1999) highlights three main elements that put the beach user at risk of harm: water depth, breaking waves and surf zone currents.

- Water depth presents a hazard through 1) deep water, where an inexperienced non-swimmer can potentially drown, 2) shallow water, where a plunging or surging breaking wave can propel a swimmer into the seabed, creating an impact risk, particularly spinal injuries and 3) variable water depth, often present with bar/rip morphology whereby a beach user/swimmer may find themselves moving quickly into a zone of different depth.

- Breaking waves impact beach users in the surf zone, often disorientating them, and holding them underwater. High, more energetic waves are more hazardous, as are plunging or surging wave that release more energy in the shorter distance.

- Surf zone currents, and particularly rip currents, represent the core threat to the beach user in the surf zone. Accounting for the vast majority of documented rescues and drownings in nearly every nation with a lifeguard patrol network (Engle, 2003; Lascody, 1998; Short and Hogan, 1994), rip currents typically reach velocities of 1 ms^{-1} and some have been reported as high as 2 ms^{-1} at Palm

Beach, Australia (Short, 1985) moving bathers unwillingly around the surf zone, and often into areas of greater hazard.

Further work by Short and Hogan (1994) identified specific hazards typically present within a range of beach types, documented in work by Wright and Short (1984) and Masselink and Short (1993), producing schematic illustrations of key characteristics, hazards and risk ratings for each state for wave dominated (Figure 1.19) and tide modified beaches (Figure 1.20).

Tides represent another key hydrodynamic components to hazard levels. tidal level oscillations modify the nature of the surf zone potentially incurring marked changes in prevailing beach hazards in a single tidal cycle. It has been well documented in previous studies that rip current systems are modulated by tidal level, increasing in velocity with decreasing sea level (Brander and Short, 2001; MacMahan et al., 2005) whereby the presence of rip current and their associated hazards are often synonymous with lower tide levels (Engle, 2002; Lascody, 1998; Lushine, 1991; McKenzie, 1958; Shepard, 1941; Short and Hogan, 1994).

Strong winds also create a number of hazards within the surf and nearshore zone. Strong onshore and oblique winds generate surface currents that can manifest in strong alongshore currents potentially displacing bathers from a safe to a more hazardous zone. Onshore winds also cause premature breaking of the wave crests, generating an apparently disorganized and confusing sea to the beach user (Short 1999).

Headlands, inter-tidal hard rock exposures, sub-tidal reefs and man made structures like breakwaters, groynes, harbours and sea walls additionally present a significant hazard to the beach user. These features can modify wave breaking, fixing and intensifying surf zone currents (rip currents) and present collision and cut off hazards to the beach user.

Early application of this scientific knowledge of beach processes to problems of beach safety occurred in Australia in the late 1980's. Short (1993) constructed a database of every beach in Australia with regard to its location, physical characteristics, modal wave climate and regional hydrodynamics, morphology, physical hazards, facilities and beach user risk rating. Conducted in collaboration with Surf Life Saving Australia (SLSA) this
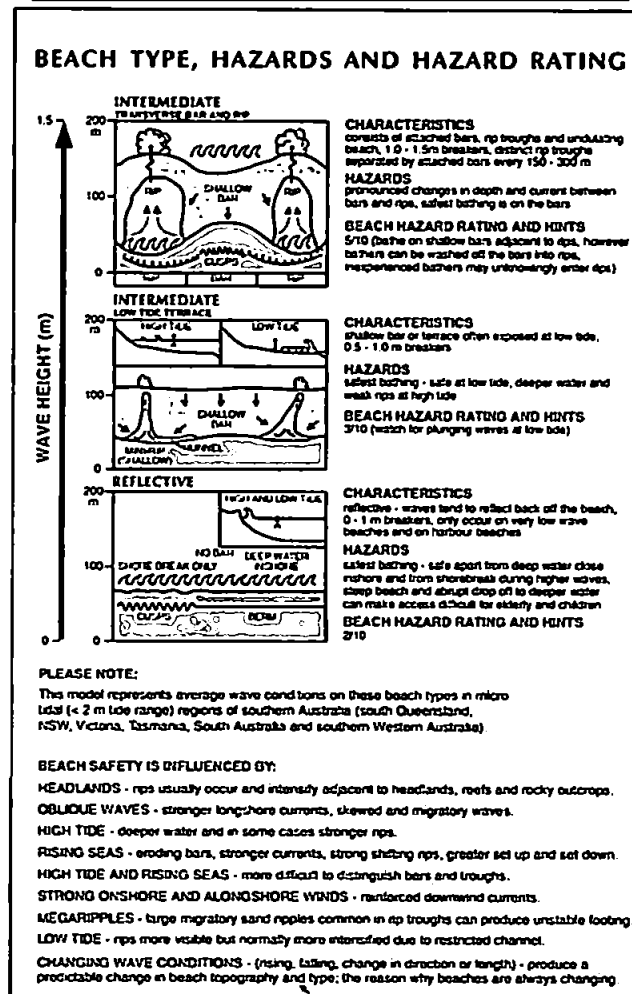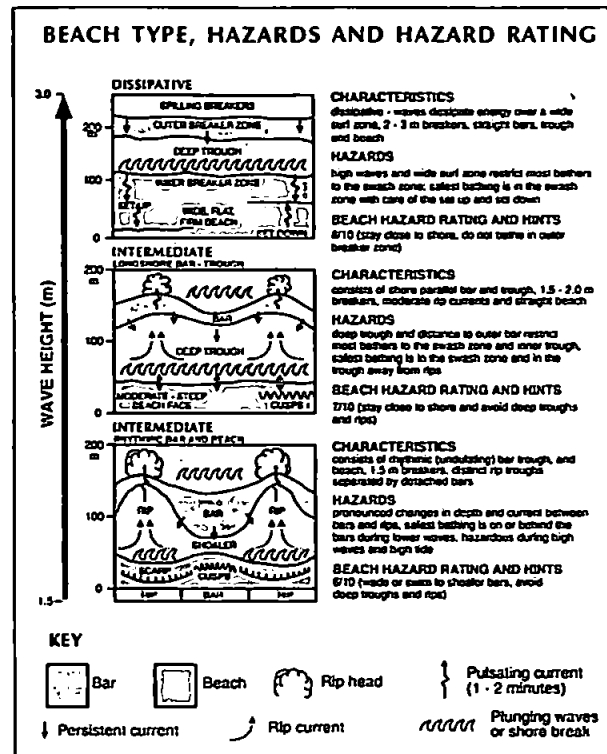
Figure 1.19. - Key hazards illustrated for Reflective to Dissipative wave dominated beaches (Short, 1999).

Figure 1.20. - Key hazards illustrated for tide dominated and tide modified beaches (Short, 1999).

project was called the Australia Beach Safety and Management Program (ABSAMP), which, driven by this underlying dataset, provided lifeguards with a management tool for use in patrolling the popular Australian beaches. Incorporated in the ABSAMP is a beach hazard rating (Short, 1996; Short and Hogan, 1994b) developed to enable empirical quantification of the level of beach hazard present for wave dominated and tide modified beaches (Figure 1.21). Generated from a prevailing wave height value and a beach type class each location has an associated range of hazard ratings (between 1 and 10). Modal hazard rating can be calculated from the modal wave height. To generate a more informed view of the relative risk to the beach user associated with hazardous beach environments, the incorporation of levels of exposure, in this case population is required. This probabilistic/likelihood approach was used by Short and Hogan (1994), Short (1999) and Hartman (2006) in the assessment of reported rescue levels and drowning statistics.

Recent beach safety research in Florida (East Central Florida) has concentrated on the prediction of rip currents along the Floridian coast. The empirical rip current forecasting technique LURCS (LUshine Rip Current Scale) developed by Lushine (1991), assuming strong onshore winds were the dominant mechanism for rip current generation, was developed and adapted for use in east central Florida (ECFL LURCS) by Lascody (1998) who reported the importance of long period swell through an analysis of east central Florida rip current rescues (75% occurred on days when long period swells were the primary formation mechanism). Engle (2002) examined lifeguard rescue logs from Daytona Beach, Florida. Rip current related rescues were correlated to concurrent hydrodynamic data on an intermediate shoreline where bar rip morphology is commonly observed. The study showed an increase in rip related rescues associated with shore normal wave incidence and lower tide levels.

These results were applied to modifying the ECFL LURCS model, being used as the National Weather Service's (NWS) rip current forecasting model to include wave direction and tidal stage as predictive parameters. The inclusion of these new parameters and the elimination of two wind parameters resulted in more accurate forecasting of days with a high number of rip current rescues (Engle, 2002) (Figure 1.22). At present this model provides the basis for NWS's daily rip current forecasts in the United States that form part of the NWS national Rip Current Program to inform the public when rip currents will pose the greatest hazard to beachgoers. The daily rip

Figure 1.21. - Matrix for calculating the prevailing beach hazard rating, based on beach type and prevailing wave height and, on tide modified beaches, state of tide (Short, 1999).

current risk is typically communicated via a 'Surf Zone Forecast' (termed SRF), which also provides forecasts for other beach hazards, weather, and surf conditions. Figure 1.23 is an example of a Surf Zone Forecast produced by the Weather Forecast Office (WFO) in Tampa Bay with the qualitative rip current forecast highlighted. Within the SRF, a qualitative rip current outlook is provided using one of three tiers in a Low-Moderate-High scheme:

- Low Risk: Wind and/or wave conditions are not expected to support the development of rip currents. However, rip currents can sometimes occur, especially in the vicinity of groins, jetties, and piers. Know how to swim and heed the advice of the beach patrol.

- Moderate Risk: Wind and/or wave conditions support stronger or more frequent rip currents. Only experienced surf swimmers should enter the water.

- High Risk: Wind and/or wave conditions support dangerous rip currents. Rip currents are life-threatening to anyone entering the surf.

Further examples of active beach hazard forecasting systems can be seen in Hawaii. Produced by the Hawaii Lifeguard Association in conjunction with several local authorities and the University of Hawaii these forecasts provide an overall beach hazard rating unique to distinct coastal regions based on wave model forecasts. Similar to the NWS forecast it uses a three-tiered rating system and is available to the media and the public (http://oceansafety.soest.hawaii.edu).

Figure 4. Modified ECFL LURCS checklist. A rip current warning is issued if the rip current threat is greater than five.

Figure 1.22. – Example of the Modified ECFL LURCS checklist (Engle, 2002).

Figure 1.23 – Example SRF forecast for the WFO for Tampa Bay. Rip forecast is highlighted.

1.4 SUMMARY

A number of general conclusions can be drawn from the reviewed material presented here:

- The coast of England and Wales is one of the most diverse coastlines in the world with varying combinations of sediment size (fine sand to boulders), tidal range (micro- to mega-tidal) and wave climate (low-energy wind wave to high-energy swell wave dominated) imposed upon a coast with a broad spectrum of geologic characteristics from hard to soft rock, varying coastal geomorphology and contrasting sedimentary environments.

- There is a relative lack of knowledge of beach morphodynamic systems within a macrotidal context specifically relating to the UK environment where the characteristics of the coastal setting are not represented well within existing beach state models.

- Reviews of these traditionally used beach state/classification models by a number of authors suggest the situation may be more complex in environments which have significant influence from a complex geologic history, where recent glacial history has left antecedent morphological features, affecting sediment abundance and the nature of the bounding geologic framework, a mixed (often high-energy) wind/swell wave climate and a high macro- to mega-tidal sea level excursion.

- Previous research has theoretically linked beach hazards to beach type through a basic understanding of the principal driving mechanisms posing a hazard to the surf zone bather and the typical surf zone characteristics associated with a variety of identifiable beach states.

- Drowning and rescue statistics in micro- and mesotidal environments indicate that rip currents are the principal hazard to bathers (approximately 80% in both the United States and Australia).

- Little is known about beach hazard characteristics and levels within the UK, a coastal environment that is very different from that of the United States and Australia. An introduction 50 years ago of a lifeguard service in England indicates that significant bathing hazards are present in many locations around the coast.

- Although there has been a increase in rip related research in recent years, much of the effort has been directed toward micro- and mesotidal environments. The documented role of rip currents in intermediate beach morphologies (especially

in recent studies of macrotidal environments) and as key drivers of hazard within microtidal environments indicates that a clear knowledge gap exists with regard to the influence and characteristics of rip current systems within macrotidal wave-dominated beaches of the UK.

- Some success at providing basic beach/rip hazard forecasts has been achieved in the US in recent years, although the forecast models, developed in a microtidal context, are based on empirically derived thresholds and do not include effects of morphological state. The author is unaware of testing of these models outside of the development region.

2. METHODOLOGY

2.1 INTRODUCTION

A wide range of data types and collection techniques were used during the course of this study. Many of these, specific to individual sections of the work, are described within the relevant chapters. This chapter details some of the principal methods that relate to a number of sections of the study and that are referred to throughout the thesis, as well as some technical descriptions of data types and collection techniques that are more appropriate for inclusion in this dedicated methods chapter. The data collection and processing techniques described within this chapter include: (1) inter-tidal morphological measurements and processing at a range of timescales; (2) Argus video: system overview and analytical techniques; (3) surface sediment collection and particle size analysis; and (4) UK wave climate analysis, wave models, buoys and analytical techniques.

2.2 BEACH SURVEYING

2.2.1 Overview

The acquisition of beach surface topographic measurements is an integral component of most field studies investigating coastal processes. Throughout this study, understanding of the morphological characteristics of the beach system is required for assessment of both beach type and hazard. Recent developments in the technical capability of remote sensing and surveying equipment have meant that the rapid measurement of an entire beach surface in three dimensions is now possible, something that was beyond the capacity for previous instrumentation traditionally limited to the collection of two-dimensional data.

For the purpose of this study a real time kinematic (RTK) Global Positioning System (GPS) was used. This system provided both a rapid, flexible, (inter-tidal) technique for collecting spatially high-resolution positional measurements of a desired accuracy that are appropriate for the spatial scale of the study sites (Bilker, 2002; Morton et al., 1993; Trimble, 2009). Due to the macro- and megatidal ranges and the intermediate/dissipative nature of the beaches within the study region a large component of the nearshore system is exposed during a spring tidal cycle, increasing the value of an

inter-tidal survey; however, surveying seaward of MLWS remained problematic due to the high-energy nature of the environment under study and the logistics and cost involved in regular bathymetric data acquisition. Improved understanding of nearshore morphological adjustment and the behavior of neashore bars was gained, largely qualitatively, within this study through oblique photography and more quantatively through use of remote video imaging techniques, of which details can be found in section 2.3.

2.2.2 Survey equipment and accuracy

Equipment used for beach surveys and analysis included:

- 2 x Trimble 5800 RTK GPS (Dual frequency L1/L2) receivers (Figures 2.1 and 2.2).

- Trimble 4000 SSi Dual Frequency GPS Receiver and L1/L2 antenna with ground plane for acquisition of ground control points.

- Yamaha Grizzly 450cc all terrain vehicle (ATV) with antenna mount and appropriate personal protective equipment (Figure 2.2).

- Custom built trolley with receiver mount to conduct surveys on foot.

- PC and data processing software packages Trimble Geomatics Office (TGO) and Matlab.

RTK GPS systems have become recognised as standard beach survey tools and are now used routinely in both research and commercial coastal process survey applications. The RTK GPS system used here provides measurement accuracies well within that required to capture the dynamics of the beach environment in question. Published horizontal and vertical instrument measurement accuracies for the system are within ±10 mm and ±20 mm, respectively (accuracy and reliability may be subject to anomalies such as multipath, obstructions, satellite geometry, and atmospheric conditions). To enable rapid acquisition of topographic data of the desired spatial coverage and resolution, beyond recording static point measurements, both mobile trolley and ATV based instrument platforms were introduced. This survey technique combined with the ability of the system to auto-acquire positions at set spatial or temporal intervals allowed collection of up to 30,000 data points (using ATV) within a 6-hour period. Ground point position determination using both ATV and trolley mounted systems simply involved mounting the GPS receiver and pole securely to the vehicle using a specifically engineered clamp Figure 2.2. A simple offset from phase centre of the vertically
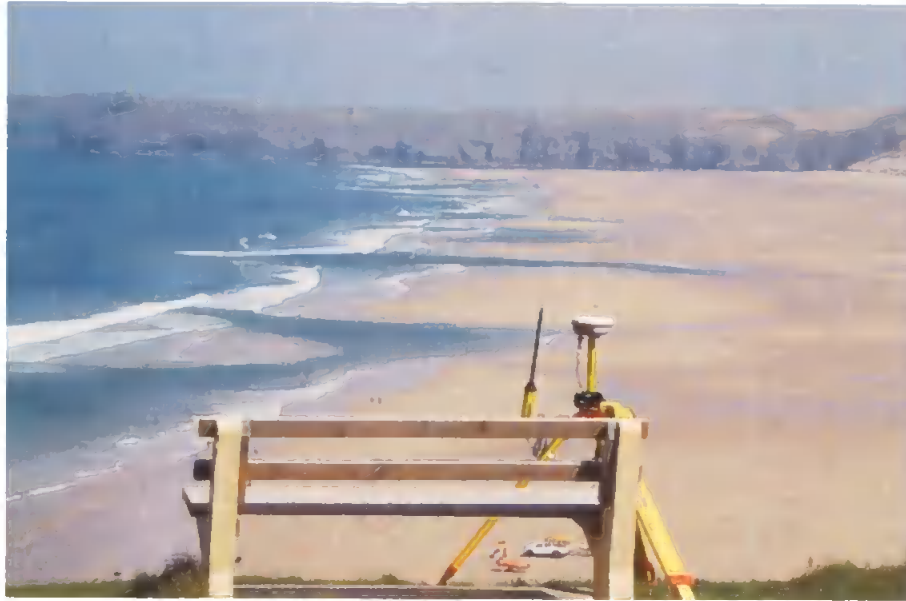
Figure 2.1 - Reference base station for the RTK GPS survey system. Trimble 5800 dual frequency receiver and radio with battery pack (12Ah). Perranporth beach in the background provides a good example of typical low-tide morphology in the region.

Figure 2.2 - ATV mounted RTK GPS system in use conducting a beach survey. Trimble 5800 dual frequency receiver is mounted on front bars and TSC survey controller on the handlebar mount. All data links are wireless via Bluetooth.

mounted receiver to the beach surface is required to compute the beach surface elevation. Within this system, there is a potential for the generation of systematic positional error through vehicle tilt due to beach slope.

Within the intermediate to ultra-dissipative, macro- to mega-tidal environments under investigation the maximum likely beach section slope would be expected to be in the range of 3°. A receiver elevation (z_r) of 1.5 m (typical for ATV) under a tilt of 3° would create a receiver deviation with a horizontal position error (x_e) of 0.08 m and a vertical position error (z_e) of 0.002 m. To reduce error the trolley system ($z_r \sim 0.75$ m) was employed for beaches with slopes >1.5° where x_e = 0.039 m and z_e = 0.001 m on a 3° slope. Typical open beach slopes at selected study sites were between 0.5–1.5° where x_e = 0.018–0.052 m and z_e = 0.00008–0.0006 m. These errors were deemed acceptable in the context of the scale of the survey region and although localized errors could arise around defined bar morphology, the benefit of spatial coverage using the ATV outweighed the potential systematic errors. Of more significance are the elements of the survey open to human error: (1) measurement of rover antenna height; (2) measurement of base antenna height; (3) conducting comprehensive ground control point checks pre- and post-survey to determine daily environmental and operator error; (4) resolution of survey grid and morphological coverage and (5) errors generated through selection of subsequent data interpolation technique.

2.2.3 Experimental design and methods

2.2.3.1 Ground control points

In order to position the survey within a known context or co-ordinate system, reference points, termed 'ground control points' (GCP) must be acquired or found, which provide a framework (co-ordinate reference frame) for the survey, enabling site calibration and error checking for positional accuracy. A control network is essential if comparisons are to be made of multiple surveys at a site. In some cases Environment Agency benchmarks, with relevant specification documentation, were already established within proximity to the beach. In cases where no reliable GCPs where present they had to be installed. This process used a Trimble 4000 SSi Dual Frequency GPS Receiver and L1/L2 antenna with ground plane to make a static 3-hour observation over an installed permanent survey marker. This observation could subsequently be post-processed with positional data from the surrounding active GPS control network, maintained by the Ordnance Survey in combination with precise ephemeris information to generate three-
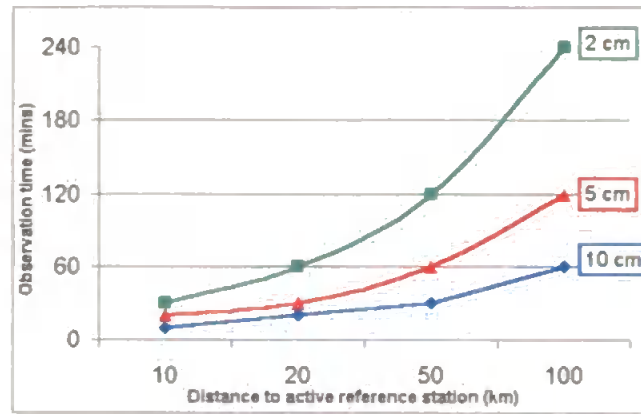
Figure 2.3 - Approximate horizontal accuracies as a function of observation time and baseline length (image courtesy of Ordnance Survey).

dimensional GPS baseline solutions between points, using post processing module within TGO (Trimble, 2002). Accuracies of the processed positions vary and are dependant on baseline length and number of satellites observed. Installed GCP locations were always within 30 km of the nearest reference station and occupations were at least 3 hours in length (Figure 2.3). Re-occupation tests on selected GCPs gave accuracies of x_e <1 cm and z_e <3 cm.

The Ordnance Survey in the UK created the National Grid called OSGB36 (Ordnance Survey Great Britain 1936, based on the Airy 1830 ellipsoid), Great Britain's national co-ordinate system for topographic mapping. The local vertical datum in Great Britain is termed Ordnance Datum Newlyn and provides an orthometric height that refers to a historic reference elevation at the port of Newlyn, referring to a historic mean sea level that is now +0.2 mODN. In order to align collected GPS positions (WGS84) to this system a geodetic co-ordinate transformation is required. The most recent models OSTN02 (grid transformation) and OSGM02 (geoid model) were used to accomplish this.

2.2.3.2 Survey plan

Prior to surveying, an RTK GPS reference base station was established on a GCP within line of sight of the survey area in order to broadcast the RTK corrections to the roving unit on the beach. Before the commencement of each beach survey, control point checks were conducted to assess levels of environmental and operator-based error. At least two GCP's were used for each check with an accepted maximum error level of x_e = 1 cm and z_e = 3 cm. If RTK GPS positions were within tolerance the beach survey could

51

commence. Subsequent survey tracks varied depending on individual beach characteristics. Generally, observations began during the ebbing tide with shore parallel lines being recorded from at least MHWS (where possible as much of the active upper beach was included) progressing seaward. Cross-shore line spacings of 10–30 m were acquired depending on morphology and beach area. A flexible survey grid was followed as it was crucial to be able to follow and capture morphological features that often migrated between surveys. These morphologically based lines more accurately represent the true morphology when processing spatial data. Following this principle, wider cross-shore spacing was permitted within more planar beach sections. Figure 2.4 illustrates a typical survey track at Perranporth beach. A small number of fixed cross-shore profiles were collected at each site. Large tidal ranges and rapid cross-shore tidal translation rates meant that timing was critical to enable maximum coverage at MLWS, which in many cases was the region of greatest morphological complexity. Regions of standing water greater than 0.5 m were surveyed on foot with telescopic pole. On completion of the survey, post survey error checks were conducted against site GCPs.

Principle survey limitations and hazards were generated through 1) adverse (storm) weather conditions driving increased sea surface elevation through set-up (reducing beach width) and increased infra-gravity swash excursions (extending up to 200 m on occasion during high-energy conditions) and 2) changing morphology and beach elevation creating standing water and hard rock obstacles limiting accessible survey region. Risk assessments were conducted prior to surveying.

2.2.4 Data processing

To enable analysis of spatial and temporal morphological variation at each of the study sites a certain level of processing of the geospatial data was required. Of primary importance was the ability to compare multiple surveys through time to assess sediment transport dynamics and to generate a digital elevation model (DEM) of the survey region that represented key morphological features of interest. To this end a process of cleaning, preparing and interpolating the dataset was established that produced a final surface that represented the real beach surface within acceptable error levels (Figure 2.5). Data preparation involved a visual, three-dimensional inspection of the survey data, identifying and fixing/discarding obvious erroneous data points. Following this quality control process the data was transformed onto a local cross-shore/alongshore grid system for each site. Subsequently, a quadratic loess interpolation

Figure 2.4 - Image showing typical survey track at Perranporth beach. Alongshore orientated lines enable maximum morphological coverage throughout the low-tide region due to rapid cross-shore tidal translation rates.

routine was applied within MATLAB (Plant et al., 2002; Schlax and Chelton, 1992) that enabled data interpolation onto a pre-defined grid. This interpolation routine utilizes a scale-controlled interpolation method that minimizes the adverse affects of measurement errors and aliasing. A form of linear interpolation, in which the estimates are a linear combination of the observations, the quadratic loess interpolation allows for an estimation of unavoidable interpolation errors. Additionally, an analysis of interpolation errors can be performed independently of actual observations, which allows for optimization of survey sampling strategies by ensuring that dominant scales are either resolved or largely removed (Plant et al., 2002).
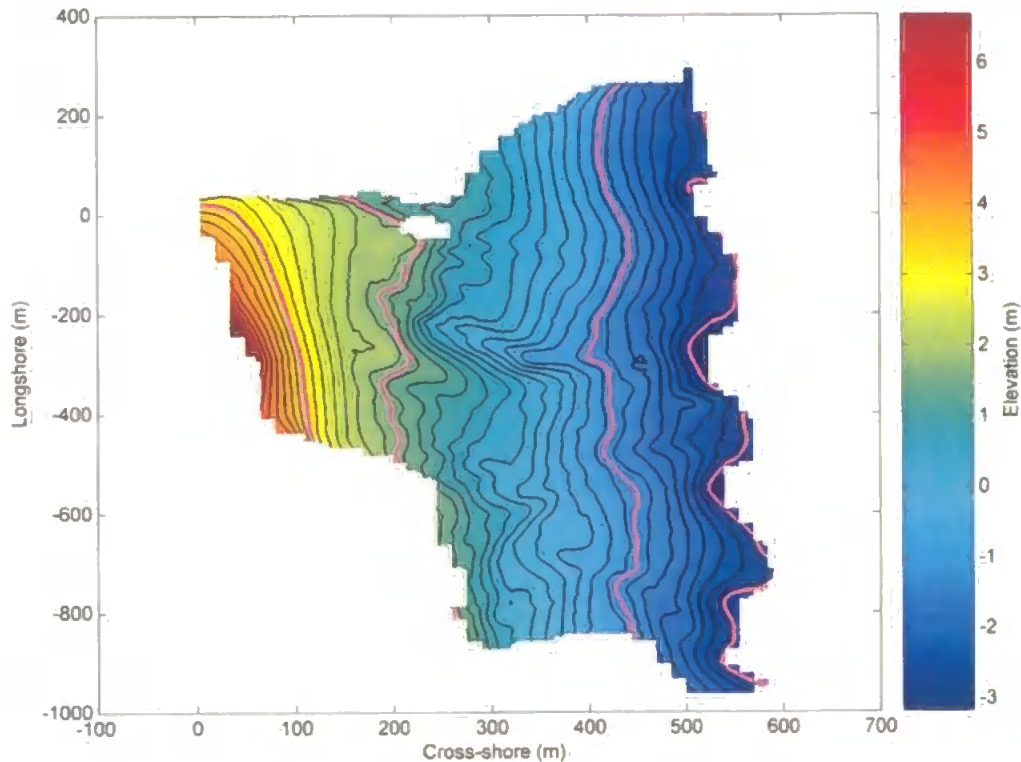
Figure 2.5 - Typical resultant interpolated surface DEM from Perranporth using quadratic loess interpolation routine. Interpolation scales $(\lambda_x) = [5; 10; 30; 50]$ m; Grid spacing $(x) = 5$ m; and permissible vertical interpolation error levels set at 0.05 m. Magenta lines indicate mean tidal levels. Black lines are contoured elevation at 0.25 m intervals.

A number a guidelines are suggested by Plant *et al.* (2002) to optimize grid spacing and interpolation window length scales in the context of desired morphological length scales: 1) smoothing scales (λ_x) can be selected to preserve a length scale of interest (L), $\lambda_x<(L/2)$; 2) grid spacing (x) should be selected so as not to over-resolve the pass band, $x=\lambda_x/4$; and 3) in the case of high-density observations, over-sampling can reduce the accuracy of interpolation error estimates, re-sampling using a running average can reduce this effect (suggested running average half width of $\lambda_x/8$).

With these recommendations in mind, a variety of interpolation length scales can be applied until the resolved data best suits the analytical needs. Finally, cross-shore profiles are extracted from the DEM at set intervals. Profiles are linearly interpolated at 1 m intervals in the cross-shore.

2.3 ARGUS VIDEO MONITORING

During the course of the study, video data were made available from an Argus monitoring station at Perranporth beach. The station was set up originally by the Coastal Imaging Lab at Oregon State University, as part of the CoastView Program (OSU; http://cil www.coas.oregonstate.edu: 8080), to develop tools to exploit the low-cost, long-term optical measurements available from Argus to solve a range of Coastal Zone Management problems (Holman and Stanley, 2007). The Perranporth video monitoring station, mounted on a headland to the south of the beach affording extensive visual coverage of the beach and nearshore, comprises two video cameras (based on Scorpion SCOR-14SOC cameras) that record images of dimension 1024×768 pixels (Figure 2.6). One camera collects images of the low-tide and nearshore region, the other the mid- and high-tide regions (Figure 2.7). In addition, the system consists of a computer with communications link to the World Wide Web for control and data return plus a timing module to synchronize collections between the cameras.

To enable the estimation of the geometry of each view, Ground Control Points (GCP) are also required in combination with predicted tidal levels for Perranporth (no real sea-level elevation data were available for the duration of this study). These GCPs were collected throughout the inter-tidal image view using a total station to a target board identifiable in the captured images. The acquisition of geometries then allows for the transformation of the image information into a locally derived co-ordinate system for comparison and analysis in conjunction with additional data sources like topographic and bathymetric survey data (Figure 2.7). For the purposes of this study, effects of set-up, run-up and surf beat are not accounted for in the image transformation, although previous work by for example Van Enckevort and Ruessink (2001), has generated models to improve accuracy of positions due to these phenomenon. These calculations and transformations are enabled through specifically designed ARGUS specific toolboxes for use within Matlab software.

The principal image products from this system that are used in this study are the single snapshot and the time-exposure images. The single snapshot image, collected at 30-min interval provides a qualitative assessment of the image (Figure 2.7). The second image product, the time-exposure (or timex) images (Figure 2.7), collected at 30-min interval represent the mean of all of the frames collected at 2 Hz over a 10-min period of sampling. Non-moving objects onshore are rendered as they appear in

Figure 2.6 - Argus video cameras at Perranporth at an elevation of 47.87 mODN (B) and indication of the extent of the field of view (inset A).

a snapshot, but moving features such as waves are averaged out with only their mean brightness returned. These images provide mean wave breaking intensity patterns within areas of the surf zone where wave dissipation is occurring. As sandbars induce wave breaking, wave dissipation patterns can be used to extract information on bar crest locations and patterns of nearshore bar morphology and rip channels (Holman and Stanley, 2007; Lippmann and Holman, 1989). Further research has found some discrepancies in this link in the cross-shore due to tidal elevation and variations in wave height, but to an extent these errors can be quantified and corrected for if required (Kingston et al., 2000; Van Enckevort and Ruessink, 2001).

Quantitative data extraction from images within this study involved the identification of alongshore rip locations during mid- and low-tide water levels (see Chapter 6). The alongshore region of interest at Perranporth ranged from -1000–100 m. The pixel resolution within this region ranged from X_{res} < 5 m and Y_{res} < 5 m in the near-field to X_{res} < 5 m and Y_{res} ~ 10–15 m in the far-field (Figure 2.8). Rip channels and their locations were the features of interest within this study. A sensitivity analysis of extracted alongshore low-tide rip locations was performed. Rip head locations were manually picked from the plan view timex image using a rip picking routine within Matlab (Figure 2.9). For each of three rip systems within the image (near-, mid- and far-field), 50 manual assessments of the rip head location were conducted for each to identify to potential error in visual identification and point extraction throughout the

(A) Snapshot images

Camera 1   Camera 2

(B) Timex (time exposure) images

Camera 1   Camera 2

(C) Plan view (geo-rectified) image

(D) Transformed plan veiw image with topographic survey overlay
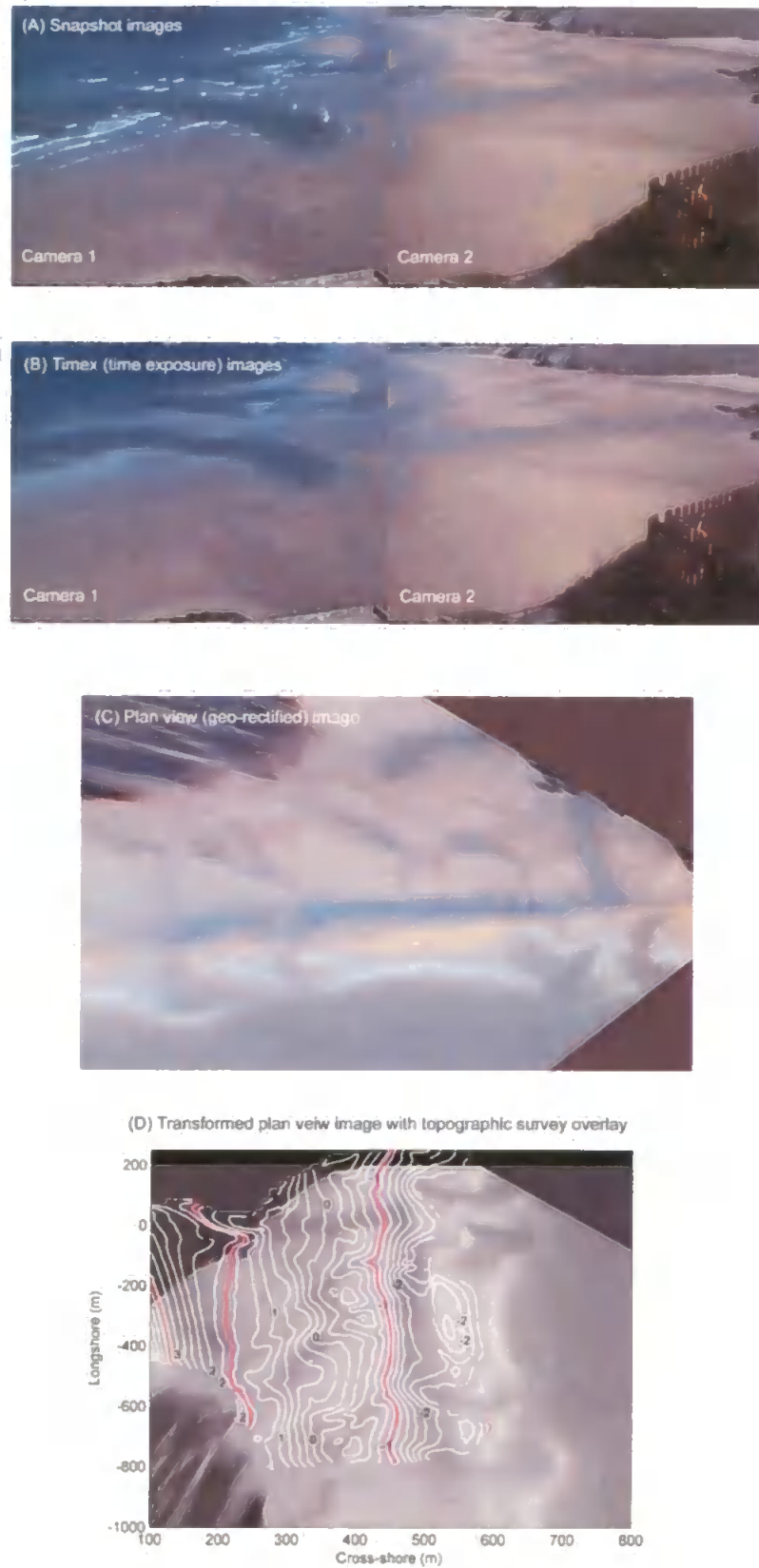
Figure 2.7 - Example Argus video products from Perranporth station: (A) snapshot images; (B) timex images; (C) plan view (geo-rectified) image; and (D) example of low-tide plan image transformed into local co-ordinates for merge with survey data.
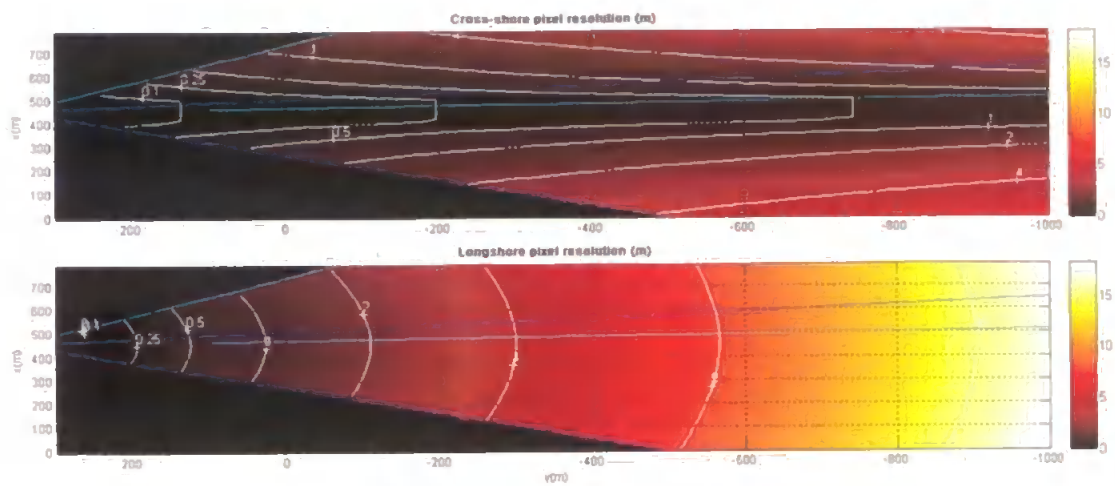
Figure 2.8 - Calculated pixel resolutions for the Argus video cameras at Perranporth.
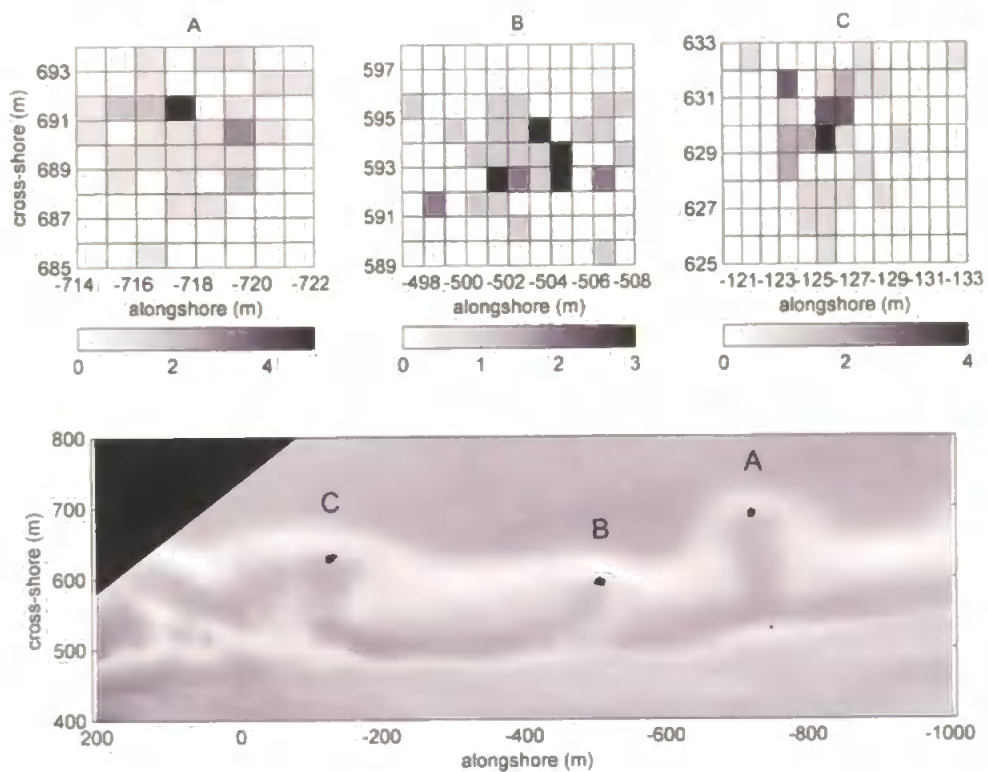
Figure 2.9 - Sensitivity analysis of observational consistency during manual rip picking routine. Top three panels show picked rip head locations for 150 acquired points. The three rip locations are indicated on the Argus plan timex image in bottom panel.

field of view. The standard deviations of alongshore positions for each rip marked A, B and C in Figure 2.9 were 2 m, 2.7 m and 3.4 m respectively. The range of extracted rip head locations in the alongshore for each rip system was 8.1 m, 11.2 m and 12.2 m for rip A, B and C, respectively. This level of observational consistency was acceptable in the context of rip systems under investigation that were mostly 50–100 m in width. Little variation in observational precision was identified due to loss of image resolution in the far-field.

2.4 SEDIMENT ANALYSIS

The properties of beach sediments provide a fundamental control on the morphodynamic state of the beach system and as such surface sediment samples were taken during every topographic survey. Due to the macrotidal context of most of the study sites, multiple samples, covering the lower and upper beach, were taken so a representation of cross-shore variability in sediment characteristics was possible. Samples were collected along fixed cross-shore profiles for each site, so repeat samples were comparable, from the upper active layer of the beach (top 1 cm). Group averaging, where required, of multiple samples enabled an overall view of lower-, mid- and upper-beach particle properties reducing local variations due to small-scale bedforms.

Sediments were analysed using a settling tube to determine settling velocity and associated statistics. The settling velocity is a direct measure of interest in the consideration of the morphodynamic implications of sediment type in the nearshore. This sedimentologic measure also enables accurate calculation of morphodynamic indices traditionally used to parameterize the beach environment thus enabling a reliable assessment of collected data in the context of previous studies and morphodynamic frameworks. The settling tube used had a nominal height of 2.205 m and internal diameter of 0.22 m. Electronic scales recorded sediment weight from release point at 2 Hz and data were logged directly to a PC.

Prior to settling, the sediment samples were processed. Once collected, samples were washed over a 63 μm sieve and oven dried. Samples were then sieved where necessary to remove any coarse fraction >2 mm prior to settling as it was deemed inappropriate to settle these grains because of insufficient tube width to accurately determine the settling velocity. Split into 10 sub-samples using a rotary splitter, alternate samples were taken

Figure 2.10 - Automated settling tube used to determine the sediment fall velocity distribution.

for analysis. Approximately 10 g of sediment was used for each sample drop. The settling process was repeated three times and results averaged for each sample analysed.

The fall velocity data were then used to characterize standard properties of the mean (Equation 2.1), sorting (Equation 2.2) and skewness (Equation 2.3) of the settling distribution using graphical methods as outlined by Folk and Ward (1957). The psi measure ($\psi = -\log_2 w$) was used, as introduced by Middleton (1967), in place of the standard phi measure ($\varphi = -\log_2 d$) for grain size. Percentiles were taken from the cumulative weight distribution.

$$Mean = \frac{\psi_{16} + \psi_{50} + \psi_{84}}{3} \tag{2.1}$$

$$Sorting = \frac{\psi_{84} - \psi_{16}}{4} + \frac{\psi_{95} - \psi_5}{6.6} \tag{2.2}$$

$$Skewness = \frac{\psi_{16} + \psi_{84} - 2\psi_{50}}{2(\psi_{84} - \psi_{16})} + \frac{\psi_5 + \psi_{95} - 2\psi_{50}}{2(\psi_{95} - \psi_5)} \tag{2.3}$$

Where estimates of grain size parameters were required during the study, Equation 2.4, developed by Furguson and Church (2004), was used. The equation results from a dimensional analysis that derived a simple explicit form for all grain sizes. The formula assumes that the relation must reduce to Stokes' law (fall velocity increasing as the square of particle diameter) for fine sediment and a constant drag coefficient (fall velocity varies as only the square root of particle diameter) for coarse sediment.

$$w = \frac{RgD^2}{C_1 v + (0.75 C_2 RgD^3)^{0.5}}$$

(2.4)

where w denotes the particle's fall velocity, D its diameter, R its submerged specific gravity (1.65 kg m^{-3} for quartz in water), g the acceleration due to gravity, v the kinematic viscosity of the fluid (1.0 x 10^{-6} kg m^{-1} s^{-1} for water at 20°C) and C_1 a constant with a value of 20 for nominal grain diameters of natural sands. C_2 is the constant asymptotic value of the drag coefficient $C_D = 4RgD/3w^2$ at 10^3 < Re < 10^5 (where Re is the Reynolds number = wD/v) and is 1.1 for nominal diameters of natural sands.

From Equation 2.4 a seventh order polynomial function was derived to enable the calculation of a reasonable estimate of grain size D from the graphical quantities of the settling distribution. Figure 2.11 plots a comparison of the calculation of grain size from fall velocity data using Equation 2.4 and that obtained from a laser sizer (Malvern Mastersizer 2000) for 40 samples from a range of study sites. Linear regression indicates a good fit with an R^2 of 0.93 and linear fit indicates that the settling values for grain size are consistently 20% smaller than that of laser derived sediment sizes. These systematic discrepancies can be attributed to the fundamentally different theoretical principals being used to determine the same statistic. Recent studies have documented the tendency for laser sizing to over predict size of platey grains as measured size can be dominated by their large projected area not borne out in their settling velocity (McCave et al., 2006). The estimation of grain size from settling using the above method was deemed suitable for the purposes of this study and is used throughout with the exception of particle size analysis of significant fractions greater than 2 mm, which was performed using traditional sieving techniques.
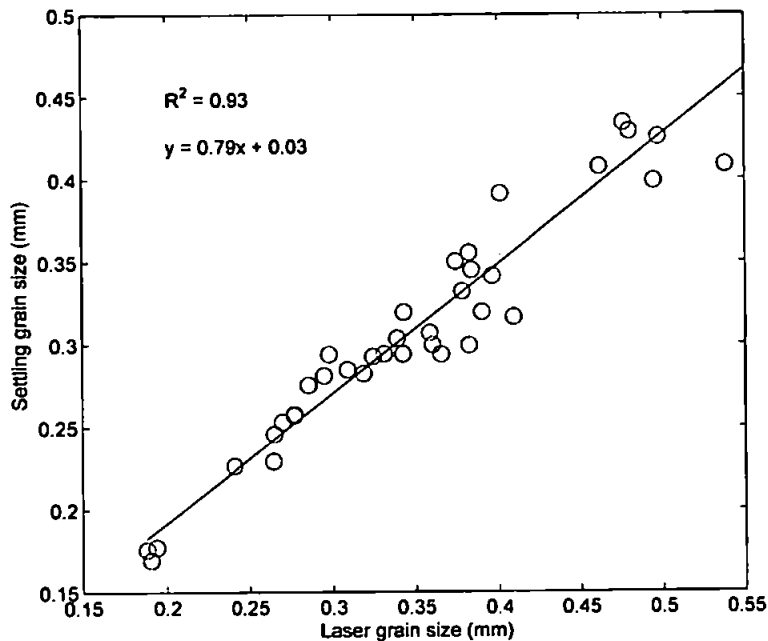
Figure 2.11 - Comparison of estimation of mean grain size from settling tube data and that derived from laser size analysis for 40 samples. Solid line indication results from a linear regression.

2.5 WAVE CLIMATE

In order to understand the relationships and driving environmental mechanisms of beach type/morphology and state in the UK coastal environment, a realistic representation of dominant wave conditions is needed. In the UK this is not straightforward due to the variability in both the character of the coastal morphology and wave climate throughout the country. Chapter 4 investigates beach types and their hydrodynamic setting within the UK where beach sites were sub-divided into 6 distinct wave climate regions: the North Sea (F), the English Channel (E), the Atlantic Ocean (C), the Irish Sea (B) and Liverpool Bay (A). A further sub-division is that of Lyme Bay (D) that is situated within the transition between the Atlantic and English Channel wave climates. The following wave climate analysis will treat these regions separately (Figure 2.12).

Within the context of the investigation reported in Chapter 4 the required wave breaker characteristics for each beach site were calculated in a number of ways. For beaches within proximity of a near-shore directional wave buoy, an annual data record was used. For beaches where local nearshore recorded wave buoy data were not available, data
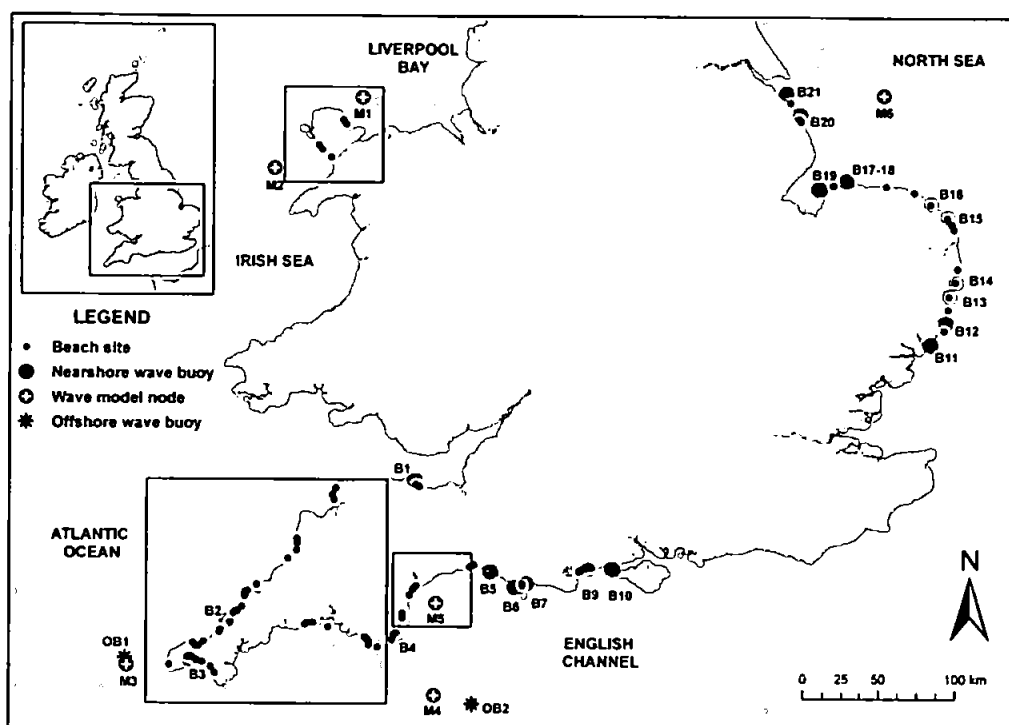
Figure 2.12 - Overview map of wave data sources used in the study. UK beach study sites are marked by black filled circles. Boxes indicate regions where nearshore wave modelling was performed using MIKE21.

from the MetOffice UK waters wave model was used to drive a numerical wave transformation model (MIKE21SW) providing simulated nearshore wave climate statistics. Figure 2.12 gives an overview of the wave climate regions and the data sources available for each region and Table 2.1 provides associated metadata connected to these data sources. A variety of offshore wave data sources, measured and modelled, were assessed and compared for their suitability for input as boundary conditions in the wave transformation model MIKE21SW.

2.5.1 Measured wave data

2.5.1.1 MAWS Marine Automatic Weather Station network

The Met Office Marine Automatic Weather Stations (MAWS) was developed as part of an early warning system for severe weather and sea conditions. The network includes eleven moored wave and weather observing buoys and seven lightship and island systems, mostly located in open-ocean locations to the west of the British Isles (ODAS), and two in coastal inshore waters. Within this study, the Seven Stones Lightship (50°6'9" N 6°6'0" W, 60 m depth) and the Channel Lightship (49°54'0" N 2°54'0" W; 66 m depth) were used to provide offshore wave climates for the Atlantic west and

63

Table 2.1 – Summary of wave data sources.

Location	Source	Code	Position	Record type	Record dates	Water depth
OFFSHORE						
Liverpool Bay	MetOffice	M1	53.5°N 4.08°W	Model	01/01/07 – 31/12/07	~40m
Irish Sea	MetOffice	M2	53.06°N 4.92°W	Model	01/01/07 – 31/12/07	~55m
SW approaches	MetOffice	M3	50.06°N 6.08°W	Model	01/01/07 – 31/12/07	~60m
Channel coast	MetOffice	M4	49.95°N 3.75°W	Model	01/01/07 – 31/12/07	~66m
Lyme Bay	MetOffice	M5	50.5°N 3.25°W	Model	01/01/07 – 31/12/07	~25m
East coast	MetOffice	M6	53.5°N 1.09°E	Model	01/01/02 – 31/12/02	~25m
62107	WW3	M7	50°N 6.25°W	Model	01/01/07 – 31/12/07	~60m
62103	WW3	M8	50°N 3.75°W	Model	01/01/07 – 31/12/07	~60m
Seven Stones Buoy	MAWS	OB1	50.10°N 3 6.1°W	ODAS Buoy	01/01/03 – 31/12/07	~60m
Channel Lightship	MAWS	OB2	49.9°N 2.9°W	ODAS Buoy	01/01/07 – 31/12/07	~66m
INSHORE						
Minehead	CCO	B1	51.22881°N 3.47136°W	Datawell Buoy	01/01/07 – 31/12/07	~10m
Perranporth	CCO	B2	50.35335°N 5.17518°W	Datawell Buoy	01/01/07 – 31/12/07	~10m
Penzance Bay	CCO	B3	50.11421°N 5.50282°W	Datawell Buoy	01/04/07 – 31/03/08	~10m
Start Bay	CCO	B4	50.29143°N 3.61712°W	Datawell Buoy	01/04/07 – 31/03/08	~10m
West Bay	CCO	B5	50.69311°N 2.74956°W	Datawell Buoy	01/01/07 – 31/12/07	~10m
Chesil Beach	CCO	B6	50.60209°N 2.52336°W	Datawell Buoy	01/01/07 – 31/12/07	~10m
Weymouth	CCO	B7	50.62300°N 2.41388°W	Datawell Buoy	01/01/07 – 31/12/07	10.6m
Swanage Pier	CCO	B8	-	Guage	01/01/07 – 31/12/07	N/A
Boscombe	CCO	B9	50.71138°N 1.83959°W	Datawell Buoy	01/01/07 – 31/12/07	10.4m
Milford	CCO	B10	50.71256°N 1.61503°W	Datawell Buoy	01/01/07 – 31/12/07	11m
Donna Nook	EA/Guardline	B21	53°31'.80N 0°7'.20E	Nortek AWAC	03/10/06 - 03/10/07	11m
Theddlethorpe	EA/Guardline	B20	53°24'.00N 0°15'.00E	Nortek AWAC	06/08/06 - 03/10/07	11m
Sunk Sand	CEFAS	B19	52°57'.30N 0°24'.70E	Nortek AWAC	09/10/06 – 07/08/07	10m
Walcott	EA/Guardline	B17	52°50'.64N 1°30'.42E	EA gauge	08/09/02 - 07/09/03	7.5m
Horsey	CEFAS	B16	52°45'.52N 1°39'.77E	Nortek AWAC	09/10/06 – 06/10/07	8m
Off Bawdsey Cliff	CEFAS	B11	52°0'.29N - 1°26'.44E	Valport 730DT	21/08/03 - 21/08/04	4.2m
Sudbourne	EA/Guardline	B12	52°7'.76N - 1°35'.80E	Nortek AWAC	03/10/06 - 22/09/07	6m
Dunwich Bay	EA/Guardline	B13	52°17'.19N - 1°38'.57E	Nortek AWAC	12/10/06 - 22/09/07	5m
North Southwold	EA/Guardline	B14	52°22'.14N - 1°42'.75E	Nortek AWAC	12/10/06 - 22/09/07	7m
Southwold (North)	EA/Guardline	B15	52°22'.14N - 1°42'.75E	Valport 730D	21/08/03 - 21/08/04	4.6m
Scolt Head	EA/Guardline	B17	53°0'.03N - 0°41'.07E	Nortek AWAC	10/10/06 - 19/12/06	8m
Scolt	EA/Guardline	B18	53°0'.00N - °41'.04E	EA gauge	07/09/02 - 08/09/03	9m

southwest coasts (OB1 and OB2 in Figure 2.12). The significant wave height is calculated as four times the root mean square (RMS) value of a 17.5 min record leading up to the observation time. The wave period parameter is calculated from the average zero-crossing period. Historically with the buoys considered in this study the wave sensor has failed 4 times over a cumulative operational period of 125 years and 10 locations (Halliday and Douglas, 2008).

2.5.1.2 Channel Coastal Observatory: nearshore wave observations

The Channel Coastal Observatory (CCO) maintains a series of observing stations covering the SW-SE coasts of England from Minehead in Somerset to the Isle of Grain in North Kent. The network comprises of a system of moored directional wave rider buoys spanning the region from the Solent to the Bristol Channel. The buoys are located in 10–15 m water depth with data being telemetered to shore in real-time. Standard integrated parameters representing wave conditions are generated from the directional wave spectrum (Bradbury et al., 2004).

2.5.1.3 WaveNet wave monitoring network

A Defra commissioned strategic wave monitoring network for England and Wales, run by the Centre for Environment, Fisheries & Aquaculture Science (Cefas) provides a network of nearshore wave data recorders. Instruments include directional wave buoys and Nortek AWACs (Acoustic Wave And Current profilers). Data from the WaveNet archive provided annual measured nearshore (~ 8 m depth) wave statistics for the East Coast region.

2.5.2 Modelled offshore wave data

Within the UK waters, model data were obtained from both the third generation NOAA WaveWatch III model and the second generation MetOffice UK Waters Wave Model. NOAA WaveWatch III uses a coarse (1.25x1 degree) model grid that gave insufficient resolution to successfully model the inshore wave conditions for UK coastal regions of interest. The MetOffice UK water model, which has a 12 km grid, was deemed adequate for use as boundary conditions for the regional wave transformation model used in this analysis (MIKE21). What follows is a summary and validation of the MetOffice UK waters wave model.

2.5.2.1 MetOffice second generation wave models: UK waters model

The MetOffice second generation wave model data was used to simulate/hindcast the wave climate for this study. The Met Office 2nd Generation spectral wave model runs with both global and nested regional configurations. The UK Waters Wave Model is nested within and forced by the MetOffice Global Wave Model. The wave models are forced using hourly wind fields generated in Met Office Numerical Weather Prediction (NWP) models, which include observational data from satellite, ship and data buoy networks in their assimilation schemes. Based on the local wind speed and direction, energy is input to waves through a parameterisation of the exponential growth of existing wind sea energy (linear growth in the early development stage). Wind sea spectral peakedness and peak frequency are used to select an appropriate member of the JONSWAP family of spectra to describe the growing wind sea energy distribution in frequency space. Wave energy is advected through the model domain using a 2nd order Lax-Wendroff scheme. In shallow water (< 200 m depth) wave group speed depth dependency, bottom friction and refraction are represented in the model physics. Operationally, the models are configured with a spectral resolution of 13 frequency bins and 16 directional bins, representing waves with a range of periods between 25 seconds and 3 seconds (deep water wavelengths from 975 m to 15 m).

Wave conditions worldwide are forecast using the Global Wave Model on a 5/9 degree latitude by 5/6 degree longitude grid (approximately 60 km square grid at mid-latitudes), a further increase in resolution is made for the UK Waters Wave Model, which is nested using boundary conditions from the Global Wave Model. The UK Waters Wave Model grid covers the northwest European continental shelf from 12°W between 48°N and 63°N. The UK Waters Wave Model is forced by high resolution (~ 12 km grid) Mesoscale NWP 10m winds and includes effects of time-varying currents on the UK continental shelf as generated by the Met Office's operational Storm Surge Model. This model was introduced into the operational suite in March 2000 and is run four times daily using analysis times 0000, 0600, 1200 and 1800 UTC.

From the two-dimensional frequency-direction spectrum standard integrated parameters representing wave conditions are generated (e.g. significant wave height, wave peak and zero up-crossing period and principal wave direction).

The coastline in the model is coarsely represented by the land ocean boundary of the model grid providing limited resolution of nearshore wave transformations. The nearest grid points to the land are generally too far away from the shoreline to be used directly in coastal process simulations (Bradbury et al., 2004). Therefore wave transformation was performed using MIKE21 SW (Spectral Waves) to estimate the inshore wave climate. Wave model grid locations, for use in the regional wave transformation model were selected to best represent the coastal regions of interest and be co-located where possible with offshore wave buoys (non-directional) for validation. For more localised areas of interest, data from the most landward limit of the model grid was utilised (Lyme Bay).

2.5.2.2 Model validation: Offshore waves

The UKMO UK waters model was validated against the Seven Stones wave recorder for H_s and T_z during 2007 (Figure 2.13). The buoy location and model output node can be considered to be co-located. Validation of mean/peak wave direction and peak period was not possible as these integrated parameters are not recorded at this ODAS buoy location. Agreement between modelled and measured wave heights at this exposed west coast location (M3, OB1) was reasonable. The model tending to over predict 3hr average significant wave heights (23.2% on average during 2007), with low wave conditions (< 1.5 m) performing worse than high wave conditions. This phenomenon is attributed to the ability to predict the onset and decay of wave events. Annual average wave heights were over predicted by 18%. This tendency for over prediction by the model is consistent with other studies of model performance at deep water sites on the continental shelf (Bidlot et al., 2002) and has been attributed to the over estimation of 10 m winds in the Met Office system. A direct comparison with zero up-crossing wave period (Figure 2.13) indicates that the model consistently under predicts wave period, on average by 25%. It is suggested that this is at least in part due to the representation of the frequency resolution within the model being coarse, impacting on the ability of the model to represent growth of the wave period in a well defined manner. The range of periods from 3.1–5.2 s is represented in the model by just 3 frequency bins and the lower limit of frequency resolution is 3.1 s. The frequency resolution of the UK Waters model is represented by only 13 frequency components in total, and the peak period is defined by the component with maximum energy. As the wave buoy record doesn't calculate peak period no comparison was possible but previous authors have conducted a global analysis of similar scatter diagrams indicating the Met Office models tend to
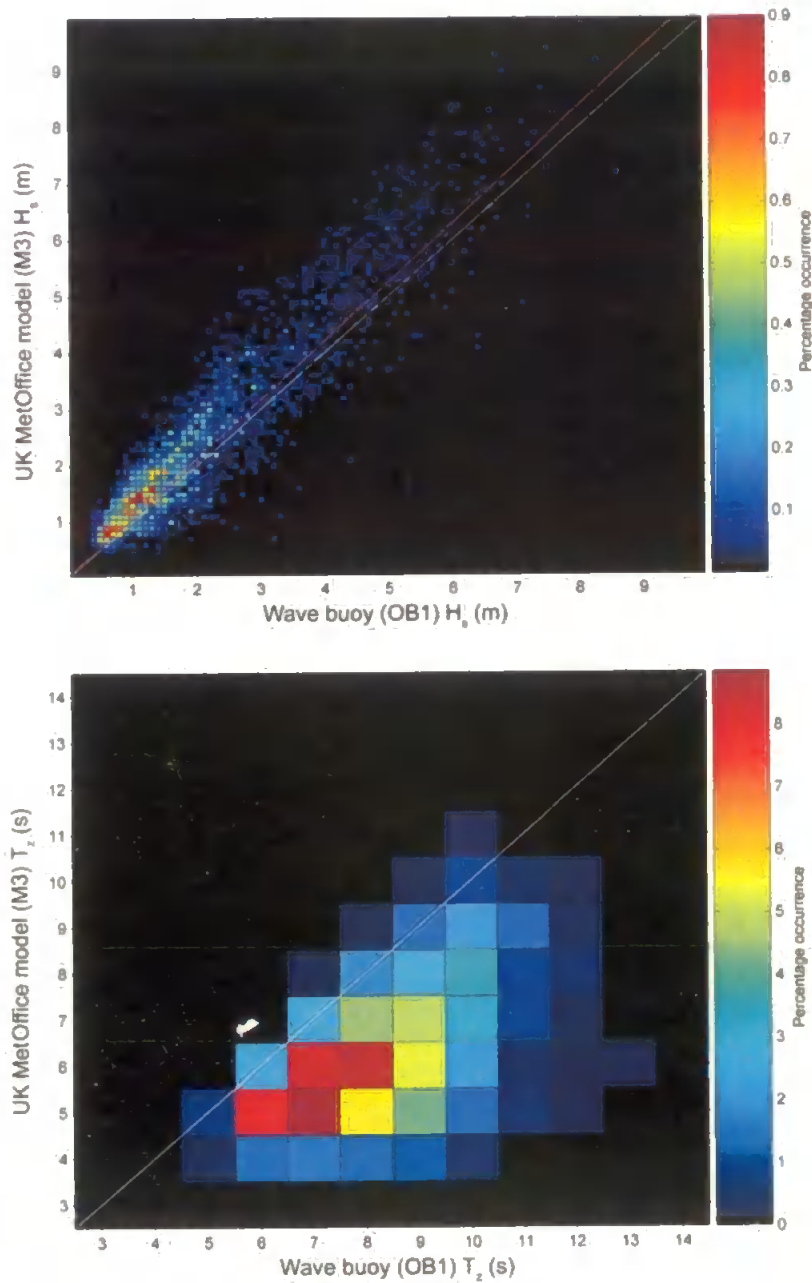
Figure 2.13 - Seven Stones Buoy (OB1) versus UKMO UK waters model (M3), 2007. Top panel shows significant wave height and bottom shows zero up-crossing wave period.

overestimate the peak period (Bidlot et al., 2002). For the purpose of near-shore wave modelling using MIKE21 SW a requirement for a value of peak period is required for generation of the wave spectrum from integrated parameters. Therefore, as the only data source available, the MetOffice UK Waters Model record was used with caution.

Event time series

Sample time series from both modelled and measured wave data at the co-located west coast location (M3, OB1) over two 40-day periods are illustrated in Figure 2.14. Representing a range of high- and low-energy conditions, it shows that for this sample, the UK waters model performs well at tracking the higher resolution fluctuations in wave height at the buoy. The model record appears to over predict wave heights during the falling limb of a high-wave event and in many cases during the sample time series over-predict the peak wave heights during significant wave events. There are examples where both models over-predict the peaks of wave events. This phenomenon has been assessed by Bidlot et al. (2002) to be due to inaccuracies in the forcing wind data in the associated atmospheric models, through grid resolution or ground-truthing problems.

Comparison of the UK waters wave model record with measured data for 2007 shows reasonable overall agreement. Although several limitations in model accuracy have been highlighted it was concluded that the UK Waters Wave Model would provide an acceptable tool for estimating regional offshore wave climate.
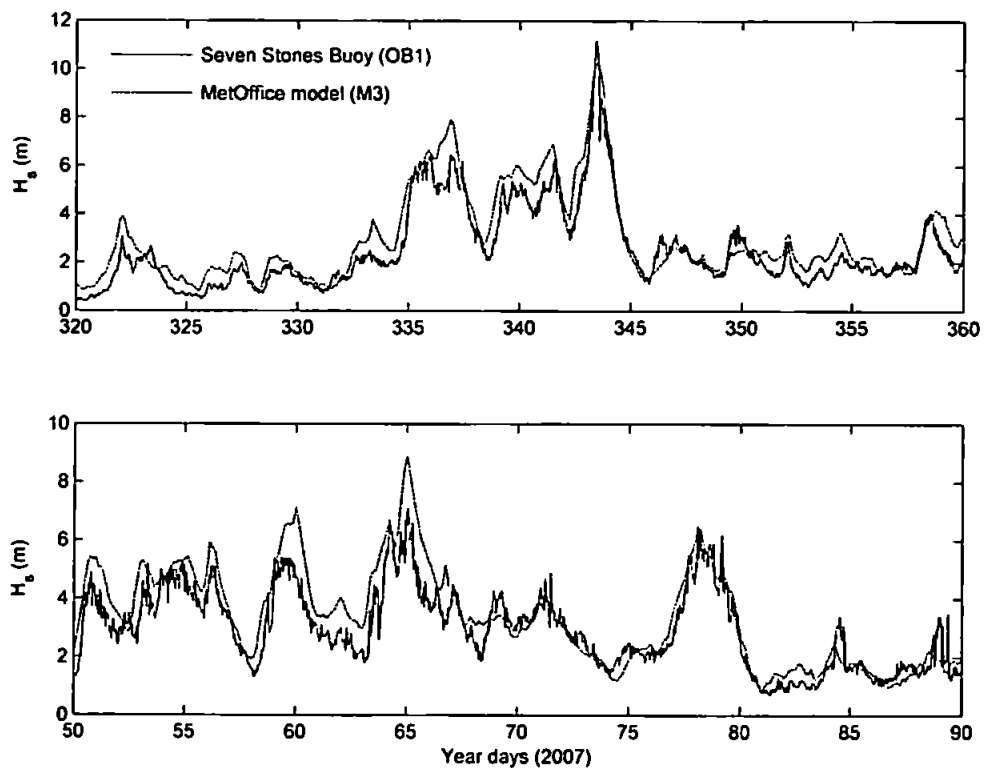
Figure 2.14 - Significant wave height sample timeseries comparison between the OB1 buoy (1-hr timestep) and M3 Met Office UK waters model record (3-hr timestep).

Importantly, it provides the desired temporal and spatial coverage and the required integrated parameters (H_s, T_p, $Dirp$) for the near-shore wave model (MIKE21 SW).

2.5.3 Regional wave climate analysis

Regional wave climates were assessed with attention paid to the orientation of the coastal region of interest, and the requirements of the wave transformation model to enable the best and most appropriate estimation of near-shore wave climates for the selected beach study sites. Assessment criteria were to define:

- swell wave, mixed swell/wind or wind dominated wave climate
- directional modality, separate relevant modal segments (max width 90°)
- $H_{s,50\%}$, $H_{s,10\%}$, $H_{s,90\%}$, T_p and mean and residual energy flux direction for each defined directional segment.

Wave energy flux (wave power), defined as the power per unit wave crest, was calculated as (Komar, 1998):

$$P = \frac{1}{8}\rho g H_s^2 C \frac{1}{2}\left[1 + \frac{2kh}{\sinh(2kh)}\right] \tag{2.5}$$

$$C = \frac{gT}{2\pi}\tanh\left(\frac{2\pi h}{L}\right) \tag{2.6}$$

where ρ is the density of sea water (1025 kg m^{-3}), g is gravitational acceleration (9.81 ms^{-2}), k is the wave number, h is the water depth and C is the wave celerity. As the wave outputs are located in intermediate depth the full general expression for C is used and L_{int} (wave length, intermediate depths) was calculated using an approximation derived from the dispersion equation given by (Eckart, 1952).

$$L_{(int)} = L_\infty\left[\tanh\left(\frac{2\pi h}{L_\infty}\right)\right]^{0.5} \tag{2.7}$$

The regional wave characteristics were assessed for all previously defined study regions using data from the MetOffice UK waters wave model for 2007. Due to issues of data availability only one year of data was used to approximate the typical annual wave

climate. The majority of morphological and sedimentological data collection, in regions where modelled wave data were used to represent the wave climate, occurred in October and November of 2007, with the exception of data from Anglesey, North Wales. As model run times prohibited calculating a complete annual time series, the annual direction spectrum was broken down into identifiable segments, each representing a percentage of the annual observations. These segments and associated integrated wave parameters were transformed to the coast and recombined to approximate the annual wave climate in the near-shore. This procedure was deemed suitable and a vast improvement on previous investigations that estimated wave breaker heights from offshore wave data using linear wave theory (e.g. Jackson et al., 2005), without considering the effects of regional and local coastal and beach orientation on the inshore wave transformations and hence the accuracy of breaker height estimation for individual sites. Each region was assessed separately and a characteristic wave climate generated.

2.5.3.1 Near-shore wave transformation using MIKE21

At locations where near-shore wave buoy data was unavailable the MIKE21 Spectral Wave Model was used. The model was used to transform characteristic values of the offshore wave statistics for each region for 2007. Due to the representative nature of the forcing boundary conditions the inclusion of regional wind forcing was not possible. Some previous studies have indicated that the exclusion of the local wind forcing generally has little effect within a high-energy swell wave dominated environment (Strauss et al., 2007).

The offshore wave data were analysed as described above for each region and broken down into key directional bins with regard to the dominant conditions affecting the region of interest and the orientation of the coastal zone. Within each discrete zone, mean wave power direction, annual 10% and 50% exceedance significant wave heights, along with the mean peak period and an approximation of directional spreading in the region are needed to drive the spectral wave module in MIKE21. Wave output nodes in the model were located over the 15 m depth contour or 1 km from the mean shoreline, depending on the distance of the 15 m contour from the beach. These gave good estimates of regional variations in wave conditions but were not able to resolve local, small scale $O(100m)$ variations in wave climate, due to the regional nature of the model domain (computational efficiency) and limitations in bathymetric resolution. To generate the final breaker wave values for each beach site, the percentage annual

contribution of each wave sector was taken into account when calculating and annual weighted value for each parameter.

Model description

MIKE 21 SW is a third-generation spectral wind wave model based on unstructured meshes. The model was developed by the Danish Hydraulic Institute (DHI) and the model simulates the growth, decay and transformation of wind generated waves and swells in offshore and coastal areas. The discretisation in geographical and spectral space is performed using a cell-centered finite volume method. The source functions take into account the near-shore effects of refraction, shoaling, wave breaking, bed friction, and wind wave growth (Holthuijsen et al., 1989; Sorensen et al., 2004).

Mesh generation

The model is based on flexible mesh and therefore is particularly applicable for simultaneous wave analysis on both regional and local scale. Flexible mesh allows for coarse spatial resolution for offshore area and high resolution mesh in shallow water and at the coastline. This dramatically reduces the computation load and enables the generation of large regional model domains. A depth controlled mesh was generated for each wave climate region with a coarse offshore grid size increasing in resolution shoreward to the nearshore. Figure 2.15, an example of the mesh for the Atlantic west coast model run, represents at typical mesh with 30367 elements and 15623 nodes. The mesh resolution at the shoreline is approximately 200–300 m. Depth information within the model domains was obtained from Edina Marine Digimap in the form of digital bathymetric charts. This dataset, largely digitized from original bathymetric charts has a resolution of 100 m x 100 m and provides an appropriate source for the regional scale modeling performed in this study, but lacks both the detail and accuracy in the nearshore to perform more high resolution modeling than described here. This bathymetric data is interpolated onto the generated mesh for each model domain (Figure 2.16).

Model inputs

Further to the model formulation and mesh generation, careful consideration of boundary conditions and model settings were essential in order to obtain reliable results from the model. An open offshore boundary is specified for each model domain to which values of offshore wave conditions H_s, T_p, mean wave direction and a value for the directional spreading index (not available from MetOffice model, therefore
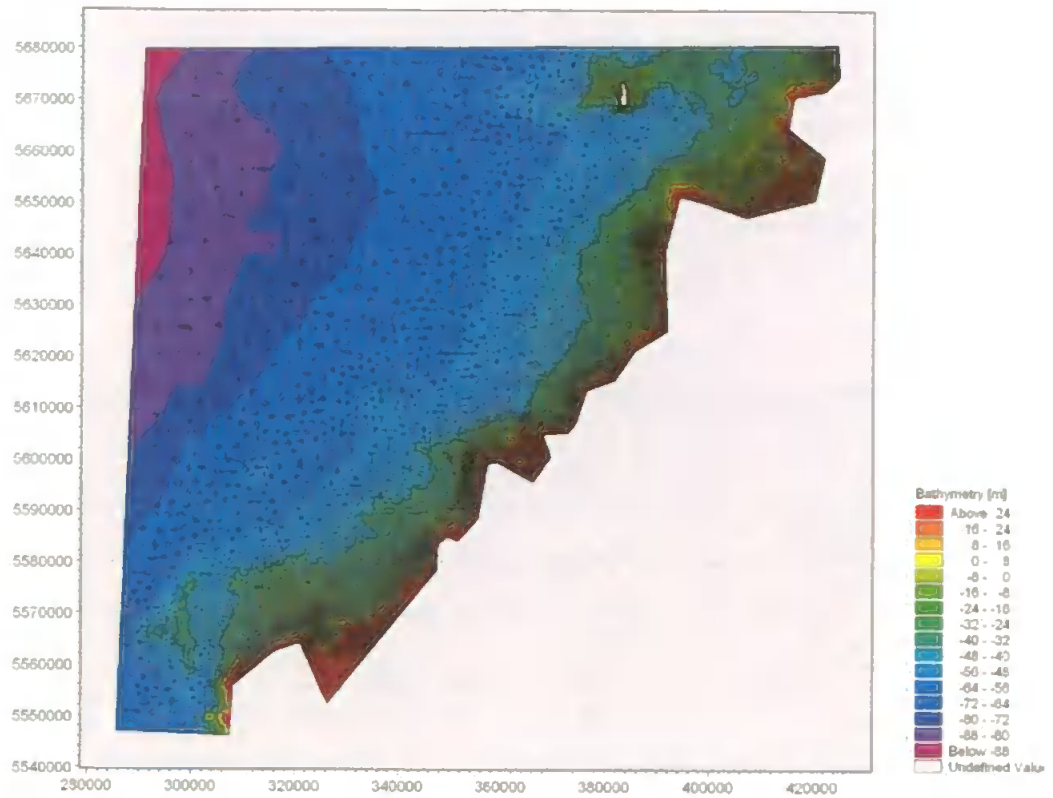
Figure 2.15 – Example of MIKE21 flexible mesh model domain for the Atlantic west coast.
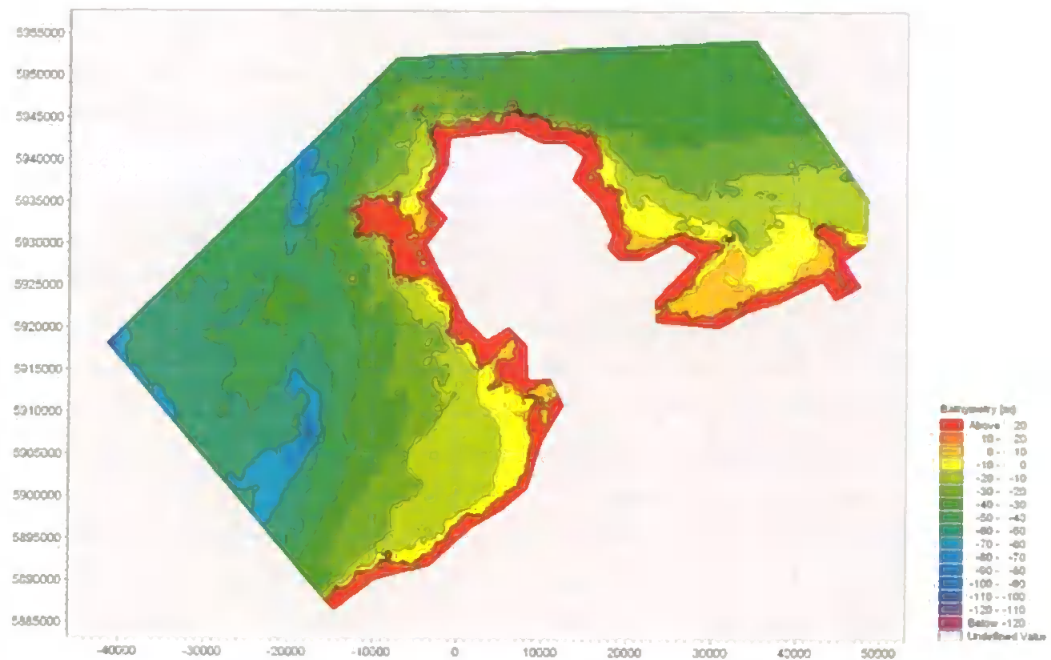
Figure 2.16 – Example interpolated bathymetry for the Irish Sea and Liverpool Bay model domain.

estimated from available wave buoy deployments in the region) are inputted. On each side of the open boundary, lateral boundaries are specified where a one-dimensional calculation of the basic equations is solved along the boundary line. The information of the incoming waves in the start point and the end point of the line are obtained from the connected boundary lines. Finally the land boundary is regarded as a closed boundary, where there is no wave transmission and all waves are fully absorbed. Wave breaking and bottom friction are the two key calibration factors within the model. For wave breaking the default values for α (rate of energy dissipation after breaking) and γ (amount of depth-related breaking) were used as the initial settings (Battjes and Janssen, 1978). A calibrated value for bed roughness (Nikuradse roughness, k_N) of 0.01 m was applied uniformly across the model domain; this value is commonly used in literature for sandy beds (Martinelli et al., 2006). Finally, the model was run with a fixed water level to simulate mean sea level and within the spectral discretisation the directional sector 0°–360° was resolved into 16 directions. Figure 2.17 illustrates examples of four model runs.

Model validation

The wave model results using MIKE21 were validated for the Atlantic west coast and South coast model domain against recorded nearshore wave data from the directional waverider buoys at Perranporth (west coast) and Penzance Bay (southwest coast) respectively. Model results for the Lyme Bay model domain were validated against the only available wave data in that region from a Rosemount WaveRadar Rex, located on Teignmouth Pier covering the period March 2008 to Present. The latter only afforded a general wave climate comparison due to the mismatch between the observed record date and the more shoreward location of the WaveRadar compared to the model output node. The resultant calibrated value for bottom friction was applied to all domains, including the Irish Sea and Liverpool Bay domains, even though no near-shore wave data was available for model verification. Table 2.2 shows annual wave statistics for both measured and modelled data for each of the calibration sites using $k_N = 0.01$ m constant in domain.

A comparison between modelled and, measured values for $H_{s10\%}$ and $H_{s50\%}$ at all sites in Table 2.2 show a satisfactory skill when applied to both open (Perranporth) and sheltered (Penzance Bay and Teignmouth) locations with the largest difference being an under prediction of 17% occurring in $H_{s50\%}$ at Perranporth. In both co-located data sets
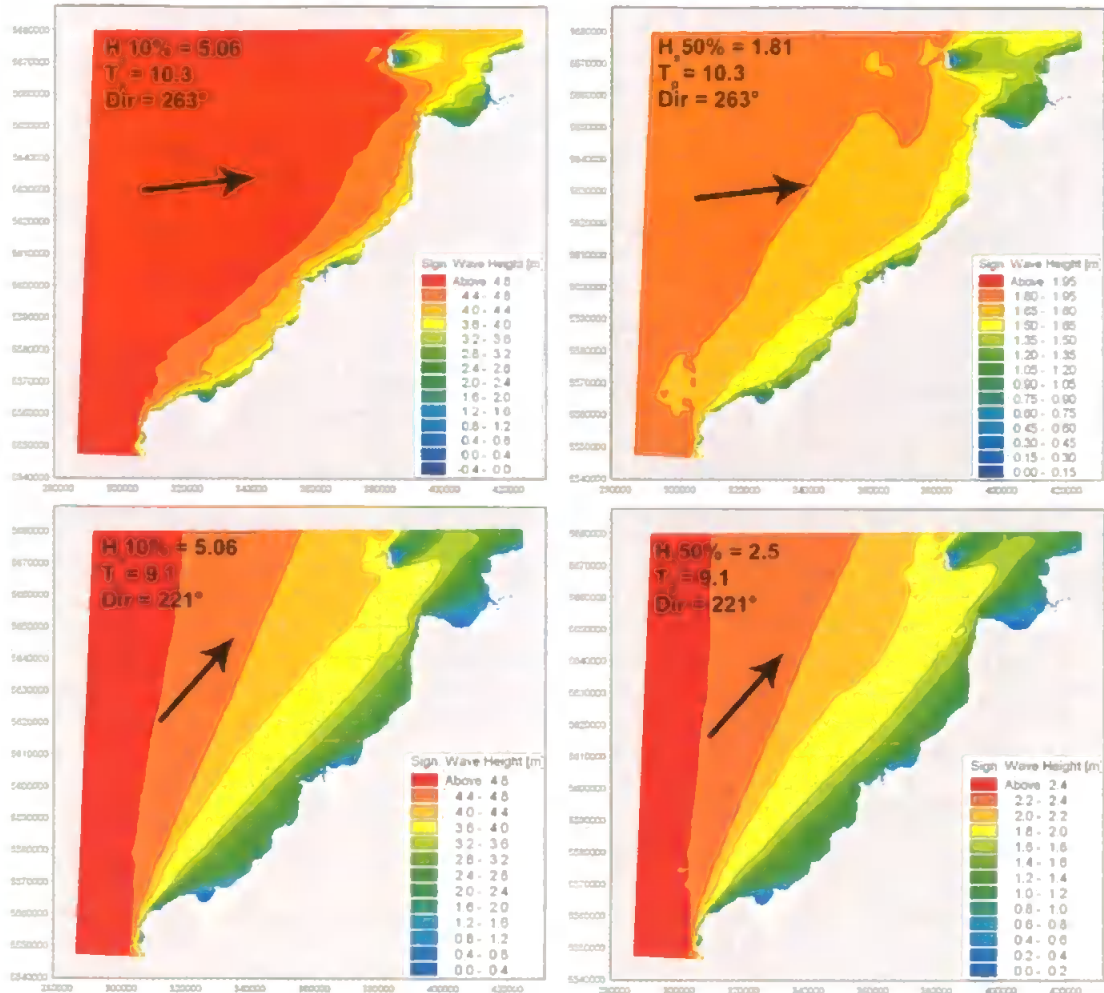
Figure 2.17 – Example of four model runs for the Atlantic west coast representing the $H_{s,10\%}$ and $H_{s,50\%}$ exceedence levels (left to right) for both west and southwest swell directions (top to bottom).

(Perranporth and Penzance) values for peak wave period T_p are reasonably predicted with an over prediction of 17% at Penzance, possibly due to the value for bottom friction being too high to represent the fine sediments of Penzance Bay leading to an increase in T_p and reduction in H_s. In sheltered cases values for T_m are over estimated, up to 93% at Penzance Bay and this may be attributed to local wind fields not being included in the model. In these regions with a mixed wind/swell wave climate only the swell component is represented in the model. In the Lyme Bay region this effect is partially resolved by driving the model using a UKMO model node from within the sheltered region where a bi-directional wind/swell wave spectrum allows for an improved separation of the wind (easterly) and swell (westerly) components. Fortunately for all wind dominated mixed wind/swell beach locations outside of Lyme

Table 2.2 – Final measured and modelled values for; 10% and 50% exceedence significant wave height; and peak and mean wave period for selected calibration sites.

Data source	Data type	$H_{s10\%}$ (annual)	$H_{s50\%}$ (annual)	T_p (annual)	T_m (annual)
Atlantic west coast model – Perranporth	model	3.58	1.30	10.0	8.3
Perranporth nearshore wave buoy	measured	3.45	1.57	11.4	6.2
South coast model - Penzance	model	1.29	0.47	10.0	8.3
Penzance wave buoy	measured	1.23	0.48	8.5	4.3
Lyme Bay model - Teignmouth	model	1.14	0.50	7.4	6.2
Teignmouth wave recorder	measured	1.05	0.45	9.1	3.7

Bay, measured wave buoy data was available. Model predictions for exposed swell dominated coasts were deemed satisfactory for nearshore wave climate estimation.

2.5.3.2 Resultant nearshore wave climate

Combining transformed wave model data and measured nearshore buoy data, an approximation of the nearshore wave conditions (proxy to breaker height) were obtained for all beach study sites within each region. In cases where a beach location is considered equidistant between two wave buoy locations, a linear interpolation was made between the two resultant annual wave records. Appendix 1 contains calculated nearshore integrated wave parameters for all beach sites.

2.6 SUMMARY

Within the study a wide range of hydrodynamic and morphodynamic data were collected and analysed using an array of techniques, in many cases generating novel and expansive datasets new to the UK environment. The analysis, evaluation and synthesis of these data enabled new insights into UK beach morphodynamics, associated hazards and characteristics of risk to the beach user. These form the basis of the subsequent chapters.

3. BEACH RESCUE STATISTICS, NEARSHORE MORPHOLOGY AND HAZARDS: A CASE STUDY FOR SOUTHWEST ENGLAND

3.1 INTRODUCTION

As alluded to in Chapter 1, due to its location and geologic setting, the UK possesses a very broad spectrum of beach environments around its more than 5,000-km long shoreline. This provides an important public amenity that attracts visitors throughout the year. However, the beach environment is inherently hazardous and exposes people to risk and to understand and manage this risk, a comprehensive understanding of UK beach environments and their associated hazards is needed. A lifeguard service is a response to these risks posed within the beach environment, and aims to protect and educate the beach user. To best perform this task a comprehensive knowledge of site-specific physical beach hazards, hence beach morphodynamics, is needed.

Beach hazards in this study represent any phenomena that place the beach user at risk, henceforth termed the 'insea' beach user, of harm through interaction with the shoreline and surf zone. These bathing hazards are related to beach morphology and nearshore hydrodynamics and their definitions are in line with those investigated in studies relating to beach safety in Australia (Short and Hogan, 1994) and the US (Lushine, 1991; Lascody, 1998) (see Section 1.3.4.2). The character and combined severity of these bathing hazards can vary spatially in the alongshore between regions of high and low hazard, and also in the cross-shore between high and low tide (potentially significant on macrotidal beaches). The nature of this spatio-temporal variation in bathing hazard within a specified region is hereon in referred to as the 'temporal hazard signature' describing the instantaneous distribution of type and severity of hazard along the shoreline of interest. The temporal hazard signature may vary throughout a range of timescales from incident waves to decades. This chapter addresses the annual spatial (between beach) variation in bathing hazard throughout the southwest region of England. Chapter 5 addresses the sub-seasonal variation of the temporal hazard signature in this region.

This chapter focuses on the coasts of Devon and Cornwall in the southwest of England. This region, as well as being a popular tourist destination during the spring/summer months with over 20 million visitors in 2005 (Devon County Council, 2006) exhibits a broad range of tide, wave and sedimentological environments. On western coasts 10% exceedence wave heights ($H_{s,10\%}$) reach 2.5 to 3 m (Draper, 1991) and MSR ranges from 4.2 to 8.6 m (Admiralty, 2005). This wave climate is characterised by a mixture of Atlantic swell and locally generated wind waves. The spectrum of beach environments and the location of the majority of RNLI patrol units within the region mean it is ideally suited as a study area for this project and provides the setting for Chapters 3, 5 and 6.

This specific aims of this chapter are:

- to improve understanding of the spatial variation in beach systems (morphology, hydrodynamics and sediments) and beach hazards in Devon and Cornwall (and by proxy the UK);

- to quantify the various environmental hazard types within the recorded incident record for 2005;

- to make a preliminary assessment of the level of association between hazard and beach type within the regions patrolled beaches;

- to draw comparisons between the investigated beach environments and those that have been the subject of previous related research.

The outputs of this investigation form the baseline rational for the subsequent investigations documented in the following chapters.

3.1.1 Lifeguarding in the UK

Surf life saving began in Australia in the early 1900s as a response to the increase in drowning events, partly due to the growth in coastal urban populations and an interest in swimming in the sea. Starting as a group of local residents rescuing people from the sea, over the years the beach lifeguard service provision has became a more professional operation. In the UK, beach lifeguard services first began in 1955 when the Surf Life Saving Association of Great Britain was formed (SLSGB) as volunteer clubs began to patrol beaches in Bude and St Agnes in Cornwall and Brighton on the south coast of England. At present, the RNLI represents the contemporary face of beach lifeguarding, providing well-equipped and highly-trained services to beaches around the UK. The RNLI Lifeguards, a sub-division of the established RNLI Lifeboats founded in 1824, began
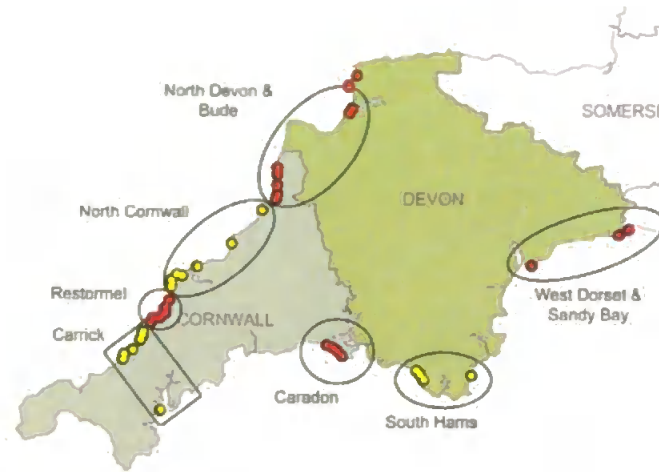
Figure 3.1 – Map of the southwest peninsula indicating the location of RNLI beach patrols, and their associated regions, in operation within the southwest region during the period of the study in 2005.

providing beach lifeguard services within the UK in 2001 with 37 beaches. By 2005, when the data for this study were collected, the RNLI lifeguarding services had expanded to include 62 beaches throughout south and southwest England (Figure 3.1). In 2009, the RNLI has expanded around the UK providing services to 141 beaches throughout Wales and the east, northeast, south and southwest of England. They respond to more than 9,000 incidents per year and since its inception in 2001 the service has assisted a total of 68,658 people and saved 367 lives (RNLI, 2009). The RNLI's vision is to be recognised universally as the most effective, innovative and dependable lifeboat and lifeguard service, existing to save lives at sea. To this end, their commitment to funding work to improve the core understanding of the physical environment they are working in and the hazards it presents, indicates their belief that a strong scientific base is essential in expanding and improving their service.

3.1.2 Beach classification and safety management

The merging of lifeguarding and the physical sciences is not new. As detailed in Section 1.4.3, Australian studies have associated physical hazards with beach state and temporal variation in environmental conditions leading to the development of the Australian Beach Safety And Management Program (ABSAMP), aimed at improving safety services for Australian beaches (Short, 1993; Short, 2001). Introducing the concept of beach morphodynamics to physical bathing hazards enabled an improved understanding of the variability of hazard with beach state, which in turn led to methods of hazard assessment

for vast swathes of the Australian coastline and the collection of physical beach data, led by Short (1998) of the Coastal Studies Unit, University of Sydney, for every beach throughout the entire coastline of the nation (Short, 1993; Short and Hogan, 1994; Short and McLeod, 1998; Short, 1999; Short, 2001).

This union was based largely on conceptual models of beach state and its dynamic transition under varying hydrodynamic and morphological conditions, developed in the late 1970's and early 1980's. The culmination of this pioneering work on modelling beach morphodynamic states was represented by the seminal and widely cited paper of Wright and Short (1984) in Australia who developed a beach classification model for microtidal, wave-dominated coasts using the dimensionless fall velocity (Ω) shown in Equation 1.2. This was further extended by Masselink and Short (1993) to include meso/macrotidal environments by defining an additional dimensionless parameter, the relative tidal range (*RTR*) shown in Equation 1.3 (for detailed review see section 1.4.1). Incorporating both morphological and hydrodynamic factors, a sequence of characteristic beach morphologies can be identified on the basis of Ω and *RTR*, leading to the identification of distinct morphodynamic states. It is the understanding of these states that was central to the early work on association of beach hazards and beach type (Short, 1993; Short and Hogan, 1994; Short, 1999; Short, 2001). Chapter 1 provided a summary of the hazard rating matrix produced by Short and Hogan (1994) whereby identified beach types, within the continuum of reflective to dissipative surf zone regimes, were allocated generic hazard ratings dependant on the prevailing wave conditions. In general, hazard levels increased from reflective to dissipative beach types, and from low to high wave conditions. Some attempt was made to incorporate tide-modified and tide-dominated beaches, based on those occurring around the Australian coast. Specifically, it was acknowledged that levels of hazard can vary from low- to high-tide within a macrotidal environment.

3.2 STUDY SITE: SOUTHWEST ENGLAND

3.2.1 Introduction

Regardless of the importance of its beaches to the local and regional economy and the fact that the majority of the RNLI lifeguard patrols are located within it, as a study site, the region of Devon and Cornwall, within the southwest of England, provides a valuable insight into the geomorphology of the UK coast. As a region, it possesses a wide spectrum

Figure 3.2 – Photographs illustrating the coastal diversity within the study region: A) Sennen Cove, West Cornwall (sand only); B) Seaton beach, East Devon (mixed sand/gravel); and C) Spekes Mill Mouth, West Devon (gravel/boulder, shore platform).

of beach environments both in terms of wave height, tide range and sediment size/abundance, as well as contrasting coastal geomorphology (Figure 3.2). What follows in this section is a brief review of the geologic and sedimentary characteristics of the region, both onshore and offshore, followed by a summary of the spatial distribution of the beaches within the region in association with their sedimentology and backshore morphology and

some indication of the regional hydrologic and hydrodynamic character. Geographical locations for location names referred to in the text can be viewed in Figure 3.3.

3.2.2 Coastal geomorphology

Due to Holocene sea-level rise and the downward movement of the coastline of southern Britain (see Section 1.3.1 for more details), the south-west peninsula is a drowned landscape. The majority of the coast from Start Point on the South Devon coast to Porlock in the Bristol Channel to the north is composed of hard Devonian and Carboniferous rocks with no cover of glacial material. Headlands are derived from harder sediments, geological structure and volcanic rocks. In combination with drift filled river valleys, that are drowned (or partially drowned) in their lower reaches, the observed highly indented coastline can be explained by regions composed of sedimentary rock that show a marked variability in hardness (lower Devonian and Culm measures). This, combined with the large number of complex sills and dykes as well as many minor faults, drive the present physiology of the coast creating the headlands and bays apparent around the entire coastline (Futurecoast, 2002).

3.2.2.1 South Coast overview

The south coast, specifically the region between Start Point in the east and Lands End in the west, is a highly indented coastline dominated by small embayed coves often within larger scale headland controlled bays. On a regional scale, the intersection of numerous rias of varying sizes (of which the Fal, Helford, Tamar, Erme and Yealm are good examples) along this coastal stretch characterises the complexity of the coastal planform that has been little affected by any of the Pleistocene glaciations and shows an absence of glacial deposits along the coasts. The presence of long intermittent exposures of raised beaches and head deposits have been suggested as a potential sediment source along this coast and the continued presence of these deposits indicates the lack of coastal erosion during the Holocene (c.10, 000 years BP). In many places these head and raised beach deposits sit on a fossil beach platform c. 2 to 5 m ODN in front of rock cliffs.

Further east, stretching from Start point to Portland Bill, the coastline has been retreating, eroding and changing orientation over the last millennia in response to sea level fluctuations, dominated by the inundation of the English Channel associated with marine transgression throughout the Holocene (Keen, 1998). This region is broadly defined by the
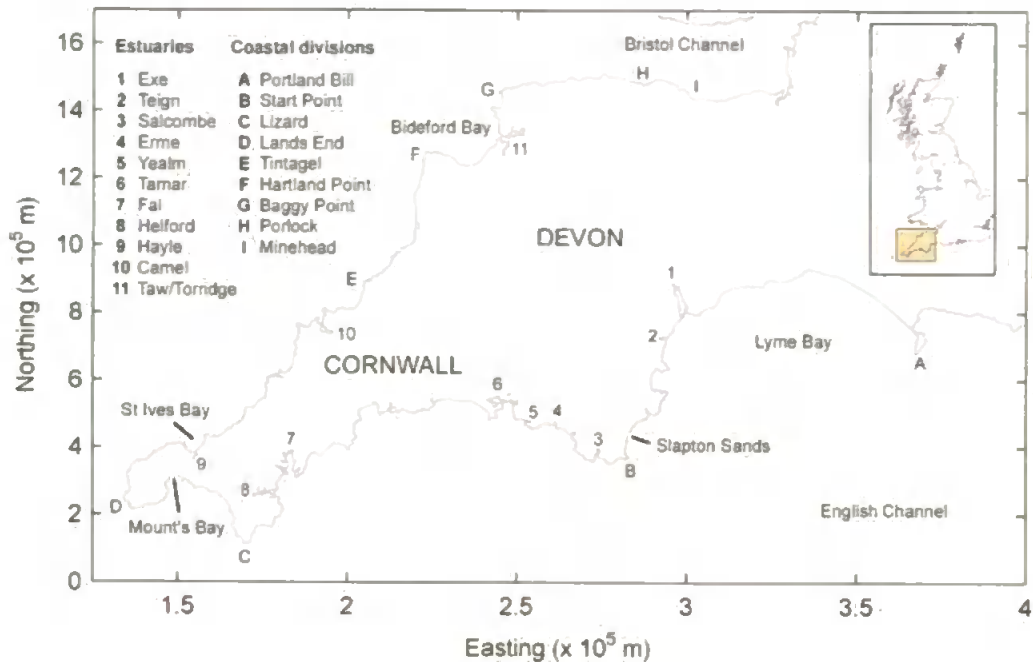
Figure 3.3 – Map indicating geographical locations of features relating to the coastal system of Devon and Cornwall. Estuaries, coastal division and bays only represent those referred to in the text.

large, shallow embayment of Lyme Bay to the east, associated with a sequence of Permo-Triassic and Jurassic strata to Portland Bill, and a region to the south of the Teign estuary that is defined by a succession of smaller, headland embayments. This stretch of coast is dominated by cliffs, rocky platforms and mostly coarse clastic beaches. The only exceptions are the two major estuaries (Exe and Teign), where banks, bars and shoals have accumulated both landward and seaward of estuary mouths (SOCPAC, 2004). The only stretches of coastline where geological structure and lithology are not controlling the coastal morphology are where gravel barrier beaches have been driven shorewards through rising sea-level. Slapton Sands, between Torcross and Strete provides a classic example. It has been suggested that prior to the Holocene transgression, when sea levels were 100–120 m below present, a prototype continuous 'super' barrier between Portland Bill and Start Point may have been present (Hails, 1975; Morey, 1983; SDADCAG, 2009).
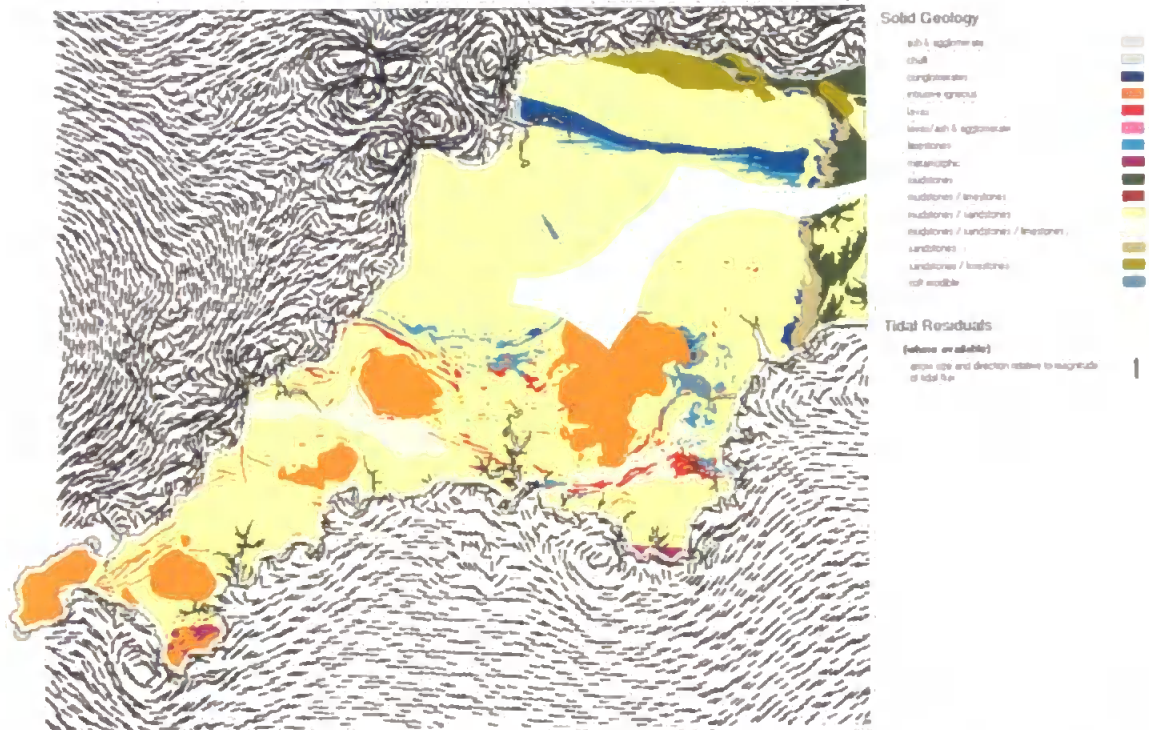
Figure 3.4 – Vector plot of mean tidal residuals around the southwest peninsula and onshore solid geological characteristics, from Futurecoast (2002).

3.2.2.2 North Coast Overview

The north coast of the southwest region can be divided into four different sections based on the solid rock lithology illustrated in Figure 3.4. The stretch from the most southern point at Lands End to St Ives Bay is composed of granite throughout, followed by the silty and sandy slates, mudstones, sandstones with lower order igneous and limestone sections up to the promontory of Boscastle near Tintagel. Subsequently, moving northward, the section extending to the headland of Baggy Point (associated with Croyde Bay, North Devon) is dominated by Carboniferous mudstones and sandstones, moving up the Bristol channel into Devonian slates, sandstones with mudstones, mudstones with siltstones, and thin limestones reaching Minehead (Steers, 1946; Keene, 1996; Futurecoast, 2002). The regional variations in lithology described above determine the form of the coast, with the massive jointed granite coast around Land's End having a different form from the steeper cliffed coast of sandstone and slate south of Hartland Point. The detailed form of the coast is commonly the result of the local joint and fault patterns (the coastline around Tintagel being a good example) (Wilson, 1971).

3.2.2.3 Drainage

On a regional scale this cliffed form is broken only by occasional river valleys. Along the south coast of Devon and Cornwall, the lower courses of these valleys have been inundated by the sea to form rias (e.g. the Fal estuary). The north coast, well known for its high steep-cliffed, high-energy coastline, only provides shelter through a handful of estuarine systems (e.g. Hayle, Camel and Taw/Torridge estuaries) that are also, in many cases, associated with regions of higher sediment abundance. More locally, drainage networks within the region (Figure 3.5), both cutting across the geological trend and following the faulting and joint trends (north coast granite regions) have a significant role in coastal geomorphology, especially beach morphology, as rivers and streams flow out over and through the beach sediment accumulations at the drowned lower reaches of drainage systems and indented bays. This has implications from the event to seasonal temporal scale for the hydraulic characteristics of the beach and hence its morphodynamic response.

3.2.2.4 Sediments

The southwest peninsula lay at the southern limit of the main Pleistocene ice sheets. Late Devensian ice sheets extended to the Isles of Scilly and apart from deposits of large erratic boulders on the modern coast by ice sheets or icebergs during the Pleistocene, glacial sediments are largely absent from the sea bed within the offshore regions. This has led to the presence of only a thin covering of Holocene sediment and for many kilometres off the coast, typically only a metre deep. Thicker accumulations of sediment are found within some bays (e.g. Mount's Bay). Some estuaries have sand bars at their entrance (e.g. Salcombe and Yealm) but other estuaries (Helford) display no such bar. Most of the region underwent a prolonged period of deep weathering through the Tertiary and Pleistocene, the products of which were not removed by subsequent glacial erosion. The weathering of granites leads to the release of quartzitic sands that were washed onto the continental shelf and provided a sediment source for the region's beaches. Because of the resistant nature of the bedrock forming the coast, natural recession, and hence locally derived sources of sediment, is negligible. The shallow inshore rock platform typical of areas around Britain formed of softer rocks, is very narrow or absent within the southwest region. Measurable coastal retreat is found very locally where unconsolidated Quaternary sediments are subject to marine erosion. The nearshore zone off the south coast of Devon is largely comprised of thin gravel sediment with a more sandy nature at increased depth. This has a carbonate content of between 25 to 50%, decreasing eastwards. On the north Cornwall coast sandy
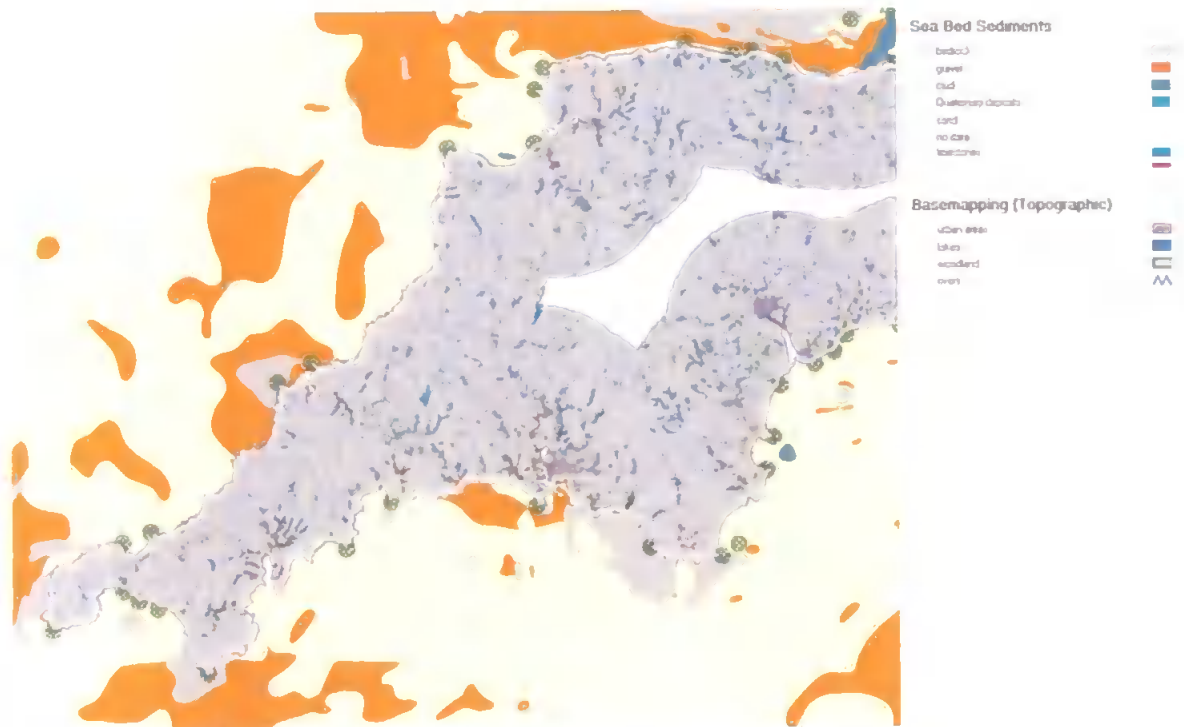
Figure 3.5 – Offshore seabed sediments and onshore hydrological characteristics for the southwest peninsula, from Futurecoast (2002).

gravel and gravely sand predominate throughout with a carbonate content commonly reaching 75%. Early effects of human influence of sediment supply were seen when substantial volumes of sand and mud were contributed to the coastal system through the extensive mining for tin and china clay in the 19th and 20th centuries. Subsequent cessation over recent decades has led to beach sediment depletion on some locations. Apart from some of the beaches and seafront associated with the bays and estuaries of Lyme Bay (e.g. Torbay, Teignmouth and Exmouth), there are relatively low levels of large-scale coastal defence/protection when compared to other parts of Britain, but human influences in this regard have been apparent in the region from the mid/late 19th century to protect the urban development and infrastructure related to tourist amenities and resources. Other human influences within the region include removal of beach sediment for engineering projects and dredging of navigation channels.

3.2.2.5 Offshore processes and bathymetry

From Start Point in the southeast, through Land's End to Hartland Point in the northwest, the coast is open and exposed to Atlantic wave energy. This region is affected by stronger wave action than any other part of southern Britain. The sea bed falls steeply away from the

coast and water depths in excess of 50 m are reached within a few kilometres of shore around most of the coast. At depths of 50 to 70 m the seabed flattens, continuing to the inner continental shelf. Tidal currents in the area are generally less than 0.75 ms^{-1} off the north Cornwall coast and less than 0.5 ms^{-1} off the southern coast of the peninsula (Futurecoast, 2002). They increase close to the headlands, exceeding 1.5 ms^{-1} off Land's End, and locally at estuary mouths (e.g. Exe and Teign) where maximum spring ebb current velocities can exceed 3.0 ms^{-1} (Duvivier, 1998; SDADCAG, 2009). The tidal residual flows deduced by Pingree and Griffiths (1979) from numerical modelling suggest the only areas of significant, although generally weak, net sand transport were to the northwest along the north Cornwall coast and to the east along the east Devon coast (east of the Teign) (Figure 3.4). In the context of its effect on coastal geomorphology, the tidal control on sand transport is weak and regionally uncertain, with the volumes of sand involved being less than that of other parts of the English coast. Wave induced currents are more important in controlling sediment movement. This motion is largely derived from the west and southwest components of the wave climate composed of fetch-unlimited swell and local short-fetch waves driven by prevailing winds from the south and west. Although less frequent winds with an easterly component can produce significant movement of sediment in south coast regions. Storm events can drive sediment movement on the inner shelf but the effects are greatest in shallower nearshore zone.

3.2.3 Beaches of Devon and Cornwall

To obtain an overview of all the beach systems in Devon and Cornwall, an inventory of all beaches >50 m in length was established. A combination of topographic and geological maps, site visits, web material including online environmental GIS databases (Defra, 2006) and geo-referenced aerial imagery, was used for assessment of beach geometries, sediment types, physical beach characteristics and associated estimates and predictions of the local mean tide/wave conditions. Each beach was assessed in terms of wave/tide conditions, sediment texture, and coastal setting, geometry, structures and backshore geomorphology.

The total number of beaches >50 m in length is 690. Of these, 204 (30% by number) possess predominantly sandy inter-tidal zones, of which 59 (9% by number) have an upper beach composed of gravel/boulder sediments (Table 3.1; Figure 3.6). Spatially, these sand-dominated beach forms are well distributed throughout the entire coastline with the exception of east Devon (east of the Exe), the Bristol Channel coast and the southern

Table 3.1 – Geological and structural statistics of beach groups represented in Figure 3.6 (modified group is not exclusive and represents beaches modified by engineering structures).

High-water	Inter-tidal	Number (n)		Area (m²)		Length (m)		Width (m)
		total	%	mean	%	mean	%	mean
Gravel / boulder	Sand	59	9	116000	14	600	11	150
Sand	Sand	145	21	155500	47	600	28	200
Gravel / boulder	Gravel / boulder	135	20	35000	10	450	21	50
Beach	Rock	253	37	25000	13	200	15	50
Other		98	13	29100	16	300	25	72
Modified		151	23	140011	45	700	37	150

stretch of Bideford Bay (Hartland Point to Westward Ho!). But those beaches entirely dominated by sand (upper and inter-tidal) are more prevalent on the west facing coasts of Devon and especially Cornwall. With average widths of 200 m, these beaches represent an important economic resource of the region as they attract the largest number of visitors representing 45% of the entire region's beach area (at mean spring low tide). In contrast, beaches with gravel/boulder sediments throughout are on average only 50 m in width and represent 20% by number of the region's beaches ($n = 135$) but only 10% by inter-tidal area.

Due to the limited sediment supply to much of the coast and its geomorphological history, the presence of shore platforms and inter-tidal rock outcropping is not uncommon. This is confounded by the observation that 37% of all beaches by number ($n = 253$) possess some form of inter-tidal rock formation, which were on average, associated with beaches 50 m wide. A survey of coastal geomorphology (Table 3.2) showed that the majority of these beaches were associated with shore platforms ($n = 240$). It is also worth noting that 11% (by number) of beaches are submerged at high water. These beaches are found in cliff-backed regions and can drive the segmentation of beaches into a number inaccessible coves during the upper limit of the tide. This can be a significant source of hazard and will be discussed in detail later in the chapter.

The prevailing hydrodynamic regime varies in its level of wave and tidal energy constituents. Figure 3.7 illustrates the estimated hydrodynamic character for each beach
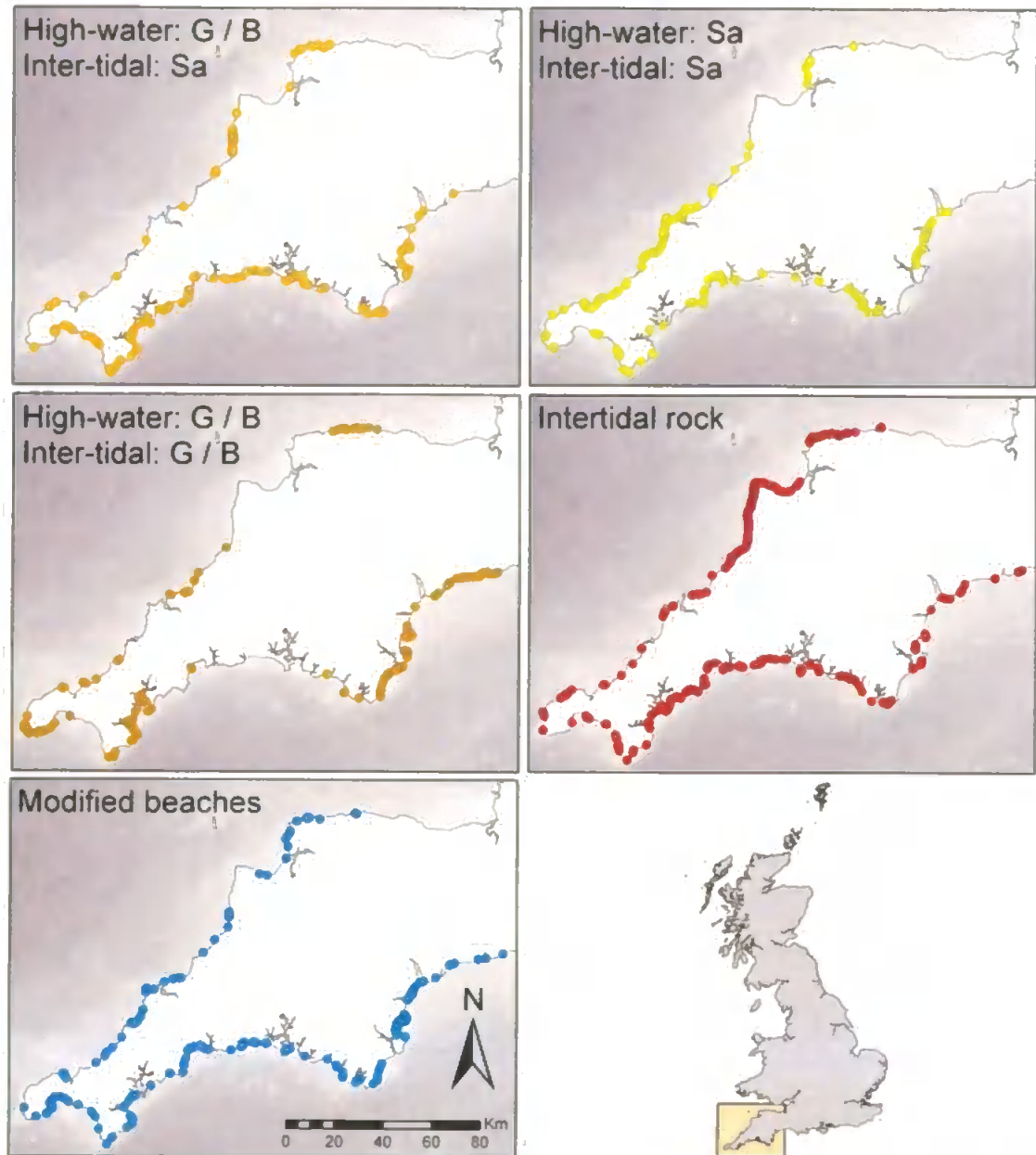
Figure 3.6 – Plots display range of beach sediment types and their distribution around Devon and Cornwall. Sediment categories represent a selection of the total. G = Gravel; B = Boulders; Sa = Sand; and Modified beaches are those that have being anthropogenically altered by hard engineering structures including: groynes; breakwaters; piers; seawalls; harbours; and jetties.

Table 3.2 – Coastal morphology and hydrodynamics associated with the beaches of Devon and Cornwall. Beach database combined with coastal classification from Masselink (2004).

Morphology	Beaches num	Beaches %	Low-cliff	High-cliff	Dunes	Beach length avg (m)	Beach length sum (km)	Beach length %	Beach width avg (m)	H$_{s50\%}$ avg (m)	H$_{s10\%}$ avg (m)	MSR avg (m)
Barrier beach	16	2.4	5	3	12	1497	24	8.1	184	0.8	1.6	4.9
Mainland beach	229	35	30	163	19	630	143.1	48.6	124	0.7	1.5	5.3
Tidal flat + beach	4	0.6	0	0	1	325	1.3	0.4	263	0.7	1.4	6.5
Shore platform + beach	240	36.7	25	181	4	374	88.9	30.2	129	0.9	1.7	5.9
Cove (with bench)	93	14.2	4	76	0	225	20.9	7.1	82	0.5	1.2	4.9
Low cliffs + sub-beach	7	1.1	0	0	0	371	2.6	0.9	86	0.7	1.5	4.9
High cliffs + sub-beach	65	9.9	0	0	1	215	13.8	4.7	70	0.9	1.7	5.7

derived from NOAA's WaveWatch III 3G model output for each region identified. 50% exceedence significant wave height clearly indicate the effect of exposure to the Atlantic on the west coast with values of up to 1.5 m decreasing along the south coast moving east until reaching Lyme Bay, where very little westerly swell reaches the beaches that are largely dominated by southern and eastern wind wave events. A similar situation occurs within the Bristol Channel where increased shelter from the predominant westerly swell reduces 50% exceedance significant wave heights to below 0.9 m. These wave energy variations occur alongside a marked variation in mean spring tidal range, which is at its peak in the mega-tidal Bristol Channel beaches (>9 m) reducing sharply southward to the southern limit of the west coast (~ 5.4 m). Eastwards along the southern coasts the reduction continues at a reduced gradient to 3.7 m in the far southeast of Devon.

The combination of hydrodynamic regime and sediment distribution plays a significant role in the spatial distribution of beach width characteristics, which can be seen in Figure 3.8. It is clear that the region's macrotidal high-energy west coast beaches with a sufficient supply of sandy quartzite and carbonate material are the the regions widest beaches (>150 m) representing 15.8% of all beaches. These wide inter-tidal zones are significant, both because of their increased beach user carrying capacity and their rates of horizontal shoreline translation. It is also noted that the region's widest beaches (>300 m) are predominantly located in proximity to estuaries and regions of abundant finer sandy sediments. The majority of narrow beaches (<50 m) are largely confined to meso-/macrotidal south coast and are associated with coarser sediments and shore platforms.
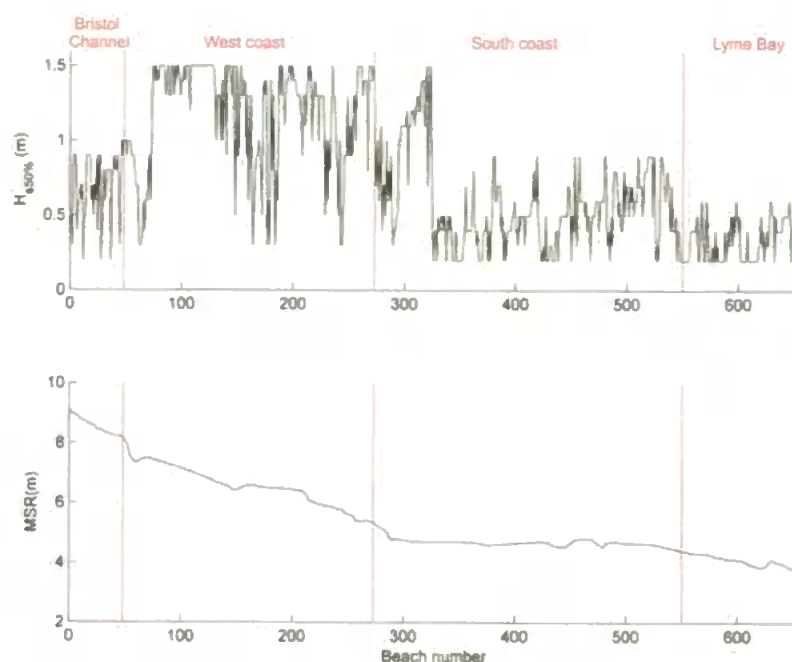
Figure 3.7 – 50% exceedence wave height (calculated from a simple linear regression model relating the effect of wave exposure to modelled offshore/nearshore wave heights in the region and applied to modelled offshore waves from the period 2003 - 2008), and mean spring tidal range (linear interpolation between standard and secondary ports around the coast) for all beaches in Devon and Cornwall (Admiralty, 2005). Beach number represents 'along-coast' beach sequence and red line separate coastal regions of interest.

The sandy and mixed sediment mainland beaches and beaches with shore platforms account for 72% of all beaches around the region. It is the aesthetic and practical attraction (access, infrastructure and scale) of these beaches, often spectacularly backed by high cliffs (73% > 20 m high) and dune systems (5%), which draw the largest visitor numbers during the summer season. Hence, these beaches are seen as having high economic importance to the region. Due to this, in an attempt to manage risk posed to the beach user within the beach environment, the RNLI lifeguard patrol units are often associated with these types of beaches.

3.3 METHODOLOGY

Data collection consisted of two main phases: 1) the collection of RNLI lifeguard incident records and daily logs for the 2005 patrol season at all locations within the southwest region; and 2) collection of associated beach morphological, sedimentary and hydrodynamic data to enable a physical characterization of beaches and hazards. An
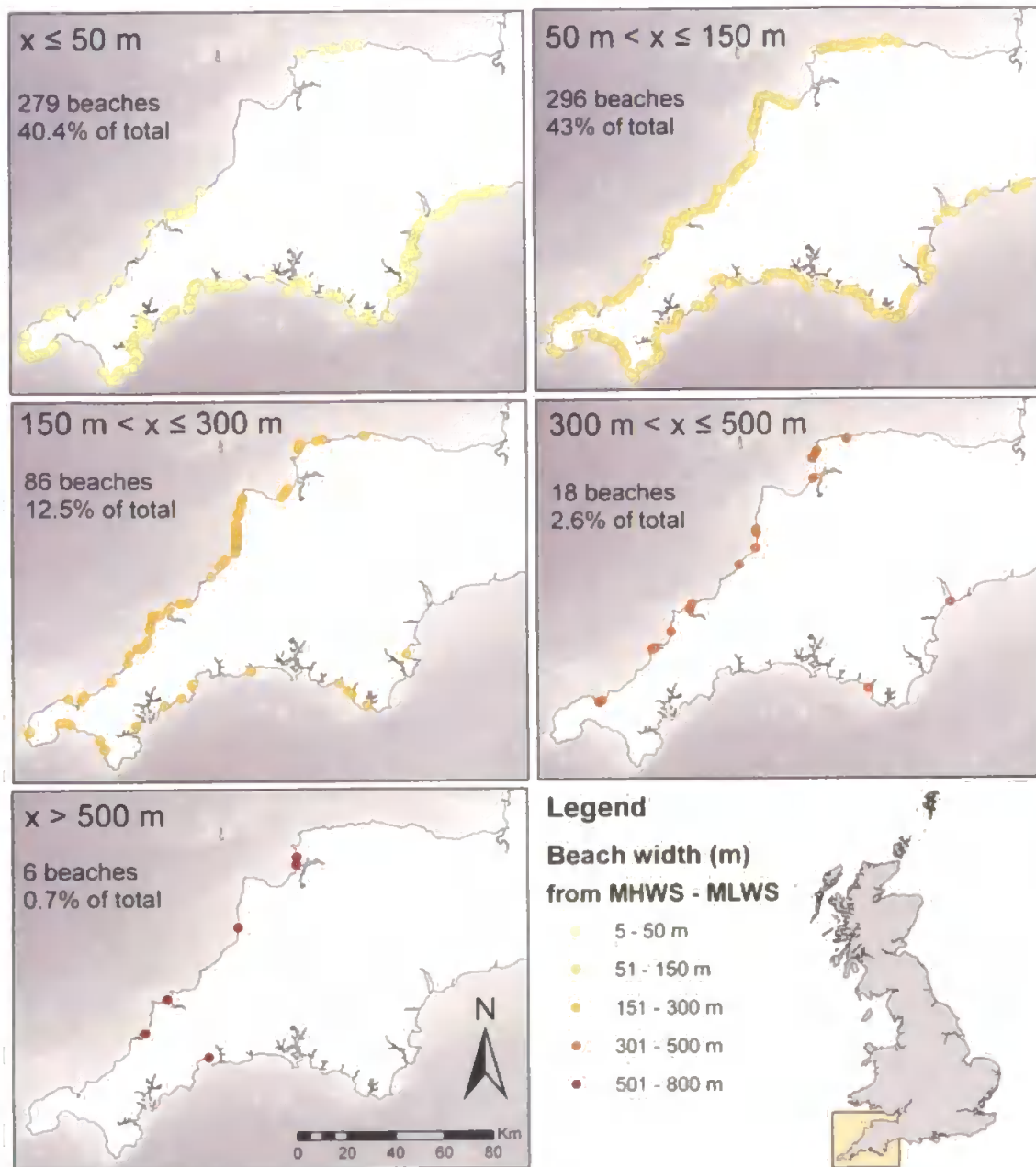
Figure 3.8 – Plots display the range of beach width and their spatial distribution within Devon and Cornwall.

overview of hydrodynamic conditions throughout the region was obtained both through visual observations of wave breaker heights recorded hourly by the RNLI lifeguards, use of statistical wave conditions from Draper (1991) and predicted tidal information from the Admiralty (2005).

3.3.1 Beach hazards: RNLI data

This study uses RNLI incident statistics and logs of observed daily conditions collected for 62 locations within the southwest of England for the 2005 patrol season (1st May to 1st October). This is a comprehensive dataset that was collected by the lifeguards through the use of incident forms and daily logs.

3.3.1.1 Incident data

RNLI lifeguards log number of people and the environmental cause for every incident that they attend throughout the patrol season. This information was used in this study to indicate the nature of the hazards affecting the insea beach user during the 2005 patrol season. Each incident recorded is associated with an event containing one or more individuals that required RNLI lifeguard assistance beyond solely preventative actions and incorporates details of the number of people assisted. Termed the environmental cause of incident, the main physical (morphological/hydrodynamic) drivers to be associated with the assist/rescue were assessed by the lifeguards involved and categorised into specific physical hazards.

- Rip currents: incident caused in part by the potential to transport the insea beach user through the rip current surf zone circulation and associated seaward-directed current flow to deeper water and hence a region of increased hazard.
- Littoral currents: alongshore current hazard, causing the relocation of the insea beach user parallel to the shoreline. This is often associated with a rip current hazard as rip current hazard levels are commonly variable in the alongshore.
- Estuarine currents: current hazard associated with hydrodynamics of estuaries, inlets and river mouths.
- High seas / heavy surf: high surf zone energy and waves can increase submersion, and disorientation limiting the ability of the insea beach user to escape the region of elevated hazard.
- Surging waves: associated with swash events and surging waves, the rapid lateral movement of the shoreline acts to overpower the beach user either transporting

them seawards to a region of increased hazard, or creating a collision hazard through falling (e.g. on slipway).

- Plunging / dumping waves: responsible for increased submersion, disorientation and seabed collision hazard through more energetic wave breaking.

- Bed return flow: term for any offshore current flow at bed-level that acts to undermine the beach user, increasing susceptibility to submersion and disorientation.

- Strong winds: effect of strong winds through level of visibility, surface transport of floating bather and any craft and effect of wind chill on body temperature.

- Offshore winds: transports floating bather/craft offshore, often to a region of increased hazard.

- Tidal cut-off: modulation of tidal level creates a temporal reduction in beach area and can increase water depth that needs to be passed to reach a region of reduced hazard (dry beach), often associated with headlands and cliff-foot beaches that are submerged at high water.

- Sandbars / sandbanks: beach morphology in the form of sandbars and sandbanks creates a hazard through spatially variable water depth within the inner surf zone.

3.3.1.2 Daily logs

Supplementing the incident report records, all lifeguard units make a series of hourly observations relating to the environmental conditions and visitor population dynamics at the beach. These hourly logs, running between 10:00 – 18:00 hrs for each day for the season (1st May to 1st October in 2005) and for all of the 63 lifeguard patrols, provide a valuable dataset for the assessment of beach user activity and prevailing wave conditions. The beach user count provided a key dataset for this study. The proportion of the population which is interacting with the surf- and nearshore zone is critical in making any comment on relative hazard levels, environmental risk, or incident probability/likelyhood within the beach environment. Beach user numbers represent an estimate through lifeguard observation each hour. The RNLI commissioned an external study to investigate the accuracy of beach user counts across a range of beaches indicating that, on average, beach user counts were accurate to within 10% of the true population. It was suggested that the largest source of error was introduced during the estimations of very large beach populations. This error was suggested to be due to the adoption of different visual estimation techniques when dealing with high, densely populated beaches. Within this investigation, the interest lies in the insea

beach user population estimates (smaller population sizes), providing hourly values for the surf- and nearshore zone population.

Hourly breaking wave heights were also visually estimated by the lifeguards on patrol and were designated one of 5 categories: flat; 1-2 ft; 3–4 ft; 5–6 ft; and >6 ft. Unfortunately, no measured nearshore wave data were available within the region during the study period to validate the observations. The large volume of data collected throughout the season at each beach (~2420 hourly observations per beach) may go some way to reducing the influence of observational error at any particular location, enabling the calculation of more reliable seasonal statistics, although this will have no effect on any systematic error present within and between lifeguard patrols.

3.3.2 Beach environment: morphology, waves and tides

In order to investigate the extent to which identified hazards are associated with nearshore morphology, a campaign of data collection of regional beach morphology was conducted. Twelve beaches were selected to complement the principal research goals (Figure 3.9). The range of beach sites were chosen to represent examples of both key high and low risk beaches, indicated through the assessment of RNLI incident records, as well as those representing examples of the significant spatial morphological variation observed throughout the region.

The morphological assessment of these 12 selected sites involved a combination of 3D beach surveys using an ATV mounted Trimble RTK GPS system conducted during several spring tide cycles from August to September, 2006, enabling the generation of a digital terrain model of each selected beach site. This was combined with sediment sampling, low-tide photographic imagery and time averaged coastal images from an Argus video station (Perranporth only) enabling a comprehensive morphological assessment. The beach survey procedures and techniques, as well as sediment sample strategy, collection techniques and particle size analysis employed have been discussed in Chapter 2.

The assessment of the hydrodynamic climate required both annual mean wave statistics as well as a time series, synchronous with the recorded incident events, associated with the 2005 lifeguard season. Data from Draper (1991) collated numerous measured and shipborne observed wave data from around the UK, defining exceedence wave height
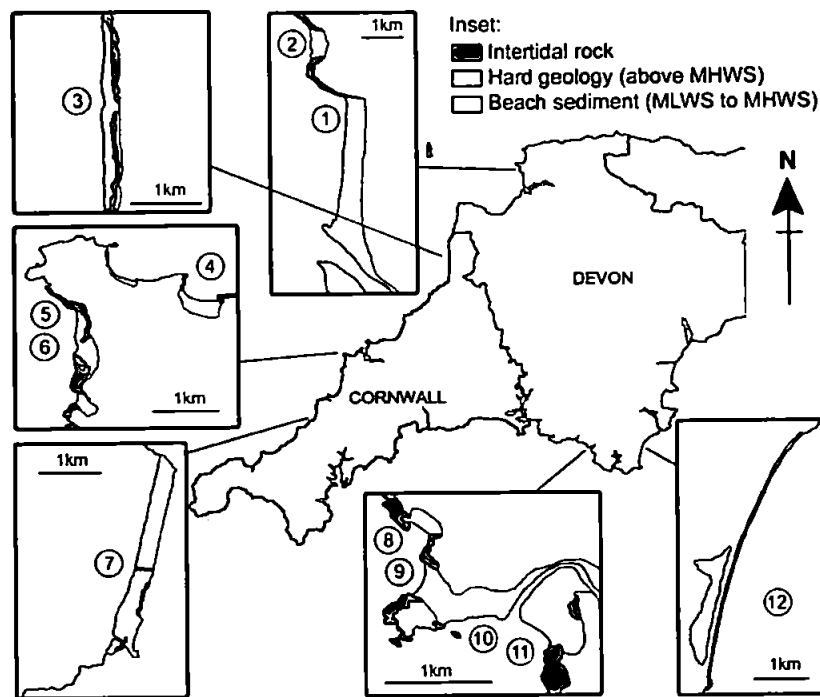
Figure 3.9 – Regional map and schematic plan views of each selected study site indicating beach shape, aspect of the coast and inter-tidal geology

statistics and associated periods for the entire coast of Britain. At the time of the study, these data provided the best available estimate of the general annual offshore wave climate around the southwest peninsula. The requirement for an increased temporal and spatial resolution to assess wave conditions in relation to RNLI incidents meant that the hourly/daily wave height observations recorded in the Daily Log as described above represented the only available dataset and were therefore used to define wave breaker height characteristics for the assessment of hazards.

3.3.3 Beach type: reference to literature

Morphodynamic parameters Ω and RTR (Equations 1.2 & 1.3), associated with the conceptual models of Wright and Short (1984) and Masselink and Short (1993) were used to gain an understanding of the observed beach morphologies and hydrodynamics of the study region as well as to place the systems in the context of previous research.

3.4 RESULTS AND DISCUSSION

3.4.1 Beach population dynamics

Seasonal trends within the records of beach population dynamics throughout the region's 62 RNLI patrolled beaches are illustrated in Figure 10. The average seasonal beach population was significantly correlated ($R^2 = 0.91$; $p < 0.01$) with the insea user population. Throughout the season, including all beaches, the insea user population was 19% of the whole beach population. Figure 3.11 illustrates the spatial variation among the RNLI beaches. This data provided a number of insights into the spatial distribution of insea population numbers throughout the study region:

- The lowest seasonal average for insea population (8 people) coming from Torcross, a reflective gravel beach on the low energy Lyme Bay coast, South Devon.

- Those beaches with a seasonal average of between 15 and 30 people insea occur across the south and north coasts of Devon and Cornwall. The lower insea population at these beaches is often due to a reduction in the accommodation space of the surf zone because the beaches are either embayed and relatively small (<300 m in length), for example Challaborough in South Devon, or submerged at high water creating a significant temporal variation in carrying capacity (surf zones often closed by lifeguards at high-tide in these cases).

- Beaches accommodating > 30 people on average are predominantly located on the west coasts. These beaches are typically longer (> 300 m) with a lower inter-tidal gradient and higher tidal range, resulting in larger inter-tidal and surf zone widths.

- Those with insea populations of between 30 and 50 people where mostly associated with the more rural locations, with limited facilities (e.g. Sandymouth beach and Constantine Bay in North Cornwall). At these popular beaches the limited infrastructure and access controls levels of beach use.

- Increases up to an average of 100 people insea appears to be again related to the size (length and width) of the beach and surf zone, but also the predominance of sandy beaches without significant inter-tidal rock exposures and increasing infrastructural capacity to accommodate large numbers of beach visitors.

- Finally, those beaches with >100 people insea on average were all wide (> 500 m) high-energy Atlantic coast sandy beaches popular for surfing.

97
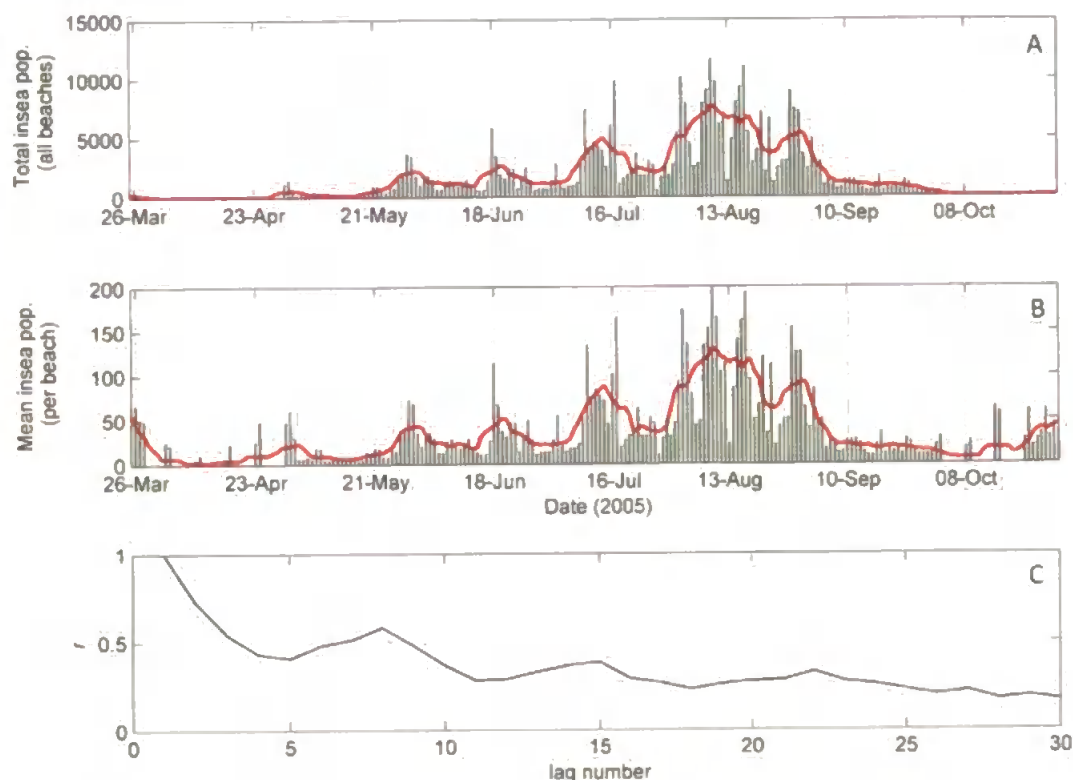
Figure 3.10 – A) seasonal distribution of total insea population per day throughout all RNLI beaches; B) seasonal distribution of mean insea population per beach; and C), the autocorrelation function of mean insea population, for the lags up to 30 days. Red lines represent distributions with 7-day moving average applied in both A and B.

The insea population in this study is a combination of the surfing and bathing populations, but the data suggest there is no significant relationship between the proportion of surfers and the size of the insea population. Although, among the sandy west coast beaches with insea populations >100 people, all are located in proximity to town or localities that cater for large numbers of tourists and are very popular surfing destinations for all abilities (e.g. Perranporth, Polzeath and North Fistral). For these locations the surfing population accounts for at least 50% of the insea population (most have a surfing population that is on average larger than that of bathing) and all have a high level of facilities and services that enable increased contact with the surf zone, for example surf/wetsuit hire, water sports retail outlets and surf schools.
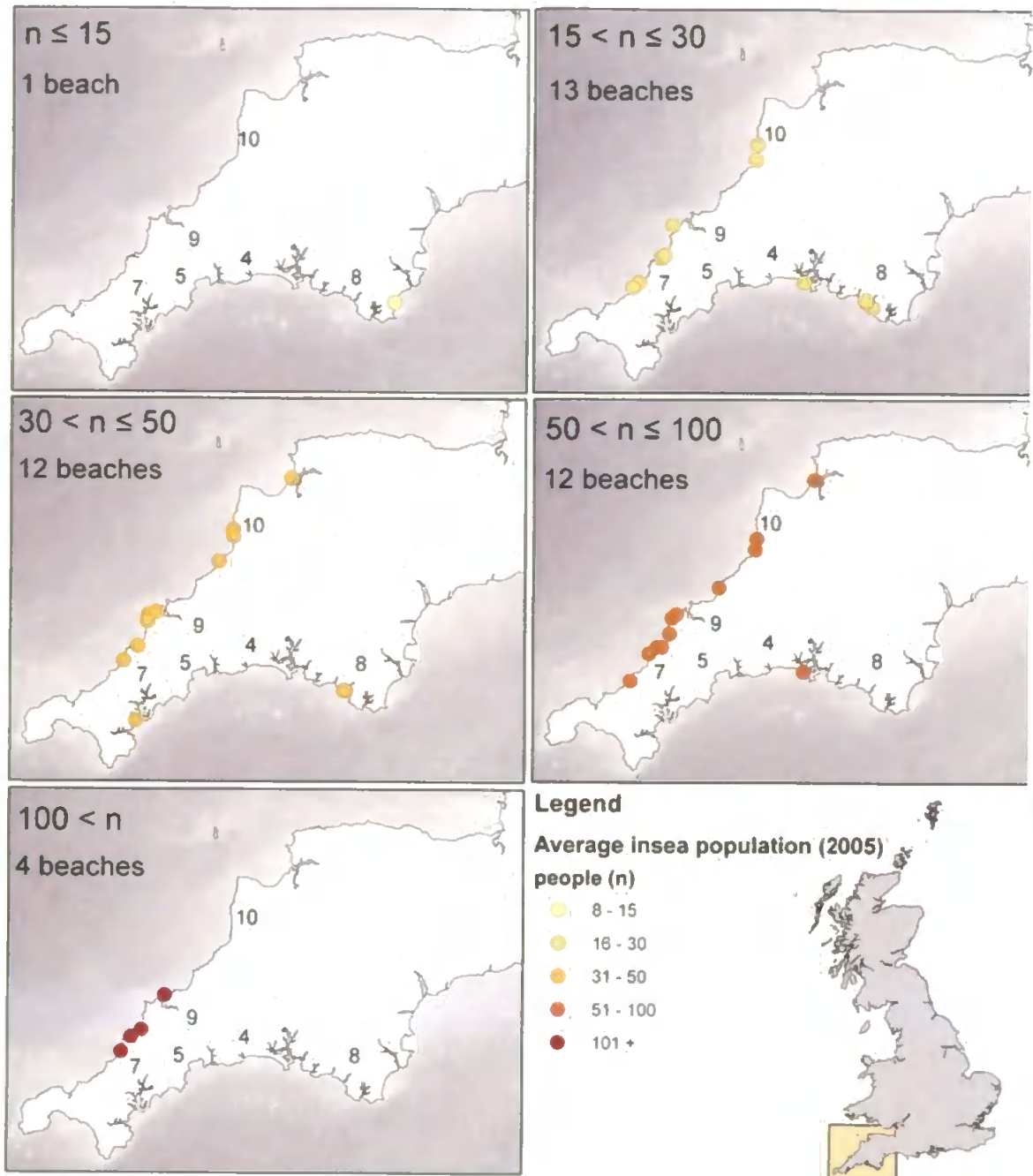
Figure 3.11 – Spatial distribution of the average number of people insea at any given RNLI beach location between 10:00 and 18:00 during the 2005 patrol season (1st May to 1st October). Number codes represent regional boroughs.

An understanding of the temporal variation of the insea user population is valuable in improving the understanding of variations in risk (vulnerability to hazard) and for the effective resource management of RNLI staff and equipment. Figure 3.10 shows the seasonal time series of the total (regional) insea population during 2005. There is a clear increase in the insea population during the summer months (late July to early September), peaking in August at over 10,000 people insea at all RNLI beaches at any one time. A clear picture of relative beach population loadings is given by plot B, where the per beach user populations (season lengths can vary slightly from beach to beach) indicate some higher resolution peaks and troughs in population numbers. Although it is possible these are linked to wave and weather conditions the general trends appear to coincide in part with school and public holidays occurring 26th May – 3rd June, 25th July – 2nd September. On a shorter timescale (< 7 days), there is a strong indication that a weekly periodicity is present within the data as indicated through the autocorrelation function (r) in Figure 3.10 with significant lag peaks around 7 ($r = 0.65$) and 14 days ($r = 0.4$), indicating consistently higher insea populations at weekends.

3.4.2 Incident statistics

Analysis of incident data clearly shows that during 2005 both the environmental cause of incident and the number of incidents vary significantly around the coasts of Devon and Cornwall (Figure 3.12). A dominance of rip current related incidents (47% of all incident events for 2005) is seen in most regions. Rip currents account for 49% of incident events in west coast regions where $H_{s,10\%}$ is 2.5–3 m and MSR $\approx$ 7 m, as opposed to the south coast regions where, $H_{s,10\%} = 0.5$–2.5 m, MSR $\approx$ 4.7 m and rip currents cause 25% of total incident events. In south coast regions surging waves and tidal cut-off, account for 8% and 10% of total recorded incident events respectively, showing an increased prevalence compared to west coast regions where the role of surging waves (3% of total incidents) and tide cut off (3% of total incidents) is less significant. In many cases on the south coast, the increase in tidal cut-off is associated with beaches that have significant portions of their length submerged or segmented at high-tide.

When incidents are broken down into the number of individuals assisted/rescued within each event (Figure 3.13), rip currents are shown to play a role in 71% of incidents occurring within Devon and Cornwall during the 2005 season. Offshore winds, sandbars, bed return flow, high surf, strong winds, tidal cut-off and dumping waves individually represent no
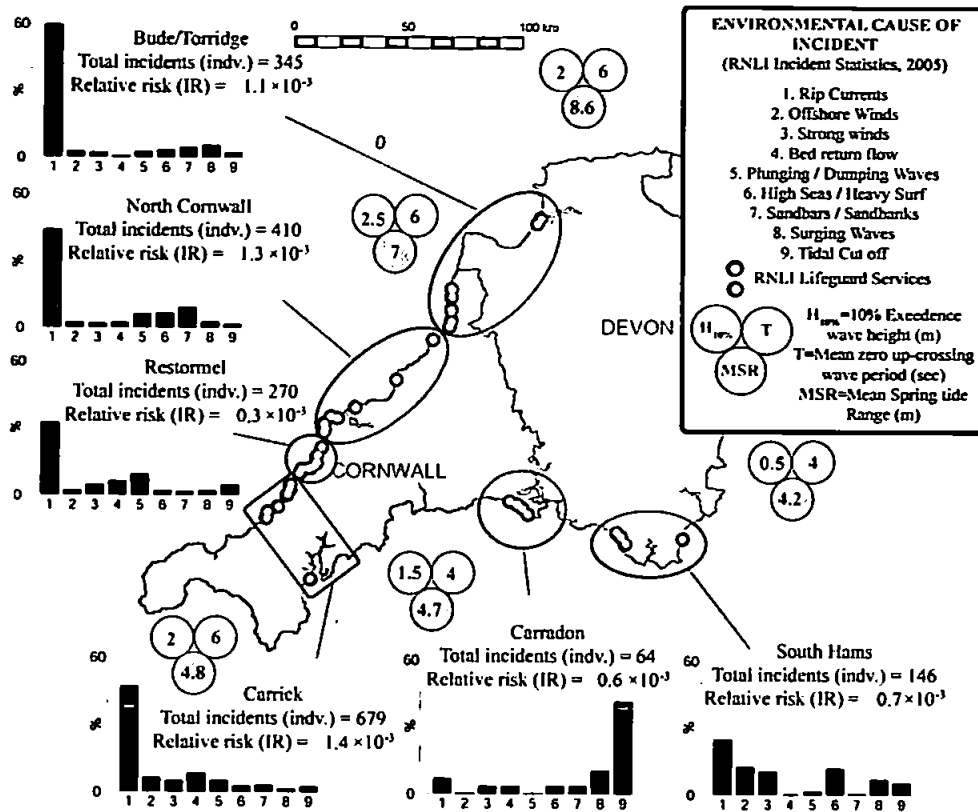
Figure 3.12 – Plots illustrating percentage distribution of the environmental cause of incident for all cases of active assistance at RNLI-patrolled beaches in Devon and Cornwall during 2005. Total number of individuals (indv.) assisted and relative risk posed by physical beach hazards (IR=incidents.hr^{-1}/ insea.hr^{-1}) are displayed for each region. Circles represent 10% exceedence significant wave height (Draper, 1991), mean zero up-crossing wave period (Draper, 1991) and mean spring tidal range (UKHO, 2003). The histograms show the environmental cause of incident.
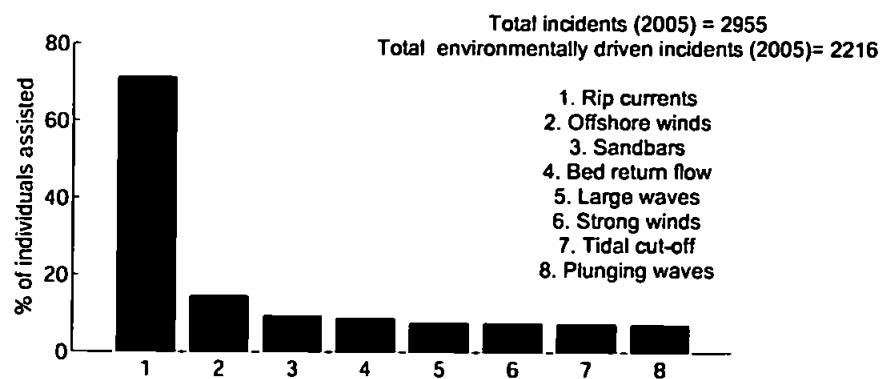
Figure 3.13 – Plot illustrates percentage frequency distribution of environmental cause contributing to each individual assisted during the 2005 season (some assists involve more than one environmental cause)

more than 15% of all incidents. Some of these environmental causes occur in conjunction with rip currents in 30% of incidents, suggesting risk to the beach user is often compounded with a combination of hazards, such as large waves and littoral currents, that can drive the spatially unaware beach user into areas of increased rip current hazard.

Individual locations were analysed to further understand the beach hazard characteristics and specifically the influence of rip currents in rescue incidents. This analysis includes calculation of a level of risk for each location for the 2005 season. A risk parameter IR is derived through two statistics: (1) the average number of people estimated to be in the water at hourly intervals (P) between 10:00 and 18:00 hrs during the 2005 season; and (2) the average number of individuals assisted/rescued per hour (Re) at a specific location (calculated from the total number of insea assists/rescues per season divided by the number of hours in a season at each location). The ratio between these two statistics is the probability of an incident occurring:

$$IR = \text{Re}/P \qquad\qquad (3.1)$$

The probability of rip current related incidents IR_{RIP} was also calculated:

$$IR_{RIP} = \text{Re}_{RIP}/P_{RIP} \qquad\qquad (3.2)$$

where Re_{RIP} is the number of rip incidents per hour at each location. Figure 3.14 illustrates the spatial distribution of IR_{RIP} around the region highlighting a number of interesting points. Firstly, it is evident from the spatial distribution that most beaches with a high IR_{RIP} are located on the high-energy west coast region. Secondly, these beaches within the west coast regions, and in fact those with the highest IR_{RIP} on the south coast, are the most exposed to the dominant swell direction (west and southwest). This phenomenon can be clearly seen in Figure 3.14b and Figure 3.14c, where more sheltered north and northwest facing beaches have low values of IR_{RIP} compared to their more exposed counterparts, even when the beaches are within close proximity.
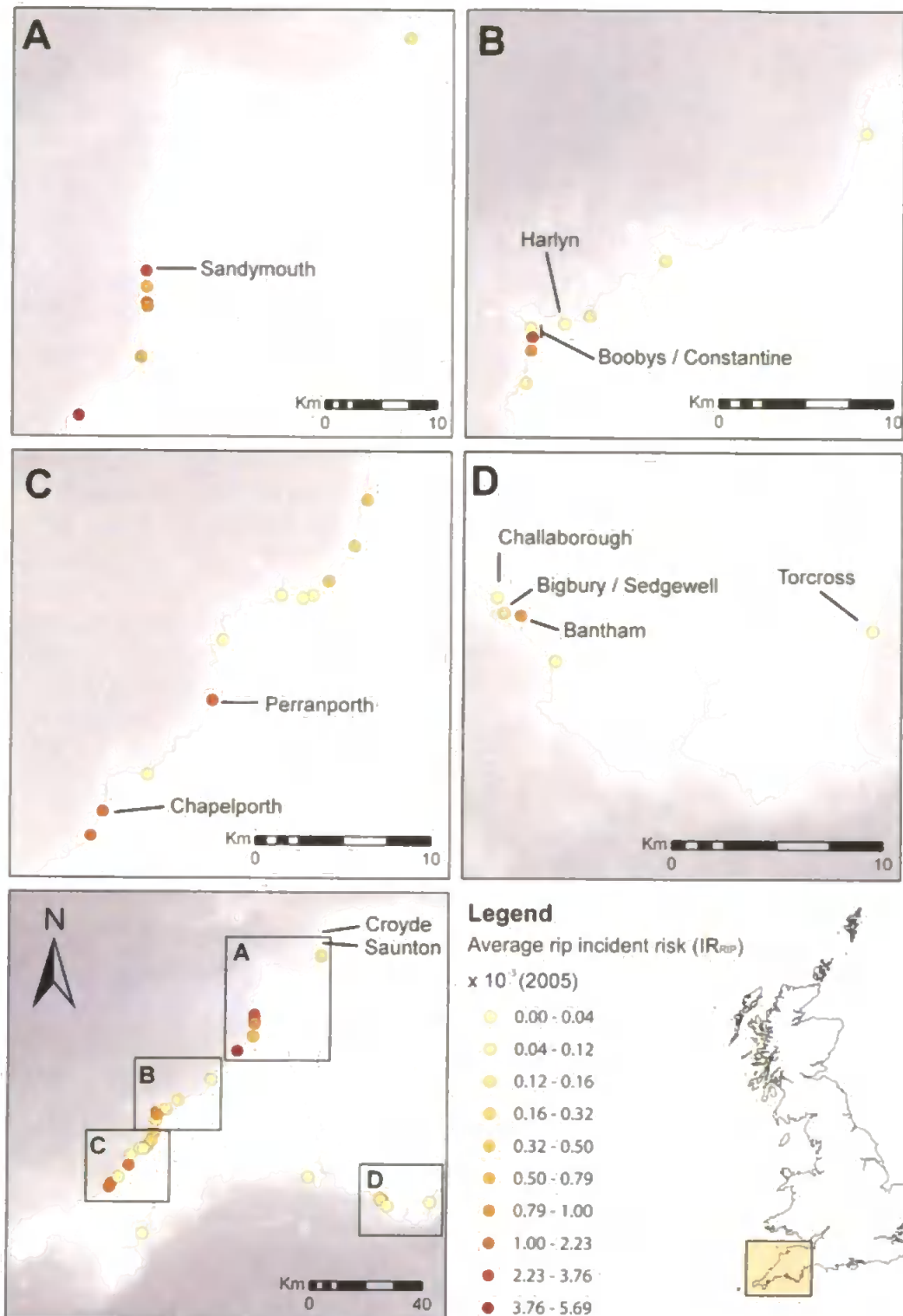
Figure 3.14 = Spatial distribution of rip risk (IR_{RIP}) within RNLI beach sites in Devon and Cornwall. Calculated from incident statistics collected during the 2005 patrol season (1st May to 1st October). Insets A, B, C and D represent regional enlargements.

3.4.3 Beach hazards and morphology

To better understand mechanisms behind these spatial variations in IR and specifically IR_{RIP} a number of beach sites were chosen for further investigation. A morphological and hydrodynamic assessment of these sites enabled insights into the role that waves, tides and morphology play in modifying the hazards and hence risk of these lifeguarded beaches. Selected beaches, marked in grey in

Table **3.3** and highlighted in Figure 3.9 and Figure 3.15 were targeted to elucidate these aims and hence they included beaches that represented the end members of the IR_{RIP} spectrum and those that displayed a marked difference in IR_{RIP} within the same visitor catchments and locality. In addition, these sites represented a cross-section of the beach morphologies and coastal environment within the study region, and to this end, two non-RNLI beaches were included in the morphological analysis, Croyde Bay and Saunton Sands that represented an example of an ultra-dissipative end member.

Reviewing the RNLI incident data, it is clear that the type and level of hazards vary with location. Morphological data from the survey data collection at these sites is shown in Figure 3.15. The exposed intermediate beaches on the west coast (2, 3, 5, 6 and 7), having a $H_{s10\%}$ of approximately 2.5–3 m, represent some of the highest values of IR_{RIP}, with values at locations 6 (Constantine) and 7 (Perranporth) reaching 3.76 and 2.01 (per 1000 individuals) respectively. Perranporth and Constantine also received the most incidents during 2005 with 379 and 201 individuals rescued, respectively. Low IR_{RIP} values consist of beaches located within sheltered areas of the west coast (location 4) and the south coast (see Figure 3.15). These areas have a reduced $H_{s10\%}$ due to the aspect of the coast. The high-energy westerly Atlantic swell waves which are dominant throughout the year have to refract through 45–90° to arrive at the sheltered north and south facing beaches. Harlyn Bay (location 4) had an average of 80 individuals insea hr^{-1} during the season compared to 48 at the neighboring Constantine Bay, but only 14 environmentally driven rescues occurred during the season as opposed to 201 at Constantine Bay. At south coast locations mean observed H_b was between 0.1 m and 0.4 m at patrolled beach locations 8, 9, 10, 11 and 12 during the 2005 season. These locations had the lowest calculated rip current risk values. In some cases other environmental hazards were more prevalent. On the south coast, in combination with lower energy conditions, the dominant winds from the western quadrant blow offshore in many locations, increasing the risk of the beach user
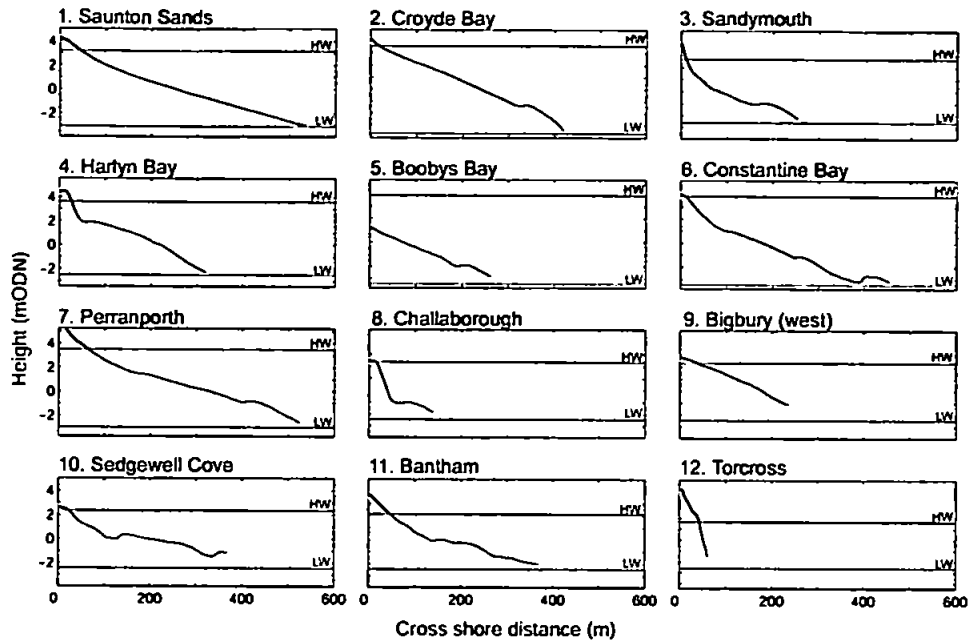
Figure 3.15 – Summary of cross shore profiles and tide ranges at study sites around Devon and Cornwall (height measured in meters above Ordnance Datum Newlyn).

drifting offshore. Significant tidal cut-off hazards are present at many locations where the large tidal range causes submerged high water beaches. The ease of beach access and characteristics of backshore geology control the severity of this hazard. Much of the tidal cut-off hazard is also present on the west facing coasts but levels of hazard are dwarfed by those posed through rip currents.

Surveyed cross-shore profiles (Figure 3.15) and wave, tide and sediment characteristics (Figure 3.16) provide a general insight into the two-dimensional inter-tidal geometry at all the sample beaches. Inter-tidal widths range from ~ 600 m at exposed fine sand high-energy west coast beaches, with morphology most similar to the Ultra-Dissipative beach type (e.g. Saunton Sands) to < 40 m at coarse sand/gravel steep beaches that are observed along the sheltered southeast facing coasts (e.g. Torcross) that would be termed a Reflective beach. Between these end members a number of beach profile geometries were observed from those with distinct breaks in slope, associated with significant changes in beach gradient (steep upper beach; wide, shallow lower beach) resembling the Low-Tide Terrace beach form, to those with significant inter-tidal and sub-tidal bar systems. The medium- to high-

105

Table 3.3 – Table of incident statistics for all RNLI beaches in 2005 in Devon and Cornwall. Incident numbers represent individuals. Risk indicator defines level of risk (total and rip current related) through; $IR = Re/P$. Shaded rows indicate selected study sites. Crackington (highest risk beach) was not used as a study site due to the short length of the patrol season at that location. Only 10 of the 12 beaches are highlighted because 2 beaches (Saunton Sands and Croyde Bay did not have RNLI lifeguard patrols during the study period. Region number relates to borough that is displayed in Figure 3.11.

Region	Beach	Incidents All	Incidents Env.cause	Beach users Beach	Beach users Swim	Beach users Surf	P (insea total)	Incidents/hr (Re) ($\times 10^{-2}$) Re (inc./hr)	Incidents/hr (Re) ($\times 10^{-2}$) Re_{RIP} (rip inc./hr)	Risk (IR) ($\times 10^{-3}$) IR (tot.risk)	Risk (IR) ($\times 10^{-3}$) IR_{RIP} (rip risk)	Rip risk ranking
9	Crackington	135	113	195.0	33.2	5.8	39.0	24.353	22.198	6.24	5.69	1
9	Constantine	201	192	403.3	35.4	12.7	48.1	18.182	18.087	3.78	3.76	2
10	Sandymouth	102	99	160.0	23.2	7.4	30.5	9.900	9.800	3.24	3.21	3
7	Porthtowan	201	187	341.3	33.5	35.8	69.3	17.444	15.485	2.52	2.23	4
7	Chapel Porth	83	81	134.8	15.2	14.0	29.3	7.556	6.157	2.58	2.10	5
7	Perranporth	379	334	749.1	72.5	45.3	117.8	26.763	23.718	2.27	2.01	6
10	Crooklets	59	55	169.0	27.6	7.6	35.2	5.413	5.413	1.54	1.54	7
9	Treyarnon	62	57	296.3	47.1	3.9	50.9	5.610	5.118	1.1	1.00	8
8	Bantham	86	78	281.8	29.7	14.5	44.3	6.250	4.247	1.41	0.96	9
10	Summerleaze	89	84	345.8	36.5	15.9	52.4	6.731	4.968	1.28	0.95	10
10	Black Rock	26	23	111.4	21.0	6.3	27.3	2.264	2.165	0.83	0.79	11
10	Northcott	9	9	77.0	21.8	4.7	26.6	1.940	1.940	0.73	0.73	12
10	Widemouth	67	41	197.5	31.5	19.6	51.1	3.285	3.285	0.64	0.64	13
7	Perran Sands	41	27	134.8	16.9	17.8	34.7	2.519	2.146	0.73	0.62	14
5	Mawgan Porth	50	47	350.5	44.1	25.7	69.8	4.451	3.504	0.64	0.50	15
5	Porth	13	12	149.1	20.9	0.8	21.7	1.136	0.947	0.52	0.44	16
5	North Fistral	97	76	701.0	51.5	126.9	178.5	6.169	5.682	0.35	0.32	17
5	Watergate Bay	43	37	385.9	38.9	84.7	123.6	3.504	2.841	0.28	0.23	19
5	Crantock	81	72	1014.1	239.3	25.0	264.3	6.818	5.777	0.26	0.22	20
5	Great Western	22	13	95.0	11.1	23.3	34.5	1.231	0.568	0.36	0.16	23
4	Sharrow	4	3	77.7	14.9	1.3	16.3	0.264	0.264	0.16	0.16	24
10	Westward Ho!	35	30	155.7	34.0	15.1	49.1	2.841	0.758	0.58	0.15	25
8	Sedgewell Cove	40	30	290.3	24.2	9.3	33.5	2.953	0.492	0.88	0.15	26
9	Polzeath	52	35	525.9	76.8	88.5	165.3	2.804	1.923	0.17	0.12	28

9	Porthcothan	5	3	150.5	24.9	5.1	30.0	0.295	0.295	0.1	0.10	29
9	Trevone	16	3	204.9	21.5	8.9	30.3	0.295	0.295	0.1	0.10	30
8	Burgh Island	5	4	177.6	23.6	5.9	29.4	0.394	0.197	0.13	0.07	31
8	Challaborough	43	19	198.7	20.8	5.0	25.8	1.870	0.098	0.73	0.04	34
4	Tregonhawke	67	55	98.6	20.3	5.2	25.5	5.208	0.095	2.04	0.04	35
10	Sandymere	11	4	129.7	31.7	19.8	51.6	0.379	0.189	0.07	0.04	36
7	St Agnes	27	21	100.2	18.0	9.9	28.0	1.959	0.093	0.7	0.03	37
5	Tolcarne	10	7	200.3	36.2	24.9	61.1	0.663	0.189	0.11	0.03	38
5	South Fistral	6	5	232.3	47.0	50.6	97.5	0.473	0.284	0.05	0.03	39
5	Towan	10	1	228.6	25.5	3.5	29.0	0.081	0.081	0.03	0.03	40
4	Tregantle	4	4	221.2	51.9	7.3	59.1	0.442	0.000	0.07	0.00	48
4	Freathy	2	2	61.6	15.1	1.6	16.6	0.439	0.000	0.26	0.00	49
7	Holywell	11	1	296.6	46.6	17.4	64.0	0.095	0.000	0.01	0.00	50
7	Gyllyngvase	37	28	261.9	25.6	5.4	31.1	2.612	0.000	0.84	0.00	51
8	Thurlestone	16	8	222.0	22.1	6.3	28.4	1.538	0.000	0.54	0.00	52
9	Booby's	2	1	75.9	14.3	6.2	20.6	0.098	0.000	0.05	0.00	56
9	Trebarwith	3	1	374.3	51.7	9.5	61.3	0.098	0.000	0.02	0.00	57
9	Harlyn	13	5	496.5	61.3	18.5	79.8	0.401	0.000	0.05	0.00	58
8	Torcross	20	7	157.7	6.9	0.6	7.6	1.346	0.000	1.78	0.00	59
	TOTALS	2955	2216									

energy, medium to coarse sand beach systems commonly displayed clear bar/rip morphologies in the MLWN to MLWS region (beaches 2, 3, 5, 6, 7 and 11) in addition to inter-tidal bars (most commonly slip-faced bars) of varying significance. The beaches were characterized by a wide range of coastal morphologic settings including enclosed/embayed (locations 2, 4, 6 and 8), quasi-open coast (locations 1, 3 and 7), estuarine influenced (locations 1, 10 and 11), barrier (location 12) and significantly geologically constrained (locations 3, 5 and 6) beaches which in combination with varying sediment abundance, characteristics and hydrodynamic conditions generated a diverse range of beach systems and forms, all of which experience surf zone bather interaction.

A summary of the combined general morphologic and hydrodynamic and incident observations ranked by IR_{RIP} is displayed in Figure 3.16. The highest levels of IR_{RIP} during the season were associated with those beaches with well-developed low-tide bar/rip

systems, high-energy wave conditions and in many cases with a significant presence of hard rock geologic features within and bounding the inter-tidal zone (locations 6 and 3). With decreasing IR_{RIP} and IR, hazards other than rip currents are observed to drive incidents. Tidal cut-off and strong winds have a significant influence within Bigbury Bay (locations 10 and 11), which is characterized by significant systems of slip-face bars and low-amplitude ridges, and experiences submerged beach sections during high water associated with an estuarine outflow system between beach units. Finally, those beaches with both low IR_{RIP} and IR commonly display little or no rip current presence due to a combination of beach type (no rip current morphology) and low-energy and wave climate (oriented away from westerly swell source) with a increasing influence from short period wind waves. The hazard signature at these beaches is controlled mainly through offshore winds and tidal cut-off.
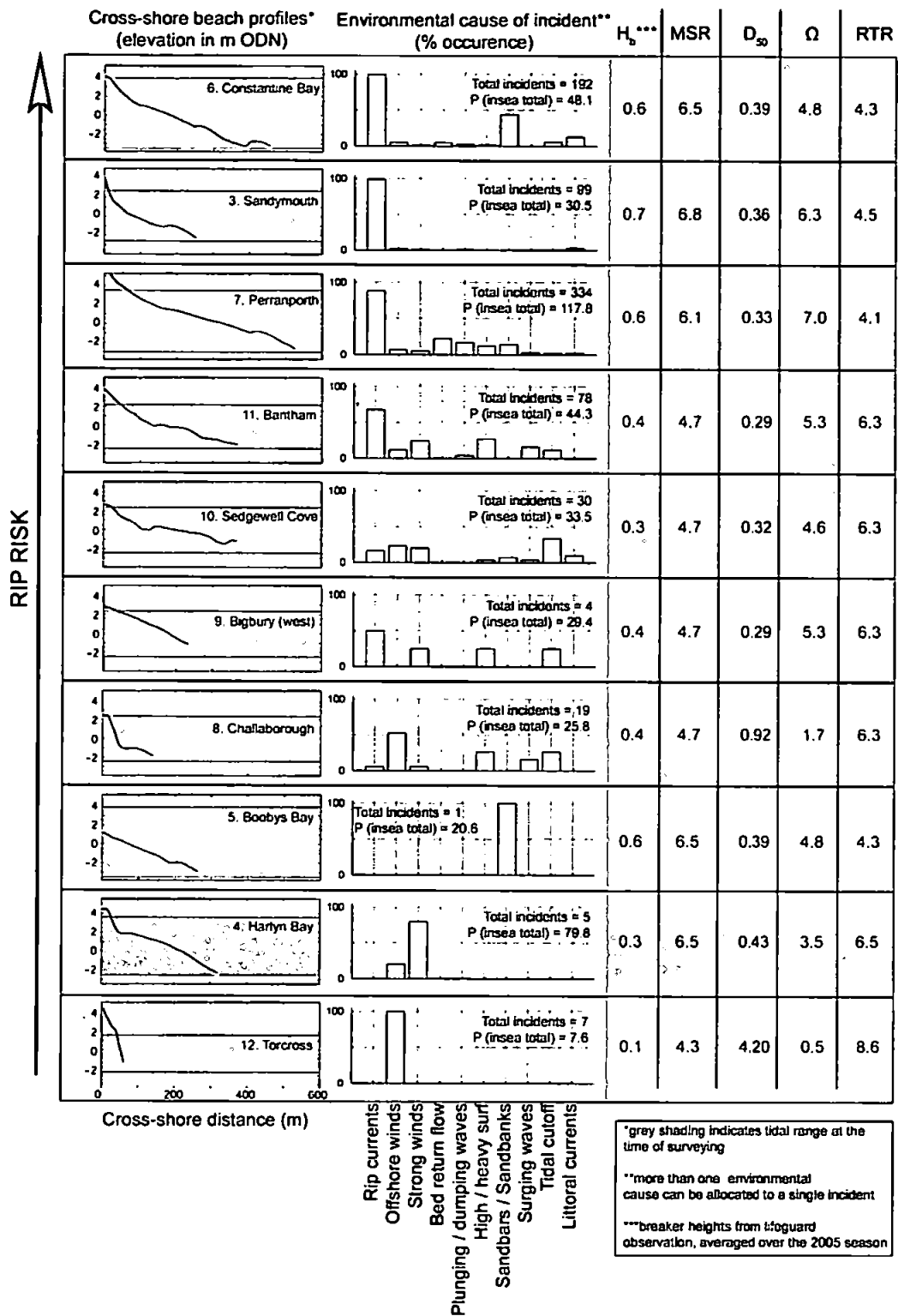
Figure 3.16 – Summary of morphodynamic, hydrodynamic, sediment size and hazard parameters associated with monitored beach sites. Associated data relating to beach profile form and incident seasonal incident levels is also presented. Ranking is 2005 seasonal values of IR_{RIP} (increasing from bottom to top).

3.4.4 Beach Types and Risks

These results indicate that the physical characteristics of the beach and its location within the hydrodynamic setting of the region play a key role in defining physical environmental hazards that are posed to the insea beach user, especially that caused by rip current activity. In turn, through human interaction with these hazards on the selected beaches studied, a general appreciation for the levels of risk within a variety of these beach environments has been assessed. The southwest coast of England displays a wide variety of medium to high energy beach types amongst varying tidal ranges. Through the use of traditional morphodynamic parameters commonly used to differentiate between a variety of beach types and surf zone regimes, the observed range of beaches within the study can assessed in the context of these specific surf zone hazards. Values of Ω and RTR for the studied beaches are shown in Figure 3.16. These values lead to some general observations on the distribution of measured levels of risk during this study illustrated in Figure 3.14. Beaches within the study can be crudely separated into three general types. Those that occupy characteristics typical of the two end members of a morphodynamic continuum displaying either highly dissipative (termed here 'ultra-dissipative') regimes or those representing highly reflective morphodynamic characteristics. These two end members were assessed, within the limited context of this study, to represent relatively low levels of risk to the insea beach user. In contrast, those beaches that fell into an increasingly dynamic intermediate group, characterized by varying levels of reflective and dissipative characteristics, often varying temporally with the tide, and commonly possessing significant bar/rip morphologies, were more likely to exhibit higher levels of risk to the beach user. Figure 3.17 summarizes these findings.

3.4.4.1 Ultra-dissipative Beaches

Ultra-dissipative high energy surf zones, for example Saunton Sands (Ω = 7.1 and RTR = 6.3), that are not well represented within previous Australian studies (Wright and Short, 1984; Masselink and Short, 1993), exhibit a very wide (> 500 m), low gradient, featureless inter-tidal profile with no significant bar morphology (Figure 3.15). Saunton Sands is characterized by a low gradient fine sand beach (D_{50} = 0.29 mm), has an MSR of 7.9 m and shows very subdued inter-tidal morphology, in part due to the significant cross-shore translation of high-energy surf zone processes during the tidal cycle. Ultra-dissipative surf zones typically have limited rip current activity due to the non-barred, dissipative nature of the wide surf and inter-tidal zone. Incident wave energy is greatly reduced when it reaches

Ultra dissipative	Intermediate (reflective/dissipative)	Reflective
Risk: Low Ω = 7.1 RTR = 6.3	Risk: Low-High Ω = 3.5 – 7.0 RTR = 4.1 – 6.5	Risk: Low Ω = 0.5 RTR = 8.6
e.g. Saunton Sands	e.g. Chapel Porth	e.g. Torcross
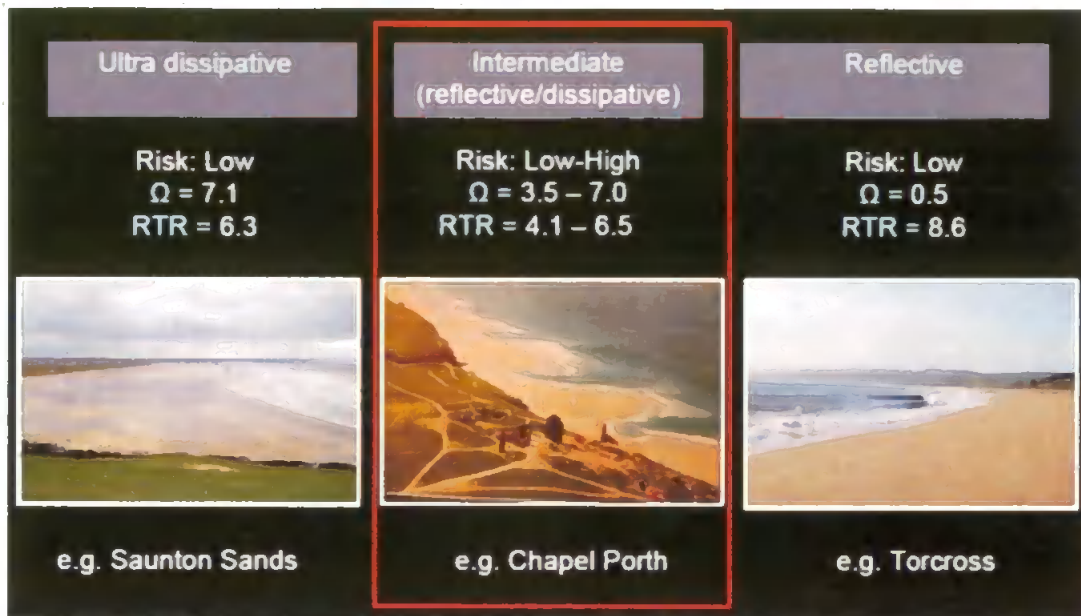
Figure 3.17 – Overview of general risk level associated with broad beach type regimes observed during the study.

the bathing zone, which under medium- to high-energy conditions is fully saturated. This means an increase in incident wave height would have little effect on the prevailing risk levels, although potentially an increase in infragravity energy at the shoreline can generate an increased swash hazard through large cross-shore excursion.

3.4.4.2 Intermediate (Reflective/Dissipative) Beaches

The more common intermediate beach types, with large tidal ranges (MSR ~ 6.1–7.9 m) and an energetic wave climate, are represented by low tide terrace, low tide terrace and rip, and low tide bar/rip morphologies. They are characterized by a steeper, often coarse, more reflective high water beach face, a wide (400–600 m) subdued dissipative inter-tidal zone (low-amplitude ridges and slip-face bars often present) and well developed intermediate low water bar/rip circulation systems (Figure 3.15). The beaches with the highest calculated IR_{RIP} were observed to possess morphology typical of that reported within the low-tide bar/rip and low-tide terrace and rip beach types (e.g. Constantine Bay, Perranporth, Sandymouth and Chapel Porth). These sites had values of Ω between 4.8 and 7 and *RTR* of between 4.1 and 4.5. Examples of these morphologies are illustrated in Figure 3.18 and Figure 3.19. Observations indicated that backshore geomorphology and exposed inter-tidal rock formations have a significant influence on the morphologic character and surf zone regime throughout the nearshore, but especially within the mid- to upper inter-
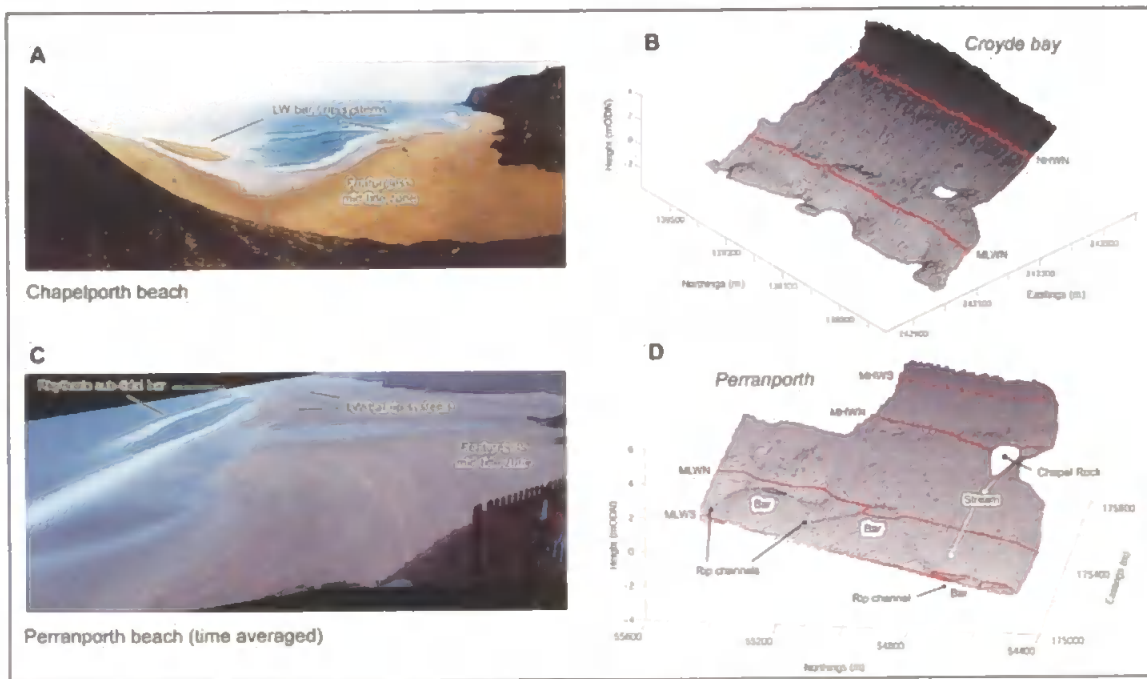
Figure 3.18 – Annotated panoramic views of Chapel Porth (A) and Perranporth (C) at spring low tide. Digital Elevation Models (right) indicate measured morphology at Croyde Bay (B) and Perranporth (D) during September 2006 with mean tidal levels represented by solid red lines.

tidal zone of many of the beaches of Devon and Cornwall. Hard rock formations at both Sandymouth and Constantine Bay (Figure 3.19) appear fundamental in generating the beach hazards. Sandymouth, with a gravel and boulder reflective high water beach, possesses an inter-tidal rock platform which topographically constrains circulation within the surf zone, consequently driving fixed topographic rip current systems. The geologic constraints at Constantine Bay act to influence surf zone circulation from high to low water, affecting morphological development modifying flow velocities and often generating deep rip channel morphologies. The combination of incised low-tide beach rips and constrained mid- to high-tide topographic rips led to Constantine Bay having the second highest rip current risk level in the region for 2005.

High rip current risk was also observed on intermediate/dissipative beaches that were relatively unconstrained by hard geologic structures like Perranporth and Chapel Porth (Figure 3.18). Both locations receive similar hydrodynamic forcing with a MSR = 6.1 m and an annual $H_{s10\%}$ = 2.5 m (Draper, 1991), and have a well defined, often rhythmic unconstrained bar and rip morphology that is commonly exposed at MLWS. During the
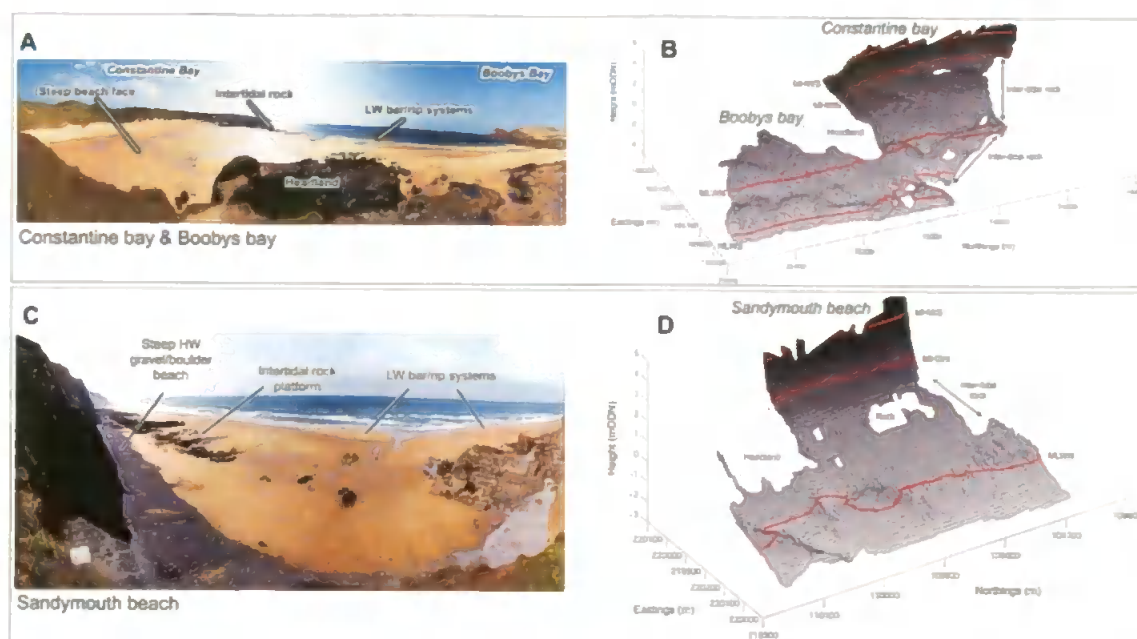
Figure 3.19 – Annotated panoramic views of Constantine and Boobys Bay (A) and Sandymouth (C) at spring low tide. Associated Digital Elevation Models indicate associated measured morphology (B & D) during September 2006 with mean tidal levels represented by solid red lines.

survey period, the unconstrained rhythmic bar and rip morphology, present at many west coast beaches had a wavelength of 300–400 m and amplitude of 1.5–2 m. With an incident breaker height of 0.5–2 m during the observation period, intense topographically driven rip systems can potentially develop as narrow rip feeders traveling within the channels between the bars, creating hazardous conditions for water users around low water at these locations (Short and Hogan, 1994; MacMahan et al., 2006). Figure 3.18 shows the observed low-tide bar and rip morphology at Perranporth (located between MLWN and MLWS) and associated oblique timex image from the Perranporth Argus station, indicating the presence of a detached sub-tidal bar system fronted by inner bar/rip morphology. Incident records suggest that rip hazards may be enhanced within the low water tidal phase during a period of maximum wave dissipation over the low-tide bar/rip morphology that, when exposed, can accommodate and attract beach users. Exposed bars are subsequently submerged during the flooding tide, activating rip currents as the surf zone passes over the morphologic template. These hypotheses are further developed and tested within Chapters 5 and 6.

3.4.4.3 Reflective Beaches

The steep reflective beaches on the south channel coast like Slapton Sands (Ω = 0.5 and *RTR* = 8.6) are coarse grained (D_{50} = 4.2 mm), narrow (~ 40 m) and associated with plunging and surging breakers within a small surf zone. Dominated by wind waves (observed summer H_b = 0.1 m), no significant rip current hazards present themselves.

3.4.5 Comparison of Australian and UK beaches

The beaches of southwest England possess a number of significant differences from those documented in previous Australian studies that form the basis of many of the commonly used morphodynamic beach models (Wright et al., 1982; Wright and Short, 1984; Short, 1986; Masselink and Short, 1993; Short, 2001; Short, 2006): 1) fine, wide, high-energy ultra-dissipative beaches like Saunton Sands; 2) steep reflective gravel beach types, like Slapton Sands of the protected south coast, with a comparatively low Ω of 0.5 but a high *RTR* of 8.6; and 3) wide largely featureless, high-energy intermediate/dissipative beaches (Ω = 4.8–7; *RTR* = 4.1–4.3) with more developed high and low water bar morphology, are not well represented within the Australian coastal environment. These differences are generated largely by the coupling of a high-energy wave climate and large tidal ranges in the UK. As a result, these beaches do not become tide-dominated with a large tidal excursion. Also, the variation in coastal geology and the present and historic sediment supply to beaches constrains the level of hydrodynamic control on beach type.

Not observed within this study and uncommon in the southwest of England but common to the UK (especially the east coast of England), are 'ridge and runnel' beaches (characterized by low-amplitude ridges) and those modified with inter-tidal coastal structures are environments that have also received limited coverage within Australian beach type models (Wright and Short, 1984; Masselink and Short, 1993). They are, however, known to represent unique UK beach morphologies and potentially unique hazard signatures.

3.5 CONCLUSIONS

As beach visitor numbers increase in the UK, understanding the physical hazards and risks posed to the beach user within a national context becomes paramount. This will underpin deployment of safety resources and enable improved understanding of the national beach environment that contributes to thousands of rescues annually. The south and southwest of England beach hazards have been found to be driven by a number of environmental factors;

strong/offshore winds, sandbars, bed return flow, large waves, tidal cut off and dumping/surging waves, but most significantly rip currents. Based on this preliminary study of the beach types, hazards, rip current characteristics and lifeguard rescue statistics the following conclusions can be drawn.

- Rip currents represented the greatest environmental threat to the insea beach user during the study. This threat can be compounded by a series of hazards working together.

- There is a significant variation in beach hazards and their severity depending on the nature of the hydrodynamic conditions and beach type. The intermediate/reflective low tide terrace and rip and intermediate/dissipative, low tide bar/rip morphologies similar to those described by Masselink and Short (1993) possess the high risk rip current systems, that are most active during wave heights of 0.5 – 2 m above which beaches are often closed to bathers.

- Moderate energy (0.5–1.5 m) Atlantic swell waves during spring and summer enable the development of rhythmic bar morphology on the intermediate beaches at the low water stand, generating morphologically controlled rip current systems.

- Large tidal ranges introduce hazards such as tidal cut-off through high water levels and rate of cross-shore shoreline movement, potentially enhancing rip current velocities on the ebbing tide.

- There is a great variation in surf zone characteristics due to beach boundary and inter-tidal hard-rock geologic structures, often constraining sand and water movement and enhancing rip current systems. With high-energy surf zones and large tidal ranges, the southwest of England experiences different hydrodynamic forcing than observed within the Australian datasets, thus generating beach environments unique to this climate.

This chapter has found that (1) there is some evidence for a link between beach type and hazard and (2) that many of the beach environments observed in the UK are fundamentally different from those observed in Australia, upon which many of the traditionally used conceptual beach state models are based. Therefore there is a need for a more comprehensive understanding of beach morphodynamics within the context of the UK beach environment to enable the successful development of a hazard referenced beach type classification that is applicable in the UK coastal environment. These issues are addressed in the following chapter.

4. UK BEACH CLASSIFICATION

4.1 INTRODUCTION

An analysis of beach hazards and rescue statistics for the Devon and Cornwall coasts in the previous chapter alluded to the influence of beach type in defining the hazard signature. Thus, an understanding of the spectrum of these beaches observed along the UK coast, with regard to their morphometrics, backshore morphology and wave, tide and sediment characteristics is integral for hazard assessment.

As previously highlighted, recent decades have seen an increase in beach research spanning a wide range of coastal environments, but attention has focussed on understanding beach morphodynamic response in micro- and meso- tidal sandy environments with relatively few studies in macrotidal regimes until recent years. Short (2006 p.27) stated that 'The 15 beach types that occur around the Australian coast also occur in similar wave-tide-sediment environments throughout the world and provide a framework for identifying many of the world's beaches. What the Australian coast does not possess, however, are tide-modified beaches exposed to higher ocean swell and storm seas, resulting in similar though higher energy beaches. It also has relatively few gravel and cobble beaches'. Short (2006) also highlighted the lack of 'ridge and runnel' beaches within the Australian environment. The diversity in wave and tide regimes, sediment distributions and geological inheritance around the UK coast make it a valuable study region within which to improve understanding of beach morphodymamics in these lesser studied environments.

The commonly used method of beach type description follows work by Wright and Short (1984) and Masselink and Short (1993) using Ω (Equation 1.2) and RTR (Equation 1.3) to position beaches within a 2D conceptual matrix based upon wave, tide and sediment characteristics. These two parameters attempt to differentiate between the forcing physical processes and the observed beach state. Recent studies (Gómez-Pujol et al., 2007; Jackson et al., 2005) have suggested that this does not explain the whole story. They state that the influence of geological inheritance and sediment supply can have a significant, if not dominant, controlling effect on observed beach state.

The three principal aims of this chapter are:

- To identify beach type variability and distribution in the UK.
- To define a range of beach groups that represents a cross-section of UK beaches and their associated hazards.
- To investigate the appropriateness of using a beach classification system to describe beach groups through the use of traditional morphodynamic parameters.

These aims were achieved through the collection and analysis of a high-quality, robust dataset capturing the spatial variability of beach types and their associated sedimentary, geometric and hydrodynamic conditions within England and Wales. This chapter identifies a number of common beach groups and proposes a conceptual morphodynamic framework as a tool to understanding beach group characteristics.

4.2   DATA COLLECTION AND ANALYSIS

Understanding the coastal setting of England and Wales is fundamental when investigating the spatial distribution of beach types and their associated morphodynamic characteristics (see Chapter 1 for a detailed description of the coastal setting of England and Wales). Antecedent environmental conditions shape the systems in which each beach site resides and will set the boundary conditions with respect to both sediment supply and sink, having a controlling effect on the morphodynamic system. To successfully summarise the beach types and associated morphodynamic regimes found in England and Wales it was deemed essential to sample from a wide cross-section of the contrasting coastal environments. With this in mind, a comprehensive campaign of data collation and collection was undertaken to generate a representative and robust dataset of morphometric and hydrodynamic attributes. The following section describes the design and process of data collection and introduces the subsequent analytical techniques used.

The study collected data from 92 beach sites within England and Wales (Figure 4.1; Figure 4.2). These sites were broken down into 5 main regions: Irish Sea and Liverpool Bay, the Atlantic southwest, Lyme Bay, the Channel Coast and the East Coast. These different regions represent a broad cross section of beach types and environmental
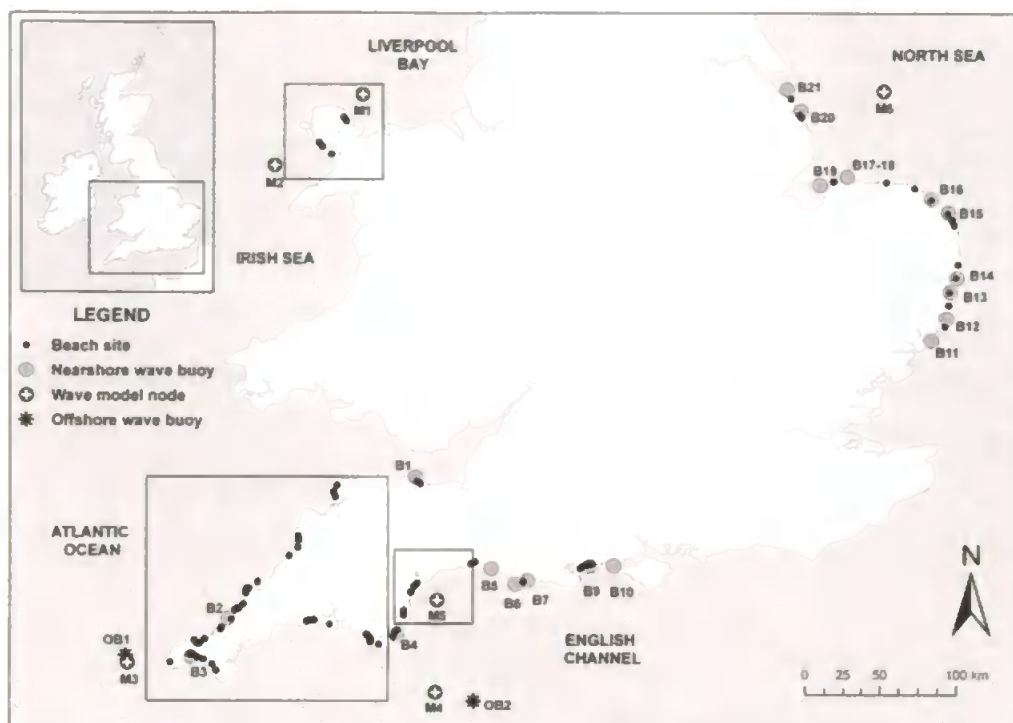
Figure 4.1 – Overview map of study region, indicating all data sources and highlighting regions where wave modelling was conducted (Map image copyright 2009, Crown Copyright Ordnance Survey, and EDINA Digimap/Joint Information Systems Committee (JISC) supplied service).
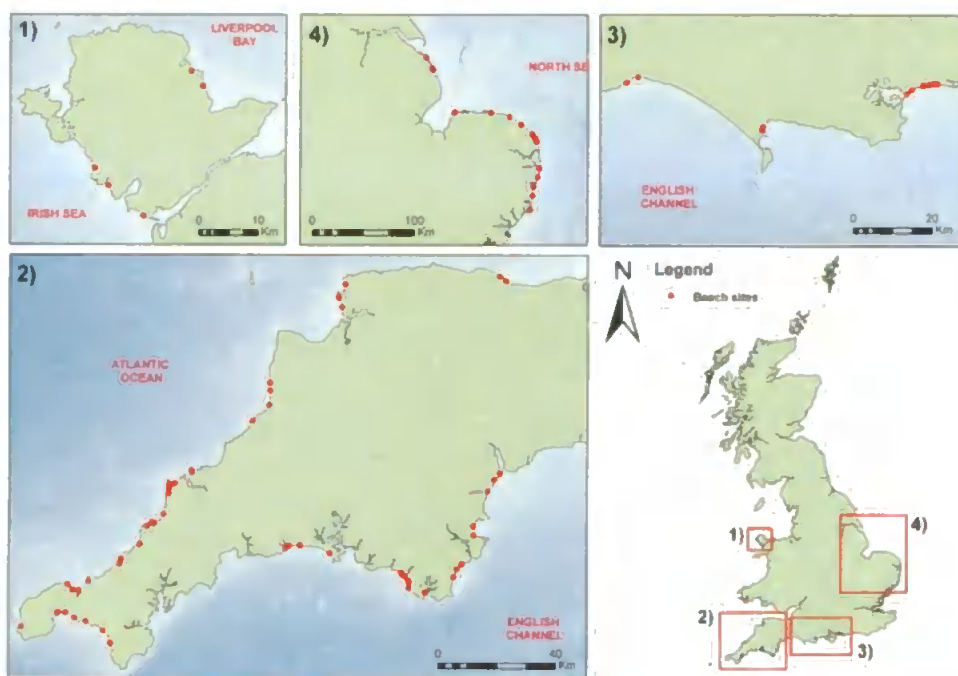
Figure 4.2 – Large scale views of selected beach sites within each region (Map image copyright 2009, Crown Copyright Ordnance Survey, and EDINA Digimap).

settings observed in the UK, possessing a marked difference in wave climate, sediment type and abundance, geological history and tidal range. Within each of these regions a campaign of data collection was undertaken between late September and early December 2007. Morphological, sedimentological and hydrodynamic datasets were collected for each beach, as well as information on the local environmental setting and extended morphological characteristics. For regions where primary data could not be collected (due to time constraints), reliable third party sources were utilised (Environment Agency, Channel Coastal Observatory, University of Wales Bangor). The data collection programme was designed to be as temporally synchronous as possible to minimise potential between site temporal variations in collected data due to changing forcing conditions.

Figure 4.3 illustrates the structure of research methods applied to this investigation. The required environmental data could be broken into two categories; 1) beach morphology, which encompassed the collection of beach profiles, sediment samples and remote imagery; and 2) hydrodynamic setting, which included the nearshore wave climate and tidal regime. The next sections detail the data collection methods and subsequent analytical techniques employed.

4.2.1 Beach morphology and sedimentology

4.2.1.1 Beach profiling

Beach profiling, using an RTK GPS system (see section 2.2 for detailed methodology), was conducted in October 2007 at locations indicated in Appendix 2, additional beach profiles were collected from third party sources (Appendix 2). Each transect was surveyed during spring low-tide to maximise the inter-tidal exposure and to enable collected profiles to extend from MHWS to MLWS. Elevations along each profile were collected at 1 m intervals, this high resolution sampling was required to resolve primary and secondary beach morphology on the range of beach sites surveyed where beach widths ranged from 15–1000 m. Collected profiles were then used for the calculation of selected morphometric variables illustrated in Figure 4.4.

4.2.1.2 Beach morphometrics

Cross-shore profiles were separated into four sections corresponding to the local mean tidal levels (MHWS, MHWN, MSL, MLWN and MLWS). The gradient for each beach section was calculated using standard linear least-squares regression techniques. The
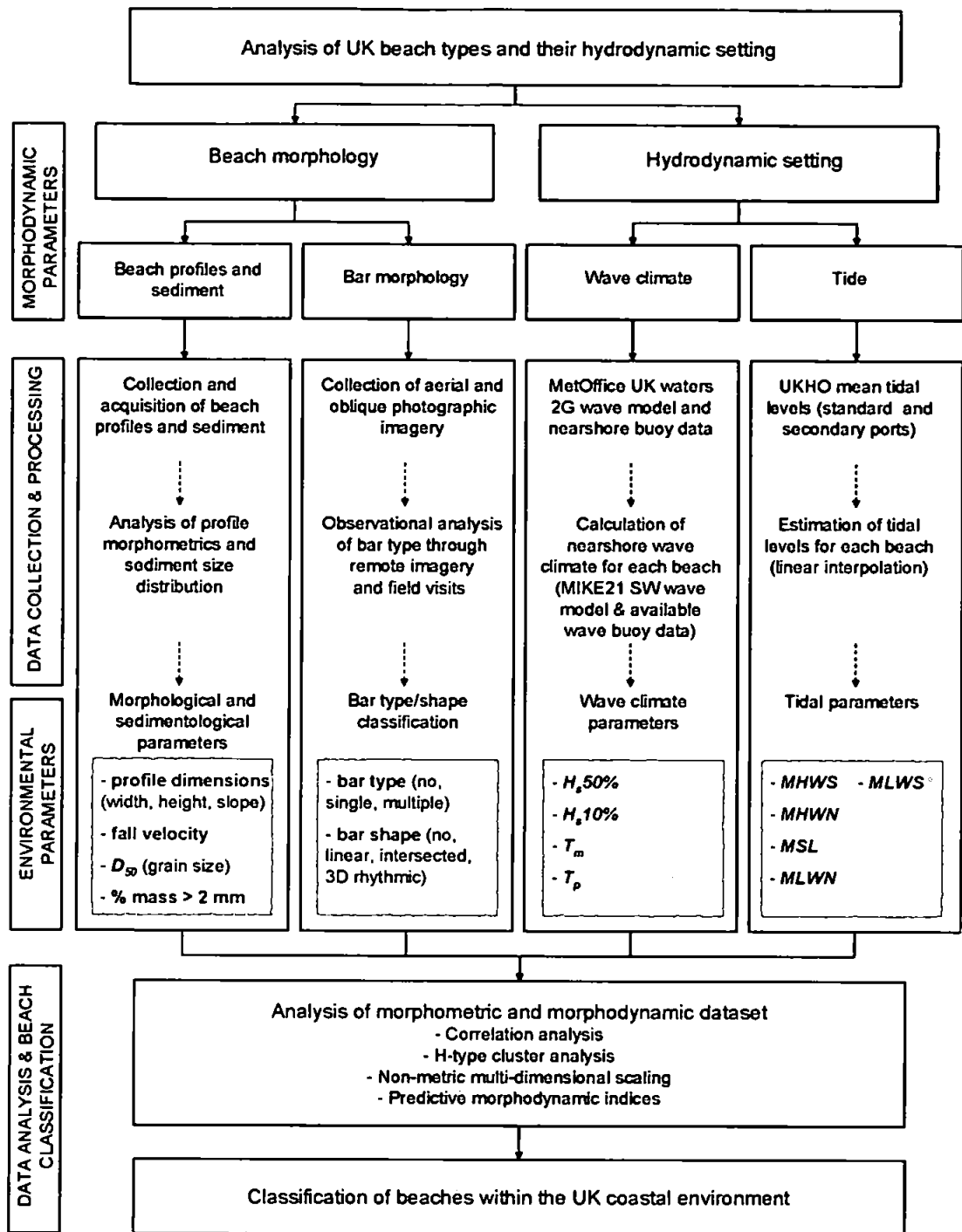
Figure 4.3 – Flow diagram of research methodology for this beach classification study.
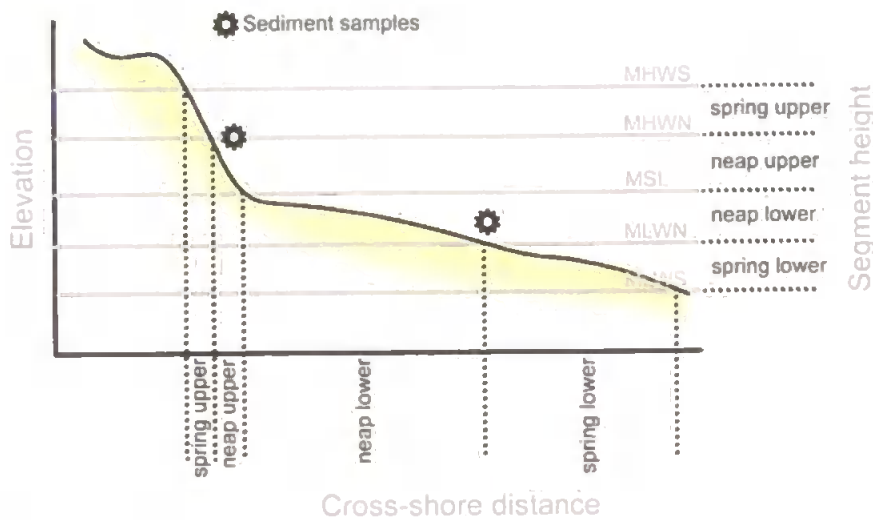
Figure 4.4 – Schematic of morphometric parameters.

cross-shore distance relating to each beach section, measured from the cross-shore locations of the profile intersection with mean tidal levels, were derived in conjunction with the overall width, height and slope of the inter-tidal zone (MHWS–MLWS). While other techniques were assessed, including delineation of sections using observed morphological features (Hegge et al., 1996), and the use of non-linear functions for regression analysis (Travers, 2007), the simple technique employed for this study provided a robust and consistent method which successfully reduced the profile form.

4.2.1.3 Sediment settling analysis

Sediment data for each profile were obtained. Where possible sediment samples were collected on the same day the beach profile was surveyed. In cases where third party survey data were used, sediment samples were generally collected within a month of the profile acquisition with five exceptions where sample separation was up to three months. Within the East coast, Liverpool Bay and Irish Sea regions, both third party survey and sedimentological data were used, both of which were collected synchronously. Summaries of sedimentological data sources for each region are displayed in Appendix 2. Surface sediment samples, collected for upper and lower beach locations (Figure 4.4) where taken from the top 1 cm of the beach surface and processed using a settling tube to acquire a mean settling velocity, sediment distribution statistics and inferred median grain diameter (D_{50}) for each sample (Ferguson and Church, 2004). A detailed description of settling tube and sediment sieving analysis, as well as calculation methods, are provided in Section 2.4. It was not appropriate to settle

sediment fractions > 2 mm therefore the coarse fraction (> 2 mm) was removed prior to settling and then weighed and sieved to calculate the percentage mass contribution and size distribution of the sample. For those samples with a significant gravel fraction, the coarse sediment distribution was included in the final calculation of D_{50}. All third party sediment size data were derived using standard sediment sieving techniques for particle size analysis (Blott and Pye, 2001).

4.2.1.4   Assessment of bar morphology

The assessment of bar morphology was crucial to the quality and usefulness of this dataset, due to the intrinsic relationship between bar morphology, surf zone circulation, rip current dynamics and hence beach hazards, alluded to in Chapter 3. Although the two-dimensional beach profiles provide an adequate measure of the beach morphology in the majority of cases, many of the beaches in the study displayed pronounced three-dimensional bar morphology. Remote imagery, acquired through oblique site photographs and aerial imagery, was utilised to assess this three-dimensionality at each site. Qualitative assessment of sub-tidal bar systems has been employed in a number of prominent studies investigating beach morphodynamics and state (Lippmann and Holman, 1990; Wright and Short, 1984) due to the difficulties in quantifying bar morphology. Ranasinghe *et al.* (2001) highlighted the problems associated with using qualitative techniques and presented a quantitative phenomenological scheme using video derived images to classify four intermediate bar morphologies. A similar scheme could not be employed in the present study due to the requirement of georectified time-averaged images for each site. Visual assessment of bar presence and type, for the purpose of this study, was deemed appropriate due to the relative ease in identifying the marked differences between the different bar states of interest. Figure 4.5 illustrates how the remote imagery was used to assess bar characteristics. Bars were classified in terms of type and shape (Figure 4.5). Bar type is defined by the presence of bars and their number. Bar shape describes the three-dimensional nature of the bar systems from linear two-dimensional to linear intersected and finally rhythmic bar systems that possess highly three-dimensional characteristics, commonly associated with rip current circulation and intermediate morphodynamic regimes (crescentic, rhythmic and transverse bar systems).
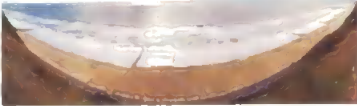
Bar type	Beach image	Bar shape
no bar		no bar
single bar		linear
multiple bar		linear intersected
		rhythmic (3D)

Figure 4.5 – Classification of bar type and shape with associated examples of remote image dataset.

4.2.2 Wave climate

Reliable information on wave climate is required in order to understand the morphodynamic relationships between beach types and hydrodynamic forcing. For the UK, this is not straightforward due to the variability in both the character of the coastal morphology and the variability of the wave climate around the coast. The beach sites in this study have been sub-divided into 6 distinct wave climate regions: the North Sea (F); the English Channel (E); the Atlantic Ocean (C); the Irish Sea (B); Liverpool Bay (A) and Lyme Bay (D). The lack of measured data, varying coastal orientation/exposure and the complexity of the changing magnitude of the bi-modal components of the regional wave spectrum meant that Lyme Bay had to be treated as a separate region. Within the context of this study the required wave breaker characteristics for each beach site were calculated using both measured and modelled nearshore wave statistics. Figure 4.1 gives

an overview of the wave climate regions and the data sources available for each region. Chapter 2 contains a comprehensive description of wave data sources (Table 2.1) and nearshore wave modelling using MIKE21 (Section 2.5.3).

Combining transformed wave model data and measured nearshore buoy data, estimations of the nearshore wave conditions (proxy to breaker height) were obtained for all beach sites within each region. In cases where a beach location is considered equidistant between two wave buoy locations, a linear interpolation was made between the two resultant annual wave records. Appendix 1 contains all calculated nearshore integrated wave parameters and associated metadata for all beach sites.

4.2.3 Tidal range

Within the UK coastal environment, an accurate understanding of the temporal variation in water level is vital to understanding the spatial variation in beach morphotypes. Mean tidal levels (MHWS, MHWN, MLWN and MLWS) were linearly interpolated between selected open coast ports at 100 m intervals to provide a continuous record of mean water elevations around England and Wales. Estimates of mean tidal elevations for individual beach sites were then extracted from this record using a minimum distance approach (Appendix 1). Resultant tidal elevations were transformed from Chart Datum (CD) to Ordnance Datum Newlyn (ODN), to enable cross-referencing with the beach profile dataset. Chart Datum, normally approximately the level of the lowest astronomical tide, varies from port to port with tidal range around the coast. Offsets to CD, published for each port, were also estimated for all individual beach sites through the same interpolation method as described above. Due to the availability of 98 standard and secondary ports within the study regions the accuracy of calculated values was considered sufficient at capturing the steep spatial gradients in tidal range.

4.2.4 Identification of morphodynamic groups

The interrelationships between morphological and environmental variables were examined to assess the presence or absence of distinct morphodynamic groups within the beach sites in the study region. Techniques of observation classification are an important suite of multivariate analysis and are widespread in science and industry and spread across a wide range of disciplines; examples include correlating tephra by means of geological fingerprinting in tephrachronology (Hermanns et al., 2000), employing multivariate cluster analysis in micropaleontology to compare microfossil assemblages

such as pollen, foraminifera or diatoms (Birks and Gordon, 1985), and assessment of surrogate approaches to vegetation description in ecology (Ramsay et al., 2006) used in data mining.

For this investigation a combination of mathematical and graphical techniques were used to interrogate the dataset and validate the resultant groupings. Firstly, the inter-relationships between morphodynamic variables were investigated through the calculation of Pearson product-moment correlation coefficients for all variables within the dataset (Pearson, 1896). Cluster analysis was then used as an exploratory tool to aid in the classification of morphodynamic variables into groups. Validations of the results from the cluster analysis were then performed using a method of non-metric multi-dimensional scaling. Finally, the ability of traditionally used predictive indices to describe distinctions in morphodynamic character between resultant beach groups was assessed.

4.2.4.1 Cluster Analysis

As a technique for identifying structure within a multivariate dataset, cluster analysis has been successfully employed in previous research in the field of beach morphodynamics and classification (Hegge et al., 1996; Travers, 2007). Cluster analysis is best thought of as a technique for illustrating graphically the relationships inherent in a distance or similarity matrix. Relationships within a correlation or similarity matrix can be represented as an easily understandable graphical tree (dendrogram), but the disadvantage is that for a large dataset some oversimplification is unavoidable (Middleton, 2000). For this investigation, a method of agglomerative hierarchical clustering analysis was used, which progressively reduces a similarity matrix to a smaller and smaller order. The reduction in matrix size is carried out by initially merging the two largest mutual similarities. These two samples are then expressed by some method of 'averaging' the similarities. This process is then repeated until all samples are represented by a single measure of similarity. The results are then expressed in the form of a hierarchical tree (Middleton, 2000). The groups resulting from this hierarchical cluster analysis are such that the most similar cases are linked most closely together. A number of authors provide comprehensive reviews of a wide range of cluster analysis techniques (Cormack, 1971; Everitt, 1980; Gordon, 1981; Middleton, 2000).

There are four main stages to performing a cluster analysis, and at each stage a range of options are available that can dramatically alter the outcome of the grouping (Middleton, 2000):

Variables and scaling

The chosen variables included within the cluster analysis were optimised through analysis of the correlation matrix where care was taken to avoid bias as much as possible by reducing the number of inter-dependant variables that were significantly correlated ($p < 0.01$). The inclusion of categorical, as well as continuous, variables within the dataset created some limitations in the methods available to calculate the similarity or distance measures between samples that were appropriate in this case.

Similarity measure

In literature, Gower's General Similarity Coefficient remains one of the most popular measures of proximity for mixed data types and has been successfully employed in cluster analysis, often in the biological sciences where mixed data types are common (Ramsay et al., 2006). This measure treats continuous and binary variables separately in the calculation of similarity, and pre-treatment of the continuous variables is unnecessary as they are scaled by range (normalised) within the algorithm. Gower's General Similarity Coefficient s_{ij} compares two cases i and j, and is defined as follows:

$$s_{ij} = \frac{\sum_{k=1}^{n} w_{ijk} s_{ijk}}{\sum_{k=1}^{n} w_{ijk}} \qquad (4.1)$$

where: $s_{ijk} = 1 - \frac{|x_{ik} - x_{jk}|}{range(k)}$ for quantitative data, $s_{ijk} = 1$ for matches of binary or multistate data and 0 for all mismatches. $w_{ijk} = 0$ for negative matches of binary data and 1 for all other situations (Gower, 1971).

Clustering method

The clustering method is the choice of algorithm used to average the similarities after merging the variables. All clustering techniques are based around this generated association matrix that defines the distance or, in the case of the present investigation, similarity between samples within a dataset, where higher values indicate increased proximity. This association provides a measure of multivariate proximity between

samples. As suggested by (Hegge et al., 1996) a sensible approach to clustering is to experiment with a range a clustering techniques. Such an approach both reduces the bias of selecting just one technique and increases the researcher's understanding of the grouping structure of the observations. Each clustering technique operates slightly differently and can give unique insights into the dataset. In this investigation four clustering methods were employed: Average linkage (weighted and unweighted), Ward's minimum variance, nearest and farthest neighbour. The statistical analysis software package Multi-Variate Software Package (MVSP) from KCS was used to perform this analysis.

Selection of cluster level

The final stage is to select the optimum number of groups for the particular application. Although there are many documented ways to perform this statistically, logic and experience of the dataset in question must be employed when analysing the results of the final cluster analysis. In practice this means that the onus remains on the researcher to select a realistic level that is most appropriate to the underlying research question (Chatfield and Collins, 1980).

When analysing the results of clustering techniques, it is important to keep in mind that a solution of structured groups will be produced regardless of whether real grouping in the data exists. Therefore, it is important to investigate and validate results thoroughly through an informed assessment as well as application of further analytical techniques.

4.2.4.2 Non-metric multi-dimensional scaling

The group structure of the resultant classification was examined using a method of non-metric multi-dimensional scaling (MDS) introduced by Kruskal (1964) and Shepard (1962) for application to problems in psychology. This is just one of a suite of multivariate tools designed to represent the samples in a data set in a reduced dimensional space (usually two-dimensional) to aid data summarization. MDS was chosen in this case due to its capacity to handle mixed data types (as discussed above). Unlike factor analysis, which requires the underlying data to be distributed as multivariate normal with linear relationships, MDS makes few assumptions about the distribution of the underlying variables. As long as the rank-ordering of distances (or similarities) in the matrix is meaningful, MDS can be used. MDS represents the samples as points in low-dimensional space such that the relative distances between the points are in the same rank order as the relative dissimilarities from the similarity matrix.

Therefore the proximity of samples within an MDS defines their similarity in community composition. The algorithm recognises the arbitrariness of absolute similarities, instead basing the ordination solely on the relative, ranked similarities (Clarke, 1993). To ensure convergence on an optimal solution the algorithm is run for multiple random restarts. The MDS ordination was performed using the PRIMER 6 software (Clarke and Gorley, 2006).

The measure of goodness-of-fit of the MDS ordination is termed the *stress* value for the required number of dimensions. This value ranges from 0 to 1 (where 0 is a perfect ordination). The *stress* value describes the level of scatter about the fitted non-parametric regression line of distance against dissimilarity according to

$$stress = \sqrt{\sum_j \sum_k \left(d_{jk} - \hat{d}_{jk}\right)^2 / \sum_j \sum_k d_{jk}^2} \qquad (4.2)$$

where $\hat{d}_{jk}$ is the distance predicted from the fitted regression line corresponding to the dissimilarity δ_{jk}. If $d_{jk} = \hat{d}_{jk}$ for all the $n(n-1)/2$ distances in this summation, the stress is zero (Clarke and Gorley, 2006). Stress levels of under 0.1 are considered to indicate an excellent ordination and levels of over 0.1 are considered unacceptable (Clarke and Gorley, 2006).

4.2.4.3 Morphodynamic indices

The suitability of a number of morphodynamic indices for describing the grouping resulting from the multivariate analysis was assessed. These indices are commonly used to describe and classify a continuum of beach morphologies and their associated morphodynamic regimes, There has been much discussion in literature of the validity of some of these indices in beach environments outside of those assessed in the original studies and the applicability of their use in mixed and sediment limited, low- and mixed-energy environments (Anthony, 1998; Gómez-Pujol et al., 2007; Hegge et al., 1996; Jackson et al., 2005; Jiménez et al., 2008; Levoy et al., 2000; Short, 2006; Travers, 2007).

This study will assess the use of three of these parameters. Firstly, the surf scaling parameter (ε) (Equation 1.1), used to describe the continuum between the reflective and dissipative surf zone regimes (Guza and Inman, 1975), recognizes that the transition

from surging to spilling breakers represents an increase in the amount of energy dissipation across the surf zone (Short, 1999). Secondly, the dimensionless fall velocity (Ω) (Equation 1.2), adapted by Wright and Short (1984) from Gourlay (1968) for use in describing beach and surf zone morphology and associated shoaling, surf and swash zones. Finally, the relative tidal range (*RTR*), defining the relative importance of shoaling, surf zone and swash processes across the inter-tidal profile.

Both the Ω and the *RTR* require a value of H_b for their calculation. In this investigation both modelled and measured wave data represent an inshore wave height (~ 10 m water depth). Previous investigations have estimated breaker height from the semi-empirical relationship provided by Komar and Gaughan (1973), based on Airy wave theory. This method significantly over predicts H_b, due to refraction and bed friction being ignored. Also, offshore non-directional wave data, used in some previous studies (e.g., Jackson et al. 2006), can potentially include wave travelling away from the coast.

4.3   SUMMARY OF ENVIRONMENTAL CONDITIONS

The final processed set of data included 92 beach sites throughout England and Wales representing a broad cross-section of morphodynamic settings enabling assessment of both beach type variability and distribution, but also associated morphodynamic regimes. This section describes the data set through a summary of the spatial morphological and hydrodynamic variability within England and Wales.

4.3.1   Regional offshore wave climate

Hydrodynamic forcing varies around the coastline of the UK. The following summaries of annual wave statistics for each study region provide an insight into this variation of offshore wave climate throughout the 5 study regions (Figure 4.1). Divisions of the directional spectrum obtained from offshore wave model records (M1–M6, Figure 4.1) represent sectors used for the inshore wave modelling within each region. The integrated wave parameters for each sector are included in Table 4.1.

Liverpool Bay (Region A, M1 model record) - Liverpool bay is a fetch-limited environment (100–150 km) with a directionally multi-modal, wind dominated wave regime. The highest energy wave events come predominantly from the W & WNW direction (peak energy direction) with a distinct second mode occurring in the E. Due to the wind-wave

130

Table 4.1 – UKMO model output statistics for selected directional sectors during 2007. Significant wave height H_s, peak wave period T_p, wave power P and resultant wave power vector angle for each sector $DirP$. Sectors represent wave rose divisions (Figure 4.6–4.10)

Sector	Obs (%)	H_s (m)					T_p (s)		P (kW m^{-1})		$DirP$ (°)
		Mean	σ	10%	50%	90%	Mean	σ	Mean	σ	
Liverpool Bay (M1, 50 m depth)											
A	46.3	1.33	0.84	2.62	1.09	0.44	6.6	2.1	19	28.2	293
B	10.7	1.06	0.6	1.91	0.97	0.38	5.0	1.2	8.9	12.3	14
C	11.2	0.92	0.46	1.66	0.88	0.38	4.6	1	5.7	7.5	87
Irish Sea (M2, 55 m depth)											
A	63.3	1.59	1.02	3.09	1.34	0.5	7.8	2.3	31.4	44.0	216
Southwest coast (M3, 60 m depth)											
A	68.4	2.42	1.69	5.06	1.81	0.81	10.3	2.3	114.1	195.4	263
B	12.3	2.81	1.62	5.06	2.5	0.84	9.1	2.1	116.4	168.5	221
Lyme Bay (M5, 25 m depth)											
A	61.2	1.34	0.90	2.62	1.12	0.34	7.9	2.5	25.2	36.1	197
B	18.7	0.88	0.51	1.59	0.78	0.31	5.5	1.2	6.8	9.4	112
East coast (M6, 25 m depth)											
A	27.7	1.17	0.55	1.88	1.06	0.59	8.2	2.7	15.3	17.2	2.7
B	23.5	1.45	0.79	2.69	1.19	0.62	6.6	1.43	23.0	27.5	79.2
C	20.9	1.37	0.65	2.28	1.22	0.66	5.7	1.26	16.6	20.6	153.8

dominated regime, wave energy is spread over a wide range of directions. Overall modal joint distribution events have a H_s of 1–1.5 m and T_p of 4.75–5.75 s (Figure 4.6). The directional spectrum was separated into 3 main sectors (A, B and C) defining key wave source directions experienced by the NE coast of Anglesey (Figure 4.6).

Irish Sea (Region B, M2 model record) - The Irish Sea is largely a fetch-limited sea to the west and north (100–150 km), but extended fetch and exposure to the Atlantic Ocean from the south, beneath the Republic of Ireland, allows the addition of a medium- to high-energy storm/swell wave signal to the wave spectrum. The Irish Sea is a mixed wind/swell wave regime. During 2007 the highest energy wave events came predominantly from the SSW & SW segments (peak energy direction) and overall modal joint distribution events had a H_s of 1.25 m and T_p of 6.25 s (Figure 4.7). The directional spectrum was separated into one main sector (A) defining the key wave source direction experienced by the SW coast of Anglesey (Figure 4.7).
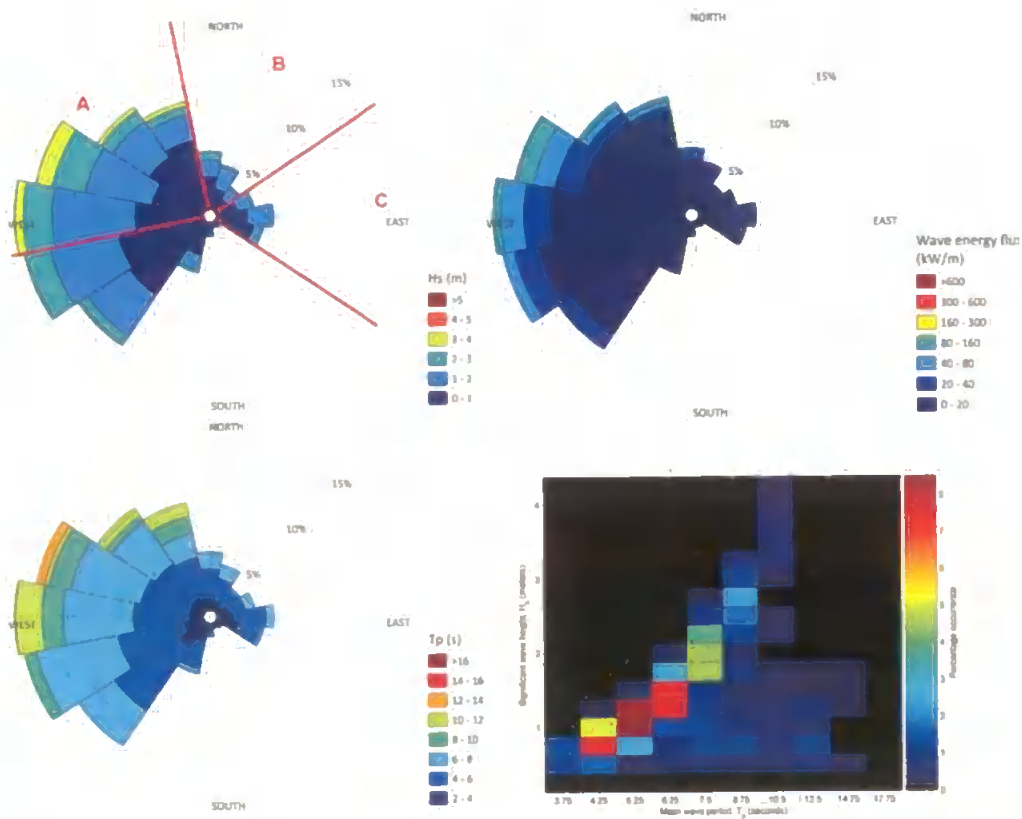
Figure 4.6 – MetOffice UK waters model output for M1 (Liverpool Bay) virtual buoy during 2007.
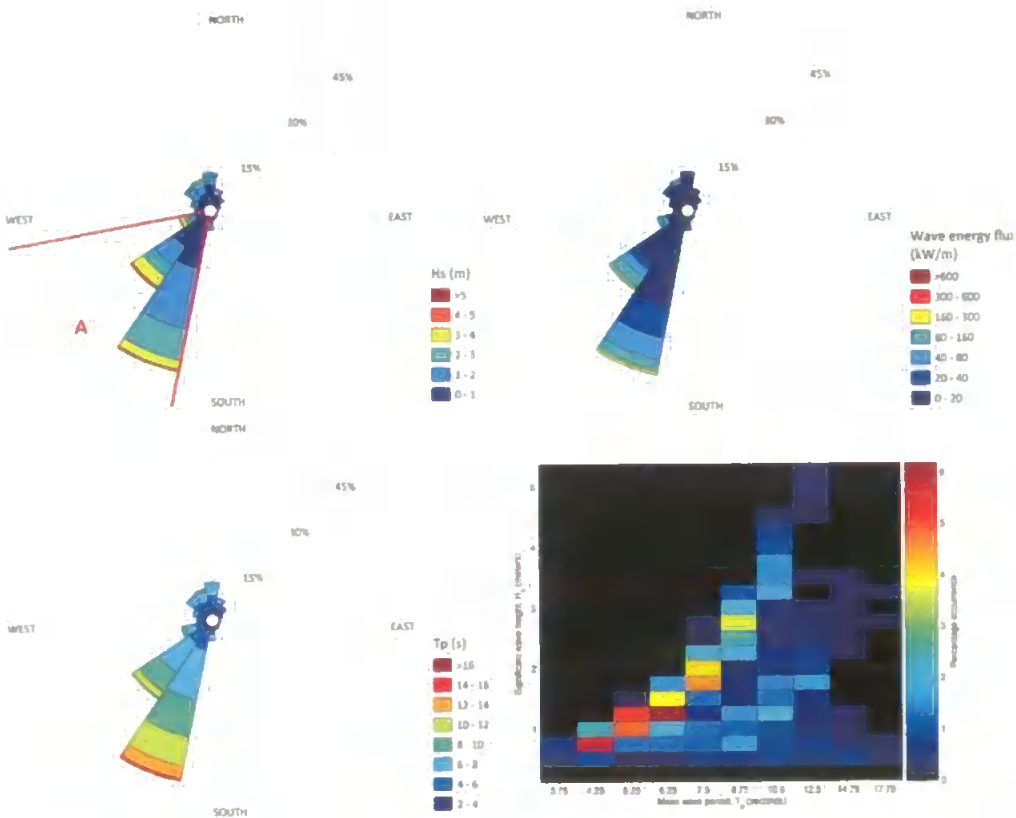
Figure 4.7 – MetOffice UK waters model output for M2 (Irish Sea) virtual buoy during 2007.
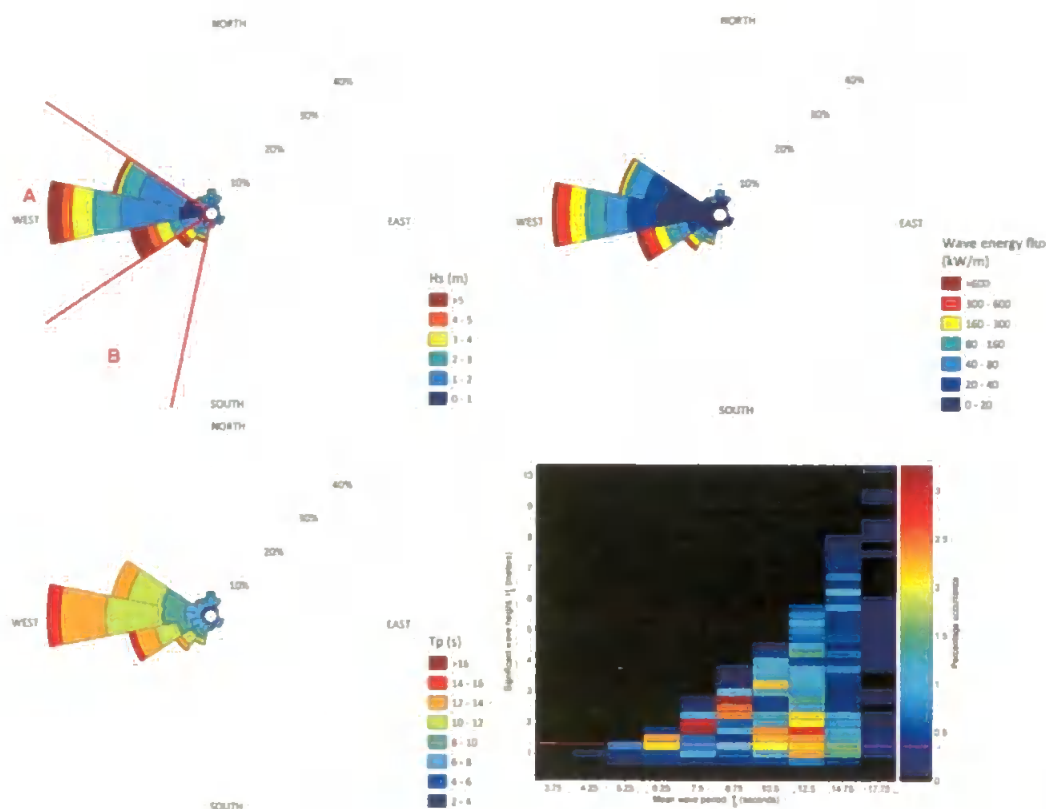
Figure 4.8 – MetOffice UK waters model output for M3 (southwest coast) virtual buoy during 2007.

Southwest coast (Region C, M3 model record) - The Atlantic west coast is a high-energy, predominantly fetch-unlimited environment, except from the N & NW where fetch is limited (100–400 km) due to the wave shadow of Wales and Ireland. The data indicates a directionally uni-modal, mixed wind/swell wave regime. During 2007 the highest energy wave events came from the W & WSW segments (peak energy direction) and overall modal joint distribution events had an H_s of 1.75–3 m and T_p of 7.5–8.75 s. The directional spectrum was separated into 2 main sectors (A and B) defining key source directions for the SW coast of Devon and Cornwall (Figure 4.8).

Lyme Bay (Region D, M5 model record) - Lyme Bay sits along a coast experiencing a mixed wind/swell wave climate. The bay is characterised by a change in coastal orientation from east-facing at the western end to progressively south-facing at the eastern end (Figure 4.2). With the predominant swell direction approaching from the west and wind waves from the southern and eastern quadrants, the region has a directionally bi-modal, mixed wind/swell wave regime. The relative contributions from both the swell and wind component varies spatially within the region due to variable shelter and fetch playing a key role in regional and local sediment transport pathways.
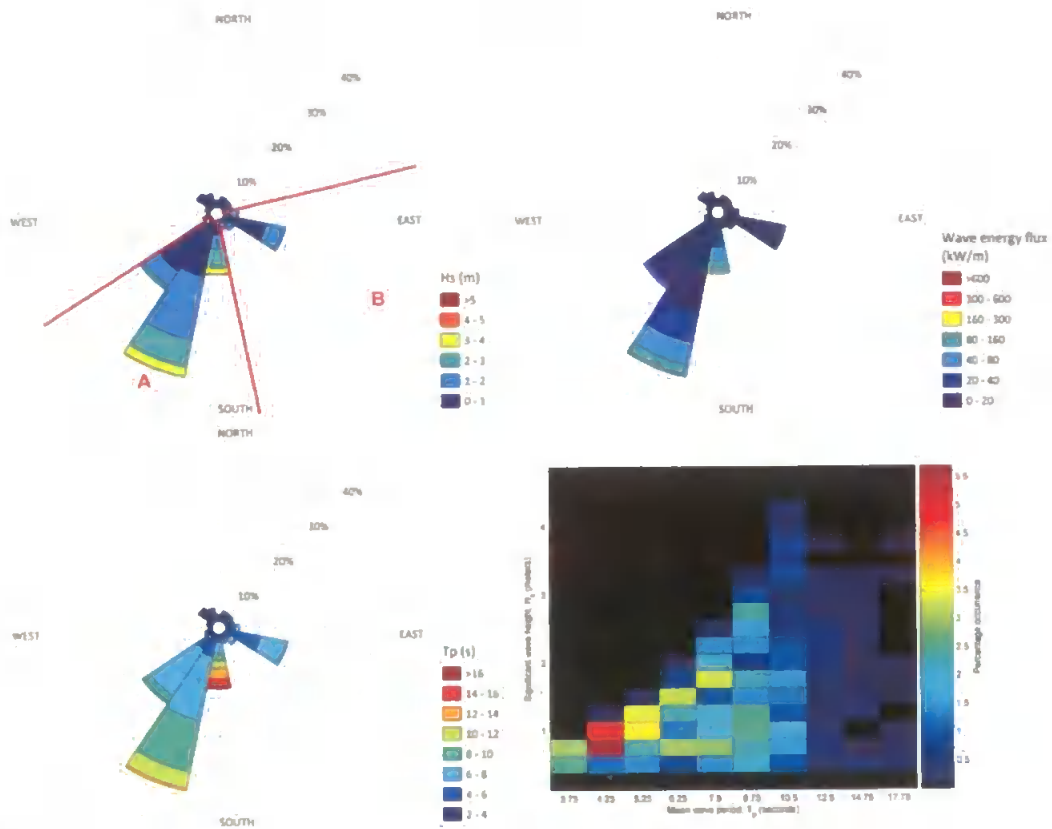
Figure 4.9 – MetOffice UK waters model output for M5 (Lyme Bay) virtual buoy during 2007.
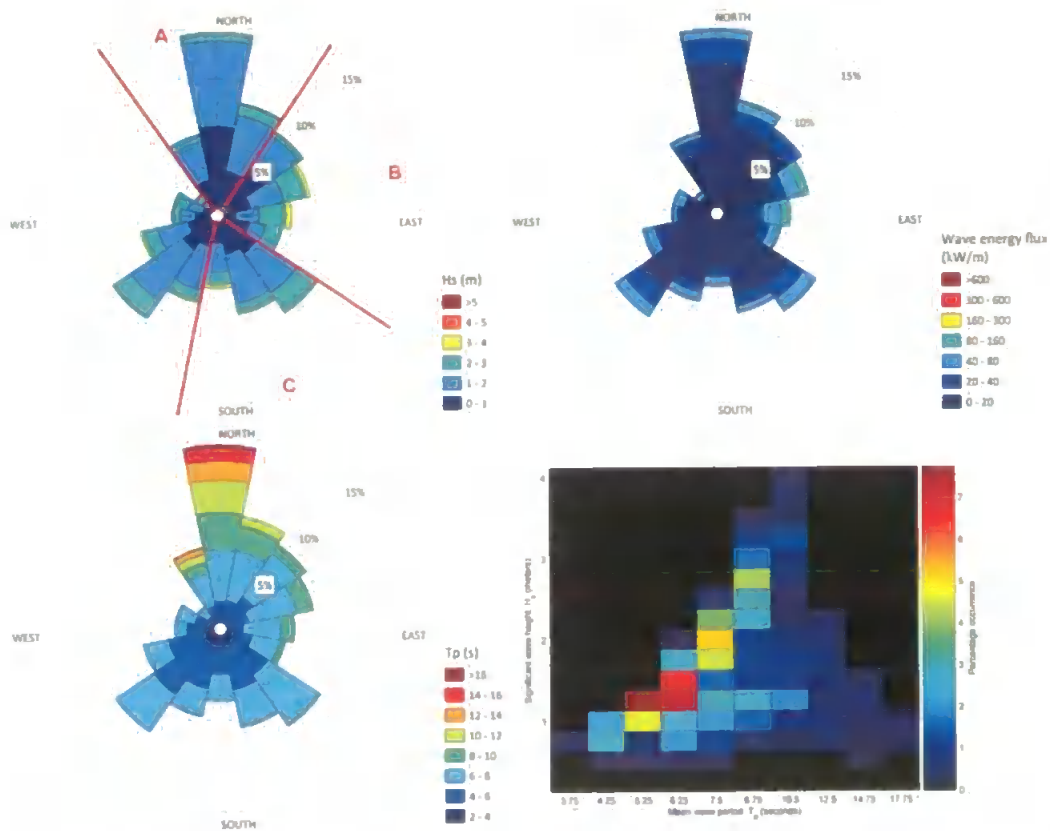
Figure 4.10 – MetOffice UK waters model output for M6 (East coast) virtual buoy during 2007.

During 2007 the highest energy wave events came predominantly from the S & SSW segments (peak energy direction). Overall modal joint distribution events had a H_s of 0.75–1 m and T_p of 4.25 s. The dominant swell-waves came from the SSW & S segments with a bi-directional wind-wave distribution from the SSW & S as well as from the ESE. The directional spectrum was separated into two main sectors (A and B) defining key wave source directions experienced by the SE coast of Devon and Dorset (Figure 4.9).

East coast (Region F, M6 model record) - The East coast has a directionally multi-modal, mixed wind/swell wave regime. Highest energy wave events come predominantly from the E & ENE segments (peak energy direction). During 2007 the overall modal joint distribution events had a H_s of 0.75–1 m and T_p of 4.25 s. The dominant swell-waves came from a fetch-unlimited northerly direction with wind waves being spread around all directions. The directional spectrum was separated into 3 main sectors (A, B and C) defining key wave source directions experienced by the E coast of Lincolnshire, Norfolk and Suffolk (Figure 4.10). The broad nature of the annual directional spectrum and the variation in the coastal orientation within the East Coast region meant that the available nearshore wave buoy data for the region were considered more appropriate than the transformed offshore model data.

4.3.2 Nearshore hydrodynamic climate

The coupling of nearshore wave buoy records and transformed wave model data, enabled an estimation of the nearshore wave climate for each individual beach. Figure 4.11 illustrates the 'round coast' variation in wave height, wave period and MSR. The six discrete regions (A – F) each represent unique combinations of these parameters describing a wide spectrum of hydrodynamic regimes. Nearshore wave characteristics for each region are a strong reflection of the offshore wave climates described previously. Region A represents a coast of low-energy, short-period waves ($H_{s50\%} < 1$ m; $T_m < 7$ s) with $H_{s10\%}$ values greater than 2 m at beaches on SW Anglesey (Region B). A macrotidal range exists throughout the region. Region C1 receives high-energy Atlantic swell waves. In the north, the Bristol Channel beaches are low-energy wind-wave dominated with an extreme mega-tidal regime (MSR ~ 10 m). In the west, the contribution of Atlantic swell and high-energy storm events to the wave climate is at a maximum. Within Region C1, fluctuations in nearshore wave height are due to local variations in beach orientation and the relative exposure (open coast, embayed or
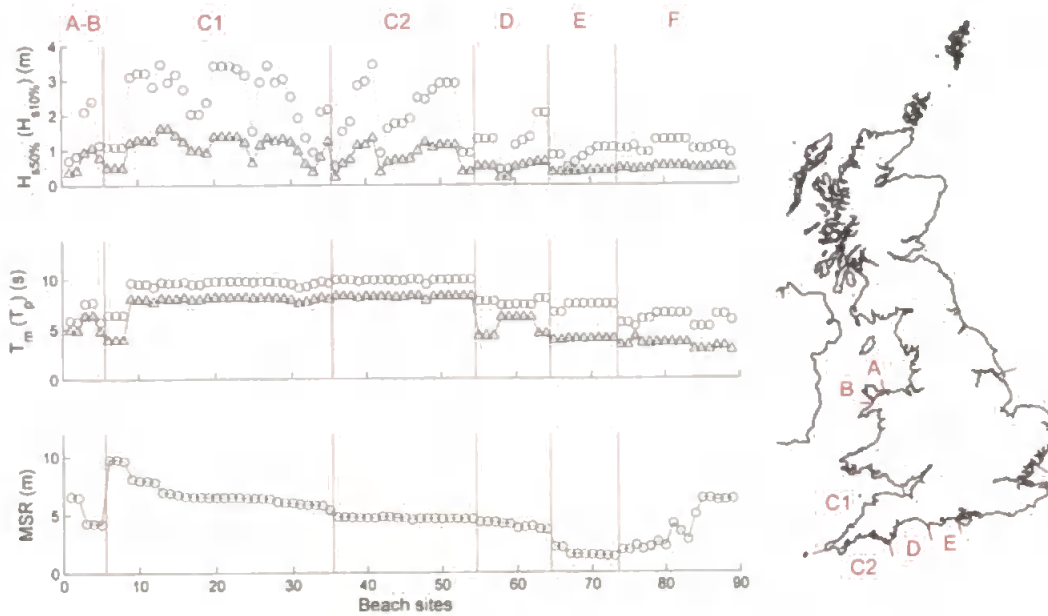
Figure 4.11 – Nearshore hydrodynamic conditions for each beach site moving anti-clockwise around the coast: (top) 50% exceedence significant wave height (triangles) and 10% exceedence significant wave height (circles); (middle) mean wave period (triangles) and peak wave period (circles); and (bottom) mean spring tidal range.

protected). Increased shelter from the Atlantic swell source in the west (regions C2 to E) drives a wave climate transition from swell-wave to wind-wave dominance. $H_{s10\%}$ remains high in a number of locations due to greater sea bed gradient relative to region C1 allowing for increased wave energy transmission to the surf zone. Finally, region F is characterised by the semi-enclosed North Sea wave climate and experiences similarly small, short period waves as region A ($H_{s50\%} < 0.6$ m, $T_m < 5$ s). Although exposed to swell from N. Atlantic and Arctic Oceans to the north, limited amounts of swell energy reach this region due to the shallow nature of the southern North Sea, where water depths, even up to 100 km offshore of region F remain on average less than 30 m.

MSR throughout the study sites is 4.9 m on average with a standard deviation of 1.9 m. This wide variance is largely due to the continental setting of the British Isles that is surrounded by constricting channels and semi-enclosed seas, modifying the N. Atlantic tidal oscillation. Figure 4.11 highlights these variations, in particular showing the results of tidal constriction in the Bristol Channel (region C1) squeezing the MSR at the selected beach sites above 10 m, as well as the effects of a degenerative amphidromic point, positioned inland of Bournemouth on the coast of southern England (region E) where a microtidal regime is observed with MSRs reaching as low as 1.2 m. A steady

136
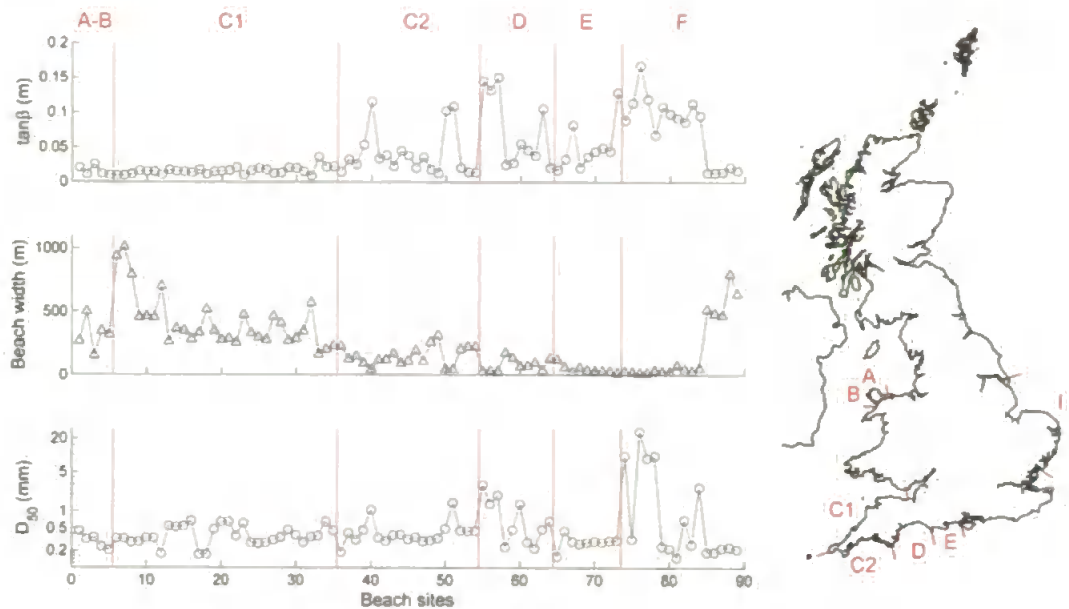
Figure 4.12 – Summary profile morphometrics and sediment size for all beach sites moving anti-clockwise around the coast: (top) mean spring inter-tidal beach slope; (middle) mean spring inter-tidal beach width; and (bottom) D_{50} for the lower inter-tidal zone at each beach site.

regional transition of MSR can be observed within the study sites from 9.77 m the Bristol Channel (Minehead) to 1.37 m in the English Channel, near Bournemouth (Fisherman's Walk). Another 'along-coast' transition occurs on the East coast where MSR is increasing northwards from 1.9 m to 6.35 m, away from the amphidromic point located in the eastern English Channel.

4.3.3 Beach morphology and sedimentology

It has been noted that within the UK, contrasting geologic environments exist with specific antecedent sedimentary characteristics. The interaction between these two environmental components provides a spatially dynamic nearshore setting throughout the UK. To some degree, the zonation on the basis of hydrodynamic parameters, depicted in Figure 4.11, is also reflected in the beach morphological parameters by gradient, width and D_{50} (Figure 4.12). Examples of the variability in profile form within the dataset are shown in Figure 4.13. Beaches throughout regions A, B and C1 are characterised by wide, flat and gently sloping profiles. Beach widths reach a maximum of 1013 m in the mega-tidal Bristol Channel and a minimum (162 m) at beaches in the sheltered macrotidal St Ives Bay. The average lower inter-tidal sediment
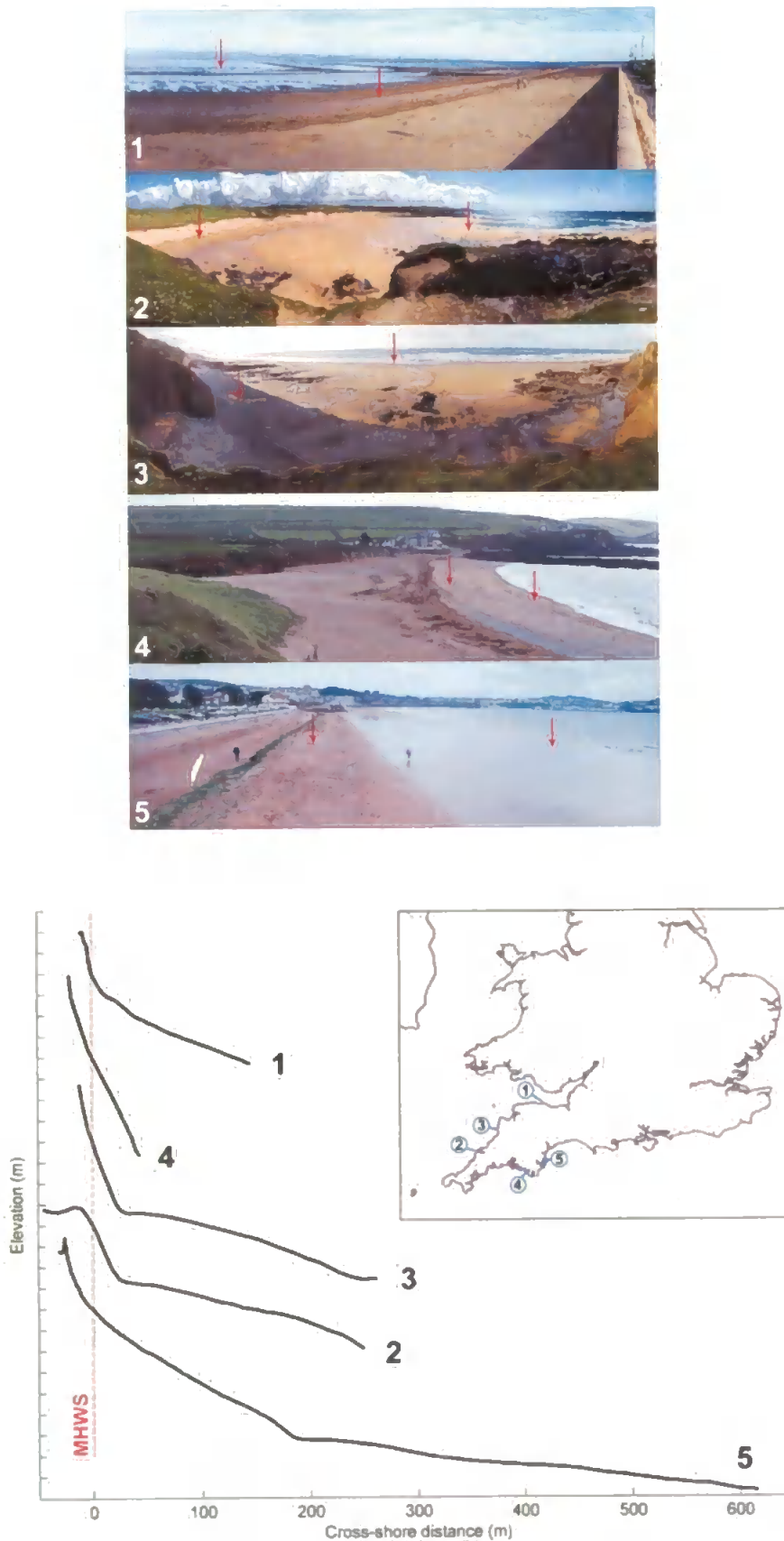
Figure 4.13 – (Top) Example oblique images of beach type variation within the dataset (numbers correspond to example sediment sites). Red arrows indicate approximate location of sediment samples. (Bottom) Cross-shore profiles of the five example locations.

size within regions A-B and C1 is 0.26 mm and 0.32 mm respectively and samples were in the sand size fraction throughout, with maximum D_{50} of 0.38 mm and 0.52 mm respectively. The south coast regions of C2, D and E show a progressive reduction in beach width in an eastward direction. Beach slopes within these regions were observed to be highly variable with an increasing occurrence of steep inter-tidal beach slopes. The steepest beach slopes occur, in most cases, with a corresponding increase in grain size. The micro- and mesotidal regions within Region E and F have a propensity for steeper, narrow beaches (minimum widths of 11 m and 13 m in Regions E and F respectively). The average lower inter-tidal sediment size within regions C2, D and E is 0.54 mm, 1.23 mm and 0.32 mm respectively with the highest grain sizes observed associated with steep gravel beaches. In region F the average grain size is 2.82 mm, but this region exhibits extremes in beach characteristics with very steep (maximum $\tan\beta$ = 0.168 at Orford Ness) beaches in Suffolk and wide, macrotidal, fine grained (minimum D_{50} = 0.19 mm at Theddlethorpe) beaches reaching widths of ~800 m.

Bi-modal, mixed sediments commonly occur throughout the UK coast. In many cases these multi-modal distributions manifest themselves as contrasting grain size distributions for the upper and lower beach sections. The different populations have different physical properties and are preferentially acted upon by different sediment transport mechanisms within the near-shore. Figure 4.14 illustrates the distribution of upper and lower beach median grain sizes (D_{50}), examples of which are shown in Figure 4.15, illustrating the broad variance of size, sorting, skewness and mineralogy within the
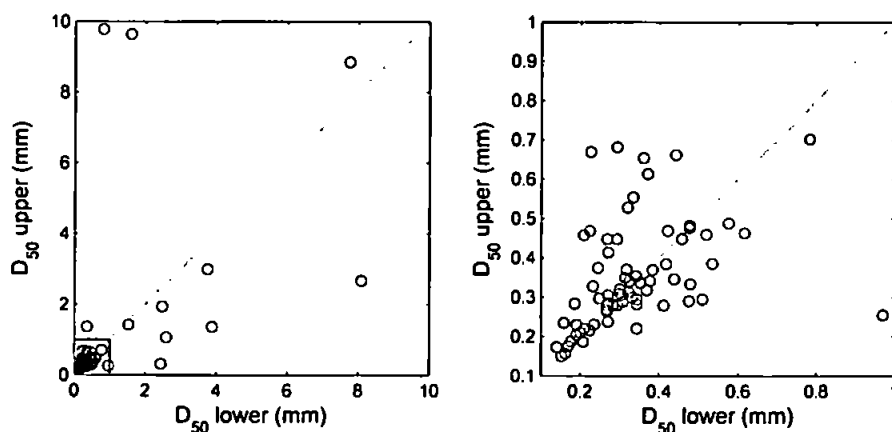
Figure 4.14 – Plots showing relationship between upper and lower D_{50} at all beach site (excluding Orford Ness where D_{50} upper = 26.32 mm and D_{50} lower = 21.05 mm): (left) all samples < 10 mm with exploded plot marked; (right) exploded view of all samples < 1 mm.

		Minehead (1)	Constantine (2)	Sandymouth (3)	South Milton (4)	Paignton (5)
UPPER BEACH	D_{50} (mm)	0.28	0.65	8 - 16	1.42	0.47
	%mass >2mm	0.0	19.6	72.1	10.8	0.7
	Mean w_s (psi)	-1.79	-3.09	-2.88	-3.92	-2.64
	Sorting w_s (psi)	0.40	0.53	0.45	0.24	0.84
	Skewness w_s (psi)	0.19	0.40	-0.06	-0.08	0.66
	Location	**Minehead (1)**	**Constantine (2)**	**Sandymouth (3)**	**South Milton (4)**	**Paignton (5)**
	Region	**C!**	**C1**	**C1**	**C2**	**D**
LOWER BEACH	D_{50} (mm)	0.19	0.36	0.33	1.52	0.22
	%mass >2mm	0.0	0.0	0.0	37.4	0.2
	Mean w_s (psi)	-0.92	-2.22	-2.09	-3.98	-1.32
	Sorting w_s (psi)	0.46	0.47	0.32	0.18	0.60
	Skewness w_s (psi)	0.24	0.12	0.25	0.05	-0.08

10cm

Figure 4.15 – Photographic examples of sediment sample at sample beach locations

region (examples correspond to those in Figure 13). Two themes seem to be apparent: within sites where sediment is coarse (gravel) throughout, the lower beach is more often coarser than the upper beach; and where one of both regions are within the sand fraction the lower beach is generally the finer.

Bar types are crucial to understanding the surf zone characteristics and hence potential bathing hazards. Broken down into observed presence/absence and abundance and three-dimensionality (non-linearity), bar characteristics can indicate the dominant hydrodynamic forcing mechanisms at each beach. Figure 4.16 maps the distribution of the simplified bar characteristics as observed from available remote imagery and field visits. The swell dominated regions of the west coast of England are the only region where strongly three-dimensional bar systems were observed (generally associated with rhythmic transverse bar/rip systems). Beaches with few or no bar features were predominantly found in lower energy mixed or wind dominated locations. Multiple bar systems were found in macrotidal, and predominantly low-energy environments in regions of sediment abundance associated with ebb-tidal deltas at estuary mouths (Masselink, 2004; Masselink et al., 2006; van Houwelingen et al., 2006). Observed cases of single linear bars were few; in all cases they were in micro- to mesotidal regimes in Poole Bay and southern Norfolk (Figure 4.16).
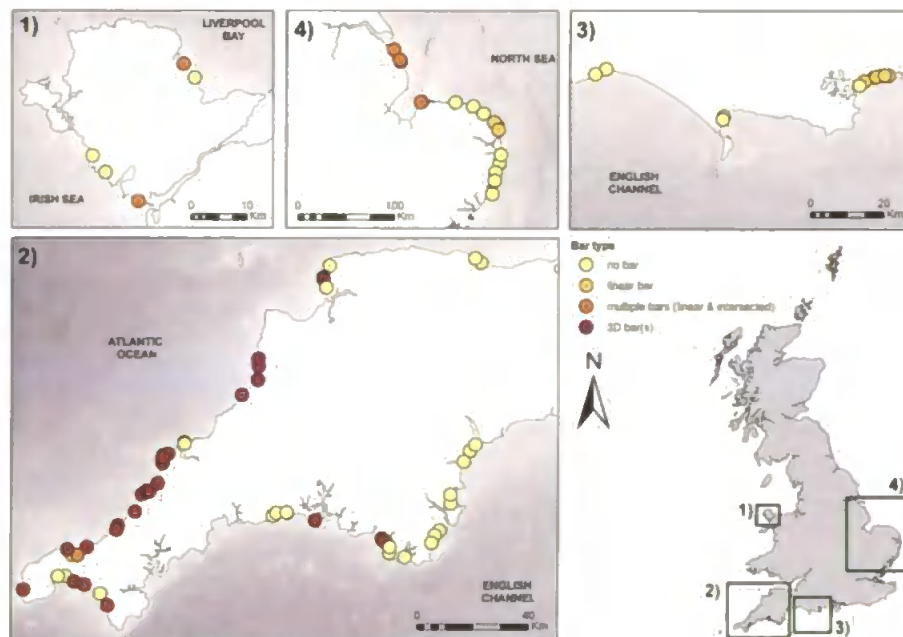
Figure 4.16 – Map illustration the distribution of bar types around the study beaches. Terminology refers to Figure 4.5.

4.4 CLASSIFICATION OF MORPHODYNAMIC GROUPS

4.4.1 Differentiation of morphotypes

Cross-correlation of morphodynamic variables shown in Table 4.2 gave an insight into inter-dependencies within the dataset. As expected, many of the morphometric variables (segment slope and width) were significantly correlated ($p < 0.01$) due to inter-dependence. Also, slope and width segments were a subsection of the inter-tidal slope and width so would be expected to provide the strongest correlations. These part-whole correlations are commonly observed in the natural world and as long as one is aware of these associations, Sokal and Rohlf (1995) state that there is nothing inherently wrong with calculating these correlations. The well documented, traditional relationship between grain size and beach slope (Bascom, 1951; McLean and Kirk, 1969) is reinforced within the sample sites where both upper and lower slope D_{50} and %mass >2 mm are strongly positively correlated with all slope parameters at the $p < 0.01$ level, with the exception of the upper beach coarse fraction and the spring low water slope. Interestingly, both lower and upper D_{50} were negatively correlated with T_p at -0.3 and -0.32 respectively ($p < 0.01$), indicating that finer grained beach profiles were in general associated with the regions of higher peak wave period. When interpreting these associations, one must be mindful of the effect the sampling strategy where regional distribution of various sites may be driving apparent dependencies. For example, fine grained beaches in the west may be due to regional sediment abundance and independent of the higher values of peak wave period associated with the region. Bar type relationships show dependencies that may have been expected: propensity for three dimensional bar/rip morphologies increases with all wave parameters ($H_{s10\%}$, $H_{s50\%}$, T_m and T_p) within the dataset; and multiple inter-tidal bar systems are positively correlated ($r = 0.55$) with $H_{s50\%}$ and MSR ($r = 0.45$) and negatively correlated with inter-tidal slope ($r = -0.45$).

The beach sites were grouped through cluster analysis on the basis of profile geometry, sedimentology and annual wave/tide climate. Analysis of the dendrogram, the graphical product of the cluster analysis and its associated agglomeration levels (Figure 4.17), enabled the grouping of beach sites based on the environmental variables detailed in Table 4.2. From the cluster analysis nine beach groups were defined at the 80% similarity level.

Table 4.2 – Correlation coefficients of environmental parameters used in the group classification. Red box highlights variables that are correlated by definition due to their inter-dependancies. Grey shading indicates correlations where *p*-values that are significant to the 0.01 level.

	Var.	S	S_SU	S_NU	S_NL	S_SL	D_SU	D_NU	D_NL	D_SL	D_TOT	H_TOT	Used_G	U_D	Lsed_G	L_D	H10	H50	Tp	Tm	B_STB	B_ITB	B_LIN	B_INT	B_B/R
Slope (intertidal)	S		0.62	0.85	0.94	0.94	-0.35	-0.55	-0.62	-0.56	-0.63	-0.55	0.43	0.48	0.78	0.58	-0.23	-0.29	-0.26	-0.39	0.13	-0.47	0.17	-0.25	-0.36
Slope (spring upper)	S_SU	0.62		0.67	0.58	0.52	-0.57	-0.57	-0.53	-0.53	-0.67	-0.57	0.55	0.44	0.54	0.46	-0.24	-0.27	-0.10	-0.18	0.22	-0.34	0.28	-0.26	-0.23
Slope (neap upper)	S_NU	0.85	0.67		0.83	0.71	-0.37	-0.71	-0.64	-0.55	-0.68	-0.62	0.46	0.51	0.65	0.56	-0.24	-0.31	-0.26	-0.37	0.20	-0.50	0.17	-0.26	-0.34
Slope (neap lower)	S_NL	0.94	0.58	0.83		0.84	-0.32	-0.55	-0.67	-0.54	-0.63	-0.58	0.41	0.42	0.74	0.47	-0.28	-0.33	-0.28	-0.41	0.14	-0.49	0.19	-0.21	-0.40
Slope (spring lower)	S_SL	0.94	0.52	0.71	0.84		-0.28	-0.45	-0.53	-0.54	-0.55	-0.47	0.33	0.31	0.71	0.43	-0.15	-0.21	-0.22	-0.35	0.12	-0.40	0.18	-0.22	-0.31
Width (spring upper)	D_SU	-0.35	-0.57	-0.37	-0.32	-0.28		0.46	0.50	0.39	0.71	0.47	-0.22	-0.14	-0.22	-0.14	0.04	0.07	-0.10	-0.09	-0.17	0.26	-0.18	0.41	0.01
Width (neap upper)	D_NU	-0.55	-0.57	-0.71	-0.55	-0.45	0.46		0.75	0.60	0.83	0.73	-0.29	-0.19	-0.36	-0.21	0.27	0.30	0.09	0.21	-0.24	0.42	-0.23	0.30	0.21
Width (neap lower)	D_NL	-0.62	-0.53	-0.64	-0.67	-0.53	0.50	0.75		0.74	0.90	0.82	-0.20	-0.22	-0.41	-0.24	0.29	0.34	0.11	0.22	-0.29	0.50	-0.28	0.30	0.30
Width (spring lower)	D_SL	-0.56	-0.53	-0.55	-0.54	-0.54	0.39	0.60	0.74		0.86	0.72	-0.27	-0.21	-0.36	-0.23	0.02	0.07	-0.12	-0.03	-0.27	0.32	-0.26	0.38	0.06
Width (intertidal)	D_TOT	-0.63	-0.67	-0.68	-0.63	-0.55	0.71	0.83	0.90	0.86		0.83	-0.30	-0.23	-0.41	-0.25	0.17	0.22	-0.03	0.07	-0.30	0.45	-0.29	0.43	0.16
Height (intertidal)	H_TOT	-0.55	-0.57	-0.62	-0.58	-0.47	0.47	0.73	0.82	0.72	0.83		-0.24	-0.28	-0.32	-0.23	0.45	0.47	0.24	0.39	-0.40	0.45	-0.49	0.17	0.39
Sediment >2mm (Upper)	Used_G	0.43	0.55	0.46	0.41	0.33	-0.22	-0.29	-0.20	-0.27	-0.30	-0.24		0.65	0.63	0.56	-0.12	-0.11	-0.22	-0.21	-0.20	-0.16	-0.16	-0.16	-0.13
D_{50} upper (mm)	U_D	0.48	0.44	0.51	0.42	0.31	-0.14	-0.19	-0.22	-0.21	-0.23	-0.28	0.65		0.54	0.87	-0.16	-0.16	-0.32	-0.24	-0.10	-0.15	-0.08	-0.08	-0.14
Sediment >2mm (Lower)	Lsed_G	0.78	0.54	0.65	0.74	0.71	-0.22	-0.36	-0.41	-0.36	-0.41	-0.32	0.63	0.54		0.66	-0.22	-0.25	-0.30	-0.34	-0.13	-0.33	-0.09	-0.14	-0.30
D_{50} lower (mm)	L_D	0.58	0.46	0.56	0.47	0.43	-0.14	-0.21	-0.24	-0.23	-0.25	-0.23	0.56	0.87	0.66		-0.14	-0.16	-0.30	-0.24	-0.09	-0.17	-0.07	-0.09	-0.15
Sig. wave ht (10% exceedence)	H10	-0.23	-0.24	-0.24	-0.28	-0.15	0.04	0.27	0.29	0.02	0.17	0.45	-0.12	-0.16	-0.22	-0.14		0.97	0.60	0.68	-0.08	0.47	-0.23	-0.26	0.72
Sig. wave ht (50% exceedence)	H50	-0.29	-0.27	-0.31	-0.33	-0.21	0.07	0.30	0.34	0.07	0.22	0.47	-0.11	-0.16	-0.25	-0.16	0.97		0.58	0.67	-0.12	0.55	-0.22	-0.21	0.73
Peak wave period	Tp	-0.26	-0.10	-0.26	-0.28	-0.22	-0.10	0.09	0.11	-0.12	-0.03	0.24	-0.22	-0.32	-0.30	-0.30	0.60	0.58		0.89	-0.03	0.18	-0.17	-0.39	0.54
Mean wave period	Tm	-0.39	-0.18	-0.37	-0.41	-0.35	-0.09	0.21	0.22	-0.03	0.07	0.39	-0.21	-0.24	-0.34	-0.24	0.68	0.67	0.89		-0.14	0.27	-0.31	-0.34	0.60
Bar type: sub tidal	B_STB	0.13	0.22	0.20	0.14	0.12	-0.17	-0.24	-0.29	-0.27	-0.30	-0.40	-0.20	-0.10	-0.13	-0.09	-0.08	-0.12	-0.03	-0.14		-0.30	0.71	-0.13	0.07
Bar type: intertidal	B_ITB	-0.47	-0.34	-0.50	-0.49	-0.40	0.26	0.42	0.50	0.32	0.45	0.45	-0.16	-0.15	-0.33	-0.17	0.47	0.55	0.18	0.27	-0.30		-0.16	0.43	0.62
Bar shape: linear	B_LIN	0.17	0.28	0.17	0.19	0.18	-0.18	-0.23	-0.28	-0.26	-0.29	-0.49	-0.18	-0.08	-0.09	-0.07	-0.23	-0.22	-0.17	-0.31	0.71	-0.16		-0.10	-0.22
Bar shape: intersected	B_INT	-0.25	-0.26	-0.26	-0.21	-0.22	0.41	0.30	0.30	0.38	0.43	0.17	-0.16	-0.08	-0.14	-0.09	-0.26	-0.21	-0.39	-0.34	-0.13	0.43	-0.10		-0.21
Bar shape: bar/rip	B_B/R	-0.36	-0.23	-0.34	-0.40	-0.31	0.01	0.21	0.30	0.06	0.16	0.39	-0.13	-0.14	-0.30	-0.15	0.72	0.73	0.54	0.60	0.07	0.62	-0.22	-0.21	

143
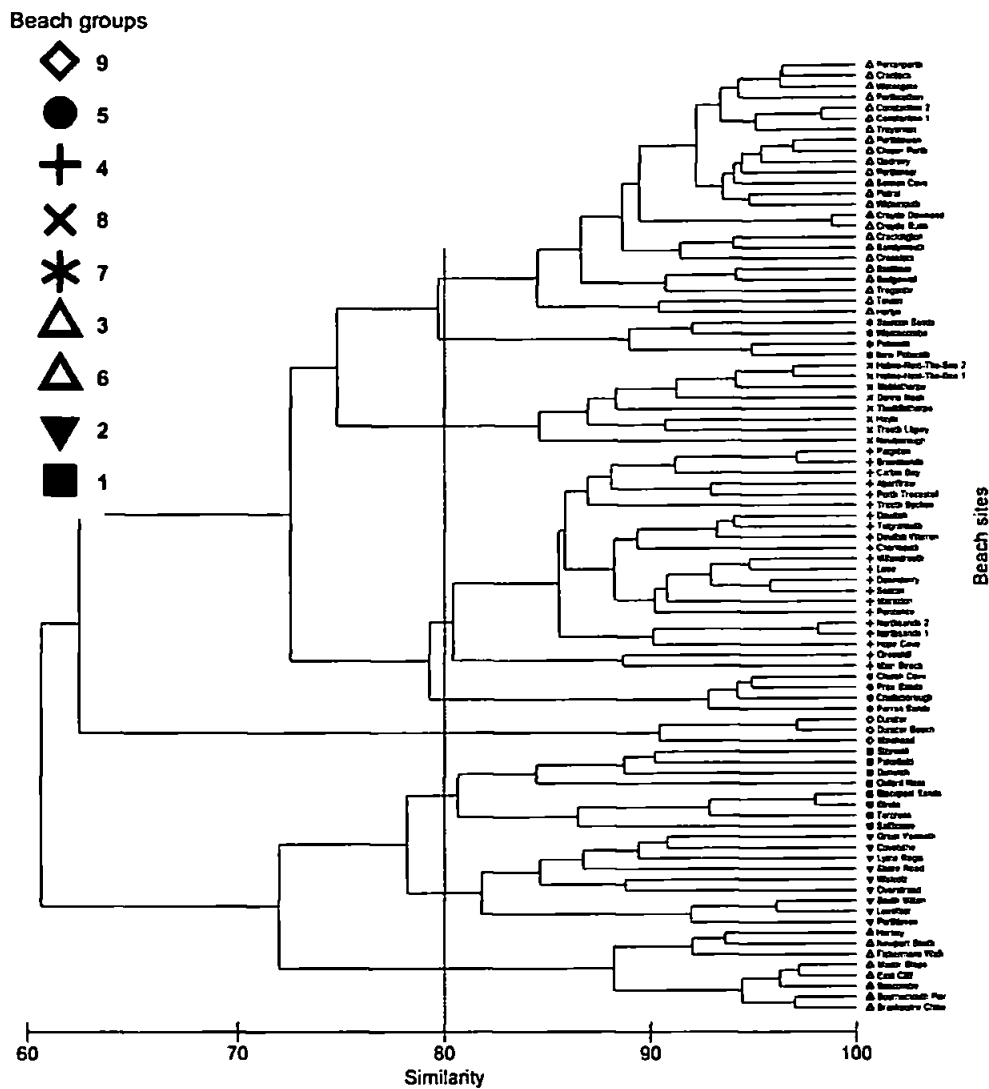
Figure 4.17 – Dendrogram clustered using unweighted pair group average (UPGMA) method. Symbols represent discrete beach groups attained using a cut-off level of 80% similarity.

The cut- off level was selected with knowledge of the beach sites in mind and represented the most appropriate resolution of classes for the number of beach sites and their observed morphological variance. Verifications of the significance of the clustering and the level of dissimilarity between groups were assessed by a graphical MDS (Figure 4.18) (Kruskal, 1964; Shepard, 1962). The ordination, with a 2D and 3D stress of 0.1 and 0.07 respectively (a measure of the goodness-of-fit), indicates a very good ordination with little possibility of additional information being gained through a three- or higher-dimensional solution (Kruskal, 1964; Clarke and Gorley, 2006). Figure 4.18 displays a reasonable level of separation within the defined beach groups (80% separation from Figure 4.17 represented as dashed lines) with the exception of groups 1,
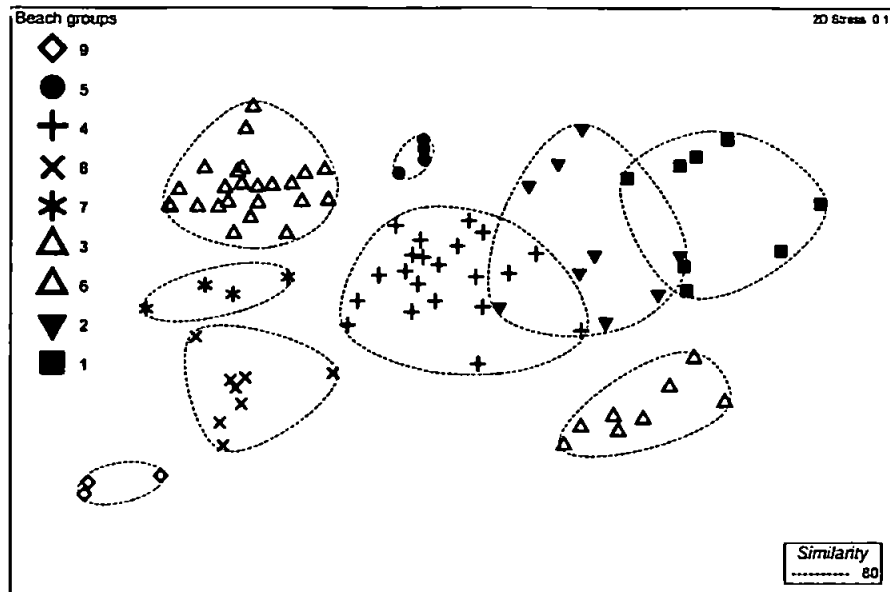
Figure 4.18 – MDS ordination plot, representing the rank order similarities in a two-dimensional space. Symbols indicate beach morphotypes generated through cluster analysis and dashed lines represent the groupings at the 80% similarity level.

2 and 4 that exhibited some overlap. This suggests that there are indeed some clear distinctions in environmental and forcing characteristics between the grouped beach types. The MDS analysis indicated that the clustering results were acceptable.

To investigate further the individual character of the defined groups the next step was to assess the within-group and between-group morphodynamic characteristics. Figure 4.19 plots all of the cross-shore profiles of group members relative to MHWS. This assessment of profile form shows immediately that beach morphometrics have a strong delineating influence on beach group membership. It is evident that both scale (MSR and inter-tidal width) and intra-profile variance of slope (i.e. beaches with clear break in slope or those with distinctive bar morphology) are important group variables. The profile groups at first glance appear to display a classic continuum from reflective to ultra-dissipative morphotypes first defined by Wright and Short (1983). Although between-group profile distinctions between: groups with steep profiles and smaller tidal ranges (1, 2 and 3); intermediate groups (4 and 5); and groups representing the transition to dissipative (6 and 7) remain unclear. This suggests that these groupings are not purely morphometric and that hydrodynamic and sedimentological parameters are also important.
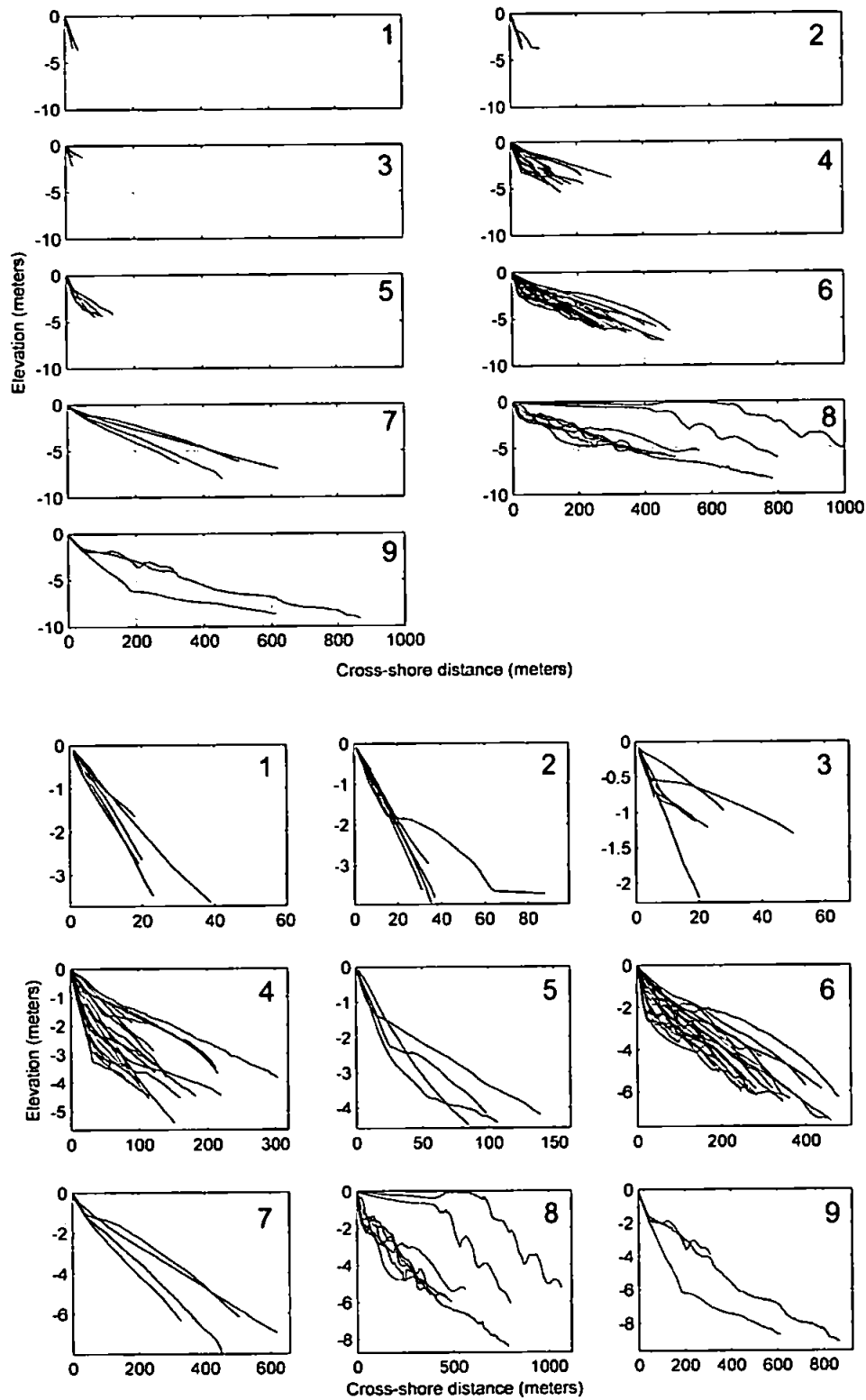
Figure 4.19 – Cross-shore profiles of beach sites within each morphotype grouping: (above) fixed scale indicates relative cross-shore and vertical extents; (below) scale to fit plots show individual profile geometries. Numbers indicate beach group.
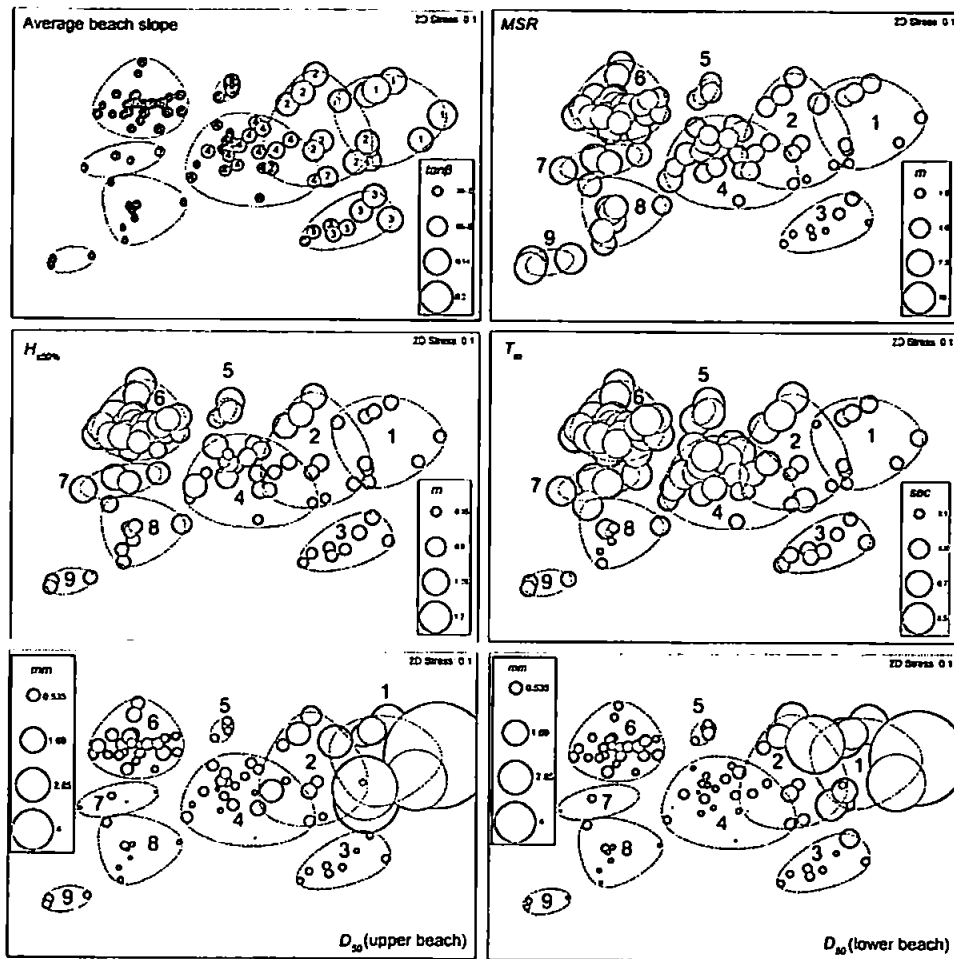
Figure 4.20 – MDS ordination of morphotype groups. Marker scaling with beach slope (tanβ), MSR, $H_{s50\%}$, T_m and upper and lower beach D_{50} allows graphical assessment of trends within and between groups). Levels of 2D Stress provide an indication of goodness-of-fit. Numbers indicate beach group.

The range of values of hydrodynamic and sedimentalogical variables associated with each group were assessed through MDS analysis (Figure 4.20). Clear trends in environmental conditions can be seen across the groups. Beach slope, a principle controlling mechanism in the reflective or dissipative nature of the surf zone, as was suggested through observation in Figure 4.19, contributes to the definition of clustered groups in one dimension, but hydrodynamic variables appear to be a controlling delineation between groups with common slope characteristics. Analysis of the relationships between wave height and tide range in Figure 4.21 indicates that in addition to beach slope, many of the beach groups are hydrodynamically distinct, with characteristic ranges of wave height and tide range. Due to the interdependence
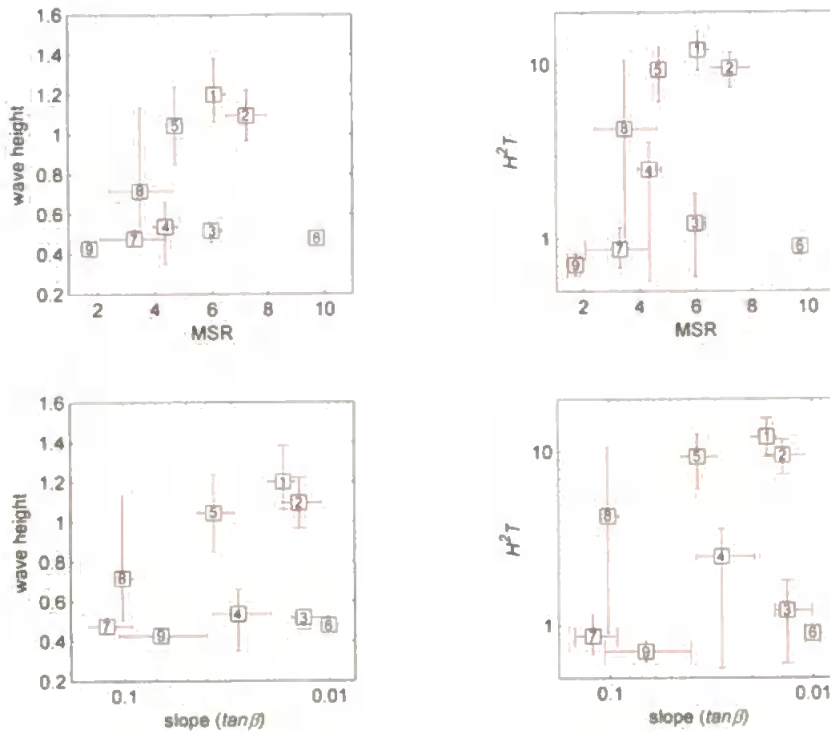
Figure 4.21 – Beach group relationships between tide range and slope are presented against both wave height and wave energy: (top left) wave height ($H_{s50\%}$) against mean spring range (MSR); (top right) wave energy scaling parameter ($H_{s50\%}^2.T_m$) against MSR; (bottom left) wave height against beach slope ($tan\beta$) parameter; and (bottom right) wave energy against slope. Boxes indicate modal values for each group and stems indicate values of the 25th and 75th percentiles of the group distribution.

apparent in tide range, beach slope and grain size; wave height, and hence wave energy, seems to be a key environmental control on the clustered beach types.

The ability of wave height and energy flux to define groups through MSR and beach slope was graphically explored in Figure 4.21. Beach slope appears to better distinguish between groups than MSR. Values for beach slope were significantly correlated to MSR and grainsize parameters within the dataset suggesting that slope provides more information on beach morphodynamics than MSR in this case. Figure 4.20 shows that wave height and MSR vary through the groups upon the same axis (both variables decrease from top left to bottom right) whereas slope and grain size vary perpendicular to the hydrodynamics (both decreasing from top right to bottom left) suggesting that it should be expected that wave energy flux and slope provide a better definition of groupings. In fact, wave height and slope in Figure 4.21 provide the best separation of
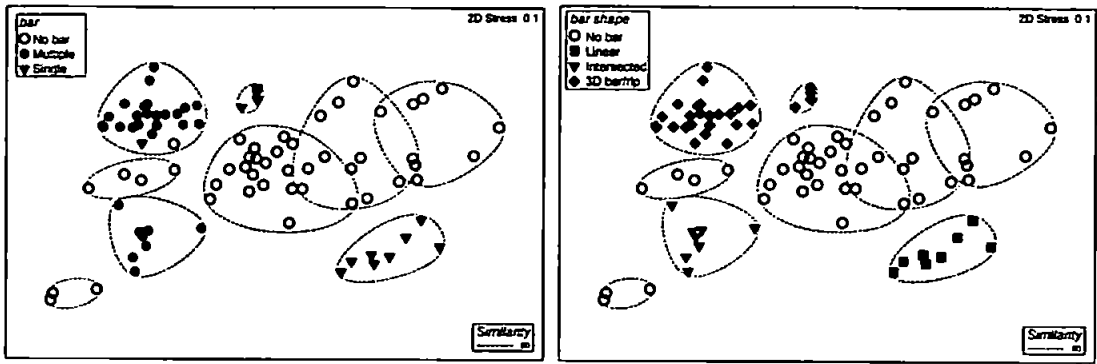
Figure 4.22 – MDS ordination with markers indicating bar type; (left) bar number; (right) bar shape.

groups with the least overlap, effectively differentiating beaches with observed three-dimensional bar morphology. Interestingly, bar type distribution throughout the groups, summarised in Figure 4.22, differentiates between beach groups of similar slope angle. As bar morphologies are known to be strongly dependant on absolute values of wave forcing it is not surprising that distinction of wave energy flux levels may also be important in defining bar characteristics between groups with similar slope. A number of trends within the dataset due to sampling must be borne in mind when viewing these relationships, particularly for application in a broader context, firstly, the high-energy sampled beaches are nearly all upper macrotidal and secondly, low-energy sampled beaches are mostly lower macro- to microtidal.

The improved understanding of the relative contributions of the morphodynamic variables that define beach group character (grain size, wave energy flux, beach slope and bar morphology), enable the classification of the identified groups (1-9). Where appropriate, for consistency, these group characterisations follow those well documented in literature (Masselink and Short, 1993; Wright and Short, 1984):

Reflective gravel: R(G) (group 1)

Highly reflective, steeply sloping beaches with slope angles ranging from 4° to 9°. Characterised by medium to coarse gravel on the upper and lower beach face, the grain size appears to be a significant controlling factor in beach type with sites occurring throughout micro- to macrotidal environments. Beaches occur in low-energy regions of Lyme Bay and the East Coast ($H_{s50\%}$ ~ 0.5 m, T_m ~ 6-7 s). These beaches typically observed to maintain a step feature at the base of the swash-zone (Wright and Short, 1984).

Reflective sand: R(S) (group 2)

Reflective, steeply sloping beaches comprised of beach slopes ranging from 5° to 6.5°. Occurring in micro- to macrotidal environments, grain sizes range from medium sand to fine gravel (commonly 10–15% gravel content) and one difference from group 7 is the occasional presence of a finer submerged terrace. These beaches occurred in a wave climate where $H_{s50\%}$ and T_m range from 5–1.1 m and 6–10 s respectively. These beaches were found along the southwest, south and east coasts of England.

Linear sub-tidal barred: STB (group 3):

A predominantly reflective beach face with inter-tidal slopes observed between 1.2°–7.2° and a sub-tidal linear bar characterise this group of beaches. They occur in a mainly microtidal environment. They appear to represent the transition to the classic linear barred beach type, more often observed in microtidal beaches worldwide, and associated with the two-dimensional end of the intermediate spectrum (Masselink and Short, 1993; Wright et al., 1986). Upper beaches observed consisted of medium sand with a medium to coarse sand lower beach. Little or no coarse fraction was found at the sites. Due to the apparent requirement of a microtidal range for development, it is no surprise that these beaches were contained within the south (Poole Bay) and east coasts of England.

Low-tide terrace / non-barred dissipative (low-energy): LTT/NBD(LE) (group 4)

A group, containing a range of beach morphologies from low-tide terrace with a distinct break in slope to highly featureless dissipative, is characterised throughout by a lack of significant bar systems. The group represents a bar-less transition through intermediate and dissipative regimes with inter-tidal slopes ranging from 0.8°–3.1° degrees. Observed in meso- and macrotidal settings, grain sizes (D_{50}) range from medium to coarse sand/gravel in the upper beach with gravel fraction reaching up to 50% in some cases, and a lower beach of fine to medium sand with coarse fractions reaching up to 25% on occasion. A textural discontinuity in some samples is often associated with a break in slope and a low-tide terrace beachform and groundwater seepage face (Turner, 1993) and is reported as being commonplace within high-latitude coasts (Carter, 1988). The group has a low-energy mixed wave climate with $H_{s50\%}$ from 0.2–1.1 m, and T_m from 4–8 s. Separated through observed profile geometry, 38% of beaches could be

considered dissipative with no significant slope break during period of observation. Beaches were found in Wales (Liverpool Bay, Irish Sea) and southwest, south and Lyme Bay regions of England.

Low-tide terrace and rip: LTT+R (group 5)

A small collection of beaches within the southwest coast of England appear to possess the required setting within the study to form beaches with a low-tide terrace structure in addition to three-dimensional bar systems, often characterised by rip current activity. Ranging from 1.4°–3° in slope, these beaches occur within a macrotidal (4–5m), regime with medium sand size and negligible coarse material (<5%). Importantly, the wave climate is higher energy than group 4 ($H_{s50\%} \sim 0.7$–1.4 m, $T_m \sim 8$ s), specifically characterised by a large increase in $H_{s10\%}$ (1.8–3.5 m).

Low-tide bar rip: LTBR (group 6)

Representing the largest sample group, these high-energy ($H_{s50\%} \sim 0.8$–1.6 m, $T_m \sim 8$ s, and $H_{s10\%} \sim 1.5$–3.5 m) beaches predominantly exist on the west and southwest coasts of England. With slopes of 0.57°–1.26° and inter-tidal zones 200–450 m wide, these macrotidal beaches can be considered dissipative in overall nature. In many cases the dissipative characteristics are tidally induced (increase in RTR). The presence of mid- and particularly low-tide bar and rip current morphologies display many characteristics of high-energy barred micro- to mesotidal intermediate beaches in literature (Masselink and Short, 1993; Wright and Short, 1984). Sample sites had medium-coarse sand upper beaches with occasionally a significant gravel component. Lower beaches were of medium sand with no coarse fractions. Although common in overall slope, this group exhibits a range of profile forms from those approaching a low-tide terrace to those closer to a dissipative beach.

Non-barred dissipative: NBD(HE) (group 7)

Bar morphology is generally absent from these dissipative beaches. Located on the high-energy Atlantic west coast, with $H_{s50\%} \sim 1$–1.2 m and $T_m \sim 8$ s these beaches are swell dominated. The presence of homogeneous fine to medium sands throughout all sites meant beach slopes were observed between 0.63°–0.92° degrees, leading to very wide (300–700 m) inter-tidal zones within the macro- to mega-tidal settings.

Multiple inter-tidal barred: MITB (group 8)

The occurrence of multiple inter-tidal barred beaches appears to be associated with abundant sediment sources, often in proximity to ebb-tide deltas of estuaries occurring throughout the coastal regions (Masselink, 2004). Sites occurred in macrotidal environments where sand was fine to medium throughout (samples taken on bar crests). Beaches were typically characterised by slopes of 0.52°–1.26°, widths of 300–800 m, and a low-energy wave climate with $H_{s50\%}$ in the range of 0.4 – 0.7 m, and T_m from 3 – 5 s. The only exception to this is Hayle where $T_m = 7.7$ s.

Ultra-dissipative and tidal flats: UD(+TF) (group 9)

With only 3 samples identified, this is a small sample of a group of beaches that are isolated to mega-tidal regions. Tidally dominated, they generally occur in channels and mouths of large estuaries/inlets. Examples include the Bristol Channel and southern English Channel (Levoy et al., 2000), which have the required basin structure and/or 'funnel effect' to generate extremely high tidal ranges. This often leads to low-energy, semi-sheltered wave climates like the Bristol Channel, where $H_{s50\%} = 0.5$ m and $T_m = 4$ s. These mega-tidal (MSR = 9.7 m) sites had flat and wide inter-tidal zones of 800–1000 m with slopes of 0.52°–0.63° and no bars. The tidally dominated lower inter-tidal zone had slopes of 0.34°–0.4° throughout the sites. Sediments were medium sand in the upper beach and very fine – fine sand in the lower beach. These beaches represented the transition to tidal flats as identified in Short (1999).

4.5 DISCUSSION

4.5.1 Morphodynamic domains

The beach dataset was analysed within the context of traditional morphodynamic indices expressed in Equations 1.1–1.3. This enabled important comparisons with previous work and created a context by which to assess the morphodynamic relationships between the identified beach groupings.

4.5.1.1 Surf scaling parameter

Values of the surf-scaling parameter (ε) for each beach site (Figure 4.23) were in general agreement with surf zone conditions observed at each site, confirming ε is useful in discriminating between reflective and dissipative extreme beach states, although, as identified in previous studies, ε performed poorly in characterizing intermediate states (Bauer and Greenwood, 1988). It was expected that ε would be an effective discriminant, due to its inclusion of beach slope as well as wave steepness in its generation, shown in section 4.4.1 to be a reasonable group descriptor.

Some disagreement occurs within the reflective beach types, where many fall into the reflective end of intermediate. These beaches represent, in most cases, the first features of the transition to a low-tide terrace form with the slope break often located around MLWS. In addition, as ε does not account for grain size, some gravel reflective beaches (type-controlled by grain size) have values in the intermediate range. The LLT/NBD group also displays values of ε that indicate intermediate and dissipative surf zone conditions highlighting the effect that extending the width of the low-tide terrace, often through an increase in tidal range, has on the overall surf zone regime. The range of values seen in the STB type can be explained by both, the difficulty in establishing a representative inter-tidal beach slope within the microtidal climate and resolution of the tidal interpolation routine within the highly spatially variable tidal characteristics within Poole Bay. The surf scaling parameter defines the overall regime well, indicating that the defined beach groups delineate differences in morphodynamic regimes and that in one dimension, beach groups are separated by means of a combination of wave steepness and inter-tidal beach slope.

Figure 4.21 shows that the beach groups are in part defined by the average annual hydrodynamic conditions and the MSR. The wave height and period indicate the

absolute level of wave energy flux, and hence level of infragravity energy within the surf zone (Goda, 1975; Guza and Thornton, 1985). Therefore, the combined effect of these variables have an impact on: beach scale, characteristics of bar morphology (through wave dissipation, long wave dynamics) and tidal translation rates (sweeping of surf zone processes across the inter-tidal profile). Figure 4.24 indicates that when plotted against deep water wave energy flux (H^2T), group definition is improved though the separation of groups with different bar morphologies. The rhythmic barred intermediate beaches (groups 5 and 1) clearly occur within the higher energy wave climates differentiating between the LTT/NBD and STB (groups 9 and 4) beach types in lower energy conditions. Of course, it is important to recognise that additional factors associated with individual regions, specifically the geological setting, nearshore slope characteristics and sediment size distribution and mineralogy could also be controlling factors in bar presence as well as wavelength variability (Short, 1999). The principal drawback of ε is that it requires the knowledge of beach slope. Previous studies have indicated that the dimensionless fall velocity Ω can be used to predict the occurrence (Dalrymple, 1992; Dean, 1973; Sunamura and Trenhaile, 1989) and type (Wright and Short, 1984) of bar morphology, although some have suggested this may not be the case in low energy and Ω fluctuating environments (Gómez-Pujol et al., 2007; Masselink and Pattiaratchi, 2001; Masselink and Short, 1993).

4.5.1.2 Dimensionless fall velocity and relative tidal range

The next approach was to assess the ability of the combination of the Ω and RTR to describe and categorise the morphodynamic characteristics of the beach groups. This approach, proposed as a two-dimensional conceptual matrix for beach classification by Masselink and Short (1993) is used widely but in some cases caution of its uncritical application has been urged due to the limited number of beach sites originally incorporated into the model and its simplistic nature (Jackson et al., 2005). A number of researchers have suggested its application is not always practical in the presence of constraining or modifying conditions such as the presence of very coarse sediments, nearshore reefs and low energy conditions (Hegge et al., 1996; Sanderson and Eliot, 1999).

When applied in this relative context, the beach sites within this study exhibited some clear distinctions in their location within the two-dimensional matrix (Figure 4.25).
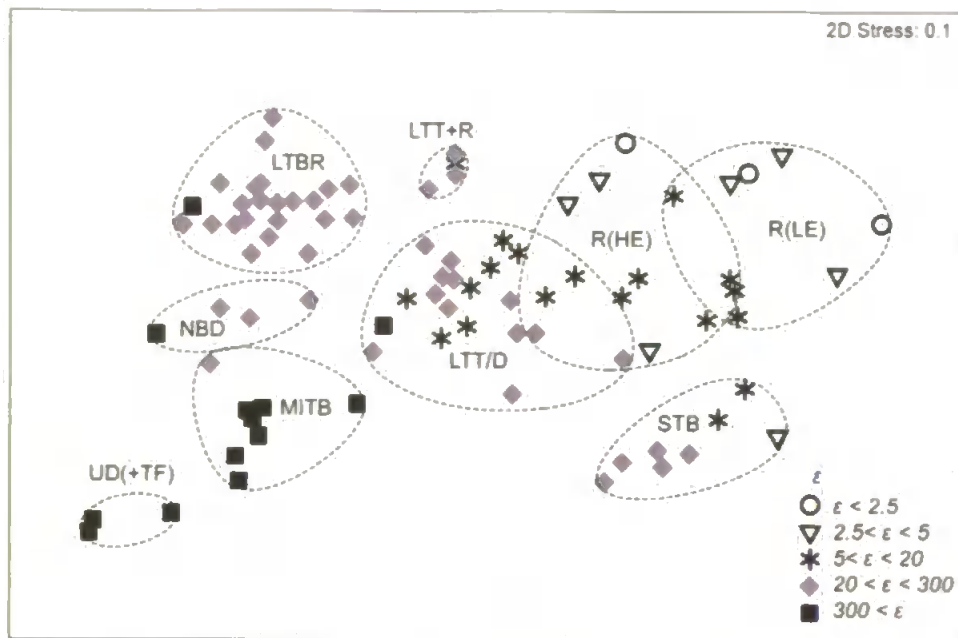
Figure 4.23 – MDS ordination with markers indicating values of the surf scaling parameter describing wave dissipation characteristics in surf zone. Beach type code indicates beach group associated with each dashed region.
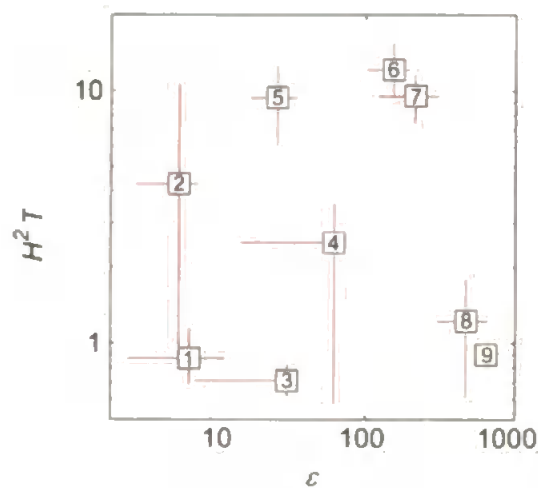
Figure 4.24 – Plot of deep water wave energy flux scaling parameter ($H_{s50\%}^2.T_m$) against the surf scaling parameter. Boxes indicate modal values for each group and stems are values of the 25th and 75th percentiles of the group distribution.

Variations in Ω from group to group describe the transitions from reflective to dissipative beach types quite well although in some cases a degree of scatter was observed. The use of *RTR* to define the additional importance of tidal effects enabled the definition of the transition from R to a LTT/NBD beach state and eventually to UD+TF. Significantly, the beach group identified as LTT/NBD appeared to show a large degree of within-group division. The use of Ω and *RTR* appears to clearly distinguish between a low-tide terrace form with a significant reflective upper beach and a non-barred dissipative form where the reflective upper beach has all but disappeared (Ω dimension). In essence, the group contains a range of low-energy beach forms that display no significant bar morphology and are of similar scale (MSR and inter-tidal width) where values for Ω and *RTR* are very sensitive to changes in hydrodynamic and sedimentary conditions. Due to the low-energy waves, mixed sediments and relatively high tidal ranges that characterise many of these beaches, relative contributions of each will be significant in controlling beach form and scale. Also, a higher variation in values of Ω and *RTR* is unavoidable within expected error levels through point sediment sampling and nearshore wave estimation. Therefore, the significance of this grouping within this relative context must be viewed with appropriate caution.

Absolute wave energy

Considering all beach groups, Ω appears to struggle to define the bar morphologies within the intermediate groups. Ω seems capable of describing the sequence of morphologies from R (no bars), through LTT+R and LTBR with bar/rip systems to NBD(HE) (planar) within the high energy environments, but the STB and LTT/NBD beaches plot within a similar relative context and have contrasting bar morphologies.

This may suggest the role of absolute wave energy flux, as indicated in Figure 4.26 is an important factor in differentiating between barred and non-barred beaches within a UK context. Absolute wave energy, historically correlated with infragravity wave motion in the surf zone, is considered key to the formation of three-dimension bar systems associated with rip currents and cell circulation (Wright et al., 1979). Typically in a microtidal (intermediate/dissipative beaches) environment, infragravity wave height in the surf zone is 20 – 60% of the offshore wave height (Goda, 1975; Guza and Thornton, 1985). Masselink and Short (1993) highlighted this issue of the potential importance of absolute wave energy level as a cautionary note in the context of their conceptual beach state model.
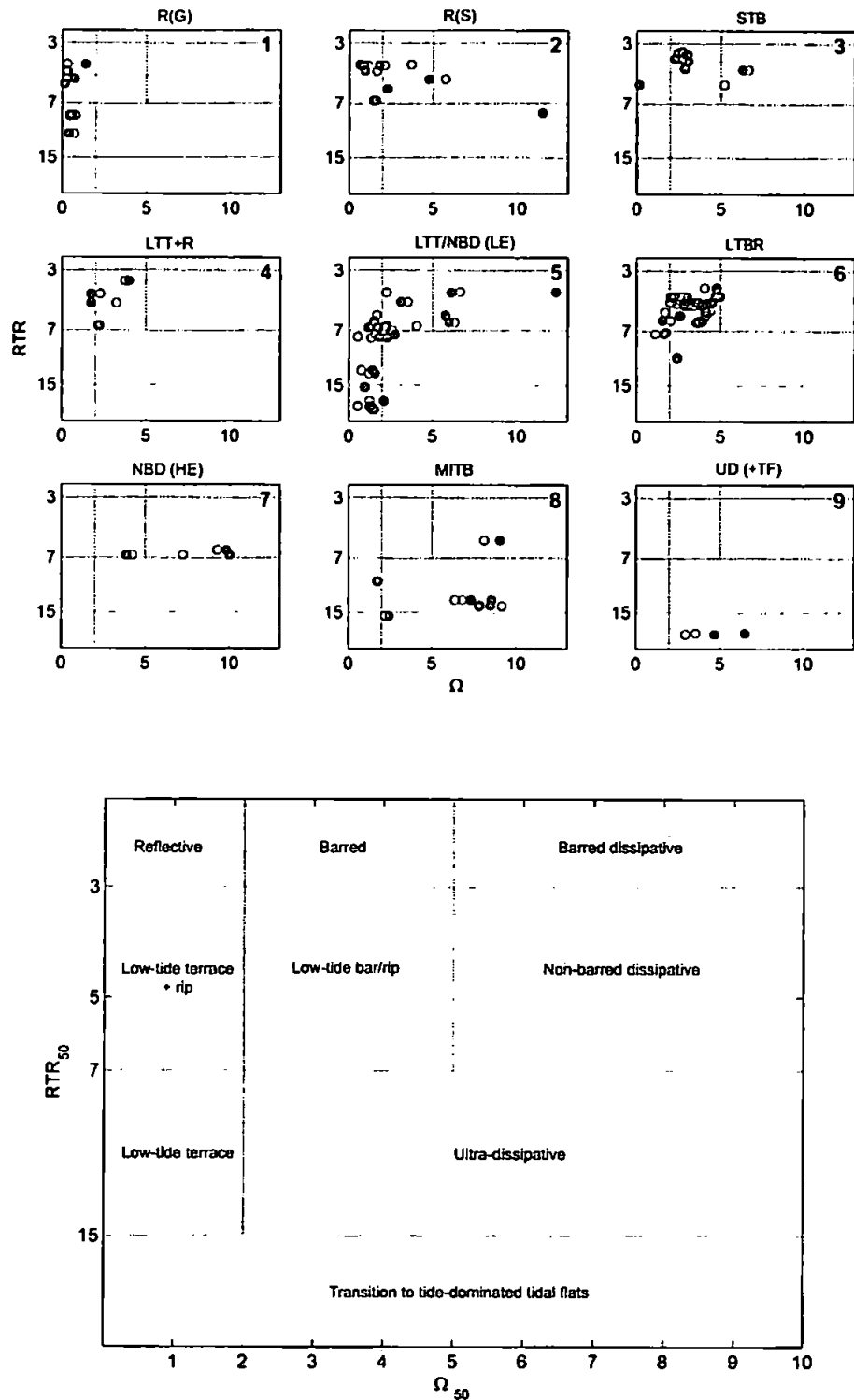
Figure 4.25 – Top: Subplots show values of Ω and RTR for each beach group. Grey and white circles indicate lower and upper beach values for omega, respectively. Framework of grey lines indicate delineations as suggested by (Masselink and Short, 1993). Bottom: Beach types as defined in (Masselink and Short, 1993).
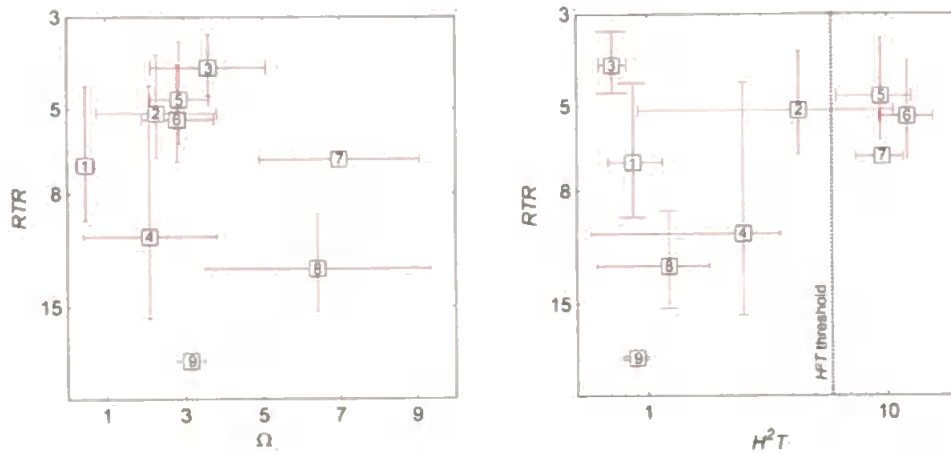
Figure 4.26 – Plot of Ω (upper beach) against RTR (left) and deep water wave energy flux $(H_{s50\%}^2.T_m)$ against RTR (right). Boxes indicate modal values for each group and stems are values of the 25th and 75th percentiles of the group distribution. Numbers indicate beach group.

Absolute tide range

Absolute values of tidal range, within a coastal environment such as the UK, will also be a significant controlling factor in beach type and indeed it appears to be an important factor in the grouping of beach types through the cluster analysis (Figure 4.20; Figure 4.21). Absolute tide range has two key influences on beach morphology. It controls scale, as increasing tide range will inevitably increase the beach inter-tidal width, leading to the presence of an increasingly lower gradient, wider and eventually more tidally dominated lower beach. Also, increased tidal translation rates, the rate of change of the shoreline and surf zone across the beach, have a strong influence in the capacity of the surf zone processes to develop beach morphology at any given location (Short, 1999). High levels of tidal translation inhibit resonant growth of sub-harmonic and infragravity oscillations deemed important in moulding beach morphologies especially in microtidal environments (Guza and Davis, 1974; Wright et al., 1982). Therefore, development is restricted to the high- and low-tide periods of relative stationarity. It is also interesting to note that a lower level of infragravity energy is experienced in macrotidal environments as opposed to microtidal intermediate-dissipative beaches (Masselink and Hegge, 1995; Wright et al., 1982). This may be an influencing factor in any designation of threshold values to separate beach groups.

Grain size

Scatter and overlap of beach sites within Figure 4.25, after consideration of wave energy levels, occurs principally among the R(S) and LTT/NBD beach groups. These beach groups exemplify the effects of absolute values on position within a relative context like that of Ω and RTR. The two groups contain beaches from a wide number of regions with tide ranges from 1 m to > 4 m. Specifically, within these sites, the role of sediment size and between-site and within-site distribution will have a significant control on beach form and stability through the contrasting sediment transport pathways of the often multi-modal sediment fractions and hence the effect of beach drainage on form and stability (Turner, 1993). Variants of the R to LTT/NBD beachform are in many cases controlled by the tide range and sediment characteristics, as well as the local coast geomorphology and drainage characteristics. Groundwater outcropping mid-beach often occurring at the slope break on LLT beaches leads to a highly saturated lower beach and a comparatively dry upper beach. This contrast affects drainage capacity and infiltration/exfilltration characteristics, and in turn sediment mobility and morphodynamic characteristics (erosive/accretionary) of the two zones. This effect is enhanced by the decoupling of the groundwater table within the beach face in regions of higher tide ranges where water levels decrease faster than the drainage capacity of the beach (Short, 1999; Turner, 1993).

Environmental setting

Finally, consideration must also be paid to beach system boundary conditions limiting the development of potential beach forms, particularly geological control (Gómez-Pujol et al., 2007; Jackson et al., 2005). The underlying geology establishes the framework within which the beach forms is set. The geometry of the substrate boundary can limit the morphological evolution via the shape and volume of accommodation space (McNinch, 2004), and the nature, source and abundance of beach materials. Where there is an abundance of re-workable sediment available to the beach, and the substrate constraints are limited, the beach form will be largely controlled by the prevailing and antecedent hydrodynamic conditions. In cases where this is not the case, profile development may be constrained. This is exemplified by the MITB sometimes termed 'ridge and runnel' beach forms (low-amplitude ridges), that, although requiring a low gradient (dissipative/ultra-dissipative) are known to occur largely in regions of high sediment abundance, often in proximity to ebb-tide deltas associated with estuaries (Kroon and Masselink, 2002; Short, 1991).

159

4.5.1.3 Overview

With the previous description of the UK coastal environment and its Holocene evolution in mind, sediment type, source and abundance, as well as drainage characteristics through local coastal geomorphology and absolute tidal and wave energy characteristics, will almost certainly have a role in the measured beach forms within this investigation. The role of absolute wave height has been highlighted as a key factor in differentiating beach types and highlights some of the drawbacks of using the relative parameters Ω and RTR. Figure 4.26 provides an overview of the beach group locations within the Ω and RTR and H^2T and RTR two-dimensional space. The combined representations provide a comprehensive overview of the beach group morphodynamics. On one hand, Ω accounts for the important influence of sediment size, and wave energy flux accounts for bar type distinctions, providing a useful tool for developing an understanding of beach morphodynamics within the context of this study and the UK coastal environment. On the other hand, the addition of a wave energy flux parameter, in this case, enables the improved differentiation of beach groups based on bar type. To enable a simplified three-dimensional view, it would be useful to derive a threshold wave energy value (H^2T), which could distinguish between high- and low-energy environments. In this case, a threshold wave energy flux (deep water) of $H^2T = 5$ m^2s is the most appropriate to differentiate between these beach groups.

4.5.2 Classification of UK beach systems

A conceptual summary of the beach groups, within the context of Ω and RTR, are shown in Figure 4.27. Due to the important role of absolute wave energy flux, beach types are broken down into two groups; those occurring in a low-energy environment; and those occurring in a high-energy environment. In this case the deep water wave energy flux threshold of $H^2T = 5$ m^2 s was used. In the study dataset this was represented approximately by values of H_b and T_m of 0.8 m and 8 s, respectively. Although this provides a useful idealised summarising tool for this dataset, it must be remembered that it is data driven and group boundaries are largely dependant on the selected beach sites. It is therefore not designed to be a predictive tool, rather an aid to understanding the relative contributions of wave, tide and sediment characteristics to the morphodynamic system. The nature of generating static boundaries between the beach types is unrealistic, and these beach types truly represent a dynamic spectrum that is subjected to local and regional variation in constraining and modifying factors. Within this summary, the LTT/NBD beach type was split into two sub-groups: LTT and NBD
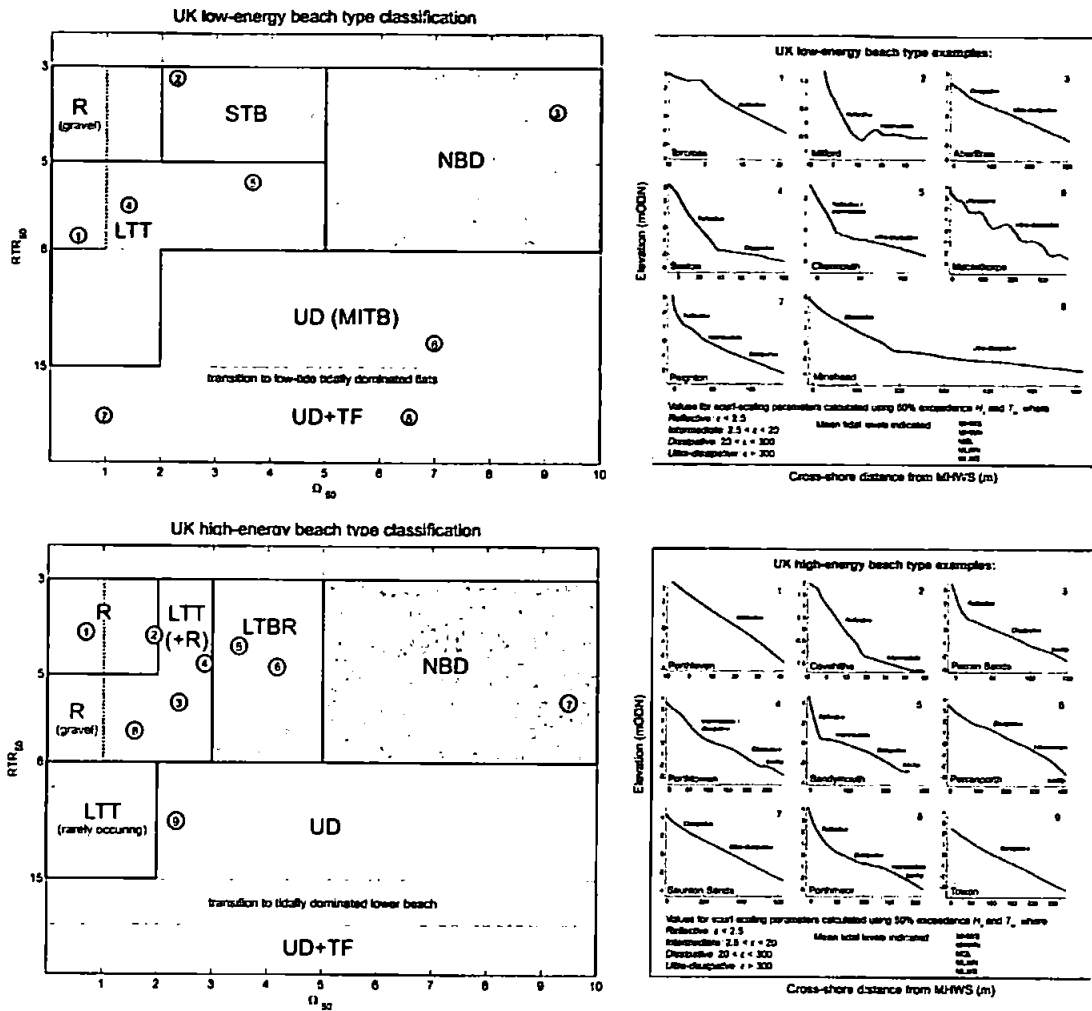
Figure 4.27 – Summary of data based beach classification for low- and high-energy beaches (upper and lower panels, respectively) based on the UK sample sites within this study with reference to prior work by (Masselink and Short, 1993). Example cross-shore profiles and associated values of the surf scaling parameter (right panels), calculated for annual $H_{s50\%}$ inshore wave conditions at each site, are presented (mean values of Ω and RTR for each site are represented in the associated left panel). Within this investigation threshold of transition between low- and high-energy environments occurs approximately at around 0.8 m wave height, and 8 sec wave period ($H^2T = 5$ m^{2}s), essentially describing the level of Atlantic swell energy contributing to the wave spectrum.

(low-energy) to better aid interpretation. With this in mind the group characteristics can be summarised as follows.

Reflective groups: $\Omega < 2$ (R(S), R(G))

Reflective beaches fall into two categories. Firstly those strongly sediment-driven gravel beaches with their dynamic control being RTR (enabling an extension to 8 in cases of gravel beaches) as insufficient wave energy would feasibly be available to modify the type. This is the dominant reflective type on higher-energy coasts. Secondly, finer, sandy reflective beaches which are dynamic in both Ω and RTR, and where an increase in H_b lead to a transition to LTT or STB types. These types were restricted to the rare microtidal low-energy coasts.

Intermediate groups: $1 < \Omega < 5$ (STB, LTT, LTT+R, LTBR)

The most wide ranging subset, containing beaches that are most commonly identified by dynamic profile morphology and seasonal adjustment, frequently found in environments of mixed sediment types, and in many cases defined by their bar systems. Mostly variants of the LTT form, they are broken into low- and high-energy types within the classification. The largely planar low energy forms display a clear break in slope, separating a reflective upper beach and dissipative (ultra-dissipative) lower beach, often with the presence of a strong seepage face, in many cases separating contrasting grain size distributions. This can create a tidally decoupled saturated lower beach encouraging an erosive dissipative morphodynamic regime contrasting with the accretionary upper beach (Turner, 1993). At the other extreme, the inter-tidal zone can be dominated by a wide dissipative/ultra-dissipative beach, driven by either sediment fining, or increase in tide range. Within microtidal regions, an increase in incident wave height can create a STB beach type with single linear bars developing, backed by a runnel at the base of the reflective upper beach. With increasing tide, the transition from STB to LTT can lead to the presence of subdued inter-tidally exposed linear bars cut by drainage channels. The high-energy forms, predominantly occurring within meso- to macrotidal regions in the UK, in most cases possess three-dimensional bar/rip morphologies. These bar systems are enabled by the increased presence of infragravity frequency energy within the surf zone. Many of the beaches within the study fell into a dynamic equilibrium between the LTT+R and LTBR beaches where, potentially, small changes in wave height, tide range and/or sediment size could drive beach state variation on occasion reaching the extremes of LTT and NBD states. The transition within the predominantly

intermediate/dissipative LTBR form comes through the generation of a reflective berm feature in low-energy spring/summer swell wave conditions and generation of an often three-dimensional mid-tide bar. This transition can, in some cases, be enabled though lunar sea-level fluctuations, rapidly returning to a flat planar beach through the onset of storm wave conditions.

Dissipative groups (high- and low-energy): $\Omega > 5$ (NBD(LE+HE))

Inevitably, within a country where the average spring tidal range is > 4 m and in many systems fine sediments are in abundance, beaches that are dissipative in nature are widespread. In this classification, the NBD beach type is almost entirely dominated by a flat, wide, featureless inter-tidal zone. In some cases a relatively small reflective coarse upper beach may be present due to locally derived or relict coarse sediments. Typically occurring in high-energy macro- to mega-tidal regions (RTR > 3), the rate of tidal translation of surf zone processes inhibits the formation of any bars. Under low-energy conditions, NBD (LE) forms occur due to the presence of fine sediments.

Ultra-dissipative groups: $\Omega > 2$; RTR > 7 (MITB, UD+TF)

Where $\Omega > 5$, the UD beach is an extension of the NBD type sharing similar morphological features. Where Ω is between 2 and 5 an increasingly concave upward profile is present. Although not exclusively, many of the 'ridge and runnel' or MITB beaches occur within this space. Controlled by additional factors like sediment abundance, these low-energy beach forms are often spatially clustered in proximity to ebb-tide deltas (Short, 1999). Finally, when RTR > 15, confined within mega-tidal regions, the lower beach can begin to become tidally dominated. Beach processes may persist to higher values of RTR within higher-energy wave climates. The surf zone regimes of these beaches vary greatly from high- to low-tide. Lower beach gradients, and very wide surf zones drive breaker height down due to bed friction (Levoy et al., 2000) increasing the tidal dominance, while at high-tide, a reduction in wave attenuation and surf zone width can lead to a more intermediate surf zone character.

4.5.3 Conceptual morphodynamic framework

Figure 4.28 presents a conceptual morphodynamic overview that represents the dynamic relationships between beach types, and their transitions in relation to the relative contribution of waves, tides and sediments. The lack of defining thresholds is in
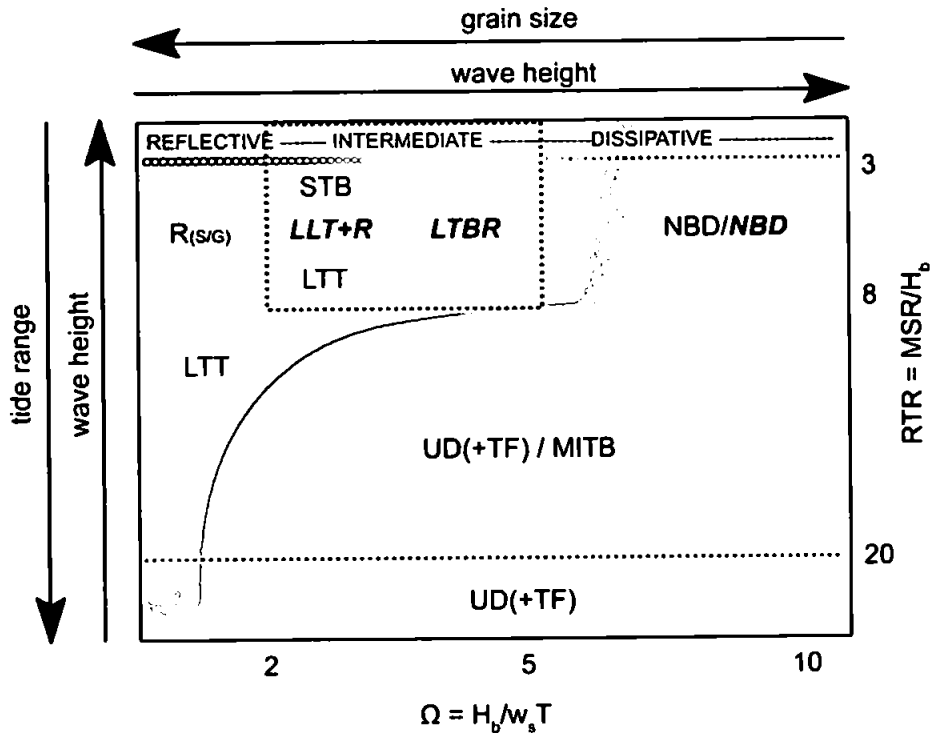
Figure 4.28 – Conceptual morphodynamic framework for sampled UK beaches. Dark and light shading indicate transition from reflective to dissipative surf zone conditions respectively. Black dashed box indicates region where high-energy conditions ($H^2T > 5$ m^2 s) induce 3D bar formations and bold italics represent high-energy beach types.

response to the observed scatter within the dataset (lack of clear boundaries) that has been suggested to be a result of both the role of absolute values of wave energy, tides and sediment characteristics, as well as the controls exerted by geological setting in many locations and the awareness of potential error in the estimation of environmental parameters. Absolute wave energy is represented through the presence or absence of three-dimensional bar morphology within the intermediate beaches where within high-energy environments LTT+R and LTBR beaches occur; under low-energy conditions STB and LTT beaches may be observed.

4.5.4 Limitations

The sample of beaches from the UK coastal environment highlight the contrasts in the geological settings and hydrodynamic systems associated with the broad spectrum of beach forms that exist. In the quest to provide a comprehensive assessment and subsequent classification of this observed spectrum of beach forms and their general morphodynamic characteristics, a high-resolution dataset of environmental parameters for nearly 100 beaches was generated. Limitations in the techniques in estimating and

sampling of these complex environmental parameters induced a significant amount of bias into the dataset. This was reduced as much as possible, but some key assumptions must be borne in mind when assessing the dataset.

- **Temporal stability:** analysis of groups assumed that sampled profiles and sediments represented an equilibrium state with respect to the annual average nearshore wave climate.

- **Wave climate approximation:** in many regions where calculation of wave climate was based on model data, limited measured data was available for validation. Particular attention must be paid to the use of the modelled wave period, which in sheltered locations over-represented the swell wave fraction due to absence of local wind fields over model domains.

- **Sediment uniformity:** sediment sampling, particularly of coarse fractions assumed spatial and temporal uniformity. In many of the mixed beaches, sediment composition was observed to have has strong cross-shore spatial gradients.

- **Two-dimensional beach profiles:** assessment of beach profiles assumes alongshore uniformity. This limitation was reduced by representative on-site profile selection, although a two-dimensional approach is limited in highly three-dimensional systems. A qualitative assessment of bar type using observations and photographs from site visits and remote imagery provided some information on three-dimensional beach form.

- **Seaward extent:** due to surveying constraints, profile information was limited to the inter-tidal zone down to MLWS. Due to the importance of sub-tidal morphology in both the morphodynamic signature of the beach and the prevailing bathing hazards, a visual assessment of the sub-tidal and inter-tidal bar morphology was performed.

4.6 CONCLUSIONS

This chapter has documented an investigation to further the understanding of the spectrum of beaches observed along the UK coast. The collection and analysis of a high-quality, robust dataset including 98 beaches provided insights into the spatial variability of beach types and their associated sedimentary, geometric and hydrodynamic conditions within England and Wales. The morphodynamic relationships between these groups were then assessed in the context of traditional morphodynamic parameters. The investigation provided the following insights:

- 9 distinct beach groups were identified through the analysis of the collected dataset that included 92 beaches from England and Wales, each having a unique morphodynamic signature.

- Beach groups could be defined well, based upon the characteristics of environmental forcing i.e. tide, wave and slope.

- An assessment of the ability of relative morphodynamic parameters to distinguish between beach groups identified the need for an understanding of absolute wave energy when trying to differentiate between the presence/absence of three-dimensional bar morphology. A threshold deep water wave energy flux level of $H^2T = 5$ m^2 s was used to define this group boundary.

- Analysis of the applicability of morphodynamic indices to distinguish between groups suggested that while ε performed well in combination with H^2T, its reliance upon beach slope was a disadvantage. Ω and RTR provided an acceptable conceptual morphodynamic framework within which to describe the relationships between beach groups and associated environmental forcing and characteristics within the UK. In addition, the use of an energy flux threshold was useful to distinguish between low- and high-energy intermediate/dissipative beach types.

- In addition to the roles of waves, tides and sediments in driving beach type, other important site-specific controls were identified. The effects of geologic setting, absolute energy contribution of waves and tides and the limitations in the accuracy of estimation of environmental and morphological variables suggest that the application of fixed beach group boundaries is impractical and an unnecessary exercise. With this in mind,

a simple conceptual framework describing the morphodynamic relationships between the beach groups identified within this study is presented in Figure 4.28.

5. BEACH MORPHODYNAMICS AND HAZARD

5.1 INTRODUCTION

In this chapter, an attempt is made to further the understanding of the relationship between beach type and hazard through an assessment of both the between-group and within-group relationships of the beach types identified in Chapter 4. The investigation focuses on beach types characterised by rip current morphology (LTT+R and LTBR). An improved understanding of the temporal variation in beach morphodynamics is paramount in assessing the spatio-temporal variation of rip current activity and hence hazard. Observations from Chapter 4 suggest the within-group variations in morphology amongst the identified intermediate beaches in this study are similar to bar type transitions documented in previous studies amongst intermediate beach sequences in micro-tidal environments (Bowen and Inman, 1971; Sonu, 1973; 1984; Lippmann and Holman, 1990). These macrotidal intermediate beaches are of particular interest to beach safety managers and the RNLI due to their prevalence and popularity within the Atlantic west coasts of the UK.

The three principal aims of this chapter are:

- to improve the understanding of how the environmental hazard signature varies throughout the classified UK beach types, associated with RNLI beaches, through an assessment of all RNLI incident data collected between 2005 and 2007;

- to investigate the extent of the temporal variation of beach morphology and its affect on type and levels of hazard among the high risk RNLI beaches;

- to generate an improved understanding of the key environmental forcing mechanisms behind temporally varying hazards; specifically identifying key high risk 'scenarios';

- to investigate the hypothesis generated in Chapter 3 that rip hazards are enhanced during the low tidal phase through tidal modulation of rip currents.

To address these aims and objectives, field campaigns were conducted to assess temporal (annual and seasonal) morphologic and hydrodynamic variation at selected RNLI beaches in the southwest between 2006 and 2008 with particular focus on the 2007 lifeguard season from May-October. The implications of these findings to beach safety were then examined through an analysis of lifeguard incident and beach user

data, leading to the identification of key environmental factors affecting temporal variation in beach hazard. The next section details an analysis of incident records across all RNLI beaches, grouped using the classification framework specified within Chapter 4. These findings provide the basis with which beach sites were selected for further assessment within this chapter.

5.1.1 Beach type and hazards

In Chapter 3 the levels of hazard presented to the beach user were determined through incident counts and the levels of usage throughout a spring/summer/autumn season. The combination of these data enabled an approximation of the level of beach risk as a function of the hazard and usage levels. In this section the distribution of hazards and risks across the wide range of RNLI beach types were analysed using all RNLI incident reports recorded between 2005 to 2007 and the beach group classifications defined in Chapter 4. Sub-dividing the LTT/NBD beach group (Group 4 in Section 4.4.1) into 2 sub groups; LTT and NBD(LE), as described in Section 4.5.2, was continued in this chapter as it aided hazard characterisation and assessment within a beach safety context. Figure 5.1 illustrates the locations of all RNLI patrol units that were active between 2005 and 2007. 71 of 76 active beaches during this period were located in the southwest of England. Within the southwest region, 38 units were located on the south coasts of Cornwall, Devon and Dorset and 38 on the Atlantic west coasts of Devon and Cornwall. Classified beach types are not distributed evenly among these various geographical regions. Table 5.1 shows that of the 32 LTT+R and LTBR beach types present, 25 are located on the Atlantic west coasts of Cornwall and Devon with the more sheltered regions (SE. Devon, Dorset and Norfolk) being dominated by R and LTT types.

Schematic conceptual representations of each beach type where there was an RNLI presence (there were no patrolled ultra dissipative beaches during the study period) are presented in Figure 5.2, highlighting key morphological features that have been assessed to have controlling influences on hazard levels. Some representation of observed temporal variation in principal morphological features is included, derived from a monthly photographic records of beach state, collected throughout the study period at a number of beach locations in Devon and Cornwall. This has enabled qualitative morphological assessments of the region's beaches. The greatest
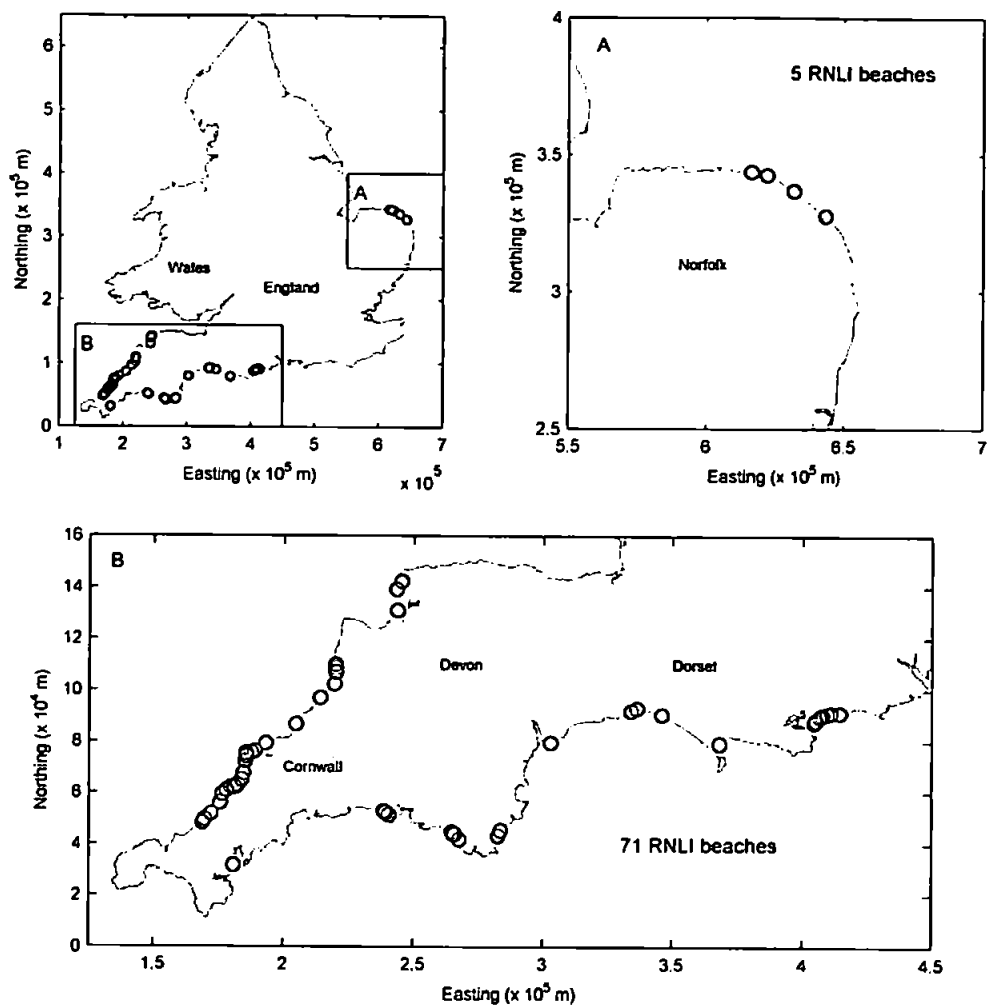
Figure 5.1 – Map of all 76 RNLI beach locations active between 2005 and 2007. Subplots A and B display exploded views of the east coast and southwest regions respectively.

Table 5.1 – Count of beach types associated with the various regions containing RNLI patrol units between 2005 and 2007.

County	Beach types									
	R (S)	R (G)	LTT	STB	LTT+R	LTBR	MITB	NBD (LE)	NBD (HE)	UD(+TF)
Dorset	3	3	8	10	0	0	0	0	0	0
N.Cornwall	0	0	1	0	16	7	0	0	6	0
N.Devon	0	0	0	0	0	2	0	0	2	0
Norfolk	0	0	3	1	0	0	1	0	0	0
S.Cornwall	0	0	1	0	4	0	0	0	0	0
S.Devon	2	1	0	0	3	0	1	1	0	0

morphological variation, with respect to sandbar morphology, occurred among the LTT+R and LTBR beaches. LTT+R and LTT represent the highest proportion of the 76 RNLI beaches totalling 23 and 12 respectively. Least represented with only 1 beach is the NBD (LE) beach type as well as the MITB type (2 beaches).

Analysis of the incident data indicates that 68% of all recorded incidents (individuals rescued/assisted) were due to rip currents, supporting preliminary findings from Chapter 3 and representing a similar percentage to beach rescues in Australia and the USA. Figure 5.2 illustrates the percentage cause of incident over the same period for the different beach types patrolled. Incidents driven by strong and offshore winds, as well as littoral currents, present the greatest cause of incident on beaches that are commonly without rip current activity. Interestingly, beach type division through absolute wave energy, in some cases, also reveals significant differences in the hazard signature. LTT and NBD beaches both show a strong dominant influence of incidents driven by the effects of offshore winds as well as strong winds within the low-energy beaches, with the high-energy beaches being more influenced by rip currents and high-energy surf zone hydrodynamics like plunging/dumping waves and bed-return flow/swash events. Reflective beaches show fewer differences between high- and low-energy types although the low-energy beaches are accompanied by an increase in incidents driven by offshore winds. This is likely to be related to the reduced shoreline energy within the low-energy beach allowing increased bathing and inflatable access; this is supported by the higher insea user numbers at the low-energy as opposed to high-energy beach (11.3 and 3.6 people per hour respectively). Although tidal cut-off does not appear to be a significant contributor to the overall beach hazard levels, the high levels of incident due to sandbank/sandbars on beach types with low wave heights and typically large tidal excursions suggests cut-off through sandbank and zonal isolation is an important hazard driver on low-energy LTT and MITB types.

LTBR and LLT+BR beaches have greater than 80% of all incidents being caused by rip currents, and with 2269 and 3253 incidents from 2005 to 2007, respectively, they constitute 78.1% of all recorded incidents over that period. LTBR and LLT+BR beaches represent 46.6% of all patrolled beaches and with an average of 33.6 and 42.9 people in the sea per hour (May to October) during the 3-year period making these the most popular bathing beaches that are patrolled by the RNLI.
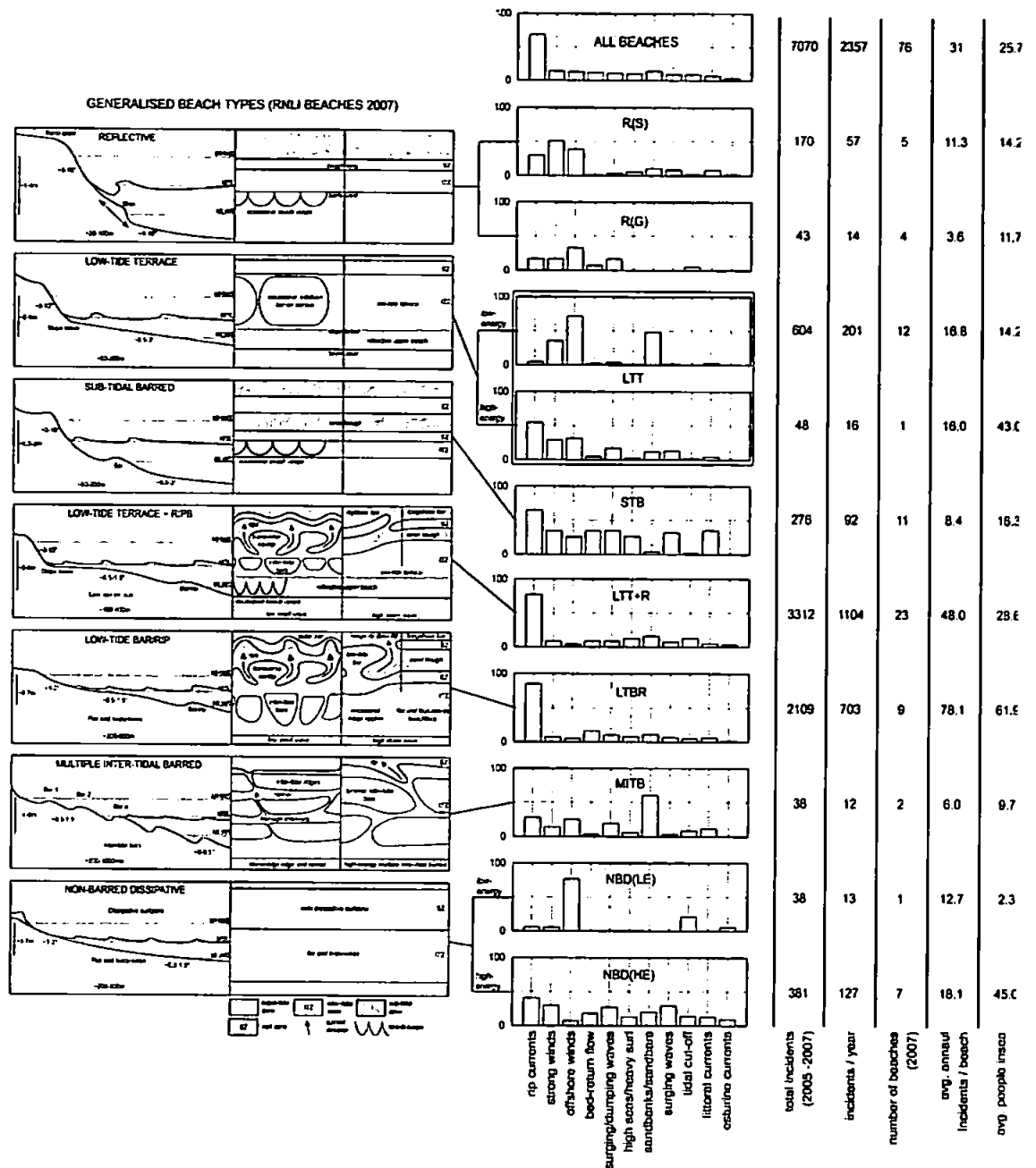
Figure 5.2 – Percentage occurrence of all environmental causes of incidents (recorded by RNLI) for observed UK beach type groupings (2005 to 2007). There were no RNLI patrolled ultra dissipative beaches during the study period.

Due to the high levels of rip current hazard, dynamic bar morphology, popularity and large carrying capacity, the intermediate LTBR and LLT+BR beaches on the high-energy west coast of Devon and Cornwall are the focus of field investigations within the rest of this chapter that investigates the temporal morphodynamic variation and associated hazard within these beach environments.

5.2 METHODOLOGY

5.2.1 Site selection

An inventory was conducted of all beaches within Devon and Cornwall. Within the west coast regions LTBR and LTT+R beaches represent 59% (62% by length) of all beaches with sandy lower inter-tidal zones. These beaches with rip morphologies are mostly located on the high-energy west facing coasts (Figure 5.3) with lower and upper beach sediment grain sizes ranging from 0.3–0.48 mm and 0.29 mm–gravel/boulder respectively. Nine field sites were selected that were patrolled by the RNLI, represented a range of LLT+R and LTBR beaches and experienced high beach user numbers. In addition the chosen sites possessed a variety of rip current types (beach and topographic rips) and varying degrees of geologic control. These beaches were located on the west coasts of Devon and Cornwall (Figure 5.3). Of these nine beaches, six were chosen as core monitoring stations for quantitative assessment of beach morphodynamics.

5.2.2 Data collection

An evaluation of beach morphodynamics and hazards for six field sites, four LLT+R beaches (sites 2, 4, 6 and 8) and two LTBR beaches (sites 1 and 7) were made between July 2006 and March 2008 through analysis of hydrodynamic forcing, wind conditions, beach morphology, rip current activity and RNLI incident and hourly beach population counts (Figure 5.3). A higher resolution assessment of seasonal morphodynamic variation was conducted during the 2007 lifeguard season (May–October).

5.2.2.1 Hydrodynamic and wind conditions

Hydrodynamic conditions during 2007 were monitored with a Datawell near-shore directional waverider buoy at Perranporth beach (50.35379°N, 5.17497°W; 10 m water depth) maintained by the Channel Coastal Observatory (Figure 5.3). Offshore (~30 km) non-directional wave conditions, spanning the entire monitoring period, were provided by the Seven Stones Lightship (50.103°N, 6.100°W; 60 m water depth). Sea surface elevations throughout the period were obtained from a combination of predicted tides for Perranporth beach (Admiralty, 2005; Admiralty, 2006; Admiralty, 2007) and surge residuals recorded by the Newlyn tide gauge located at the tip of the southwest peninsula in Cornwall. Surge residual levels are produced for each high- and low-tide and calculated from the difference between predicted and observed sea level. The surge
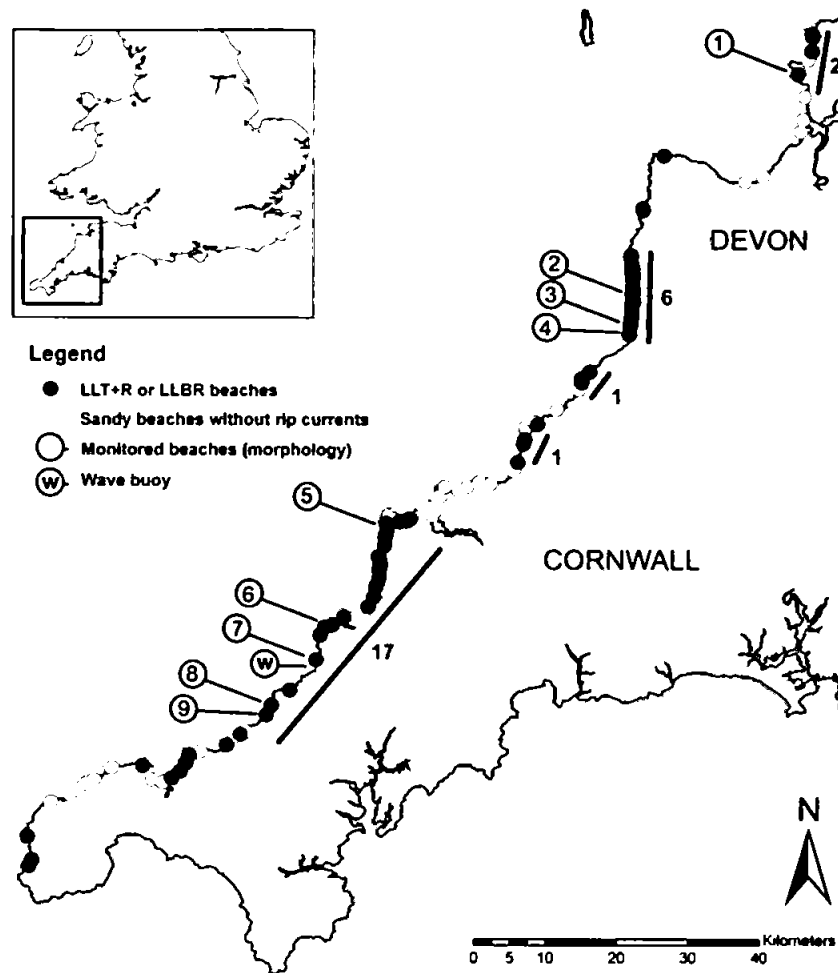
Figure 5.3 – Map showing the nine study sites where morphological monitoring was conducted: 1) Croyde Bay; 2) Sandymouth; 3) Northcott mouth; 4) Crooklets; 5) Constantine Bay; 6) Fistral Bay; 7) Perranporth; 8) Chapel Porth; 9) Porthtowan. All beaches in the west coast region are marked with circles. Black and dark white fill represent beach types with and without rip current morphology (LTT+R and LTBR) respectively.

data were supplied by the British Oceanographic Data Centre as part of the function of the National Tidal & Sea Level Facility. Hourly mean wind statistics were recorded both at St Mawgan airfield near Perranporth and at the Seven Stones Lightvessel, and were supplied by the MetOffice.

5.2.2.2 Beach morphology

Beach morphology was measured both bi-annually (summer/winter) during the monitoring period and monthly during the 2007 season (May to October). Surveys were conducted using ATV based RTK GPS survey system (see section 2.2 for detailed survey methodology) at the sites which had appropriate access points and agreements in place (beaches 1, 5 and 7). Those beaches where ATV access was not possible or

agreements were not in place, trolley based RTK GPS surveys were conducted on foot. Each monthly survey campaign lasted approximately 6 days. Sites were surveyed as close to monthly intervals as possible.

Survey data were analysed using the Loess interpolation procedure, developed by Plant (2002) to generate a digital elevation model of the beach surface (Section 2.2.4). A pre-existing Argus video station at Perranporth beach provided both snapshot and 'timex' (time averaged) rectified beach and surf zone images at 30-minute intervals (Section 2.3). Background photographic monitoring of all 9 selected west coast beach sites was conducted throughout the monitoring period. Frequency of the photographic data collection was increased during the 2007 patrol season when each location was photographed at bimonthly intervals. Photographic monitoring entailed capturing panoramic photographs from fixed locations at each study site. Images were 'stitched' using Autostitch software, developed by Brown and Lowe (2007) at Columbia University. This dataset enabled a qualitative assessment of beach morphology that gave supporting information on beach conditions, bar state and drainage characteristics.

5.2.2.3 Rip current activity

Daily assessments of rip severity at all tidal levels were estimated by the RNLI lifeguards at 4 sites that represented LTBR and LTT+R morphologies, with both beach and topographically controlled rip currents (beaches 2, 5, 6 and 7 shown in Figure 5.3), providing a qualitative comprehension of spatial and temporal variation in rip current characteristics. Rip current assessment forms were completed daily for low-, mid- and high-tide when possible within patrol hours. The assessment required the lifeguard to enter details on rip presence, number of rips within a defined area and an estimation of the severity of those rips from 1–5 (Appendix 3). Each patrol was provided with a document clearly describing the assessment routine and providing descriptions in real terms of the rip strength severity levels to improve continuity in assessment between units. It is acknowledged that this technique is open to subjectivity but it was deemed to provide a valuable insight into a system that is rarely monitored daily over a period of months.

5.2.2.4 Incidents and beach population

The assessment of beach hazards and beach user numbers used the same data source as described in Section 3.3.1. Comprehensive RNLI lifeguard incident records provided information of hazard levels. Hourly estimated beach user counts, recorded within

RNLI patrol hours, provided temporal insea beach usage statistics throughout the monitoring period.

.

5.3   RESULTS AND DISCUSSION

5.3.1   Annual beach change

5.3.1.1   Environmental conditions

The wave climate of the west coast of Devon and Cornwall is both high-energy and highly seasonal. Mean significant wave heights between 2006 and 2008 at Seven Stones Light Vessel vary from 3.1 m in winter to 1.3 m during summer (Table 5.2). During the high-energy winter months 10% exceedance wave heights reach 5.1 m. An annual mean wave period of 8.2 s varies from 9.3 s in winter to 7.3 s in summer. Macro-tidal (> 4 m) and mega-tidal (> 8 m) mean spring tidal ranges exist along the entire west coast of Devon and Cornwall from 4.1 m at the southern tip to 9.6 m in the northwest. The west coast beaches studied are all approximately west facing and receive similar wave energy throughout the year. This high-energy climate drives the seasonal sediment transport observed along the coast.

The study period includes two high-energy winters (Figure 5.4). Between October 2006 and April 2008 daily averaged offshore significant wave heights were frequently between 4 m and 6 m and mean wave periods above 10 s. Two significant storm events occurred in December 2007 and March 2008 where daily averaged offshore wave heights exceeded 6 m. During both observed summer periods (June to August), daily averaged offshore wave heights never exceeded 4 m. Near-shore wave heights, available from January 2007, recorded mean significant wave heights of 2.3 m and 1.2 m for winter and summer respectively. Zero up-crossing wave periods ranged from 6.8 s in winter to 5.5 s in summer and peak wave periods from 13.2 s to 8.6 s respectively. Wave conditions during both the annual and seasonal survey periods are illustrated in Figure 5.4.

The mean wave angle (bathymetrically controlled) was 280°. During the energy peak of the winter 2007/2008 storm events, in ~ 10 m water depth, 30-min averaged significant wave heights exceeded 7 m and maximum wave heights exceeded 9 m. Mean offshore winds recorded from Steven Stones Light Vessel display a clear seasonality where mean hourly 10 m wind speeds exceeded 34.9 kts 10% of the time in winter months and 22.9

Table 5.2 - Offshore wave climate statistics from 2006 to 2008 at Seven Stones Light Vessel. H_s is significant wave height and T_m mean wave period.

	H_s (m)		H_s exceedance (m)			T_m (sec)	
	Mean	s.d.	10%	50%	90%	Mean	s.d.
Annual	2.0	1.4	4.0	1.6	0.7	8.2	2.0
Winter	3.1	1.5	5.1	3.0	1.3	9.3	3.1
Spring	2.0	1.3	3.7	1.7	0.7	8.2	2.0
Summer	1.3	0.7	2.3	1.1	0.5	7.3	1.3
Autumn	1.7	1.0	3.1	1.5	0.7	7.9	1.7
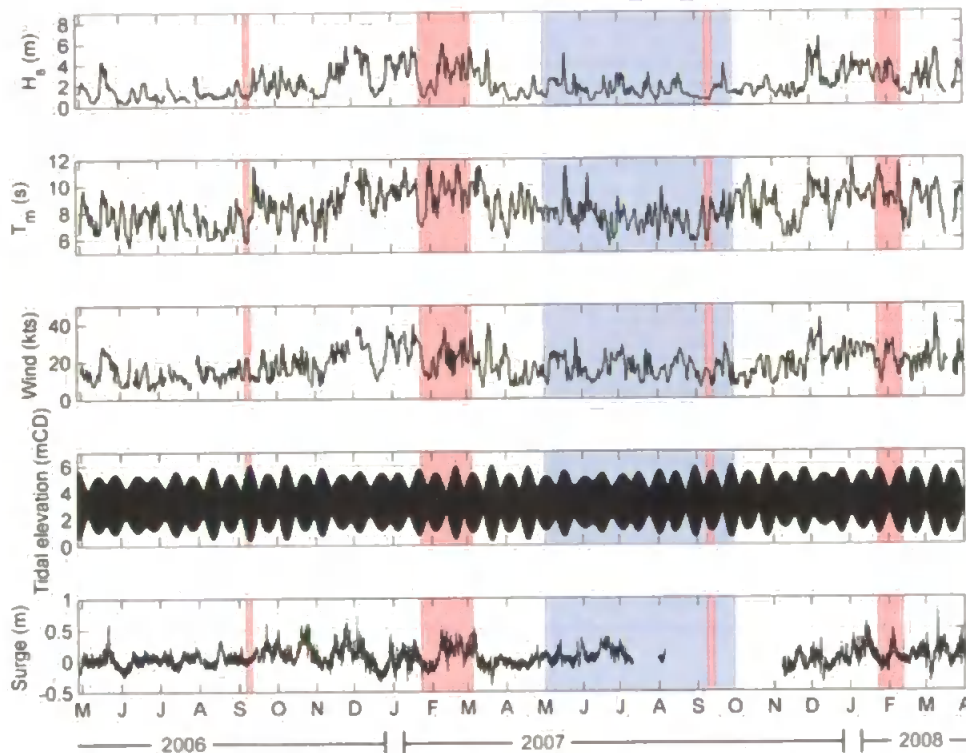
Figure 5.4 – Environmental conditions observed during the monitoring period (From top) Offshore wave record (daily averaged) showing (upper) significant wave height (H_s) and (lower) mean wave period (T_m), mean wind speed (24-hour averaged) from Seven Stones Lightvessel, predicted tidal elevation at Perranporth measured to Chart Datum and surge residual recorded at Newlyn. Red regions indicate periods when annual winter/summer beach surveys were conducted and blue regions indicate the high resolution seasonal survey period.

kts in summer. Mean 10 m winds reduced from 23.2 kts in winter to 14.1 kts in summer throughout the monitoring period.

5.3.1.2   Morphological transition

During the study period, high volume sediment transport was observed as beach morphologies adjusted to the changing hydrodynamic climate. A general trend of large scale erosion of sediment from the inter-tidal zone occurred at all monitored LLT+BR and LTBR beaches along the west coast of Devon and Cornwall. This took the form of beach lowering from 0.2-0.5 m which locally exceeded 1 m at some locations. Beach lowering occurred in association with transition from highly developed low-tide bar/rip systems and enhanced mid-tide bar systems during the lower energy swell-wave dominated summer months, to increasingly shore parallel offshore bars and planar featureless mid-tidal zones during the high-energy, storm dominated winter months. This transition is well illustrated in the captured 2006/7 summer/winter photographic series from Chapel Porth, West Cornwall (Figure 5.5). The following sections illustrate and quantify, with examples, this seasonal winter/summer transition at four contrasting beach sites between 2006 and 2008.

Figure 5.5 – Summer/winter low-tide images of Chapel Porth beach, 10/09/06 to 05/03/07.

Perranporth - An exposed beach in West Cornwall with an average grain size (D_{50}) of 0.32 mm. Classed as a LTBR beach, it experienced a marked annual transition, both in beach morphology and volume between the 09/06 and 02/08 (Figure 5.6). Erosion of - 154 and -210 m^3 m^{-1} occurred from 11/09/06 to 20/03/07 and 12/09/07 to 08/02/08 respectively along a cross-shore profile between MLWS and MHWS (Table 5.3). This erosion constituted a mean reduction of the beach elevation of 0.25 and 0.45 m. During the winter/summer transition between 20/03/07 and 12/09/07 an accretion of 146.2 m^3 m^{-1} was recorded, with a mean beach elevation change of 0.42 m. Argus timex images (Figure 5.6) illustrate the annual variation in bar morphology with a tendency for more shore-parallel longshore sub-tidal bar/trough systems during months of high wave energy and more well-developed transverse bar/rip systems during lower energy periods.

Table 5.3 – Annual winter/summer beach volume and surface elevation changes for the studied beaches

Dates		Volume change		
from	to	m^3m^{-1}	Δz	$\sigma(\Delta z)$
		Perranporth		
11/09/06	05/03/07	-154	-0.25	0.19
05/03/07	12/09/07	146.2	0.42	0.12
12/09/7	08/02/08	-210.3	-0.45	0.33
		Croyde		
07/09/06	02/02/07	-100.7	-0.25	0.37
02/02/07	14/09/07	82.68	0.19	0.39
14/09/07	12/02/08	-110.76	-0.24	0.39
		Sandymouth		
06/09/06	23/01/07	-163.57	-0.69	0.29
23/01/07	13/09/07	103.38	0.42	0.6
13/09/07	07/02/08	-97.484	-0.42	0.4
		Constantine		
09/09/06	23/01/07	15.966	0.04	0.52
23/01/07	13/09/07	-63.87	-0.19	0.59
13/09/07	07/02/08	-55.164	-0.17	0.44
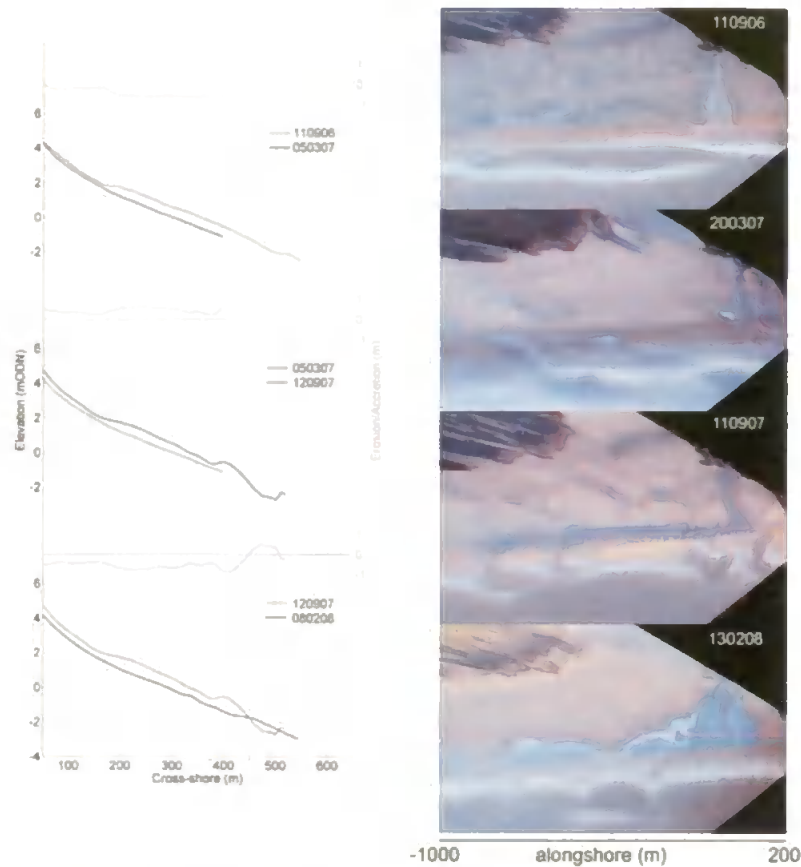
Figure 5.6 – Seasonal morphological transition at Perranporth beach from summer 2006 to winter 2008; (left) cross-shore profiles illustrate seasonal beach change and along-profile elevation change (Δz). Horizontal lines represent mean tidal levels; (right) rectified timex video images indicate observed 3D morphological changes associated with each profile (image date is closest available).

This transition is illustrated by the development of inter-tidal bar formation within the neap low-tide region at a cross-shore location (X) of 400–450 m. Under low-energy conditions the accumulation of sediment in the form of secondary bar morphology within the mid-tide region is common. Subsequent removal of these inter-tidal secondary bar formations occurs with the onset of higher energy conditions.

Croyde Bay - The beach volume dynamics at Croyde Bay (D_{50} = 0.38 mm), another LTBR beach, display similar trends to Perranporth (Figure 5.7). Croyde Bay experienced erosive transitions during both winters of -100.7 and -110.76 m^3 m^{-1} respectively (Table 5.3), with an accretion of 82.86 m^3 m^{-1} during the intervening winter/summer period. Mean elevation changes were of the same order as Perranporth although the development and destruction of the bar morphology, present throughout the entire inter-tidal profile, was more pronounced with a standard deviation of cross-
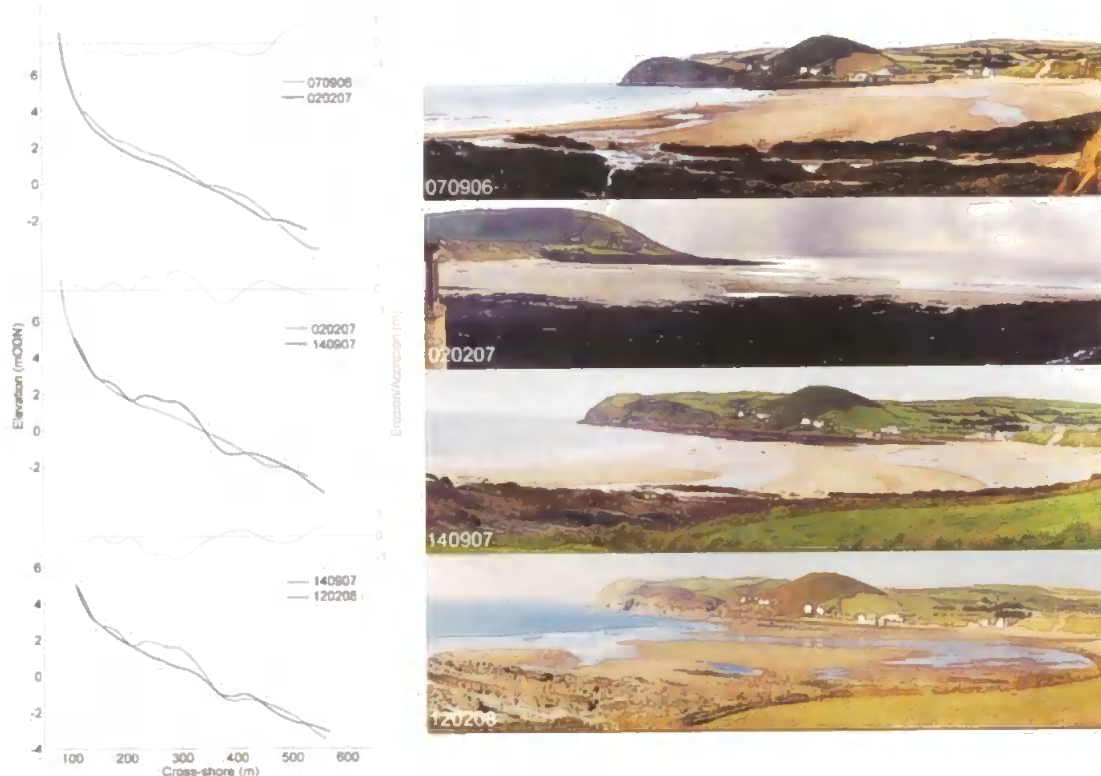
Figure 5.7 – Seasonal morphological transition at Croyde Bay from summer 2006 to winter 2008; (left) cross-shore profiles illustrate seasonal profile change and along-profile elevation change (Δz). Horizontal lines represent mean tidal levels; (right) panoramic photographic images indicate observed 3D morphological changes.

shore surface elevation change between surveys of 0.37 m to 0.39 m. Photographs in Figure 5.7 show large regions of saturated beach during summer and winter periods.

Sandymouth - As an example of a LTT+R beach type, Sandymouth possesses a coarse, steep, gravel/boulder high water beach ($X \sim 50$–100 m) and a wide sandy lower inter-tidal zone ($D_{50} = 0.39$ mm), characterised by significant bar formations below mean low water neaps. Inter-tidal geologic exposures of hard substrate, often part of a shore platform, are a significant feature at the beach due to limited sediment availability. This was exemplified during the summer/winter transitions that occurred during the monitoring period where inter-tidal erosion volumes of -163.57 and -97 m³ m⁻¹ (Table 5.3) were measured along one cross-shore profile (Figure 5.8). These transitions amounted to mean reductions in surface elevation of -0.69 m and -0.42 m respectively during the 2006/7 and 2007/8 seasons. Profiles show that in the region of mean low
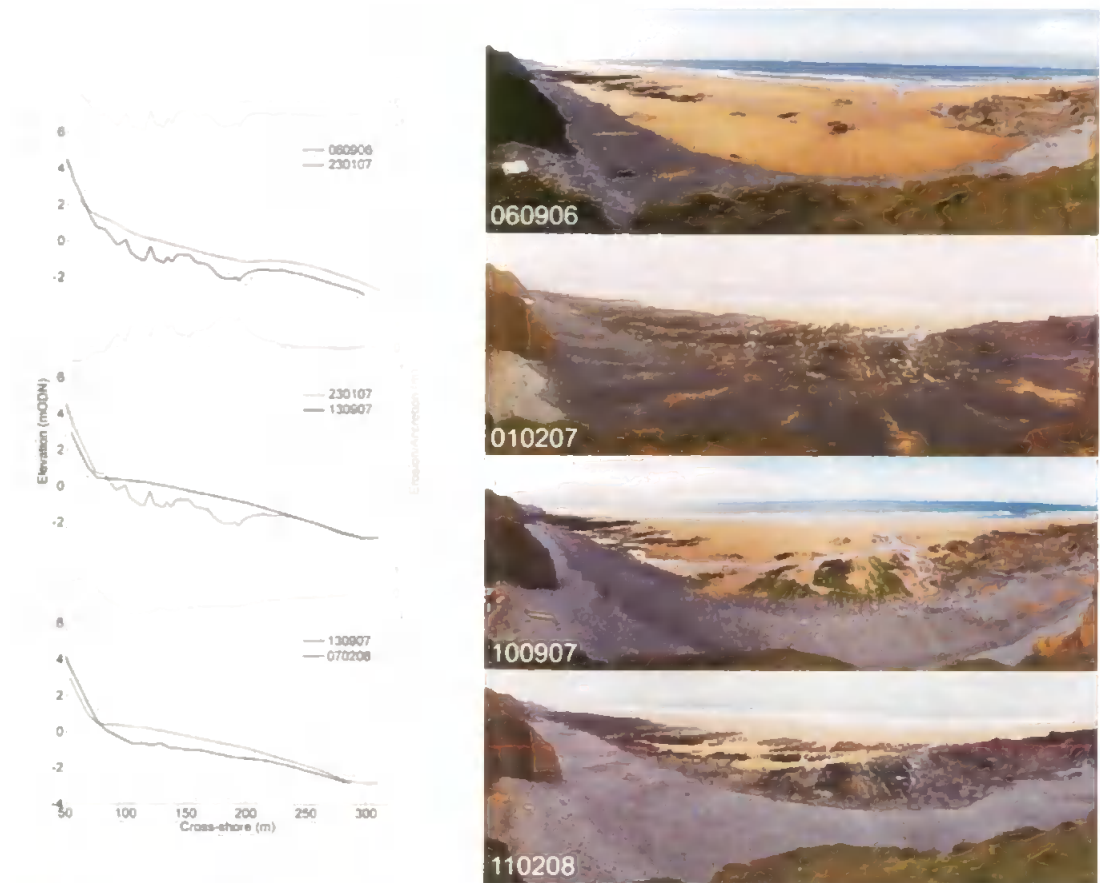
Figure 5.8 – Seasonal morphological transition at Sandymouth from summer 2006 to winter 2008; (left) cross-shore profiles illustrate seasonal profile change and along-profile elevation change (Δz). Horizontal lines represent mean tidal levels; (right) panoramic photographic images indicate observed 3D morphological changes.

water neaps to mean high water neaps erosion of more than 1 m occurred in some locations during 2006/2007. The transitions at Sandymouth were characterised by the increase in bedrock exposure during the winter surveys. The removal of sediment offshore of MLWS, between 06/09/06 and 01/02/07, left 35% bedrock exposure on 01/02/07 (an increase from 4% on 06/09/2006). Bedrock exposure between MHWN and MLWN in the 23/01/07 survey restricted the ability of the beach to respond to the prevailing hydrodynamic conditions, constraining sediment transport pathways, reducing depths to bedrock and hence altering drainage properties and sediment mobility, and driving bedrock constrained surf zone currents (rip currents) during the mid and high tide. An appreciation of the spatial extent of the observed morphological transition and bedrock exposure can be gained from the panoramic images in Figure 5.8. Subsequent to the high-energy winter of 2006/2007 the beach volume did not recover to its previous level before the onset of the next winter season. Little evidence of the

presence of low-tide and sub-tidal bar morphology can be found in the cross-shore profiles, although the panoramic images and field observations suggest their presence through three-dimensional morphology and breaker dissipation patterns observed. Accretional transitions appear to drive a steepening and raising of the coarse upper beach face and berm crest, accompanied by an observed landward movement of the gravel/sand transition (slope break) of up to 25 m.

Constantine Bay - An example of another LTT+R beach type, the morphologically dynamic Constantine Bay is sandy throughout the inter-tidal profile ($D_{50} = 0.48$ mm) and, like Sandymouth, is influenced by hard rock exposures to the north and south of the bay constraining sediment transport pathways narrowing the beach width seaward from high-water to low-water. Panoramic images and field observations show that well defined berm growth ($X \sim 100$–200 m) and highly dynamic and developed three-dimensional bar/rip system, present throughout the beach and particularly around low- and sub-tidal regions are common. Interestingly, given these observations, no evidence of significant volume changes along a selected cross-shore profile were evident during the monitored summer/winter transitions. This could be due to the significant three-dimensional nature of the morphodynamic change at the beach limiting the effectiveness of a two-dimensional monitoring approach. Observed highly active bar dynamics at and below mean low water within the photographic record suggest much of the morphological change is not captured within the surveyed inter-tidal profile. The three-dimensional nature of beach change is investigated further in the next section.

The ability of morphodynamic indices Ω and RTR to describe the observed temporal morphological transitions is explored in Figure 5.10. The values are calculated for the summer/winter transition from 09/07 to 02/08 due to availability of nearshore wave buoy data for this period (Perranporth wave buoy). Statistical wave parameters were calculated from a 3-month period prior to the survey date to take account of antecedent wave conditions. Sediment fall velocities were taken from the mid-tide region for each survey and tidal ranges were obtained from the mean spring tidal range values published for each beach. Results compare well to the observed morphological changes. As observed, the beaches assessed to be LTBR translate to the LTBR region of the UK beach classification framework (Figure 5.10) with a Ω_{summer} values of 5.1–5.2, and those that were classed LTT+R (Constantine Bay and Sandymouth) have lower values of $\Omega_{summer} = 3.4$–4.8. Calculated parameters for the winter measurements show a clear
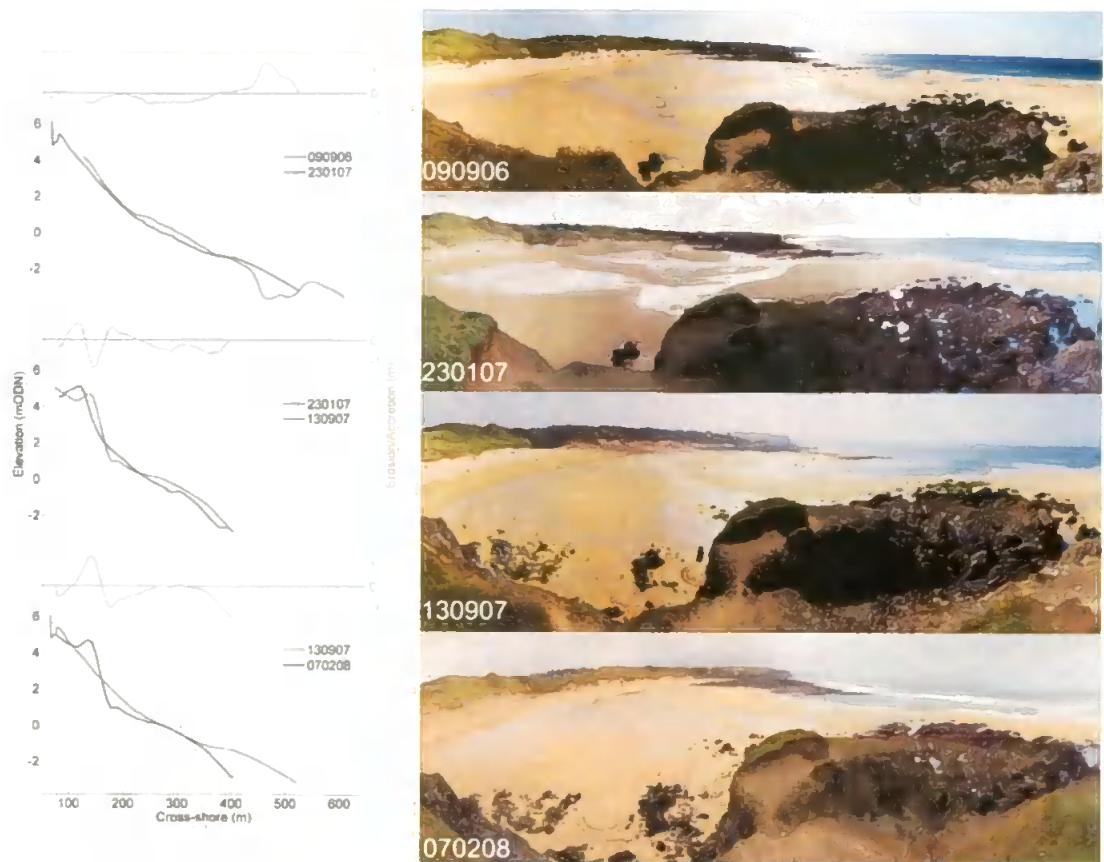
Figure 5.9 – Seasonal morphological transition at Constantine Bay from summer 2006 to winter 2008; (left) cross-shore profiles illustrate seasonal profile change and along-profile elevation change (Δz). Horizontal lines represent mean tidal levels; (right) panoramic photographic images indicate observed 3D morphological changes.

translation to higher values of Ω and lower values of *RTR* putting most of the beaches within the NBD category. Interesting, the one exception is Constantine Bay which remains within the LTBR region, potentially giving some explanation for the continuing three-dimensional bar/rip activity observed during the winter surveys. The calculated morphodynamic indices indicate that Perranporth should theoretically experience the greatest transition in beach state during the measurement period.
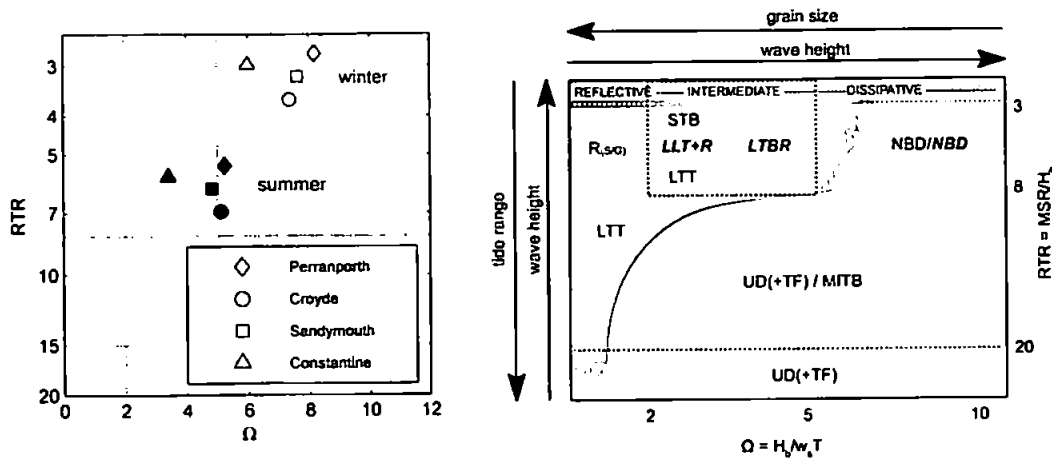
Figure 5.10 – (Left) Annual variation in morphodynamic variables Ω and RTR between summer 2007 and winter 2008 for the studied beaches. (Right) Conceptual UK beach classification framework (see Figure 4.28).

5.3.2 Seasonal morphological transition

5.3.2.1 Environmental forcing

The hydrodynamic and meteorological conditions during the winter/summer period of 2007 are summarised in Figure 5.11. The timeseries of environmental conditions illustrates the transitions from high-energy conditions during the winter/early spring period A (01/01/07-20/04/07) where nearshore, 6-hr averaged, significant wave heights and peak periods regularly exceeded 4 m and 12 s respectively. During this period high-energy wave events were typically associated with rainfall rates of over 10 mm/day. The subsequent period until 05/05/07 was dominated by low waves and rainfall. Long period low- to medium-energy swell waves continued during period B until approximately 15/06/07 when the first topographic surveys began. The period C between the first and second survey campaigns was characterised by unseasonably high levels of rainfall throughout. Mean wind speeds increased to 11.9 kts during this interval accompanied by higher, steeper wave conditions ($H_s \sim 1.5$ m and $T_p \sim 8.4$ s) with three storm wave events where $H_s > 3$ m. A decrease in mean wave height ($H_s \sim 1.0$ m and $T_p \sim 8.4$ s), wind speeds ($U \sim 8.3$ kts) and rainfall characterised the following period (D) between the second and third survey campaign. Finally, period E between the third and forth survey campaigns consisted of a continuation of low-energy wave conditions ($H_s \sim 0.8$ m and $T_p \sim 7.6$ s) and very low rainfall levels. With a mean H_s of 1.1 m and maximum H_s of 4.4 m during the survey period, the nearshore wave record shows high-
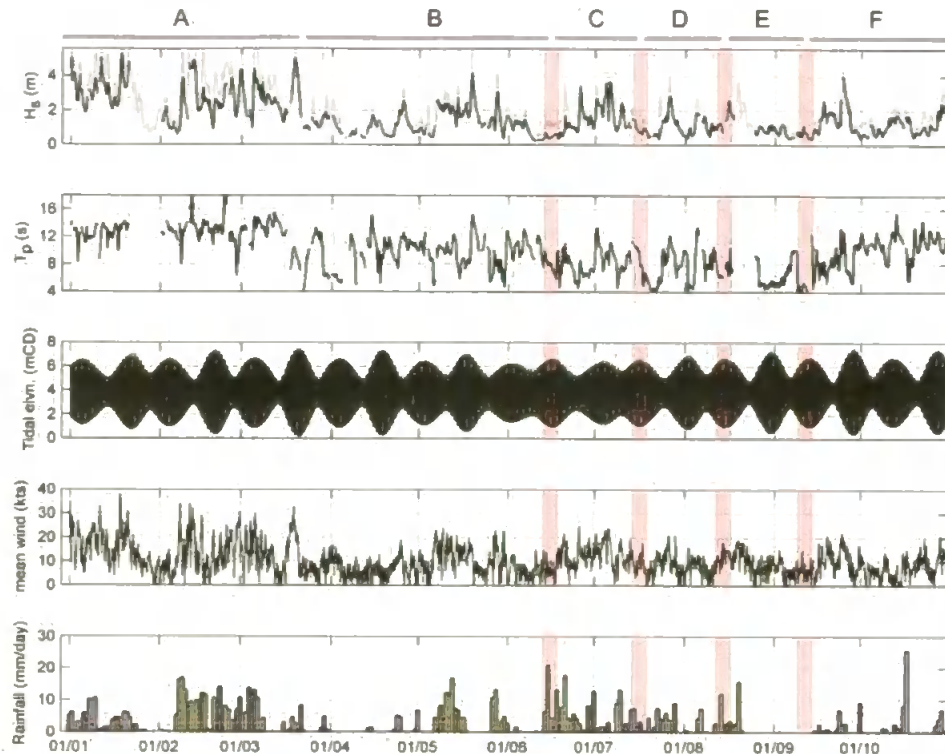
Figure 5.11 – (from the top) Offshore wave record (6 hour averaged) during study period (H_s and T_p) Grey line shows simultaneous 6 hr averaged offshore wave record from Seven Stones Lighvessel; predicted tidal elevation (mCD); mean hourly wind speed and daily rainfall totals from St Mawgan airfield. Red regions highlight survey periods.

energy wave events during the first half of May and start of July, followed by relatively low-energy conditions until the end of September. A mean and maximum T_p of 8.2 s and 16.7 s respectively indicates the presence of swell wave conditions throughout the study period. The mean spring tidal range at Perranporth is 6.1 m, typically decreasing by approximately 2 m during neap tides. Towards the end of the study period (autumnal equinox) the tidal range varies from 1.67 m (20/9) to 7.17 m (28/9).

5.3.2.2 Bar morphology

Surveyed morphology and video image capture during the monitoring period at Perranporth recorded the seasonal transition of beach and bar morphology at an open coast, LTBR beach. Residual and difference surfaces from each of the survey campaigns, shown in Figure 5.12, capture the seasonal inter-tidal morphological transition where a planar beachface, observed during survey A (05/04/07) shows a general accretionary trend throughout the season toward the development of highly three-dimensional low- to mid-tide bar systems that are observed in the final survey D
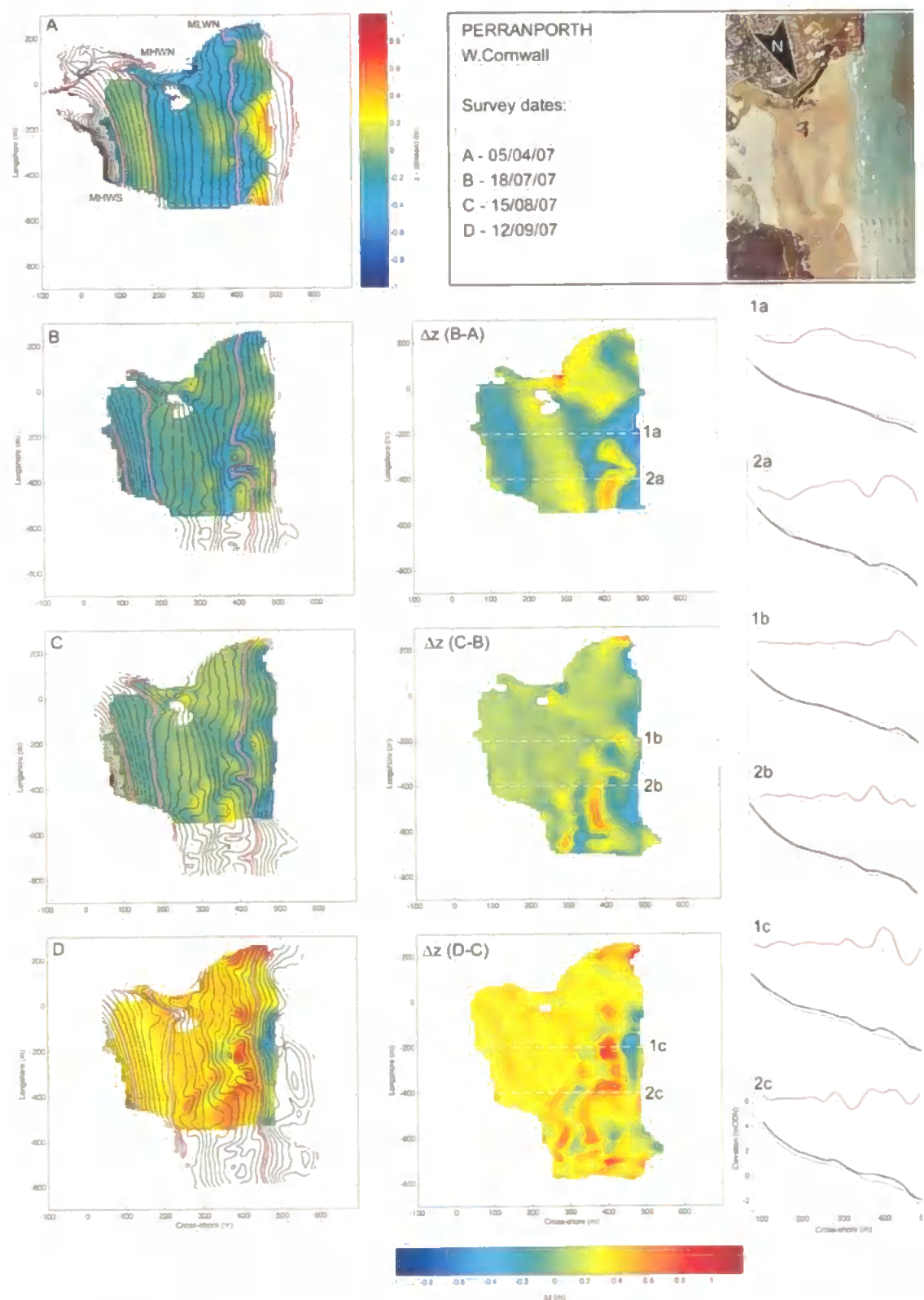
Figure 5.12 – (left) Plots show residual morphology from the mean beach surface with surveyed topography shown as black contours, mean tidal levels marked in magenta; (central column) Difference plots indicating regions of erosion/accretion between surveys; (right) Cross-shore profile taken from transects marked on central column show two-dimensional beach morphological change, grey and black lines indicate before and after profiles while red lines indicate residual elevation. Horizontal grey lines indicate mean tidal levels.

(12/09/07). Within the survey region, a net monthly accretion was observed. Rates of accretion increased during the survey period from Δz = 0.03 m (9175 m^3 by volume within survey area) between survey A-B, to Δz = 0.08 m (21375 m^3 by volume within survey area) and Δz = 0.34 m (90025 m^3 by volume within survey area) between B-C and C-D respectively. The largest accretion event between surveys C-D occurred in conjunction with a period of low-energy wave conditions and low rainfall (highlighted as period E in Figure 5.12). The bar morphology within the mid- and low-tide regions is shown to be highly dynamic. Within the cross-shore, profiles associated with each survey (Figure 5.12) indicate surface elevation changes, through bar dynamics, of greater than 0.5 m in many cases. Initially these morphological changes appear to be restricted to the lower inter-tidal zone (below MLWN) during the first two survey periods, subsequently bar systems are present up to MHWN. To investigate the distribution of the topographic variability within the along as well as cross-shore components a measure of alongshore bathymetric non-uniformity (*BNU*) was calculated (Feddersen and Guza, 2003), which is the alongshore depth variance, defined as:

$$BNU = \frac{1}{L_y} \int_0^{L_y} \left[z(x,y) - \overline{z(x)} \right]^2 dy \qquad (1)$$

where $z(x,y)$ is the surface elevation, $\overline{z(x)}$ is the alongshore mean cross-shore profile, L_y is the alongshore integration distance and d_y the alongshore grid spacing. Data from the RTK surveys are used to compute *BNU*.

Approximately representing a region below MHWN, developments of the alongshore mean cross-shore profile in Figure 5.13 show a clear accretion between X ~ 375–475 m through time. The values of *BNU* in the cross-shore indicate regions of increased alongshore surface variance from the mean profile associated with bar/rip presence. Figure 5.13 shows a growth and landward progression of peaks in *BNU* through subsequent surveys from a single low-tide peak in survey A, developing into a double (C-D) and then triple peak by survey D. These peaks were confirmed through observations in the three-dimensional survey data (Figure 5.14). The peaks in *BNU* can be attributed to the development of bar/rip systems throughout the inter-tidal zone.

Combining these findings with observations from the sub-tidal zone, through inclusion of rectified timex video images, provided evidence of an accretionary bar state
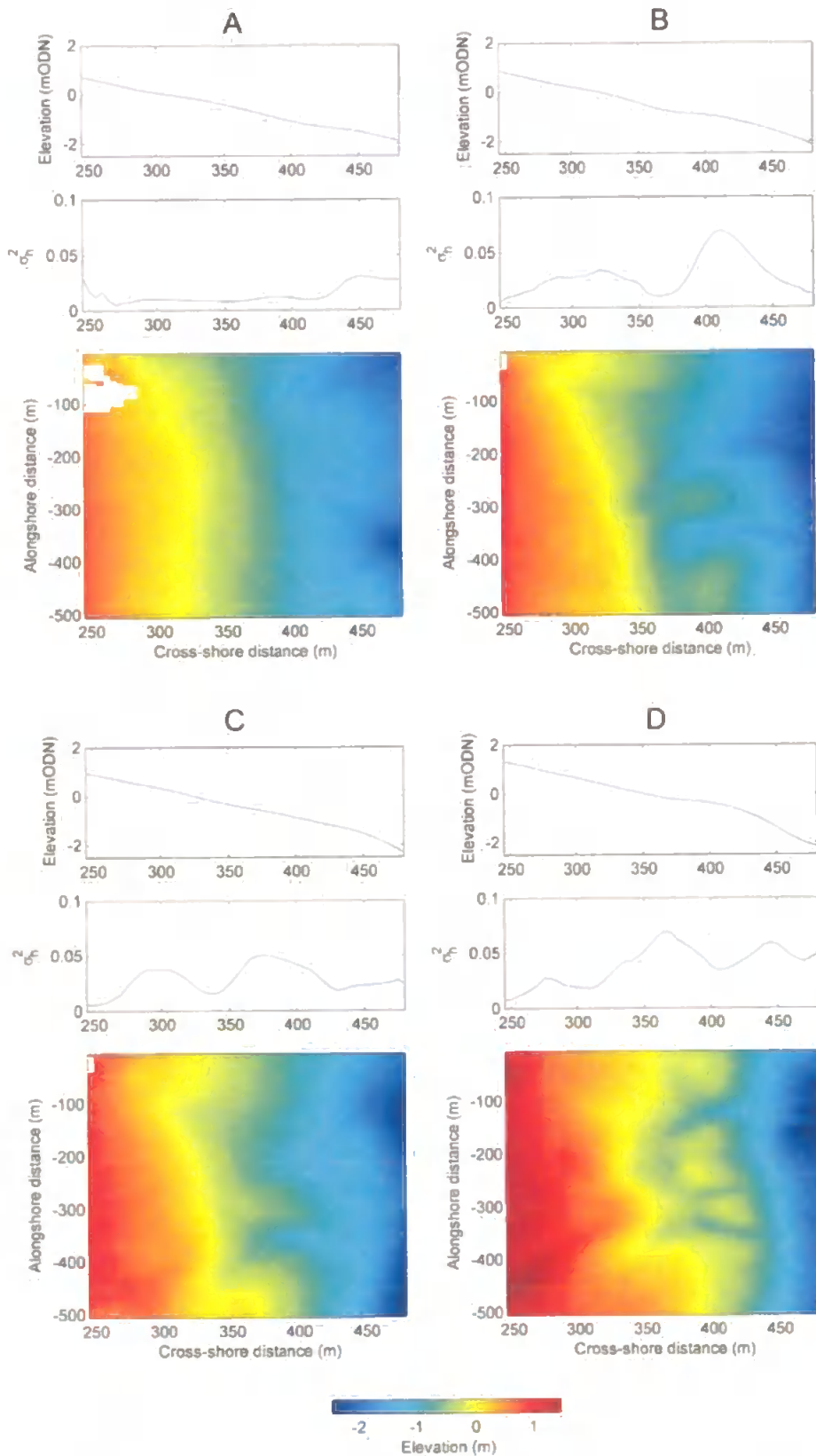
Figure 5.13 – Panels A-D show, for selected region; (from top) alongshore averaged cross-shore profile; cross-shore variation in bathymetric non-uniformity (σ^2_b); and three-dimensional surface elevation for Perranporth beach. A – 05/04/07; B – 18/07/07; C – 15/08/07; and D – 12/09/07.

190
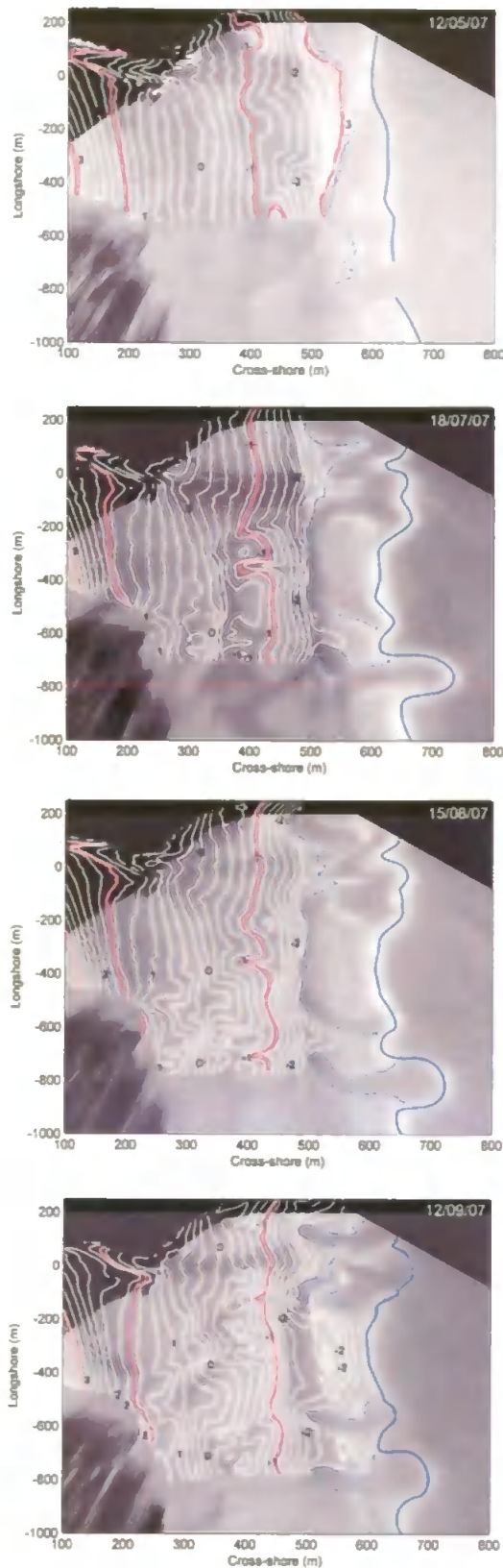
Figure 5.14 – Contoured morphology from four surveys at Perranporth beach including; mean tidal levels (magenta); rectified timex image indicating regions of wave breaker dissipation (background); and extracted bar crest locations for inner breaker zone/shoreline (dashed blue) and outer breaker intensity maximum/bar crest (solid blue).

191

transition typical to those observed in micro-tidal environments as classified by Wright and Short (1984). In this case the bar morphology is constrained to the low-tide region where tidal stationarity is sufficient to enable their development. The observed down-state transition, as displayed in Figure 5.14 and identified from the breaker dissipation patterns, is from a longshore bar/trough (LBT) through rhythmic bar/beach (RBB) to transverse bar/rip (TBR) bar state. Bar state transitions of this type have been observed in upper meso-tidal environments, for example on the high-energy French Aquataine coast (Castelle, Bonneton et al., 2007) a spectrum of bar states from LTT to D were recorded throughout a number of investigations but few observations of these bar state transitions have been reported in strongly macro-tidal settings.

The observed temporal variations in bar states drive the changing template morphology that will influence location and characteristics of rip current circulation characteristics throughout the season. The supposition is that there is indeed a significant temporal variation in rip current beach morphological characteristics throughout a sample lifeguard season, and hence this could induce a temporal rip current hazard signal. Also, the observation that, during an accretionary phase, it is possible to generate a quadruple bar/rip system extending from MHWN seaward, will lead to a highly complex temporal variation in rip current characteristics throughout the tidal excursion.

5.3.2.3 Sediment supply, geological control and beach drainage

At many of the studied locations there are significant modifications of the general morphological transition observed. The beaches of Devon and Cornwall, and indeed the UK, are highly variable in their sediment characteristics and abundance, as well as in backshore geology. Many beaches within the study region accommodate drainage systems, mostly in the form of streams, from local catchments, which during periods of heavy rainfall, provide additional sediment transport mechanisms and also cause the beaches to be saturated throughout the tidal cycle affecting the mobility of the beach sediment. The following examples highlight the importance of the role of inter-tidal geology and beach drainage in modifying the capacity of a beach to respond to the prevailing hydrodynamic conditions within this study area within a single spring/summer season.

As observed at the LTBR beach sites, significant morphological adjustment occurred during the season at the LTT+R beaches monitored (Section 5.3.1.2). These beaches

also had significant geological constraints and were influenced by beach drainage systems; they were highly dynamic in all cases. Geologic intervention between mid- and high-tide regions, in addition to beach drainage fluctuations, generated seasonally dynamic mid-tide bar/rip systems that appeared largely decoupled from the low-tide and sub-tidal bar state.

At both Constantine Bay and Crooklets beach large-scale erosion was measured throughout the inter-tidal beach between the first and second survey periods (surveys A and B in Figure 5.15 and Figure 5.16). It is thought that the scale of the measured erosion (A-B) was in part due to the preceding 3-month accretionary period of relatively small waves and low rainfall (period B in Figure 5.11) where monthly rainfall records were 97% and 29% of the long-term means for March and April, respectively. This period of accretion was subsequently followed by a period of high waves and unseasonably high rainfall rates (period C in Figure 5.11) during which rainfall totals were 202% and 230% of the monthly means for June and July, respectively.

This response was not evident in the Perranporth record, possibly due to the earlier date of the first survey. This erosive period accounted for inter-tidal volume changes of -64,300 m^3 (Δz = -0.51 m) at Constantine Bay and -4580 m^3 (Δz = -0.09 m) at Crooklets Beach. At Constantine Bay local surface elevation changes of up to -2 m were measured. Both these locations have geological constraints within the mid-tide region, through which drainage systems discharge. During rainfall events discharge mechanisms were observed as both surface run-off within a stream channel and groundwater outflow, with a seepage face commonly being associated with the break in slope at approximately MSL-MHWN (Figure 5.17).

Volume changes at both sites during this event (A-B) were principally through incising and deepening of drainage/rip channels. In both sites the channel morphology developed adjacent to hard rock constrictions at both sides of the embayment (Figure 5.15 and Figure 5.16). In the case of Constantine Bay, erosion occurred through a recession of the berm in the vicinity of the principal drainage source [X, Y] ~ [150 m, 320 m], where X and Y are the local cross-shore and alongshore co-ordinates. Figure 5.17 illustrates the extent of the surface drainage and beach saturation during the 16/07/07 survey at Crooklets Beach. Further visual examples of the extent of beach saturation and surface drainage during periods of high rainfall are displayed in Figure 5.18 under both low-
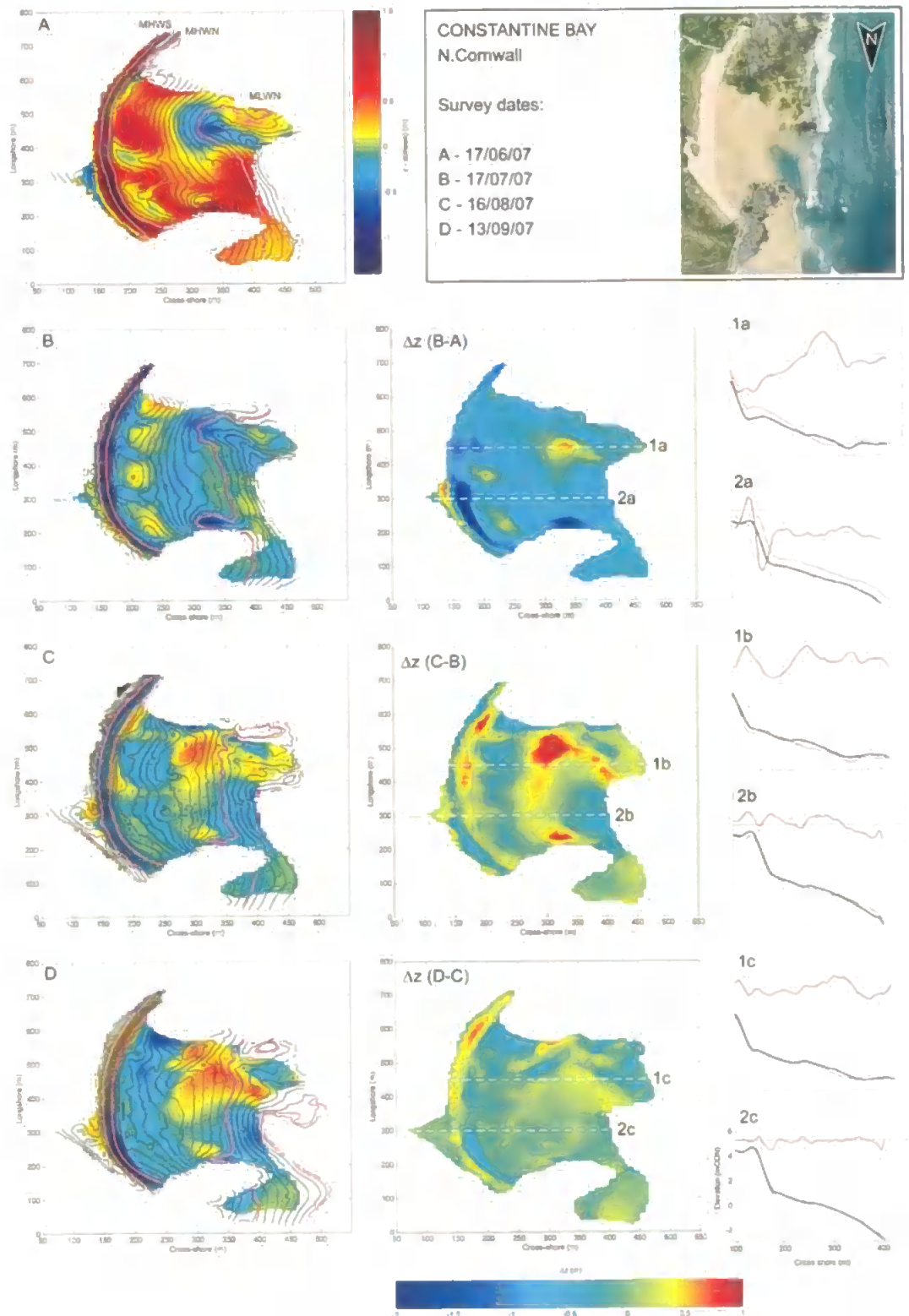
Figure 5.15 - (left) Plots show residual morphology from the mean beach surface at Constantine Bay, with beach surface shown as black contours, mean tidal levels in magenta; (central column) Difference plots indicating regions of erosion/accretion between surveys; (right) Cross-shore profiles (from marked transects) show two-dimensional beach morphological change, grey and black lines indicate before and after profiles while red lines indicate residual elevation. Horizontal grey lines indicate mean tidal levels.
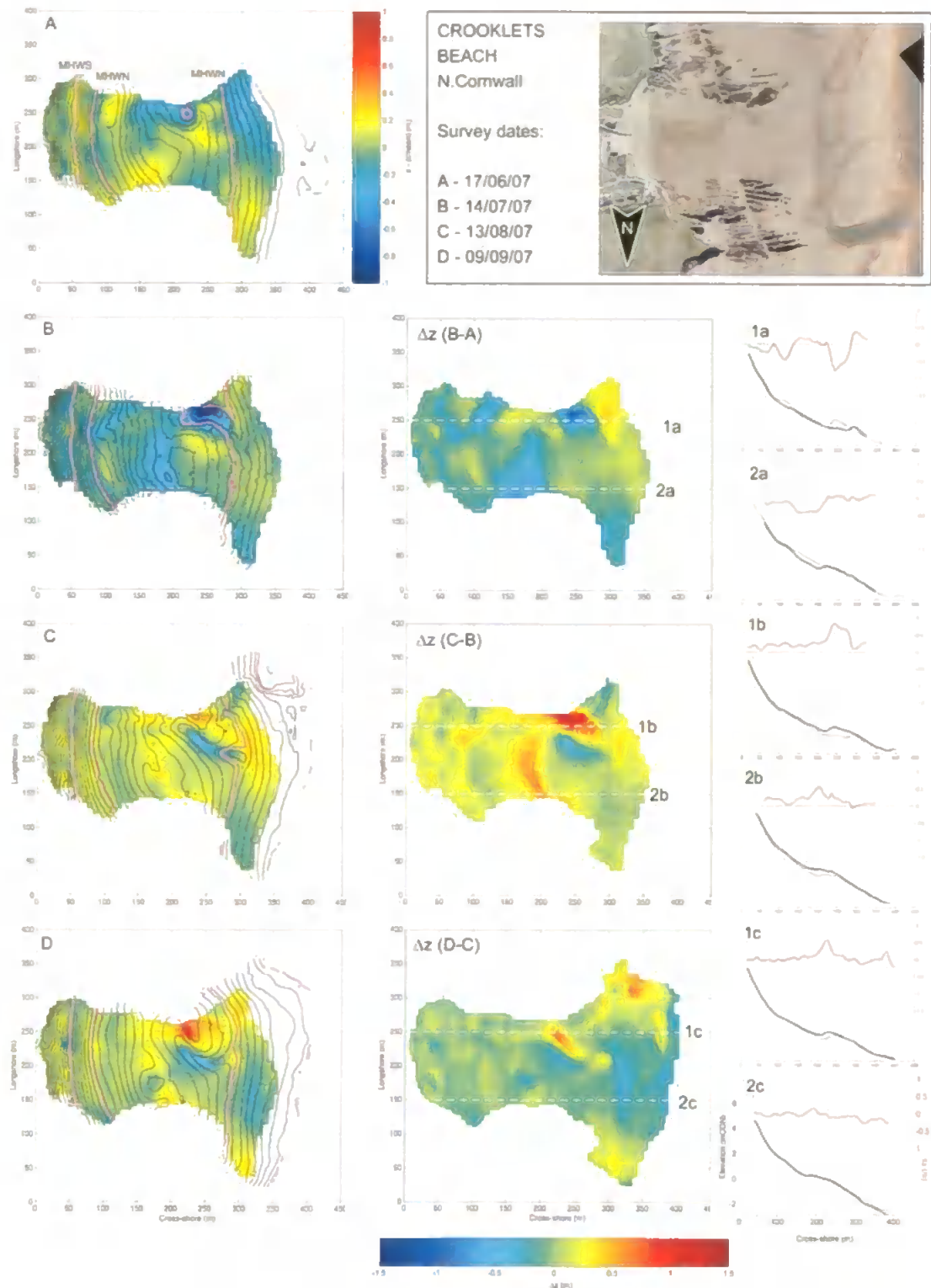
Figure 5.16 - (left) Plots show residual morphology from the mean beach surface at Crooklets Beach, with beach surface shown as black contours, mean tidal levels in magenta; (central column) Difference plots indicating regions of erosion/accretion between surveys; (right) Cross-shore profiles (from marked transects) show two-dimensional beach morphological change, grey and black lines indicate before and after profiles while red lines indicate residual elevation. Horizontal grey lines indicate mean tidal levels.

Figure 5.17 – Panoramic photograph of Crooklets beach on 16/07/07 illustrating surface and groundwater drainage through the inter-tidal beach.

and high-energy wave conditions. These images provide evidence, unlike observations at Perranporth, of instances where mid-tide morphology appears de-coupled from the low- and sub-tidal bar morphology, under environments where a degree of geological control exists (example of constrained upper and open lower beach morphology is shown in Figure 5.19).

Analysis of the monthly variation in *BNU* at Crooklets (Figure 5.20) shows peak values at $X \sim 200\text{-}250$ m associated with the point of maximum geological constriction. This peak remains within this region throughout the season but steadily decreases. It is suggested that this decrease in BNU could be due to the steady reduction in rainfall and hence drainage discharge through the beach throughout the season, with channel infilling occurring under accretionary conditions.

Subsequent surveys at both sites recorded an initial accretionary response in the third survey campaign (survey C in Figure 5.15 and Figure 5.16) with a mean elevation change of 0.09 m and 0.18 m and Constantine Bay and Crooklets Beach respectively. The fourth survey period (D), associated with a preceding period of low wave energy and low rainfall (period E in Figure 5.11), measured no significant net volume change (measured change is less than that due to potential instrument error) within the surveyed region. Unfortunately no quantitative information is available for beach elevation on or below MLWS. Therefore limited comment can be made on the dynamics and state of low- and sub-tidal bar/rip systems at these sites. Qualitative field observations and bimonthly photographic records suggest the unconstrained low-tide bar/rip systems at

196

all nine study sites possess similar dynamic characteristics to those previously discussed at Perranporth (Section 5.2.2.8).

A surveyed beach section of the open, but geologically constrained Sandymouth beach is presented in Figure 5.21. This set of beach surveys provides further evidence of the dynamic nature of inter-tidal bar morphology within the region. Headland constraint in association with a surface drainage system at $Y \sim 200$ m drives dramatic monthly morphological changes of the order +/- 1 m. Large-scale variations in alongshore location of low- and sub-tidal bar/rip morphology are observed throughout the monitoring period.

Throughout the study sites, observations show that confined mid- and upper-beach regions often flow into open coast domains within the lower-beach. When the constrained beach width is less than the alongshore wavelength of the low-tide bar/rip system, the lower-beach in these cases can be in phase with either the larger scale open coast rip embayment or the adjacent shoal. The alongshore configuration of this system potentially has a significant effect on the rip current hazard signature at low-tide.

Figure 5.18 – Panoramic photographs of Crooklets inter-tidal zone illustrating beach drainage characteristics under low-energy swell wave and high-energy storm wave conditions. Images captured (from top) on 01/08/07 and 11/03/08.
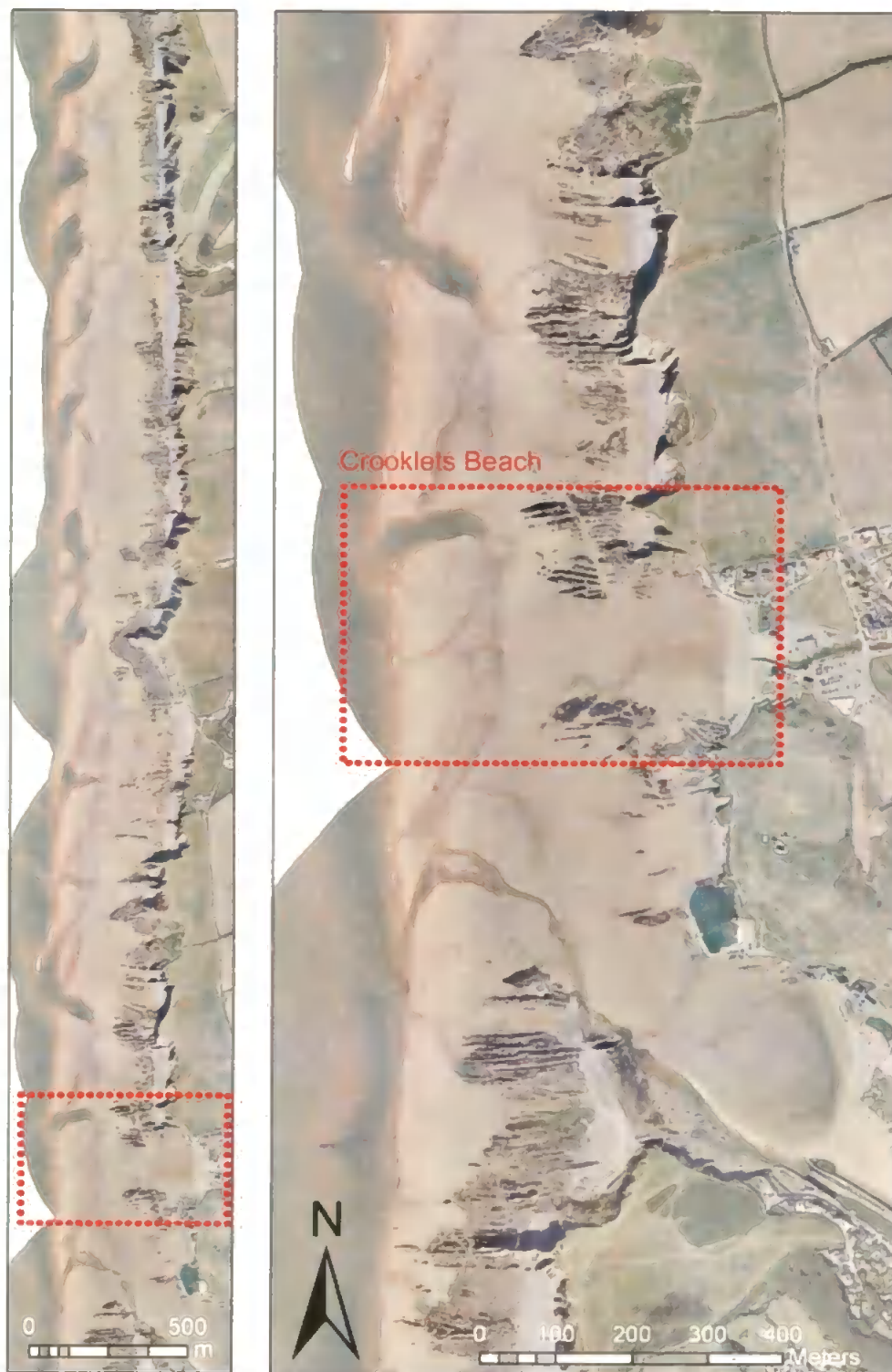
Figure 5.19 – Aerial images of Crooklets beach (September 2006) and associated constrained upper inter-tidal morphology and open lower inter-tidal bar systems. Images provided by the Environment Agency.
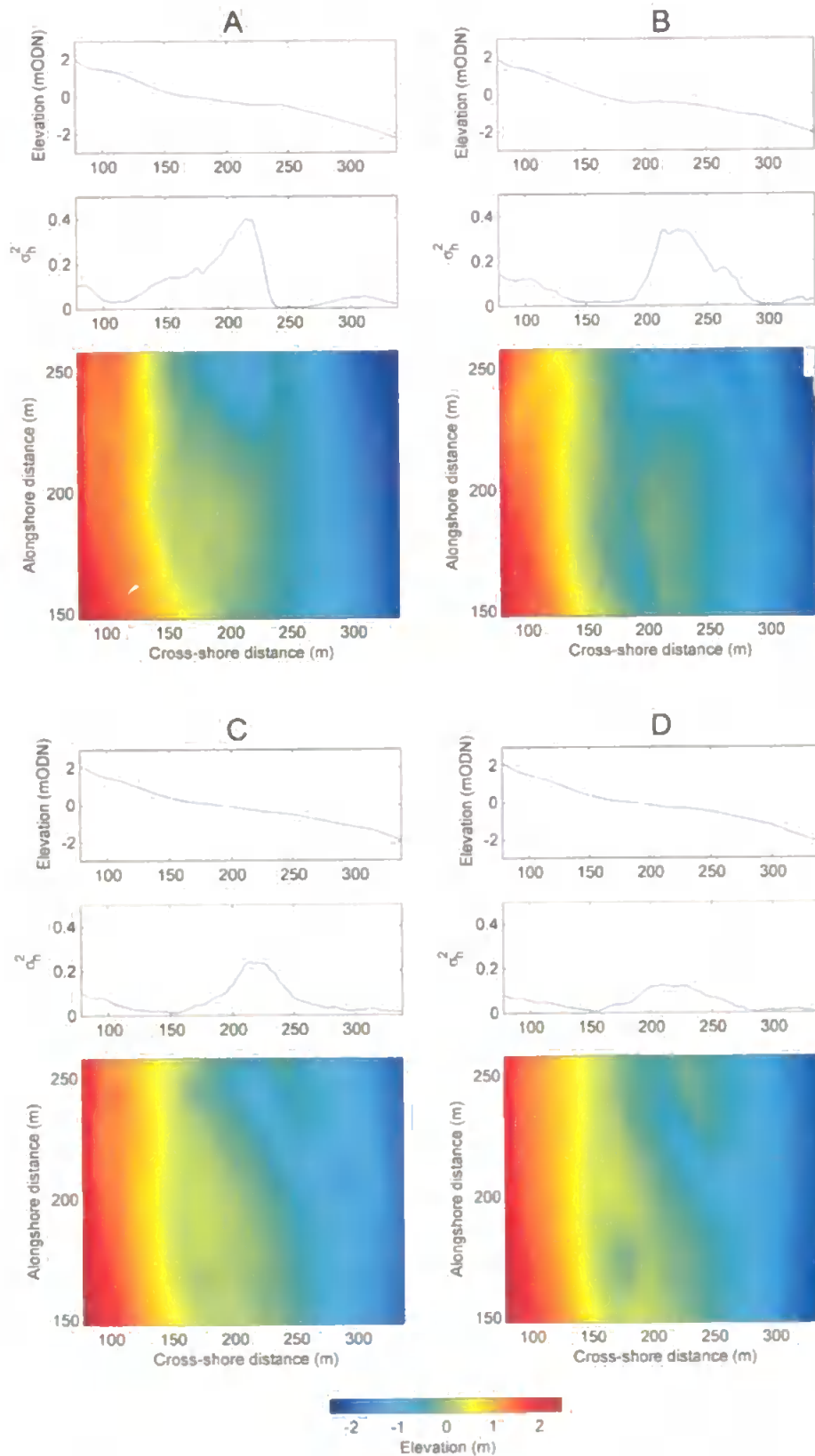
Figure 5.20 – Panels A-D show, for selected region; (from top) alongshore averaged cross-shore profile; cross-shore variation in bathymetric non-uniformity (σ^2_h); and three-dimensional surface elevation for Crooklets beach. A – 17/06/07; B – 14/07/07; C – 13/08/07; D – 09/09/07.
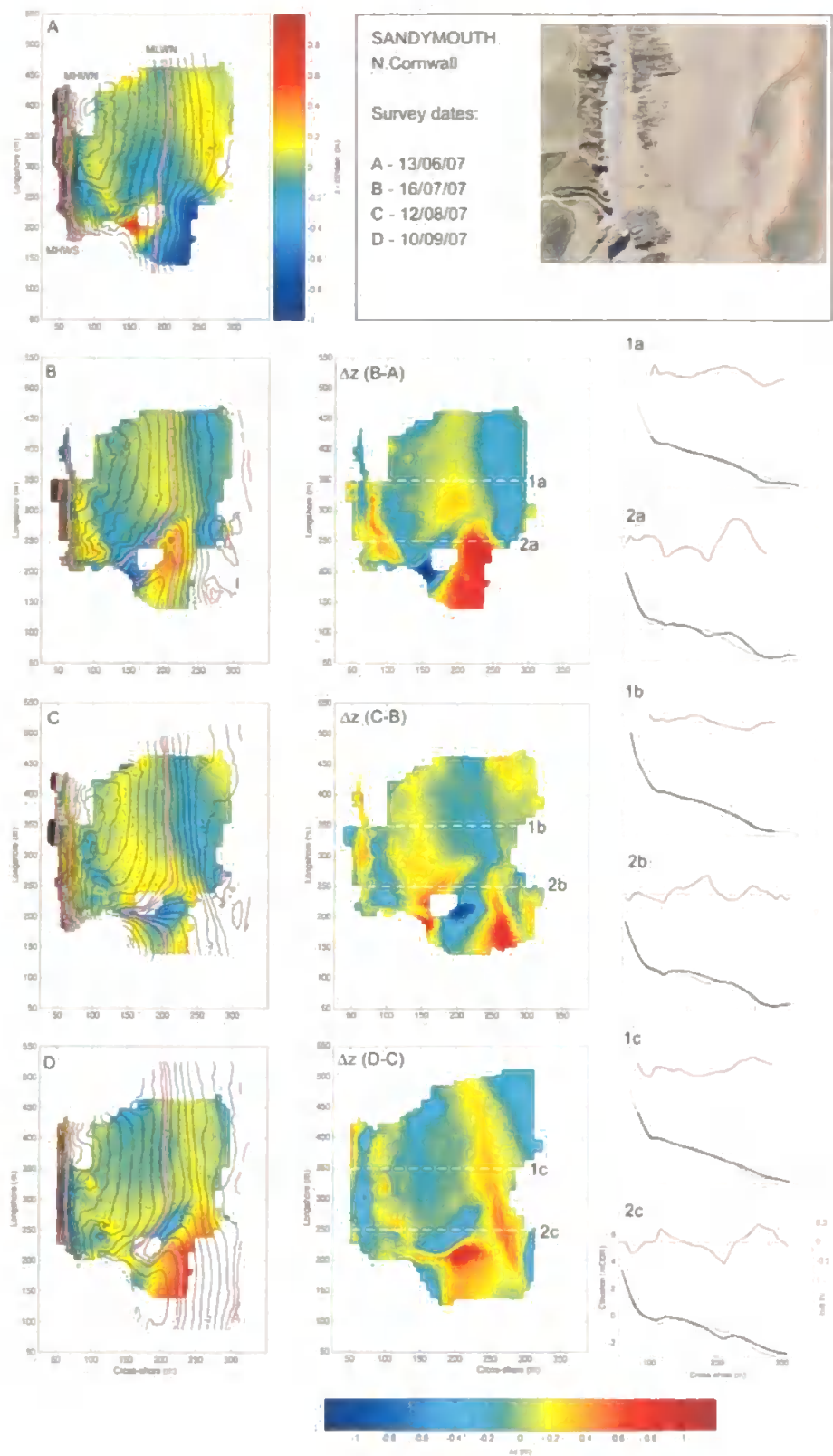
Figure 5.21 – (left) Plots show residual morphology from the mean beach surface at Sandymouth, with beach surface shown as black contours, mean tidal levels in magenta; (central column) Difference plots indicating regions of erosion/accretion between surveys; (right) Cross-shore profiles (from marked transects) show two-dimensional beach morphological change, grey and black lines indicate before and after profiles while red lines indicate residual elevation. Horizontal grey lines indicate mean tidal levels.

5.3.2.4 Rip current type, variability and density

Observed daily at low-, mid- and high-tide, a scaled, qualitative assessment of rip current severity was made by experienced lifeguards at 4 beach sites shown in Table 5.4. Severity was estimated by determining the hazard the rip current would pose to an average swimmer (Appendix 3). Rip current types for the purpose of this assessment were classified as accretionary and erosive beach rips (B) and geologically/topographically controlled rips (G). Beaches dominated by beach rips (B) show a decrease in mean rip severity and mean rip number from low- to high-tide. Sandymouth and Constantine, both LTT+R beaches, possess geologically controlled rip systems in the mid- and high-tide regions. This appears to be reflected in the mean severities that are similar throughout the inter-tidal zone at Sandymouth and enhanced in the mid-tide region at Constantine. Interestingly, the low-tide beach rips at all sites have a similar mean rip wavelength of λ_{rip} = 267–280 m where beach widths are greater than two mean wavelengths. Mean wavelengths decrease at higher tidal stages within the embayed and constrained beaches where values of embaymentisation (Short, 1999), the ratio between arc and chord dimensions, increase as does the likelihood of topographic rip currents at embayment boundaries. In addition, temporally exposed constraining rock outcrops within the shore platform at Sandymouth drive fixed rip currents within the mid- and high-tide regions reducing the mean rip wavelength. Variations in severity between beaches were not considered significant at the recorded levels due to the level of subjectivity in visual assessment.

Table 5.4 – Mean rip current severity and rip number with tidal stage at selected Atlantic west coast beaches. Data represents all observations collected during the 2007 patrol season.

Beach name	Beach type	Rip types	Low-tide			Mid-tide			High-tide		
			Rip severity	Rip number	Mean λ (m)	Rip severity	Rip number	Mean λ (m)	Rip severity	Rip number	Mean λ (m)
Perranporth (7)	LTBR	B	3.9	3.6	278	3.5	2.6	385	3	1.9	316
North Fistral (6)	LLT+R	B	3	2.5	280	2.4	1.7	412	2.1	1.6	250
Sandymouth (2)	LLT+R	B+G	3.2	1.5	267	3.2	1.7	176	3.3	2	150
Constantine (5)	LLT+R	B+G	2.9	1.7	294	3.8	1.9	211	3	2.6	192

Rip types indicate the presence of Accretionary and Erosional Beach rip systems (B) and Geologically controlled rip systems (G). Rip severity represents mean observed rip strength daily at three tide levels (where data was available). Data scaled from 0 (no rips) to 5 (extreme). Rip number is mean observed number of rip present at each observation.

5.3.3 Implications for beach safety

5.3.3.1 Incident records and environmental conditions

What is important for beach safety is the link between temporal changes in beach morphology and surf zone characteristics and the temporal hazard signature. Through an assessment of hazard levels throughout the season, temporal and spatial correlations of the hazard signature with morphologic, wave, tidal and weather conditions were investigated.

RNLI lifeguard incident and beach usage records, logged between 01/05/07 and 01/10/07 for all the LTT+BR and LTBR beaches studied (Figure 5.3), were analysed in combination with hydrodynamic (near-shore wave buoy data and predicted tidal elevations for Perranporth beach), mean wind speed (St Mawgan airfield, Newquay) and rip current morphology at Perranporth (Figure 5.22). Weekly averaging of the insea user numbers reduced bias occurring due to high weekend counts and individual rescue events providing an insight into background incident forcing.

Values for P are highest during July and August, the main holiday season, where values reach 500 insea/hr. This period is also associated with the highest weekly incident counts peaking at over 200 incidents during the week surrounding 31/07/07. The timeseries of IR shows a general upward trend throughout the 2007 lifeguard season until the end of August when a sharp reduction in IR occurred. Amongst the background trends, three significant peaks in IR were recorded during weeks surrounding 03/07/07, 31/07/07 and 28/08/07. A separation of rip related rescues in the analysis (Figure 5.22) showed that they consistently contributed to almost all incidents recorded in the weekly totals.

The availability of video data at Perranporth enabled assessment of morphological changes at a high sample rate throughout the monitoring period. Due to this, Perranporth was used as an indicator of general morphological trends throughout the studied beaches. To assess the temporal variations in rip number and configuration at Perranporth, all time-averaged rectified video images available at low- and mid-tidal stages during the monitoring period were used to extract the location of the rip head which was used to represent the rip current location in the alongshore (Figure 5.22).
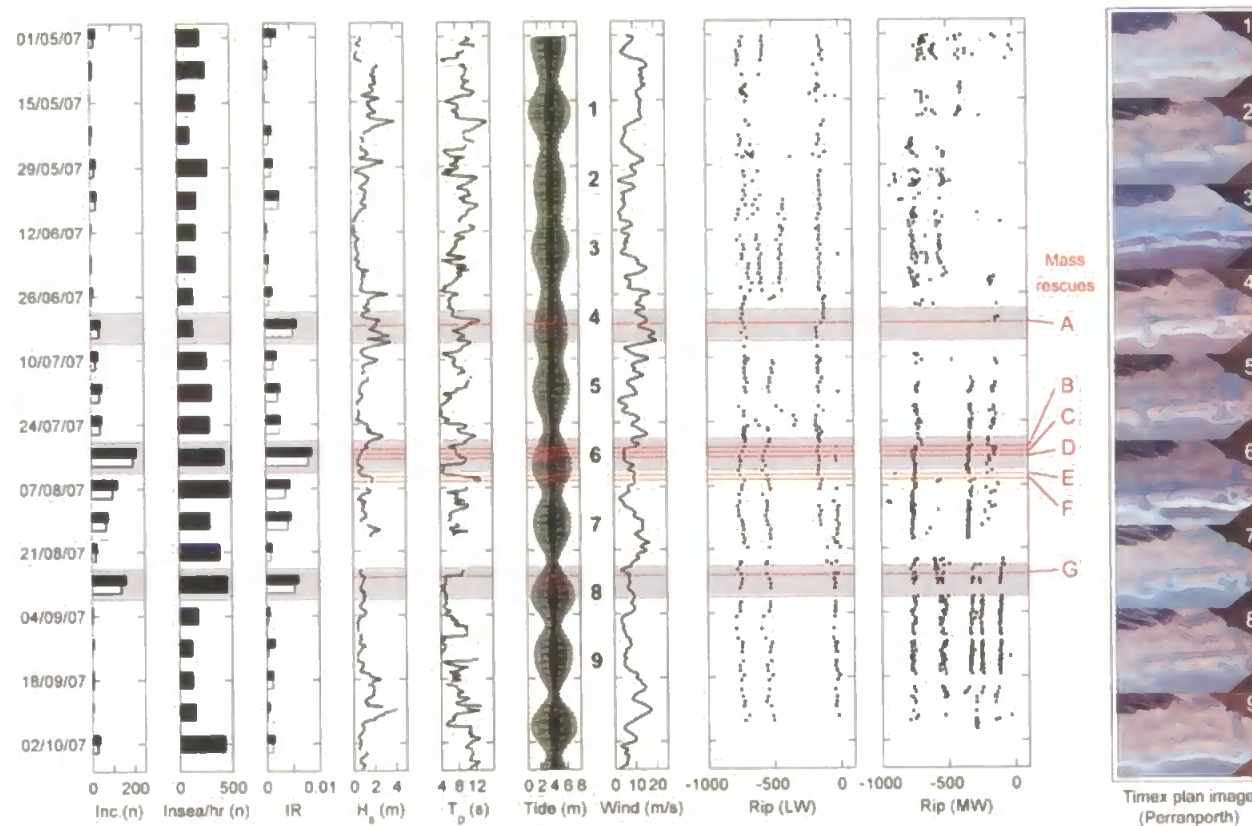
Figure 5.22 – Plot shows data from all LTBR and LTT+BR beaches studied, from left to right; individuals rescued per week (total rescues and rip related rescues shown as dark and light bars respectively); averaged people in sea per hour for each week; *IR*, total and rip rescues divided by number of people in sea per hour (a measure of the probability of an incident occurring per hour); nearshore H_s and T_p (6hr average); and predicted tidal elevation (meters from Chart Datum). Grey bands highlight weeks of high *IR*. Argus Timex video images illustrating bar morphology and general morphological transition. Red lines indicate significant coast-wide 'mass rescue' events.

Data gaps are due to either lack of image (technical); very small (no wave breaking) or large wave conditions (wave breaking occurred in rip channels). Rips were located through a reduction in alongshore pixel intensity associated with reduced wave breaking (for methodology see Section 2.3).

No systematic alongshore migrations of rip current locations were identified. The largest changes in rip morphology occurred during prolonged periods of high winds and large waves (> 2 m). Mid-tide rip systems were more dynamic and were absent for a large part of the record. They are distinct from the low-tide systems and are predominantly phase offset in the alongshore. A period of high waves in May was associated with mobile rip locations both in the low- and mid-tide regions. The subsequent cessation of wave energy during June led to the development of distinct fixed rip current channels within the low-tide ($Y \sim$ [-730; -600; -450; -150 m]) and mid-tide ($Y \sim$ [-750; -550 m]) regions. The increase in wave energy, wind and precipitation during end June/early July drove a reset of bar morphology, removing identifiable rip morphology in the mid-tide region and reducing the low-tide rip number to two ($Y \sim$ [-700; -150 m]). From this point to the end of the patrol period environmental conditions led to the development of low- and mid-tide bar systems that reached an apparently stable state during the low-energy wave conditions and large spring tidal ranges between 21/8 and 18/9. During this period, morphological enhancements of the mid-tide rip systems under low waves and high spring tidal conditions, suggests they may be incised by tidal drainage. Lack of rip current activity under the small wind waves during this period was observed to be accompanied by infilling of low-tide rip channel morphologies.

The three peaks in *IR* shown in Figure 5.22 indicate weeks in which risk associated with environmental hazards was high. The environmental conditions associated with these periods, also shown in Figure 5.22, indicated that spring tidal conditions occurred during all three high risk weeks. Considering the statistics associated with individual incidents and the corresponding tidal range (Figure 5.23) it is evident that there is indeed a greater number and a higher probability of incidents occurring during tidal ranges greater than the mean for the monitoring period. Both incident count and probability of incident peaked at the 5 m tidal range. When considering the morphological characteristics and cross-shore tidal excursion at Perranporth it is clear that tide range is a key factor driving temporal hazard levels. From video observations,
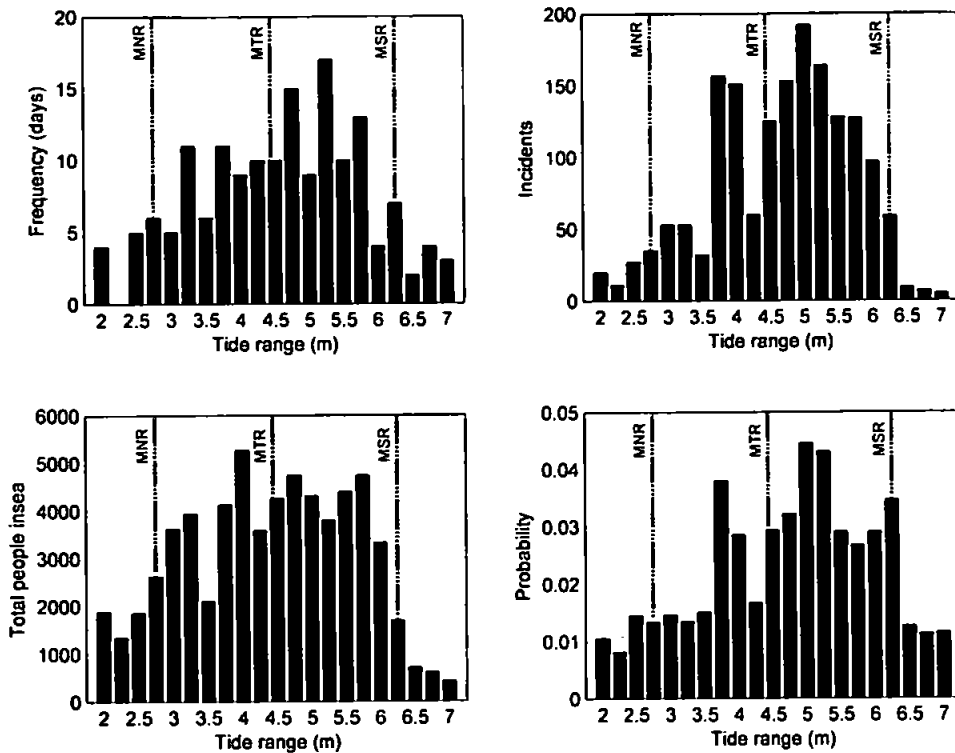
Figure 5.23 – Histograms of tidal range characteristics (top left) and associated incident frequency (top right) and insea population (bottom left) leading to probability of incident *IR* against tidal range (bottom right) during the 2007 patrol season at studied west coast beaches. Dash lines indicate mean neap range (MNR), mean tidal range (MTR) and mean spring range (MSR).

it appears that only under tidal ranges greater than the mean is the low-tide level such that the low-tide bar/rip systems become active, hence increasing levels of hazard.

In addition to the spring/neap variation, it is important to understand the semi-diurnal tidal controls on the temporal hazard signature. Tidal levels associated with individual incidents throughout the season showed some temporal variation, which can be associated with the changing morphology presented in Section 5.3.2.2. Figure 5.24 provides evidence of this temporal response, with values of incident, normalised by tidal elevation frequency, showing incident signatures throughout the tidal range for early (May-June), mid (July-August) and late season (Sept-October). The change in response shows some relation to morphological change quantified at Perranporth through values for *BNU* (Figure 5.13). Peaks in the inter-tidal *BNU* lie within the low-tide region during early season and progressively develop throughout the mid and upper inter-tidal
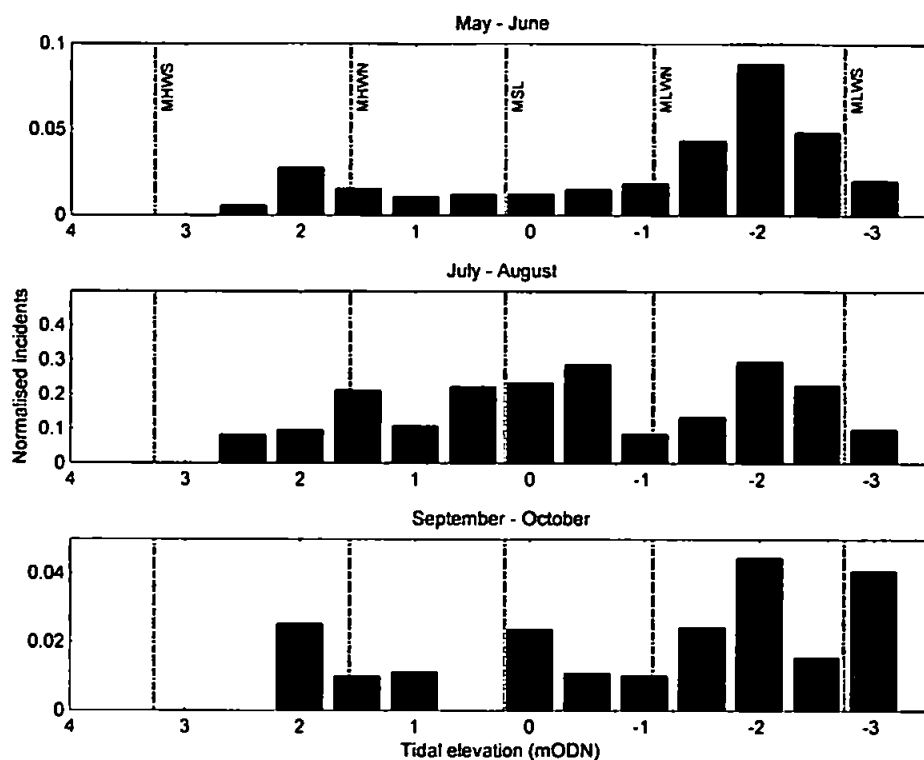
Figure 5.24 – Incident occurrence at Perranporth, normalised by frequency of tidal elevation, within 0.5 m invervals for early, mid and late season. Dashed lines indicate mean tidal levels.

zones as the season progresses. Significantly, the levels of *BNU* are unknown for the spring low-tide and sub-tidal regions where video evidence has already indicated the presence of well-developed rip systems. Figure 5.24 indicates the presence of a persistent low-tide rip hazard throughout the season identified through high normalised incident values, especially between MLWN and MLWS. Through video observations shown in Figure 5.22 the time series of rip channel locations throughout the monitoring period suggests rip current activity at low-tide. The significant variation in normalised rip incident levels comes in the mid-tide region as bar development between $X \sim$ -1–1 m, indicated by peaks in *BNU*, during July-August leads to associated increases in normalised incident levels. Within September-October low-tide incidents dominate again with a significant signal maintained within the well developed mid-tide bar systems as indicated by heightened values of *BNU* below -1 m and a continuing intersected bar presence within the mid-tide region. Analysis of morphological, incident and tidal data at Perranporth provides evidence in support of the hypothesis that incident occurrence is linked to morphology and particularly bar/rip presence and that temporal variability in morphology and sea level control hazard levels.

Trends in wave conditions and their role in controlling hazards were less clear. The two mid-season *IR* peaks highlighted in Figure 5.22 (31/7 and 28/8) were dominated by low wave heights (associated with low-energy swell wave conditions). The early season *IR* peak was dominated by higher energy swell waves, $H_s \sim 2$ m. Conditions during the high *IR* weeks (1st, 7th and 8th August) surrounding those mid-season peaks were dominated by low-energy swell waves $H_s \sim 1$ m and $T_p > 8$ s.

The joint wave distribution of the entire patrol season showed that the highest frequency wave heights were between 1.5-2 m with peak wave periods between 4–12 s (Figure 5.25). Joint distribution clusters identified short period medium-energy events and low-energy long period events as most common. Incident counts show long period low-energy wave conditions ($H_s \sim 0.5$–1 m; $T_p \sim 6$–10 s) to be associated with the highest number of incidents (241 incidents) representing 28% of all incidents at the selected beaches during the season. Unsurprisingly, the largest number of people were insea during low-energy conditions ($H_s < 2$ m), under peak wave periods of 4–12 s. Probability of incident, where insea populations are applied, yield the highest risks associated with high-energy wave conditions and peak wave periods > 10 s. These results reflect a small number of incidents occurring during the early season when insea population totals are very low. This highlights the well known hazardous nature of high-energy conditions on bar/rip beach types, although typically under these conditions, due to the low insea population exposure to these hazards are often minimal. On the other hand, illustrated by the insea population statistics and incident counts, it is clear that 75% of beach users during the season were in the sea during low-energy wind and swell wave conditions ($H_s \sim 0.5$–1.5 m; $T_p \sim 6$–12 s) and that it is under the longer period swell component of these conditions that a large proportion (36%) of the seasons incidents occurred. This highlights the importance of understanding hazard levels associated with lower-energy conditions where there are high levels of beach user interaction with the surf zone.

5.3.3.2 Mass rescue events

Throughout the season a number of high daily incident totals appeared to stand out from the background trends discussed in this section. These events have a large effect of the seasonal statistics and contribute significantly to the annual rescue totals. Anecdotal evidence from the RNLI suggested that frequently during summer months, coast-wide
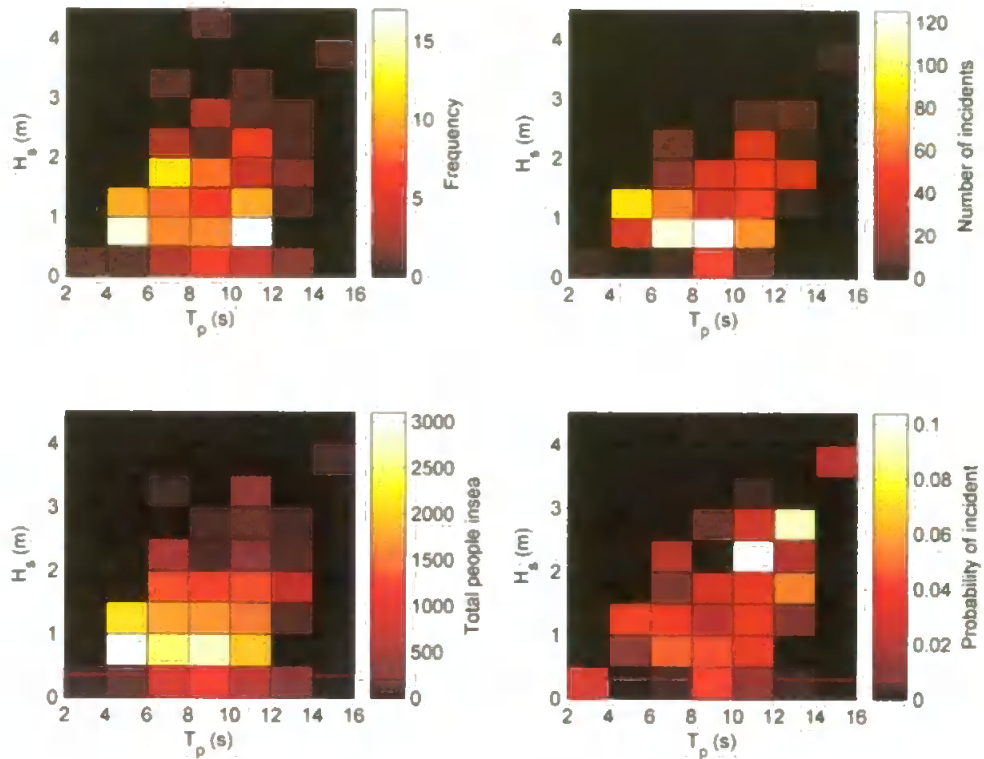
Figure 5.25 – 2D frequency matrices of joint wave distribution associated with; (top left) frequency; (top right) number of incidents; (bottom left) cumulative daily insea average; and (bottom left) probability of incident during the 2007 patrol season.

'mass rescue' (MR) events were reported to occur. Whether or not they were driven by specific environmental conditions, they evidently stretched lifeguard resources and hazard identification and mitigation procedures and therefore warranted further investigation. Within the context of MR events, the next section aims to identify the potential environmental forcing behind specific scenarios responsible for generating short-lived high risk events.

Reported MR events during the study period occurred at multiple locations on the same day and were reported to be caused by rip currents. To identify and assess these observations it was important to investigate rip incidents in relation to the number of people in-sea on any given day. Hourly people counts at each beach enabled calculation of daily mean estimates for people in-sea over the entire west coast during 2007 (27 RNLI sites). During the course of the monitoring period, short periods of high rip current incident density were recorded. These events can be seen in Figure 5.26 (inset) as 7 outliers from the bulk of the data which displays a good linear relationship ($R^2 =$

0.54) considering the inherent scatter expected in the data. By normalising incidents by the associated insea population these outlier events can be clearly identified in time. All occurring in July and August, the 7 highlighted events exceed 2 standard deviations from the mean.

Identification

This analysis was specifically interested in identifying events where high levels of rip incidents were occurring at multiple locations on the same day, enabling an insight into regional environmental conditions that may be key drivers in the cause of these events. Identifying environmental conditions in this way, of course, will not identify all the days when these optimal environmental conditions exist as identification requires an insea population, hence Figure 5.26 shows a higher density of normalised rip incidents during the peak summer months of July and August. Likewise, an assumption is made that all locations are proportionally staffed with lifeguards of equal ability to mitigate against incidents.

Event characterisation

Assessment of the incident characteristics and environmental conditions during the highlighted (A to G) MR events in Figure 5.22 indicated that except for A, all events involved ≥ 10 beaches (Table 5.5) with 15 beaches contributing to event D. Event A included only 3 beaches, one of which contributed 90% of the incidents, and is therefore not considered a spatially widespread incident. The remaining events fall into 3 distinct periods: 1) B, C and D, occurring on consecutive days totalled 264 rip incidents, with between 12 and 15 beaches involved each day; 2) E and F occurred on consecutive days totalling 171 rip incidents and involved 10 and 11 beaches respectively; 3) event G, saw 151 incidents in one day spread among 12 beach sites.

These events had a number of key environmental characteristics in common. Small to medium sized swell waves (H_s = 0.5–1.7 m; T_p = 7.6–12.8 s) were the dominant wave conditions during all the MR events. All the MR events occurred during a tidal range large enough to expose the low tide bar/rip morphology (spring) and in this region spring low water always occurs during patrol hours, often coinciding with the middle of the day, leading to higher potential hazard exposure. All events occurred during a period of high rate of change of tidal range. Events D, C, D, E and F occurred during a period where tidal range varied by 3.7 m within 6 days and event G occurred during a period where tidal range varied by 4.6 m in 6 days. These dramatic temporal variations create a
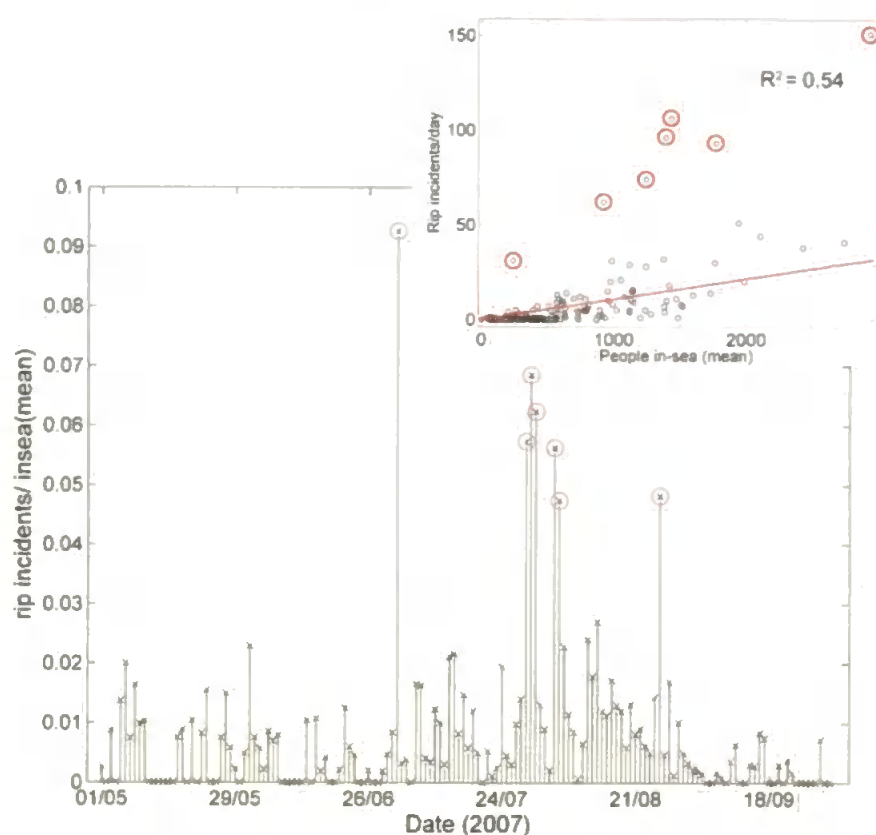
Figure 5.26 – (Inset) Scatter plot of rip incidents per day vs. people insea (daily mean), indicating linear fit and outliers. (Main) Stem plot of normalised rip incidents (daily) vs. date, with outliers (> 2σ) circled.

Table 5.5 – Outlier rip incident event ('mass rescue') data.

Event	LW times (height mCD)	Date (2007)	No. of beaches	Incidents	Highest contributors (%) primary(secondary)	H_s (m) 6hr avg.	T_p (s) 6hr avg.	Wind (kts) mean	Wind dir (°)
A	1218 (1.3)	2/7	3	31	**90**(7)	2.3	10.9	13.7	235
B	1046 (1.5)	29/7	13	62	**23**(21)	1.0	7.6	6.5	10
C	1124 (1.2)	30/7	12	106	**59**(10)	0.7	8.2	5.5	259
D	1203 (1.0)	31/7	15	96	**20**(14)	0.5	10.1	5.6	113
E	1452 (1.2)	4/8	10	77	**26**(26)	1.7	10.9	10.5	174
F	1540 (1.6)	5/8	11	94	**30**(17)	1.7	12.8	10.8	252
G	0947 (1.8)	26/8	12	151	**22**(17)	1.0	9.6	8.3	12

211

very different temporal hazard signature at a given beach from one day to the next, leading to a potential situation where, under similar wave forcing, low-tide rip systems may be inactive under one tide and active under the subsequent tide. Wind speeds during the MR events were commonly on or below the average of the study period (10 kts) with direction showing no trend.

In all the examined MR events, 3D survey and photograph/video imagery supported the observation that the low- and mid-tide bar/rip systems were well developed along the coast as illustrated in the example plan view video images of Perranporth in Figure 5.22 and Figure 5.27. Perranporth, the only beach to be implicated in all MR events had both well developed rip feeder systems that enabled isolation of the seaward bar crests at low-tide and mid-tide bar/rip systems that were well developed and offset in the alongshore from the low-tide rip channels (highlighted in Figure 5.27).

Times of rip incident occurrence, related to tidal stage during each MR event (Figure 5.27), indicate that the majority of rip incidents occurred within the mid- and low-tide periods and in D, E, F and G the transition between low- and mid-tide generated the highest incident frequency. This finding was similar to the general background incident trend throughout the season discussed in 5.3.3.1. During this transition period, locations of rip current hazard can migrate rapidly through high tidal translation rates, tidal elevation can modulate rip current velocities 'switching' systems on and off, and tidal cut-off on exposed low-tide bars during the flooding tide can force bathers to return landward through the active rip feeder channel once a critical depth over the bar in reached (1–2 hours after low-tide). The presence of phase offset three-dimensional bar systems within the mid-tide region adds complexity to the system with rapidly migrating alongshore rip locations and increased temporal persistence of rip hazards throughout the semi-diurnal cycle. The importance of the rate of change of the temporal hazard signature is illustrated in Figure 5.28. During a spring tide in 18/06/07 and 14/09/07 at Croyde Bay, Devon, the rate of tidal translation reaches up to 5 m min^{-1} within the mid-tide region in both surveys. This causes dramatic alongshore translation of rip hazards throughout the tidal cycle. Understanding these hazard variations is crucial in safely managing recreational beach users.

MR events appear to occur under certain scenarios when the combination environmental conditions and insea population dynamics are optimum for generating high hazard and
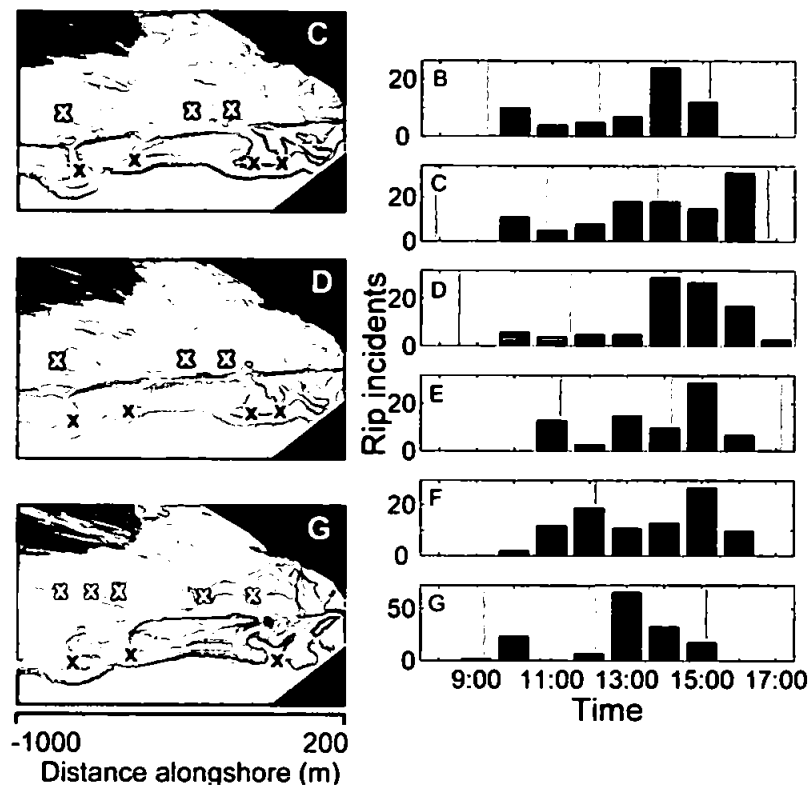
Figure 5.27 – (Left) Time averaged, rectified, low-tide video images of Perranporth during events C, D and G; sea is located at the bottom of each image, land at the top. West is oriented down-page; black markers locate approximate positions of low-tide rip currents, white locates mid-tide rip channel morphology. (Right) Histograms of incident times for each event from all beaches. Dark shading indicates 3 hour low-tide period and light shading the mid-tide.

particularly high risk bathing conditions. The generation of these optimum conditions is encouraged by the fact that during the peak summer period where maximum insea population counts are observed, small swell wave conditions are most common and proximity to the autumnal equinox means large spring tidal ranges are commonly experienced. In addition, specific to the region, low tide during spring tides periods occurs during patrol hours and commonly around midday
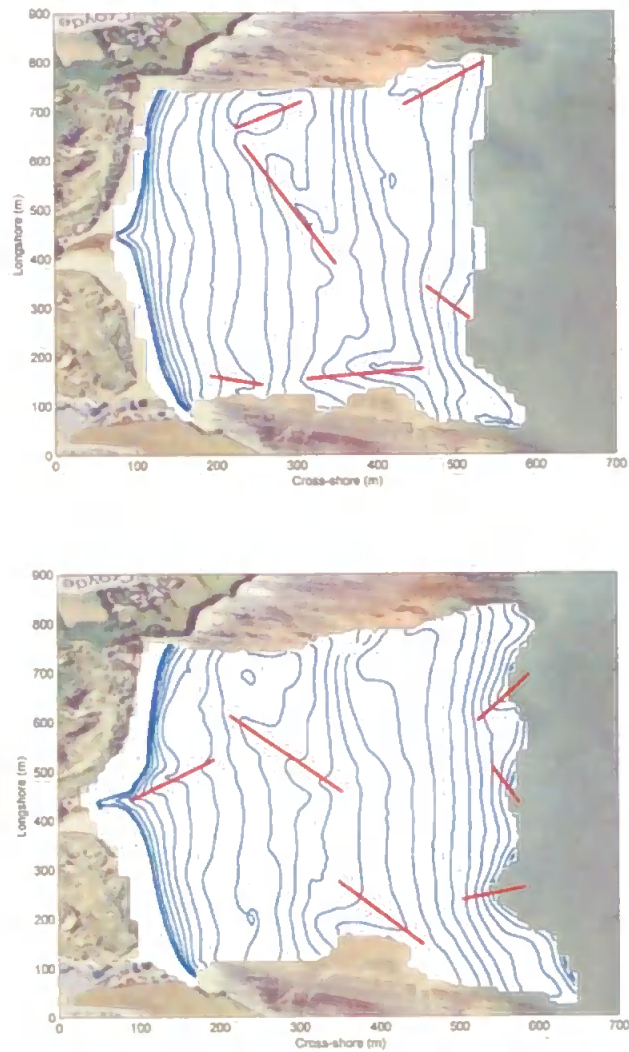
Figure 5.28 – Plots A and B show 15 minute shorelines at Croyde Bay, North Devon during spring tides on the 18/06/07 and 14/09/07 respectively. Bold red lines indicate regions of heightened rip current hazard.

5.4 CONCLUSIONS

An assessment of the temporal variation in beach volume and morphology along the high-energy (10% exceedence significant wave heights of 3–4 m), macro/mega-tidal (4.1–6.9 m) west coast of Devon and Cornwall, southwest England were made between summer 2006 and winter 2008. Significant temporal morphological change was observed:

- Low-energy summer morphologies with low tide bar/rip systems and three-dimensional mid-tide bars (RBB & TBR) were modified through high volume offshore sediment transport during winter causing inter-tidal beach lowering of ~ 0.5–1 m along all studied beaches. Planar inter-tidal beach morphologies with quasi-linear, shore-parallel, sub-tidal bars (LBT) occurred during winter.

- Sediment supply, geologic exposure and drainage characteristics modified and restricted the envelope of potential morphological transition at some locations.

The collation of detailed lifeguard incident data with that of beach morphology and hydrodynamic conditions enabled an assessment of both the implications of temporal morphological transition for beach safety and the spatial extent and characteristics of rip currents within the study region. From this investigation of the period between 01/05/07 and 01/10/07 the following key insights were gained:

- High risk LTBR and LTT+R beaches represent 59% (62% by length) of all sandy west coast beaches within Devon and Cornwall.

- Beach rip severity was observed to be highest at low tidal levels and geologically constrained rips highest at mid- and high-tidal levels.

- Temporal variation in the severity and location of rip current hazards were shown to be controlled by the characteristics of the bar morphology, specifically the development of low-tide bar/rip systems throughout the winter/summer transition. Variability in exposure of inter-tidal geologic formations in sediment poor environments controlled levels of constrained rip current hazard. While development of mid-tide bar systems during summer accretion extended the rip hazard further into higher inter-tidal regions.

- The forcing wave conditions that present the risk to the insea beach user were relatively small, long period swell waves (H_s ~ 0.5–1 m; T_p ~ 6–10 s) that allow

for shoaling to extend to the inner transverse bar and the development of strong rip currents. These conditions also maintain easy surf zone access and have a high occurrence during the summer season (hazard exposure).

- Tidal elevation played a significant role in controlling the temporal hazard signature, principally through the modulation and activation of rip currents throughout the lower inter-tidal zone. Spring tides increased exposure of low-tide bar/rip morphologies increasing rip hazards during the lower tides. Variations in tidal range from neap to spring tides created significant semi-diurnal variations in the temporal hazard signature.

- The rate of cross-shore translation of the surf zone during spring tides increased the rate of change of the temporal hazard signature, having significant implications for lifeguard beach safety management.

- Analysis of 6 coast-wide 'mass rescue' events identified that under 'optimum' combinations of the above environmental conditions as well as high insea populations, peak hazard and risk levels can overstretch lifeguard services. Specifically, these high risk scenarios were identified to be driven by the effect of spring/neap and semi-diurnal tidal variations on the interaction with the 'optimum' template morphology controlling the temporal hazard signature under the 'optimum' wave forcing conditions.

6. RIP CURRENT DYNAMICS AND HAZARDS

6.1 INTRODUCTION

Previous chapters have clearly established the importance of rip currents in contributing to beach bathing hazards in the UK and worldwide. In Chapter 5, key environmental conditions were identified which appear to control the level of hazard, particularly rip current hazard over scales of months down to days and hours through assessment of beach morphological state, nearshore hydrodynamics (waves and tides) and remote video imagery. Throughout this approach both observed RNLI incidents and qualitative lifeguard observations have been the only measures of rip current strength and activity. Therefore, the direct measurement of a rip system, within the context of these previous findings enabled further hypothesis testing through quantitative hydrodynamic observations.

During periods of high rip current hazard, it has been suggested that environmental controls present themselves as an 'optimum' combination of beach morphological state (presence of bar and rip morphology) and the prevailing hydrodynamic conditions (wave and tide). These 'optimum' environmental conditions as well as the temporal variation of the hazard signature are observed to be a key factor driving periods of high bathing risk levels during the busy summer months when these conditions have been shown to be associated with coast wide 'mass rescue' events. It is hypothesized here that one of the principal causes of these events is the tidal modulation of rip currents, where periods of low water have been qualitatively associated with increased rip current activity and the 'switching' on and off of rip currents leading to high numbers of rip current incidents. This chapter, while continuing to focus on the macrotidal west coasts of Devon and Cornwall, documents a field investigation measuring Eulerian and Lagrangian flows in a rip current system at Perranporth beach during August 2008 to investigate the circulation and dynamics and assess the forcing mechanisms behind a typical macrotidal low-tide beach rip system.

Rip currents, a well studied phenomenon in micro- and mesotidal tidal regions (1997; Bowman, 1988; Brander, 1999; Brander and Short, 2001; Castelle et al., 2006; Huntley, 1988; MacMahan et al., 2005a; McKenzie, 1958; Shepard, 1941; Sonu, 1972), have been shown to be an integral component of nearshore cell-circulation, returning water

seawards from within the surf zone, largely as a confined energetic jet. While many field experiments, like those using dye and person floats conducted in Australia and New Zealand (Brander and Short, 2000; Brander and Short, 2001), generally support such circulation, recent work by (2004; MacMahan et al., 2006; MacMahan et al., 2005) has demonstrated the rotational nature of rip currents within the surf zone, illustrated by high levels of retention of Lagrangian drifters. MacMahan *et al.* (in press) extended these observations to locations in both micro/meso and macrotidal environments. This observation runs contrary to common advice given to both lifeguards and the public worldwide, suggesting that the classic scenario may be an oversimplification of the true circulation occurring in some environments.

Increasing rip current attention and improved technological capabilities in the last decade have led to a greater number of quantitative investigations of rip current dynamics, but few of these have been in macrotidal environments. Rip currents are known to be modulated by tidally-induced changes in water level (Brander and Short, 2000) and while rip currents are forced by the incoming wave energy, they may be strongly influenced by tidal elevation (Aagaard, 1997; Brander and Short, 2001). The tide may modulate rip currents such that decreases in tidal elevation increase rip current flows to a relative maximum (Aagaard, 1997; Brander, 1999; MacMahan et al., 2005a). Brander and Short (2001) presented evidence that topographic confinement enhanced rip flow at low tide, raising the question as to whether morphological control is manifest by distinct flow channelization or by the enhancement of set-up gradients caused by wave dissipation over varying morphology. Sonu (1972) states that wave breaking over nearshore bars is essential to the formation of rip circulation and that the intensity of breaking, controlled by the tide, corresponds to a proportionally stronger circulation.

However, the findings of Brander and Short (2001) provide some support for the idea of morphologic flow constriction, with the observation that narrow rip channels with pronounced banks were more sensitive to tidally-induced water depth changes. Short (1985) hypothesizes that flow velocity is stable whilst constrained within the channel, but that once the banks are overtopped with increasing water depth the flow dramatically reduces. Perhaps more importantly, tidally induced changes in water depth modify the interaction of incident waves and existing morphology. The presence of transverse or significantly incised shore parallel sandbars in the intertidal/nearshore

zone affect wave breaking and changes in water depth create a temporal pattern of wave breaking over these bars.

When considering the extent of the typical breakpoint excursion within a macrotidal environment where significant transverse bar and rip systems are present within the low-tide region, at high- and mid-tide the proportion of waves breaking over the bars will be small and hence there will be little in the way of an alongshore gradient in set-up. As the water level falls, wave breaking increases over the bar crests and an alongshore set-up gradient is established. Therefore at some critical water depth over the bar, the set-up gradient and hence rip current flow will be maximized. This hypothesized 'switching' on and off and the apparent alongshore movement of rips as the tide translates through mid-, low- and mid-tide would increase the temporal beachface hazard signature and could be a key driver in 'mass rescue events' occurring on certain beaches.

This chapter aims to investigate:

- the extent to which the typical rip current system, observed at Perranporth, exhibits rotational circulatory behaviour, and the variation of rip circulation behaviour in relation to bathing hazard;
- the effect that tidal modulation of the sea surface has on both rip current dynamics and circulatory behavior;
- the relative contribution of mechanisms controlling rip current flow velocities, wave breaking and morphological constraint.

The chapter begins with a brief introduction of the field site at Perranporth (detailed in previous chapters) and an overview of experiment logistics, followed by a description of the data collection methods and instrument used. Results are then summarized for both the Eulerian (in-situ) and Lagrangian observations at which point selected data are presented that investigate the stated hypotheses. The principal findings are then discussed with reference to the implications they have for beach safety. Finally the chapter is summarized in a set of brief conclusions.

It is acknowledged here the collaborative team that provided both logistical support in the design and planning of the experiment, practical assistance in the field and guidance and technical support in processing and analysing the collected datasets. Dr Martin

Austin was co-investigator with the author for this experiment. His accumulated expertise in surf zone field deployments and collection and analysis of hydrodynamic data enabled the provision of key support and guidance throughout. Dr Austin provided significant contributions to Section 6.2.2.2 and Section 6.3.3. Specifically, his technical contribution with the Eulerian instrument deployment and data processing (MatLab code) and subsequent analysis was essential to the viability and success of this research within the time period available. Dr Jamie MacMahan provided technical support during the preparation, deployment and processing of the lagrangian GPS drifter deployments through the provision of GPS logging units and echo sounder, graduate students Jeff Brown and Jenna Brown (field assistance) and technical support (MatLab code) with drifter GPS data processing. The team of field assistants from the University of Plymouth and the University of Southampton also provided the man power during the experiment that was essential to make it a success.

6.2 METHODOLOGY

6.2.1 Field site

A 10-day field experiment was conducted at Perranporth, Cornwall, UK during August 2008. As described in previous chapters, Perranporth is a macrotidal beach with a mean spring tide range of 6.3 m and it falls at the transition between the low tide bar/rip and dissipative morphological states and exhibits pronounced low-tide bar/rip morphology (Chapter 5). In order to better understand the key driving mechanisms and characteristics of rip current systems similar to those representing the highest hazard to beach users as discussed in Chapter 5, it was critical to target the experiment during the following combination of conditions: a period of well developed rip morphology that is commonly associated with the low energy spring/summer period; spring tides; as well as low-energy swell wave conditions. To improve the probability of collecting observations under these conditions, beach morphological state was monitored at Perranporth over a 3-month period between June and August, 2008, to assess the optimum experiment timing and rip system location. Held between 31st July and 9th August, this period coincided with large spring tides and summer swell wave conditions (H_s = 0.83 – 1.32 m; T_p = 7.1 – 9.1 s). The low-tide, transverse bar/rip morphology was well developed during this period (Figure 6.1). The experiment period coincided with a period of high visitor numbers leading to the potential for an associated rescue signal. Perranporth was considered an ideal site due to its high incident levels, consistent bar/rip morphological presence, infrastructure and association with an Argus video monitoring program.

6.2.2 Data collection and instrumentation

MacMahan *et al.* (2006) stated that a complete rip current experiment requires three types of measurements, assuming the conditions exist for the generation of rip currents: 1) comprehensive velocity measurements within the rip channel and neighboring shoal, 2) accurate measure of the bathymetry, and 3) offshore directional waves. With this in mind the following section details the data collection program for this study.

6.2.2.1 Beach morphology and bathymetry

Regular inter-tidal beach-face surveys were carried out using a survey-grade real-time kinematic global positioning system (RTK-GPS) mounted on an all-terrain vehicle (ATV) during low tide. Surveys of the inter-tidal beach morphology were conducted
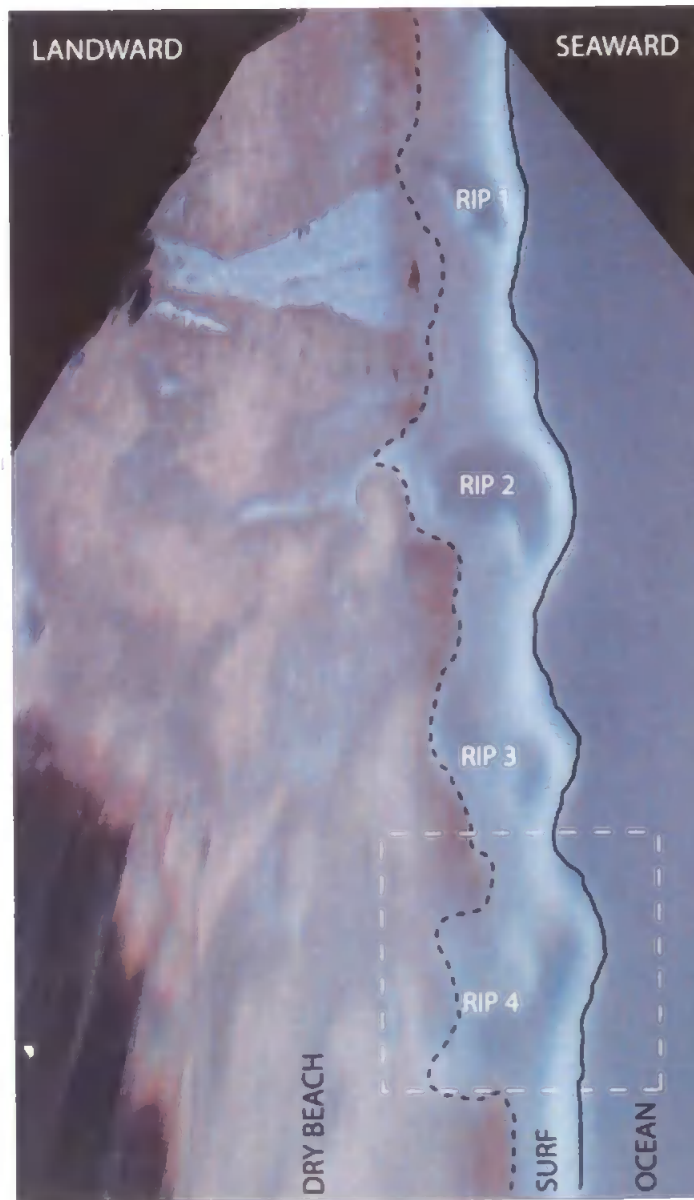
Figure 6.1 – Rectified low tide ARGUS image of rip currents at Perranporth during experiment period. The dashed and solid black lines represent the shoreline position and the seaward edge of the surf zone. The four rips are separated by transverse bars and retained within the surf zone by a longshore bar (sinuous bright band demarcating outer surf zone). The boxed area represents experiment region.

during LT3, LT8 and LT13; a more detailed explanation of the beach survey techniques and technical specifications can be found in Chapter 2. A survey-grade RTK-GPS system mounted on a single-beam sonar-equipped RNLI inshore rescue boat enabled a bathymetric survey of the studied rip current system and surrounding morphology, conducted during the high-tide period on 8th August, 2008, covering the low-tide

transverse bar system to approximately 600 m offshore of MLWS and 500 m alongshore of the rip system both to the north and south via the collection of cross-shore lines at 50 m intervals. Adverse weather and logistical restrictions allowed for only one bathymetric survey during the study period. All positions were transformed into a local co-ordinate system [X, Y]. The morphology during the field experiment was characterized by extensive bar/rip systems located around the low water level (-3 m) and a sub-tidal bar located in 7 m water depth (Figure 6.2). The incised rip channels were quasi-periodic with a spacing O(400 m) (Figure 6.1).

6.2.2.2 Eulerian measurements

In-situ measurements of surf zone hydrodynamics during the experiment were collected using an RBR TWR2050 pressure transducer (Tide Wave Recorder) located on the crest of the inter-tidal bar recorded water depth for 8.5 min bursts every 10 min (TWR in Figure 6.3). The TWR was mounted on a secure vertical steel tube with a sensor height of 0.7 m above the bed with a sensor elevation of -2.54 mODN. All nearshore instruments were sampled synchronously and logged at 4 Hz. Offshore waves were measured by a directional waverider buoy (DWR) moored in 10 m water depth. Rip current dynamics were monitored using a small array of current meters and pressure transducers located within the low tide transverse bar/rip system. Flow dynamics within a rip channel and adjacent incised shore-parallel low-tide bar/feeder region were measured with two Nortek Vector 3D-ADVs (Acoustic Doppler Velocimeter) with integrated pressure transducers also equipped with an external PT, OBS and battery pack (PUVC). The head of the ADVs and co-located sensors were mounted 0.2 m above the bed (Figure 6.3). This configuration enabled observations of pressure p, cross-shore current u and alongshore current v in burst logging mode. Two free-standing stainless steel mobile rigs were used to mount the equipment (Figure 6.3), enabling the ability to adjust the rig position between low-tides in case of morphodynamic re-configuration of the rip system and well as for ease of deployment and recovery (for data download and adverse conditions). Deployment occurred between tides 3 and 9 within the region, X = 650 m, Y = -800 m (Figure 6.2).

The instrument rigs were located in the feeder flow at the bar edge to the north of the TWR and in the rip channel adjacent to the TWR. The extent of the spring/neap tide range variations in this region means that only a small window is available in which instruments can be deployed and recovered to the required depth, after which they are
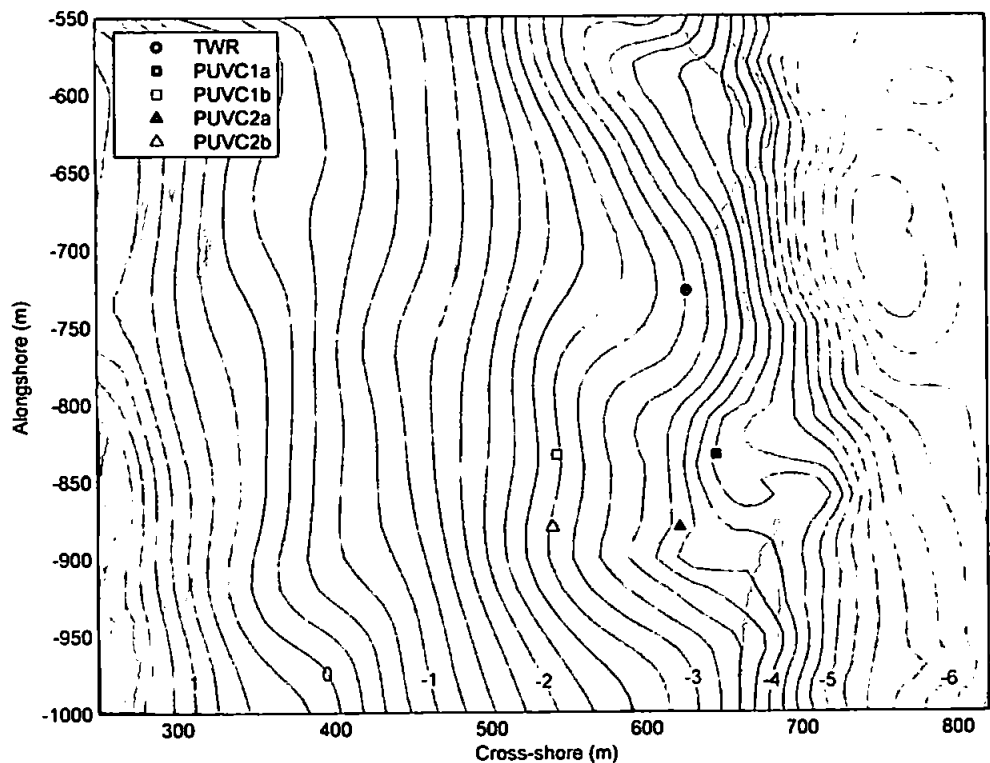
Figure 6.2 – Combined results of the inter-tidal morphology (RTK-GPS survey, LT3) and nearshore bathymetry indicating the instrument positions. PUVC positions where moved landward during LT7 due to the reduction of the spring tidal range, enabling access for post-experiment recovery during LT9. Contours indicate beach surface elevation relative to Ordnance Datum Newlyn (mODN). Back contours indicate the approximate minimum low water elevation during deployment (-2.5 m) and mean sea level (0 m). Background example rectified Argus video image taken during the survey indicates typical wave breaking and dissipation patterns (bar configuration) within the surf zone during a spring low-tide.

inaccessible without a inshore vessel for the subsequent lunar cycle, during which period they present a hazard to bathers/surfers and are vulnerable to storm damage and burial. With this in mind PUVC positions were moved landward during LT7 due to the reduction of the spring tidal range, enabling access for post-experiment recovery during LT9 (Figure 6.2).

A certain amount of processing of the ADV current data was required to generate a dataset that was suitable for analysis. Once collected, calibration constants were set for each sensor as well as sensor offsets for the deployments (taking into account redeployments of rigs). The raw ADV velocity data (v, u and w) was then quality

Figure 6.3 – Free-standing mobile instrument frame (one of two) showing Nortek Vector 3D – Acoustic Doppler Velocimeter (ADV), Pressure Transducer (PT) and Optical Back Scatter probe (OBS). Image on left indicates sensor elevations above the bed. Bottom image shows instrument frame deployment.

checked by filtering using minimum amplitude and correlation cut-offs that are set as minimum data quality standards. The filtered data was then despiked removing outliers exceeding two standard deviations from the mean. Once the quality checking procedure was completed tide, wave and current statistics were calculated and the data records from the ADVs were combined with the TWR data and separated into individual tides for analysis. Additional processing of the TWR data required correction for depth

attenuation. All sensor records were visually inspected before and after quality checking and despiking to ensure that all sensors were functioning correctly and that only poor data was removed prior to data analysis.

6.2.2.3 Lagrangian GPS drifters

Lagrangian flows in the nearshore were measured using GPS drifters similar to the design of Schmit (2005) and MacMahan (2009b). Drifters were constructed of a 10 cm UPVC buoyancy cylinder, 0.4 m in height, mounted on a circular plywood dampener, reducing vertical motions and surfing effects. Ballast was added through the addition of a steel bottom plate to maintain the water level at the base of the 0.7 m mast which was affixed to the top of the central buoyancy cylinder (Figure 6.4). Low-cost, hand-held, L1 (1575.42 MHz) Global Positioning Systems were used to track the drifter positions, specifically using a Dolorme Earthmate Blue Logger (DEBL) GPS encased in a waterproof Otterbox attached to the base of the mast. The external GPS patch antenna was fixed on a 7 cm diameter aluminium disk, acting as a groundplane, on top of the mast to reduce the effects of multi-path. The DEBL has both internal battery and data logger allowing for the recording of 5400 positions including carrier phase information (MacMahan et al., 2009a; MacMahan et al., 2009b) which amounts to a potential deployment period of ~3 hrs at the maximum sampling rate of 0.5 Hz. The positional accuracy was increased through post-processing GPS location data using a fixed, high-precision Trimble 5800 RTK GPS base station (1–2 cm horizontal accuracy). After investigation, MacMahan (2009b) stated the position error for dynamic surveys using this configuration to be 0.4 m and the velocity error on land relative to a survey-grade system was 0.01 m s^{-1}. MacMahan (2009b) also conducted experiments combining drifter and dye releases indicating that drifter observations are valid Lagrangian estimates as well as comparing well with stationary in-situ observations (MacMahan et al., 2008). The positional data were quality controlled to remove erroneous points (greater than 3 velocity standard deviations from mean), and gaps in the time series were interpolated linearly when greater than 10 s and spline interpolated for gaps less than 10 s, consistent with surf zone drifter observations by Spydell et al. (2007).

12 drifters were constructed for this experiment (Figure 6.4) and were released in groups of 4. During the experiment period a deployment area boundary was implemented that surrounded the rip system, approximated by the dashed box indicated in Figure 6.1. Treated as 'soft' boundaries, drifters were retrieved once they passed
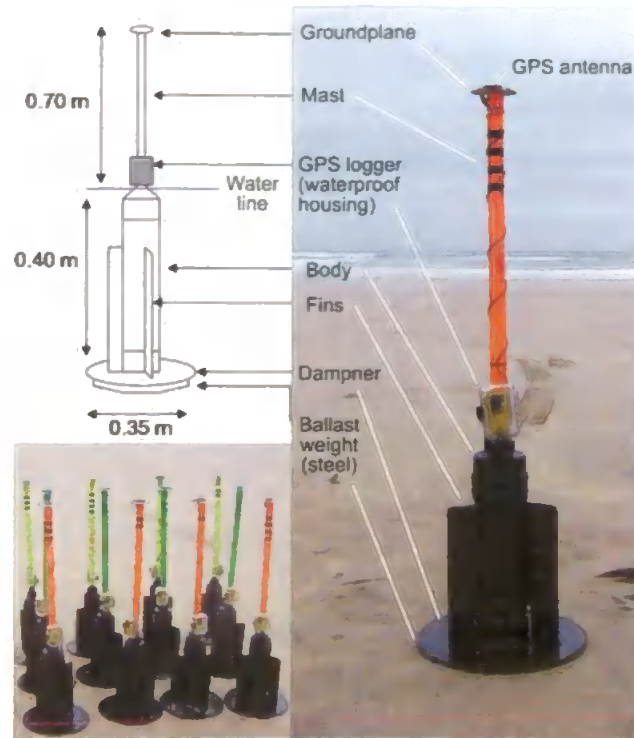
Figure 6.4 – Picture (right – not to scale) and diagram (upper left) of the inexpensive surf zone drifter that the GPS was deployed on. The main body buoyancy is built of upvc tube and welded end caps on top of a round, flat, plywood (marine) disk to dampen and prevent surfing. Below this a steel plate acts as ballast. The design is based on that of (MacMahan et al., 2009b; Schmidt et al., 2005).

through these lateral boundaries or washed up onto the shoreline and then re-released as clusters of four wherever possible. Drifters exiting the surf zone offshore were collected once they were judged to have permanently left the influence of the rip circulation. Due to the proximity of the lifeguarded bathing zone to the north of the experiment these limits had to be strictly adhered to for safety reasons. Drifters were deployed during 5 low-tides (LT3, LT5, LT7, LT9 and LT13). No deployment occurred during low-tides 10–12 due to the onset of energetic wave conditions limiting the ability to manually recover the drifters.

Drifter deployments occurred during the low-tide period when the rip currents were observed to be active over the low-tide bar/rip morphology. Deployment durations ranged from 46 to 199 minutes covering both ebb and flood transitions through the low- and mid-tides. Typical wind speeds during drifter deployments were approximately 2 m s^{-1} with a maximum of 6 m s^{-1}. MacMahan et al. (2008) experienced similar wind speeds to this study and assuming wind slippage is similar to that of Murray (1975),

Figure 6.5 – Photograph (above) of GPS drifters in the surf zone during the experiment. Drifters circled in black, with waterline at the base of the mast. Photograph (below) manpower required to safely conduct the experiment without PWC assisted pick-up.

who had used a similar drifter with a longer mast of the same diameter, they estimated the maximum biased error for the experiment to be 0.06 m s^{-1}. The drifter design proved robust with no losses or breakages during the experiment.

6.2.2.4 Remote imagery

An Argus video monitoring system, maintained by the University of Plymouth, was present at the Perranporth site. Images were collected at 30 minute intervals and provided rectified time-averaged plan views of the study area indicating regions of wave

breaking, providing qualitative information on bar configuration and wave dissipation (especially at the rip head).

6.3 RESULTS

6.3.1 Tide and wave climate

The experiment was conducted over the peak spring tide period and tidal ranges were in excess of 5.5 m (Figure 6.6). Significant wave height and peak period were 1–2 m and 7–12 s, respectively and were similar at both offshore and inshore locations, which is indicative of swell conditions. Between 04/08 and 05/08, T_p reduced sharply as strong NW winds caused local wave generation accompanied by an increase in H_s observed to be wind wave dominated (Figure 6.6). A significant swell wave event occurred between the 5th and 7th August ($H_{smax} \sim 1.9$ m; $T_{pmax} \sim 12.5$ s) during which time no equipment was deployed. The mean wave direction was -19° (south of shore normal), except for during periods of local wave generation when it was ~0° (Figure 6.6). Although the swell waves approached slightly oblique to the shoreline, refraction due to the local bathymetry between the DWR and the shoreline created near-normal incidence and resulted in relatively weak net alongshore currents, although alongshore currents associated with rip circulation were present. The experiment period experienced diminishing tidal ranges throughout from a spring-tide peak during LT3 of 6.35 m (Table 6.1).

6.3.2 Morphology and bathymetry

Morphological change, monitored throughout the experiment, was deemed insignificant in context of its effect of rip channel morphology. Due to the decreasing tidal range, collecting comparative surveys of the exposed inter-tidal region of the rip morphology at low-tide was not possible. A detailed bathymetric survey was conducted on the 8th August after previous attempts to survey the bar/rip morphology around the study region were aborted due to poor wave conditions. Representative bathymetry from here in is compiled from a detailed survey conducted during the largest spring tide on 2nd August merged with the bathymetry collected on the 8th August as presented in Figure 6.2.

6.3.3 Eulerian flow observations

A range of statistical hydrodynamic parameters was computed from the 2048 samples (~8.53 min) collected every 10 minutes (Figure 6.7). The in-situ instruments were
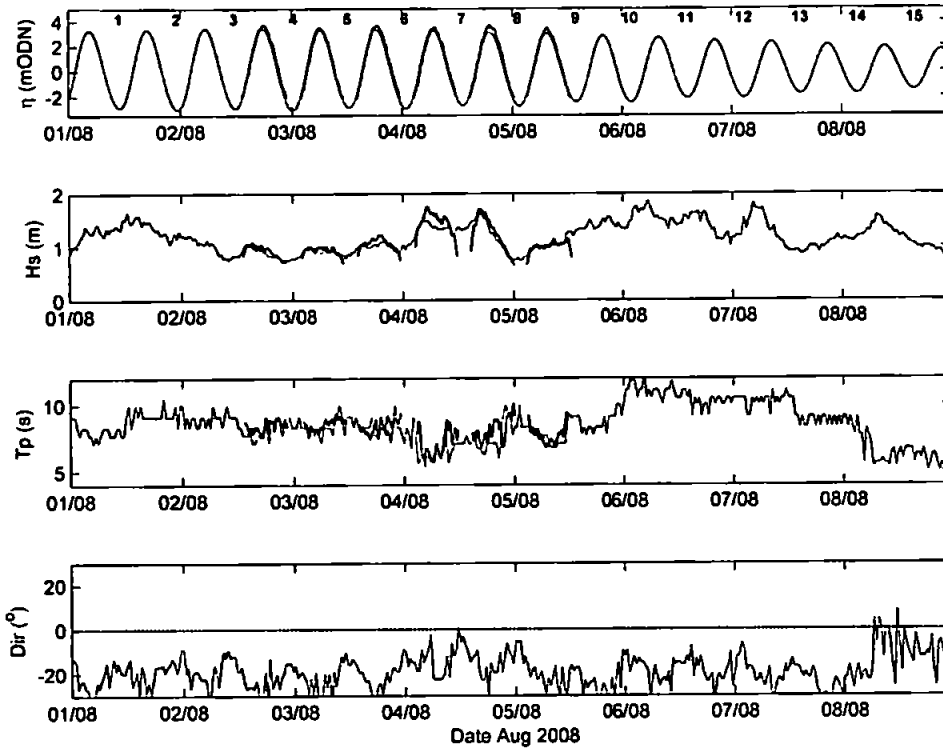
Figure 6.6 – (Top) Tidal elevation record from a UoP prediction model (grey) and the TWR (black); (below) Wave record from the DWR (grey) and TWR (black), showed measured values for significant wave height (H_s, T_p) and wave direction relative to shore normal. The DWR is located ~1 km from the shore in 10 m water depth.

deployed below the MLWS elevation and water depth over each tide varied between 0.5 and 7.5 m (Figure 6.7). The offset in water depth after the data gap during the 4th August is due to a shoreward relocation of the mobile rigs (PUVCs). H_s at all instrument locations was typically ~1 m during high-tides and increased to a maximum ~1.8 m during 4th August at the bar crest (TWR) position. Wave height was clearly modulated by water depth, consistently decreasing during low-tide (sensor within the surf zone). This is more apparent on the bar than in the deeper rip and feeder rigs as the sensor was dry at spring low-tide.

Several field studies have demonstrated that a dimensionless parameter for local relative wave height is useful when describing wave energy and wave breaking characteristics within the surf zone. Thornton and Guza (1982), amongst others, illustrated the relationship between root-mean-squared wave height (H_{RMS}) and local water depth, termed the *attenuation coefficient*, $<\gamma>$. The parameter $<\gamma_b> = H_b/h_b$ is widely used as

230

Table 6.1 – Wave and tidal observations during the experiment where H_s is mean significant wave height, T_p is peak period, and θ is mean wave direction from the DWR (10 m depth). η is predicted tidal range associated with the tide number.

LW number	H_s (m)	T_p (s)	θ (°)	η (m)
3	0.83	8.3	274	6.35
5	0.84	9.1	280	6.2
7	1.31	7.1	286	5.97
9	1.32	9.1	272	5.47
13	0.85	9.1	271	4.12

breaking criterion (Osborne and Greenwood, 1992). Values from field and laboratory work in literature range widely, largely driven by the dependence on beach slope due to hydraulic hysteresis, allowing waves on steeper slopes to break in shallower water (Galvin, 1968). Hence $\langle \gamma_b \rangle$ increases with steeper slopes and decreases with increasing wave steepness. As well as indicating the point of wave breaking and saturation, $\langle \gamma \rangle$ can also be used across the inner surf zone to describe surf zone characteristics and energy dissipation (relative contribution of unbroken, breaking, unsaturated wave and saturated bores) as H/h is predicted (Keller et al., 1960; Vincent, 1985), and has been observed in the field to increase shoreward (Vincent, 1985). On a quasi-planar beach, this enables the use of H/h as an indication wave breaking and of cross-shore location within the surf zone. H_s/h was used here to provide a spatial and temporal context for the comparison of wave breaking characteristics during the experiment. Values for relative wave height (H_s/h) suggest that wave breaking occurred at all instrument locations during low-tide ($H_s/h > 0.4$), although at the rip rig (PUVC2) minimal breaking occured during LT4 and LT5. Observed values for relative wave height at all locations increase inversely to water depth with PUVC2 reaching a maximum during LT3 and LT4 of ~1 m. Truncated values for TWR position are due to sensor elevation relative to the low-tide level. After shoreward movement of PUVC1 during LT5, pressure observations indicate sensor drying (0.2 m above bed) during the LT8 elevation minima.

Analysis of the flow velocity data from the 2 mobile instrument rigs shown in Figure 6.8 indicates significant tidal modulation of the currents with maximum flows around low water at both PUVC rigs. Mean cross-shore flows $\langle u \rangle$ are generally offshore and
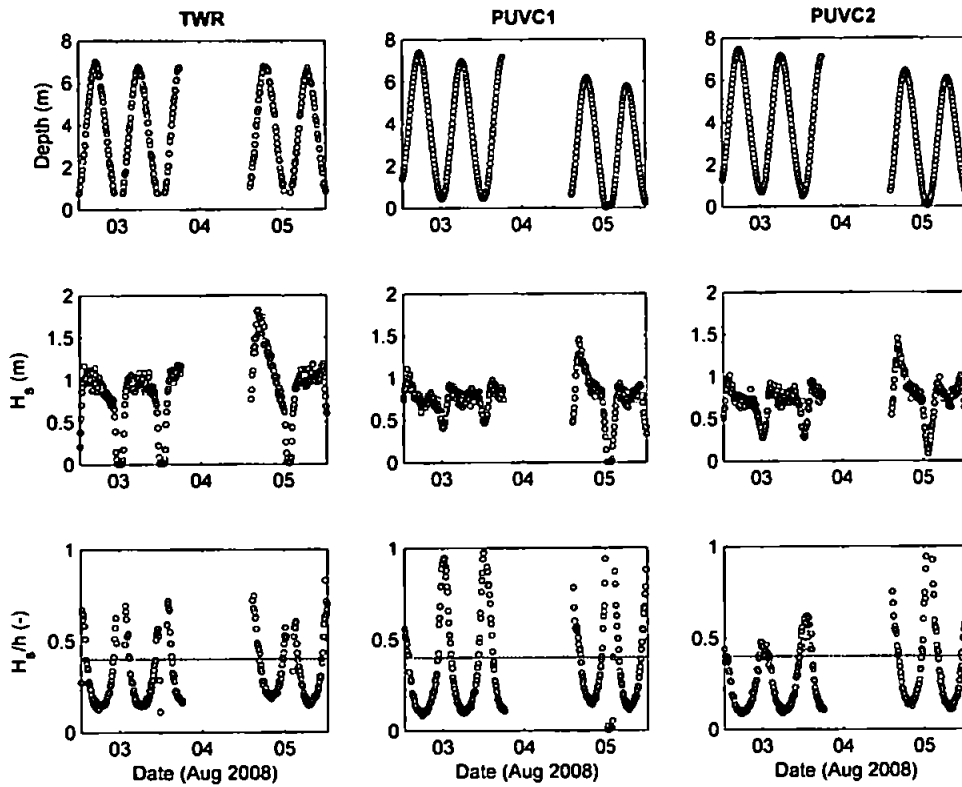
Figure 6.7 – Summary of statistics of measured sea surface elevation from the in-situ instruments at 10 minute intervals. (Top) Mean water depth above the instrument position. (Middle) Significant wave height, H_s. (Bottom) A measure of relative local relative wave height, H_s/h. The dashed line on bottom panel at $H_s/h > 0.4$ indicates approximately value for the onset of wave breaking (Thornton and Guza, 1982).

reach -0.5 m s^{-1}, whilst cross-shore orbital velocities are 0.5–1.5 m s^{-1}. Mean alongshore currents $\langle v \rangle$ were recorded up to 0.5 m s^{-1} to both the north and south with maximum orbital velocities of 0.6 m s^{-1}. Due to the circulation around the bar/rip, flow was not always directed in either a cross- or alongshore direction so the mean return speed U_r was computed as ($= \sqrt{u^2 + v^2}$). Maximum values of U_r where recorded up to 0.7 m s^{-1} and coincided with the lowest tidal stages.

Histograms in Figure 6.9 show 8.5 min mean cross- and alongshore current velocities throughout the entire experiment for both PUVC instrument rigs. The feeder rig (PUVC1) observed 41% offshore directed cross-shore velocities and 51% northward directed alongshore velocities during the experiment. The rip rig (PUVC2), as expected, observed an increased percentage of offshore-directed cross-shore velocities at 44% and
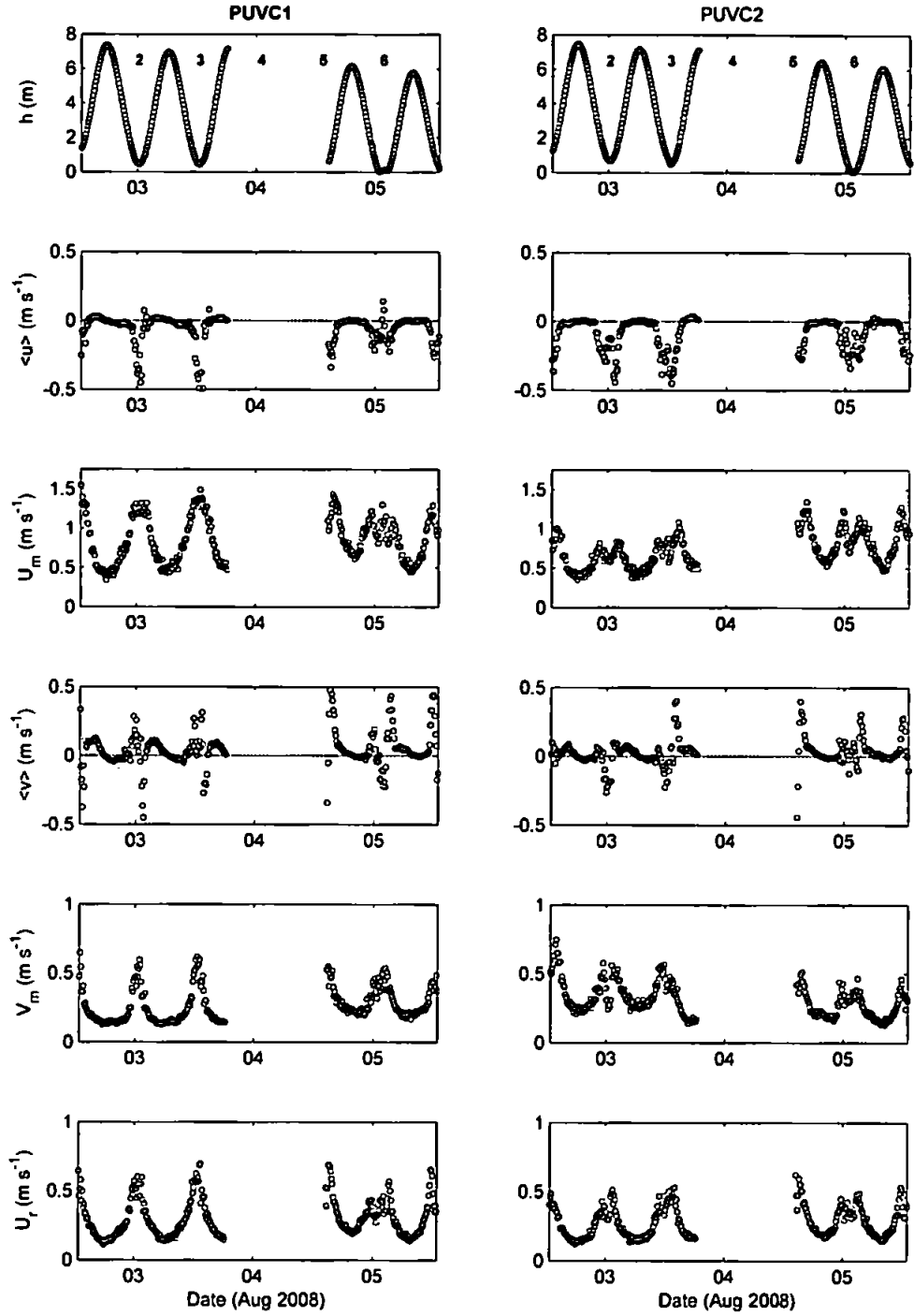
Figure 6.8 - Summary of statistics of measured flow from the in-situ instruments at 10 minute intervals for the rip (PUVC1) and feeder (PUVC2) locations. (From top) Water depth h; mean cross-shore flow velocity $\langle u \rangle$, positive onshore; maximum cross-shore orbital velocity U_m; mean longshore flow velocity $\langle v \rangle$, positive north; maximum longshore orbital velocity V_m; and U_r mean return speed. Numbers in the upper panel indicate the low tide number. LT4 is missing due to an instrument failure.

233

a reduced number of northward directed alongshore velocities at 47%. The large proportion (~50% in cross-shore; ~30% in alongshore) of velocities ~0 m s^{-1} at both rigs represents the high-tide periods where instruments are in deep water and the rip current was inactive.

Comparison of mean return flow U_r, and significant wave height H_s with water depth h was investigated for the flood and ebb tide phases. Figure 6.10 shows that this phenomenon was not apparent during the experiment. In fact, U_r was consistently greater on the flood tide at both rig locations. This appears to be matched by higher flood values of H_s up until the point of breaking, after which values for H_s are similar for both flood and ebb tides. Measured values for H_s/h at the point of breaking are consistent with the adopted threshold of 0.4. Interestingly, observations of U_r from both rigs indicate a reduction in velocity from ~0.5 m to 0 m.

6.3.3.1 Rip scaling

The rip flow velocity is clearly dependant on the tidal elevation. In this study, observed mean cross-shore currents begin to increase in the offshore direction once a threshold depth of ~3 m is reached, and although more variable in direction, the alongshore currents also increase below this threshold. As described previously, this is a phenomenon that has been observed during previous field investigations (Aagaard, 1997; Brander, 1999; Brander and Short, 2001; MacMahan et al., 2005; Sonu, 1972) over a range of morphologies, wave forcing and tidal elevations. The variety of wave and tidal conditions experienced during the experiment has indicated the existence of a relationship between wave energy and water depth within the studied rip system. The calculation of a dimensionless measure of rip current velocity (Froude number), introduced by Haller (2002) and MacMahan (2005)

$$Fr = U_r / \sqrt{gh}$$ (6.1)

where U_r is the mean return speed, g is gravity and h the local water depth, when assessed as a function of the local relative wave height H_s/h, parameterizing the forcing intensity, enabled the assessment of rip current velocities under variety of wave and tidal conditions. The dimensionless rip current velocity was observed to have a good
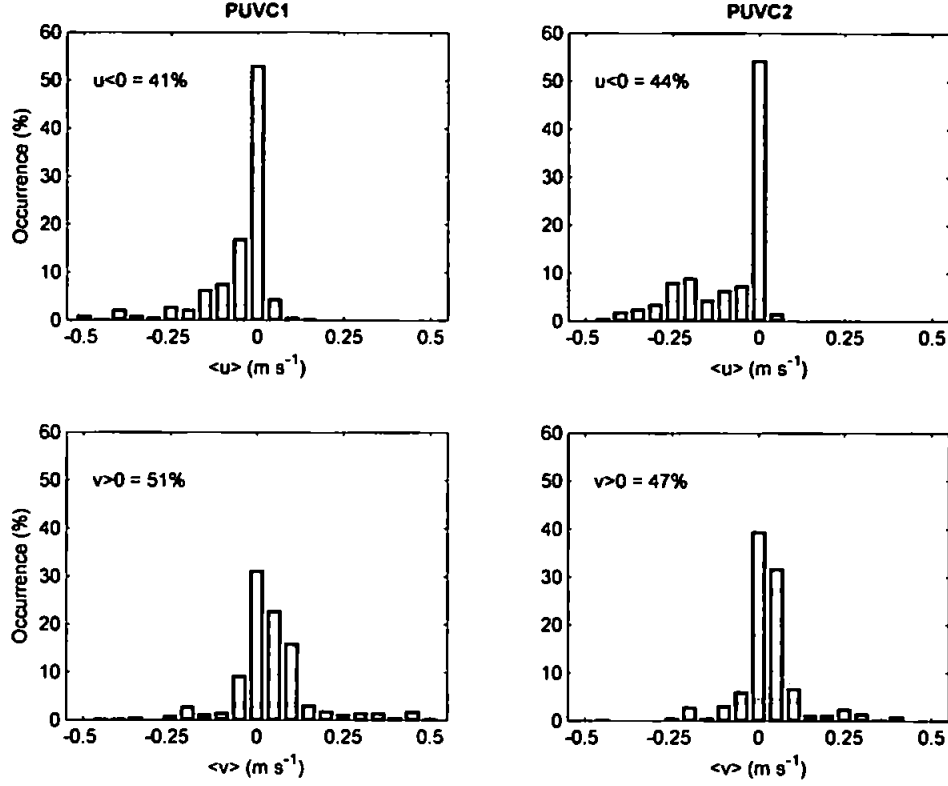
Figure 6.9 – Histograms of 8.5 min mean velocities of; (top) cross-shore, onshore directed; and (bottom) longshore, northward flows from the rip (PUVC1) and feeder (PUVC2) instrument locations. Measurements represent observations from LT(3, 4, 5, 7 and 8).

linear relationship with the relative wave height H_s/h with r^2 values of 0.59 and 0.73 for PUVC1 and PUVC2, respectively (Figure 6.11). Note the relative wave height has been computed using the significant wave height and water depth as measured on the bar crest rather than the offshore wave height as used by MacMahan *et al.* (2005); however, the wave height on the bar crest and at the DWR in 10 m water depth are very similar. An alternative scaling of the rip velocity was suggested by Brander and Short (2001) as

$$\frac{U_r}{H_s/T_p} \propto \frac{h}{h_{ht}} \tag{6.2}$$

where h_{ht} is the water depth at high tide. This scaling, which normalizes the rip speed with the wave steepness, provides a similar result to the Froude scaling and offshore directed current observations, with the rip speeds increasing significantly below $h/h_{ht} \sim$ 0.5, from mid-tide, peaking at the minimum tidal elevation ($h/h_{ht} \sim 0.1$) (Figure 6.12).
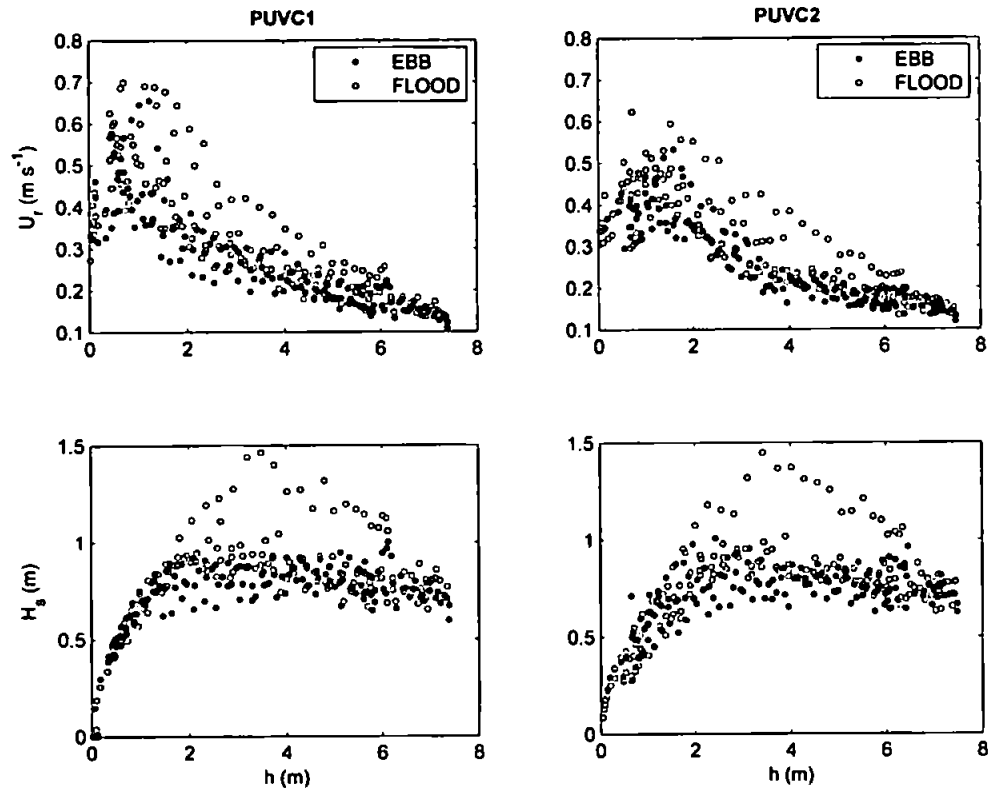
Figure 6.10 – Return flow velocities U_r during the flood and ebb tides (top) for feeder and rip rigs (PUVC 1 and 2 respectively). (Bottom) Comparison of observed significant wave height H_s during the flood and ebb tides. Data are observations from entire deployment.
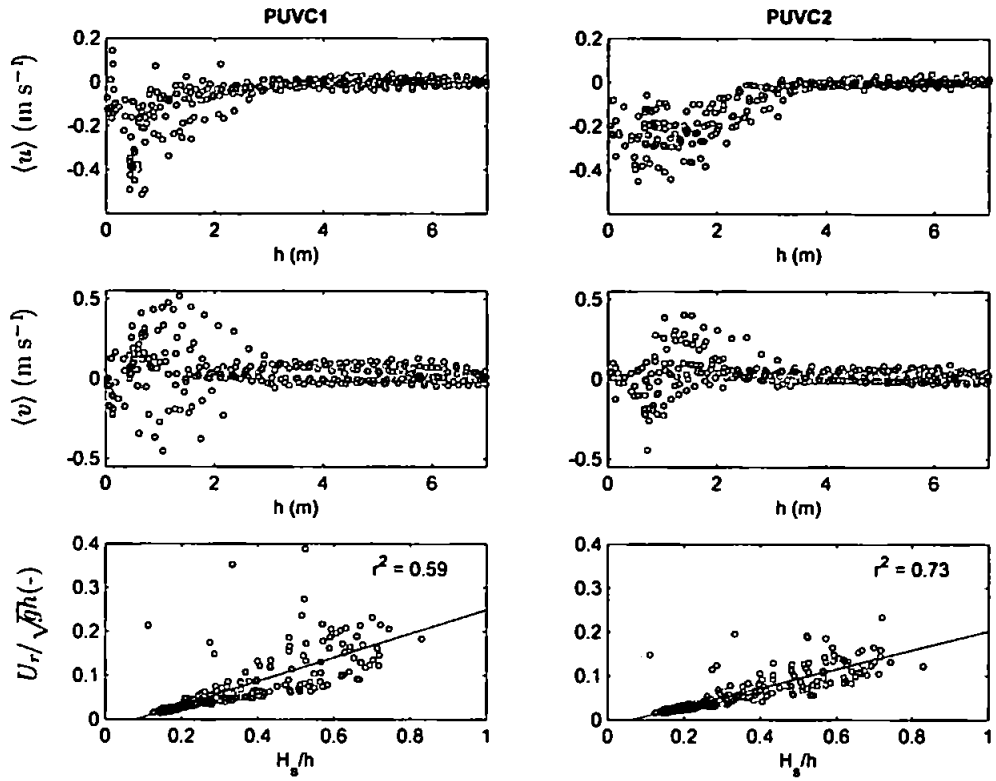
Figure 6.11 - Scatter plots of (top) mean cross-shore current and (middle) mean longshore current vs. water depth; and (bottom) Froude number vs. relative wave height on the bar crest indicating linear fit.
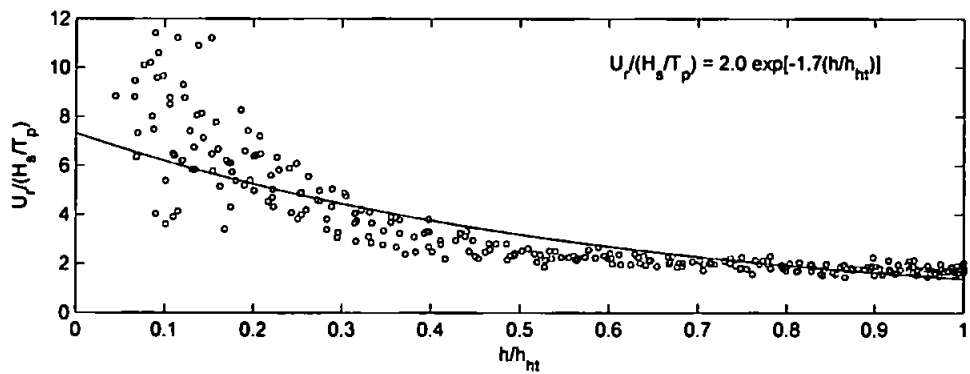
Figure 6.12 − Plot illustrating the relationship between mean rip return flow, non-dimensionalised by wave steepness (H_s/T_p). Curve represents the exponential relationship of rip velocity scaling from Brander and Short (2001).

6.3.3.2 Bathymetric non-uniformity

The strong linear correlation between U_r and H_s/h observed in this study suggests that the modulation of the intensity of wave breaking on the bar crest has a significant control on rip current strength (SONU, 1972). Therefore, it can be hypothesized that the variation in alongshore wave breaking intensity should give some indication of rip current activity. With an established link between wave breaking and water depth, it follows that a measure of the alongshore variation in depth (morphological elevation) throughout the nearshore, could be a controlling factor in rip current activity. Alongshore bathymetric non-uniformity (Feddersen and Guza, 2003) is the alongshore depth variance, $\sigma_h^2(x)$, defined as

$$\sigma_h^2(x) = \frac{1}{L_y} \int_0^{L_y} \left[z(x,y) - \overline{z(x)} \right]^2 dy \qquad (6.3)$$

where $z(x,y)$ is the bottom elevation, $\overline{z(x)}$ is the alongshore mean cross-shore profile, L_y is the alongshore integration distance and d_y the alongshore grid spacing. Data from the RTK-GPS inter-tidal beach and bathymetric surveys and are used to compute $\sigma_h^2(x)$.

The cross-shore profile envelope and distinct maxima in the alongshore depth variance can be seen in Figure 6.13. Maxima correspond to the nearshore incised bar/trough morphology associated with the instrument locations at $X \sim 630$ m and the outer extent of the rhythmic bar system associated with the seaward extend of the surf zone during the experiment ($H_s \sim 1$ m) at X ~ 730 m. An estimation of the theoretical break point locations and cross-shore excursion throughout a tidal cycle were calculated following the empirical breakpoint criterion (Sallenger and Holman, 1985):

$$\langle \gamma_b \rangle = 0.3 + 3.2 \tan \beta \qquad (6.4)$$

where $\tan\beta$ is beach slope ($\tan\beta = 0.017$) giving a breaker index $\langle \gamma_b \rangle = 0.36$. Assuming a significant wave height of 1 m (approximate for study period) breaker depth can be calculated as $h_b = H_s/\langle \gamma_b \rangle = 2.8$ m. The calculated breakpoint excursion throughout the tide extends ~400 m to X ~720 m. Cross-shore velocities from the rip rig indicate that rip activation occurs below ~3 m water depth (-1 mODN). Under these theoretical conditions, it is clear that the onset of rip activity occurs in association with wave
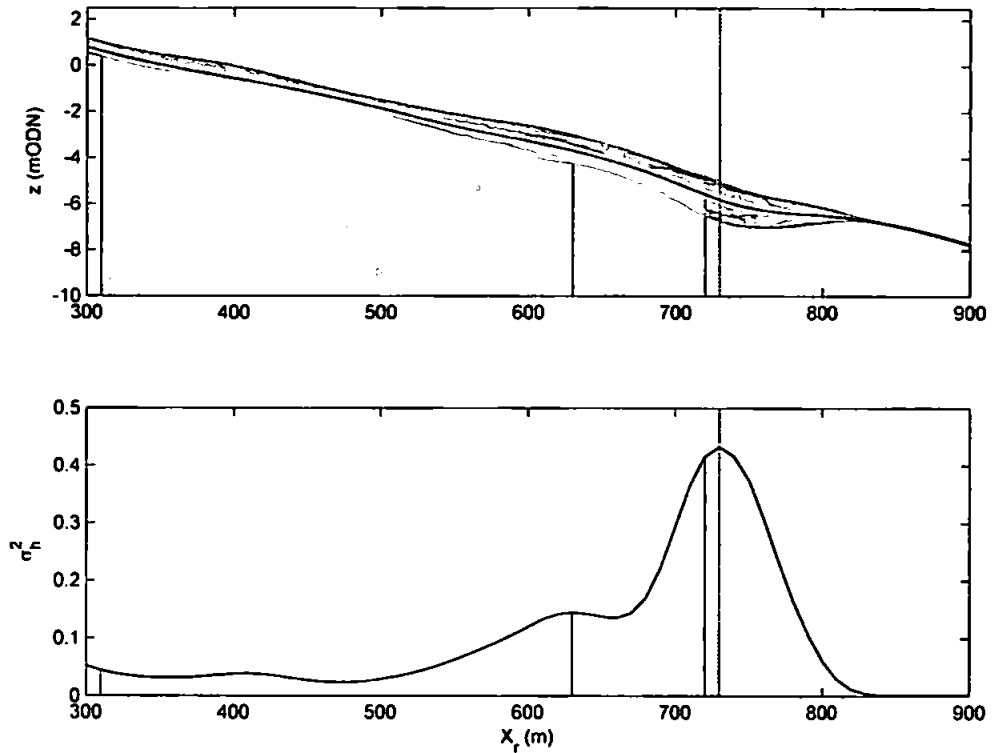
Figure 6.13 – Alongshore bathymetric variability: (top) cross-shore profile envelope (grey) and mean profile (black) occurring within the study region; (bottom) alongshore bathymetric non-uniformity, $\sigma_h^2(x)$. Shaded regions represent the approximate breakpoint excursion (H_s = 1 m) using the empirical relationship $<\gamma b>$ = 0.3 + 3.2$\tan\beta$ from Sallenger and Holman (1985), during the highest and lowest tidal elevations during the study period. Darker shading indicates the region in which the rip current was typically active (z < -1 mODN).

breaking at the shoreward maximum in alongshore depth variance extending to the seaward maxima (rhythmic bar) at the low-water extreme, where wave breaking occurs on the rip head bar in conjunction with an observed temporary decrease in mean return flows.

6.3.4 Lagrangian GPS drifters

Lagrangian observations obtained using GPS drifters enabled a synoptic assessment of rip circulation patterns and velocities over the larger spatial extent of the system than the in-situ Eulerian observations. Observations provided an insight into the temporal variation of the rip current circulation patterns and tracked drifter trajectories within the surf zone.

6.3.4.1 Mean circulation

To enable the calculation of a mean circulation pattern the spatial extent of the nearshore was split into 10 m x 10 m bins and the drifter observations during each low-tide deployment (LT3, LT5, LT7, LT9 and LT13) averaged within each bin. A drifter was considered as an independent observation when within a particular bin. If a drifter re-entered the same bin, it was considered a new independent observation if $t > l_g/U$ had elapsed, where l_g is the length of the bin and U is the average speed for all drifter observations in that bin. Bins with at least 5 independent observations were considered statistically significant (Spydell et al., 2007).

It is clear from Figure 6.14 that a large rotational rip current circulation was present within the surf zone during the course of the experiment with cross- and alongshore length scales of ~200 m. The rip circulation was counter-clockwise and traveled offshore through the surf zone under an angle to the south until reaching the seaward breaker line. The flow then turned alongshore for ~75 m before returning through the surf zone over the shallow intertidal bar at approximately $[X, Y] = [650 \text{ m}, 750 \text{ m}]$. There were several points in the circulation pattern where drifters would exit the surf zone to seawards, be ejected into adjacent rip systems or meander in very shallow water to landwards. For all tides, except LT13 (07/08/08), the rotational eddy was observed to be present with varying degrees of persistence and velocity. LT5 and LT7 exhibited the most developed circulation cells with mean velocities indicating high levels of surf zone retention and only a few surf zone exits. LT9 and LT13 appear to be dominated by alongshore current movement with very limited significant surf zone eddy circulation observed during the deployments.

The mean significant flow speeds (per tide) recorded by the surf zone drifters from within the rip current circulation are within the range 0.01–1.27 m s^{-1} with the maximum tide integrated speeds recorded during LT5 and LT7, which were the tides associated with the most intense rip circulation. Modal drifter speeds during the experiment ranged from 0.3–0.5 m s^{-1}, peaking at 0.55 m s^{-1} during LT7. Mean return speeds are comparable with the mean rip return speeds recorded by the in-situ instrumentation (0.35–0.4 m s^{-1}), but there is a greater proportion of higher speeds and lower speeds (Figure 6.15). This is probably due to the higher number of spatial observations recorded by the drifters in the region of maximum and minimum circulation compared to the single points of current measurement intentionally deployed
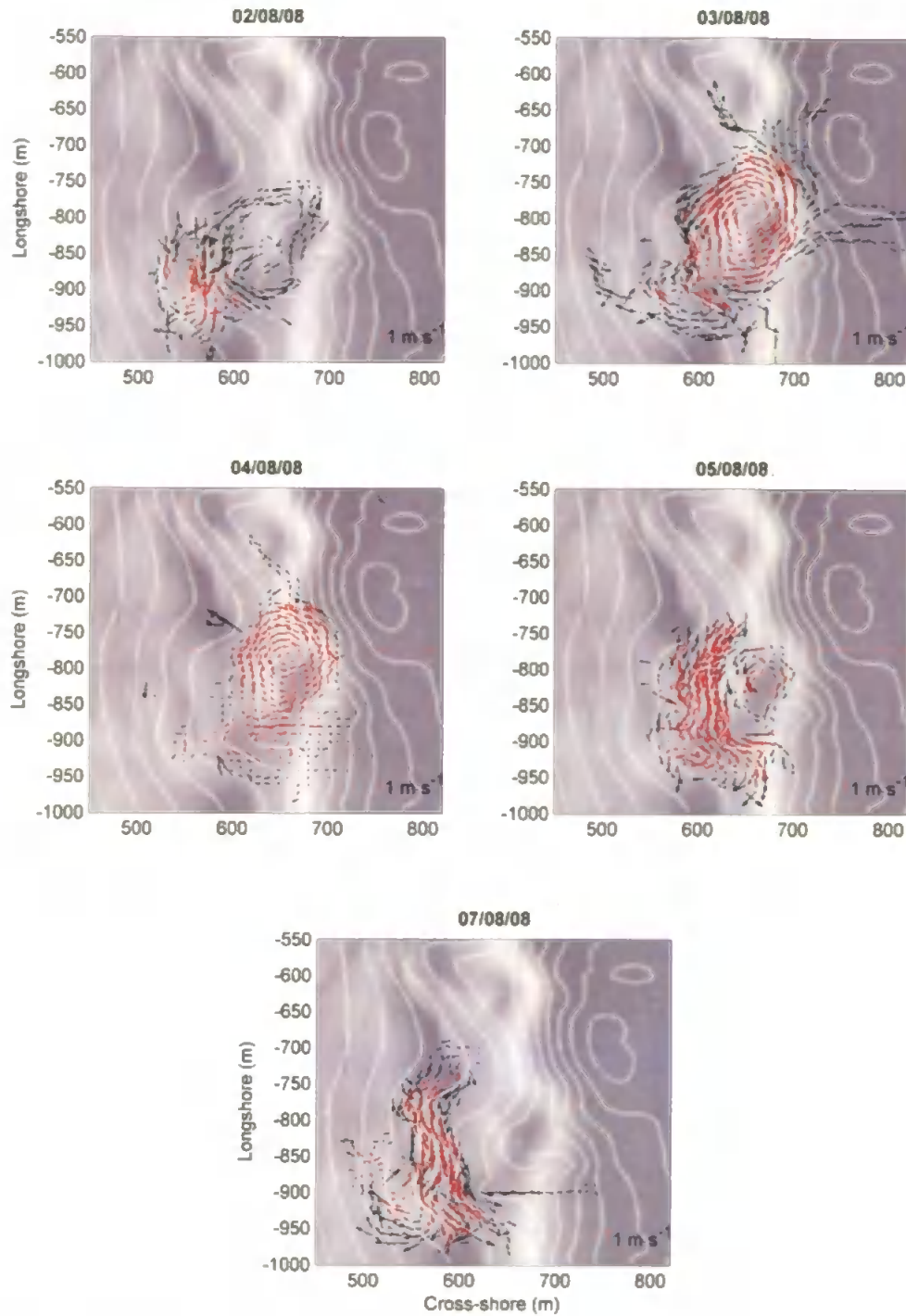
Figure 6.14 – Mean drifter velocity observations for each deployment (LT3, LT5, LT7, LT9, LT13 chronologically). Scaled vectors represent drifter velocity direction and strength. Each vector represents mean independent drifter observations (n) within 10 m x 10 m bins. Red vectors represent statistically significant velocities (n > 5). Beach morphology and bathymetry are contoured in the background (08/08/08 bathymetry) along with a rectified video timex image showing wave breaker intensity.
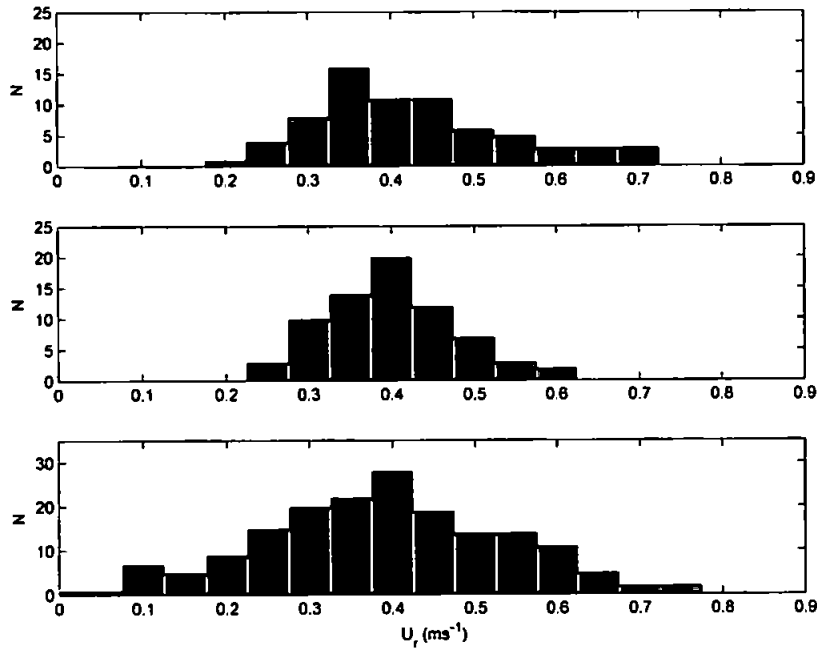
Figure 6.15 - Comparison of Eulerian and Lagrangian drifter speeds U_r. Mean rip current speeds at PUVC1 (top) and PUVC2 (middle) during periods when the rip current was active (η < -1 mODN). (Bottom) Rip speed from the statistically significant mean drifter circulation during periods when drifter and in-situ instruments were synchronous.

within the feeder and rip channels. With a limited morphological variation it is clear that variations in circulation pattern are driven by changes in the wave and tide conditions.

6.3.4.2 Circulation pattern classification

A variety of drifter track behaviors was observed during the experiment. In order to understand the dominant behavior of released drifters during each deployment, circulation patterns were divided into 6 categories (Figure 6.16; Table 6.2): (1) Wash-up, where dominant motion of drifter is shoreward, washing up on the shoreline; (2) Meandering, where drifter paths follow no significant circulation and meander around the inner surf- and swash-zone at low speed; (3) Alongshore, where subsequent to release drifter travels alongshore, without circulating or moving offshore within the rip circulation; (4) Rotation, where drifter tracks indicate rotational (including offshore directed) trajectories associated with the rip current cell circulation; (5) Exit, where a track exits the surf zone through the rip neck; and finally (6) Exit and re-entry, where an exiting drifter subsequently, possibly through Stokes drift and/or wind slippage, re-enters the surf zone. The number of cycles within the surf zone was calculated for those that entered the rip circulatory system (Rotation and Exit). Rotational rip current tracks
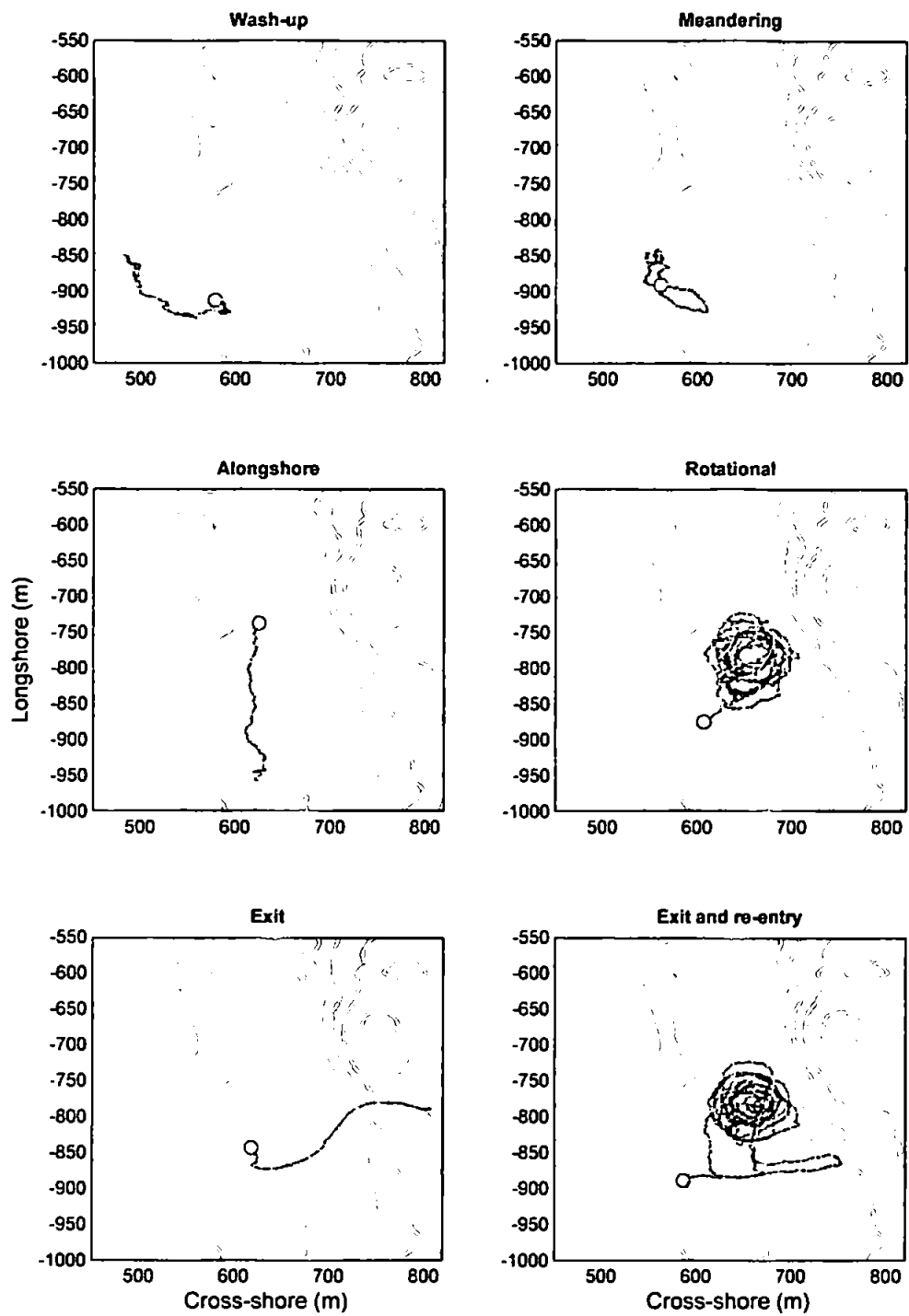
Figure 6.16 – Examples of drifter track classifications.

Table 6.2 – Statistics of drifter track classifications during each deployment. Duration is time between release of first and last drifter in each deployment. Mean and max cycles represents the number of full cycles of the rip system on a single release (only includes those drifters within the rotation class).

LW number	Duration	Wash-up	Meandering	Alongshore	Rotation		Cycles	
	min	%	%	%	%	% exit	mean	max
3	46	3.85	7.69	69.23	19.23	3.85	1	2
5	144	10.26	2.56	0	79.49	23.07	2.96	10
7	146	25	3.13	3.13	59.38	18.75	6.63	24
9	120	4.26	8.51	78.72	6.38	2.13	4.67	9
13	199	20	7.5	70	2.5	2.5	0	0

dominated the circulation for LT5 and LT7 (79% and 59% respectively), with alongshore tracks dominating for LT3, LT9 and LT13 (69%, 79% and 70% respectively). During LT5 and LT7 when the most significant rip cell vortices were observed, surf zone retention was high, with mean cycles per drifter within the rip current of 3 and 6.6 for LT5 and LT7 respectively. In some cases the drifters would exceed 10 cycles over periods greater than 45 minutes. A maximum of 24 cycles was observed during LT7. Although this aids the understanding of the characteristics of the specific rip current circulation over a period of time, the key question is: what is the effect of tidal modulation on these observed rip circulation behavioral patterns? Hydrodynamic conditions for each drifter deployment are summarized in Table 6.3.

6.3.4.3 Tidal modulation of circulation pattern

In order to investigate tidal modulation of rip circulation, Lagrangian drifter observations for each deployment were divided into elevation bins of 0.5 m. An unbroken tidal record was required. The fixed in-situ TWR provided the most accurate sea-surface elevation record in the surf zone. This record had data gaps during extreme low-tides, during which the sensor was dry, therefore the predicted tidal curve for Perranporth was considered. A cross-correlation of the predicted and measured record shows a high correlation with a lag of -20 mins (Figure 6.17). The offset predicted record was subsequently used to simulate the missing data. Drifter tracks were categorized into designated elevation bins associated with their release times. For illustration, tracks were classified into one of three behaviors; wash-up/meander; alongshore; and rotation/exit. Video images represent those captured during the associated elevation period.
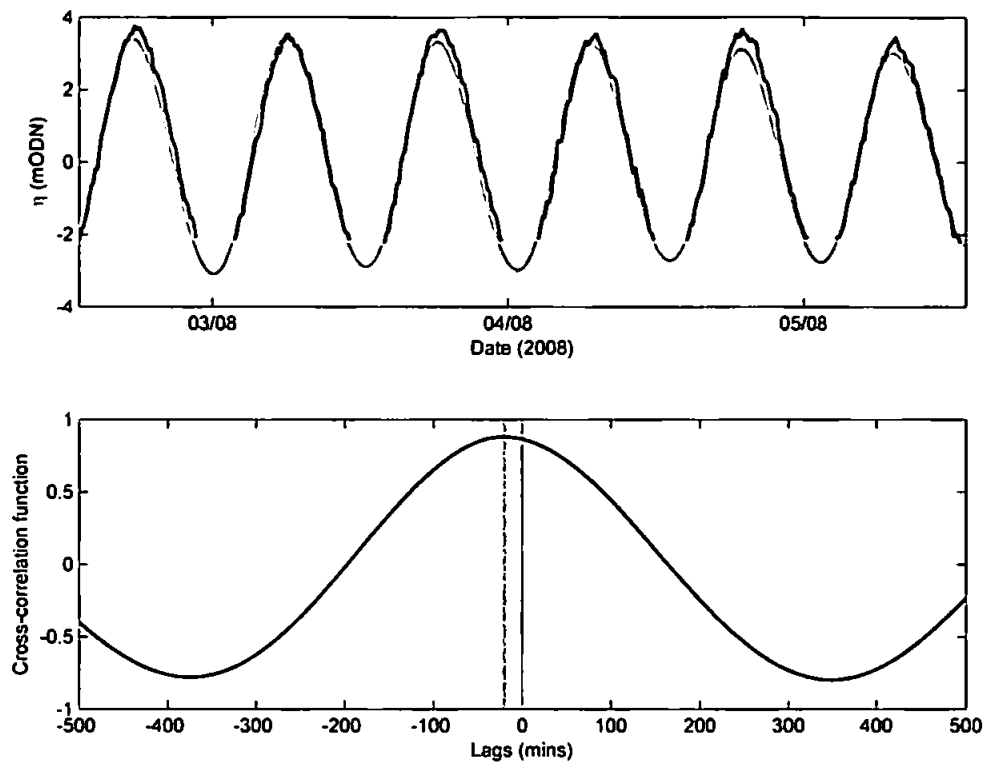
Figure 6.17 – Comparison of predicted and measured sea-surface elevation. (Top) predicted tide (grey) and measured surface elevation, η (black). A consistent lag on the falling limb of the tide can be seen in the TWR data. Lag is also observed on the rising limb to a lesser extent. (Bottom) The cross-correlation function of the time series in the upper panel indicating a negative lag of 20 mins (dotted line).

Table 6.3 – Summary of hydrodynamic conditions observed during drifter deployments at a water depth of 10 m. Shoreline orientation is 293°.

LW number	H_s (m)	T_p (s)	θ (°)	$\Delta\eta$ (m)
3	0.83	8.3	274	6.35
5	0.84	9.1	280	6.2
7	1.31	7.1	286	5.97
9	1.32	9.1	272	5.47
13	0.85	9.1	271	4.12

LT3 (02/08/08)

Dominated by small swell waves (H_s = 0.83 m; T_p = 8.3 s) and large spring tides ($\Delta\eta$ = 6.35 m), alongshore drifter movement dominated during a deployment (46 mins) that did not include the extreme low-tide. Wave angle in 10 m depth is -19 degrees to shore normal. Elevations between -1 and 0.5 mODN were captured. Video images indicate a reduction in wave breaking on adjacent bars as tidal elevation increases, accompanied by a reduction in rotational drifter tracks. Alongshore movement was the only behavior between -0.5 and 0.5 mODN. Rotational tracks associated with rip current activity only occurred between -1 to -0.5 mODN (Figure 6.18).

LT5 (03/08/08)

Under similar conditions to LT3, small swell waves dominated the deployment (H_s = 0.84 m; T_p = 9.1 s) during large spring tides ($\Delta\eta$ = 6.2 m). Wave angle in 10 m depth is -13 degrees to shore normal. Deployment spanned the full extent of the low-tide (144 mins). Elevation from -3 to -0.5 mODN were entirely dominated by a highly retentive rotational rip current vortex accounting for greater than 80% of drifter circulation patterns with a mean and maximum of 3 and 10 cycles, respectively, during the deployment. No evidence of the presence of an alongshore dominant current was observed. Between -2 to -1 mODN a reduction in rotational behavior occurred ending in 100% wash-up/meandering between -1.5 and -1 mODN. A reduction in wave breaking over the bar/rip system was observed simultaneously to the observed reduction in rotational behavior. Of the rotational tracks, 23% exited the surf zone at some point.

LT7 (04/08/08)

The deployment during LT7 extended throughout the ebb and flood limbs surrounding the low-tide stand (deployment of 146 mins) with a spring tidal range of $\Delta\eta$ = 6 m With an increase in wave height and reduction in period (H_s = 1.31 m; T_p = 7.1 s) with a wave angle of -7 degrees from shore normal. Rotational circulation dominated throughout with only 3% alongshore tracks. The deployment observed tracks between tidal elevations of -3 to -2 mODN. High levels of surf zone retention led to rotational track cycling 6.6 times on average with a maximum of 24 cycles during one release, retaining the drifter for 153 mins. Of the rotational tracks 18.8% exited the surf zone at some point. Evidence of a smaller counter circulation to the north was observed.

LT9 (05/08/08)

After LT7, tidal ranges began to significantly reduce. An increase in wave period signaled the onset of a higher energy wave climate (H_s = 1.32 m; T_p = 9.1 s) with wave angles increasing to -21 degrees from shore normal. A 120 min deployment during the low-tide period covered a single tidal elevation bin of -2.5 to -2 mODN. During this deployment, 79% of tracks were classified as alongshore (to the north) and only 6.3% entering a rotational behavior. Wave breaking (observed on the associated video image indicates) occurred predominantly on the seaward extent of the rhythmic longshore bar, including in the rip head.

LT13 (07/08/08)

Deployment during LT13 occurred during low-energy swell waves (H_s = 0.85 m; T_p = 9.1 s), after a period of higher energy waves, before which the instrument rigs were decommissioned (LT9). The mean wave angle was -22 degrees to shore normal in 10 m water depth. Alongshore track behavior to the north dominated (70% of releases) during the 199 min deployment, with only one release indicating a rip circulation between tidal elevations -2 and -1.5 mODN that exited the surf zone immediately. The smaller tidal range led to little or no morphological isolation of rip channel and adjacent shoals at low-tide.

Significant variations in drifter track behavior were observed during varying tidal elevation. Strong rotational behavior, associated with rip current vortices within the surf zone, was observed to be more prevalent during low-tidal levels, particularly during tidal elevation of less than -2 mODN. The reduction of tidal elevation led generally to increased wave breaking over the adjacent bars and particularly wave breaking in the rip head on the low-tide. On the lowest tides, the reduction in tidal elevation increasingly isolated the rip circulation morphologically. Significantly, the bar to the north begun to dry below -2 mODN, constricting alongshore current flow.
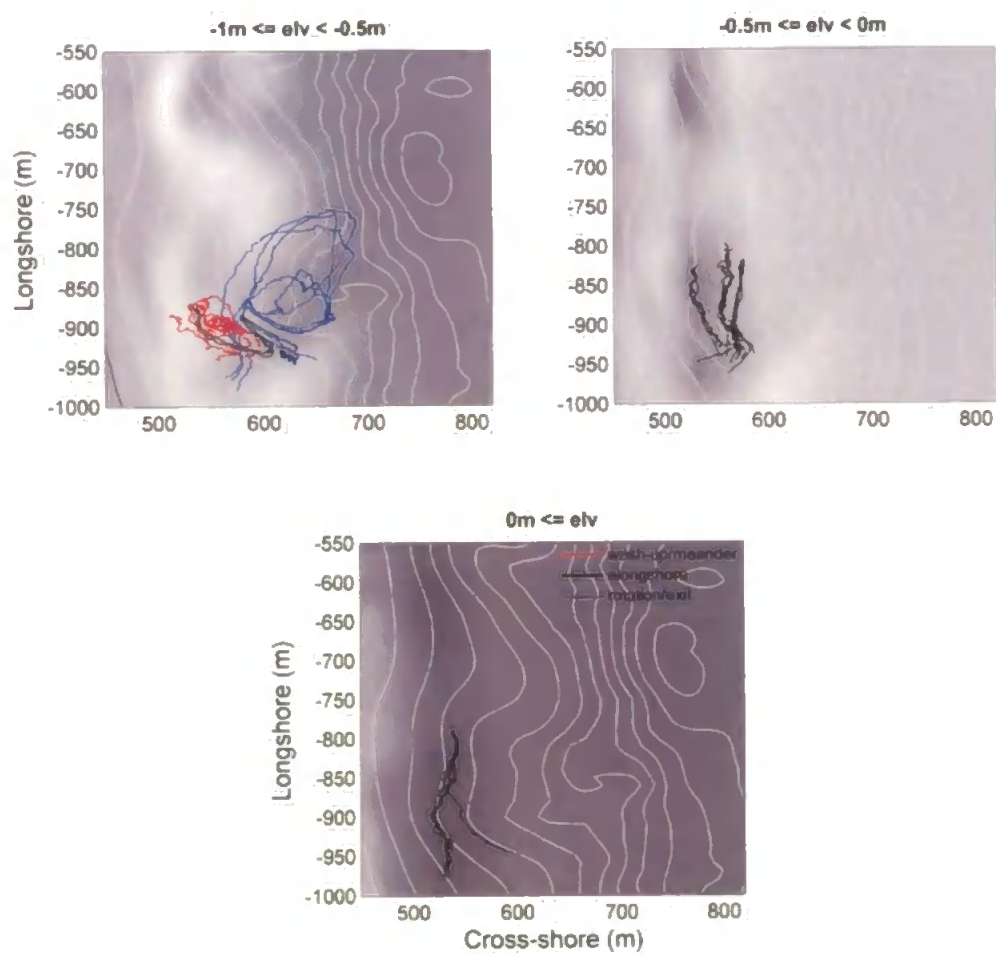
Figure 6.18 – Drifter tracks for LT3 (02/08/08), separated into 0.5 m sea-surface elevation bins. Colours represent associated behavioral classification. Background rectified video image represents nearest capture to the bin midpoint.
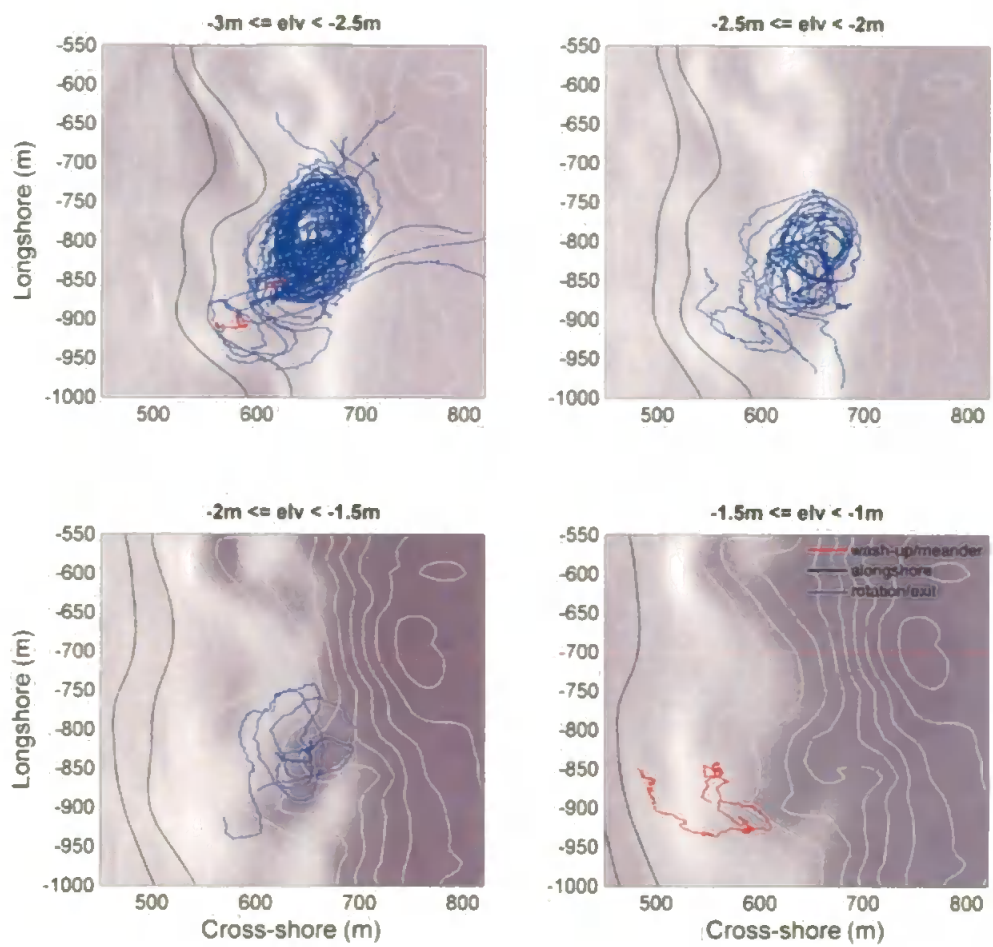
Figure 6.19 – Drifter tracks for LT5 (03/08/08), separated into 0.5 m sea-surface elevation bins. Colours represent associated behavioral classification. Background rectified video image represents nearest capture to the bin midpoint.
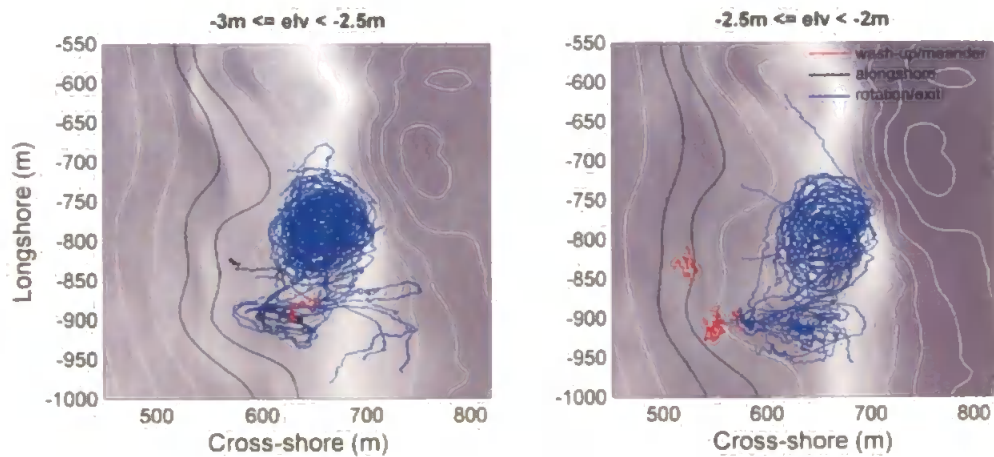
Figure 6.20 – Drifter tracks for LT7 (04/08/08), separated into 0.5 m sea-surface elevation bins. Colours represent associated behavioral classification. Background rectified video image represents nearest capture to the bin midpoint.
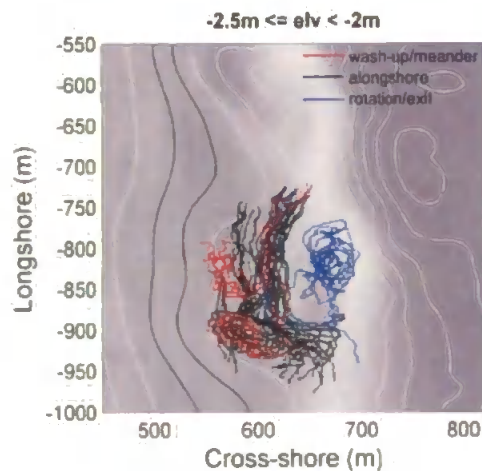
Figure 6.21 – Drifter tracks for LT9 (05/08/08), separated into 0.5 m sea-surface elevation bins. Colours represent associated behavioral classification. Background rectified video image represents nearest capture to the bin midpoint.
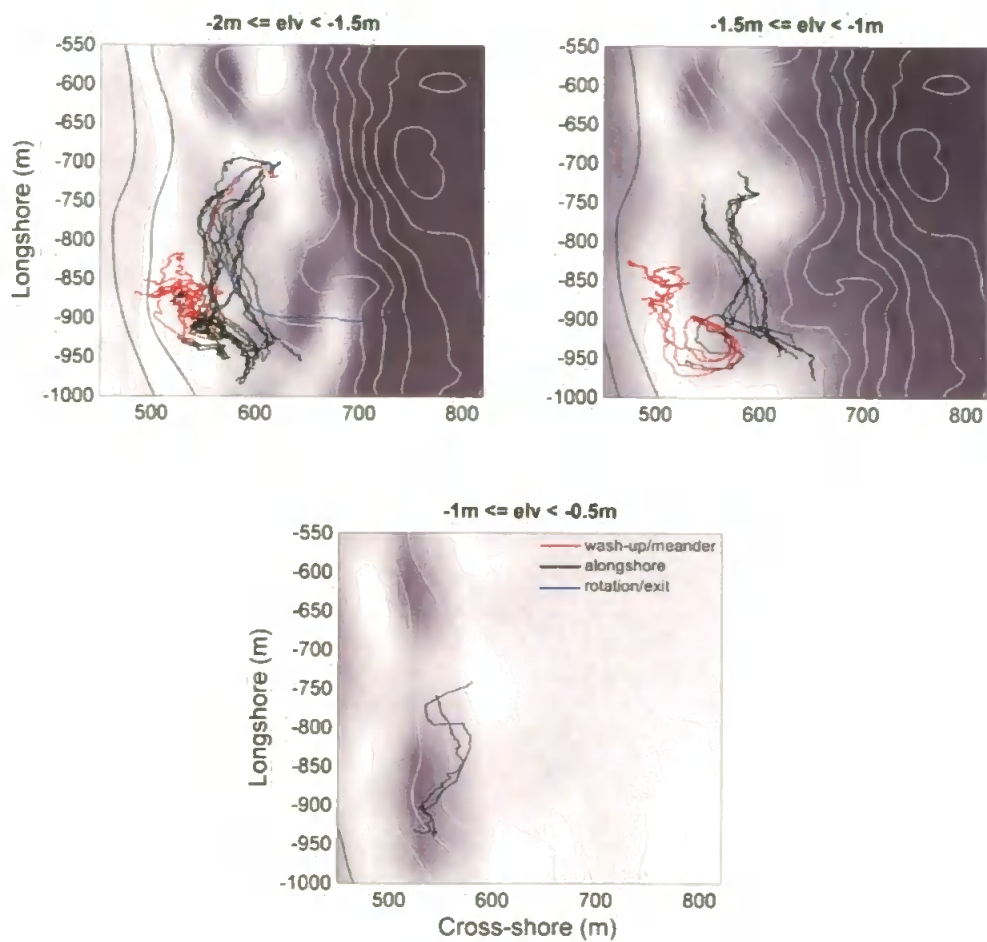
Figure 6.22 – Drifter tracks for LT13 (07/08/08), separated into 0.5 m sea-surface elevation bins. Colours represent associated behavioral classification. Background rectified video image represents nearest capture to the bin midpoint.

6.3.4.4 Environmental controls of mean rip circulation and dynamics

To gain an insight into mean rip current circulation and dynamics under various wave and tidal conditions, all collected Lagrangian drifter observations were integrated using the dimensionless parameter of the local relative wave height H_s/h. H_s and h were taken from the bar crest TWR, approximately adjacent to the rip neck, giving an appropriate scale of wave forcing. Gaps in H_s/h record (water depth on bar crest < 0.3 m) during the low-tide stand were linearly interpolated.

Drifter track classifications

Separated into H_s/h bins of 0.5, deployments cover the range 0.2 to 0.8. Figure 6.23 details combined tracks from LT3, LT5 and LT7 (deployments with simultaneous in-situ measurements). From the data available during these deployments for the rip current system under study, it is clear that rip current activity is related to local relative wave height. The observed rip current eddy circulation begins to be active at $H_s/h \sim 0.4$ where a combination of rotating and alongshore drift was observed. Values greater than 0.5 were associated with dominant rotational track patterns, and values below 0.4 were characterized by alongshore drift, meandering and wash-up behaviors. Although data is limited, there is some evidence to suggest an isolation of the rip circulation occurs at values of H_s/h greater than 0.7. This is hypothesized to be a result of drying of adjacent bar crests and an increase in wave breaking in the rip head, isolating the rip into an apparent morphological 'hole'. This may explain the apparent reduction in mean return flow from Eulerian measurement during the lowest tides as the drying bar crests indicate the seaward movement of maximum rip velocities toward the center of the rip vortex. Also, no surf zone drifter exits were observed while H_s/h was greater than 0.7.

It is acknowledged that there is an apparent contradiction between the linear correlation between Fr and H_s/h illustrated in Figure 6.11 and the concept of a threshold to activate the rip current. This appears to be due to the use of U_r to calculate Fr therefore including the longshore current component of velocity. It is this longshore component which is observed to increase steadily, during the ebbing tide, prior to rip current activation in the form of surf zone generated alongshore current. The rip current activation H_s/h threshold then refers to the initiation of the rip current cell circulation observed in the drifter data. This explanation is supported by the PUVC2 (feeder) instrument rig, located in the longshore current prior to rip activation, showing a stronger linear correlation in Figure 6.11.

252

Mean circulation and rip speeds

As a function of H_s/h, the combined mean rip circulations observed during LT3, LT5 and LT7, displayed in Figure 6.24, provided further insight into circulation dynamics and particularly drifter velocities and their spatial distribution. Mean flow velocities highlight regions in which spatially consistent flows were generated throughout the experiment during similar ranges of H_s/h. As established through the drifter track behaviors, the mean circulation scales with the local relative wave height, in this case indicating the spatial velocity distribution. Once the circulation is active at $H_s/h > 0.4$ until $H_s/h \sim 0.7$, the alongshore directed flow from the bar crest to the bar edge is consistently strongest with maximum velocities of 0.71 m s^{-1} ($0.5 < H_s/h < 0.6$) increasing to 0.85 m s^{-1} ($0.6 < H_s/h < 0.7$). Mean return speeds within the rip channel are initially strong at activation ($0.5 < H_s/h < 0.6$) reaching ~ 0.6 m s^{-1} but as H_s/h increases to 0.7 southward directed alongshore velocities associated with the eddy transition from the rip head to bar crest [X, Y] = [680 m, 750 m] and the northward bar crest to bar edge flow [X, Y] = [620 m, 770 m] begin to dominate with maximum velocities of 0.85 m s^{-1}. Finally, the highest significant mean flow velocities were observed when $H_s/h > 0.7$ corresponding to the lowest tide levels where all parts of the rip circulation recorded significant mean flows of > 0.6 m s^{-1} reaching a maximum of 1 m s^{-1}.
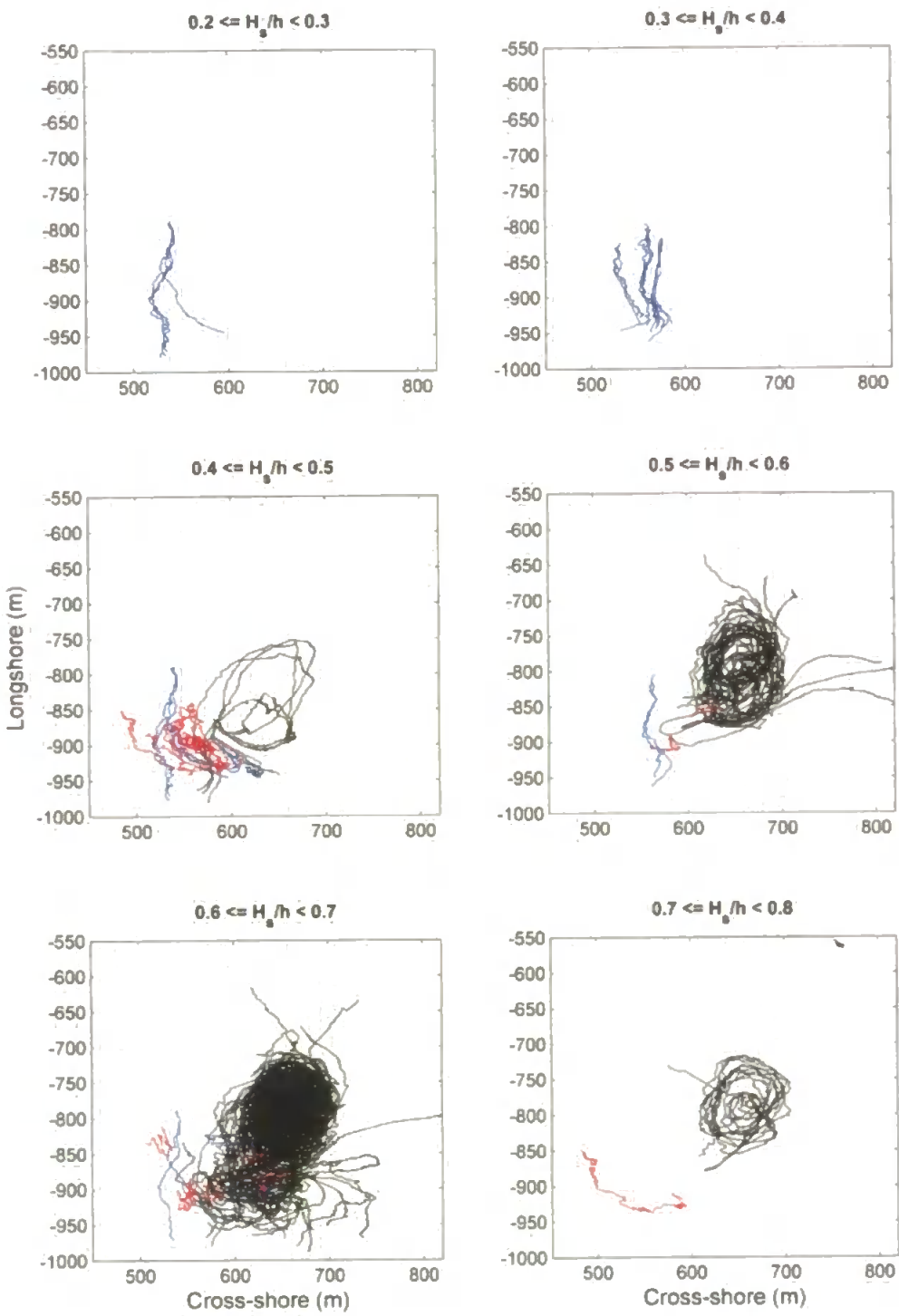
Figure 6.23 – Combined drifter tracks from LT3, LT5 and LT7, separated into H_s/h bins of 0.5. Colours represent associated behavioural classification: rotation (black); alongshore (blue); and wash-up/meander (red). Measured bathymetry represented in background.
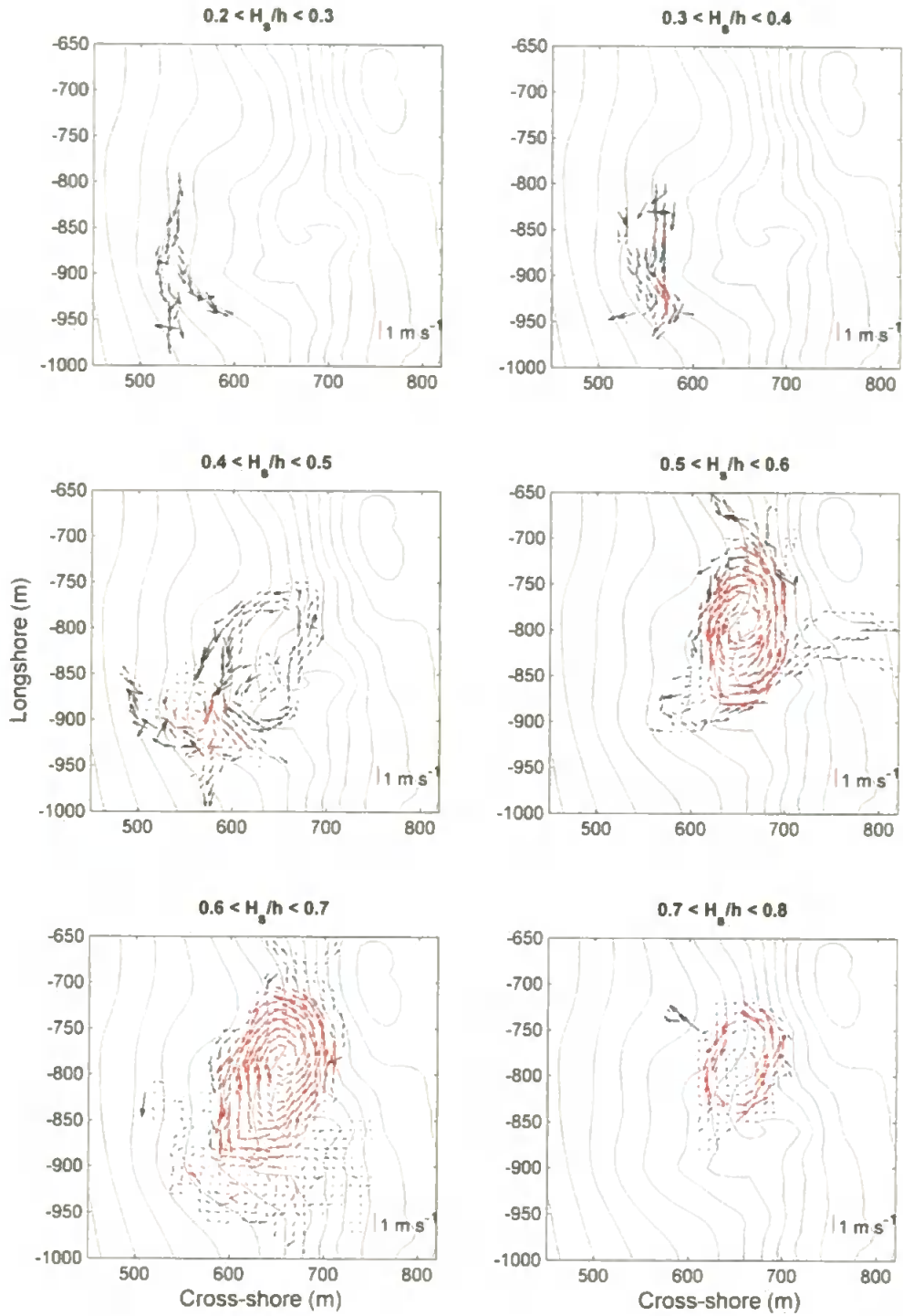
Figure 6.24 – Observed mean Lagrangian rip circulation associated with each H_s/h bin (width 0.5). Red vectors represent significant velocities (> 5 independent observations). Colours indicate mean return speeds associated with each 10 m x 10 m bin. Bathymetry is contoured in background.

6.4 DISCUSSION

6.4.1 Rip current circulation and dynamics

This chapter has presented results of a rip current experiment during typical wave, tidal and morphological conditions associated with summer (low-energy; mean $H_s < 1$ m) accretionary conditions at Perranporth Beach, a low-tide bar/rip macrotidal west coast beach in the UK (mean annual $H_s \sim 2.5$ m), classified following Short (1986) as a high-energy beach. The low-tide region during the experiment was in a transverse bar/rip morphodynamic state (Wright and Short, 1984). The results have shown that, as traditionally associated with these beach morphologies in micro- and mesotidal regions, rip current systems are present within the low tide bar/rip morphological system at the study site. These morphologies are characteristic of many beaches within the region; therefore, associated findings suggest that qualitative observations of rip current flows, commonly associated with these beach morphological systems, have some validity.

When at its most active during the experiment, the rip current system under investigation showed cross- and alongshore length scales of ~ 200 m. The rip circulation was counter-clockwise and traveled offshore through the surf zone, at approximately 45° to shore normal towards the south, until reaching the seaward breaker line. The flow then turned alongshore to the south for ~ 75 m before returning through the surf zone over the shallow inter-tidal bar at approximately $[X, Y] = [650$ m, 750 m]. Although there was presence of a subdued rip feeder channel, much of the flow feeding into the rip channel was observed to come from the side of the bar. These rip dimensions fall between recent rip current investigations in low-energy systems where alongshore rip spacing was ~ 125 m and surf zone widths were ~ 100 m during experiments conducted by MacMahan et al. (2009a) in Monterey Bay, CA and 200 m and $120 - 150$ m during experiments by Brander (1999) at Palm beach Australia and dimensions recorded within high-energy rip systems where rip spacing was 500 m and surf zone width was 400-500 m recorded by Brander and Short (2000) in Muriwai, New Zealand. With mean and maximum Lagrangian flow velocities of $0.01-0.8$ m s^{-1} and $0.6-1$ m s^{-1} respectively, rip current speeds were, in general, of similar magnitude during the period of this study to previous low-energy rip current experiments mentioned above where H_s ranged from $\sim 0.5-1.5$ m and mean and maximum instantaneous rip flow velocities were of the order of $0.2-0.6$ m s^{-1} and $0.8-1.2$ m s^{-1} respectively (Brander and Short, 2000).

In contrast, this investigation used novel techniques for investigating Lagrangian rip current circulation patterns within a macrotidal environment. The recent development of low-coast GPS units enabled the use of drifters to quantify rip circulation behaviour with an increased spatial coverage. Observations by MacMahan et al. (2009b) using this technique provided new insights about the behaviour of rip currents and surf zone exchange for open coast rip channeled beaches. They observed beach rip current circulation consisting of semi-enclosed vortices that retained material within the vortex center and remained within the surf zone. Their drifter observations support findings by Talbot and Bate (1987) that indicate that despite the large velocities in the rip channel, diatoms, pollution, and other floating material are only rarely transported offshore and are instead retained and concentrated within the rip current vortices inside of the surf zone. The present study lent more support to these findings where during periods of rip current activity strong rotational eddies were observed within the surf zone, which exhibited high levels of surf zone retention. Thus suggests cross-shore material exchange outside the surf zone was limited under the observed conditions. In the most extreme case a single drifter was retained within the rip current circulation for 24 cycles over a period of 144 min. During tides when the rip eddy circulation was the dominant drifter behavior, surf zone exits were ~ 20%. This exit rate is of the same order as that observed in recent drifter deployments in Monterey Bay, CA and Truc Vert, France where exit percentages of 20–30% were commonly observed (MacMahan et al., 2009b).

It has been well documented that rip current velocities are modulated at the tidal frequency (Brander, 1999; Brander and Short, 2000; Brander and Short, 2001; MacMahan et al., 2006) explained by both a modification of the cross- and alongshore location of wave breaking as well as the variable effect of morphological constraint on the rip current channel flow. The effect of variable sea surface elevation during the present study, located within a macrotidal regime, was significant. Throughout the experiment, modulation of rip current dynamics and circulatory behaviour were quantitatively observed, in a macrotidal setting. The observed modulation is significantly more step-wise than previous observations of tidal modulation (e.g. Brander and Short, 2001) and indicates that in addition to the flow velocity modulation the rip is essentially being 'switched' on and off by tidal-frequency water level variations. In general, flow velocities increase with the falling tide from approximately -1 mODN from which point rip current flows were active during a 3-hour period around low tide. The maximum mean Eulerian flows were recorded at low water and were

directed offshore with peak velocities of -0.5 m s^{-1}. Alongshore flow velocities were of the same order of magnitude and also peaked at low water. No evidence of increased mean return velocities were observed during the ebb tidal phase, in fact a slight velocity increase on the flood phase was measured.

Rip current speed, parameterized as a Froude number, scaled well with the relative wave height on the inter-tidal bar crest ($r^2 \sim 0.65$). This suggests that wave breaking across the regions adjacent to the rip channels is necessary to drive the rip currents. An estimation of the break point location during the period of rip current activity ($\eta < -1$ mODN) indicated that wave breaking occurred over the region of maximum alongshore bathymetric non-uniformity associated with the low-tide transverse bar/rip morphology and maximum alongshore gradients in wave energy dissipation.

Tidal modification of rip circulation behavior, as a function of local relative wave height over the bar crest, correlated well with in-situ velocities throughout the study period. Although initially velocity increases were associated with alongshore drifter behavior at $H_s/h \sim 0.4$–0.5, above this rip circulation surf zone vortices develop, fixed over the rip current morphology. As H_s/h increases to 0.8 (associated with a relative lowering of sea-level) the surf zone eddy becomes increasingly isolated with decreasing alongshore movements and increased surf zone retention until circulation is entirely confined to the surf zone with minimal cross-shore exchange. This suggests that although wave breaking over the rip morphology is driving the circulation, the local rip system morphology plays a significant role in combination with the tide in the temporal modification of circulatory behavior.

To further quantitatively investigate the role of morphological constraint in the modification of the rip current a planar trend surface was computed and local bathymetry was de-trended identifying the residual bar/rip morphology. As the study region represented a section of a relatively wide flat inter-tidal zone, a planar surface performed better than a higher order surface. The resulting residual morphology, shown in Figure 6.25, clearly indicates the bar/trough configuration around the active rip current highlighting the seaward extent of the northern adjacent shore-connected shoal, which appears to merge with the offshore sub-tidal bar. Significantly, there is a relatively   deep   incised   channel   between   these   two   regions   of
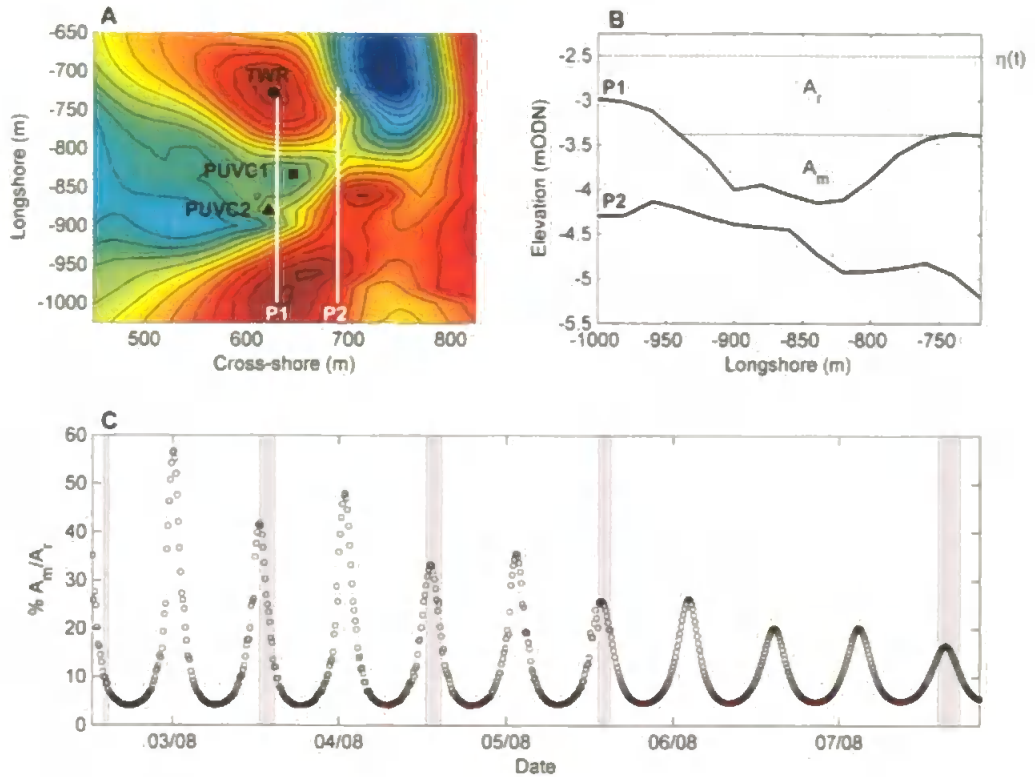
Figure 6.25 – Morphological characteristics of the rip channel. (A) Residual morphology highlighting areas of positive (red) and negative (blue) relief; indicating the cross-section through the rip channel P1 and transition to rip head P2 (white lines); and indicating in-situ instrument locations. (B) Cross-sections P1 and P2 through the rip channel, P1 indicates the profile used for derivation of the area available for rip flow A_r and the morphological area of the channel A_m. (C) Temporal variation in the percentage of A_r/A_m. Shaded regions indicate the periods of rip drifter deployment.

positive relief, which constitutes the rip neck area. A dimensionless parameter representing the level of morphological constraint on the rip current neck was computed as a percentage of morphological cross-sectional area within the rip neck (A_m) to the total cross-sectional area available for rip flow (A_r). An alongshore oriented cross-section was located by the residual morphological peak over the rip bar (TWR location) at $[X, Y] = [630, -720 \text{ m}]$ and the northern extent of significant drifter data $[X, Y] = [630, -1000 \text{ m}]$ (Figure 6.25) A_m was calculated at the tidal elevation where both adjacent bar crests were dry ($\eta = -3.38$ m) meaning that under these sea-level elevations the morphology must be a controlling factor if the rip is active. The lowest tide during the experiment was -3.1 m. At higher tidal levels, the morphological area is relatively insignificant when compared to the total area available for flow, so the morphology could be regarded as a less significant flow constraint. This parameter provides a means

259

to quantify the morphological control of the rip during changing tidal elevations. A timeseries of A_m/A_r was generated for the whole experiment using constructed tidal record from the bar crest (Figure 6.25C). Interestingly, A_m/A_r decreased rapidly during successive tides with the onset of smaller tide ranges (neap tides).

To assess the relationship between mean Lagrangian rip circulation and morphological constraint drifter observations were classified in relation to their associated A_m/A_r values. As expected, A_m/A_r classified circulation characteristics ($5\% < A_m/A_r < 45\%$) show significant relation to the underlying morphology (Figure 6.26). Circulation patterns show similar characteristics to H_s/h as both are affected by sea-level elevation. Circulation patterns defined by the morphological index show more defined structure suggesting the morphology may exert a stronger role on the specifics of vortex shape. As seen through the relation with wave breaking, there appears to be a critical A_m/A_r threshold ($A_m/A_r = 15\%$) where rip circulation activates below which alongshore currents dominate. The active rip vortex center is consistently located at $[X, Y] \sim [650, -800]$. Beginning with a strong alongshore dominance, the offshore flow through the rip neck becomes increasingly confined at higher values of A_m/A_r, reducing the northerly alongshore flows and deflecting them offshore through the rip neck. Background residual morphology in Figure 6.26 indicates significant morphological control of flow through the well-defined rip neck. The strongest rip neck flows are located on the northern side of the incised channel. As A_m/A_r increases the feeder channel area decreases and the rotational nature of the circulation (apparent vorticity) increases and reaches an observed maximum between $30\% < A_m/A_r < 35\%$, after which the rotational circulation appears to become increasingly isolated.

Rip speeds relative to contributions of wave breaking and morphological control were calculated by defining feeder, bar and rip neck regions within which flow statistics could be extracted for each class. Defined rip regions, illustrated in Figure 6.27 were based on observed circulation/data limits which were well defined by residual morphological thresholds. H_s/h binned mean and maximum rip speeds for each region presented in Figure 6.28 show an increasing offshore directed U_r after rip circulation becomes active up to a mean and maximum of 0.57 m s^{-1} and 1 m s^{-1} in the highest recorded bin ($0.7 < H_s/h < 0.8$). A_m/A_r also shows a critical activity threshold
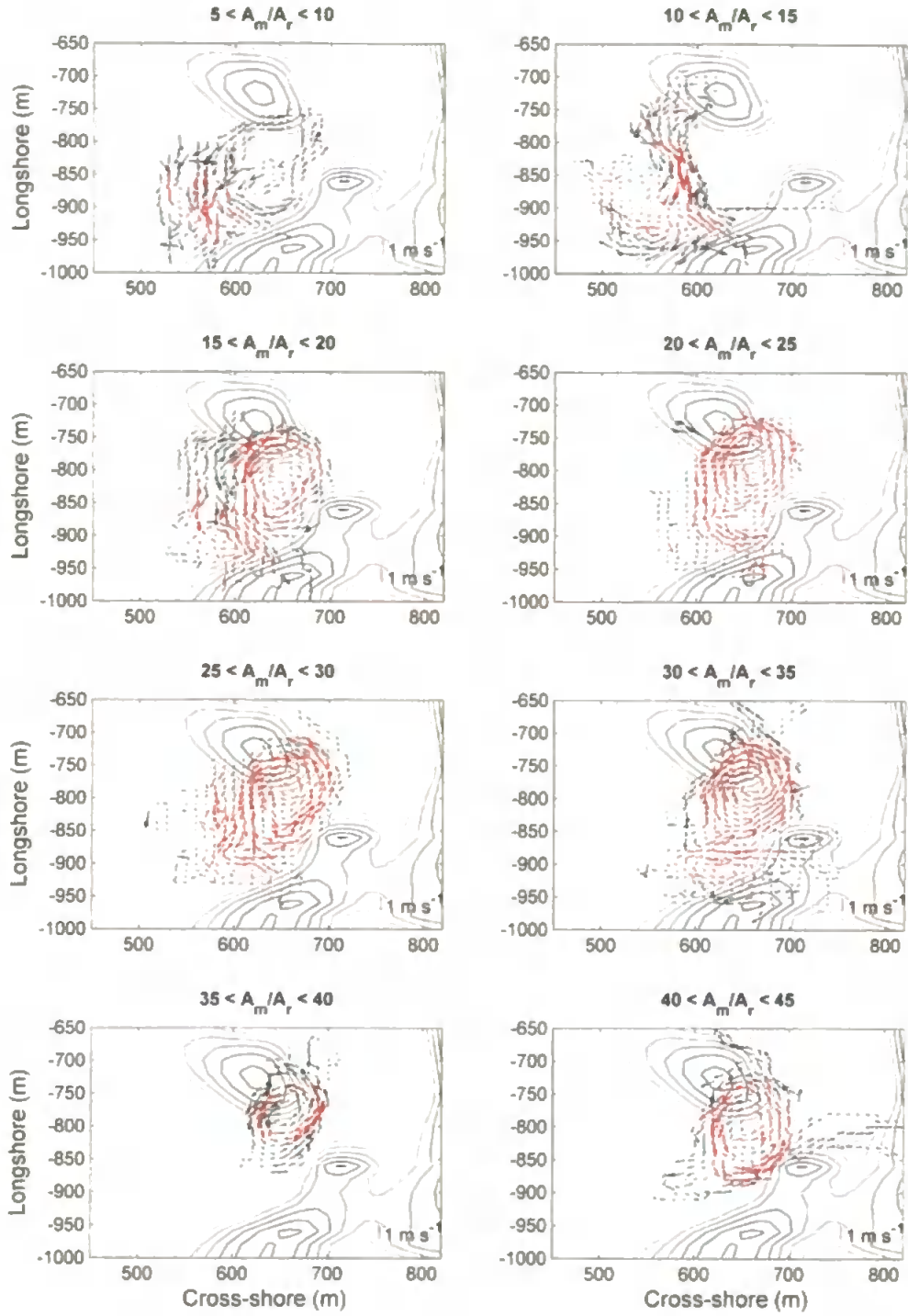
Figure 6.26 – Mean Lagrangian rip circulation separated into A_m/A_r classes. Shading indicates mean rip speed U_r within each spatial bin for all observations. Vectors (red) represent rip speed for those bins classified as statistically significant (> 5 independent observations). Residual bathymetry is contoured in the background.

($A_m/A \not> 10\%$) and mean and maximum rip neck speeds increase to a peak between 25% and 40% at 0.55 m s^{-1} and 0.89 m s^{-1}, but reduce towards maximum A_m/A_r (40% < A_m/A_r < 45%). Bar speed characteristics in relation to both A_m/A_r and H_s/h show a similar trend to the rip neck region although onshore-directed bar speeds are generally higher than the rip neck under both cases when values are just above the critical activation threshold. At high values of both indices rip neck speeds are generally greater than over the rip bar region.

This phenomenon is thought to be due to the complex roles of both wave dissipation and morphological constraint driven by sea-level elevation. Initially, before a critical rip activation depth threshold is reached, alongshore (named feeder in Figure 6.27) flows dominate, then as sea-level lowers past a threshold elevation, wave breaking over the rip bar drives alongshore set-up gradients initiating cell circulation. Initially the depth over the adjacent morphology is not sufficient to constrain and redirect offshore flows through the rip neck then subsequently, as the water level lowers, channelization of flow increases through constraint at which point the rip current vortex is most intense. As feeder area reduces and the rip bar becomes exposed the rip is increasingly fed directly through bar side drainage. Finally, at the lowest tidal elevations, the rip becomes increasingly isolated until the seaward migration of the surf zone leaves the rip bar crest dry and wave breaking on the sub-tidal bar and in the rip head reduced the alongshore set-up gradient and the cell circulation loses intensity and becomes a 'hole', free of wave dissipation within the surf zone.

During this study morphological flow constriction was tidally-modulated at the semi-diurnal and spring- neap timescales. The overall morphological configuration of the nearshore bars and troughs varies at the seasonal and storm-event timescales. Brander (1999) describes this variation in terms of down-state morphological transitions during the accretionary phase of the Wright and Short (1984) model, during which there is a steady decrease in the cross-sectional area of the rip channel, infilling of the alongshore feeder channels and an increase in rip flows. It is clear that during this experiment the reduction in tidal elevation around low water acts conceptually in the same manner as the wide-spread accretion during beach state changes to maximise bar relief, flow channelization and rip speeds at the semi-diurnal timescale. Further modulation of the rip occurs at the spring-neap timescale due to the reduction in tidal range from > 6 m during springs to < 3 m during neaps. The effect of this is two-fold in that it influences
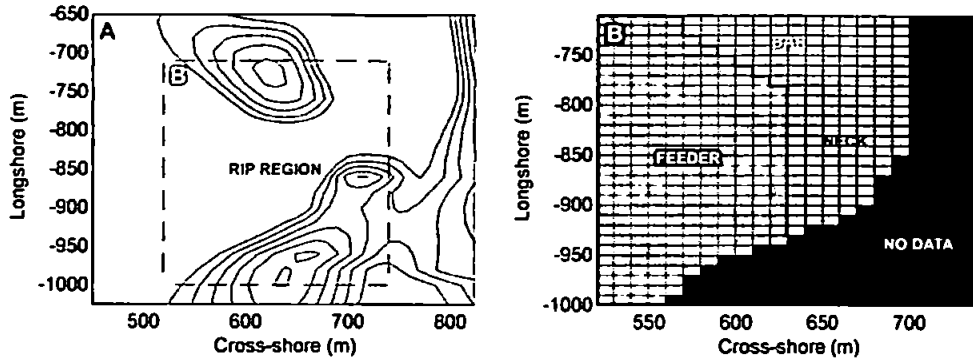
Figure 6.27 – Definition of rip regions. (A) Indicates rip region area of interest in association with residual morphology. Residual morphology used as a rip neck boundary threshold. (B) Illustrates drifter bin allocation to each defined rip region. Black area indicates regions where insufficient data was available to calculate representative rip flows (rip head and northern shoal).
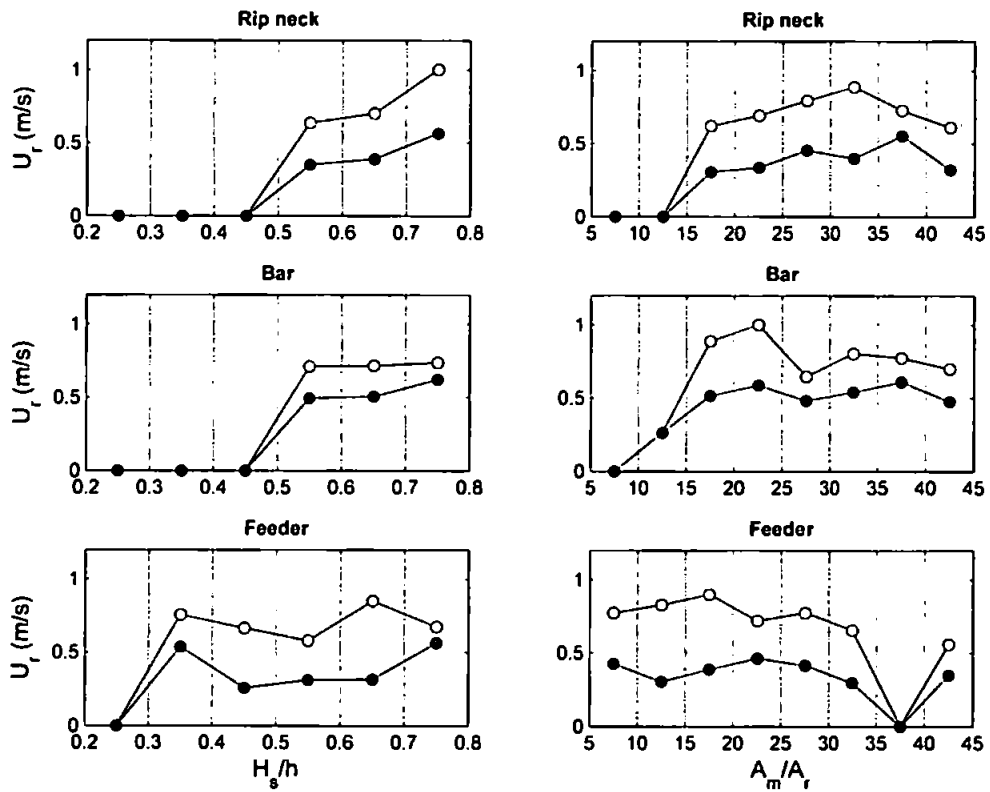
Figure 6.28 – Mean and maximum rip speeds U_r associated with rip neck (offshore-directed), bar (onshore-directed) and feeder regions. Values are separated into H_s/h (left) and A_m/A_r (right) classes. Dashed lines indicate class boundaries.

both the dissipation and morphological control mechanisms. During the neap tide phase, greater water depths are maintained over the inter-tidal bars during low-tide, minimizing the morphological control and preventing depth-limited wave breaking. This was clearly evident during the later period of the field experiment (LT 9 and 13) where rip circulation was replaced by a strong net alongshore current. It should be noted that there is no rip-head bar such as that described by Brander (1999) at the seaward end of the rip channel, rather it is suggested that this bar has already welded to the seaward slope of the adjacent northern bar and forms part of the secondary sub-tidal bar system. Wave breaking observed in the rip head during the lowest tides is though to be in part due to wave-current interaction.(Yu and Slinn, 2003).

6.4.2 Implications for beach safety

Put simply, rip current bathing hazards are concerned with the transport of a person within the surf zone from a situation of a known hazard to one with an increased hazard. The mechanism for this is generally the transport of the person willingly or unwillingly by the rip current circulation from shallow to deep water, in some cases this may involve a significant alongshore as well as offshore-shore directed component. It has been established that the vast majority of incidents on RNLI beaches are driven by rip currents, and previous chapters have identified scenarios of 'optimum' conditions where rip current hazard and risk to the bather are at their highest. The quantitative results from this field experiment have provided dynamical basis by which these qualitative and conceptual relationships can begin to be tested. Although only a snapshot of a single system over a limited number of tides, the findings from this dataset provide an insight into the mechanisms that are driving bathing hazard within the surf zone.

Findings that are of direct relevance to beach safety are as follows:

- The observed 'switching' on and off of rip activity through the mid- to low-tide phases associated with low-tide bar/rip morphology drives increased variation and rate of change of the temporal hazard signature. This observation, where rips were active for 3-4 hours around low-tide, confirms the presence of a phenomenon that was hypothesized to be a key mechanism driving observed 'mass rescue' events.

- Interestingly, strongest flows in many cases occurred in an alongshore direction across the bar directly into the rip channel. This finding, if found to occur within similar rip systems, supports anecdotal evidence (RNLI lifeguards, personal

communication) that the alongshore currents associated with the flow off the bar crest and potentially feeder channel are a principal driver in the initiation of 'mass rescue' events displacing the bathing/surfing population laterally towards a region of increased hazards (rip channel).

- Tidally induced temporal variations in flow speed and circulation patterns create rapid variations in the temporal hazard signature. The dynamic rotational structure of the rip circulation is more complex than conveyed through present public safety advice.

- Relatively high rip velocities (up to 1.2 m/s) were observed during relatively small wave events during which access to the surf zone for recreational bathing is improved, and therefore exposure to hazard and hence risk increases.

- Surface rip circulation diminished under higher waves, driving alongshore current

- Surf zone drifter exits were low during the experiment and surf zone retention very high. Exit mostly occurred for the period when the rip was active but little wave breaking was occurring over the bar.

- The sensitivity of rip flow characteristics to the morphological index indicated that as previously suggested the effect of the spring-neap tidal range variation can have significant implications on the temporal rip current characteristics maintaining the temporal rip hazard signature in constant flux, even under identical wave and morphological conditions.

6.5 CONCLUSIONS

Field observations of rip current flows have been obtained to investigate their dynamic behaviour within a macrotidal environment. A number of key hypotheses were investigated resulting in new insights into rip circulation and dynamics:

- This study has emphasized the strong tide-induced modulation of the rip flows and in common with previous investigations has highlighted that the strongest flow speeds occur around low water; moreover, it has indicated that there was a threshold depth of ~ 3 m, above which the rip flows appeared to cease.

- Lagrangian drifters demonstrated that the rip current flow was strongly rotational, consisting of a large $O(200$ m) eddy contained within the limits of the surf zone.

- During the high- and mid-tide periods when the rip was not active, strong alongshore currents dominated.

- The results of this study also indicate that with the large spring-neap variations in tidal height, there are periods during the neap tides when water depths remain too deep to permit rip circulation.

- The rip current dynamics appear to be controlled by a combination of wave dissipation and morphological flow constriction driven by tidal elevation. Measurements indicate that local relative wave height over the inter-tidal bar crest was generally well correlated with rip flow speed where the rip circulation activate above 0.4 initiating with peak rip flows occurring over the bar (onshore-directed); however, in shallower water morphological constriction increases to what appears to be an optimum combination of wave and morphology producing an intense rotational eddy vortex ($25 < A_m /A_r < 40$). At lowest water levels wave dissipation over the adjacent bars reduces and feeder area reduces, leaving the rip isolated within the incised channel and fed from the bar edge. Eventually, in this example, wave breaking on the sub-tidal bar and in the rip head reduced the alongshore set-up gradient and the cell circulation loses intensity and becomes a 'hole', free of wave dissipation within the surf zone.

- The study has provided quantitative evidence supporting hypothesized mechanisms for the generation of high hazard signatures under 'optimum' MR conditions and illustrated how the temporal hazard signature for a single rip system may be highly dynamic.

Although this study has attempted to determine whether macrotidal rip circulation can be attributed to either wave dissipation or morphological control, it seems that both processes ultimately combine to force the rip current. Variations in the pattern of wave dissipation and hence set-up gradients seem to trigger the rip circulation, but there are periods, as water depth shallows when morphology appears to exert the greater control on rip circulation and characteristics. The combination of forcing and constraining mechanisms is complex, and it is noted that this is a single case and it is suggested that this balance may vary from system to system, largely due to the template morphology through spatial dimensions and orientation of bar, feeder channel, rip channel and rip head bar morphology. In addition, the cross-shore location in relation to tidal phase will affect the temporal residence of wave breaking over the maximum non-uniformity and the extent to which morphodynamic interaction with swash, surf and shoaling zone processes can maintain or disperse the rip template morphology throughout the tidal cycle. This

study represents a snapshot in both forcing conditions and evolutionary morphological state of a macrotidal rip system. Obviously, much more investigation is required to make general statements of macrotidal rip morphodynamics.

7. SYNTHESIS

7.1 INTRODUCTION

Throughout this thesis, the relationship between beach hazards and the prevailing morphodynamic/environmental conditions have been investigated on a range of temporal and spatial scales within the UK coastal environment. A number of important findings and new concepts have been revealed that represent insights into beach morphodynamics and hazards on three key timescales: annual, seasonal and tidal. In Chapter 4, a new beach classification system for beaches in the UK is presented consisting of 12 beach types, each characterized by a distinct annual morphodynamic expression and associated hazard signature. In Chapter 5, then, the characteristic seasonal morphologic and hydrodynamic transitions at selected sites have been identified in association with their dynamic hazard signatures for the high-risk beach groups. Furthermore, in Chapters 5 and 6, the dynamics and characteristics of the beach rip current systems within spring/neap and semi-diurnal timescales were investigated at these selected sites. This provided new insights into the environmental, morphologic and forcing mechanisms behind observed incidents and coastal-wide, high-risk, 'mass rescue' scenarios.

The aim of this chapter is to synthesize the key project outcomes to provide important new insights into the fundamental controls on the temporal hazard signature within high risk beach environments in the UK. It will also highlight some of the implications and applications of this research summarizing these outcomes in relation to the stated project aims.

7.2 TEMPORAL HAZARD SIGNATURE

Beach hazards, like beach morphodynamincs, vary on a range of timescales. For the successful provision of beach safety services it is crucial to have an understanding of the temporal variability of the prevailing hazards from a strategic and operational viewpoint. Figure 7.1 provides a conceptual summary of the key findings of the project within the context of the temporal hazard signature for the highest risk recreational bathing beaches in the UK. This framework provides a structure for beach hazard assessment where hazard characteristics are initially defined by beach type and environmental setting, and modified by temporal variation in morphology and hydrodynamic forcing.
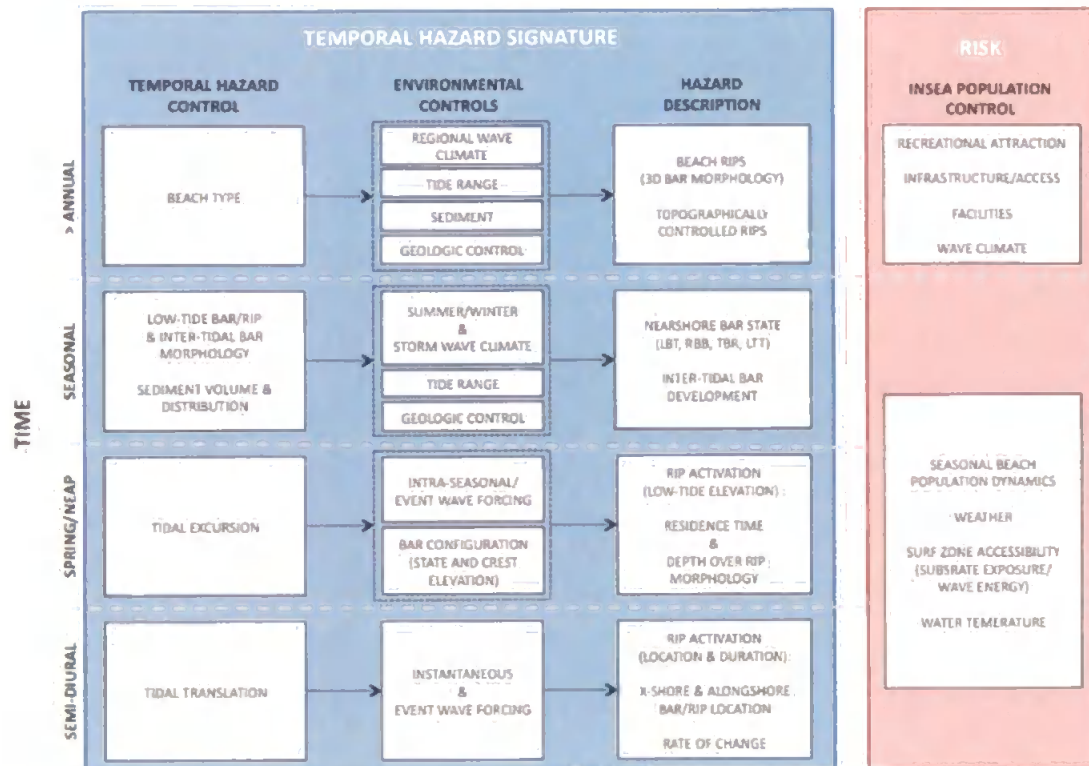
Figure 7.1 – Conceptual summary of principal controls of the temporal hazard signature (rip current hazard) for high risk beaches and key insea population controls for a range of temporal scales. Summary is in specific relation to beaches monitored in this study and represents only the principal mechanisms identified to drive rip hazard levels.

This approach represents an extension of that used by Short and Hogan (1994) that provided modal, and wave height-modified, beach hazard ratings for each beach state described by Wright and Short (1984) and Masselink and Short (1993). While they tentatively included tidally-modified and tide-dominated beaches, the approach taken was one derived from micro-tidal environments, defining hazard levels increasing linearly from reflective to ultra-dissipative states, and increasing from low to high waves (Figure 1.19, page 34). In contrast, this investigation considers the intermediate beach groups (LTT+R and LTBR) as the most hazardous with the dissipative and ultra-dissipative groups representing some of the lowest hazard. Rip currents represent the largest recreational beach hazard at RNLI beaches, and the relatively low hazard rating for (ultra-) dissipative beaches is attributed to the lack of bar morphology and a fully saturated surf zone, leading to low rip current activity.

7.2.1 Beach type

Few researchers, other than Short (1993, 1994, 1999 and 2001) and Short and Hogan (1994), have included concepts of morphological state and beach type in hazard evaluation. In many cases only wave height, period and direction have been used (e.g. Lushine, 1991). Eight of the nine identified beach groups were represented within the RNLI lifeguard service during this study. These contrasting beach environments provided a unique opportunity to identify specific hazard characteristics associated with beach types that have received little attention in previous hazard research (Section 4.5.2). In line with rescue statistics from the US and Australia, RNLI incident records revealed the dominance of rip current activity as the causal hazard for 68% of all reported incidents between 2005-2007. Unique hazard signatures were apparent on beaches where rip activity was low, for example, in regions characterized by low-energy wind waves, mega-tidal ranges and/or sediment distributions that were restrictive of bar formation. These non-rip hazards were mainly tidal cut-off (increased by low-sediment supply/hard rock exposures and large tidal range) and offshore winds (increased by dominant meteorological climate and beach orientation). It is clear, therefore, that a single hazard rating for the beach groups defined in this study that is solely based on the wave height will not provide sufficient information to effectively characterize the general hazard signature required for representative beach hazard assessments.

Previous beach hazard research used the morphodynamic indices Ω and RTR, and conceptual beach state models of Wright and Short (1984) and Masselink and Short (1993) to identify beach types. Prior to this study the usefulness of these parameters to delineate beach type in the UK beach environment was unknown. Several recent studies have challenged the applicability of Ω to define and predict beach state change, and have highlighted confounding factors such as response times (e.g., Gómez-Pujol et al., 2007; Jiménez et al., 2008) and geological control (Jackson et al., 2005). This investigation of UK beach types assumed that sampled beaches were in equilibrium with their annual mean wave and tidal conditions, and due to the wide range of beach types under investigation, the observed intra-annual fluctuations in beach form were less significant than the spatial differences between sites. Even under these assumptions, Ω and RTR proved useful in parameterizing the environmental conditions that characterized the different beach groups. However, the absolute wave height was also found to be important. The importance of wave energy levels is related to minimum wave energy thresholds for transport (Masselink and Short, 1993) and specifically in the

beach groupings presented in Chapter 4 threshold energy levels required for generating infragravity waves (Guza and Inman, 1975) and rhythmic bar morphology. Low- and high energy intermediate beach groups, characterised by absence and presence of bar/rip morphology, respectively, were separated by a critical wave energy threshold $H^2T = 5$. Masselink and Short (1993) tentatively suggested a threshold of $H_b < 0.25$ m as a minimum energy level for model applicability. The beaches studied here all exceeded this, suggesting that the latter threshold is not sufficiently restrictive.

Jackson *et al.* (2005) and McNinch (2004) suggested that hard geology constrains and modifies morphodynamic processes through sediment abundance and depth to geologic substrate. Identified to be of key importance within the often sediment-limited UK environment, the influence of hard rock exposure and underlying framework controlled the scope of both morphologic adjustment and hydrodynamic processes within the surf zone. The environmental setting of a beach, including geologic control, drainage characteristics and backshore geomorphology were all revealed to influence beach response to forcing conditions and hence, in many cases, will significantly modify surf zone conditions and hazards throughout a range of temporal scales.

The combination of beach type and environmental controls (geologic/structural constraint, sediment abundance, drainage and backshore geomorphology) define the potential for rip current activity. As identified by Short (1985), rips can take on a number of forms based on their forcing and controlling mechanisms. This study has identified accretionary beach rips and topographically controlled rips as the greatest contributor to observed beach hazards. The critical importance of the temporal and spatial variations of these rips was revealed throughout the study sites where, due to the large tidal excursion, distinct hazard signatures were defined from low- to high-tide. Low-tide regions were dominated by beach rips within the sub- and low-tide rhythmic bar systems. At high tide these systems were often in > 8 m water depth and surf zone processes interacted with a steeper upper beach (LTT+R examples). In cases with significant geologic control, separate bar systems and/or geologic constraints drove beach and topographic rips located up to 500 m landward of the low-tide shoreline (Table 5.4). Observations in Section 5.3.2.3 (Figures 5.19 and 5.20) suggested the combination of geologic constraint and stream drainage constrained morphological adjustment within the upper beach resulting in the decoupling of the high/mid- and low-tide rip systems. These observations emphasize the importance of accounting the

temporal variation in the hazard signature throughout the tidal cycle within macrotidal beaches. Illustrated in Figure 1.18, this approach was initiated by Short (1999) for macrotidal beaches in Australia.

Section 5.3.3.1 showed that the distribution of incidents with respect to tidal elevation varied with the rip morphology throughout the spring/summer season (using regions of maximum alongshore bathymetric non-uniformity as a proxy to the cross-shore location of bar/rip morphology). This indicated that for the sites studied, beach rips were the greatest cause of incident. These systems occurred within LTT+R and LTBR beaches that represented 59% of sandy beaches along the west coasts of Cornwall and Devon. Unlike some of the more reflective or ultra-dissipative beach groups, where state change is restricted by large tidal ranges or sediment size, the intermediate dynamic LTT+R and LTBR beaches exist around critical thresholds of Ω (Davidson and Turner, 2009). Variation of Ω around these threshold values is driven by typical intra-annual wave conditions, controlling the dominance of erosive or accretionary surf zone conditions.

7.2.2 Temporal morphodynamic change

Data collection in Chapter 5 documented key inter-annual and seasonal morphological change within studied LTT+R and LTBR beaches. Offshore sediment transport (below MLWS) and inter-tidal beach lowering occurs during high-energy winter periods, resulting in flat featureless inter-tidal zones and quasi-linear LBT sub-tidal bar systems. Accretion and re-establishment of rhythmic, and then transverse, lower inter-tidal bar systems occurs during the lower energy summer period (Section 5.3.2.2). Also development of inter-tidal bars (slip-face bars) within the MLWN–MSL region provided the template morphology to extend rip current activity throughout more of the tidal cycle, playing an important role in magnifying temporal rip hazards.

It is wave forcing over the dynamic template morphology that drives the identified rip current systems (Haller et al., 2002; Sonu, 1972). This concept is the basis for all present rip prediction tools (Section 1.4.3). Previous research suggests rip current flow speeds scale with wave height (MacMahan et al., 2006). While this may be true, when considering rip strength relative to wave energy, it has been observed here that rips in combination with significant morphological constraints can have high flow speeds in relation to the forcing wave energy through flow channelization by rip channel morphology. In particular, low-energy long period swell wave conditions, associated

with summer accretionary periods, shoal to the inner transverse bars generating strong alongshore variations in wave breaking and are responsible for these relatively strong rip flows. These typical summer low-energy conditions ($H_s \sim 0.5{-}1$ m; $T_p \sim 6{-}10$ s), commonly occurred in conjunction with high insea populations (75% of insea beach use), were responsible for a large proportion (36%) of incidents recorded in 2007.

7.2.3 Tidal control

Recent approaches to rip hazard prediction have begun to incorporate an element of tidal modulation (Engle, 2002). Tidal level has been widely observed to modify rip flows in previous studies, enhancing flow speeds at lower tides (e.g. Sonu, 1972; Aagaard et al., 1997; Brander, 1999; Brander and Short, 2001; MacMahan et al., 2005). The role of tidal control on rip dynamics within the studied macrotidal beaches has been identified as a principal mechanism controlling the instantaneous and event scale dynamics of the temporal hazard signature. In combination with the template morphology and wave forcing conditions, tidal modulation of hazards is exerted through two principal key mechanisms:

Tidal excursion

In many cases tidal excursion across the low-tide bar/rip system was observed to control a conceptual morphological down-state (ebb tide) and up-state (flood tide) transition, similar to that observed by Brander (1999), but as a function of tidal level and observed through the wave dissipation patterns (Figure 7.2). Observed at Perranporth during August 2008, at the MLWN level the typical wave dissipation pattern represented a LBT/RBB system and rip circulation was weak with alongshore flows dominating. As tidal elevation decreased towards the MLWS level, the wave dissipation pattern represented TBR morphology and the combination of wave dissipation and morphological constriction resulted in the strongest rip flows. Finally, during the lowest observed tides the rip system became isolated, representing the TBR/LTT configuration. Within this model there are two hazardous transitions: (1) falling tide from LBT/RBB to TBR (down-state); and (2) rising LTT to TBR (up-state). The extent of tidal excursion within the spring/neap cycles will control the extent of these transitions and hence the levels of low- and mid-tide rip activation. In addition, the exposure of the low-tide bar crest attracts bathers onto the low-tide bar/rip systems. During the subsequent flood, the bar crest submerges and the feeder channel and rip system become active (TBR stage) as the insea population pass through the feeder channel to reach the beach. This

represents a key peak hazard, high risk scenario. This highlights the importance of tidal level and particularly the role of the spring/neap cycle in driving daily modification to rip activity.

Tidal translation

Tidal translation refers to the rate of change in the shoreline location and is identified here as a key mechanism driving the high risk scenarios investigated (Section 5.3.3). While the tidal excursion defines the extent of rip channel exposure throughout the tidal cycle, the tidal translation controls the rate at which changes in the hazard signature occur. Many of the studied beaches have a tidal range > 6 m with a horizontal tidal excursion of up to 600 m. An example from Croyde Bay (Figure 5.28) illustrates that translation rates during large spring tides can reach 100 m in 15 minutes. This has significant implication for beach safety management when, during 'optimum' morphological configurations, low-tide bar/rip systems are backed landwards by alongshore phase-offset inter-tidal bar/rip systems, driving a rapid alongshore migration of rip channel location throughout the tidal cycle. In addition, the large variation between spring and neap tidal range around the autumnal equinox, where tidal range at Perranporth can vary from 2 m to 7 m within 7 days, suggesting the tidal excursion, tidal translation and hence the temporal hazard signature will vary significantly on a daily basis, even under identical wave forcing conditions.

7.2.4 Rip circulation

Investigation of rip circulation and dynamics on the smallest spatial and shortest temporal scale revealed that strongly rotational eddy structures represent the principal circulation of the transverse rip current system studied. A similar circulation pattern was observed by MacMahan *et al.* (in press) at beaches from micro- to mesotidal environments, and represents a new concept which contradicts the long-standing notion of seaward flowing jets expelling bathers from the surf zone. In addition, the present study observed alongshore-directed rip flows over the bar edge of equal, often with greater speeds than the offshore flowing rip neck, revealing an additional hazardous component of the rip system potentially driving bathers from the 'safe' bar crest laterally toward a region of higher hazard.

These identified complexities of rip current circulation patterns, flow speeds and the tidal modulation of the system are rarely understood by experienced lifeguards. Without
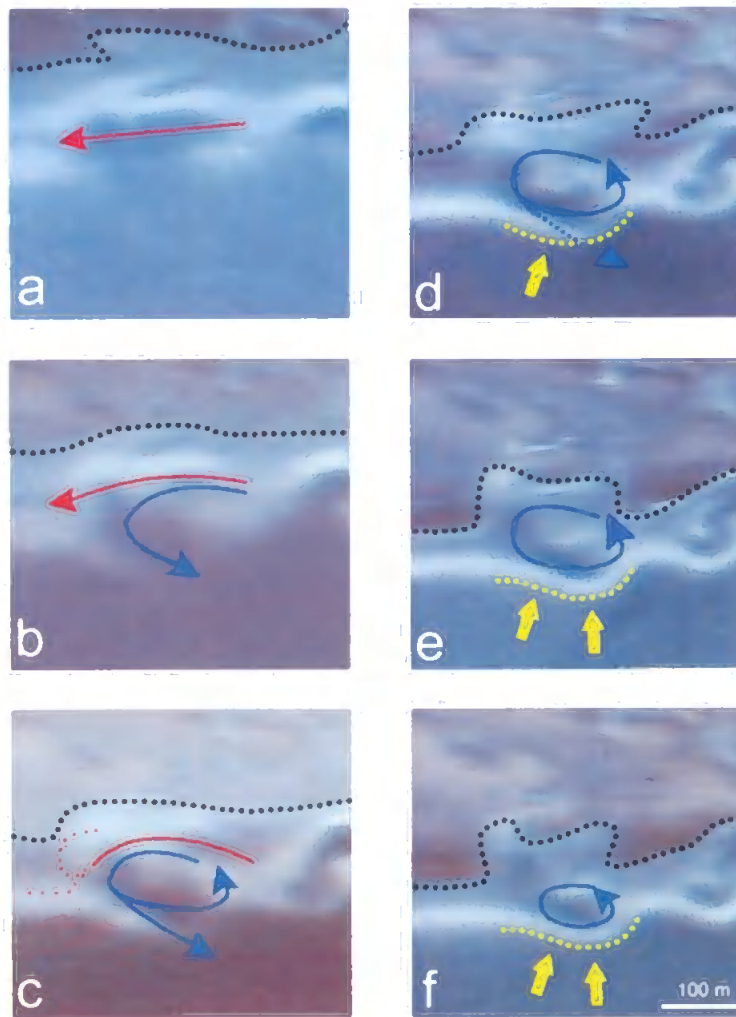
Figure 7.2 – Conceptual sequence of the temporal evolution of the observed macrotidal rip current cell at Perranporth. Each schematic represents 30 min time step towards spring low-tide at (f) under average measured conditions (H_s ~1 m). Black dots indicate approximate shoreline position, yellow dots indicate wave breaking on the northern shoal and rip head with yellow arrows approximating angle of wave approach. Generalised rip circulation patterns are marked in solid blue and red lines (and arrow heads) indicating rotational and alongshore behavior. Time step d) represents the optimum combination of wave forcing and morphological constraint to generate an intense eddy vortex. Each snapshot covers the same beach region. Note the breaker dissipation patterns mimic a conceptual down-state transition, as observed by Brander (1999) as a function of tidal elevation a) LBT; b) RBB; c) RBB/TBR; d) TBR and e) TBR/LTT.

this fundamental scientific knowledge of surf zone processes and the temporal hazard signature, the experienced lifeguard can only realistically provide a reactive service.

7.2.5 Controls of population

Without exposure to hazard there is no risk, therefore, a consideration of the beach population dynamics in combination with an understanding of the temporal hazard signature provides a useful tool for beach safety management. Figure 7.1 highlights population controls identified within the study region on a range of temporal scales. This project has made a number of assumptions regarding the uniformity of the insea population and its effect on the likelihood of incident. Insea population has been used purely as a tool to normalize the incident record and provide a baseline concept of hazard levels and risk. In reality the bathing population is demographically diverse, with a range of swimming abilities and experience. Undoubtedly, this will have an effect on individual risk levels. Understanding the effects of demographically variable insea populations, and the effects of conflicting activities in the surf zone, on levels of risk would be a useful area of further research.

7.3 RESEARCH APPLICATIONS AND FURTHER WORK

Close collaboration with the partnering institute has been crucial to the applicability of the project outcomes to the RNLI. The transfer of new scientific knowledge generated by this project to the RNLI can be divided into two areas: 1) The RNLI's risk assessment program for use on UK beaches which addresses the seasonal to annual timescales of the temporal hazard signature; and 2) incorporation of relevant new understanding of UK beach types and dynamics, associated hazards and macrotidal rip currents into the lifeguard/risk assessor training curriculum.

7.3.1 RNLI risk assessment program

The development of a beach classification and hazard assessment procedure has provided the RNLI with a structured approach to providing baseline data on environmental and hazard characteristics of a specific beach to the risk assessors. The procedure comprises an assessment model and a comprehensive, standardized and scientific database containing physical environmental information about beaches in the UK. The database holds information regarding beach group classification (Chapter 4), a modal and high energy (10% exceedence) hazard characterization of that beach type (Appendix 4), details about the environmental setting (hard rock intervention, drainage,

backshore geomorphology, embaymentization), as well a statistical representation of wave, tide and wind forcing for the specific location. This information is intended to provide the beach risk assessor with a comprehensive set of background data on a given beach location, to enable the establishment of a broad picture of the physical beach environment prior to a field visit and assessment, that cannot be learnt from a single beach visit, as well as a standardized approach to assessing beach hazard within the UK.

The beach and hazard database is hosted by the Marine Conservation Society and integrated as part of their online 'Good Beach Guide' (www.goodbeachguide.co.uk). Through a secure interface, risk assessors are able to download a report of a specific beach prior to field visits or to aid in the generation of the RNLI beach audits. In addition, a coastal hazard summary, including beach type, associated hazard and modifying environmental setting for a specific location, is directly included in RNLI beach risk assessment reports.

7.3.2 Lifeguard training

Education of lifeguards remains one of the most effective tools for transmission of scientific advances in beach hazard research. Providing the lifeguard with the knowledge required to understand the basic principles and processes that drive various phenomena they observe, for example rip currents, can enable improved ability to learn from observation and enable more proactive and predictive insights into the temporal hazard signature. This research has initiated ongoing improvement to training material for lifeguards and risk assessors which will result in a number of printed resources (posters, booklets) to be located at relevant patrol units providing reference material.

7.3.3 Hazard prediction

While an improved understanding of the environmental controls of beach risk levels due to rip current activity has been achieved, the level of understanding required to provide accurate prediction of rip hazard levels within a macrotidal setting has not yet been reached. Further investigations including extending field monitoring and modelling efforts are required throughout a range of rip current systems, under a broad spectrum of forcing conditions to enable more general statements to be made regarding macrotidal rip current systems. Indeed, due to the success of this PhD project partnership with the RNLI, a 3-year NERC funded partnership project with the RNLI has been proposed, to test and extend ideas generated within this present work by measuring and modelling rip

currents under a variety of wave, tide and beach conditions. Key outcomes of this proposed project are the development of rip hazard scenarios and prediction tools to assist the RNLI to better resource its rescue assets and personnel. These include simple generic rip hazard scenarios, but also a first attempt at developing a decision-support system for predicting rip hazards several days in advance that would integrate Argus video image acquisition as a tool (called 'Beach Wizard') to update template bar morphology within the XBeach model domain. Figure 7.3 shows an example rip risk plot, generated using the XBeach numerical model as a proof of concept (Austin, personal communication). Such a map can be used to manage lifeguard resource deployment, inform lifeguard decision making and provide public information. This has the potential to significantly improve public safety.
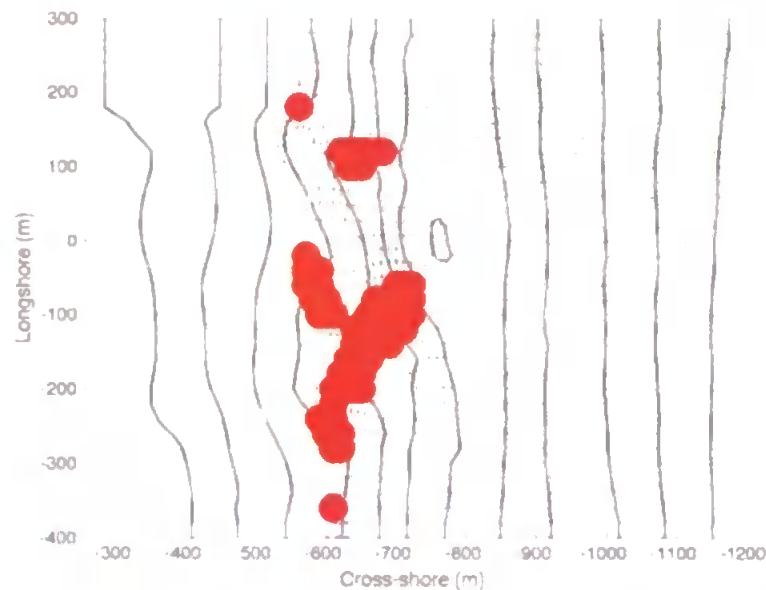
Figure 7.3 - Example of Rip Risk Plot showing the occurrence of offshore-directed mean nearshore currents exceeding 0.5 m/s. The plot was obtained using XBeach with standard parameters (uncalibrated) and the measured bathymetry (not derived from using the BeachWizard).

7.4 CONCLUSIONS

The UK beach environment has been shown to be highly diverse and relatively poorly understood, both in terms of beach hazards and morphodynamics. Dominated by macrotidal, often mixed sediment beaches, exposed to a wide range of wave climates, the understanding of the complex morphodynamics of UK beaches remains a challenge. Masselink (1993) stated that, contrary to early notions that macrotidal beaches were fundamentally different to their micro-tidal counterparts, in fact they share many things in common. It is with this concept in mind that the morphodynamics and associated hazards of macrotidal beaches within the UK were investigated, initially through an assessment of the validity of previous knowledge and understanding of beach morphodynamics within micro- to macrotidal environments and extending this through newly acquired data and understanding of macrotidal beaches and associated hazards within the UK.

The following project aims were identified in Section 1.5:

1) Identify the nature and specific causes of beach hazards through the assessment of RNLI incident records and assess the resulting hazard signatures in relation to previous research.

2) Identify beach type variability in UK and investigate the appropriateness of using a beach classification system to describe beach type groups though the use of traditional morphodynamic parameters.

3) Investigate the spatial distribution of the identified beach types and their associated morphodynamic characteristics.

4) Investigate the relationship between hazard and beach morphodynamics within the UK environment and assess whether it is similar to that observed in previous research.

5) Identify the extent to which rip currents cause hazard in UK and identify and quantify the location, circulation and dynamics of high-risk rip current scenarios.

The preceding chapters have satisfied these aims and provided new insights into both the morphodynamics of beaches common to the UK and beach recreational hazards. The nature of the UK beach environment and the presence and characteristics of

recreational beach hazards has been established. The following summarises the key findings in relation to the initial project aims:

Beach hazards

- Rip currents were responsible for 68% of all recorded incidents between 2005-2007 throughout all 76 beaches patrolled by the Royal National Lifeboat Institution (RNLI).

- Hazard type and severity varied between morphodynamically distinct beach types. Intermediate beaches with low-tide bar/rip morphology (where dimensionless fall velocity (Ω) = 2–5 and relative tide range (RTR) < 7), including Low-Tide Terrace and Rip (LTT+R) and Low-tide Bar/Rip (LTBR) beaches, presented the greatest risk to the insea beach user.

- These high risk beaches, representing 59% of the west coast beaches in Devon and Cornwall, also attracted the greatest visitor populations.

- Hazards driven by tidal-cut off (large tidal ranges) and offshore winds (coastal orientation, low wave environments) are dominant on beaches in the absence of rip currents.

UK beach types

- Detailed morphodynamic characteristics of 92 beaches within the UK were collected. Nine distinct beach groups were identified through cluster analysis, each having a unique morphodynamic signature.

- Traditional morphodynamic indices Ω and RTR were found to be effective in discriminating between beach groups. However, it was found be to important to account for absolute wave energy flux, here in the form of a threshold parameter, H^2T, whereby a critical value of 5 m^2 s was derived to differentiate between intermediate groups with (> 5) and without (< 5) three-dimensional bar systems within the presented dataset.

- The role of geologic control, sediment abundance and drainage characteristics in constraining beach morphodynamics was shown to be significant within the sites studied. It is acknowledged that, due to this site specific influence exerted by the environmental setting on beach state evolution, defining beach group boundaries within conceptual morphodynamic models is often inappropriate. Furthermore, models should be used as tools for understanding morphodynamic systems rather than beach type prediction.

-

Beach morphodynamics and hazards

- Seasonal monitoring of hydrodynamics, morphology and lifeguard incidents at LTT+R and LTBR beaches in Devon and Cornwall identified key mechanisms controlling the temporal hazard signature (THS): 1) the dynamic morphological template; 2) wave forcing; and 3) tidal excursion and translation.

- The morphological template controlled the presence, extent and intensity of beach rip current systems. Observed transition from a LBT sub-tidal bar system and planar beach during high-energy winter months to the development of low/tide transverse and inter-tidal bar/rip systems during summer represented an increase in morphological hazard. Seasonal transition from an erosive to accretionary system drove significant beach elevation changes in many cases having significant implications for levels of hard rock exposure.

- Typical summer wave forcing by relatively small, long period swell ($H_s \sim 0.5$–1 m; $T_p \sim 6$–10 s) over this high hazard template morphology provided conditions that drove hazardous rip currents. Under these conditions hazard exposure was increased due to the accessibility of the relatively low energy surf zone.

- Both spring/neap and semi-diurnal tidal variations were identified as key controls on the THS. Variable tidal excursion modulated rip current activity, and tidal translation rates controlled the rate of change of the THS. The 'optimum' combination of these mechanisms results in the 'switching' on and off of rip currents during spring low tides and the subsequent rapid alongshore migration of rip channel/hazard location as the surf zone inundated the landward, often alongshore phase offset, inter-tidal bar system.

- In conjunction with high insea population, these 'optimum hazard scenarios' drove high risk, coast-wide 'mass rescue' events identified in the incident records that in some cases caused > 150 incidents across 12 beaches during one day.

Rip current circulation, dynamics and hazard

- Incident occurrence was shown to be strongly influenced by the location, elevation and development of bar/rip morphology within the tidal cycle. Throughout the 2007 spring/summer season incident occurrence was observed to be strongly controlled by regions of maximum alongshore bathymetric non-uniformity, a proxy to the cross-shore location of bar/rip morphology.

- While topographic rip currents were observed to extend rip hazards into mid- and high-tide regions of beaches with hard rock geologic constraints, the low-tide accretionary beach rips were responsible for most incidents throughout the 2007 spring/summer season.

- Lagrangian drifters experiments, within a typical low-tide transverse bar/rip system demonstrated that the rip current flow was strongly rotational, consisting of a large $O(200 \text{ m})$ eddy contained within the limits of the surf zone. Observed strong onshore/alongshore flow speeds over the sides of the bar revealed an important mechanism for driving bathers from the bar crest into the rip circulation.

- These quantitative measurements of rip dynamics identified strong tide-induced modulation of the rip flows. In common with previous investigations the strongest flow speeds occurred around low water (peak lagrangian $U_r \sim 1 \text{ m s}^{-1}$). Moreover, it has indicated that there was a threshold depth of $\sim 3 \text{ m}$ (when $H_b \sim 1 \text{ m}$) above which the rip flows appeared to cease, effectively 'switching' off and remaining inactive apart from a period of 3–4 hrs around spring low-tide. In fact, under some neap low-tide conditions, depths over the bar crest remained too deep for the rip currents to activate.

- A complex interplay of wave dissipation, constraining rip channel morphology, adjacent shoal elevation, feeder channel geometry and cross-shore bar crest location have all been shown to influence the specific character of rip circulation and its temporal signal under variable combinations of tidal level and wave forcing. These observations provided an insight into rip circulation and dynamics under conditions similar to those identified to be responsible for the recorded 'mass rescue' events.

REFERENCES

Aagaard, T., Greenwood, B. and Nielsen, J., 1997. Mean currents and sediment transport in a rip channel. Marine Geology, 140(1-2): 25-45.

Admiralty, 2005a. Admiralty Tide Tables. Chart NP201. Admiralty Charts and Publications, Volume 1. United Kingdom Hydrographic Office, Taunton.

Admiralty, 2006. Admiralty Tide Tables. Chart NP201. Admiralty Charts and Publications, Volume 1. United Kingdom Hydrographic Office, Taunton.

Admiralty, 2007. Admiralty Tide Tables. Chart NP201. Admiralty Charts and Publications, Volume 1. United Kingdom Hydrographic Office, Taunton.

Admiralty, A., Admiralty Tide Tables. Volume 1, 2006, Admiralty Charts and Publications, Chart NP201, United Kingdom Hydrographic Office, Taunton (2005). 2005b. Admiralty Tide Tables. Chart NP201. Admiralty Charts and Publications, Volume 1. United Kingdom Hydrographic Office, Taunton.

Anon, 2002. Futurecoast: Final Project Report, DEFRA.

Anthony, E.J., 1998. Sediment-wave parametric characterization of beaches. Journal of Coastal Research, 14(1): 347-352.

Anthony, E.J., Levoy, F., Monfort, D. and Degryse-Kulkarni, C., 2005. Short-term intertidal bar mobility on a ridge-and-runnel beach, Merlimont, northern France, pp. 81-93.

Anthony, E.J., Levoy, F. and Monfort, O., 2004. Morphodynamics of intertidal bars on a megatidal beach, Merlimont, Northern France. Marine Geology, 208(1): 73-100.

AS/NZS, 1999. Risk Management, Joint Standards Australia/Standards New Zealand Commitee OB/7.

AS/NZS, 2004. Risk Management AS/NZS 4360:2004, Joint Standards Australia/Standards New Zealand Commitee OB/7.

Bascom, W.N., 1951. The relationship between sand-size and beach-face slope. Transactions of the American Geophysical Union, 32: 866–874.

Bauer, B.O. and Greenwood, B., 1988. Surf-zone similarity. Geogr. Rev., 78: 137–147.

Baxter, P.J., 2005. The east coast Big Flood, 31 January - 1 February 1953: a summary of the human disaster. Philosophical Transactions of the Royal Society Series A - Mathematical Physical and Engineering Sciences, 363: 1293-1312.

Bidlot, J.R., Holmes, D.J., Wittmann, P.A., Lalbeharry, R. and Chen, H.S., 2002. Intercomparison of the Performance of Operational Ocean Wave Forecasting Systems with Buoy Data. Weather and forecasting, 17,: 287-310.

Bilker, M., 2002. RTK GPS - Quality in the field, Proceedings of the XIV General Meeting of the Nordic Geodetic Commission, Espoo, Finland.

Birks, H.J.B. and Gordon, A.D., 1985 Numerical methods in quaternary pollen analysis. Academic, London.

Blott, S.J. and Pye, K., 2001. GRADISTAT: a grain size distribution and statistic package for the analysis of unconsolidated sediments. Earth Surface Processes and Landforms, 26: 1237-1248.

Bowen, A.J. and Inman, D.L., 1969. Rip Currents 2. Laboratory and Field Observations. Journal of Coastal Research, 74(23): 5479-5490.

Bowen, A.J. and Inman, D.L., 1971. Edge Waves and Crescentic Bars. Journal of Geophysical Research, 76(36): 8662–8671.

Bowman, D., Rosen, D.S., Kit, E., Arad, D., Slavicz, A., 1988. Flow Characteristics at the Rip Current Neck under low energy conditions. Marine Geology, 79: 41-54.

Bradbury, A.P., Mason, T.E. and Holt, M.W., 2004a. Comparison of the Met Office UK-Waters Wave Model with a network of shallow water moored buoy data, Proceedings of the 8th International Workshop on Wave Hindcasting and Forecasting, Hawaii.

Bradbury, A.P., Mason, T.E. and Holt, M.W., 2004b. Comparison of the performance of the Met office UK-waters wave model with a network of shallow water moored buoy data, 8th International Workshop of Wave Hindcasting and Forecasting, North Shore, Oahu, Hawaii.

Brander, R.W., 1999. Field observations on the morphodynamics evolution of a low-energy rip current system. Marine Geology, 157: 199-217.

Brander, R.W. and Short, A.D., 2000. Morphodynamics of a large-scale rip current system at Muriwai Beach, New Zealand. Marine Geology, 165(1-4): 27-39.

Brander, R.W. and Short, A.D., 2001. Flow kinematics of low-energy rip current systems. Journal of Coastal Research, 17(2): 468-481.

Bray, M.J. and Hooke, J.M., 1997. Prediction of soft-cliff retreat with accelerating sea-level rise. Journal of Coastal Research, 13: 453-467.

Bridges, E.M., 1998. Classic Landforms of the North Norfolk Coast. The Geographical Association, Sheffield.

Brown, M. and Lowe, D., 2007. Automatic Panoramic Image Stitching using Invariant Features. International Journal of Computer Vision, 74(1): 59-73.

Brunsden, D. and Goudie, A., 1997. Classic Landforms of the West Dorset Coast. The Geographical Association, Sheffield.

Carrier, G. F. and Greenspan, H. P., 1958. Water waves of a finite amplitude on a sloping beach. Journal of Fluid Mechanics. 4, 97-109.

Carter, R.W.G., 1988. Coastal environments: An Introduction to the physical, ecological, and cultural systems of coastlines. Academic Press, London, 617 pp.

Castelle, B., Bonneton, P., Dupuis, H. and Sénéchal, N., 2007. Double bar beach dynamics on the high-energy meso-macrotidal French Aquitanian Coast: A review. Marine Geology, 245(1-4): 141-159.

Castelle, B. et al., 2006. Dynamics of wave-induced currents over an alongshore non-uniform multiple-barred sandy beach on the Aquitanian Coast, France. Continental Shelf Research, 26(1): 113-131.

Castelle, B. et al., 2009. Rip current system over strong alongshore non-uniformities: on the use of HADCP for model validation, 10th International Coastal Symposium (ICS 2009). Coastal Education & Research Foundation, Lisbon, POLAND, pp. 1746-1750.

Castleden, R., 1996. Classic Landforms of the Sussex Coast. The Geographical Association, Sheffield.

Chatfield, C. and Collins, A.J., 1980. Introduction to Multivariate Analysis Chapman and Hall, London and New York, 246 pp.

Church, J.A. and White, N.J., 2006. A 20th century acceleration in global sea-level rise. Geophysical Research Letters, 33(doi:10.1029/2005GL024826).

Clarke, K., 1993. Non-parametric multivariate analyses of changes in community structure. Australian Journal of Ecology, 18: 117-143.

Clarke, K. and Gorley, R., 2006. PRIMER v6 User Manual/Tutorial, Plymouth.

Clayton, K. and Shamoon, N., 1998. New approach to the relief of Great Britain II. A classification of rocks based on relative resistance to denudation. Geomorphology, 25: 155-171.

Cormack, R.M., 1971. A review of classification. Journal of the Royal Statistical Society, B(34): 321-367.

Cowell, P.J. and Thom, B.G., 1994. Morphodynamics of coastal evolution. In: R.W.G. Carter and C.D. Woodroffe (Editors), Coastal evolution, Late Quaternary shoreline morphodynamics. Cambrich University Press, pp. 33-86.

287

Cowell, P.J. and Thom, B.G., 1997. Morphodynamics of coastal evolution. In: R.W.G. Carter and C.D. Woodroffe (Editors), Coastal evolution, Late Quaternary shoreline morphodynamics. Cambrich University Press, pp. 33-86.

Dalrymple, R.A., 1992. Prediction of storm/normal beach profiles. J. Waterway, Port, Coastal, Ocean Engng, 118: 193–200.

Davidson, M., Huntley, D., Holman, R., George, K., 1997. The Evaluation of Large-scale (km) Intertidal Beach Morphology on a Macrotidal Beach using Video Images Proceedings Coastal Dynamics '97: 385-394.

Davidson, M.A., Russell, P.E., Huntley, D.A. and Hardisty, J., 1993. Tidal asymmetry in suspended sand transport on a macrotidal intermediate beach. Marine Geology, 110(3-4): 333-353.

Davidson, M.A. and Turner, I.L., 2009. A behavioural-template beach profile model for predicting seasonal to interannual shoreline evolution. Journal of Geophysical Research - Earth Surface 114:F1.

Davies, J.L., 1980. Geographical Variation in Coastal Development Longman, New York.

Davies, R.A. and Hayes, M.O., 1984. What is a wave dominated coast? Marine Geology, 60: 313-329.

Dean, R.G., 1973. Heuristic models of sand transport in the surf zone, Proc. 1st Australian Conf. on Coastal Engineering, Engineering Dynamics in the Surf Zone, pp. 208-214.

Defra, 2006. Multi-Agency Geographic Information for the Countryside (MAGIC). www.magic.gov.uk.

Devon County Council, 2006. Tourism trends in Devon 2005. ISBN 1-85522-960-9, Exeter.

Draper, L., 1991. Wave Climate Atlas of the British Isles, Offshore Techology Report, OTH 89 303 Department of Energy, HMSO, London.

Duvivier, P., 1998. Lyme Bay and South Devon Shoreline Management Plan, 3 Volumes. Report to Lyme Bay and South Devon Coastal Group.

Dyer, K.R. and Moffat, T., J., 1998. Fluxes of suspended matter in the East Anglian plume Southern North Sea. Continental Shelf Research 18: 1311-1331.

Engle, J., MacMahan, J., Thieke, R.J., Hanes, D..M. and Dean, R.G., 2002. Formulation of a rip current predictive index using rescue data. In: L. Tait (Editor), 15th Annual National Conference on Beach Preservation Technology. Florida Shore & Beach Preservation Association, Biloxi, Ms, pp. 285-298.

Engle, J.A., 2003. Formulation of a Rip Current Forecasting Technique through Statistical Analysis of Rip Current-Related Rescues, Master of Science Thesis., University of Florida, Florida.

Everitt, B.S., 1980. Cluster Analysis. Halsted Press, New York, 136 pp.

Fairbanks, R.G., 1989. A 17,000-year glacio-eustatic sea level record: Influence of glacial melting rates on the Younger Dryas event and deep-ocean circulation. Nature, 342: 637-642.

Feddersen, F. and Guza, R.T., 2003. Observations of nearshore circulation: Alongshore uniformity. Journal of Geophysical Research 108(C1): 10.1029/2001JC001293.

Ferguson, R.I. and Church, M., 2004. A simple universal equation for grain settling velocity. Journal of Sedimentary Research, 74(6): 933-937.

Flather, R.A., 1987. Estimates of extreme conditions of tide and surge using a numerical model of the northwest European continental-shelf. Estuarine Coastal and Shelf Science, 24: 69-93.

Folk, R.L. and Ward, W.C., 1957. Brazos River Bar: A study in the significance of grain size parameters. Journal of Sedimentary Petrology, 27(1): 3-26.

French, P.W., 2004. The changing nature of, and approaches to, UK coastal management at the start of the twenty-first century. Geographical Journal, 170: 116-125.

Futurecoast, 2002. Final Project Report, DEFRA.

Galvin, C.J., 1968. Breaker type and classification on three laboratory beaches. Journal of Geophysical Research, 73: 3651-3659.

Goda, Y., 1975. Irregular Wave Deformation in the Surf Zone. Coastal Engineering in Japan, 18: 13-26.

Gómez-Pujol, L. et al., 2007. Morphodynamic classification of sandy beaches in low energetic marine environment. Marine Geology, 242(4): 235-246.

Gordon, A.D., 1981. Classification: Methods for the Exploratory Analysis of Multivariate Data. Chapman & Hall, London, 193 pp.

Gourlay, M.R., 1968. Beach and dune erosion tests. Rep. m935/m936, Delft Hydraul. Lab., Delft.

Gower, J.C., 1971. A General Coefficient of Similarity and Some of Its Properties. Biometrics, 27(4): 857-871.

Guza, R.T. and Davis, R.E., 1974. Excitation of edge waves by waves incident on a beach. J. Geophys.Res., 79(9): 1285-1291.

Guza, R.T. and Inman, D.L., 1975. Edge waves and beach cusps Journal of Geophysical Research, 80(C21): 2997-3012.

Guza, R.T. and Thornton, E.B., 1985. Observation of surf beat. J. Geophys. Res, 90(C2): 3161-3172.

Hails, J.R., 1975. Sediment distribution and Quaternary history of Start Bay, Devon. Journal of the Geological Society, London, 131: 19—35.

Haller, M., Darlrymple, R. and Svendesen, 2002. Experimental study of nearshore dynamics on a barred beach with rip channels. Journal of Geophysical Research, 107(14): 1-21.

Halliday, R. and Douglas, N.G., 2008. Baseline Survey of Available Wave Data. The Crown Estate, pp. 126.

Hartmann, D., 2006. Drowning and Beach-Safety Management (BSM) along the Mediterranean Beaches of Israel—A Long-Term Perspective. Journal of Coastal Research 1505.

Hegge, B., Eliot, I. and Hsu, J., 1996. Sheltered sandy beaches of Southwestern Australia. Journal of Coastal Research, 12(3): 748-760.

Herlihy, A.J., 1982. Coast Protection Survey 1980, Department of the Environment, London.

Hermanns, R.L., Trauth, M.H., Niedermann, S., McWilliams, M. and Strecker, M.R., 2000. Tephrochronologic constraints on temporal distribution of large landslides in northwest Argentina. Journal of Geology, 108(1): 35-52.

Holman, R.A. and Stanley, J., 2007. The history and technical capabilities of Argus. Coastal Engineering, 54(6-7): 477-491.

Holthuijsen, L.H., Booij, N. and Herbers, T.H.C., 1989. A prediction model for stationary, short-crested waves in shallow water with ambient currents. . Coastal Engineering 13: 23–54.

HSE, 2006. Five steps to risk assessment, revised 06/06, Health and Safety Executive.

Huntley, D.A., Hendry, M.D., Haines, J., Greenidge, B., 1988. Waves and rip currents on a caribbean pocket beach. Journal of Coastal Research, 4(1): 69-79.

Jackson, D.W.T., Cooper, J.A.G. and del Rio, L., 2005. Geological control of beach morphodynamic state. Marine Geology, 216(4): 297-314.

Jiménez, J.A., Guillén, J. and Falqués, A., 2008. Comment on the article "Morphodynamic classification of sandy beaches in low energetic marine environment" by Gómez-Pujol, L., Orfila, A., Cañellas, B., Alvarez-Ellacuria, A., Méndez, F.J., Medina, R. and Tintoré, J. Marine Geology, 242, pp. 235-246, 2007. Marine Geology, 255(1-2): 96-101.

Keen, D.H., 1998. The Quaternary History of the Dorset, South Devon and Cornish
Coasts. In: S.C.e. al. (Editor), Quaternary of South-West England. Geological
Conservation Review, London, pp. 157-169.

Keene, P., 1996. Classic Landforms of the North Devon. The Geographical Association,
Sheffield.

Keller, H.B., Levine, D.A. and Whitlam, G.B., 1960. Motion of a bore over a sloping
beach. Journal of Fluid Mechanics, 7: 302-316.

King, C.A.M., 1972. Beaches and coasts Arnold, London 570 pp.

King, C.A.M. and Williams, W.W., 1949. The formation and movement of sand bars by
wave action. . Geographical Journal 113: 70–85.

Kingston, K.S., Ruessink, B.G., van Enckevort, I.M.J. and Davidson, M.A., 2000.
Artificial neural network correction of remotely sensed sandbar location. Marine
Geology, 169(1-2): 137-160.

Komar, P.D. and Gaughan, M.K., 1973. Airy wave theories and breaker height
prediction, Proc. 13th Coastal Engineering Conf. ASCEM, pp. 405–418.

Kroon, A. and Masselink, G., 2002. Morphodynamics of intertidal bar morphology on a
macrotidal beach under low-energy wave conditions, North Lincolnshire,
England. Marine Geology, 190(3-4): 591-608.

Kruskal, J.B., 1964. Multidimensional scaling by optimizing goodness of fit to a
nonmetric hypothesis. Psychometrika(29): 1-27.

Lascody, R.L., 1998. East Central Florida Rip Current Program. Natl. Wea. Dig., 22(2).

Leahy, S., McLeod, K. and Short, A.D., 1996. Beach Management Plan, Surf Life Saving
Australia Ltd, Sydney.

Levoy, F., Anthony, E.J., Monfort, O. and Larsonneur, C., 2000. The morphodynamics
of megatidal beaches in Normandy, France. Marine Geology, 171(1-4): 39-59.

Lippmann, T.C. and Holman, R.A., 1989. Quantification of sand bar morphology: A
video technique based on wave dissipation. Journal of Geophysical Research, 94:
995– 1011.

Lippmann, T.C. and Holman, R.A., 1990. The spatial and temproal varability of sand bar
morphology. Journal of Geophysical Research, 95(C7): 11575-11590.

Lushine, J.B., Rip Currents: Human Impact and Forecastibility.

Lushine, J.B., 1991. A study of rip current drownings and related weather factors.
National Weather Digest, 16: 13–19.

MacMahan, J. et al., 2009a. Mean Lagrangian Flow Behavior on an Open Coast Rip-
channeled Beach: A New Perspective. Marine Geology.

MacMahan, J., Brown, J. and Thornton, E., 2009b. Low-Cost Handheld Global Positioning System for Measuring Surf-Zone Currents. Journal of Coastal Research, 25(3): 744-754.

MacMahan, J.H., Reniers, A., Thornton, E.B. and Stanton, T.P., 2004. Surf zone eddies coupled with rip current morphology. Journal of Geophysical Research-Oceans, 109(C7): 15.

MacMahan, J.H., Thornton, E.B. and Reniers, A., 2006. Rip current review. Coastal Engineering, 53(2-3): 191-208.

MacMahan, J.H., Thornton, E.B., Reniers, A., Stanton, T.P. and Symonds, G., 2008. Low-Energy Rip Currents Associated With Small Bathymetric Variations. Marine Geology, 255(3-4): 156-164.

MacMahan, J.H., Thornton, E.B., Stanton, T.P. and Reniers, A.J.H.M., 2005b. RIPEX: Observations of a rip current system. Marine Geology, 218(1-4): 113-134.

MAFF, 1994. Coast Protection Survey of England: Summary Survey Report, Ministry of Agriculture Fisheries and Food, Department of Environment, London.

Marino-Tapia, I., Russell, P.E., O'Hare, T., Davidson, M.A. and Huntley, D.A., 2007. Cross-shore sediment transport on natural beaches and its relation to sandbar migration patterns. Part 1: Field observations and derivation of a transport parameterization. . Journal of Geophysical Research, 112(C03001).

Martinelli, L., Zanuttigh, B. and Lamberti, A., 2006. Hydrodynamic and morphodynamic response of isolated and multiple low crested structures: Experiments and simulations. Coastal Engineering, 53(4): 363-379.

Masselink, G., 1993. Simulating the effects of tides on beach morphodynamics. Journal of Coastal Research(Special Issue No. 15): 180–197.

Masselink, G., 2004a. Classification of the coastline of England and Wales. Internal report, University of Loughborough.

Masselink, G., 2004b. Formation and evolution of multiple intertidal bars on macrotidal beaches: application of a morphodynamic model. Coastal Engineering, 51(8-9): 713-730.

Masselink, G. and Anthony, E.J., 2001. Location and height of intertidal bars on macrotidal ridge and runnel beaches. Earth Surface Processes and Landforms, 26(7): 759-774.

Masselink, G., Austin, M., Tinker, J., O'Hare, T. and Russell, P., 2008. Cross-shore sediment transport and morphological response on a macrotidal beach with

intertidal bar morphology, Truc Vert, France. Marine Geology, 251(3-4): 141-155.

Masselink, G. and Hegge, B., 1995. Morphodynamics of meso- and macrotidal beaches: Examples from central Queensland, Australia. Marine Geology, 129(1-2): 1-23.

Masselink, G. and Hughes, M., 2003 Introduction to coastal processes and geomorphology. London, United Kingdom. Arnold, 354p.

Masselink, G., Kroon, A. and Davidson-Arnott, R.G.D., 2006. Morphodynamics of intertidal bars in wave-dominated coastal settings -- A review. Geomorphology, 73(1-2): 33-49.

Masselink, G. and Pattiaratchi, C.B., 2001. Seasonal changes in beach morphology along the sheltered coastline of Perth, Western Australia. Marine Geology, 172(3-4): 243-263.

Masselink, G. and Short, A.D., 1993. The Effect of Tide Range on Beach Morphodynamics and Morphology - a Conceptual Beach Model. Journal of Coastal Research, 9(3): 785-800.

May, V.J. and Hansom, J.D., 2003. Coastal geomorphology of Great Britain. Geological conservation review series 28. Joint Nature Conservation Committee, Peterborough

McCave, I.N., Hall, I.R. and Bianchi, G.G., 2006. Laser vs. settling velocity differences in silt grainsize measurements: estimation of palaeocurrent vigour. Sedimentology, 53(4): 919-928.

McKenzie, P., 1958. Rip-current systems. Journal of Geology, 66: 103–113.

McLean, R.F. and Kirk, R.M., 1969. Relationships between grain-size, size-sorting and foreshore slope on mixed sand-shingle beaches. New Zealand Journal of Geology and Geophysics, 12: 138-155.

McNinch, J.E., 2004. Geologic control in the nearshore: shoreoblique sandbars and shoreline erosional hotspots, Mid-Atlantic Bight, USA. Marine Geology, 211: 121–141.

Michel, D. and Howa, H.L., 1999. Short-term morphodynamic response of a ridge and runnel system on a mesotidal sandy beach. Journal of Coastal Research, 15(2): 428-437.

Middleton, G.V., 1967. Experiments on density and turbidity currents, III. Deposition of sediment. Can. J. Earth Sci. , 4: 475-505.

Middleton, G.V., 2000. Data analysis in the earth sciences using MATLAB. Prentice Hall, New Jersey, 260 pp.

Morey, C.R., 1983. The Evolution of a Barrier-Lagoon System - A Case Study from Start Bay. Proc Ussher Society, 5: 454-459.

Morton, R.A., Leach, M.P., Paine, J.G. and Cardoza, M.A., 1993. Monitoring beach changes using GPS surveying techniques. Journal of Coastal Research, 9 (3): 702-720.

Motterhead, D., 1996. Classic Landforms of the South Devon Coast. The Geographical Association, Sheffield.

Munk, W., 1949. Surf beats. Eos Trans. AGU, 30: 849–854.

Osborne, P.D. and Greenwood, B., 1992. Frequency dependent cross-shore suspended sediment transport, 2. A barred shoreface. Marine Geology(106): 25–51.

Pearson, K., 1896. Mathematical contributions to the theory of evolution. III. Regression, heredity and panmixia. Philos. Trans. Royal Soc. London Ser. A , 187 pp. 253–318

Pingree, R.D. and Griffiths, D.K., 1979. Sand transport paths around the British Isles resulting from M2 and M4 tidal interactions. Journal of the Marine Biological Association, U.K, 59: 197-513.

Proundman, J. and Doodson, A. J., 1924. The principal constituent of the tides of the North Sea. Philos. Trans. Royal Soc. London Ser. A224, 185-219.

Plant, N.G., Holland, K.T. and Puleo, J.A., 2002. Analysis of the scale of errors in nearshore bathymetric data. Marine Geology, 191(1-2): 71-86.

Ramsay, P.M., Kent, M., Reid, C.L. and Duckworth, J.C., 2006. Taxonomic, morphological and structural surrogates for the rapid assessment of vegetation. Journal of Vegetation Science, 17(6): 747-754.

Ranasinghe, R., Hacking, N. and Evans, P., 2001. Multi-functional artificial surf breaks: A review, NSW Department of Land and Water Conservation, Center for Natural Resources, Parramatta, Australia.

Ranasinghe, R., Symonds, G., Black, K. and Holman, R., 2004. Morphodynamics of intermediate beaches: a video imaging and numerical modelling study. Coastal Engineering, 51(7): 629-655.

Reading, H.G. and Collinson, J.D., 1996. Clastic coasts. In: H.G. Reading (Editor), Sedimentary Environments: Processes, Facies and Stratigraphy. Blackwell Science, Oxford, pp. 154-231.

Reichmüth, B. and Anthony, E.J., 2007. Tidal influence on the intertidal bar morphology of two contrasting macrotidal beaches. Geomorphology, 90(1-2): 101-114.

Reniers, A.J.H.M., Roelvink, J.A. and Thornton, E.B., 2004. Morphodynamic modeling of an embayed beach under wave group forcing. . J. Geophys. Res., 109(C01030).

RNLI, 2009. 2008 RNLI Lifeguards annual report.

Roelvink, J.A. and Stive, M.J.F., 1989. Bar-generating cross-shore flow mechanisms on a beach. . Journal of Geophysical Research, 94: 4785–4800.

Russell, P.E. and Huntley, D.A., 1999. A cross-shore transport "shape function" for high energy beaches. Journal of Coastal Research, 15(1): 198–205.

Sallenger, A.H. and Holman, R.A., 1985. Wave energy saturation on a natural beach of variable slope. Journal of Geophysical Research, 90: 11939-11944.

Sanderson, P.G. and Eliot, I., 1999. Compartmentalisation of beachface sediments along the southwestern coast of Australia. Marine Geology, 162(1): 145-164.

Schlax, M.G. and Chelton, D.B., 1992. Frequency domain diagnostics for linear smoothers. J. Am. Stat. Assoc., 87: 1070-1081.

Schmidt, W.E., Guza, R.T. and Slinn, D.N., 2005. Surf zone currents over irregular bathymetry: Drifter observations and numerical simulations. Journal of Geophysical Research-Oceans, 110(C12).

SDADCAG, 2009. South Devon & Dorset Shoreline Management Plan Review - Consultation Draft.

Sedrati, M. and Anthony, E.J., 2007. Storm-generated morphological change and longshore sand transport in the intertidal zone of a multi-barred macrotidal beach. Marine Geology, 244(1-4): 209-229.

Selma van, H., Gerhard, M. and Joanna, B., 2006. Characteristics and dynamics of multiple intertidal bars, north Lincolnshire, England, pp. 428-443.

Shennan, I. and Andrews, J.E., 2000. Holocene Land-Ocean Interaction and Environmental Change around the North Sea. Geological Society Special Publication 166. Geological Society Publishing House, Bath, 299-319 pp.

Shennan, I. and Horton, B., 2002. Holocene land- and sea-level changes in Great Britain. Journal of Quaternary Science, 17: 511-526.

Shepard, F.P., 1949. Dangerous currents in the surf. Physics Today 2: 20-29.

Shepard, F.P., Emery, K.O., La Fond, E. C., 1941. Rip Currents: A process of geological importance. Journal of Geology, XLIX: 337-369.

Shepard, F.P. and LaFonda, E.C., 1940. Sand movement along the Scripps Institution Pier. American Journal of Scince, 238: 272-284.

Shepard, R.N., 1962. The analysis of proximities: multidimensional scaling with an unknown distance function. Psychometrika(27): 125-140.

295

Sherker, S., Brander, R., Finch, C. and Hatfield, J., 2008. Why Australia needs an effective national campaign to reduce coastal drowning. Journal of Science and Medicine in Sport, 11(2): 81-83.

Short, A.D., 1975. Three-dimensional beach stage model. Journal of Geology, 87: 553–571.

Short, A.D., 1978 Wave power and beach-stages. A global model, Proceedings of the16th International Conference on Coastal Engineering. ASCE, pp. 1145-1162.

Short, A.D., 1985. Rip-current type, spacing and persistence, Narrabeen Beach, Australia. Marine Geology, 65(1-2): 47-71.

Short, A.D., 1986. A note on the controls of beach state and change, with examples from south-east Australia. Journal of Coastal Research, 3 (3): 387–395.

Short, A.D., 1991. Macro-Meso Tidal Beach Morphodynamics - an Overview. Journal of Coastal Research, 7(2): 417-436.

Short, A.D., 1993. Beaches Of The New South Wales Coast, Australian Beach Safety and Management Project. Sydney University Press, Sydney, 358 pp.

Short, A.D., 1996. The role of wave height, period, slope, tide range and embaymentisation in beach classifications: A review. Revista Chilena De Historia Natural, 69(4): 589-604.

Short, A.D., 2001. Beaches of the Southern Australian Coast and Kangaroo Island. Australian Beach Safety and Management Project. Sydney University Press, Sydney, 346 pp pp.

Short, A.D., 2006. Australian Beach Systems - Nature and Distribution. Journal of Coastal Research, 22(1): 11-27.

Short, A.D., Editor, 1999. Handbook of beach and shoreface morphodynamics.

Short, A.D. and Hogan, C.L., 1994. Rip currents and beach hazards: Their impact on public safety and implications for coastal management. Journal Coastal Research, Special Issue(12): 197-209.

Short, A.D. and McLeod, K., 1998. Australian Beach Data: Site selection, attributes and quality control, Australian Government, DEH.

SOCPAC, 2004. Coastal Sediment Transport Study.

Sokal, R.R. and Rohlf, J.F., 1995. Biometry : the principles and practice of statistics in biological research. Freeman, New York ; Oxford, 887 pp.

Sonu, C.J., 1972. Field Observation of Nearshore Circulation and Meandering Currents. Journal of Geophysical Research, 77(18): 3232-&.

Sonu, C.J., 1973. 3-Dimensional Beach Changes. Journal of Geology, 81(1): 42-64.

Sonu, C.J. and Vanbeek, J.L., 1971. Systematic Beach Changes on Outer Banks, North Carolina. Journal of Geology, 79(4): 416-&.

Sorensen, L.S., Kofoed-Hansen, O.R., H. and Rugbjerg, M., 2004. A third-generation spectral wave modelusing an unstructured finite volume technique, International Conference on Coastal Engineering, pp. 894-906.

Spydell, M., Feddersen, F., Guza, R. and Schmidt, W., 2007. Observing surf-zone dispersion with drifters. J. Phys. Ocean, 37 (12): 2920-2939.

Steers, J., 1960. The Coast of England and Wales in Pictures. Cambridge University Press, London.

Steers, J.A., 1946. The Coastline of England and Wales. Cambridge University Press, Cambridge.

Strauss, D., Mirferendesk, H. and Tomlinson, R., 2007. Comparison of two wave models for Gold Coast, Australia. Journal of Coastal Research, SI 50: 312 - 316.

Sunamura, T. and Trenhaile, V.C.L.a.A.S., 1989. Chapter 6 Sandy Beach Geomorphology Elucidated by Laboratory Modeling, Elsevier Oceanography Series. Elsevier, pp. 159-213.

Talbot, M.M. and Bate, G.C., 1987. Rip current characteristics and their role in the exchange of water and surf diatoms between the surf zone and nearshore. Estuar. Coast. Shelf Sci., 25(6): 707-720.

Taylor, J.A., Murdock, A.P. and Pontee, N.I., 2004. A macroscale analysis of coastal steepening around the coast of England and Wales. Geographical Journal, 170: 179-188.

Thornton, E.B. and Guza, R.T., 1982. Energy saturation and phase speeds measured on a natural beach. J. Geophys. Res., 87: 9499–9508.

Tinker, J., O'Hare, T., Masselink, G., Butt, T. and Russell, P., 2009. A cross-shore suspended sediment transport shape function parameterisation for natural beaches. Continental Shelf Research, 29(16): 1948-1960.

Travers, A., 2007. Low-Energy Beach Morphology with Respect to Physical Setting: A Case Study from Cockburn Sound, Southwestern Australia. Journal of Coastal Research, 23(2): 429-444.

Trimble, 2002. Trimble Geomatics Office- User Guide: v1.6, Trimble Navigation Limited, Dayton, USA.

Trimble, 2009. Trimble R8 GNSS, R6, 5800 User Guide v4.00, Trimble Navigation Limited, Dayton, USA.

Tucker, M.J., 1950. Surf beats: sea waves of 1 to 5 min. period. Proceedings of the Royal Society of London, 202: 565-573.

Turner, I., 1993. Water-Table Outcropping on Macro-Tidal Beaches - a Simulation-Model. Marine Geology, 115(3-4): 227-238.

Van Enckevort, I.M.J. and Ruessink, B.G., 2001. Effect of hydrodynamics and bathymetry on video estimates of nearshore sandbar position. Journal of Geophysical Research, 106: 16969-16980.

van Houwelingen, S.T., Masselink, G. and Bullard, J.E., 2006. Characteristics and dynamics of multiple intertidal bars, north Lincolnshire, England, pp. 428-443.

Vincent, C.L., 1985. Depth-Controlled Wave Height. Journal of Waterway, Port, Coastal and Ocean Engineering, 111: 459-475.

WHO, 2003. Guidelines for safe recreational waters Volume 1 - Coastal and fresh waters, World Health Organization.

Wijnberg, K.M. and Kroon, A., 2002. Barred beaches. Geomorphology, 48: 103– 120.

Wilson, G., 1971. The influence of rock structure on coastline and cliff development around Tintagel, North Cornwall. In: J.A. Steers (Editor), Geographical Readings: Introduction to coastline development. Macmillan, London, pp. 133-161.

Wright, L.D., Chappell, J., Thom, B.G., Bradshaw, M.P. and Cowell, P., 1979. Morphodynamics of Reflective and Dissipative Beach and Inshore Systems - Southeastern Australia. Marine Geology, 32(1-2): 105-140.

Wright, L.D., Guza, R.T. and Short, A.D., 1982a. Dynamics of a high-energy dissipative surf zone. Marine Geology, 45(1-2): 41-62.

Wright, L.D., Nielsen, P., Shi, N.C. and List, J.H., 1986. Morphodynamics of a bar-trough surf zone. Marine Geology, 70(3-4): 251-285.

Wright, L.D., Nielsen, P., Short, A.D. and Green, M.O., 1982b. Morphodynamics of a Macrotidal Beach. Marine Geology, 50(1-2): 97-127.

Wright, L.D. and Short, A.D., 1983. Morphodynamics of beaches and surf zones in Australia. In: P.D. Komar (Editor), Handbook of Coastal Processes and Erosion. CRC Press, Boca Raton, pp. 35– 64.

Wright, L.D. and Short, A.D., 1984. Morphodynamic Variability of Surf Zones and Beaches - a Synthesis. Marine Geology, 56(1-4): 93-118.

Wright, L.D. and Thom, B.G., 1977. Coastal depositional landforms: a morphodynamic approach. . Progress in Physical Geography 1: 412-459

Yu, J. and Slinn, D.N., 2003. Effects of wave-current interaction on rip currents. Journal of Geophysical Research 108(3088).

298

APPENDIX

Appendix 1 – Calculated representative wave climate statistics for each of the beach study sites in Chapter 4.

Beach Index	Location	Region	Wave data name	Data source	%	Annual H, 10%	Annual H, 50%	T$_p$	T$_m$	MSR
1	Traeth Bychan	Anglesey	M1	Model	68.2	0.7	0.35	5.9	4.9	6.60
2	Traeth Lligwy	Anglesey	M1	Model	68.2	0.82	0.41	5.8	4.8	6.50
3	Porth Trecastell	Anglesey	M2	Model	63.3	2.1	0.92	7.6	6.3	4.31
4	Aberffraw	Anglesey	M2	Model	63.3	2.4	1.05	7.7	6.4	4.27
5	Newborough	Anglesey	M2	Model	63.3	1.14	0.77	5.8	4.8	4.20
5	Dunster Beach	Someset	B1	Measured		1.09	0.48	6.5	3.9	9.77
6	Dunster	Someset	B1	Measured		1.09	0.48	6.5	3.9	9.77
8	Minehead	Someset	B1	Measured		1.09	0.48	6.5	3.9	9.64
9	Woolacombe	N.Devon	M3	Model	80.7	3.09	1.2	9.7	8	8.11
10	Croyde Ruda	N.Devon	M3	Model	80.7	3.2	1.28	9.5	7.9	7.93
11	Croyde Downend	N.Devon	M3	Model	80.7	3.2	1.28	9.5	7.9	7.94
12	Saunton Sands	N.Devon	M3	Model	80.7	2.81	1.24	9.2	7.7	7.81
13	Sandymouth	Bude	M3	Model	80.7	3.47	1.61	9.7	8.1	6.96
14	Crooklets	Bude	M3	Model	80.7	2.95	1.6	9.6	8	6.88
15	Widemouth	Bude	M3	Model	80.7	3.17	1.41	9.7	8	6.74
16	Crackington	N.Cornwall	M3	Model	80.7	2.74	1.22	9.8	8.1	6.58
17	New Polzeath	N.Cornwall	M3	Model	80.7	2.04	0.97	9.5	7.9	6.52
18	Polzeath	N.Cornwall	M3	Model	80.7	2.04	0.97	9.5	7.9	6.52
19	Harlyn	N.Cornwall	M3	Model	80.7	2.37	0.91	9.8	8.1	6.49
20	Constantine	N.Cornwall	M3	Model	80.7	3.42	1.38	9.8	8.1	6.49
21	Constantine	N.Cornwall	M3	Model	80.7	3.42	1.38	9.8	8.1	6.49
22	Treyarnon	N.Cornwall	M3	Model	80.7	3.42	1.38	9.8	8.1	6.48
23	Porthcothan	N.Cornwall	M3	Model	80.7	3.35	1.38	9.8	8.1	6.47
24	Watergate	W.Cornwall	M3	Model	80.7	3.15	1.21	9.8	8.1	6.42
25	Towan	Newquay Bay	M3	Model	80.7	1.55	0.63	9.7	8.1	6.39
26	Fistral	W.Cornwall	M3	Model	80.7	2.95	1.14	9.8	8.1	6.40
27	Crantock	W. Cornwall	M3	Model	80.7	3.44	1.34	9.8	8.1	6.34
28	Perranporth	W.Cornwall	M3	Model	80.7	2.95	1.24	9.7	8.1	6.10
29	Chapel Porth	W.Cornwall	M3	Model	80.7	3.04	1.32	9.7	8	6.02
30	Porthtowan	W.Cornwall	M3	Model	80.7	2.55	1.23	9.5	7.9	6.01
31	Godrevy	Hayle Bay	M3	Model	80.7	1.92	0.97	9.1	7.6	5.88
32	Hayle	Hayle Bay	M3	Model	80.7	1.35	0.6	9.3	7.7	5.83
34	Carbis Bay	St Ives	M3	Model	80.7	0.94	0.38	9.6	7.9	5.81
35	Porthmeor	W.Cornwall	M3	Model	80.7	2.1	0.79	9.8	8.1	5.78
36	Sennen Cove	SW Cornwall	M3	Model	80.7	2.17	1.24	9.6	8	5.37
37	Penzance	SW Cornwall	M4	Model	80.7	0.54	0.23	10	8.3	4.79
38	Marazion	S.Cornwall	M4	Model	80.7	1.53	0.62	10	8.3	4.77
39	Perran Sands	S.Cornwall	M4	Model	80.7	1.82	0.73	10	8.3	4.75
40	Praa Sands	S.Cornwall	M4	Model	80.7	2.85	1.13	9.8	8.1	4.73
41	Porthleven	S.Cornwall	M4	Model	80.7	2.96	1.15	10	8.3	4.70

42	Church Cove	Gunwalloe	M4	Model	80.7	3.45	1.35	9.9	8.2	4.70
43	Looe	Looe Bay	M4	Model	80.7	0.92	0.38	10	8.3	4.80
45	Millandreath	Looe Bay	M4	Model	80.7	1.61	0.64	9.9	8.2	4.78
46	Seaton	Whitsands Bay	M4	Model	80.7	1.76	0.7	9.9	8.2	4.70
47	Downderry	Whitsands Bay	M4	Model	80.7	1.76	0.7	9.9	8.2	4.70
48	Tregantle	Whitsands Bay	M4	Model	80.7	1.9	0.75	10	8.3	4.54
49	Challaborough	S.Devon	M4	Model	80.7	2.5	0.98	10	8.3	4.64
50	Bigbury West	Bigbury Bay	M4	Model	80.7	2.46	1.21	9.5	7.9	4.64
51	Bigbury East	Bigbury Bay	M4	Model	80.7	2.46	1.21	9.5	7.9	4.64
52	Sedgewell	Bigbury Bay	M4	Model	80.7	2.46	1.21	9.5	7.9	4.64
53	Bantham	Bigbury Bay	M4	Model	80.7	2.72	1.06	9.9	8.2	4.63
54	Leesfoot	Bigbury Bay	M4	Model	80.7	2.92	1.13	9.9	8.3	4.63
56	South Milton	Bigbury Bay	M4	Model	80.7	2.92	1.13	9.9	8.3	4.63
59	Hope Cove	S.Devon	M4	Model	80.7	2.92	1.13	9.9	8.3	4.63
60	Northsands	Salcombe	M4	Model	80.7	2.56	0.99	10.1	8.3	4.60
62	Torcross	S.Devon	B4	Measured		1.32	0.52	7.8	4.3	4.35
63	Strete	S.Devon	B4	Measured		1.32	0.52	7.8	4.3	4.33
64	Blackpool Sands	S.Devon	B4	Measured		1.32	0.52	7.8	4.3	4.32
65	Broadsands	Torbay	M5	Model	79.5	0.27	0.12	7.2	6	4.20
66	Paignton	Torbay	M5	Model	79.5	0.45	0.21	7.4	6.1	4.15
67	Teignmouth	E.Devon	M5	Model	79.5	1.14	0.5	7.4	6.2	3.82
68	Dawlish	E.Devon	M5	Model	79.5	1.27	0.56	7.4	6.1	3.90
69	Dawlish Warren	E.Devon	M5	Model	79.5	1.38	0.61	7.4	6.1	3.97
70	Lyme Regis	W.Dorset	B5	Measured		2.06	0.65	8	4.5	3.71
71	Charmouth	Lyme Bay	B5	Measured		2.06	0.65	8	4.5	3.66
72	Shore Road	Poole Bay	B8-B9	Measured		0.5	0.35	13.3	5.9	1.55
73	Branksome Chine	Poole Bay	B8-B9 int	Measured		0.65	0.36	7.5	4	1.54
74	Bournemouth Pier	Poole Bay	B8-B9 int	Measured		0.8	0.39	7.5	4	1.50
75	East Cliff	Poole Bay	B8-B9 int	Measured		0.95	0.4	7.5	4	1.48
76	Boscombe	Poole Bay	B9	Measured		1.07	0.41	7.5	4	1.44
77	Manor Steps	Poole Bay	B9	Measured		1.07	0.41	7.5	4	1.40
78	Fishermans Walk	Poole Bay	B9	Measured		1.07	0.41	7.5	4	1.37
79	Milford	Poole Bay	B10	Measured		1.45	0.44	8.4	4.1	1.60
80	Main Beach	Weymouth	B7	Measured		0.85	0.35	6.6	3.8	2.18
81	Greenhill	Weymouth	B7	Measured		0.85	0.35	6.6	3.8	2.14
82	Pakefield	Suffolk	B14	Measured		1.04	0.47	5.6	3.4	1.90
83	Covehithe	Suffolk	B14	Measured		1.04	0.47	5.6	3.4	1.90
84	Oxford Ness	Suffolk	B11	Measured		1.12	0.43	5.2	4.1	2.30
85	Boyton (Oxford Ness)	Suffolk	B11	Measured		1.12	0.43	5.2	4.1	1.97
86	Dunwich	Suffolk	B13	Measured		0.93	0.44	6	3.5	1.97
87	Sizewell	Suffolk	B13	Measured		0.93	0.44	6	3.5	2.19
88	Great Yarmoth	Norfolk	B16	Measured		1.29	0.52	6.5	3.6	2.59
89	Newport South	Norfolk	B16	Measured		1.29	0.52	6.5	3.6	2.26
90	Overstrand	Norfolk	B16	Measured		1.29	0.52	6.5	3.6	4.18
91	Walcott	Norfolk	B16	Measured		1.29	0.52	6.5	3.6	3.49
92	Horsey	Norfolk	B16	Measured		1.29	0.52	6.5	3.6	2.79
93	Salthouse	Norfolk	B17	Measured		1.02	0.46	5.2	2.9	4.97
94	Holme-Next-The-Sea	Norfolk	B17	Measured		1.02	0.46	5.2	2.9	6.32
95	Holme-Next-The-Sea	Norfolk	B17	Measured		1.02	0.46	5.2	2.9	6.35
96	Mablethorpe	Lincolnshire	B20	Measured		1.09	0.49	6.4	3.2	6.18

| 97 | Theddlethorpe | Lincolnshire | B20 | Measured | 1.09 | 0.49 | 6.4 | 3.2 | 6.19 |
| 98 | Donna Nook | Lincolnshire | B21 | Measured | 0.9 | 0.46 | 5.8 | 2.8 | 6.27 |

Appendix 2 – Summary of data sources for beach profile and sediment data used in Chapter 4.

Location	Sediment			Beach profile		
	Source	Date	Analysis	Source	Date	Method
Traeth Bychan	Dixey	1965	sieve	Dixey	1965	Level
Traeth Lligwy	Clark.M	1995	sieve	Clark.M	1971	Level
Porth Trecastell	Dixey	1965	sieve	Dixey	1965	Level
Aberffraw	Dixey	1965	sieve	Dixey	1965	Level
Newborough	Davis	11/04/1975	sieve	Davis	11/04/1975	Level
Dunster Beach	Scott	12/11/2007	settling	PCO	12/11/2007	RTK GPS
Dunster	Scott	12/11/2007	settling	PCO	22/05/2007	RTK GPS
Minehead	Scott	12/11/2007	settling	PCO	13/11/2007	RTK GPS
Woolacombe	Scott	12/11/2007	settling	PCO	29/09/2007	Lidar
Croyde Ruda	Scott	14/09/2007	settling	Scott	14/09/2007	RTK GPS
Croyde Downend	Scott	14/09/2007	settling	Scott	14/09/2007	RTK GPS
Saunton Sands	Scott	01/08/2006	settling	PCO	03/02/2007	Lidar
Sandymouth	Scott	10/11/2007	settling	Scott	10/09/2007	RTK GPS
Crooklets	Scott	10/11/2007	settling	Scott	26/07/2007	RTK GPS
Widemouth	Scott	10/11/2007	settling	PCO	01/10/2007	RTK GPS
Crackington	Scott	10/11/2007	settling	PCO	24/03/2007	Lidar
New Polzeath	Scott	09/11/2007	settling	PCO	12/09/2007	RTK GPS
Polzeath	Scott	09/11/2007	settling	PCO	12/09/2007	RTK GPS
Harlyn	Scott	09/11/2007	settling	Scott	05/04/2007	RTK GPS
Constantine 1	Scott	17/07/2007	settling	Scott	17/07/2007	RTK GPS
Constantine 2	Scott	17/07/2007	settling	Scott	25/10/2007	RTK GPS
Treyarnon	Scott	09/11/2007	settling	Scott	25/10/2007	RTK GPS
Porthcothan	Scott	09/11/2007	settling	PCO	28/10/2007	RTK GPS
Watergate	Scott	09/11/2007	settling	PCO	26/09/2007	RTK GPS
Towan	Scott	09/11/2007	settling	PCO	27/09/2007	RTK GPS
Fistral	Scott	09/11/2007	settling	PCO	27/10/2007	RTK GPS
Crantock	Scott	09/11/2007	settling	PCO	01/04/2007	RTK GPS
Perranporth	Scott	15/11/2007	settling	Scott	12/10/2007	RTK GPS
Chapel Porth	Scott	14/07/2007	settling	Scott	14/07/2007	RTK GPS
Porthtowan	Scott	08/11/2007	settling	Scott	30/09/2007	RTK GPS
Godrevy	Scott	08/11/2007	settling	PCO	14/10/2008	RTK GPS
Hayle	Scott	08/11/2007	settling	PCO	28/09/2007	RTK GPS
Carbis Bay	Scott	08/11/2007	settling	PCO	28/09/2007	RTK GPS
Porthmeor	Scott	08/11/2007	settling	PCO	29/09/2007	RTK GPS
Sennen Cove	Scott	13/11/2007	settling	PCO	14/09/2007	RTK GPS
Penzance	Scott	13/11/2007	settling	PCO	28/10/2007	RTK GPS
Marazion	Scott	13/11/2007	settling	PCO	28/10/2007	RTK GPS
Perran Sands	Scott	13/11/2007	settling	Scott	29/10/2007	RTK GPS
Praa Sands	Scott	13/11/2007	settling	PCO	30/10/2007	RTK GPS
Porthleven	Scott	13/11/2007	settling	PCO	26/10/2007	RTK GPS
Church Cove	Scott	13/11/2007	settling	PCO	27/10/2007	RTK GPS
Looe	Scott	07/11/2007	settling	PCO	10/10/2007	RTK GPS
Millandreath	Scott	07/11/2007	settling	PCO	10/10/2007	RTK GPS
Seaton	Scott	07/11/2007	settling	PCO	10/10/2007	RTK GPS
Downderry	Scott	07/11/2007	settling	PCO	10/10/2007	RTK GPS
Tregantle	Scott	07/11/2007	settling	PCO	10/10/2007	RTK GPS
Challaborough	Scott	30/08/2006	settling	Scott	10/09/2007	RTK GPS

Sedgewell	Scott	11/11/2007	settling	Scott	01/09/2007	RTK GPS
Bantham	Scott	17/11/2007	settling	Scott	30/08/2007	RTK GPS
Leesfoot	Scott	11/11/2007	settling	PCO	27/10/2007	RTK GPS
South Milton	Scott	11/11/2007	settling	PCO	27/10/2007	RTK GPS
Hope Cove	Scott	11/11/2007	settling.	PCO	04/12/2007	RTK GPS
Northsands 1	Scott	11/11/2007	settling	PCO	24/02/2008	RTK GPS
Northsands 2	Scott	11/11/2007	settling	PCO	19/05/2007	RTK GPS
Torcross	Buscombe	12/10/2007	sieve	PCO	20/10/2007	RTK GPS
Strete	Buscombe	12/10/2007	sieve	PCO	20/10/2007	RTK GPS
Blackpool Sands	Buscombe	21/1/2007	sieve	PCO	28/10/2007	RTK GPS
Broadsands	Scott	16/11/2007	settling	PCO	26/10/2007	RTK GPS
Paignton	Scott	16/11/2007	settling	PCO	27/10/2007	RTK GPS
Teignmouth	Kulkarni	Nov-99	sieve	PCO	13/09/2007	RTK GPS
Dawlish	Scott	17/11/2007	settling	PCO	11/09/2007	RTK GPS
Dawlish Warren	Scott	17/11/2007	settling	PCO	12/09/2007	RTK GPS
Lyme Regis	Scott	17/11/2007	settling	CCO	23/03/2007	RTK GPS
Charmouth	Scott	17/11/2007	settling	CCO	07/03/2007	RTK GPS
Shore Road	Scott	19/11/2007	settling	CCO	13/09/2007	RTK GPS
Branksome Chine	Scott	19/11/2007	settling	CCO	13/09/2007	RTK GPS
Bournemouth Pier	Scott	19/11/2007	settling	CCO	13/09/2007	RTK GPS
East Cliff	Scott	19/11/2007	settling	CCO	13/09/2007	RTK GPS
Boscombe	Scott	19/11/2007	settling	CCO	13/09/2007	RTK GPS
Manor Steps	Scott	19/11/2007	settling	CCO	13/09/2007	RTK GPS
Fishermans Walk	Scott	19/11/2007	settling	CCO	13/09/2007	RTK GPS
Main Beach	Scott	20/11/2007	settling	CCO	05/03/2007	RTK GPS
Greenhill	Scott	20/11/2007	settling	CCO	05/03/2007	RTK GPS
Pakefield	EA	01/08/2003	sieve	EA	10/08/2003	RTK GPS
Covehithe	EA	01/08/2003	sieve	EA	12/08/2003	RTK GPS
Oxford Ness	EA	01/08/2003	sieve	EA	04/08/2003	RTK GPS
Dunwich	EA	01/08/2003	sieve	EA	23/07/2003	RTK GPS
Sizewell	EA	01/08/2003	sieve	EA	09/08/2003	RTK GPS
Great Yarmoth	EA	31/10/2002	sieve	EA	18/11/2002	RTK GPS
Newport South	EA	23/08/2002	sieve	EA	18/11/2002	RTK GPS
Overstrand	EA	23/08/2002	sieve	EA	18/11/2002	RTK GPS
Walcott	EA	19/08/2002	sieve	EA	18/11/2002	RTK GPS
Horsey	EA	19/08/2002	sieve	EA	18/11/2002	RTK GPS
Salthouse	EA	10/08/2002	sieve	EA	18/11/2002	RTK GPS
Holme-Next-The-Sea 1	EA	31/10/2002	sieve	EA	18/11/2002	RTK GPS
Holme-Next-The-Sea 2	EA	31/10/2002	sieve	EA	29/03/2002	RTK GPS
Mablethorpe	van Houwelingen	Feb 2001	sieve	van Houwelingen	Oct-01	RTK GPS
Theddlethorpe	van Houwelingen	Feb 2001	sieve	van Houwelingen	Oct-01	RTK GPS
Donna Nook	van Houwelingen	Feb 2001	sieve	van Houwelingen	Oct-01	RTK GPS

Appendix 3 – Example of rip current assessment form for N.Fistral, Cornwall (Chapter 5).

North Fistral
Rip Current Assessment Form   Observer(s) _____

| Date ⎣ \ _ \ ⎦   Time ⎣ _ : _ ⎦   Tide height: Low ☐   Mid ☐   High ☐ |

| Are rip currents present?   Yes ☐   No ☐

 How many rip currents are present? ⎣_____⎦ | Tide times   High water ⎣ _ : _ ⎦

 Low water ⎣ _ : _ ⎦ |

What area of the beach is being assessed?   Whole beach ☐
Patrol area ☐
Other ⎣_____⎦

Strength/Severity of rip current(s): ☐ Weak (present but no hazard posed to swimmer)
☐ Mild (potential hazard to weak swimmer)
☐ Strong (current faster than average swimmer speed)
☐ Severe (hazardous to any swimmer)
☐ Extreme (extremely hazardous to any water user)

Fill in sketch map with symbols below:

← Arrow marks location
and direction of
rip current

✗ Cross marks flagged
bathing zone

⊠ Box cross marks flagged
surf/craft zone

◯ The circle identifies the
location
of a sandbar/sandbank

Low water

High water

Pentire
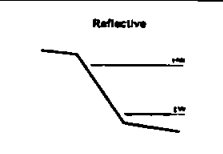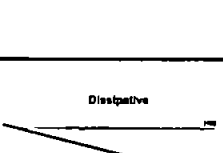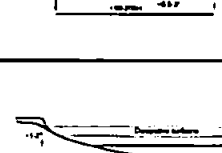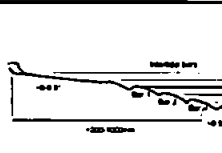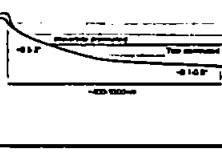
Comments:
(i.e. wave/wind
conditions) ⎣_____⎦

305

Appendix 4 – UK beach type classification system for the RNLI risk assessment program.

High-energy UK beach types to be used with University of Plymouth Beach Hazard Assessment Model.

Type	Sub-Type (HW/LW)	Name	Illustration	Beach Type Characteristics	Physical hazards modal (high energy)	UK examples
Reflective 	Reflective / Reflective	Reflective		**Wave**: high-energy mixed to swell wave dominated regime. HW: surging-plunging. LW: surging-plunging **Sediment**: coarse sand to gravel/boulder. **Tide**: micro-tidal to macro-tidal **Surf-zone width**: narrow **Comments**: enhanced step created beneath point of wave breaking which moves with the tide creating a large increase in water depth within a few meters of shore. Wave run-up/swash can far exceed MHWS moving sediment over the berm crest. During high-energy (storm) conditions the narrow surf-zone can be extremely energetic as all wave energy reaches shoreline with large run-up heights and high swash velocities. These extreme events can dramatically modify the shoreline position and alter profile slope. Strong alongshore currents and backwash can be present. General stability: high.	**Rip currents**: HW: low, LW: low **Wave breaking**: HW: medium (high), LW: medium (high) **Surf-zone energy**: HW: medium (v high), LW: medium (v.high). **Beach gradient**: HW: medium-high, LW: medium-high **Swash**: HW: medium (v.high), LW: medium (v.high) **Tidal cut-off**: low **Littoral currents**: HW: medium (high), LW medium (high) **Summary**: low-medium hazard under modal conditions. There are two main hazards: beach gradient, as a bather can move out of depth suddenly due to submerged beach step and steep beach-face, and high-energy wave conditions can lead to powerful plunging/surging waves and large, high-energy swash/backwash. Steep beach means high-energy waves can approach at an angle generating strong littoral currents. Hazard Rating: low - medium.	Porthleven, Cornwall Chesil, Dorset Thurlestone, Devon
Intermediate 	Reflective / Intermediate	Sub-tidal barred		**Wave**: high-energy mixed to swell wave dominated regime, HW: surging-plunging, LW: plunging-spilling **Sediment**: HW: medium sand to gravel, LW: fine-coarse sand **Tide**: micro-tidal to meso-tidal. **Surf-zone width**: HW: narrow-medium, LW: medium-wide **Comments**: Common to many regions of the US and Australia. In the UK these beach types are rare due to the lack of high-energy micro-/meso-tidal environments. HW: majority of wave energy reaching HW beach, possible formation of runnel at the foot of the HW beach. LW: Horizontally segregated surf-zone with bars and often rips. Plunging waves break on bar and setup cell-circulations in the surf-zone. Bar systems can vary from almost linear two-dimensional form, intersected by transverse rip channels to three-dimensional rhythmic bar systems. Waves can break heavily on bars and reform in troughs, re-breaking at shoreline. Strong alongshore as well as cross-shore currents often present. Multiple sub-tidal bars may be present. General stability: low	**Rip currents**: HW: medium-high (high), LW: medium-high (v.high) **Wave breaking**: HW: low-medium (high), LW: medium (high) **Surf-zone energy**: HW medium (high), LW medium (high). **Beach gradient**: HW: medium, LW: medium-high **Swash**: HW: low (medium), LW: low (medium) **Tidal cut-off**: low **Littoral currents**: HW: medium (high), LW: medium (high). **Summary**: medium-high hazard under modal conditions. Beach rip currents main hazard throughout tide varying with beach morphology. Dynamic bar systems with troughs and rip channels mean beach gradient hazard is also significant. Longshore trough shoreward of bar can be deep and strong longshore currents can be present under higher energy conditions. Hazard levels can change rapidly (days) due to dynamic beach morphology. Hazard Rating: medium - high.	Machrihanish, Mull of Kintyre Europie, Lewis Dail Mor, Lewis
	Reflective / Dissipative	Low tide terrace		**Wave**: high-energy mixed to swell wave dominated regime, HW: surging-plunging. LW: plunging-spilling **Sediment**: HW: coarse sand to gravel/boulder, LW: fine-medium sand **Tide**: micro-tidal to macro-tidal **Surf-zone width**: HW: very narrow-medium, LW: medium-very wide **Comments**: HW: majority of wave energy reaching HW beach, narrow surf-zone can be energetic as all wave energy reaches shoreline, occasional presence of longshore trough at the slope break. During storm conditions possible surf-zone extension over terrace increasing wave attenuation to the shoreline, LW: beach exhibits clear break in slope at approximately MSL, often accompanied by change in sediment size and groundwater seepage. Terrace is flat and featureless. Occasional presence of subdued inter-tidal bars. General stability: medium.	**Rip currents**: HW low (medium), LW: low-medium (medium). **Wave breaking**: HW: low-medium (high), LW: low (medium). **Surf-zone energy**: HW: medium (high), LW: low (medium). **Beach gradient**: HW: low-medium, LW: v.low-low **Swash**: HW: medium (high), LW: low (medium). **Tidal cut-off**: low - medium. **Littoral currents**: HW: low-medium (high), LW: low-medium. **Summary**: low-medium hazard under modal conditions. Plunging/surging wave breaking and high-energy surf-zone at high-tide is a significant hazard, especially under high energy conditions. Potential tidal cut-off hazard due to increased tidal translation rates across low tide terrace. Potential heightened transient rip and littoral current hazards during high-energy conditions. Hazard Rating: low - medium.	Newgale, Pembrokeshire Harlyn, Cornwall Westward Ho!, Devon
	Reflective / Intermediate	Low tide terrace + bar/rip		**Wave**: high-energy mixed to swell wave dominated regime, HW: surging-plunging. LW: plunging-spilling **Sediment**: HW: medium sand to gravel/boulder, LW: fine-medium sand **Tide**: meso-tidal to mega-tidal **Surf-zone width**: HW: narrow-medium, LW: medium-wide **Comments**: HW: majority of wave energy reaching HW beach, possible wave breaking on mid tide bars during storm conditions or neap tides, occasional presence of longshore trough at the slope break. LW: beach exhibits clear break in slope at approximately MSL, often accompanied by change in sediment size and groundwater seepage. Inter-tidal bars and rip current systems present, especially between MLWN and MWLS. Low- and sub-tidal bar systems are often very dynamic both on a seasonal (winter/summer) and on an event (storm) scale. Bar configurations can range from a linear longshore bar/trough to more 3D transverse bar/rip with inter-tidal bar development. Under prolonged high energy conditions beach can, in some cases, move closer to a low-tide bar/rip state. General stability: low – medium.	**Rip currents**: HW: low (medium-high), LW: medium-high (v.high). **Wave breaking**: HW: low-medium (high), LW: medium (high). **Surf-zone energy**: HW: medium (high), LW: medium (high) **Beach gradient**: HW: medium, LW: high. **Swash**: HW: low-medium (medium-high), LW: low (medium). **Tidal cut-off**: medium-high. **Littoral currents**: HW: medium (high), LW: medium (high). **Summary**: medium hazard under modal conditions. Beach rip currents main hazard at low-tide varying with beach morphology, dynamic bar systems with troughs and rip channels mean beach gradient hazard is also significant. Longshore trough shoreward of bar can generate strong longshore currents. Significant tidal cut-off hazard due to isolation on low- to mid-tide bars and rapid tidal translation across wide low-tide terrace in macro- and mega-tidal regions. Strong dumping waves can occur at high tide on steeper upper beach presenting collision hazard. Hazard Rating: medium - high	Praa sands, Cornwall Church Cove, Cornwall Sennen Cove, Cornwall Sandymouth, Cornwall Constantine, Cornwall Fistral, Cornwall
Dissipative 	Intermediate / Intermediate	Low tide bar/rip		**Wave**: high-energy mixed to swell wave dominated regime, HW: plunging-spilling (occasionally plunging-surging), LW: plunging-spilling **Sediment**: HW: medium-coarse sand (occasionally gravel/boulder), LW: fine-medium sand **Tide**: meso-tidal to mega tidal **Surf-zone width**: HW: medium-wide (occasionally narrow-medium), LW: medium-wide **Comments**: HW: intermediate/dissipative surf zone with plunging/spilling breakers. Berm development unusual (occasionally relict/local coarse sediment at HW creates steep HW reflective beach). LW: wide, flat and featureless lower inter tidal zone with subdued mid tide bar(s). 3D low tide bar/rip morphology present between MLWN and MLWS. Energetic plunging breakers over low tide bars. Rip current activity is commonly enhanced around low tide. Mid tide bar(s) become more developed during low-energy periods. Beach mega-rips can form during storm conditions on open beaches. Low- and sub-tidal bar systems are often very dynamic both on a seasonal (winter/summer) and event (storm) scale. Bar configurations can range from a linear longshore bar/trough to more 3D transverse bar/rip with inter tidal bar development. Under prolonged low energy conditions beach can, in some cases, move closer to a low tide terrace + rip state. General stability: medium.	**Rip currents**: HW low (medium), LW: medium-high (v high). **Wave breaking**. HW: low (medium), LW: medium (high). **Surf-zone energy**: HW: low-medium (medium), LW: medium (high). **Beach gradient**: HW: low, LW: high **Swash**: HW: low (medium-high), LW: low (high). **Tidal cut-off**: medium-high **Littoral currents**: HW: low-medium (high), LW: medium (high). **Summary**: medium hazard under modal conditions. Beach rip currents main hazard at low-tide varying with beach morphology. Dynamic bar systems with troughs and rip channels mean beach gradient hazard is also significant. Bars in mid- and low-tide during lower-energy spring/summer swell conditions lead to strong spatially and temporally variable beach rip currents controlled by tidal level. Significant tidal cut-off hazard due to isolation on low- to mid tide bars and rapid tidal translation across wide low-tide terrace in macro- and mega tidal regions. Generally, prevailing hazard is lower at high-tide with intermediate/dissipative wave breaking across the surf-zone and reduced rip current activity. Hazard Rating: high	Croyde, Devon Perranporth, Cornwall Holywell, Cornwall Crantock, Cornwall
	Dissipative / Dissipative	Non-barred dissipative		**Wave**: high energy mixed to wind wave dominated regime, HW: spilling (occasionally plunging-surging), LW: spilling (occasionally plunging) **Sediment**: HW: fine-medium sand (occasionally gravel/boulder), LW: fine sand **Tide**: meso-tidal to macro-tidal **Surf-zone width**: HW: wide (occasionally narrow-medium), LW: wide-very wide **Comments**: HW: dissipative surf-zone with spilling (occasionally plunging) breakers. Berm development unusual (occasionally relict/local coarse sediment at HW creates steep HW reflective beach). LW: wide, flat and featureless lower inter-tidal zone with little or no bar presence. Very little incident wave energy reaches shoreline. Swash movements of the shoreline occur at periods on the scale of wave sets and can be large under storm conditions. Can experience high storm surge under extreme conditions. General stability: medium - high	**Rip currents**: HW low (medium), LW: low (medium). **Wave breaking**: HW: low (medium), LW low (medium). **Surf-zone energy**: HW low (medium), LW: low (medium) **Beach gradient**: HW: low, LW: v low **Swash**: HW: v low (medium), LW: v low (medium). **Tidal cut-off**: low - medium **Littoral currents**: HW: low (medium), LW: low (medium) **Summary**: low hazard under modal conditions. Potential tidal cut-off hazard due to increased tidal translation rates across wide, flat inter tidal beach. Elevated surge high-water during storm conditions could also increase tidal cut-off hazard. Potential heightened rip (transient) and littoral current hazards during high-energy conditions. Hazard Rating: low	Polzeath Beach, Cornwall Towan Beach, Cornwall
Ultra-dissipative 	Dissipative / Ultra-dissipative	Ultra dissipative		**Wave**: high-energy wind to mixed wave dominated regime, HW: spilling (occasionally plunging-surging), LW: spilling **Sediment**: HW: fine-medium sand (occasionally coarse sand/gravel), LW: fine sand **Tide**: mega-tidal **Surf-zone width**: HW: wide-very wide (occasionally narrow-medium), LW: very wide **Comments**: HW: dissipative/ultra-dissipative surf-zone with spilling breakers (occasionally relict/local coarse sediment at HW creates steep HW reflective beach). LW: wide, flat and featureless lower inter-tidal zone with only occasional subdued wave driven bars present. MLWN to MLWS is increasingly tide modified. Under high energy conditions long period fluctuations in the shoreline (wave sets) dominate inner surf-zone dynamics and surf-zone can become very wide. Tide can move rapidly across the very wide inter-tidal zone. Can experience high storm surge under extreme high energy conditions. General stability: high	**Rip currents**: HW low (medium), LW: v low (low). **Wave breaking**: HW: v low (low), LW: v.low (low) **Surf-zone energy**: HW: low (medium), LW: low (medium). **Beach gradient**: HW: low LW: v low **Swash**: HW v low (medium), LW: v low (medium). **Tidal cut-off**: medium. **Littoral currents**: HW: low (medium), LW: low (medium). **Summary**: low hazard under modal conditions. Tidal cut-off is a hazard especially at lower tidal levels due to extremely rapid tidal inundation across the very flat, wide lower beach and possible isolation around bar formations. Tidal translation rates can be rapid at the peak of the tide. Increased wave breaking and surf zone energy at high-tide due to very large tidal ranges allowing increased wave energy reaching shoreline. Surge high-tides during storm increase swash, rip and littoral current hazards. Under high energy conditions long period (wave set timescale) shoreline movements can increase swash hazards. Hazard Rating: low	Rossili Beach, Gower Saunton Sands, Devon

Low-energy UK beach types to be used with University of Plymouth Beach Hazard Assessment Model.

Type	Sub-Type (HW/LW)	Name	Illustration	Beach Type Characteristics	Physical Hazards modal (high energy)	UK examples
Reflective	Reflective / Reflective	Reflective		*(text illegible)*	*(text illegible)*	*(examples illegible — Devon, Poole, Norfolk)*
Intermediate	Reflective / Intermediate	Sub-tidal barred		*(text illegible)*	*(text illegible)*	*(examples illegible — Hampshire, Dorset, Norfolk)*
	Reflective / Dissipative	Low tide terrace		*(text illegible)*	*(text illegible)*	*(examples illegible — Dorset, Devon, Cornwall)*
Dissipative	Dissipative / Dissipative	Non-barred dissipative		*(text illegible)*	*(text illegible)*	*(examples illegible — Devon, Cornwall)*
Ultra-dissipative	Dissipative / Dissipative	Multiple inter-tidal barred (Ridge and Runnel)		*(text illegible)*	*(text illegible)*	*(examples illegible — Lincolnshire, Anglesey, Lancashire, Merseyside)*
	Dissipative / Ultra-dissipative	Dissipative + tidal flats		*(text illegible)*	*(text illegible)*	*(examples illegible — Somerset)*

Appendix 5 – First author publications.

Beach Rescue Statistics and their Relation to Nearshore Morphology and Hazards: A Case Study for Southwest England

T. Scott† P. Russell†, G. Masselink∞, A. Wooler§, and A. Short‡

† School of Earth, Ocean and Environmental Sciences University of Plymouth PL4 8AA UK timothy.scott@plymouth.ac.uk	∞ School of Geography University of Plymouth PL4 8AA UK	§ Royal National Lifeboat Institution West Quay Road BH15 1HZ UK	‡ Coastal Studies Unit University of Sydney NSW 2006 Australia

ABSTRACT

SCOTT, T., RUSSELL, P., MASSELINK, G., WOOLER, A., and SHORT, A., 2007. Beach rescue statistics and their relation to nearshore morphology and hazards: a case study for southwest England. Journal of Coastal Research, SI 50 (Proceedings of the 9th International Coastal Symposium), 1 – 6. Gold Coast, Australia, ISSN 0749.0208

The coasts of Devon and Cornwall in the southwest of England experience some of the most energetic wave conditions ($H_{x,10\%} = 2$–3 m) and largest tide ranges MSR = (4.2–8.6 m) in the UK. They are also a popular tourist destination during the summer months with over 10 million visitors per year. The energetic wave/tide conditions pose a considerable physical risk to beach users and 62 beach environments in this region are therefore patrolled by Royal National Lifeboat Institution (RNLI) lifeguards. Beach rescue statistics collected by the RNLI during spring and summer (1 May to 1 October) were analysed to examine and quantify the risk posed by physical beach hazards to beach users. Rip currents were found to be the main hazard and were responsible for 71% of all recorded incidents. The most hazardous beaches were found on the exposed west coast of the study area. Beaches here can be classified as morphodynamically intermediate and are characterized by low-tide tide bar and rip systems, often topographically-constrained by intertidal geology. The rip currents are generally most active around low tide. Beaches in Devon and Cornwall exhibit morphologies that are significantly different from previously studied beaches in Australia due to the combination of high energy surf zones, large tides and variable coastal geology. This work represents a first step towards the generation of standardized beach risk assessments in the UK.

ADITIONAL INDEX WORDS: *Beach safety, Rip currents, Beach type, High energy, Macro-tidal.*

INTRODUCTION

Due to its location and geological setting, the United Kingdom (UK) possesses a very broad spectrum of beach environments around its more than 5,000 km long shoreline. UK beaches attract a large number of visitors annually for their aesthetic, sport and recreational appeal, providing pivotal support to the tourism industry in many regions. However, the beach environment is inherently hazardous and exposes people to risk. To understand and manage this risk, a comprehensive understanding of UK beach environments and their associated hazards is needed.

Beach hazards in this study represent any phenomena which place the beach user in danger and are related to beach morphology and nearshore hydrodynamics. Hydrodynamically-driven hazards manifest themselves as breaking waves, bores and set up; variable water depth; and nearshore currents, driven by waves, tide and wind. In association with beach morphology, these forces can move people unwillingly around the nearshore zone, placing them at risk. Intertidal and backshore geology constrains the characteristics of the beach and surf zone, and introduces localised hazards such as reefs, rocks and shore platforms (SHORT and HOGAN, 1994).

As one of the most diverse coastlines in the world, the UK experiences Mean Spring tide Ranges (MSR) of 1.5–15 m, and a wave climate gradient from exposed ocean swell to fully protected wind-wave environments. Wind, wave and tidal processes produce dynamic nearshore current systems that play an important part in forming the wide range of beach morphodynamic states that exist around the UK. The geological setting of these beach environments includes high hard-rock cliffs, low soft-rocks cliffs, embayed coves and open ocean beaches, river mouths, tidal inlets, estuaries, spits and barriers. Beach sediments range from fine sand to boulders, and gravel beaches are particularly well represented in the UK due to its glacial history (MAY et al., 2003). With high population density in coastal areas, human modification is a significant feature around the UK beaches and has acted to alter beach shape and hydrodynamics through the implementation of groynes, breakwaters and sea walls (FRENCH, 2001).

This study focuses on the coasts of Devon and Cornwall in the southwest of England. This region, as well as being a popular tourist destination during the summer months with over 10 million visitors a year, experiences some of the most energetic wave conditions in the UK with 10% exceedence wave heights ($H_{s,10\%}$) reaching 2.5 to 3 m on western coasts (DRAPER, 1991). This wave climate is characterised by a mixture of Atlantic swell and locally generated wind waves, and exhibits a MSR ranging from 4.2 to 8.6 m (UK HYDROGRAPHIC OFFICE, 2003). In conjunction with the Royal National Lifeboat Institution (RNLI), who provide beach lifeguarding services to 62 beaches in the region, this study analyses the beach rescue statistics in association with physical beach characteristics and hydrodynamic conditions, examining the hazards posed to the beach user through interaction with the beach
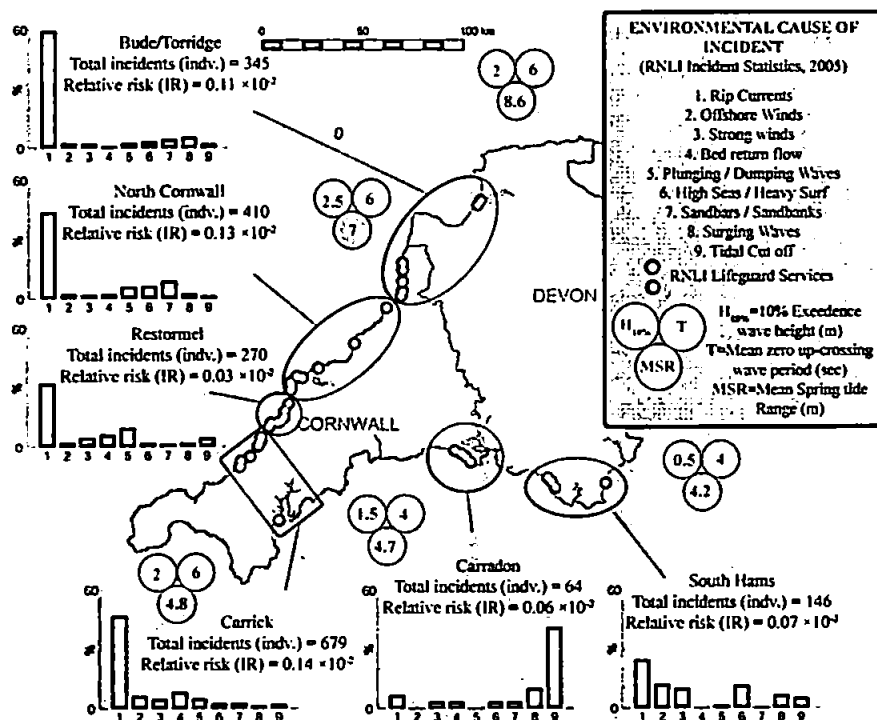
Figure 1. Plots illustrating percentage distribution of the environmental cause of incident for all cases of active assistance at RNLI-patrolled beaches in Devon and Cornwall during 2005. Total number of individuals (indv.) assisted and relative risk posed by physical beach hazards (IR=incidents.hr^{-1}/people in-sea.hr^{-1}) are displayed for each region. Circles represent 10% exceedence significant wave height (DRAPER, 1991), mean zero up-crossing wave period (DRAPER, 1991) and mean spring tidal range (UKHO, 2003). The histograms show the environmental cause of incident.

and nearshore zone under typical spring/summer season conditions (1st May to 1st October). An improved understanding of beach hazards in Devon and Cornwall represents an initial step towards the generation of a standardised beach risk assessment for the UK.

Lifeguard services began in the UK in 1955 when the Surf Life Saving Association of Great Britain was formed (SLSA) as volunteer clubs began to patrol beaches in Bude and St Agnes in Cornwall and Brighton on the south coast of England. At present, the RNLI represent the contemporary face of beach lifeguarding, providing well-equipped and highly-trained services to 62 beaches in the southwest of England. A lifeguard service is a response to the risks posed within the beach environment and it aims to protect and educate the beach user. To best perform this task a comprehensive knowledge of site-specific physical beach hazards, hence beach morphodynamics, is needed.

Much of the pioneering work on modelling beach morphodynamic states and their associated hazards was conducted in Australia. WRIGHT and SHORT (1984) developed a beach classification model for micro-tidal, wave-dominated coasts using the dimensionless fall velocity ($\Omega = H_b/w_sT$, where H_b is breaker height, w_s is sediment fall velocity and T is wave period) to differentiate between reflective ($\Omega < 1$), intermediate ($\Omega = 1$–6) and dissipative ($\Omega > 6$) regimes. MASSELINK and SHORT (1993) extended this work to meso/macro-tidal environments by defining an additional dimensionless parameter, the relative tidal range (RTR = MSR/H_b), to describe the relative importance of shoaling, surf zone and swash processes across the intertidal profile.

Incorporating both morphological and hydrodynamic factors, a sequence of characteristic beach morphologies can be identified on the basis of Ω and RTR, leading to the identification of distinct morphodynamic states. Recent Australian studies have associated physical hazards with beach state and temporal variation in environmental conditions, and have led to the development of the Australian Beach Safety and Management Program (ABSAMP), aimed at improving safety services for Australian beaches (SHORT, 2001).

METHODOLOGY

This study uses RNLI incident statistics and logs of observed daily conditions collected for 62 locations within the southwest of England for the 2005 lifeguarding season (1st May to 1st October) to investigate the specific hazards present within this coastal environment. Data of physical beach characteristics were collected through a campaign of 3D beach surveys using a quad mounted Trimble RTK GPS system conducted during several spring tide cycles from August to September, 2006. This was combined with sediment sampling, low-tide photographs and video from an Argus station (Perranporth only). Hydrodynamic conditions were obtained both through visual observations of wave breaker heights recorded hourly by the RNLI, statistical wave conditions from DRAPER (1991) and tidal information from the UK HYDROGRAPHIC OFFICE (2003). Estimation of beach user numbers was obtained from the RNLI daily logs where the number of beach users was estimated each hour between 10:00 and 17:00 hrs.

1. Rip currents
2. Offshore winds
3. Sandbars
4. Bednehm Flow
5. Large waves
6. Strong winds
7. Tidal cut-off
8. Plunging waves
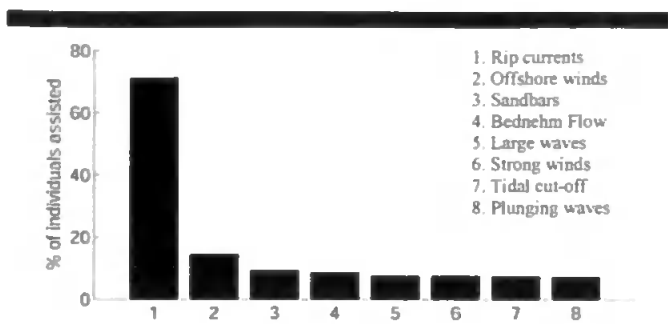
Figure 2. Plot illustrates percentage frequency distribution of environmental cause contributing to each individual assisted during the 2005 season (some assists involve more than one environmental cause)

REVIEW OF RESULTS

Incident statistics

A comprehensive database has been compiled, containing information on all RNLI incidents (a logged event of active assistance which can involve multiple individuals), daily conditions and beach population during the 2005 season from late April to early October (dates within which RNLI serviced beaches are patrolled). Incidents recorded range from a situation requiring assistance to a life threatening rescue. Detailed information is logged for each incident including the cause of incident and specific environmental factors. Figure 1 summarises the environmental cause of incident statistics for all recorded incidents during the 2005 season within each regional division.

This dataset clearly shows that during 2005 both the environmental cause of incident and the number of incidents vary

significantly around the coasts of Devon and Cornwall. A dominance of rip current related incidents (47% of total incidents for 2005) is seen in most regions. Rip currents account for 49% of incidents in west coast regions where $H_{s,10\%}$ is 2.5–3 m and MSR $\approx$ 7m, as opposed to the south coast regions where, $H_{s,10\%} = 0.5$–2.5 m, MSR $\approx$ 4.7m and rip currents cause 25% of total incidents (Figure 1). In south coast regions surging waves and tidal cut-off, account for 8% and 10% of total recorded incidents respectively, showing an increased prevalence compared to west coast regions where the role of surging waves (3% of total incidents) and tide cut off (3% of total incidents) is less significant. When incidents are broken down to the number of individuals assisted/rescued (Figure 2), rip currents are shown to play a role in 71% of incidents occurring within Devon and Cornwall during the 2005 season. Offshore winds, sandbars, bednehm flow, high surf, strong winds, tidal cut-off and dumping waves individually represent no more than 15% of all incidents. Some of these environmental causes occur in conjunction with rip currents in 30% of incidents, suggesting risk to the beach user is often compounded with a combination of hazards i.e. large waves and littoral currents can drive the spatially unaware beach user into areas of increased rip current hazard.

To further understand the beach hazard characteristics and specifically the influence of rip currents in rescue incidents, individual locations were analysed (Table 1). This analysis included calculation of a coefficient of risk for each location for the 2005 season. This risk coefficient IR was derived through two statistics: (1) the average number of people estimated to be in the water per hour (P) between 10:00 and 17:00 hrs during the 2005 season; and (2) the average number of individuals assisted/rescued per hour (Re) at a specific location (calculated from the total number of insea assists/rescues per season divided by the number of hours in a season at each location). The ratio between these two statistics represents the probability of an incident occurring:

Table 1: Summary of beach safety and beach type statistics for selected locations in Devon and Cornwall.

ID	Location	P (hr⁻¹)	Re (indv.season⁻¹)	IR (×10⁻²)	Re_rip (indv.season⁻¹)	IR_rip (×10⁻²)	Hb (m)	MSR (m)	D₅₀ (mm)	Ω	RTR
					West coast						
1	Saunton Sands	-	-	-	-	-	-	7.9	0.19	7.1	6.3
2	Croyde	-	-	-	-	-	-	7.9	0.37	5.2	6.3
3	Sandymouth	31	102	0.324	98	0.321	0.7	6.8	0.36	6.3	4.5
4	Harlyn	80	13	0.005	0	0.000	0.3	6.5	0.43	3.5	6.5
5	Booby's Bay	21	2	0.005	0	0.000	0.6	6.5	0.39	4.8	4.3
6	Constantine Bay	48	201	0.378	191	0.376	0.6	6.5	0.39	4.8	4.3
7	Perran Sands	35	41	0.073	23	0.062	0.6	6.1	-	7.0	4.1
8	Perranporth	118	379	0.227	296	0.201	0.6	6.1	0.33	-	-
9	Chapel Porth	29	83	0.258	66	0.210	0.7	6.1	0.47	4.8	4.1
					South coast						
10	Challaborough	26	43	0.073	1	0.004	0.4	4.7	0.92	1.7	6.3
11,12	Bigbury (west,east)	29	5	0.013	2	0.007	0.2	4.7	0.30	4.9	6.3
13	Sedgewell Cove	33	40	0.088	5	0.015	0.3	4.7	0.32	4.6	6.3
14	Bantham	44	86	0.141	53	0.096	0.4	4.7	0.29	5.3	6.3
15	Torcross	8	20	0.178	0	0.000	0.1	4.3	4.20	0.5	8.6

P = average number of people insea per hour; Re = total number of individuals assisted per season; IR = Re./ P (risk ratio); Re_rip = total number of individuals assisted in rip related incidents per season; IR_rip = Re_rip / P (rip risk ratio); Hb = mean observed breaker height during 2005 season; D₅₀ = grain diameter; Ω = dimensionless fall velocity (Hb/w_sT);RTR = relative tidal range (MSR/Hb))

$$IR = Re / P$$

The risk of rip current related incidents IR_{rip} was also calculated:

$$IR_{rip} = Re_{rip} / P$$

where Re_{rip} is the number of rip incidents per hour at each location. West coast beach locations 6, 3, 8 and 9 have the highest rip current risk of all RNLI patolled beaches, whereas sheltered west coast beaches (4) and south coast locations 10, 11, 12, 13 and 15 have the lowest values for rip current risk with only 8 rip current related incidents between them in 2005.

Beach Hazards

Reviewing the RNLI incident data, it is clear that the type and level of hazards vary with location. The beaches listed in Table 1 were chosen for further analysis as they represent the high and low risk extremes of the RNLI beaches within the study region, and contain a representative spread of the beach types present around the coast.

The exposed intermediate beaches on the west coast (2, 3, 5, 6, 8, and 9), having a $H_{s10\%}$ of approximately 2.5 to 3m, represent some of the highest rip risks, with values at locations 6 (Constantine) and 8 (Perranporth) reaching 0.376 and 0.201 (probability of rip related rescues per hour) respectively. Perranporth and Constantine also received the most incidents during 2005 with 379 and 201 individuals rescued, respectively.

The low rip current risk values consist of beaches located within sheltered areas of the west coast (location 4) and the south coast (see Figure 4). These areas have a reduced $H_{s10\%}$ due to the aspect of the coast. The powerful westerly Atlantic swell waves which are dominant throughout the year have to refract through 45-90° to arrive at the sheltered north and south facing beaches. Harlyn Bay (location 4) had an average of 80 individuals inseahr[-1] during the season compared to 48 at the neighbouring Constantine Bay, but only 14 environmentally driven rescues occurred during the season as opposed to 201 at Constantine Bay. At south coast locations mean observed H_b was between 0.1m and 0.4m at patrolled beach locations 10, 11, 12, 13, 14 and 15 during the 2005 season. These locations had the lowest calculated rip current risk values. In some cases other environmental hazards were more
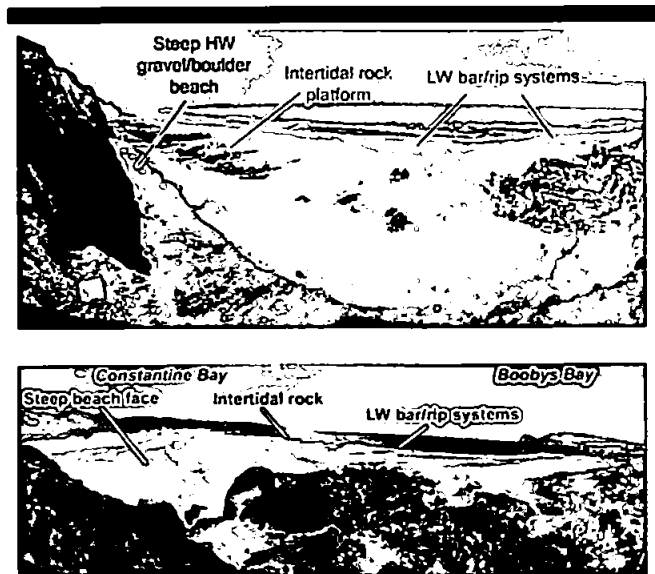
Figure 3. Annotated panoramic views of Sandymouth (above) and Constantine and Boobys Bay (below) at low tide.

prevalent. On the south coast, in combination with lower energy conditions, the dominant winds from the western quadrant blow offshore in many locations, increasing the risk of the beach user drifting offshore. Significant tidal cut off hazards are present at many locations where the large tidal range causes submerged high water beaches. The ease of beach access and characteristics of backshore geology control the severity of this hazard.

Beach types and rip risks

The physical characteristics of the beach and its location within the hydrodynamic setting of the region play a key role in defining rip current hazards and risks to the beach user. The southwest coast of England displays a wide variety of medium to high energy beach types amongst varying tidal ranges.
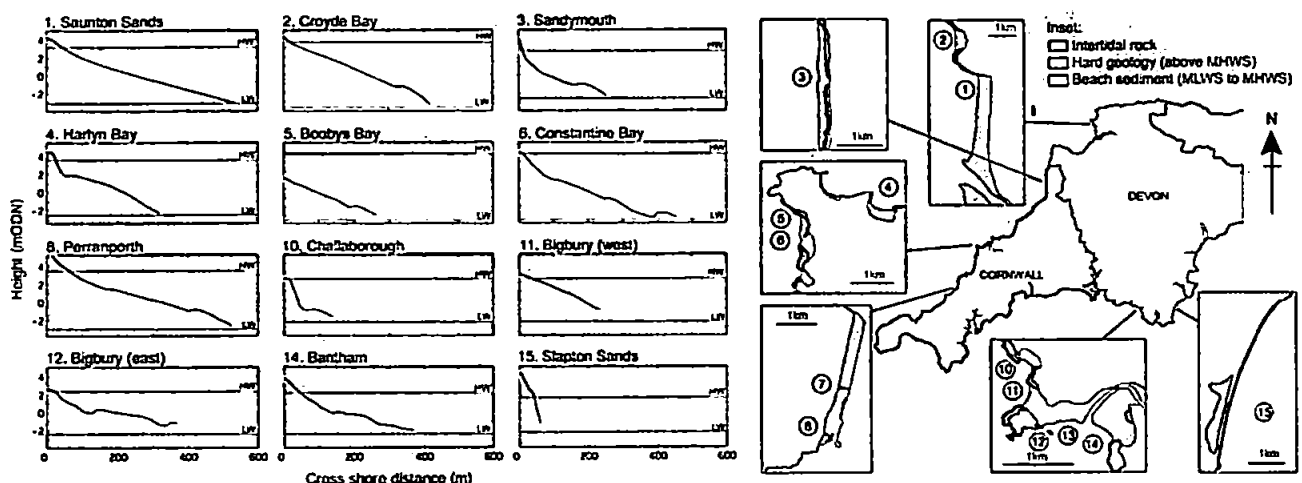
Figure 4. Summary of cross shore profiles and tide ranges at selected locations around Devon and Cornwall (height measured in meters above Ordnance Datum Newlyn), and schematic plan views of each site indicating beach shape, aspect of the coast and intertidal geology.
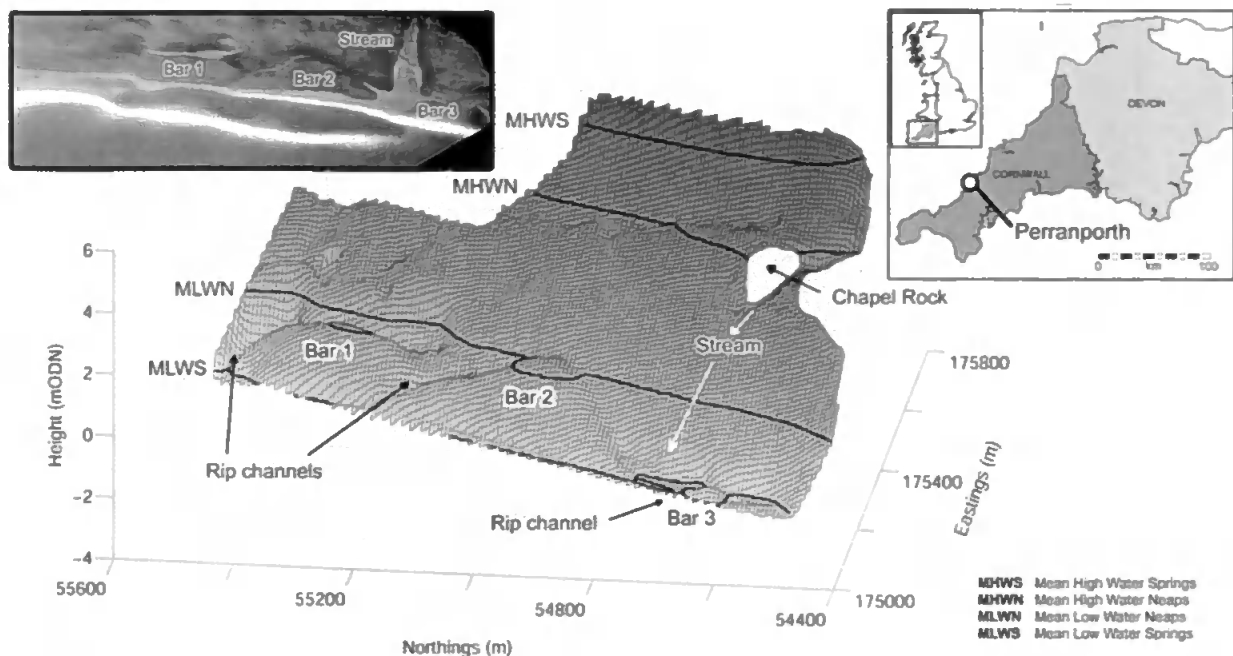
Figure 5. Digital Terrain Model of Perranporth Beach with mean tidal statistics and annotations marking main morphological features. Inset: Rectified timex image of low tide bar morphology and surf zone at Perranporth Beach from the Droskyn Argus camera station.

Ultra-dissipative beaches

Ultra-dissipative high energy surf zones like Saunton Sands (Ω=7.1 and RTR=6.3) that are not represented within previous Australian studies (MASSELINK and SHORT, 1993; WRIGHT and SHORT, 1984b), exhibit a very wide ($\approx$500 m), low gradient, featureless intertidal profile with no significant bar morphology (Figure 4). Saunton Sands, characterised by a low gradient fine sand beach (D_{50}=0.19 mm), has an MSR of 7.9 m and shows very subdued intertidal morphology due to the cross shore translation of high energy surf zone processes during the tidal cycle. Intertidal zones of this width do not occur in high energy wave climates in Australian examples. Although there is no lifeguard service at Saunton Sands, it presents a lower risk to the water user due to the lack of intense rip current systems and the non barred, dissipative nature of its wide surf zone. Thus incident wave energy is greatly reduced when it reaches the bathing zone. Consequently it is popular with novice surfers.

Intermediate (Reflective/Dissipative) Beaches

The more common intermediate beach types, with large tidal ranges (MSR between 6.1 to 7.9 m) and an energetic wave climate, are represented by low tide terrace, low tide terrace and rip, and low tide bar/rip morphologies. They are characterised by a steeper, often coarse, more reflective high water beach face, a wide (400-600 m) subdued dissipative intertidal zone (swash bar sometimes present) and well developed intermediate low water bar and rip circulation systems (Figure 4). The beaches with the highest calculated rip current risk fall into the low tide bar/rip beach type (Constantine Bay, Perranporth, Sandymouth and Chapel Porth), with a Ω of between 4.8 and 7 and an RTR between 4.1 and 4.3.

Backshore geology and intertidal rock formations have a significant influence on the characteristics of the beaches of Devon and Cornwall. At both Sandymouth and Constantine Bay

(Figures 3 and 4) these formations are fundamental in generating the beach hazards that are present. Sandymouth, with a gravel and boulder reflective high water beach, possesses an intertidal rock platform which topographically constrains circulation within the surf zone, consequently driving fixed rip current systems. The geological constraints at Constantine Bay act to influence surf zone circulation from high to low water, generating deep rip channels. These are especially severe at low water when the ebbing tide enhances rip current velocities, leading to the highest rip current risk in the region.

Other beach types associated with high rip current risk are those represented by Perranporth (Figure 5) and Chapel Porth (Figure 6). Both locations receive similar hydrodynamic forcing with a MSR of 6.1 m and an $H_{s10\%}$ of 2.5 m (DRAPER, 1991), and have a well defined often rhythmic unconstrained bar and rip morphology that is exposed at MLWS. During the survey period, the unconstrained rhythmic bar and rip morphology, present at many west coast beaches had a wavelength of 300-400 m and amplitude of 1.5-2 m. With an incident breaker height of 0.5-2 m, intense topographically driven rip systems can develop as narrow rip feeders travelling within the channels between the bars, creating high risk conditions for water users around low water at these locations (SHORT and HOGAN, 1994; MACMAHAN et al., 2006). Figure 5 and inset shows the low tide bar and rip morphology at Perranporth and a rectified timex image from the Perranporth Argus station, indicating the presence of a detached sub tidal rhythmic bar system. Rip hazards are enhanced at low water as the bars, accommodating beach users, are submerged during the flooding tide, activating morphologically constrained rip feeder currents in the lee trough placing the beach user at risk.

Reflective Beaches

The steep reflective beaches on the south, channel coast like Slapton Sands (Ω=0.5 and RTR=8.6) are coarse grained

Figure 6. Annotated panoramic image of Chapel Porth at low tide.

(D_{50}=4.2 mm), narrow ($\approx$70 m) and associated with plunging and surging breakers within a small surf zone. Dominated by wind waves (H_b=0.1 m), no significant rip current hazards present themselves.

Comparison of Australian and UK beaches

The beaches of southwest England possess a number of significant differences to those documented in previous Australian studies (WRIGHT et al., 1984a; WRIGHT and SHORT, 1984b; SHORT, 1986; MASSELINK and SHORT, 1993; SHORT, 2001; SHORT, 2006). Firstly, fine, wide, high energy ultra-dissipative beaches like Saunton Sands; secondly, steep reflective gravel beach types, like Slapton Sands of the protected south coast with a comparatively low Ω of 0.5 but a high RTR of 8.6; and thirdly, wide largely featureless, high energy intermediate beaches (Ω=4.8-7, RTR=4.1-4.3) with more developed high and low water morphology, are not well represented within the Australian coastal environment. These differences are generated largely by the coupling of a high energy wave climate and large tidal ranges in the UK. As a result, these beaches do not become tide dominated with a large tidal excursion. Also, the variation in coastal geology and the present and historic sediment supply to beaches constrains the level of hydrodynamic control on beach type.

Rare in the southwest but common to the UK (especially the east coast of England), ridge and runnel beaches and those modified with intertidal coastal structures are environments that have also received limited coverage within Australian beach type models (WRIGHT and SHORT, 1984b; MASSELINK and SHORT, 1993) but represent unique UK beach morphologies and associated hazards.

CONCLUSIONS

As beach visitor numbers increase in the UK, understanding the physical hazards and risks posed to the beach user within a national context becomes paramount. This will underpin deployment of safety resources and enable improved understanding of the national beach environment that contributes to thousands of rescues annually. The south and southwest of England beach hazards are posed by a number of environmental factors: strong/offshore winds, sandbars, bednehm flow, large waves, tidal cut off and dumping/surging waves, but the most significant is rip currents. Based on this study of the beach types, hazards, rip current characteristics and lifeguard rescue statistics the following conclusions can be drawn.

1) Rip currents represent the greatest environmental threat to the insea beach user. This threat can be compounded by a series of hazards working together.

2) There is a significant variation in beach hazards and their severity depending on the nature of the hydrodynamic conditions and beach type. The reflective low tide terrace and rip and

intermediate, low tide bar/rip morphologies as described by MASSELINK and SHORT (1993) possess the high risk rip current systems, that are most active during wave heights of 0.5-2 m after which the beaches are often closed to bathers.

3) Surf zone morphologies are not as predictable as in previous Australian studies (SHORT, 1994). There is a great variation in surfzone characteristics due to beach boundary and intertidal geology, often constraining sand and water movement and enhancing rip current systems. With high energy surf zones and large tidal ranges the southwest of England experiences different hydrodynamic forcing than Australia, thus generating beach types unique to this climate.

4) Moderate energy (0.5-1.5 m) Atlantic swell waves during spring and summer enable the development of rhythmic bar morphology on the intermediate beaches at the low water stand, generating morphologically controlled rip current systems.

5) Large tidal ranges introduce hazards such as tidal cut off through high water levels and horizontal speed of shoreline movement, and enhance rip current velocities on the ebbing tide.

LITERATURE CITED

DRAPER, L., 1991. Wave Climate Atlas of the British Isles. Department of Energy Offshore Technology Report OTH 89 303 HMSO.

FRENCH, P.W., 2001. *Coastal Defences: Processes, Problems and Solutions.* Routledge, London.

MACMAHAN, J. H., THORNTON, E. B. and RENIERS, A., 2006. Rip current review. *Coastal Engineering.* 69 (4), 589-604.

MASSELINK, G. and SHORT, A.D., 1993. The effect of tide range on beach morphodynamics, a conceptual beach model. *Journal of Coastal Research,* 9, 785-800.

MAY, V.J. and HANSOM, J.D., 2003. *Coastal Geomorphology of Great Britain.* Joint Nature Conservation Committee: Geological Conservation Review Series. 28, 754 p

SHORT, A. D., 1986. An note on the controls of beach type and change, with se Australian examples. *Journal of Coastal Research.* 3, 387-395.

SHORT, A. D., 1991. Macro-Meso tidal beach morphodynamics – an overview. *Journal of Coastal Research,* 7, 417-436.

SHORT, A. D. and HOGAN, C. L., 1994. Rip Currents and beach hazards: Their impact on public safety and implications for coastal management. *In:* FINKL, C.W. (ed.), *Coastal Hazards.* Journal of Coastal Research Special Issue No. 12. pp. 197-209.

SHORT, A D, 2001. *Beaches of the Southern Australian Coast and Kangaroo Island. Australian Beach Safety and Management Project,* Sydney, Sydney University Press 346 p.

SHORT, A. D., 2006. Australian beach systems – Nature and distribution. *Journal of Coastal Research,* 22, 11-27.

WRIGHT, L. D., NIELSEN, P., SHORT, A. D. and GREEN, M. O., 1984a. Morphodynamics of a macrotidal beach. *Marine Geology,* 50 (1-2), 97-127.

WRIGHT, L. D. and SHORT, A. D., 1984b. Morphodynamic variability of surf zones and beaches – A synthesis. *Marine Geology,* 56 (1-4), 93-118.

UK HYDROGRAPHIC OFFICE, 2006. Admiralty Tide Tables: Volume 1, United Kingdom and Ireland (including European Channel Ports). UKHO.

HIGH VOLUME SEDIMENT TRANSPORT AND ITS IMPLICATIONS FOR RECREATIONAL BEACH RISK

Tim Scott[1], Paul Russell[1], Gerhard Masselink[1], Adam Wooler[2] and Andrew Short[3]

In a coastal region where there are large pressures on the beach resources through recreational usage, understanding the levels and characteristics of risk to the beach user is paramount. A morphodynamic evaluation of beaches in the high-energy, macro-tidal southwest of England was made between July 2006 and February 2008. Levels of physical beach hazards presented to the beach user, both spatially and temporally, by waves, tides and surf-zone currents were assessed and calibrated against lifeguard rescue and usage data. Large seasonal variations in wave energy lead to significant annual morphodynamic transition of the popular west coast beaches from a erosive planar beach face with linear shore parallel bars in winter to a highly three dimensional accretionary system in spring/summer with pronounced low-tide bar/rip systems and enhanced mid-tide bar morphologies. In many locations this general transition is modified through sediment supply, geological constriction and freshwater drainage. This annual transition drives temporal variations in beach hazard through (1) the temporal variability morphology (especially rip currents, the cause of 68% of all incidents during 2005-2007); and (2) large tidal excursion during spring tide periods exposing low tide rip systems increasing the rate of change of the temporal hazard signature. Periods of high morphologically driven beach hazard coincide with seasonal peaks in beach user numbers, increasing recreational beach risk.

INTRODUCTION

Large-scale beach volume changes associated with morphodynamic variations occur on beaches along the high-energy (10% exceedence significant wave heights of 3-4 m), macro-tidal (mean spring tidal ranges of 4.2–8.6 m) west coast of Devon and Cornwall, in the southwest of England. This seasonal sediment movement can have significant safety implications in a region of outstanding natural beauty which receives 10 million visitors per year and has experienced a growing pressure of recreational and leisure activities in the beach environment. While providing pivotal support to the tourism industry in many regions, issues of risk to the beach user are increasingly important as the beach usage season now extends from the early spring to autumn. The Royal National Lifeboat Institution (RNLI), who provide lifeguarding services to 69 beaches in the region (2007), commissioned this project realising that beach safety could be

[1] Coastal Processes Research Group, Centre for Coastal Dynamics and Engineering (C-CoDE), University of Plymouth, UK.
[2] Surf Life Saving Great Britain (SLSGB), Exeter, UK (*formerly with the Royal National Lifeboat Institution, Poole, UK)
[3] Coastal Studies Unit, University of Sydney, NSW 2006, Australia.

improved through developing understanding of physical beach hazards in the UK.

The Wright and Short (1984) conceptual beach classification model, based on the Australian beach environment, has been increasingly used to describe morphological transition of beach types through the use of the dimensionless fall velocity parameter ($\Omega = H_b/w_sT$), where H_b is breaker height, w_s is sediment fall velocity and T is wave period). This differentiates between reflective ($\Omega < 1$), intermediate ($\Omega = 1-6$) and dissipative ($\Omega > 6$) regimes. Masselink and Short (1993) extended this work to meso/macro-tidal environments by defining an additional dimensionless parameter, the relative tidal range ($RTR = MSR/H_b$), to describe the relative importance of shoaling, surf and swash zone processes across the intertidal profile.

These models apply to high energy micro-tidal and low energy meso/macro-tidal environments with abundant sediment supply. Indeed, much of the present understanding of beach risk is confined to these sediment rich, medium/high energy micro-tidal environments (Short and Hogan, 1994; Short, 2001). Short (2006) identifies macro/mega-tidal beaches that are exposed to high ocean swell and storm seas and those with gravel and cobble sediments, and exposed intertidal geology, as environments requiring further investigation. With a significantly different sedimentary and hydrodynamic setting, UK beaches represent a new challenge in the understanding of beach morphodynamics and their association with risk to the recreational beach user.

In the present study annual and monthly beach morphology, hydrodynamic and coastal image data are used to quantify the seasonal variation in beach volume and morphology at six selected beaches that present high hazards to the recreational beach user. The implication of this transition for recreational beach risk is then assessed through the addition of detailed lifeguard incident records.

SITE SELECTION AND DATA COLLECTION

Beach type and hazards

Field sites were chosen based on the levels of hazard presented to the beach user and the levels of usage throughout the spring/summer/autumn season with the level of beach risk a function of the hazard and usage levels. The RNLI routinely records the environmental causes of every incident made at their beaches. Analysis of incident reports for all RNLI units from 2005 to 2007 indicates that 68% of all recorded incidents (individuals rescued) where due to rip currents, a similar percentage to beach rescues in Australia and the USA. Figure 1 illustrates the percentage cause of incident over the same period for the different beach types patrolled. These beach types are modified from the Masselink and Short (1993) conceptual model to better describe the beach environments in the UK. Rip currents are the largest cause of incident at all beach types that commonly support rip current systems. Incidents driven by
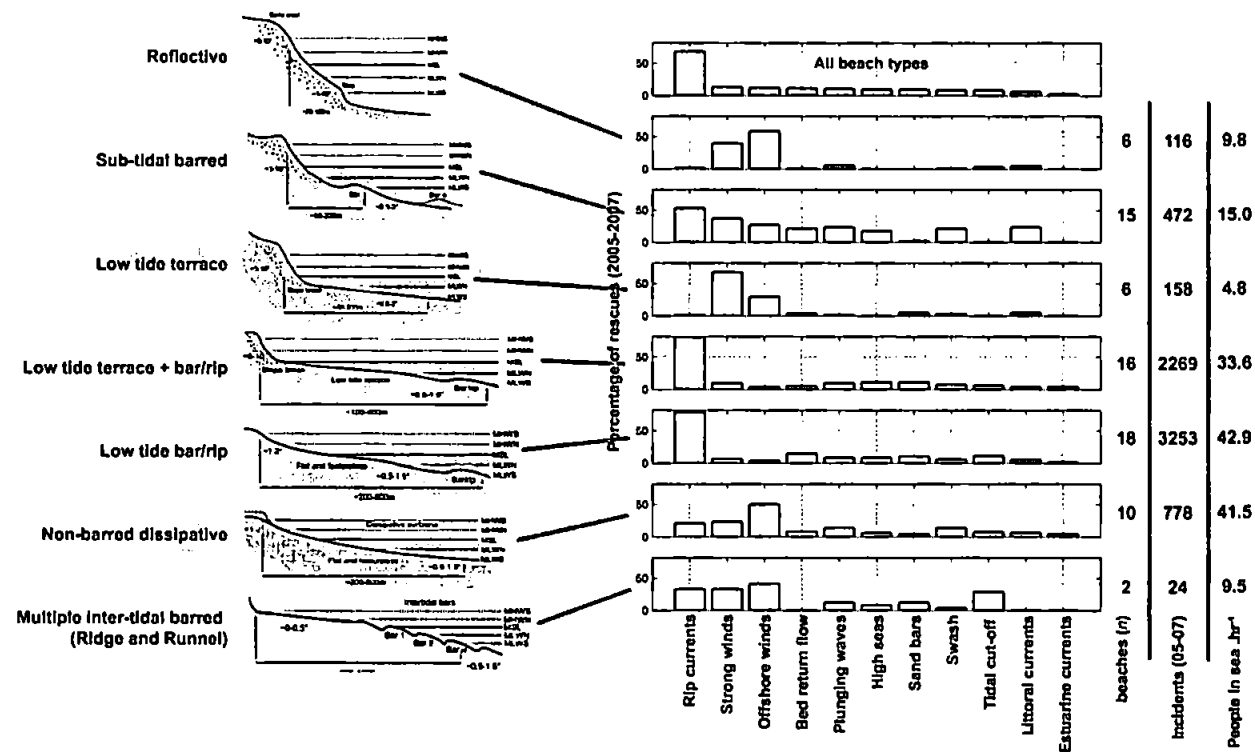
Figure 1. Percentage occurrence of all environmental causes of incidents (recorded by RNLI) for beach type groupings (2005 to 2007).

strong and offshore winds as well as littoral currents present the greatest cause on beaches that are commonly without rip current activity.

Low tide bar/rip (LTBR) and Low tide terrace + bar/rip (LLT+BR) beaches have greater than 80% of all incidents being caused by rip currents, and with 2269 and 3253 incidents from 2005 to 2007 respectively they constitute 78.1% of all recorded incidents over that period. LTBR and LLT+BR beaches represent 46.6% of all patrolled beaches and with an average of 33.6 and 42.9 people in the sea per hour (May to October) during the 3 year period making these the most popular bathing beaches that are patrolled by the RNLI. Due to the high rip current hazard, popularity and large carrying capacity of these beaches, the dynamic intermediate LTBR and LLT+BR beaches on the high-energy west coast of Devon and Cornwall (Figure 2) are the focus of this study.

Field monitoring

A morphodynamic evaluation of six field sites (three LLT+BR and three LTBR) was made between July 2006 and February 2008 through analysis of hydrodynamic forcing using long term (2003 to 2008) non-directional offshore (~30km) and short term (2007 to 2008) directional nearshore (~1km) wave buoys, seasonal and monthly 3D RTK-GPS surveys, sediment sampling, digital photography and Argus video imagery (only on Perranporth). High resolution (fortnightly) monitoring focused on the 2007 season (May to October) during which time levels and characteristics of hazard were then assessed using detailed rescue and beach usage statistics from the RNLI lifeguards incident reports and daily logs.
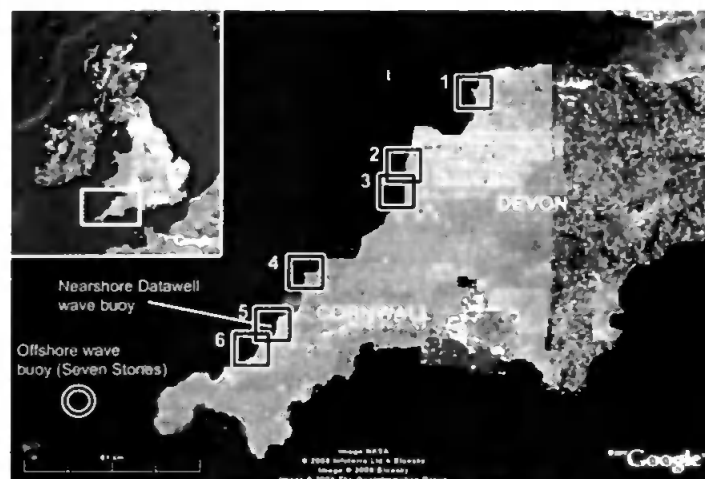
Figure 2. Field locations in Devon and Cornwall. Beaches: (1) Croyde Bay (2) Sandymouth (3) Crooklets (4) Constantine Bay (5) Perranporth (6) Chapel Porth.

ANNUAL BEACH CHANGE

Hydrodynamic climate

The wave climate of the west coast of Devon and Cornwall is both high-energy and highly seasonal. Mean significant wave heights between 2003 and 2008 at Seven Stones Light Vessel (50°6'9" N, 6°6'0" W, see figure 2) vary from 2.4m in winter to 1.2m during summer. During the high-energy winter months 10% exceedance wave heights reach 4.8m. An annual mean wave period of 8.4 s varies from 9.2 s in winter to 7.6 s in summer.

Table 1. Offshore wave climate statistics from 2003 to 2008 at Seven Stones Light Vessel. H_s is significant wave height and T_m mean wave period

	H_s (m)		H_s exceedance (m)			T_m (sec)	
	Mean	s.d.	10%	50%	90%	Mean	s.d.
Annual	1.9	1.3	3.7	1.6	0.7	8.4	1.8
Winter	2.7	1.5	4.8	2.4	1.1	9.2	1.8
Spring	1.9	1.2	3.5	1.7	0.7	8.4	1.8
Summer	1.2	0.7	2.2	1.1	0.6	7.6	1.4
Autumn	1.8	1.1	3.3	1.5	0.7	8.3	1.7

Macro-tidal (>4m) and mega-tidal (>8m) mean spring tidal ranges (MSR) exist along the entire west coast of Devon and Cornwall from 4.1m at the southern tip to 9.6m in the northwest. The west coast beaches studied receive similar wave energy throughout the year. This high-energy climate drives the seasonal high volume sediment transport seen along the coast.
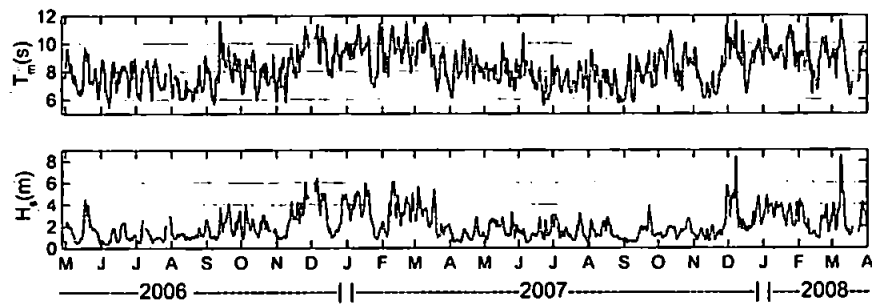
Figure 3. Offshore wave record (24 hour averaged) during study period. Plot shows (upper) significant wave height (H_s) and (lower) mean wave period (T_m).

The study period experienced two high-energy winters. Between October 2006 and April 2007 24 hour averaged off-shore wave heights were frequently between 4m and 6m and mean wave periods above 10s. Two significant storm events occurred in December 2007 and March 2008 where 24 hour averaged off-shore wave heights were greater than 8m. During both observed summer periods (June to August) 24 hour averaged off-shore wave heights never exceeded 4m.

Near-shore wave heights, available from January 2007, recorded mean significant wave heights of 2.3m and 1.2m for winter and summer respectively. Zero up-crossing wave periods ranged from 6.8s in winter to 5.5s in summer. The mean wave angle (bathymetrically controlled) was 280°. During the energy peak of the winter 2007/2008 storm events, in ~10m water depth, 30 minute averaged significant wave heights exceeded 7m and maximum wave heights exceeded 9m.

MORPHOLOGICAL TRANSITION

During the study period high volume sediment transport was observed as beach morphologies adjusted to the changing hydrodynamic climate. A general trend of large scale erosion of sediment from the inter-tidal zone occurred at all studied LLT+BR and LTBR beaches along the west coast of Devon and Cornwall. This took the form of beach lowering and transition from highly developed low-tide bar/rip systems and enhanced mid-tide bar systems during the lower energy swell-wave dominated summer months to increasingly shore parallel offshore bars and planar featureless mid-tidal zones during the high-energy, storm dominated winter months (Figure 4).

Figure 4. Summer/winter low-tide images of Chapelporth beach, 10/09/06 to 05/03/07.

The example of Perranporth beach (D_{50}=0.32mm) in Figure 5 illustrates this transition. Erosion of $210m^3$/m occurred from 12/09/07 to 08/02/08 along the cross-shore profile between MLWS and MHWS. This constituted a mean reduction of the beach elevation of 0.45m. Argus TIMEX images and 3D RTK GPS surveys (Figure 6) show the transition during the spring /summer season of 2007 where a planar beachface with linear sub-tidal bar systems during April transforms toward highly three dimensional low-to-mid-tide bar systems as the beach accretes towards September.
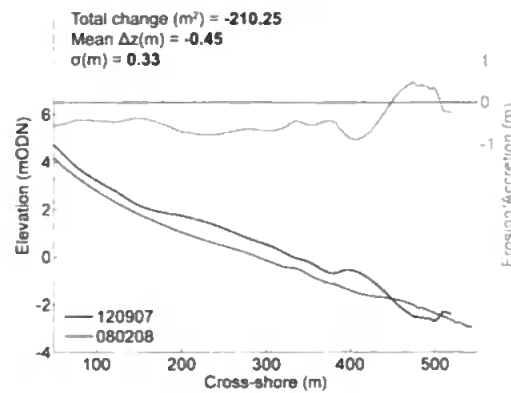
Figure 5. Morphological transition at Perranporth beach; (upper) cross-shore profiles illustrate transition between 12/09/07 and 08/02/08.
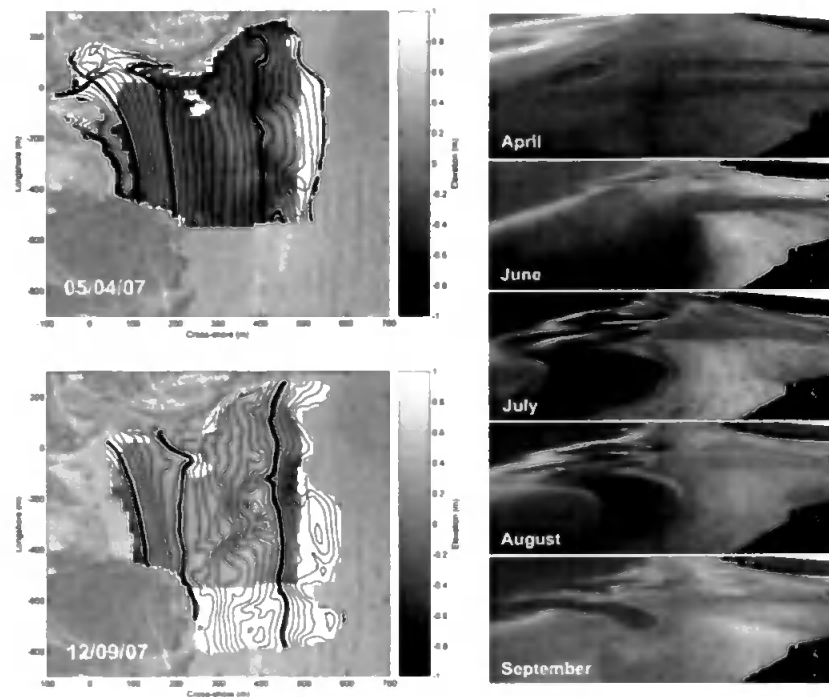
Figure 6. (left) 3D RTK GPS surveys at Perranporth shown as residual elevations from a mean surface at the start and end of the 2007 spring/summer season and (right) monthly spring low tide Argus TIMEX images give overview of observed changes during the 2007 spring/summer study period.
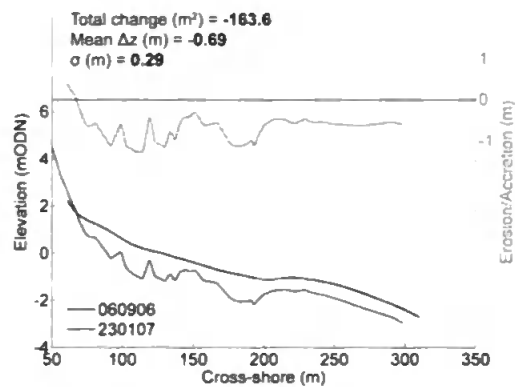
Figure 7. Morphological transition at Sandymouth beach: cross-shore profiles illustrate annual transition between 06/09/06 and 23/01/07.

Figure 8. Summer/winter images of Sandymouth beach.

Sediment supply, geological control and beach drainage

At many of the studied locations there are significant modifications of the general morphological transition observed. The beaches of Devon and Cornwall, and indeed the UK, are highly variable in their sediment characteristics and abundance, as well as in backshore geology. For example, Sandymouth beach,

Cornwall, experienced high volume sediment transport between 06/09/06 and 01/02/07: removal of 163.6m^3/m of sediment, from the cross-shore profile in Figure 7, offshore of MLWS, left 35% bedrock exposure on 01/02/07 (an increase from 4% on 06/09/2006). Figure 8 illustrates the large scale beach volume changes during this period at Sandymouth beach. The photographs clearly show the mixed nature of the beach sediment with a gravel/boulder high water beach and sandy inter-tidal/low water zone (D_{50}=0.36mm). Bedrock exposure of approximately 100m in the cross shore between MHWN and MLWN in the 23/01/07 survey restricted the ability of the beach to respond to the prevailing hydrodynamic conditions, constraining sediment transport pathways, reducing depths to bedrock and hence altering drainage properties and sediment mobility, and driving bedrock controlled surf-zone currents (rip currents) during the mid and high tide.

Many beaches within the study region also accommodate small steams from local catchments which, during periods of heavy rainfall, cause the beaches to be completely saturated throughout tidal cycle affecting the mobility of the beach sand. This case study highlights the importance of the role of intertidal geology and beach drainage in the modifying the capacity of a beach to respond to the prevailing hydrodynamic conditions within this study area.

BEACH SAFETY IMPLICATIONS
Overview

Of key importance to beach safety managers is the understanding of the implications these changes in beach morphology, generalised in the beach type, have on temporal hazard signatures presenting the recreational beach user at any given time. Once an understanding of the potential hazards is gained, temporal and spatial modification of these hazards through morphological, wave, tidal and weather variations, on the scales of minutes to seasons, need to be assessed in order to safely manage beach users in these highly dynamic beach environments.

To investigate this RNLI lifeguard rescue and beach usage records, logged between 01/05/07 and 01/10/07, for all the LLT+BR and LTBR beaches studied (Figure 2) were analysed in combination with beach elevation and hydrodynamic records (near-shore wave buoy at Perranporth, and predicted tidal elevations). Illustrated in Figure 9 are the rescue totals (total and rip-related) for each week normalised by the average number of people in the sea per hour at a location during that week, and the corresponding wave (6 hour average) and tidal record. Weekly averaging of in the sea user numbers reduces bias occurring due to high weekend counts. The right panel qualitatively illustrates the morphological change seen along the coast at every spring tide during the season through a photographic series from Chapelporth beach. The results highlighted some key environmental factors controlling rescue numbers.
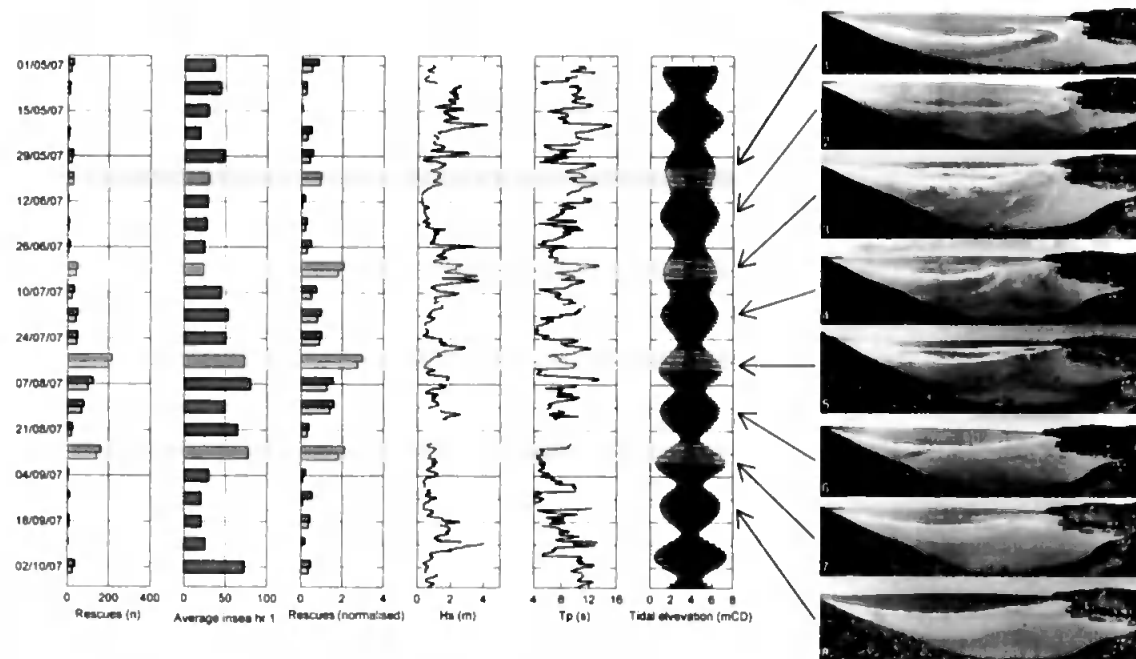
Figure 9. Plot shows data from all LTBR and LTT+BR beaches studied, from left to right; individuals rescued per week (total rescues and rip related rescues shown as dark and light bars respectively), averaged people in sea per hour for each week, total and rip rescues normalized by number of people in sea per hour, nearshore H_s and T_p (6hr average) and tidal elevation (meters from Chart Datum). Light grey bands highlight regions of interest. Photo series of Chapel Porth illustrates general regional morphological transition.

While lifeguard records indicate the number of rescues, many assumption s have to be made to utilize the data. A range of factors can affect rescues that occur on any given day including the number and experience of lifeguards on the beach per beach user, the nature of the beach user, the size of the bathing zone and local complexities in morphologies that generate hazards to the beach user. By analysing the data from a large number of locations within weekly temporal bins, the ability to assess broad trends in the data is improved. Finally, in normalising the rescues against people in the sea per hour, risk is assumed to be independent of the number of people in the sea.

Temporal variability of rip currents

Normalised rescue values show a general upward trend in rip rescues throughout the 2007 lifeguard season until the end of August when a sharp reduction in rip rescues occurred (Figure 9). The vast majority of rip incidents on the LTT+BR and LTBR beaches occur over the low tide rip systems, and the photo series of Chapelporth illustrates the presence and development of these systems until the end of August when the onset of small, short period wind waves that dominate until mid September lead to inter-tidal accretion and the infilling of the constraining rip channels (images 7 and 8 in Figure 9). This infilling of rip channels, seen in survey data at the majority of studied sites, can be associated with the reduction in rip rescues throughout late August and September.

Tidal effects

Macro-tidal and mega-tidal ranges within the region lead to large variations in the temporal hazard signature throughout the semi-diurnal cycle. Significantly, during spring tide periods, low tide bar/rip systems are exposed leading to intensification of rip current circulations. During neap tide periods, low tide bar/rip systems often remain submerged and inactive. This effect is demonstrated in the data shown in Figure 9 where peaks in the normalised rip rescue panel, highlighted in grey are all associated with weeks experiencing spring tides. The two largest peaks in normalised rip rescues during the beginning and end of August were also associated with the largest rate of change of tidal elevation from neap to spring tides (equinox tides), leading to rapid daily variation in beach exposure and horizontal translation rates.

The importance of the rate of change of the temporal hazard signature is exemplified by Figure 10 that shows 15 min shoreline contours at Croyde Bay, Devon, during a spring tide in 18/06/07 and 14/09/07. Locations of potential rip current hazards are highlighted. The rate of tidal translation reaches up to 7 m.min^{-1} within the mid-tide region in both surveys. This causes dramatic alongshore translation of rip hazards throughout the tidal cycle. Understanding these hazard variations is crucial in safely managing recreational beach users. Figure 10 also highlights the development of the low tide bar/rip morphology at Croyde Bay between 18/06/07 and 14/09/07.
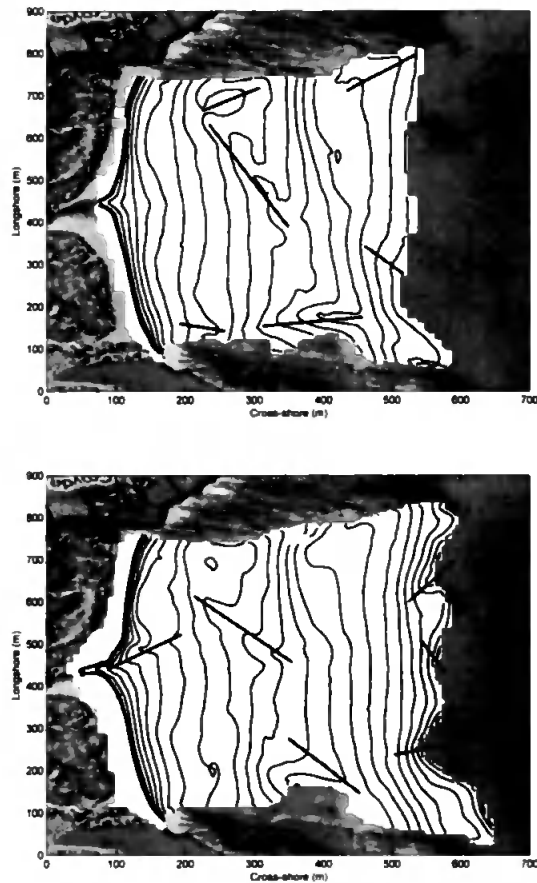
Figure 10. Plots A and B show 15 minute shorelines at Croyde Bay, North Devon during spring tides on the 18/06/07 and 14/09/07 respectively. Bold grey lines indicate regions of heightened rip current hazard.

CONCLUSIONS

An assessment of the seasonal variation in beach volume and morphology at locations along the high-energy (10% exceedence significant wave heights of 3-4m), macro/mega-tidal (4.1-6.9m) west coast of Devon and Cornwall, southwest England were made between summer 2006 and winter 2008. Significant morphological change was observed. Low-energy summer morphologies with low tide bar/rip systems and three dimensional mid tide bars were modified through high volume offshore sediment transport during winter causing inter-tidal beach lowering of ~0.5m-1m along all studied beaches. Planar inter-tidal beach morphologies with quasi-linear, shore-parallel, sub-tidal bars occurred

during winter. Sediment supply, geological exposure and drainage characteristics modified and restricted the envelope of potential morphological transition at some locations.

Implications of temporal morphological transition for beach safety were assessed. Rip current hazards were shown to increase as low-tide bar/rip systems developed throughout the winter/summer transition. Variability in exposure of inter-tidal geology in sediment poor environments controlled levels of constrained rip current hazard. Tidal elevation played a significant role in controlling the temporal hazard signature. Spring tides increased exposure of low-tide bar/rip morphologies increasing rip hazards during the lower tides. With wide inter-tidal zones and large mean spring tidal ranges, the rate of cross-shore translation of the surf-zone during spring tides increases the rate of change of the spatio-temporal hazard characteristics, having significant implications for lifeguard beach safety management. Periods of high morphologically driven beach hazard coincide with seasonal peaks in beach user numbers, increasing recreational beach risk.

REFERENCES

Masselink, G. and Short, A.D. 1993. The effect of tide range on beach morphodynamics, a conceptual beach model, *Journal of Coastal Research*, 9, 785-800.

Short, A. D. and Hogan, C. L. 1994., Rip Currents and beach hazards: Their impact on public safety and implications for coastal management, *In*: FINKL, C.W. (ed.), *Coastal Hazards*. Journal of Coastal Research Special Issue No. 12, 197-209.

Scott, T., Russell, P., Masselink, G., Wooler, A., and Short, A. D. 2007. Beach rescue statistics and their relation to nearshore morphology and hazards; a case study for southwest England, *Journal of Coastal Research*, SI 50 (Proceedings of the 9th International Coastal Symposium), 1- 6. Gold Coast, Australia

Short, A. D. 2006. Australian beach systems – Nature and distribution. *Journal of Coastal Research*, 22, 11-27.

Wright, L. D. and Short, A. D. 1984b. Morphodynamic variability of surf zones and beaches – A synthesis, *Marine Geology*, 56 (1-4), 93-118.

KEYWORDS – ICCE 2008

PAPER TITLE

High volume sediment transport and its implications for recreational beach risk

AUTHORS

Tim Scott' Paul Russell, Gerhard Masselink, Adam Wooler and Andrew Short

ABSTRACT NUMBER

911

KEY WORDS

Beaches
Sediment transport
Macro-tidal
Beach hazards
Beach safety
Rip currents

Rip current variability and hazard along a macro-tidal coast

T. Scott† P. Russell†, G. Masselink∞ and A. Wooler§

† School of Earth, Ocean and
Environmental Sciences
University of Plymouth
PL4 8AA
UK
timothy.scott@plymouth.ac.uk

∞ School of Geography
University of Plymouth
PL4 8AA
UK

§Surf Life Saving Great Britain
formerly: Royal National
Lifeboat Institution
West Quay Road
BH15 1HZ
UK

ABSTRACT

SCOTT, T., RUSSELL, P., MASSELINK, G. and WOOLER, A., 2009. Rip current variability and hazard along a macro-tidal coast. Journal of Coastal Research, SI 56 (Proceedings of the 10th International Coastal Symposium), 895 – 899. Lisbon, Portugal, ISSN 0749-0258.

The role of beach safety management is becoming increasingly important along much of the macro-tidal, high-energy Atlantic coast of England, which experiences mean spring-tidal ranges of 4.1–7.4 m and average significant wave heights of 1.2 m and 2.7 m in summer and winter, respectively. Growing pressures on beach resources due to increasing visitor numbers means an understanding of the nature of hazards surrounding the recreational beach user is paramount. Rip currents are responsible for 80% of all recorded incidents (2005–2007) along this coast. Most investigations into rip current dynamics have been reported from micro- and meso-tidal environments and macro-tidal rip systems have rarely been considered. This research assesses the spatio-temporal variability of macro-tidal rip current systems and their associated hazards along the west coasts of Devon and Cornwall between May and October 2007. Analysis of seasonal morphological and hydrodynamic datasets coupled with detailed lifeguard incident data and daily rip observations have identified some key drivers of recreational rip hazards and 'mass rescue' events on low-tide bar/rip and low-tide terrace and bar/rip beaches; 1) Small long-period swell-waves, that favour development of accretioary rip systems, shoal to the inner transverse bars generating strong alongshore variations in wave breaking and enhancing rip current activity; 2) Well developed, phase-offset low- and mid-tide bar/rip morphologies lead to the generation of active rip systems during low- and mid-tidal stages; 3) Large (spring) tidal ranges expose low-tide bar/rip systems, activating rip currents and increasing tidal cut-off potential and the rate-of-change of alongshore rip location through low- and mid-tide. Low-tide times during spring tides coincide with lifeguard patrol hours and hence times of high beach usage.

ADDITIONAL INDEX WORDS: *Beach safety, rip currents, beach type, high energy, macro-tidal.*

INTRODUCTION

With a high level of pressure from recreational beach usage along the Atlantic coast of England, the role of beach safety management is becoming increasingly important as the period of intense leisure use of the surf-zone persists into the spring and autumn months. An understanding of the physical hazards posed to the in-sea beach user by the surf-zone environment is integral to the ongoing improvement of the beach safety management service and is the key motivator for this research.

Previous investigations into beach hazards in the UK, Australia and the USA (SHORT, 1999; SCOTT et al., 2007; SCOTT et al., 2008) have indicated that rip currents are the cause of the majority of rescues and fatalities within the beach environment. Scott et al. (2008) found that 68% of all recorded incidents by the Royal National Lifeboat Institution (RNLI) in the UK were due to rip currents. 90% of these incidents were related to the contribution from beaches with identifiable rip channel morphologies: Low tide bar/rip (LTBR) and Low tide terrace + bar/rip (LLT+R) beaches (see Figure 1 and 2). In general, these two beach types share a propensity for rhythmic bar and rip current systems below mean low water neaps (MLWN) where the tidal stationarity within a high-energy, macro-tidal environment is such that the bar/rip

Figure 1. Exposed spring low-tide bar/rip morphology at Perranporth, Cornwall. A large number of recreational beach users can be seen populating the low-tide bars (T Scott).

morphological systems have the chance to develop. Tidal smearing restricts morphological development throughout the mid-tide region. Accompanying investigations (SCOTT et al.,

2008) record the dynamic nature of these systems within the seasonal wave climate cycle as the systems often transition from a featureless, linear sub-tidal multi-bar state with low frequency rythmicity during high-energy storm conditions, to highly developed low-tide bar/rip systems with increasingly developed lower mid-tidal bars during lower energy swell conditions (Figure 2). Short (1985) has classified rip systems into 4 categories: Accretionary and erosional, associated with beach rips that are fixed (low-energy) and migratory (high-energy) respectively, topographic rips that that generated through the influence of solid structures (groynes, jetties) and large scale megarips that occur during high waves. Scott *et al.*, (2007) examined rip types within a UK beach hazard context and differentiated between the low- to mid-tide accretionary beach rips and geologically (topographically) constrained rip systems that are generated at mid and hide tide due to hard rock intrusions into the surf-zone as those key to understanding levels of hazard posed to the beach user.

Most investigations into rip current dynamics have been reported from micro- and meso-tidal environments (SHORT and BRANDER, 1999; BRANDER and SHORT, 2001; MACMAHAN *et al.*, 2006) and macro-tidal rip systems have rarely been considered. This research assesses the spatio-temporal variability of macro-tidal rip current systems and their associated hazards along the west coasts of Devon and Cornwall, which experience mean spring-tidal ranges of 4.1–7.4 m and average significant wave heights of 1.2 m and 2.7 m in summer and winter, respectively. The principal aim of this investigation is to assess the contribution of key mechanisms that force and control rip current circulations with respect to their effect on the temporal hazard signature within a given spatial extent. Specifically, the study aims to investigate the reports of occasional 'mass rescue' events during the summer period.

DATA COLLECTION

A campaign of data collection was undertaken between 01/05/07 and 01/10/07 at 27 beach sites that represent both, LTBR and LTT+R beach morphologies along the Atlantic west coast of Devon and Cornwall, southwest England (Figure 3). Hydrodynamic conditions were monitored with a near-shore directional waverider buoy at Perranporth beach (50.35379°N, 5.17497°W; 10m water depth). Hourly wind statistics were
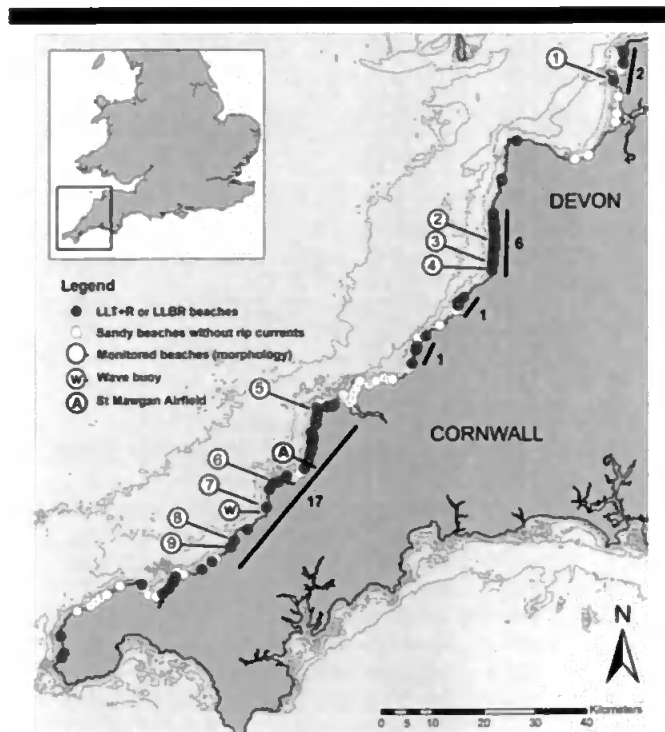

Figure 3. Map of study region and study site locations.

recorded at St Mawgan airfield. Beach morphology was measured monthly through ATV based RTK GPS surveys at selected sites, and Argus video data at Perranporth beach provided beach and surf-zone images at 30 minute intervals. Rip hazard and severity of rip currents were assessed through analysis of comprehensive incident records and beach user counts collected by the RNLI lifeguards at all 27 (indicated by numbered black bars in Figure 3) studied beach locations on a daily basis. Daily assessments of rip severity at all tidal levels were estimated by the RNLI lifeguards at 4 sites representing both LTBR and LTT+R morphologies.

REVIEW OF RESULTS

Rip current morphology and distribution

LTBR and LTT+R beaches represent 59% (62% by length) of all west coast beaches with sandy lower inter-tidal zones. These beaches with rip morphologies are mostly located on the high-energy west facing beaches (Figure 3) with lower-beach sediment sizes ranging from 0.3 mm to 0.48 mm and upper-beach from 0.29 mm to gravel/boulder. Monthly GPS surveys collected between May and October 2007 indicate that these beach types exhibit a degree of synchronicity in their response to changes in wave climate throughout the winter/summer morphological transition (see Scott *et al.*, in press, for further information). A general accretionary trend during the spring/summer transition was observed whereby low-energy swell wave conditions during summer months led to the generation of deep transverse low-tide bar/rip morphology and complex phase offset incised inter-tidal bar/rip systems (Figure 2).

Rip current severity and density

Observed daily at low-, mid- and high-tide, a scaled, qualitative assessment of rip current severity was made by experienced
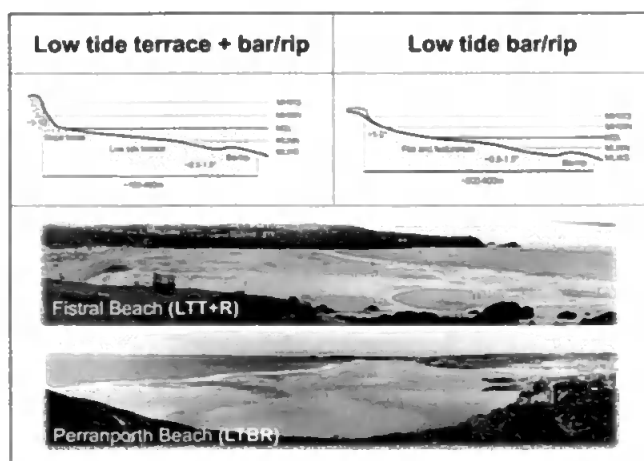

Figure 2. Illustrated description and examples of LTBR and LTT+R beach types in the UK (T Scott).

Table 1: Mean rip current severity and rip number with tidal stage at selected Atlantic west coast beaches.

Beach name	Beach type	Rip types	Low tide		Mid tide		High tide	
			Rip severity	Rip number	Rip severity	Rip number	Rip severity	Rip number
Perranporth (7)	LTBR	B	3.9	3.6	3.5	2.6	3.0	1.9
North Fistral (6)	LLT+R	B	3.0	2.5	2.4	1.7	2.1	1.6
Sandymouth (2)	LLT+R	B+G	3.2	1.5	3.2	1.7	3.3	2
Constantine (5)	LLT+R	B+G	2.9	1.7	3.8	1.9	3.0	2.6

Rip types indicate the presence of Accretionary and Erosional Beach rip systems (B) and Geologically controlled rip systems (G): Rip severity represents mean observed rip strength daily at three tide levels (where data was available). Data scaled from 0 (no rips) to 5 (extreme). Rip number is mean observed number of rip present at each observation.

lifeguards at 4 beach sites shown in Table 1. Severity was estimated by determining the hazard the rip current would pose to an average swimmer. Beaches dominated by beach rips (B) show a decrease in mean rip severity and mean rip number from low- to high-tide with Perranporth (LTBR) having a higher mean rip severity at each stage of the tide than North Fistral (LLT+R). Sandymouth and Constantine, both LTT+R beaches, possess geologically controlled rip systems in the mid- and high-tide regions. This appears to be reflected in the mean severities that are similar throughout the inter-tidal zone at Sandymouth and enhanced in the mid-tide region at Constantine.

Lifeguard rip incident records

Reported 'mass rescue' (MR) events during the study period appeared to occur at multiple locations on the same day. To identify and assess these observations it was important to investigate rip incidents in relation to the number of people in-sea on any given day. Hourly people counts at each beach enabled calculation of daily mean estimates for people in-sea over the entire coast (all 27 sites). During the course of the monitoring period, short periods of high rip current incident density were recorded. These events can be seen in Figure 4 (inset) as 7 outliers from the bulk of the data which displays a good linear relationship (R^2=0.54) considering the inherent scatter expected in the data. By normalizing incidents by people in-sea these outlier events can be clearly identified in time. All occurring in July and August, the 7 highlighted events exceed 2 standard deviations from the mean.

'Mass rescue' events

Identification

For the purpose of this study we were interesting in identifying events where high levels of rip incidents were occurring at multiple locations on the same day. This should give some insight into regional environmental conditions that may be key drivers in the cause of these events. Identifying environmental conditions in this way, of course, will not identify all the days when these optimal environmental conditions exist as identification requires people in-sea, hence Figure 4 shows a higher density of normalised rip incidents during the summer holiday months of July and August. Likewise, an assumption is made that all locations are proportionally staffed with lifeguards of equal ability to mitigate against'incidents.

Environmental conditions

Figure 5 shows a timeseries of environmental conditions (hydrodynamic, morphodynamic and wind) throughout the study period with the MR events labeled A to G. With mean H$_s$=1.2 m and maximum H$_s$=4.4 m, the nearshore wave record shows high-

energy wave events during the first half of May and start of July, followed by relatively low-energy conditions until the end of September. A mean and maximum T$_p$ of 8.8 s and 15.7 s respectively indicates the presence of swell wave conditions throughout the study period. The mean spring tidal range at Perranporth is 6.1 m, decreasing in the order of 2 m during neap tides. Towards the end of the study period (autumnal equinox) the tidal range varies from 1.67 m (20/9) to 7.17 m (28/9). Rip current locations at Perranporth were calculated from all time-averaged rectified video images available at low- and mid-tidal stages. Data gaps are due to either lack of image (technical) or very small (no rip activity) or large wave conditions (wave breaking occurred in rip channels). Rips were located through a reduction in alongshore pixel intensity associated with reduced wave breaking. The rip head was used to locate the rip in the alongshore. No systematic alongshore migration of rip current was identified. Largest changes in rip morphology occurred during prolonged periods of high winds and large waves (>2 m). Mid-tide rip systems were more dynamic and were absent for a large part of the record. They are distinct from the low-tide systems and are predominantly phase offset. Morphological enhancement of mid-tide rip systems during the low waves and high spring tidal ranges of August and September suggests they may be incised by tidal drainage.
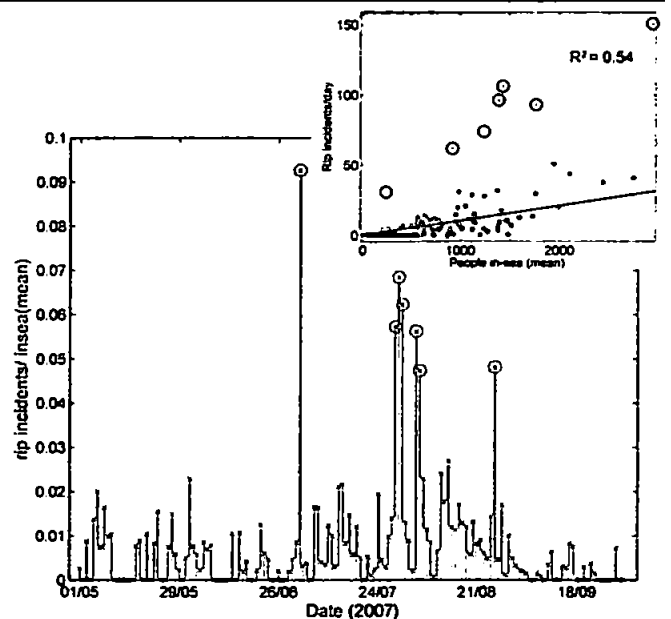

Figure 4. (Inset) Scatter plot of rip incidents per day vs. people in-sea (mean), indicating linear fit and outliers. (Main) Stem plot of normalised rip incidents (daily) vs. date, with outliers circled.
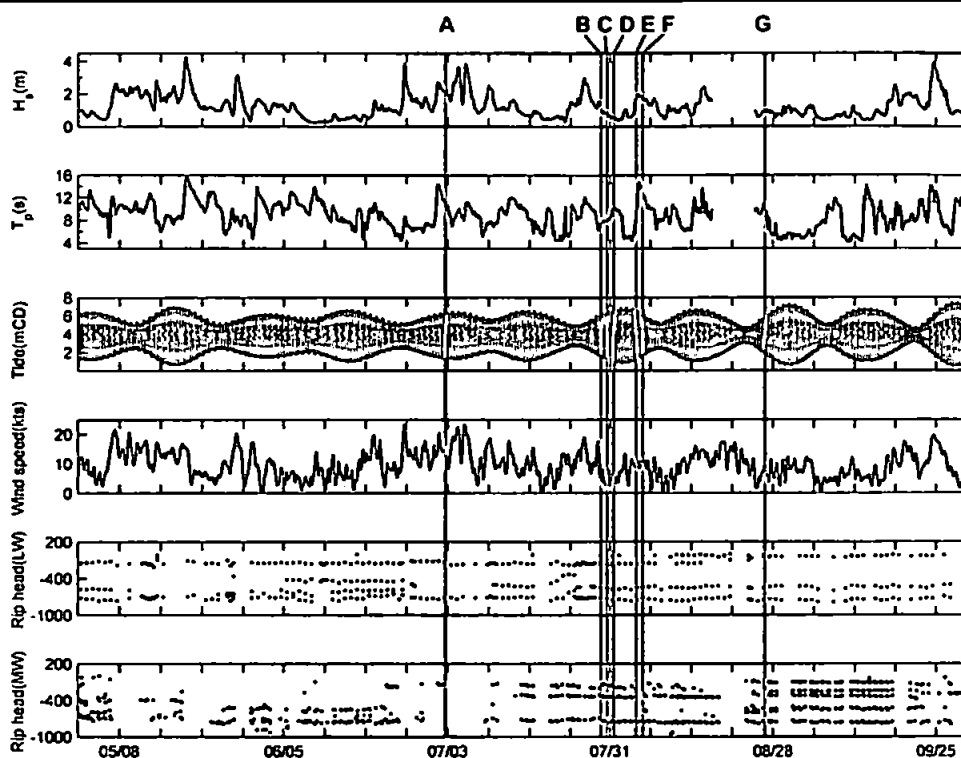
Figure 5. Overview of environmental conditions during the study period. (From top) Significant nearshore wave height (m) at Perranporth; Peak wave period (s); Predicted tidal elevation (meters relative to Chart Datum) for Perranporth; 10 m hourly mean wind speed (kts) for St Mawgan airfield; Alongshore low and mid tide rip head locations (m) at Perranporth from Argus cameras. Grey lines A to G indicate days in which outlier rip incidents ('mass rescues') occurred.

Event characterisation

Assessment of the incident characteristics and environmental conditions during the highlighted (A to G) MR events in Figure 5 indicated that except for A, all events involved ≥10 beaches (Table 2) with 15 beaches contributing to event D. Event A included only 3 beaches, one of which contributed 90% of the incidents therefore is not considered a spatially widespread incident. The remaining events fall into 3 distinct periods; 1) B, C and D, occurring on consecutive days totaled 264 rip incidents, with between 12 and 15 beaches involved each day; 2) E and F occurred on consecutive days totaling 171 rip incidents and involved 10 and 11 beaches respectively; 3) Event G, saw 151 incidents in one day spread among 12 beach sites. These events had a number of key environmental characteristics in common. Relatively small swell waves (H_s=0.5–1.7 m; T_p=7.6–12.8 s) were the dominant wave energy during all the MR events. All the MR events occurred during a tidal range large enough to expose the low tide bar/rip morphology (spring) and in this region larger tidal ranges always coincide with low water occurring during patrol hours leading to higher potential hazard exposure. Wind speeds during the MR events were commonly on or below the average of the study period (10 kts) with direction showing no trend. In all the examined MR events, 3D survey and photograph/video imagery supported the observation that the low- and mid-tide bar/rip systems were well developed along the coast as illustrated in the example plan view video images of Perranporth in Figure 6. Well developed rip feeder systems isolated the bar crests at low-tide and mid-tide bar/rip systems, incised by tidal drainage, are

well developed and offset in the alongshore from the low-tide rip channels (highlighted in Figure 6). Times of rip incident occurrence related to tidal stage during each MR event (Figure 6) indicate that the majority of rip incidents occurred within the mid- and low-tide periods and in D, E, F and G the transition between low- and mid-tide generated the highest incident frequency. During this transition period, locations of rip current hazard can migrate rapidly through high tidal translation rates, tidal elevation can modulate rip current velocities 'switching' systems on and off, and tidal cut-off on exposed low-tide bars during the flooding tide can force bathers to return landward through the active rip feeder channel once a critical depth over the bar in reached (1–2 hours after low-tide). It is suggested that this period presents a challenge, both in beach safety management and on-site interpretation and prediction of surf zone processes, as when critical thresholds are reached, a rapid mitigating response is required.

CONCLUSIONS

The results present an insight into the rip current variability and hazard along the Atlantic west coast of southwest England. The coalition of detailed lifeguard incident data with that of beach morphology and hydrodynamic conditions enabled an assessment of the spatial extent and characteristics of rip currents within the study region and the identification and investigation of reported multi-location 'mass rescue' events. From this initial investigation of the period between 01/05/07 and 01/10/07 the following has been identified:

- LTBR and LTT+R beaches represent 59% (62% by length) of all west coast beaches with sandy lower inter-tidal

Table 2: Outlier rip incident event ('mass rescue') data.

Event	LW times (height mCD)	Date (2007)	No. of beaches	Incidents	Highest contributors (%) **primary**(secondary)	H_s (m) 6hr avg.	T_p (s) 6hr avg.	Wind (kts) mean	Wind dir (°)
A	1218 (1.3)	2/7	3	31	**90**(7)	2.3	10.9	13.7	235
B	1046 (1.5)	29/7	13	62	**23**(21)	1.0	7.6	6.5	10
C	1124 (1.2)	30/7	12	106	**59**(10)	0.7	8.2	5.5	259
D	1203 (1.0)	31/7	15	96	**20**(14)	0.5	10.1	5.6	113
E	1452 (1.2)	4/8	10	77	**26**(26)	1.7	10.9	10.5	174
F	1540 (1.6)	5/8	11	94	**30**(17)	1.7	12.8	10.8	252
G	0947 (1.8)	26/8	12	151	**22**(17)	1.0	9.6	8.3	12

zones, mostly located on the high-energy west facing beaches. A degree of synchronicity in their response to changes in wave climate throughout the winter/summer morphological transition was observed.

- A general accretionary trend during the spring/summer transition was observed whereby low-energy swell wave conditions during summer months led to the generation of deep transverse low-tide bar/rip morphology and complex phase offset incised inter-tidal bar/rip systems.
- Beach rip severity was observed to be highest at low tidal levels and geologically constrained rips highest at mid- and high-tidal levels.
- Analysis of 6 coast-wide 'mass rescue' events identified possible key environmental components that when combined could be a driver for these events which overstretch lifeguard services. 1) Relatively small, long period swell waves means shoaling extends to the inner transverse bars generating increased alongshore gradient in wave breaking and therefore rip current activity. Under these conditions increased wave groupiness increases the complexity of rip current dynamics; 2) Well developed, phase offset low- and mid-tide bar/rip morphologies, present during the MR events lead to the generation of active rip systems during low- and mid-tidal stages; 3) Large tidal ranges during spring tides increase the rate of change of alongshore rips position, reducing the time for lifeguards to respond to time varying intensity and alongshore translation of rip currents during the transition from low- to mid-tide. Large spring tidal ranges allow wave breaking on low-tide bar/rip systems and enable accessibility to, and subsequent tidal cut-off of low-tide bar crests. During spring tides, low water times coincide with lifeguard patrol hours and hence times of high beach usage.

Further investigations of macro-tidal rip currents in this region are being conducted using Argus video, GPS surveying, in-situ sensors and GPS-tracked Lagrangian surf zone drifters to quantify the rip flow dynamics and circulation over a low-tide bar/rip system under optimal high hazard conditions.

LITERATURE CITED

BRANDER, R.G. and SHORT, A.D., 2001. Flow kinematics of a low energy rip current system. *Journal of Coastal Research*, 17, 468-481.

MACMAHAN, J, THORNTON, E.B. and RENIERS, A. J. H. M., 2006. Rip current review. *Journal of Coastal Engineering.* **53** (2–3), pp. 191–208.

SCOTT, T.M., RUSSELL, P.E., MASSELINK, G., WOOLER, A. and SHORT, A., 2007. Beach rescue statistics and their relation to nearshore morphology and hazards: a case study for south-west England. *International Coastal Symposium. Journal of Coastal Research, Special Issue.* 50, 1-6

SCOTT, T.M., RUSSELL, P.E., MASSELINK, G., and WOOLER, A., 2008. High volume sediment transport and its implications for recreational beach risk. *Proceedings of the 31st International Conference on Coastal Engineering (Hamburg, Germany), in press.*

SHORT, A D, 1985. Rip current type, spacing and persistence, Narrabeen Beach, Australia. *Marine Geology*, 65, 47-71.

SHORT, A.D., 1999. Beach hazards and safety. In Short A.D.(ed.), *Beach and Shoreface Morphodynamics*. John Wiley & Sons, Chichester, 292-304.

SHORT, A.D. and BRANDER, R., 1999. Regional variation in rip density. *Journal of Coastal Research*, 15, 813-822.
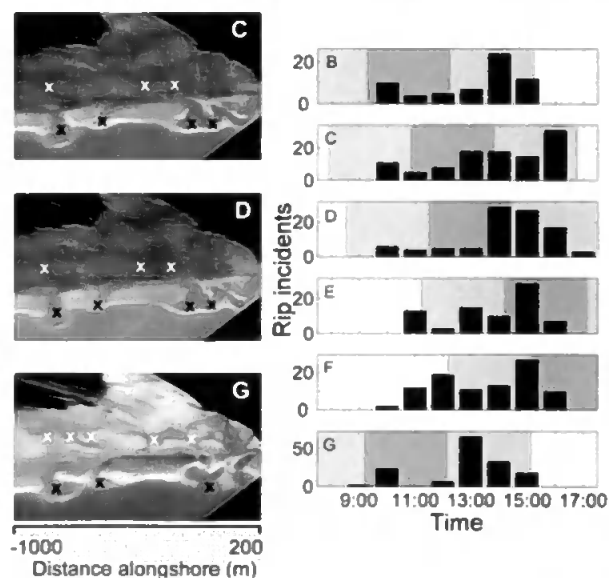
ACKNOWLEDGEMENTS

Figure 6. (Left) Time averaged, rectified, low-tide video images of Perranporth during events C, D and G; sea is located at the bottom of each image, land at the top. West is oriented down-page; black markers locate approximate positions of low-tide rip currents, white locates mid-tide rip channel morphology (Right) Histograms of incident times for each event. Dark shading indicates 3 hour low-tide period and light shading the mid-tide.